

Hydrolysis of Primary Sewage Sludge under Methanogenic, Acidogenic and Sulfate-reducing Conditions

by

**NE Ristow, SW Sötemann, RE Loewenthal,
MC Wentzel and GA Ekama**

**WRC Report No. 1216/1/05
ISBN No. 1-77005-290-5**

March 2005

Disclaimer

This report emanates from a project financed by the Water Research Commission (WRC) and is approved for publication. Approval does not signify that the contents necessarily reflect the views and policies of the WRC or the members of the project steering committee, nor does mention of trade names or commercial products constitute endorsement or recommendation for use.

Executive Summary

1. Background

Sewage sludges typically comprise 1% or less of the total volumetric flow handled by sewage treatment plants, while their treatment may represent 30 - 40% of the total costs of the sewage treatment. Of the sewage sludges, primary sewage sludge (PSS) is the largest fraction of the solids treated, approximately two thirds of the total. Treatment of these sludges is required before disposal, and anaerobic digestion is the most common treatment process, resulting in a stabilized sludge with a low residual sludge volume.

Anaerobic digestion can occur under three operating conditions: Methanogenic systems, which produce methane gas as the final COD product; sulfate-reducing systems, which require sufficient sulfate as input, and produce sulfide (aqueous, gaseous and metal sulfides precipitates) as the final COD product; acidogenic systems, which refer to anaerobic digestion systems in which methanogenic and sulfate-reducing conditions are not present, and the end product of the digestion is in the form of soluble COD.

Of these three types of systems, methanogenic systems are the most widely implemented for sludge treatment, and hence have been studied the most extensively. Conventionally, in the methanogenic treatment of PSS, acidogenic digestion and sulfate reduction are considered undesirable, as the former results in loss of methane production and the latter in odour problems. However, more recently for both situations PSS has been considered as a potential beneficial source of substrates. The products of the sequence of hydrolysis and acidogenesis (acidogenic digestion) are the volatile fatty acids (VFA) which are directly beneficial in downstream biological nutrient removal (BNR) activated sludge systems, or in the biological reduction of sulfate (internal or external to the digester) in the treatment of sulfate-rich acid mine drainage (AMD).

AMD is characterized by high concentrations of heavy metals, sulfate and total dissolved solids, coupled with a low pH. The Rhodes BioSURE[®] Process has been developed as a low cost active treatment of AMD waters. The process flow diagram consists of a series of interconnected biological and chemical unit operations that allows for the removal of heavy metals and salinity (particularly sulfate) from AMD.

The core reaction in the overall process is biological sulfate reduction using PSS as the electron donor and organic carbon source, with the concomitant production of sulfide and carbonate alkalinity. This reaction takes place in the recycling sludge bed reactor (RSBR) and a second sulfate-reducing digester. The main aim of the RSBR is to solubilize the PSS to soluble organic matter such as VFA, which then are used by the sulfate-reducing bacteria in the second sulfate-reducing digester. The sulfide and carbonate alkalinity produced in this process are recycled and contacted with the feed AMD, neutralizing the pH and precipitating the heavy metals as metal sulfides, carbonates and hydroxides. The remaining effluent from the sulfate-reducing digester is discharged to a sulfide-oxidizing reactor, where aqueous sulfide is oxidized to elemental sulfur. A high rate algal pond polishes this effluent.

Since the core reaction in the Rhodes BioSURE[®] Process is biological sulfate reduction with PSS, the design, operation and control of the process is dependent on the rate at which the PSS is utilized. A mathematical kinetic model describing and quantifying the rate of PSS utilization for sulfate reduction would be an invaluable aid in the design, operation and control of the biological sulfate reduction step in the Rhodes BioSURE[®] Process. However, such a mathematical model is not presently available and information on the rate of PSS utilization under sulfate-reducing conditions is limited, retarding development of such a model. Thus, such information needs to be developed. This would have to take account of the conditions prevailing in the RSB. These would include variations in concentration of the substrates and products as well as pH. Therefore, in order to determine the rate of PSS hydrolysis under sulfate-reducing conditions in the RSB, it is necessary that the influence of the various operating conditions on the rate be quantified. A mathematical model of the RSB would need to include these effects, and if formulated correctly, would provide a valuable tool for the optimization of the RSB operation.

Under the three operating conditions (methanogenesis, acidogenesis and sulfate-reducing), hydrolysis of the particulate PSS is the rate-limiting process, and hence the design, operation and control of these systems rely on this process being accurately quantified under different operating conditions. Several studies have investigated the digestion of PSS under each of the operating conditions (methanogenic, acidogenic and sulfate-reducing). However, systematic quantification of the PSS hydrolysis rate under all three conditions is limited. Further, no single study has investigated PSS hydrolysis kinetics under methanogenic, acidogenic and sulfate-reducing conditions in a manner that allows direct comparison of the PSS hydrolysis rates, and their interaction with system operational parameters, such as retention time, feed concentration and pH.

2. Objectives

The Water Research Commission (WRC) identified the use of PSS as electron donor for biological sulfate reduction in the remediation of AMD as of particular interest to South Africa, and accordingly contracted the Water Research Group in the Department of Civil Engineering at the University of Cape Town to investigate the kinetics of PSS hydrolysis under sulfate-reducing conditions, such as in the Rhodes BioSURE[®] Process (WRC contract no. K5/1216, April 2001 to March 2003). The original specific objectives were to:

- quantify the effects of sulfate reduction and pH on the rate of PSS hydrolysis, and to
- establish design parameters for biological sulfate reducing systems treating AMD using PSS as the electron donor/carbon source.

To quantify the effects of sulfate reduction and pH on the rate of PSS hydrolysis, the rate of PSS hydrolysis under methanogenic and acidogenic conditions needed to be quantified as a basis for comparison. This necessitated that the original objectives in the contract be expanded to include experimental investigations into, and mathematical modelling of, the rate of PSS hydrolysis under methanogenic and acidogenic conditions. During the course of the investigation on methanogenic systems, it appeared that a number of physical constraints imposed by the system influenced the rate of PSS hydrolysis, in particular retention time and influent PSS feed concentration. This required that these influences be quantified. Due to the considerable increase in the scope of the project, the research contract was extended for 1 year (April 2003 to March 2004) with additional funding.

Therefore, the principle aim of this study is to determine the rate of hydrolysis of PSS under methanogenic, acidogenic and sulfate-reducing conditions, and the influence of the system physical constraints on the rate. This also will enable a direct comparison of the rate under each of the three conditions, to determine possible influences on the rate.

In terms of this aim, the original objectives were expanded to include the following:

1. To determine the rate of hydrolysis of PSS under methanogenic conditions
2. To determine the effects of feed COD concentration, hydraulic retention time and pH on the rate of hydrolysis under methanogenic conditions
3. To develop a mathematical model for the biological processes mediating PSS hydrolysis in methanogenic systems, so that the rate of hydrolysis can be predicted for various feed COD concentrations, hydraulic retention times and operating pH, based only on the feed characterization and system operation
4. To evaluate the various rate formulations for the PSS hydrolysis at varied operating conditions, so that the most appropriate rate formulation for hydrolysis of PSS under methanogenic conditions can be identified
5. To collect data on methanogenic systems that can be used to calibrate a more extensive dynamic mathematical model for methanogenic anaerobic digestion including physical processes such as acid/base equilibria and vapour/liquid equilibria (development of this model does not form part of this research, but is part of a parallel project)
6. To determine the rate of PSS hydrolysis under acidogenic conditions
7. To determine the effects of feed COD concentration, hydraulic retention time and pH on the rate of hydrolysis under acidogenic conditions
8. To appropriately modify the mathematical model selected in 4. above, to predict the rate of hydrolysis under acidogenic conditions
9. To determine whether PSS can support internal sulfate-reduction, and to develop a greater understanding of sulfate reduction in PSS fed systems
10. To determine the rate of PSS hydrolysis under sulfate-reducing conditions
11. To determine the effects of sulfate-reduction on the rate of hydrolysis of PSS

3. Experimental Investigation

The research approach adopted was to operate 6 parallel laboratory-scale completely-mixed anaerobic digesters with PSS as influent, and to monitor the behaviour of these systems under a range of feed COD concentrations, retention times, pH and feed sulfate concentrations under stable methanogenic, acidogenic and sulfate-reducing conditions. This experimental programme required the development and construction of novel apparatus (e.g. sealed completely mixed digesters, gas flow measurement devices) and analytical methods (e.g. measurement of sulfate in the presence of organics).

4. Results and Conclusions

4.1 Methanogenic systems

Completely mixed methanogenic anaerobic digesters were operated at hydraulic retention times (= SRT) from 5 to 60d, with feed COD concentrations of 2, 13, 25 and 40gCOD/L at a controlled temperature of 35°C, see Table 1.

Table 1: Steady states measured for varying hydraulic retention times and feed COD concentrations (numbers indicate steady state period number)

Feed COD Concentration (gCOD/L)	Hydraulic Retention Time (d)							
	60	20	15	10	8	6.67	5.71	5
40			10; 11	12	21	23	28	
25		3	4	1	2	7	8	9
13			5	13	14	24	31	
9	17							
2				25	26			

For each feed COD concentration, the system hydraulic retention time was decreased step-wise until methanogenesis became unstable. Steady states periods were operated and analysed at regular retention time intervals. For these steady states:

- The minimum hydraulic retention time at which stable operation was observed was 5d at a feed COD concentration of 25gCOD/L
- Very good COD mass balances were obtained (mostly within 95 – 105%). The good COD recoveries lend credibility to the experimental data
- Reactor volatile fatty acid (VFA) concentrations were below 50mgHAc/L, and for most steady states considerably less than this

The above two observations indicate that stable methanogenic conditions had been established in all systems, a requirement for further analysis of the data

Based on an understanding of the concepts of the processes operating in the digesters:

- Characterization of the PSS is essential in order to quantify PSS hydrolysis rates correctly
- The influent PSS was characterized to give:

$$S_{ti} = S_{upi} + S_{bpi} + S_{usi} + S_{bsfi} + S_{VFai}$$

where S_{ti} is the PSS total feed COD concentration, S_{upi} is the unbiodegradable particulate concentration, S_{bpi} is the biodegradable particulate concentration, S_{usi} is the unbiodegradable soluble concentration, S_{bsfi} is the biodegradable soluble non-VFA (fermentable) concentration and S_{VFai} is the volatile fatty acids concentration.

In terms of the characterization of the PSS above, from the application of mass balance principles, the volumetric rate of PSS hydrolysis ($\text{rate}_{\text{hydrolysis}}$) was quantified for each steady state of operation (Figure 1):

- Consistent trends in the effects of SRT and PSS feed concentration were evident, substantiating data consistency
- For all feed COD concentrations, a decrease in the PSS feed concentration causes a corresponding decrease in $\text{rate}_{\text{hydrolysis}}$
- From an analysis of the data for the SRT = 60d system, the unbiodegradable particulate COD (S_{upi}) as a fraction of the total PSS COD concentration (S_{ti}) was 33.45%. Alternative analytical techniques gave the unbiodegradable particulate fraction of the COD as 33.3% for the entire data set, and hence the value of 33.45% was accepted. This value closely corresponds with the 36% obtained for the data of O'Rourke (1968).

From the literature, various rate formulations for PSS hydrolysis were identified, and evaluated against the measured methanogenic anaerobic digester data. These included (with the appropriate calibrated kinetic constants):

- First order kinetics: $\text{rate}_{\text{hydrolysis}} = k_h \cdot S_{\text{bp}}$ (1)

where $k_h = 0.992 \pm 0.492\text{d}^{-1}$

- First order specific kinetics: $\text{rate}_{\text{hydrolysis}} = k'_h \cdot S_{\text{bp}} \cdot Z_{\text{ad}}$ (2)

where $k'_h = 0.00138 \pm 0.00131 \text{ L/mgZ}_{\text{ad}} \text{ as COD.d}$

- Monod kinetics: $\text{rate}_{\text{hydrolysis}} = \frac{\mu_{\text{max}} \cdot S_{\text{bp}} \cdot Z_{\text{ad}}}{Y_{\text{ad}} (K_S + S_{\text{bp}})}$ (3)

where $\mu_{\text{max}} = 0.243\text{d}^{-1}$ and $K_S = 640\text{mgCOD/L}$

- Surface reaction kinetics: $\text{rate}_{\text{hydrolysis}} = \frac{k_{\text{max}} \left(\frac{S_{\text{bp}}}{Z_{\text{ad}}} \right)}{\left(K_S + \frac{S_{\text{bp}}}{Z_{\text{ad}}} \right)} Z_{\text{ad}}$ (4)

where $k_{\text{max}} = 11.2\text{mgCOD/mgZ}_{\text{ad}} \text{ as COD.d}$ and $K_S = 13.0\text{mgCOD/mgZ}_{\text{ad}} \text{ as COD}$, and where S_{bp} is the biodegradable particulate COD concentration (mgCOD/L) and Z_{ad} is the acidogenic biomass concentration (mgCOD/L).

From an assessment of the fit of predicted to calculated values, it could be concluded that:

- The first order kinetics and surface reaction kinetics most accurately predict the rate of PSS hydrolysis under methanogenic conditions for all hydraulic retention times and feed COD concentrations evaluated.
- Since first order kinetics are a simplification of the hydrolysis process (the acidogenic biomass is not explicitly included, nor is there an upper limit to the rate), surface

reaction kinetics (Eq 4) are the most appropriate rate formulation for PSS hydrolysis

- However, due to the simplicity of first order kinetics, and since these kinetics were able to accurately predict the PSS hydrolysis rate under all operating conditions, first order kinetics were used in this study to compare the PSS hydrolysis rates under the different operation conditions
- With the first order kinetics and a first order kinetic constant value of $0.992d^{-1}$, and an unbiodegradable particulate COD fraction of 33.45% of the total feed COD concentration, very close correlation was obtained between model predicted and calculated (from experimental data) volumetric rates of PSS hydrolysis and effluent COD concentrations under methanogenic conditions for all hydraulic retention times and feed COD concentrations, see Figures 1 and 2 respectively

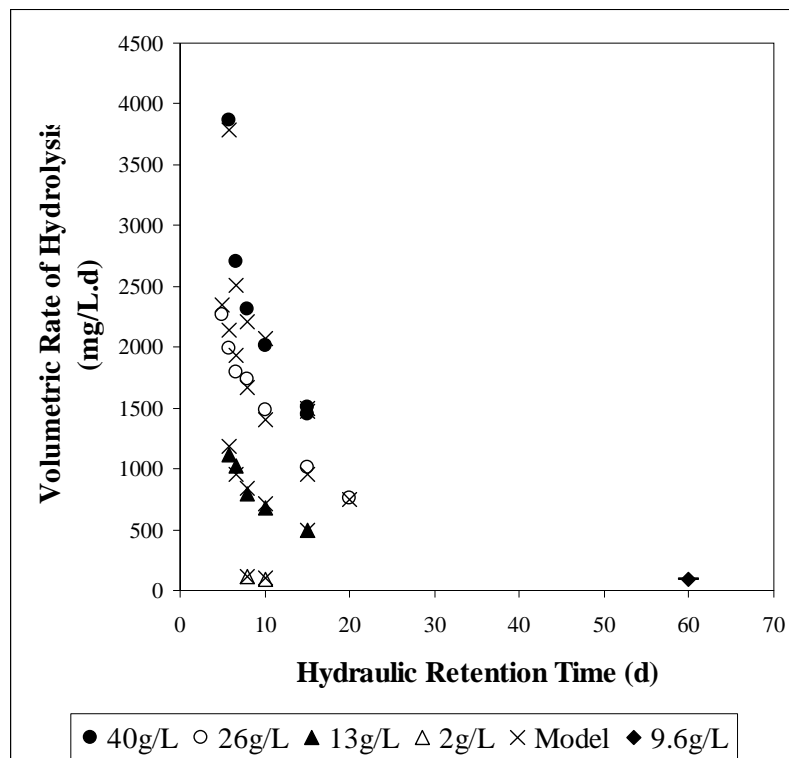


Figure 1: Calculated (from experimental data) and predicted (first order kinetics) rate of hydrolysis for each hydraulic retention time at each feed COD concentration for methanogenic systems

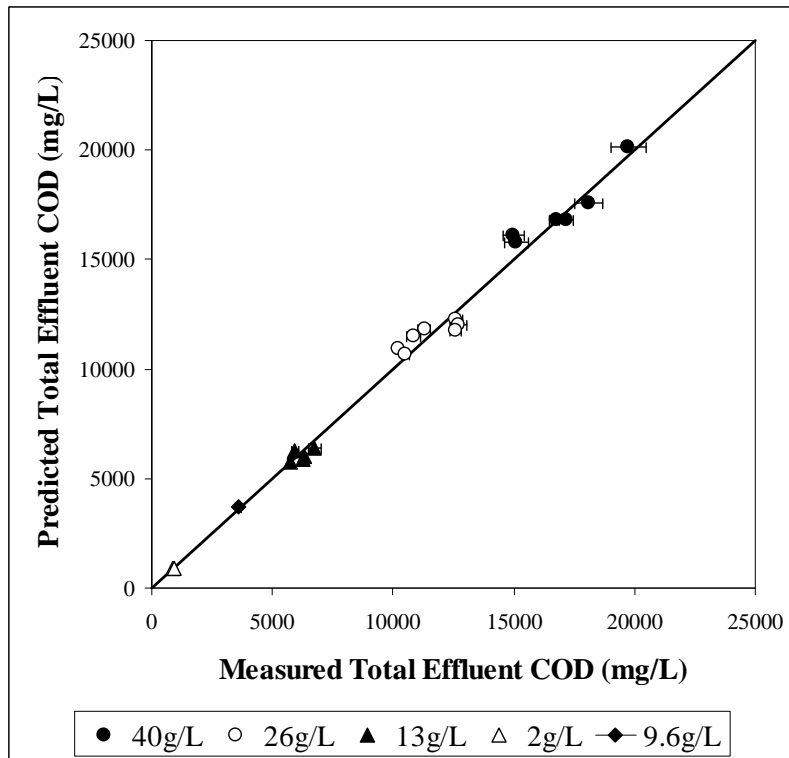


Figure 2: Predicted versus measured total effluent COD concentration for each feed COD concentration and hydraulic retention time for methanogenic systems

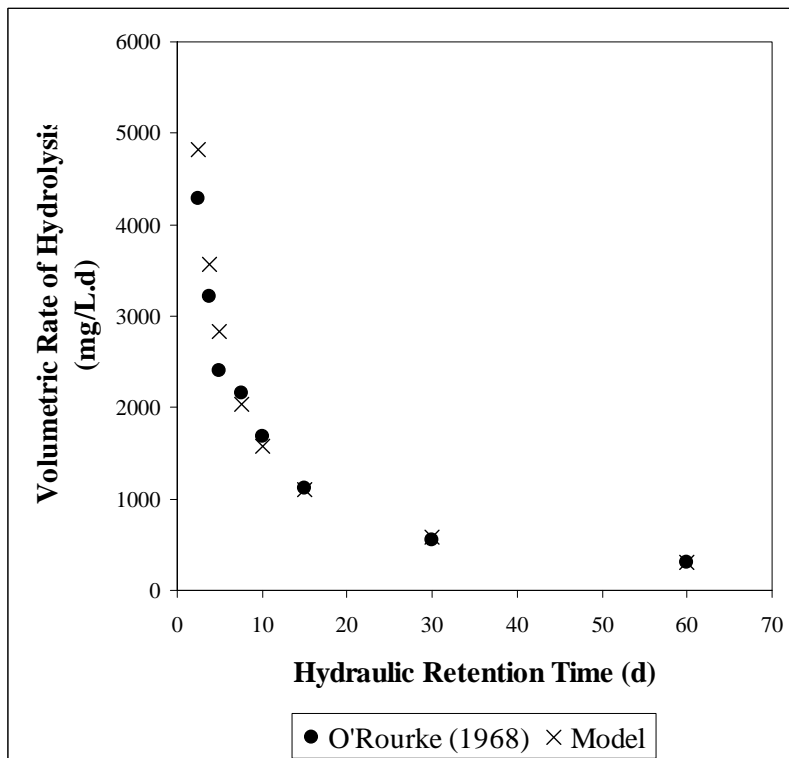


Figure 3: Calculated (from experimental data) and predicted (first order kinetics) rate of hydrolysis for each hydraulic retention time for the data of O'Rourke (1968)

- The model, as calibrated above, was applied to data collected in the independent study of O'Rourke (1968); close correlation was obtained for the longer retention times, i.e. the systems in which methanogenesis was complete, see Figure 3
- The good fits of the model predictions to the data collected in this and the independent study of O'Rourke (1968) provides powerful evidence validating the model

From an extensive investigation into the effect of pH on methanogenic anaerobic digesters (Figure 5):

- The minimum operating pH for methanogenic systems was determined at 6.38 before methanogenesis failed
- Increase in the operating pH above 6.38 has no effect on the PSS hydrolysis rate (pH = 6.38, 6.5, 7.0, 7.5, 8.0)

4.2 Acidogenic systems

Acidogenic systems were operated under varying hydraulic retention times (3.33 - 10d) and feed COD concentrations (2 – 40gCOD/L) at a constant temperature of 35°C, Table 2.

Table 2: Acidogenic steady states measured for varying hydraulic retention times and feed COD concentrations; numbers refer to steady state index, detailed results in Appendix B

Feed COD Concentration (gCOD/L)	Hydraulic Retention Time (d)		
	10	5	3.33
40		30	29
13	38	33	32
2	39	35	34

At each retention time and feed concentration, steady state periods were identified and analysed in detail:

- Very good COD mass balances were obtained (92 – 103%). This lends credibility to the experimental data
- Negligible methane gas productions were recorded
- The observations above substantiate the acidogenic condition, i.e. no methanogenesis

For each steady state of operation, the volumetric rate of hydrolysis was calculated:

- For systems fed the same feed COD concentration and operating at the same hydraulic retention time, the volumetric rates of hydrolysis were significantly lower under acidogenic conditions compared with the corresponding methanogenic conditions.

In applying the first order PSS hydrolysis kinetics developed for the methanogenic systems to the acidogenic systems:

- The value of the first order rate constant (k_h) had to be decreased significantly, substantiating the lower hydrolysis rate
- The first order kinetic constant for acidogenic conditions (k_h) is linearly dependent on the hydraulic retention time; the relationship was formulated to give:

$$k_h = 0.0883 - 0.0055.R_h \quad (5)$$

where R_h is the retention time (d)

- With the formulation above to calculate the value of the first order kinetic constant under acidogenic conditions (Eq 5), the model was able to reasonably accurately predict the rate of PSS hydrolysis under acidogenic conditions, Figure 4.

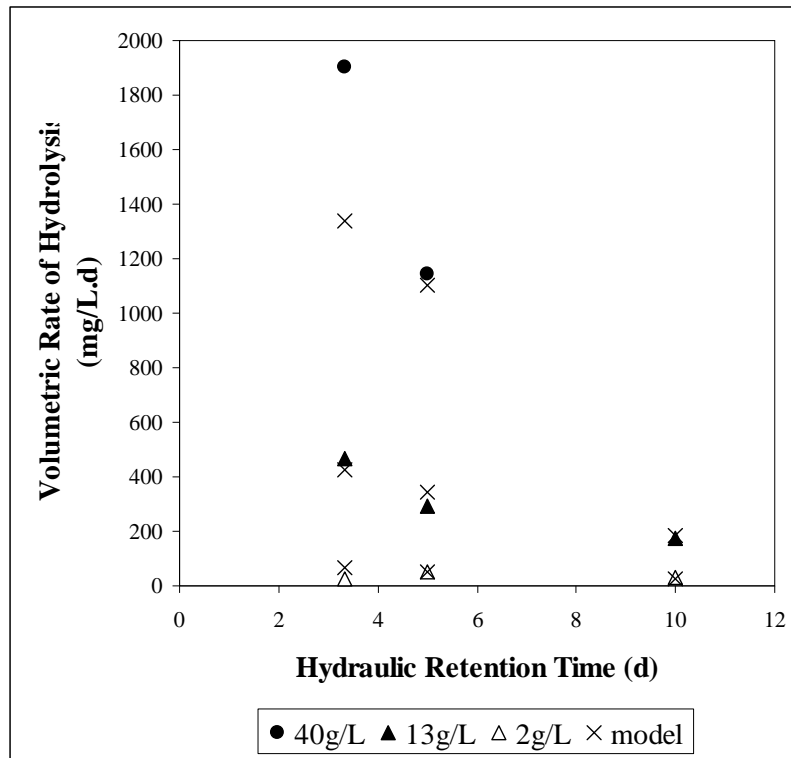


Figure 4: Comparison of the calculated and predicted hydrolysis rates for acidogenic systems using the first order rate formulation with the rate constant calculated from $k_h = 0.0883 - 0.0055.R_h$ (d^{-1})

To investigate the influence of pH on PSS hydrolysis under acidogenic conditions, further acidogenic steady state systems were operated at a constant hydraulic retention time (5d) and feed COD concentration (2gCOD/L), but with the digester operating pH controlled, and increased from the minimum pH 5 (steady state pH), to 8 at pH intervals of 1 (5.0, 6.0, 7.0, 8.0).

- The calculated rate of PSS hydrolysis under acidogenic conditions did not change when the pH was increased from 5 to 6

- However, when the pH was increased from 6 to 8, the observed rate of PSS hydrolysis increased linearly
- To include the effect above in the first order kinetics, Eq 5 was modified:

$$k_h = (0.0883 - 0.055.R_h) + 0.06 \left(\frac{\text{pH} - \text{pH}_{\text{LL}}}{\text{pH}_{\text{UL}} - \text{pH}_{\text{LL}}} \right) \quad (6)$$

where $\text{pH}_{\text{LL}} = 6.04$ and $\text{pH}_{\text{UL}} = 8.0$.

- With the modification above, first order kinetics was able to accurately predict the volumetric rate of PSS hydrolysis under acidogenic conditions for all operating pH values, see Figure 5

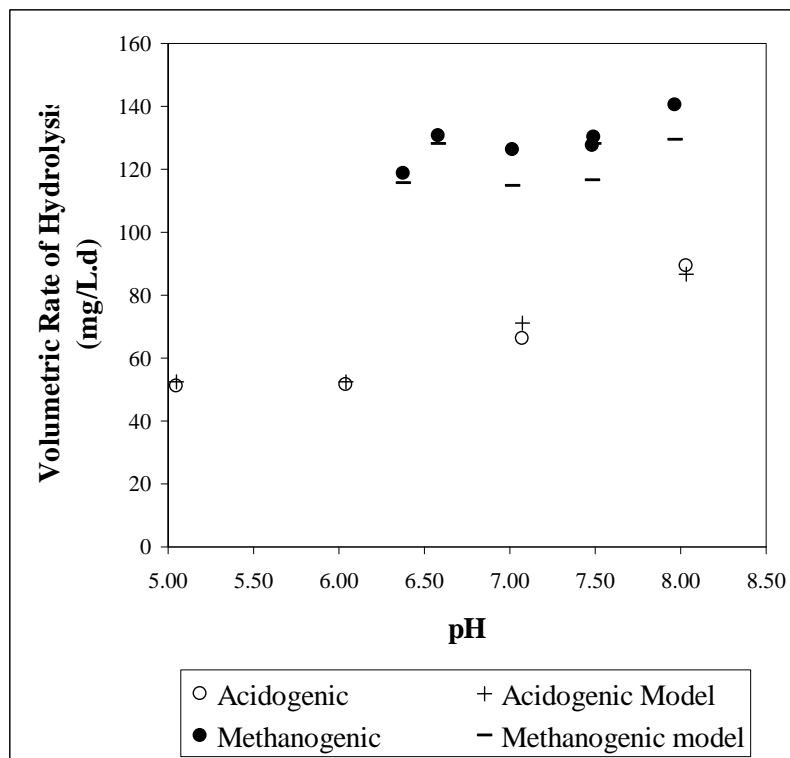


Figure 5: Calculated (from experimental data) and predicted (first order kinetics) rate of hydrolysis for methanogenic and acidogenic systems at varying operating pH values

4.3 Sulfate-Reducing systems

To quantify the rate of PSS hydrolysis under sulfate-reducing conditions and compare this rate with that for methanogenic systems, where possible these systems were operated in parallel digesters. Results from the initial experiments with limited sulfate reduction (1gSO₄/L with 26gCOD/L) showed that:

- The sulfate reduction did not influence the PSS hydrolysis rate compared with a parallel purely methanogenic system

- Methanogenesis was maintained in the digester. Therefore, a limited amount of sulfate reduction in methanogenic systems does not inhibit the hydrolysis nor methanogenesis processes, and can be treated in existing methanogenic digesters without jeopardising the process stability.

When the feed sulfate concentration was increased (9.6gSO₄/L with 13gCOD/L):

- No methanogenesis was observed
- Sulfate-reducing biomass outcompete methanogenic biomass for organic substrate
- Under sulfate-reducing conditions with low aqueous sulfide (precipitated with ferrous), the volumetric rate of PSS hydrolysis was the same as for the parallel methanogenic system
- When the aqueous sulfide was not removed, sulfate reduction was inhibited, but no information regarding the PSS hydrolysis rate was collected
- From the observations above, it can be concluded that aqueous sulfide is inhibitory to sulfate reduction

A range of systems were operated at feed COD concentrations of 2gCOD/L and feed sulfate concentrations of 2gSO₄/L, at varying retention times:

- In all systems, sulfate was slightly in excess and effluent VFA concentrations were low (< 50mgHAc/L), indicating absence of inhibitions. Thus, at lower aqueous sulfide concentrations, sulfate reduction is not inhibited

The first order rate formulation calibrated under methanogenic conditions ($k_h = 0.992d^{-1}$ and 33.45% unbiodegradable particulate COD fraction) was able to adequately predict the rate of PSS hydrolysis under sulfate-reducing conditions.

- The observation above led to the conclusion that the PSS hydrolysis rate is closely similar under methanogenic and sulfate-reducing conditions, i.e. sulfate reduction *per se* does not appear to influence the PSS hydrolysis rate

Further investigation and analysis of the data showed that:

- An operating pH between 6.5 and 7.5 did not affect the rate of PSS hydrolysis under sulfate-reducing conditions
- The mean COD:SO₄ utilisation ratio in the sulfate-reducing systems was 0.8gCOD/gSO₄, closely similar to 0.78gCOD/gSO₄ obtained by Enongene (2003). These ratios are significantly higher than the theoretical stoichiometric ratio of 0.67gCOD/gSO₄. However, taking into account COD utilization for the production of acidogen and sulfate-reducing biomasses, the theoretical ratio should be approximately 0.85gCOD/gSO₄, which is very close to the measured values
- The suspended solids concentration was significantly higher for sulfate-reducing systems compared with methanogenic systems (Figure 6), and the operating pH did not affect this concentration

- This has significant implications for sulfate-reducing systems in which solids and hydraulic retention times are uncoupled, as retention of sulfate-reducing biomass and PSS biodegradable particulate substrate may prove problematic

For acidogenic systems, the suspended solids concentration increased with increasing pH, Figure 6.

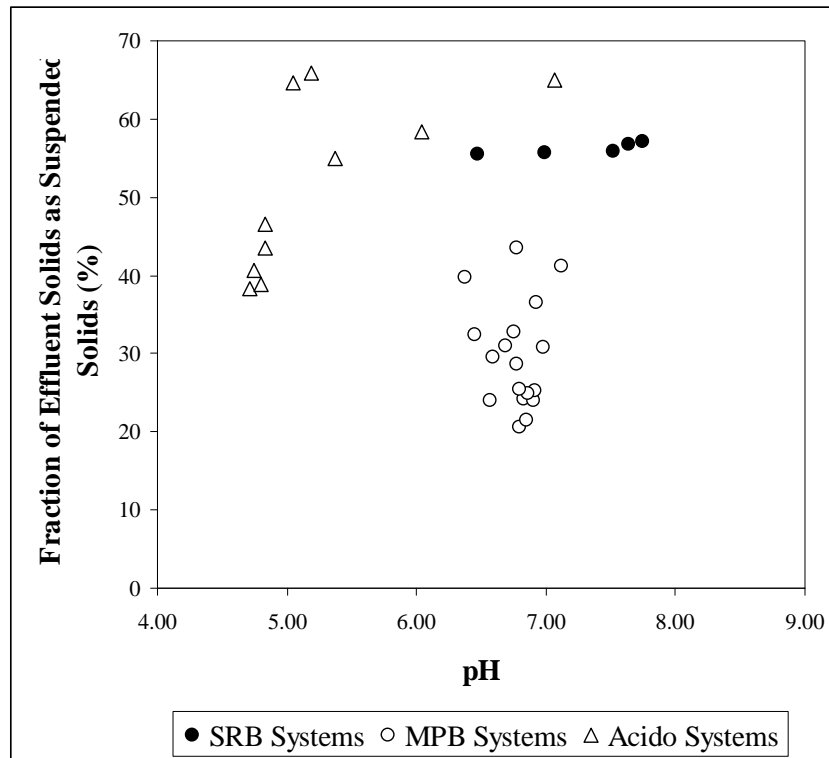


Figure 6: Ratio between the effluent suspended solids COD concentration and the effluent total particulate COD concentration (f_{SS}) for methanogenic (MPB), acidogenic (Acido) and sulfate-reducing (SRB) systems as a function of pH

A feasibility study was conducted using a UASB-type reactor for biological sulfate reduction with PSS as feed. The system was fed PSS at 1.6gCOD/L and sulfate at 1.2gSO₄/L, and operated in an upflow configuration without recycle at hydraulic retention times below 12h, with a sludge bed retention time below 5h:

- The residual sulfate concentration was below 100mgSO₄/L, with negligible soluble organic COD in the effluent, indicating near complete sulfate reduction
- Effluent particulate COD concentration of 200mgCOD/L, indicating successful sludge retention in the system

These results were encouraging, and it can be concluded that:

- This reactor configuration is a feasible option for the treatment of large volumes of sulfate-rich water such as acid mine drainage

- A feed COD:SO₄ ratio of 1.33:1 gCOD:gSO₄ is adequate for the removal of more than 90% of the feed sulfate without significant residual biodegradable organic COD concentrations

4.4 Comparison of PSS hydrolysis rates under methanogenic, acidogenic and sulphate reducing conditions

From a comparison of the PSS biodegradable particulate COD conversions for the systems operated in this study under methanogenic, acidogenic and sulfate reducing conditions (Chapter 7, Section 7.6), together with the methanogenic and acidogenic systems operated by O'Rourke (1968) (see Figure 7), it could be concluded that:

- The data gathered in this study, and substantiated by the observations of O'Rourke (1968) clearly indicates that the presence of methanogenesis substantially increases the rate of PSS hydrolysis, or conversely, the absence of methanogenesis and conditions created by acidogenesis substantially reduces the rate of PSS hydrolysis
- The effect above is not pH related; the effect of pH on PSS hydrolysis rates under acidogenic conditions is relatively small and could not account for the magnitude of the reduction in PSS hydrolysis rates
- Under the conditions which the sulfate reducing systems were operated (sulfide not inhibitory), compared with the equivalent methanogenic systems, sulfate reduction *per se* does not influence the rate of PSS hydrolysis

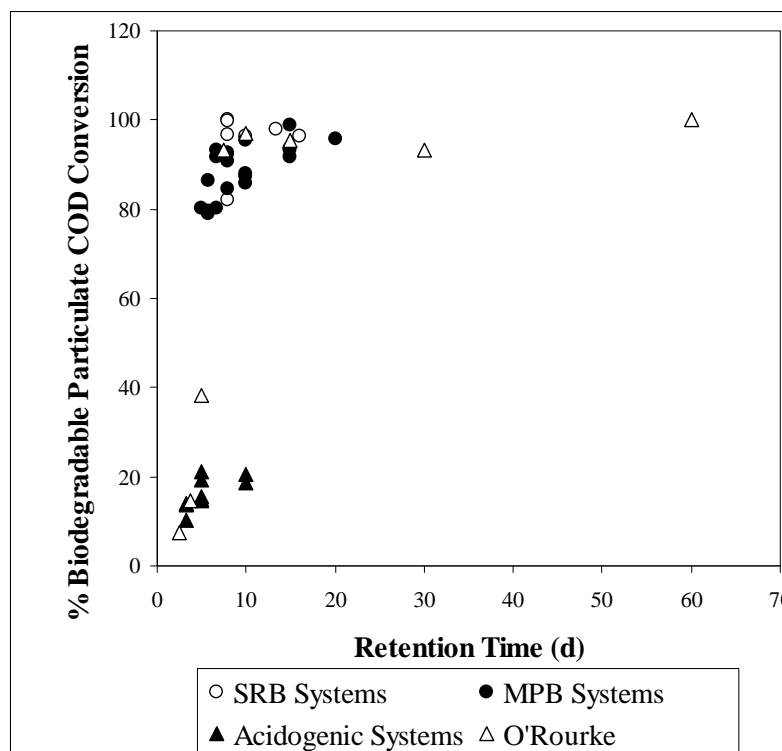


Figure 7: Biodegradable particulate COD conversions (as a % of influent PSS biodegradable particulate COD) versus retention time for the methanogenic (Chapter 4), acidogenic (Chapter 5) and sulfate reducing (Chapter 7) systems operated in this study, and the systems operated by O'Rourke (1968)

5. Closure

In this investigation, an extensive data set has been collected on anaerobic digestion of PSS under methanogenic, acidogenic and sulfate-reducing conditions, at varying retention times, feed concentrations and pH values. Through a strict attention to detail, the operating conditions for all systems were carefully controlled and completely defined.

To quantify the volumetric rate of PSS hydrolysis in such systems, a logical mathematical framework has been developed in terms of mass balance principles and characterisation of the PSS feed. This framework should provide a useful, common and systematic basis for comparisons of the hydrolysis rates for different systems. Further, a simple unified first order kinetics based model has been developed to describe PSS hydrolysis under methanogenic, acidogenic and sulfate-reducing conditions. This model takes into account the effects of retention time, feed COD concentration and pH, and the model has been validated both on data collected in this study and on data collected in independent studies.

Since PSS hydrolysis is the rate-limiting step in most methanogenic, acidogenic and sulfate-reducing systems, the subsequent processes are essentially stoichiometric. Hence, this simple model should be a valuable tool in the design, operation and control of steady state digestion systems. However, the model cannot take account of digester failure or behaviour under dynamic loading conditions. These will require development of a more extensive dynamic simulation model. In such a model, the evaluation here would suggest that surface reaction (Contois) kinetics are the most suitable for the PSS hydrolysis process. In this study, extensive data on transitions between steady states has been collected, which should prove useful for the calibration and validation of such a model.

In terms of the framework developed above, comparing the rates of PSS hydrolysis under methanogenic, acidogenic and sulfate-reducing conditions, the rates are closely similar under methanogenic and sulfate-reducing conditions, but significantly reduced under acidogenic conditions. This implies that the products of PSS hydrolysis (and subsequent acidogenesis) inhibit the PSS hydrolysis rate. If these products are removed, then PSS hydrolysis remains uninhibited, irrespective of whether the biological process that removes the products is methanogenesis or sulfate reduction.

In reviewing the literature on the hydrolysis of particulate organic wastes, it appeared that hydrolysis inhibition was linked to the lipids. Possible mechanisms for the inhibition due to VFA and/or hydrogen concentration inhibition of β -oxidation of long-chain fatty acids were proposed. However, these mechanisms are speculative, and require detailed experimental investigation.

Acknowledgements

The writers wish to express their gratitude to the members of the Steering Committee of the contract who guided the research work during the two year period:

- Mr G Steenveld Water Research Commission (Chairman)
- Mr HM du Plessis Water Research Commission
- Prof CA Buckley University of Kwazulu Natal
- Dr F Bux Durban Institute of Technology
- Prof GA Hansford University of Cape Town
- Prof STL Harrison University of Cape Town
- A/Prof AE Lewis University of Cape Town
- Prof PD Rose Rhodes University
- Mr GB Saayman City of Tshwane Metropolitan Municipality
- Dr HG Snyman ERWAT
- Dr R Van Lille University of Cape Town
- Mr OCE Hempel Water Research Commission (Committee Secretary)

Also, the writers would like to acknowledge the support of the organizations that funded the research:

- Water Research Commission
- National Research Foundation

Finally, acknowledgement is due to the technical staff in the Department of Civil Engineering at UCT, for their assistance with construction and maintenance of laboratory equipment:

- D Botha
- M Lakay
- H Mafungwa
- C Nicholas
- E von Guerard

Table of Contents

EXECUTIVE SUMMARY	iii
ACKNOWLEDGEMENTS	xvii
TABLE OF CONTENTS	xviii
LIST OF SYMBOLS	xxii
CHAPTER 1: INTRODUCTION	1
1.1 Background	1
1.1.1 Primary sewage sludge	1
1.1.2 Rhodes BIOSURE® process	2
1.1.3 Modelling anaerobic digestion	3
1.2 Research objectives	5
1.3 Research approach	6
1.4 Report layout	7
CHAPTER 2: BACKGROUND	9
2.1 Background	9
2.2 Modelling of anaerobic digestion of particulate organic matter under methanogenic conditions	9
2.2.1 Reaction scheme or mechanism	9
2.2.2 Rate limiting step	11
2.2.3 Hydrogen partial pressure effects	11
2.2.4 Inhibition	14
2.2.5 Acid/base equilibria	15
2.2.6 Vapour/liquid equilibria	15
2.2.7 Rate equations	16
2.2.7.1 Methanogenesis	16
2.2.7.2 Hydrolysis	18
2.2.8 Summary	21
2.3 Influence of methanogenesis and SRT on the hydrolysis of PSS	22
2.4 Influence of acidogenesis and SRT on the hydrolysis of PSS	26
2.5 Biological sulphate reduction	31
2.5.1 Biological sulphate reduction processes	31
2.5.2 Biological sulphate reduction with PSS as substrate	32
2.6 Closure	35
CHAPTER 3: MATERIALS AND METHODS	37
3.1 Introduction	37
3.2 Feed sludge	37
3.2.1 Feed collection and storage	37
3.2.2 Feed preparation	38
3.2.3 Feed characterisation	38
3.3 Digester design and operation	39
3.3.1 Digester design	39

3.3.2 Digester control	39
3.3.3 Feeding and sampling	39
3.4 Mass balances	40
3.4.1 Methanogenic systems	40
3.4.2 Acidogenic systems	41
3.4.3 Sulfidogenic systems	41
3.5 Analytical methods	42
3.5.1 Particulate samples preparation	42
3.5.2 Soluble sample preparation	42
3.5.3 COD and aqueous sulfide	42
3.5.4 Gas volumes and composition	43
3.5.5 VFA and alkalinity	43
3.5.6 Sulfate	44
3.5.7 Suspended solids	44
3.5.8 TKN and FSA	45
3.5.9 Total and soluble P	45
3.6 Closure	45
CHAPTER 4: METHANOGENIC SYSTEMS	47
4.1 Introduction	47
4.2 Experimental programme	47
4.3 Mathematical model	48
4.3.1 Model structure	48
4.3.2 Model assumptions	50
4.3.3 Reaction stoichiometry	50
4.3.4 Mass balances	51
4.3.4.1 Biodegradable particulate COD mass balance	51
4.3.4.2 Biodegradable fermentable soluble COD mass balance	51
4.3.4.3 Volatile fatty acid COD mass balance	51
4.3.4.4 Acidogenic biomass COD mass balance	52
4.3.4.5 Methanogenic biomass COD mass balance	52
4.4 Experimental results	52
4.4.1 COD mass balance	52
4.4.2 Minimum retention time	53
4.4.3 Methane production	54
4.4.4 pH	55
4.4.5 VFA and alkalinity	56
4.4.6 Gas composition	57
4.5 Rate of hydrolysis calculation	58
4.6 Hydrolysis rate formulations	62
4.6.1 First order kinetics	62
4.6.2 First order specific kinetics	68
4.6.3 Monod kinetics	74
4.6.4 Surface reaction kinetics	79
4.6.5 Revised data for kinetic constant determination	85
4.6.5.1 Revised Monod kinetics	85
4.6.5.2 Revised surface reaction kinetics	90
4.7 Hydrolysis rate equation selection	94
4.8 Unbiodegradable particulate COD fraction	99
4.9 Model validation	100

4.9.1 Data set of O'Rourke (1968)	100
4.9.2 Data set of Izzett <i>et al.</i> (1992)	103
4.10 Conclusions and future work	105
CHAPTER 5: ACIDOGENIC SYSTEMS	107
5.1 Introduction	107
5.2 Experimental programme	107
5.3 Mathematical model	108
5.3.1 Model structure	108
5.3.2 Model assumptions	110
5.3.3 Reaction stoichiometry	110
5.3.4 Mass balances	110
5.4 Experimental results	111
5.5 Rate of hydrolysis calculation	112
5.6 Comparison of rates of hydrolysis of PSS under methanogenic and acidogenic conditions	116
5.7 Calibration of model for acidogenic systems	117
5.8 Closure	122
CHAPTER 6: EFFECT OF pH ON THE RATE OF HYDROLYSIS UNDER METHANOGENIC AND ACIDOGENIC CONDITIONS	123
6.1 Introduction	123
6.2 Experimental programme	123
6.3 Mathematical model	124
6.4 Experimental results	124
6.5 Rate of hydrolysis calculation	126
6.5.1 Methanogenic systems	126
6.5.2 Acidogenic systems	127
6.6 Closure	129
CHAPTER 7: SULFATE-REDUCING SYSTEMS	133
7.1 Introduction	133
7.2 Experimental programme	134
7.3 Mathematical model	134
7.4 Experimental results	135
7.4.1 Experiment 1	135
7.4.1.1 Aim and experimental method	135
7.4.1.2 Results and discussion	135
7.4.2 Experiment 2	136
7.4.2.1 Aim and experimental method	136
7.4.2.2 Results and discussion	137
7.4.3 Experiment 3	141
7.4.3.1 Aim and experimental methods	141
7.4.3.2 Results and discussion	141
7.4.4 Experiment 4	143
7.4.4.1 Aim and experimental methods	143
7.4.4.2 Results and discussion	143
7.5 COD:SO ₄ utilisation ratio	147
7.6 Comparison of rates of hydrolysis of PSS under sulfidogenic, methanogenic and acidogenic conditions	147

7.7 Effluent suspended solids concentration	149
7.8 Laboratory-scale sulfate treatment process	150
7.8.1 Conceptual process design	150
7.8.2 Laboratory-scale reactor operation	151
7.8.3 Results	152
7.9 Closure	155
CHAPTER 8: CONCLUSIONS	157
8.1 Methanogenic systems	157
8.2 Acidogenic systems	160
8.3 Sulfate reducing systems	162
8.4 Comparison of PSS hydrolysis rate under methanogenic, acidogenic and sulfate reducing conditions	164
8.5 Closure	165
REFERENCES	167
APPENDIX A: FEED CHARACTERISATION	A.1
APPENDIX B: STEADY STATE DATA	B.1
APPENDIX C: TRANSIENT DATA	C.1
APPENDIX D: SULFATE MEASUREMENT METHOD	D.1

List of Symbols

AMD	Acid mine drainage
ATP	Adenosine Tri Phosphate
BNR	Biological nutrient removal
COD	Chemical oxygen demand
CSTR	Continuously fed stirred tank reactor
FSA	Free and saline ammonia
HAc	Acetic acid
HRT (R_h)	Hydraulic retention time
LCFA	Long chain fatty acids
MPB	Methane-producing bacteria
NAD	Nicotinamide Adenine Dinucleotide
OFMSW	Organic fraction of municipal solid waste
PSS	Primary sewage sludge
PST	Primary settling tank
SRB	Sulfate-reducing bacteria
SRT (R_s)	Solids retention time
TKN	Total Kjeldahl nitrogen
UASB	Upflow anaerobic sludge blanket
VFA	Volatile fatty acids
VSS	Volatile suspended solids
WAS	Waste activated sludge
b_{ad}	Acidogenic biomass decay coefficient
b_{am}	Acetoclastic methanogenic biomass decay coefficient
b_{as}	Acetoclastic sulfidogenic biomass decay coefficient
C_{be}	Bulk enzyme concentration
CF	Conversion factor
C_{me}	Enzyme concentration at microbe surface
ΔG	Change in Gibbs Free Energy
ΔG_0	Standard change in Gibbs Free Energy
K	Kelvin

k_h	First order hydrolysis kinetic constant
k'_h	First order specific hydrolysis rate constant
K_{HAc}	Acetic acid inhibition constant
k_{La}	Mass transfer coefficient
k_m	First order methanogenesis kinetic constant
k_{max}	Maximum specific rate constant for surface reaction
K_{NH3}	Ammonia inhibition constant
K_S	Half Saturation Constant
Q	Volumetric flow rate
R	Universal gas constant
$rate_{acidogenesis}$	Rate of acidogenesis
$rate_{hydrolysis}$	Rate of hydrolysis
$rate_{methanogenesis}$	Rate of methanogenesis
r_{be}	Rate of transfer of enzymes to bulk liquid
r_{me}	Rate of enzyme production from organisms
r_X	Biomass growth rate
S_{bp}	Biodegradable particulate COD in effluent
S_{bpi}	Biodegradable particulate COD in feed
S_{bs}	Biodegradable soluble COD in effluent
S_{bs}	Biodegradable soluble COD in effluent
S_{bsf}	Biodegradable soluble fermentable COD in effluent
S_{bsfi}	Biodegradable soluble fermentable COD in feed
S_{bsi}	Biodegradable soluble COD in feed
S_p	Total particulate COD in effluent
S_s	Total soluble COD in effluent
S_{si}	Total soluble COD in feed
S_{SS}	Suspended solids COD
S_t	Total effluent COD
S_T	Total aqueous sulfide concentration
S_{ti}	Total feed COD
S_{up}	Unbiodegradable particulate COD in effluent
S_{upi}	Unbiodegradable particulate COD in feed
S_{us}	Unbiodegradable soluble COD in effluent
S_{usi}	Unbiodegradable soluble COD in feed
S_{VFA}	Volatile fatty acid in feed

S_{VFAi}	Volatile fatty acids in effluent
t	time
T	Temperature
TS	Total solids
V	Reactor volume
Y_{ad}	Acidogenic biomass yield constant
Y_{am}	Acetoclastic methanogenic biomass yield constant
Y_{as}	Acetoclastic sulfidogenic biomass yield constant
Y_{xe}	Enzyme yield per unit microbe
$YXSO$	Yield coefficient
Z_{ad}	Acidogenic biomass
Z_{adi}	Acidogenic biomass in feed
Z_{am}	Acetoclastic methanogenic biomass
Z_{ami}	Acetoclastic methanogenic biomass in feed
Z_{as}	Acetoclastic sulfidogenic biomass
Z_{asi}	Acetoclastic sulfidogenic biomass in feed
Z_{hm}	Hydrogenotrophic methanogenic biomass
Z_{hmi}	Hydrogenotrophic methanogenic biomass in feed
μ_{max}	Monod maximum specific rate

Chapter 1

Introduction

1.1 Background

1.1.1 Primary sewage sludge

Solids handling, treatment and disposal in wastewater treatment plants adds significantly to the operational costs of the treatment of sewage. The sewage sludges (solids) typically comprise 1% or less (by volume) of the total flow handled by sewage treatment plants, while their treatment may represent 30 - 40% of the total costs of the sewage treatment (Knapp and Howell, 1978). In sewage treatment plants with primary settling tanks (PST), primary sewage sludge (PSS) from the underflow of the PST's is the largest fraction of the solids generated (around two thirds), the remainder being made up of waste activated sludge (WAS) and/or humus sludge (depending on the biological treatment unit process implemented).

The most common treatment method for sewage sludges is by anaerobic digestion (e.g. Pipes, 1961; Gujer and Zehnder, 1983). Anaerobic digestion refers to the biological oxidation of biodegradable organic matter in the absence of oxygen. Three main types of anaerobic digestion can be recognized: Methanogenic systems, which produce methane gas as the final COD product; sulfate-reducing systems, which require sufficient sulfate as input, and produce sulfide (aqueous, gaseous and metal sulfide precipitates) as the final COD product; acidogenic systems, which refer to anaerobic digestion systems in which methanogenic and sulfate-reducing conditions are not present, and the end product of the digestion is in the form of soluble COD (volatile fatty acids, VFA, and other soluble organics). The main advantages of anaerobic over aerobic digestion are the lower power requirements (no aeration) and associated reduced operational costs, as well as reduced final sludge production with reduced associated disposal costs (Andrews and Graef, 1971; Ray *et al.*, 1989).

In the treatment of sewage sludges, anaerobic digestion under methanogenic conditions is the most widely implemented. Methanogenic anaerobic digestion results in a stable relatively low volume sludge and produces an energy rich gas stream (CH_4 and CO_2), which can be used on site as a fuel for heating of the digesters.

Conventionally, in the anaerobic digestion of sewage sludges, acidogenic digestion only occurs because of the unintentional failure of the methanogenic processes, while sulfate-reduction is severely limited in usual operation due to an influent sulfate limitation, and in any event this process usually is considered a nuisance due to the hydrogen sulfide gas production, with associated odours (Devai and DeLaune, 1999).

However, more recently, PSS has been viewed as a valuable substrate source for the support of biologically mediated processes, other than methanogenesis. In the first steps of the anaerobic digestion of PSS, namely hydrolysis/acidogenesis, the products (mostly VFA's) are

common substrates for other biological groups, either external to the digester or internal. If the digester is operated intentionally under acidogenic conditions, the products of PSS hydrolysis/acidogenesis are the “end products”, which, once separated from the residual PSS solids, can be added to the overflow of the PST’s (settled sewage) to improve the efficiency of downstream biological nutrient (N & P) removal (BNR) activated sludge systems (Venter *et al.*, 1977; Barnard, 1984; Lilley *et al.*, 1991; Elefsiniotis and Oldham, 1993; Brinch *et al.*, 1994; Skalsky and Daigger, 1995; Hatziconstantinou *et al.*, 1996, Andreasen *et al.*, 1997; Banerjee *et al.*, 1998; Banister and Pretorius, 1998). Thus, acidogenic anaerobic digestion has an important role in generating substrates that augment BNR from sewages externally to the digester.

Furthermore, the products of PSS hydrolysis/acidogenesis have been recognized as an attractive low cost carbon source/electron donor in the biological reduction of sulfate to sulfide (Kaufman *et al.*, 1996; Whittington-Jones, 2000), in particular for the treatment of acid mine drainage (AMD) waters (Rhodes BioSURE[®] Process) (Whittington-Jones, 2000; Corbett *et al.*, 2000, Rose *et al.*, 2002).

1.1.2 Rhodes BioSURE[®] Process

The problem of AMD has been the subject of many studies (Heynike, 1981; Bekker, 1982; Toerien and Maree, 1987). AMD is characterized by high concentrations of heavy metals (Al = 50 – 2000mg/L; Fe = 10 – 6700mg/L; Zn = 10 – 100mg/L), sulfate (3000 – 30000mg/L) and total dissolved solids (1800 – 45000mg/L), coupled with a low pH (2 – 3) (Christensen *et al.*, 1996).

The Rhodes BioSURE[®] Process has been developed as a low cost active treatment of AMD waters (Rose *et al.*, 2002). The process flow diagram consists of a series of interconnected biological and chemical unit operations that allows for the removal of heavy metals and salinity (particularly sulfate) from AMD, Figure 1.1.

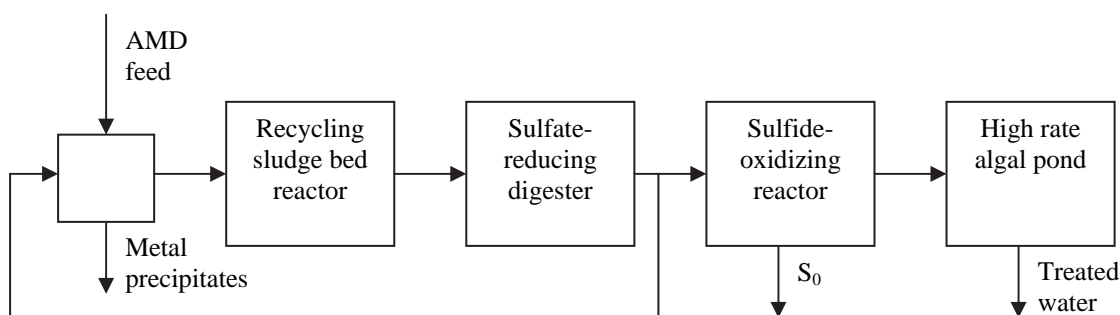


Figure 1.1: Process flow diagram of the Rhodes BioSURE[®] Process applied to the treatment of acid mine drainage wastewater (From Rose *et al.*, 2002)

The core reaction in the overall process is biological sulfate reduction using PSS as the electron donor and organic carbon source, with the concomitant production of sulfide and carbonate alkalinity. This reaction takes place in the recycling sludge bed reactor (RSBR) and the second sulfate reducing digester. The main aim of the RSBR is to solubilize the primary sewage sludge to soluble organic matter such as VFA, which then are used by the sulfate-reducing bacteria in the second sulfate-reducing digester. The sulfide and carbonate alkalinity produced in this process are recycled and contacted with the feed AMD, neutralizing the pH

and precipitating the heavy metals as metal sulfides, carbonates and hydroxides. The remaining effluent from the sulfate-reducing digester is discharged to a sulfide-oxidizing reactor, where aqueous sulfide is oxidized to elemental sulfur. A high rate algal pond polishes this effluent.

Since the core reaction in the Rhodes BioSURE[®] Process is biological sulfate reduction with PSS, the design, operation and control of the process is dependent on the rate at which the PSS is utilized. A mathematical kinetic model describing and quantifying the rate of PSS utilization for sulfate reduction would be an invaluable aid in the design, operation and control of the biological sulfate reduction step in the Rhodes BioSURE[®] Process. However, such a mathematical model is not presently available and information on the rate of PSS utilization under sulfate-reducing conditions is limited, retarding development of such a model. Thus, such information needs to be developed. This would have to take account of the conditions prevailing in the RSBR. These would include variations in concentration of the substrates and products as well as pH. Therefore, in order to determine the rate of PSS hydrolysis under sulfate-reducing conditions in the RSBR, it is necessary that the influence of the various operating conditions on the rate be quantified. A mathematical model of the RSBR would need to include these effects, and if formulated correctly, would provide a valuable tool for the optimization of the RSBR operation.

1.1.3 Modelling anaerobic digestion of PSS

In all the types of anaerobic digestion systems described above (methanogenic, acidogenic and sulfate-reducing), the first two biologically mediated processes are the hydrolysis of the PSS particulate organics (carbohydrates, proteins and lipids) to soluble organics (sugars from carbohydrates; amino acids from proteins; long-chain fatty acids (LCFA) from lipids) which then are acidified to predominantly VFA in acidogenesis. These steps are mediated by a single bacterial population group, generically called the acidogens (Gujer and Zehnder, 1983). The resultant products (VFA) then are discharged directly (acidogenic digesters) or enter the subsequent biological processes, methanogenesis or sulfate reduction (or a combination of both). Whatever the destination of the VFA, under stable operating conditions the PSS hydrolysis has been identified as the rate limiting process (e.g. Eastman and Ferguson, 1981; Ray *et al.*, 1989; Shimuzu *et al.*, 1993), and hence controls the overall net digestion rate. Thus, knowledge of the rate (kinetics) of the hydrolysis process under the various methanogenic, acidogenic and sulfate-reducing conditions, and the influence of physical constraints (e.g. retention time, feed COD concentration, feed sulfate concentration, feed COD:SO₄ ratio, pH) on the rate is essential for optimal design, operation and control.

Of all the anaerobic digestion system types, methanogenic anaerobic digestion of PSS has been the most extensively researched, and interactions between the various processes are reasonably well understood. A number of publications reviewing the anaerobic digestion processes are available, including *inter alia* the kinetics of anaerobic treatment (Pavlostathis and Giraldo-Gomez, 1991), treatment in fixed-film reactors (Henze and Harremoes, 1983), and under thermophilic conditions (Ahring, 1994). These review papers identify the microorganisms present in anaerobic digesters, as well as describe the metabolic pathways by which the digestion takes place. Further, proposed kinetic formulations and associated constants are listed for various operating conditions (and for a number of different feed types apart from PSS).

However, there is considerable variation in the kinetic formulations proposed for PSS hydrolysis and associated values for the kinetic constants (see Chapter 2). Thus, considerable

uncertainty exists as to the correct kinetic rate formulation. Also, there is uncertainty as to the calibration of the relevant rate formulations. For example, Pavlostathis and Giraldo-Gomez (1991) state that the hydrolysis step, normally rate limiting, is usually assumed to follow first order kinetics, but several values for the first order kinetic constant have been derived in the various studies. What is required is an evaluation of the various rate formulations for the hydrolysis of PSS under methanogenic conditions, in order to select a rate formulation that is able to accurately predict the rate of hydrolysis of PSS under all operating conditions studied, with comprehensive and appropriate kinetic constant calibration.

For acidogenic anaerobic digestion, studies have focused largely on VFA and soluble COD yields under a variety of operational conditions (e.g. Venter *et al.*, 1977; Gupta *et al.*, 1985; Kristensen *et al.*, 1992) and on incorporation of this digestion into, and its impact on, downstream BNR activated sludge systems (e.g. Pitman *et al.*, 1983; Barnard, 1984; Brinch *et al.*, 1994; Andreasen *et al.*, 1997; Banister and Pretorius, 1998). Some kinetic studies on PSS hydrolysis in acidogenic digestion have been undertaken, but these are largely empirical (e.g. Lilley *et al.*, 1991) and limited (e.g. Eastman and Ferguson, 1981).

In the biological sulfate reduction system with PSS as the carbon source/electron donor, since the sulfate-reducing bacteria cannot use the particulate organic matter directly, hydrolysis/acidogenesis of the particulates is required prior to sulfate reduction. Kinetic studies on the PSS hydrolysis under these conditions are extremely limited. Initial studies have concluded that sulfate-reducing (sulfide-rich) conditions resulted in “enhanced” hydrolysis of the PSS (Whittington-Jones, 2000). These results contradict the findings of Pipes (1961), who found similar volatile solids removal in sulfate-reducing systems when compared with conventional methanogenic treatment. Subsequent enzyme studies appear to confirm the enhanced hydrolysis (Whitely *et al.*, 2003), showing that the presence of sulfide may increase the activity of the hydrolytic lipase enzymes. However, similar results were obtained from experiments where carbonate and hydroxide were added instead of sulfide, suggesting that the sulfide addition was possibly indirectly responsible for the apparent increase in enzyme activity. Further studies using batch tests have also concluded that the rate of hydrolysis under sulfate-reducing conditions is significantly enhanced (Molwantwa *et al.*, 2004). Should biological sulfate reduction significantly enhance the PSS hydrolysis rate, these systems, rather than traditional methanogenic systems, could be used also for PSS disposal in regions where sufficient sulfate waste is available.

The main aim of the sulfate-reduction studies above was to evaluate the feasibility of using PSS for biological sulfate reduction, and the influence of the sulfate-reducing conditions on the microbiology and enzymology of the biological processes. Some kinetic studies were undertaken (Whittington-Jones, 2000; Molwantwa *et al.*, 2004), but these did not calculate the overall hydrolysis rate from a COD mass balance approach. Rather, substrate inhibitors were added to the batch tests: toluene to inhibit soluble sugar uptake; molybdate to inhibit sulfate reduction. The hydrolysis rate was determined by measuring the accumulation of the soluble products of hydrolysis. It is, therefore, not clear whether the accumulation of the hydrolysis products affected the hydrolysis process in some fashion. Since the studies were in short-term batch tests, from these studies development and calibration of kinetic formulations for PSS hydrolysis under sulfate-reducing conditions is not possible. Such formulations would significantly aid design, operation and control of these systems. Clearly, this is an area of considerable interest with wide practical implementation, and merits further investigation.

1.2 Research Objectives

The Water Research Commission (WRC) identified the use of PSS as the electron donor for biological sulfate reduction in the remediation of AMD as of particular interest to South Africa. Specifically, the Rhodes BioSURE[®] Process has been shown to be a potentially feasible attractive technology for the low cost treatment of AMD. In order to optimise the Rhodes BioSURE[®] Process, it is critical that the kinetics of PSS utilization within the Rhodes BioSURE[®] Process be accurately quantified. The WRC therefore contracted the Water Research Group in the Department of Civil Engineering at the University of Cape Town, to investigate the kinetics of PSS hydrolysis under sulfate-reducing conditions such as in the Rhodes BioSURE[®] Process (WRC contract no. K5/1216, April 2001 to March 2003). The original specific objectives were to:

- quantify the effects of sulfate reduction and pH on the rate of PSS hydrolysis, and to
- establish design parameters for biological sulfate reducing systems treating AMD using PSS as the electron donor/carbon source.

From the discussion above, three biological anaerobic digestion systems have been described: methanogenic, acidogenic and sulfate reducing. All three of these system types have been operated with PSS as the organic substrate, and literature studies have shown that the hydrolysis of the PSS is the biologically mediated process that is rate limiting. Further, the different operating conditions may significantly influence the PSS hydrolysis rate. Thus, in order to be able to quantify the effects of sulfate reduction and pH on the rate of PSS hydrolysis, the rate of PSS hydrolysis under methanogenic and acidogenic conditions needs to be quantified as a basis for comparison. Using the mathematical models developed for these two types of systems, the rate of PSS hydrolysis under sulfate-reducing conditions can be compared with the rate under methanogenic and acidogenic conditions. This necessitated that the original objectives in the contract be expanded to include experimental investigations into, and mathematical modeling of, the rate of PSS hydrolysis under methanogenic and acidogenic conditions.

During the course of the investigation on methanogenic systems, it appeared that a number of physical constraints imposed by the system influenced the rate of PSS hydrolysis, in particular retention time and influent PSS feed concentration. This required that these influences be quantified. Due to the considerable increase in the scope of the project, the research contract was extended for 1 year (April 2003 to March 2004) with additional funding.

Therefore, the principle aim of this study is to determine the rate of hydrolysis of PSS under methanogenic, acidogenic and sulfate-reducing conditions, and the influence of the system physical constraints on the rate. This also will enable a direct comparison of the rate under each of the three conditions, to determine possible influences on the rate.

In terms of this aim, the original objectives were expanded to include the following:

1. To determine the rate of hydrolysis of PSS under methanogenic conditions
2. To determine the effects of feed COD concentration, hydraulic retention time and pH on the rate of hydrolysis under methanogenic conditions

Chapter 1: Introduction

3. To develop a mathematical model for the biological processes mediating PSS hydrolysis in methanogenic systems, so that the rate of hydrolysis can be predicted for various feed COD concentrations, hydraulic retention times and operating pH, based only on the feed characterization and system operation
4. To evaluate the various rate formulations for the PSS hydrolysis at varied operating conditions, so that the most appropriate rate formulation for hydrolysis of PSS under methanogenic conditions can be identified
5. To collect data on methanogenic systems that can be used to calibrate a more extensive dynamic mathematical model for methanogenic anaerobic digestion including physical processes such as acid/base equilibria and vapour/liquid equilibria (development of this model does not form part of this research, but is part of a parallel project)
6. To determine the rate of PSS hydrolysis under acidogenic conditions
7. To determine the effects of feed COD concentration, hydraulic retention time and pH on the rate of hydrolysis under acidogenic conditions
8. To appropriately modify the mathematical model selected in 4. above, to predict the rate of hydrolysis under acidogenic conditions
9. To determine whether PSS can support internal sulfate-reduction, and to develop a greater understanding of sulfate reduction in PSS fed systems
10. To determine the rate of PSS hydrolysis under sulfate-reducing conditions
11. To determine the effects of sulfate-reduction on the rate of hydrolysis of PSS

The mathematical formulations to be developed will describe PSS hydrolysis under methanogenic, acidogenic and sulfate-reducing conditions, and the influence of various operational parameters on this process. These formulations will be general and should find much wider application than the biological sulfate reduction, such as acidogenic digestion of PSS to generate substrate to augment BNR.

1.3 Research Approach

The research approach adopted was to operate 6 parallel laboratory-scale anaerobic digesters with PSS as influent, and to monitor the behaviour of these systems under a range of:

- feed concentrations
- retention times
- pH
- feed sulfate concentrations

under stable:

- methanogenic
- acidogenic and
- sulfate-reducing conditions

From the application of mass balance principles, the volumetric rate of PSS hydrolysis would be quantified. From the literature, various rate formulations for PSS hydrolysis would be identified, and evaluated against the measured methanogenic anaerobic digester data. The formulation able to accommodate the observations most accurately would be selected as the most appropriate. This formulation then would be modified for acidogenic and sulfate-reducing systems, by application to the measured data. In this manner, a unified kinetic theory would be developed for PSS hydrolysis under methanogenic, acidogenic and sulfate-reducing conditions. This would enable a comparison of the relative rates under the three conditions.

1.4 Report Layout

Chapter 2 discusses the concepts of anaerobic digestion in more detail, and discusses techniques that have been used to model the biological and physical processes taking place in anaerobic digesters. Literature examples of the application of the processes (methanogenesis, acidogenesis and sulfate reduction) are also discussed, specifically for the treatment of solid wastes, and with emphasis on the hydrolysis process.

Chapter 3 describes the design, operation and control of the laboratory-scale methanogenic, acidogenic and sulfate-reducing anaerobic digesters, and the analytical methods that were used to analyze the systems.

Chapter 4 describes the results of the experiments in which the rate of hydrolysis of PSS under methanogenic conditions was determined. The effects of feed COD concentration and hydraulic retention time are quantified, and a mathematical model was developed to calculate the rate of hydrolysis at each operating point. Various forms of the hydrolysis rate equation are tested to determine which form is able to best predict the rate of hydrolysis under all operating conditions.

Similarly, Chapter 5 describes the results of the experiments to determine the rate of hydrolysis under acidogenic conditions. The rate of hydrolysis is calculated for each of the operating points in which the feed COD concentration and hydraulic retention time are varied. The mathematical model developed in Chapter 4 is appropriately modified for acidogenic conditions to determine the rate of hydrolysis.

Chapter 6 describes the effects of pH on the rate of hydrolysis under methanogenic and acidogenic conditions. The mathematical models developed in Chapters 4 and 5 are used to calculate the rate of hydrolysis for each of the two systems, and are modified appropriately to accommodate the pH effects.

Chapter 7 described the results of the experiments in which the sulfate-reducing systems are compared to methanogenic systems, to determine the effects of sulfate-reduction on the hydrolysis rate. The model developed in Chapter 4 is modified to include the sulfate-reducing bacteria, so that the rate of hydrolysis can be calculated for each operating condition.

Appendix A describes the batches of PSS used as feed for the systems and describes the changes in the feed characteristics with storage. Appendix B lists the results of the analyses performed on the systems leading up to and including the steady state of operation. Mass balance calculations are reported. Appendix C describes the transient states that were analysed in more detail. This information would be useful in calibrating a dynamic state mathematical model.

Chapter 1: Introduction

Chapter 2

Background

2.1 Introduction

From Chapter 1, the principle objective of this investigation is to determine and model the rate of hydrolysis of PSS under methanogenic, acidogenic and sulfate-reducing conditions, and interactions of this rate with the physical constraints, such as hydraulic retention time and feed COD concentration. In this chapter, the relevant literature on PSS hydrolysis is reviewed.

The most common treatment method for anaerobic digestion of PSS is under methanogenic conditions. Consequently, these systems have been studied in more detail than the acidogenic and sulfate-reducing systems. Hence, modelling of anaerobic digestion under methanogenic conditions is first reviewed, in which each of the processes and interactions in these systems are discussed. Based on these discussions, published data on methanogenic systems fed particulate wastes (in particular PSS) are presented, which highlight certain deficiencies in the published models, particularly in modelling of the hydrolysis process. With methanogenic systems as a basis, the acidogenic systems, followed by sulfate-reducing systems, are discussed in more detail, and these systems are compared with the methanogenic systems.

2.2 Modelling of Anaerobic Digestion of Particulate Organic Matter under Methanogenic Conditions

Anaerobic digestion under methanogenic conditions has been used extensively for the treatment of particulate wastes, including PSS (O'Rourke, 1968, Miron *et al.*, 2000), waste activated sludge (WAS) (Huang *et al.*, 1989, Ghosh *et al.*, 1995), mixtures of PSS and WAS (Moen *et al.*, 2001), mixtures of PSS and humus sludge (Izzett *et al.*, 1992), the solid fraction of pig slurries (Andara and Estaban, 1999 and 2002), poultry slaughter house wastes (Salminen and Rantala, 2002), raw whey (Thiele and Zeikus, 1988) and the organic fraction of municipal solids waste (OFMSW) (Kiely *et al.*, 1997).

2.2.1 Reaction scheme or mechanism

The reaction scheme proposed by Gujer and Zehnder (1983), based on the work by Kasper and Wuhrmann (1978), identifies the major pathways in the anaerobic digestion of particulate organic matter under methanogenic conditions (Figure 2.1). This reaction scheme is a practical simplification representing methanogenic anaerobic digestion. The various particulate organic substrates have been grouped together into the three main types of organics: carbohydrates, proteins and lipids. The organics are collectively degraded by a consortium of bacteria. Bacteria mediating a common reaction (process) or fulfilling a common role are grouped, to form a 'surrogate' organism, which is assigned a set of unique characteristics (similar to the approach followed for activated sludge systems, Wentzel and

Ekama, 1997).

The processes include (1) hydrolysis of complex polymers to form soluble monomers (sugars, amino acids and long chain fatty acids); (2) fermentation of the sugars and amino acids to form intermediate products (volatile fatty acids), acetic acid and hydrogen; (3) anaerobic oxidation (β -oxidation) of long chain fatty acids to form acetic acid and hydrogen; and (4) the degradation of the intermediate products to form acetic acid and hydrogen (acetogenesis). Methanogenic bacteria then degraded the (5) acetic acid and (6) hydrogen to form methane and carbon dioxide. Due to the similarity in stoichiometry and growth characteristics of the fermentation and anaerobic oxidation (and sometimes acetogenic) reactions, these often have been combined in a single process, acidogenesis, defined as the utilization of complex soluble COD to form volatile fatty acids (acetic acid) and hydrogen. Details of the reaction scheme have been discussed by Gujer and Zehnder (1983), and hence are not repeated here.

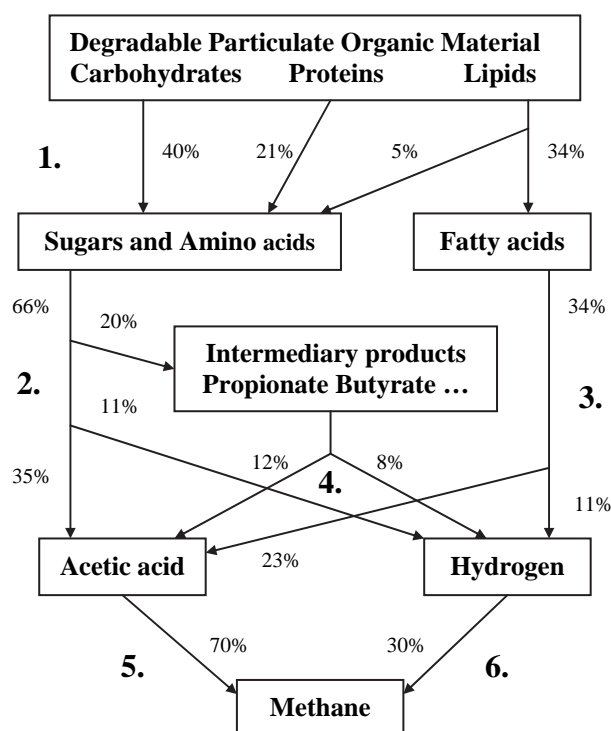


Figure 2.1: Reaction scheme from Gujer and Zehnder (1983) for the methanogenic anaerobic digestion of sewage sludge, where percentages indicate substrate flow (stoichiometrically) in the form of COD equivalents. Only the net flow of substrates through cell pools is indicated. The numbers refer to the six biological processes (1. hydrolysis; 2. fermentation; 3. anaerobic oxidation; 4. acetogenesis; 5. acetoclastic methanogenesis; 6. hydrogenotrophic methanogenesis)

The proposed reaction scheme in Figure 2.1, or modified versions, has been used as a basis to formulate a variety of mathematical models for methanogenic anaerobic digestion. The scheme was used directly in two of the published mathematical models (Bryers, 1985; Siegrist *et al.*, 1993). Massé and Droste (2000) combined the fermentation and anaerobic

oxidation steps to give a five-step scheme including hydrolysis, acidogenesis, acetogenesis, acetoclastic methanogenesis and hydrogenotrophic methanogenesis. Other published models have further simplified the reaction scheme, ranging from a four step scheme including hydrolysis, acidogenesis, acetogenesis and acetoclastic methanogenesis (Shimuzu *et al.*, 1993), a three step scheme including hydrolysis, acidogenesis and acetoclastic methanogenesis (Hill and Barth, 1977; Kiely *et al.*, 1997) and a two step scheme including hydrolysis and acetoclastic methanogenesis (Jeyaseelan, 1997). Extreme cases exist where the overall reaction scheme has been grossly simplified to a single biological reaction: hydrolysis (Jain *et al.*, 1992) or acetoclastic methanogenesis (Andrews and Graef, 1971). In all of these simplified models, the process of formation of methane from hydrogen and carbon dioxide has been ignored in the model structure, since only 25-30% of the total methane production takes place through this route (Gujer and Zehnder, 1983; Ray *et al.*, 1989). However, hydrogen may play an important regulatory role in anaerobic digestion, see below.

2.2.2 Rate limiting step

The main reason for the simplifications above to the overall scheme in Figure 2.1 is that either hydrolysis (Eastman and Ferguson, 1981; Ray *et al.*, 1989; Shimuzu *et al.*, 1993) or acetoclastic methanogenesis (Andrews and Graef, 1971; Fox and Suidan, 1990) is the rate-limiting step. These two processes are mediated by the acidogenic and acetoclastic methanogenic biomasses respectively, which are the two major groups of bacteria present in methanogenic digestion of PSS. The acidogens are typically more robust and faster growing than the methanogens, and can operate in conditions where the methanogens are inhibited (toxic compounds present in feed or produced as products by anaerobic digestion processes) or washed out (at low solids retention times, SRT). Since the methanogens are slower growing, and inhibited by high concentration of VFA, they are more sensitive to shock organic loads on the system, and recover more slowly from temperature shocks and pH shocks. They are also limited to a relatively narrow pH range, and are more sensitive to toxic substances such as acetic acid, hydrogen sulfide and ammonia than the acidogenic biomass. (Zeikus, 1977).

When anaerobic digesters ‘fail’ or ‘sour’, an accumulation of volatile fatty acids leads to a drop in the pH, suggesting that the VFA utilising biomass (acetoclastic methanogens) have failed (Andrews and Graef, 1971; Mosey, 1983; Bryers, 1985; McCarty and Mosey, 1991; Siegrist *et al.*, 1993). These observations would indicate that this group of bacteria is critical in dynamic modelling of anaerobic digestion. However, under stable methanogenic anaerobic digester operation with particulate organic as feed, the concentration of VFA’s is negligible (O’Rourke, 1968), indicating that the acetoclastic methanogen mediated process is not rate limiting. Further, under such conditions, accumulation of non-VFA soluble COD is not observed (Miron *et al.*, 2000), indicating the acidogenesis step also is not limiting. Thus, under stable operation with particulate organics as feed (such as PSS), the hydrolysis process has been identified as the rate-limiting step by a number of researchers (e.g. Eastman and Ferguson, 1981; Ray *et al.*, 1989; Shimuzu *et al.*, 1993). Since the focus of this investigation is on stable operation with PSS feed, that hydrolysis is rate limiting can be accepted here also.

2.2.3 Hydrogen partial pressure effects

Hydrogen is a significant intermediate in methanogenic anaerobic digestion of PSS, where approximately 30% (as COD) of the methane produced is via the hydrogenotrophic methanogenic process, see Figure 1. This indicates that 30% (as COD) of the products of

Chapter 2: Background

hydrolysis are converted to hydrogen. The concentration of the dissolved hydrogen plays an important regulatory role in the overall digestion. Under conditions where the hydrogenotrophic methanogenic biomass is unstable, resulting in increased concentrations of dissolved hydrogen, the various biomass groups and metabolic pathways become influenced.

Studies on the fermentation/acidogenesis of soluble carbohydrates have shown that dissolved hydrogen plays also an important role in these processes. The main route for the conversion of glucose to VFA (fermentation and acidogenesis) is via the Embden-Meyerhof pathway (Mosey, 1983). At four critical points along the pathway, the ratio of NAD^+ : NADH , controlled by the dissolved hydrogen concentration, determines which VFA species the acidogenic bacteria produce (Mosey, 1983).

The degradation of glucose (via the Embden-Meyerhof pathway) to form the various organic acids occurs according to Eqs 2.1 to 2.3 (Mosey, 1983).



From the energy (ATP) yield per mole of glucose degraded, the production of acetic acid (Eq 2.1) is favourable over the production of propionic acid (Eq 2.2) and butyric acid (Eq 2.3). However, in the reactions 2.1 and 2.2 above, the NAD consumed needs to be regenerated for the reactions to continue. In the absence of an external electron acceptor, this happens by dehydrogenation:



For this reaction to proceed, the dissolved hydrogen concentration needs to be low. Thus, under conditions of high concentrations of dissolved hydrogen, the production of propionic acid would be favourable, since hydrogen is consumed during this reaction.

An alternative reaction has been proposed with mixed acetic and propionic acids produced (Sam-Soon *et al.*, 1990):



It was proposed that the dehydrogenation in this reaction is energetically coupled to the acetic acid production (van Rensburg *et al.*, 2001).

Similarly, for PSS and other wastes with a significant lipid fraction, such as fish processing wastewaters (Palenzuela – Rollón, 1999), the lipids are hydrolyzed to long chain fatty acids (LCFA) by lipases, see Figure 2.1. The LCFA are then anaerobically oxidized to acetic acid and hydrogen via β -oxidation, except for LCFA containing an uneven number of carbon atoms, where propionic acid also will be produced in the final step. However, the β -oxidation is strongly regulated by the redox state of the cell, i.e. $\text{NAD}:\text{NADH}_2$ ratio, since the NAD consumed in the reaction would need to be regenerated, via a mechanism similar to Eq 2.4 above. Hence, similarly to that described above, the presence of elevated concentrations of dissolved hydrogen inhibits the β -oxidation process, resulting in an accumulation of the LCFA (McInerney, 1988, Palenzuela – Rollón, 1999). The elevated concentrations of LCFA

Chapter 2: Background

are inhibitory to both the methanogenic biomass and the lipid hydrolysis process, resulting in an accumulation of unhydrolyzed lipids, LCFA, acetic acid and dissolved hydrogen. However, there is no direct evidence in the literature that the dissolved hydrogen has a direct effect on the hydrolysis of lipids.

Recent studies have attempted to explain these effects from the thermodynamics of the reactions involved. By plotting the change in Gibbs Free Energy versus the hydrogen partial pressure for each of the reactions, Harper and Pohland (1986) were able to identify an operating window for the anaerobic digestion bacteria.

The change in Gibb's Free Energy can be calculated as follows (for Eq 2.1):

$$\Delta G = \Delta G_0 + RT \ln Q \quad (2.6)$$

where ΔG is the change in Gibb's Free Energy (kJ), ΔG_0 is the standard change in Gibb's Free Energy, R is the universal gas constant and T is the temperature in K.

For Eq 2.1:

$$Q = \frac{\{\text{CH}_3\text{COOH}\}^2 \{\text{CO}_2\}^2 \{\text{H}_2\}^4}{\{\text{C}_6\text{H}_{12}\text{O}_6\} \{\text{H}_2\text{O}\}^2} \quad (2.7)$$

where $\{i\}$ is the activity of the species in the system under consideration.

In order to calculate ΔG for the reaction at varying dissolved hydrogen concentrations, Eq 2.4 can be written as follows:

$$\Delta G = \Delta G_0 + RT \ln \frac{\{\text{CH}_3\text{COOH}\}^2 \{\text{CO}_2\}^2}{\{\text{C}_6\text{H}_{12}\text{O}_6\} \{\text{H}_2\text{O}\}^2} + 4RT \ln \{\text{H}_2\} \quad (2.8)$$

To determine the hydrogen partial pressure at which a particular reaction would be thermodynamically favourable, the change in Gibb's Free Energy would have to be negative for the reaction as written, with the thermodynamic limit at $\Delta G = 0$. The activities of the various reactants and products would have to be known or estimated in order to solve Eq 2.6. These values were assumed by Harper and Pohland (1986) when calculating the operating window.

Hence, if dissolved hydrogen effects are to be included in a mathematical model based on the thermodynamic principles described above, the activities of all of the products and reactants would have to be calculated, substituted into Eq 2.8, and if ΔG was less than 0, the reaction would take place. However, it is questionable whether such a thermodynamic limitation can be directly translated into a kinetic rate expression.

Accordingly, simplifications of the concepts would need to be adopted for the mathematical models. With such simplifications, the effects of hydrogen partial pressure (or dissolved hydrogen) on the system have been included in a number of mathematical models (Mosey, 1983; Costello *et al.*, 1991; Sam-Soon *et al.*, 1991; Siegrist *et al.*, 1993; Massé and Droste, 2000, van Rensburg *et al.*, 2001).

Mosey (1983) used an uncompetitive inhibition term to describe this effect, similar to Massé and Droste (2000). The uncompetitive inhibition model does not switch the rate equation off when the thermodynamic limit has been reached. Sam-Soon *et al.* (1991) and van Rensburg

et al. (2001) used a substitute simplified hydrogen gas concentration in Monod-type switching functions to implement the effects of hydrogen partial pressure with considerable success. However, there is no direct evidence to show the effects on the rates at varying hydrogen partial pressures.

Further, in modelling this phenomenon is the underlying assumption that the dissolved hydrogen is in equilibrium with the gas phase, and that the inhibitory concentration can be directly related to the hydrogen partial pressure. Studies have shown that the concentration of dissolved hydrogen in a UASB reactor was substantially higher than the expected value calculated from the hydrogen partial pressure (Pauss and Guiot, 1993), indicating non-equilibrium between the two phases. Clearly, this is an area where further kinetic studies are critical if mathematical modelling of anaerobic digestion at such an advanced level is to be developed into a useful tool.

Irrespective of whether including hydrogen partial pressure effects is reasonable or not, it is highly questionable whether these interactions will take place in a reactor treating a particulate organic waste under stable methanogenic conditions. The majority of the models incorporating hydrogen partial pressure effects have been developed and calibrated on systems treating glucose (Mosey, 1983; Costello *et al.*, 1991) or other readily biodegradable soluble carbohydrate wastes (Sam-Soon *et al.*, 1991). With particulate organic wastes operating under stable methanogenic conditions, the rate limiting hydrolysis step would probably restrict the hydrogen partial pressure to concentrations below the thermodynamic limit. This is confirmed by Siegrist *et al.* (1993) for a digester fed a mixture of primary, secondary and tertiary sludge and with acetate, propionate and formate pulse-experiments. Hydrogen partial pressures were inconsequential until external addition of formate, suggesting that they can be ignored in a completely mixed digester fed particulate organic matter only. Hence, for the purpose of this investigation where stable methanogenic anaerobic digestion of PSS is being considered, the hydrogen partial pressure effects can be safely ignored.

For acidogenic systems, where the hydrogenotrophic methanogenic biomass is not present, clearly the effects of elevated concentrations of dissolved hydrogen will be evident. In this investigation, the methods for quantifying the dissolved hydrogen concentration, the individual VFA species, the LCFA species and concentrations, and the lipid concentration were not available, since this was beyond the scope of the investigation. However, the overall rate of PSS hydrolysis will be investigated under acidogenic conditions, and the combined effects of dissolved hydrogen and other factors on PSS hydrolysis quantified.

2.2.4 Inhibition

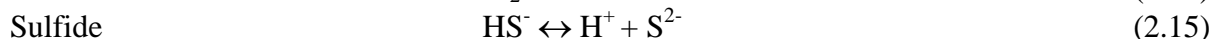
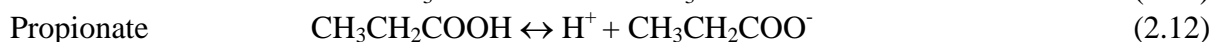
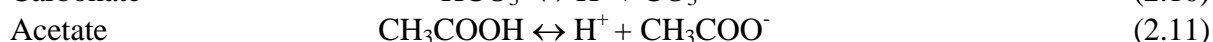
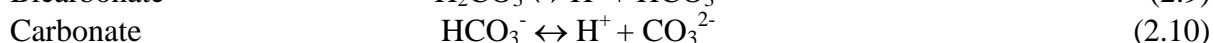
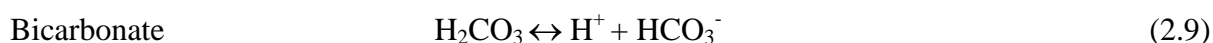
Inhibition effects that have been incorporated into mathematical models include inhibition by pH, acetic acid, ammonia, hydrogen sulfide or other contaminants. Inhibition by acetic acid, ammonia or hydrogen sulfide takes place at high concentrations of the undissociated molecule (CH_3COOH , NH_3 and H_2S) as opposed to the total species concentration. Because the pH affects the ratio between the dissociated and undissociated species via the acid-base equilibrium (see below), pH inhibition terms have seldom been used directly in mathematical models (Costello *et al.*, 1991; McCarty and Mosey, 1991). Rather, the majority of the mathematical models have simply calculated the concentration of the undissociated species from the observed pH of the system, and included these concentrations in the inhibition terms (Andrews and Graef, 1971; Hill and Barth, 1977; Kiely *et al.*, 1997; Kalyuzhnyi and Fedorovich, 1998). In contrast, the model proposed by Siegrist *et al.* (1993) includes terms

for dissociated acetate inhibition (CH_3COO), as well as hydrogen ion inhibition (H^+), rather than combining the two terms. This necessitates acid/base equilibria modelling (see below).

Whatever approach is followed for modelling undissociated species and pH effects, very little information exists in the literature on the effect of pH on the PSS hydrolysis rate under stable methanogenic conditions, while some studies have been performed on acidogenic systems; Eastman and Ferguson (1981) found a 42% increase in the soluble COD production when the pH of the acidogenic system was operated at a pH of 5.15 and 6.67. Veecken *et al.*, (2000) also found an increase in the hydrolysis rate of the organic fraction of municipal solids waste (OFMSW) when the pH was increased from 5 to 7. Since the substrate for hydrolysis in these studies was different, the hydrolysis rates could not be compared. Chapter 6 investigates the effects of pH on the hydrolysis of PSS under both methanogenic and acidogenic conditions.

2.2.5 Acid/base equilibria

The inhibition by the undissociated species of the various compounds discussed above requires that a comprehensive model predict these undissociated species concentrations from the pH of the system and the total species concentration. In order to calculate the pH, all weak acid/base species with a buffering capacity in the pH range under consideration would need to be included in the model, as well as the consumption or production of these species in the biological reactions. The following acid-base equilibria have been considered, depending on the species present, and the pH of the system:



Overall species balance and charge balance equations have been used to calculate the hydrogen ion concentration, and therefore the pH (Andrews and Graef, 1971; Hill and Barth, 1977; Bryers, 1985; Costello *et al.*, 1991; Kiely *et al.*, 1997; Massé and Droste, 2000). Alternatively, due to the dynamic nature of the above equilibria, each equilibrium has been modelled using kinetics for a forward and reverse reaction, with the two rates being linked by the equilibrium constant, K_a (Musvoto *et al.*, 1997; Musvoto *et al.*, 2000).

With the pH established via either of the techniques above, the effect of the pH on the processes, particularly the rate-limiting PSS hydrolysis step, needs to be determined. As noted above, there is little information on this aspect. Further, the dearth of information causes uncertainty in comparisons of different systems that may have established different pH values. Hence, the requirement to quantify the effect of pH on the PSS hydrolysis rate, as noted above.

2.2.6 Vapour/liquid equilibria

The production of biogas (CH_4 and CO_2) is of major importance to many wastewater treatment plants, since methane is used as a fuel to heat the digesters. Therefore, the prediction of the gas production rate and composition is an important output of any mathematical model. The expected species present in the gas from an anaerobic digester

include methane, carbon dioxide, trace amounts of hydrogen and ammonia, and depending on the system, hydrogen sulfide. The majority of these gases are soluble in the aqueous phase, and their composition in the gas phase is dependent on the vapour-liquid equilibrium. Henry's Law has generally been used to describe these equilibria (e.g. Musvoto *et al.*, 1997; Siegrist *et al.*, 1993; Vavilin *et al.*, 1995).

Methane is practically insoluble, and can be modelled as such, with no methane present in the aqueous phase; hence stoichiometric methane production can be accepted where the hydrolysis step is rate limiting, and is accepted in this research. In contrast, hydrogen and carbon dioxide may not be in equilibrium with the aqueous phase (Pauss and Guiot, 1993; Massé and Droste, 2000), and mathematical models have included mass transfer limitations to account for this phenomenon (Massé and Droste, 2000). However, under conditions of stable, completely mixed operation, equilibrium is likely.

2.2.7 Rate Equations

From the review above, it is apparent that for stable operation the overall process of anaerobic digestion has frequently been modelled with either hydrolysis or acetoclastic methanogenesis as the rate-limiting step. Hence, the choice of rate equation for these two processes is critical. In this section, the various types of rate equations that have been used for these two processes in published models are presented.

2.2.7.1 Methanogenesis

From Figure 2.1, the majority of methane (70%) is formed from acetate cleavage or acetoclastic methanogenesis:



Although acetoclastic methanogenesis takes place by the uptake of acetic acid (HAc) by the acetoclastic methanogenic bacteria, and therefore would appear dependent on this biomass concentration, Ray *et al.* (1989) and Shimizu *et al.* (1993) used simple first order kinetics to describe the production of methane:

$$\text{rate}_{\text{methanogenesis}} = k_m \cdot [\text{HAc}] \quad (2.17)$$

where k_m is the first order kinetic constant (d^{-1}).

Both of the above models were used to describe the anaerobic digestion of waste activated sludge following pre-treatment of the particulate organics. Since the emphasis of the research was on the chemical, thermal, or thermo-chemical (Ray *et al.*, 1989) and thermal, acid, alkali or ultrasound (Shimizu *et al.*, 1993) pre-treatment of the waste activated sludge, and the hydrolysis processes were modelled using a first order equation, the same form of equation was adequate for the rate of methane formation, since the hydrolysis step was rate limiting. Although the systems under investigation were similar with respect to operating conditions (temperature and pH), the value of the first order kinetic constant (k_m) differed: 12 and 4.62d^{-1} for Ray *et al.* (1989) and Shimizu *et al.* (1993) respectively. Most likely, these differences were due to the difference in biomass concentrations in each of the systems, since Ray *et al.* (1989) used an upflow anaerobic sludge bed reactor (UASB) while Shimizu *et al.* (1993) used a chemostat: Since the concentration of biomass in a UASB is higher than in a chemostat due to solid liquid phase separation, the acetoclastic methanogenesis biomass

Chapter 2: Background

concentration would be higher, and the rate of methanogenesis would be higher.

Substrate saturation kinetics (Monod, 1949) also have been used to describe the rate of acetoclastic methanogenesis, although not always coupled with the hydrolysis of particulate organic matter. The rate of growth of acetoclastic methanogen biomass (Z_{am}) on acetic acid (HAc) substrate is given by:

$$\text{growth rate} = \frac{\mu_{\max} Z_{am}}{1 + \frac{K_s}{[\text{HAc}]}} - b_{am} Z_{am} \quad (2.18)$$

where μ_{\max} is the maximum specific growth rate of the acetoclastic methanogenic bacteria (d^{-1}), K_s is the Monod saturation or half velocity constant (mgCOD/L), and b_{am} is the cell death constant/decay coefficient (d^{-1}).

The rate of acetic acid substrate utilization ($\text{rate}_{\text{methanogenesis}}$) is related to the rate of the biomass growth through the yield constant (Y_{am}):

$$\text{rate}_{\text{methanogenesis}} = \frac{\mu_{\max} Z_{am}}{Y_{am} \left(1 + \frac{K_s}{[\text{HAc}]} \right)} \quad (2.19)$$

Values for the kinetic constants used in the Monod equation (μ_{\max} and K_s) have been reported extensively, covering various operating conditions (Henze and Harremoës, 1983; Gujer and Zehnder, 1983; Bryers, 1985; Thiele and Ziekus, 1988; Pavlostathis and Giraldo-Gomez, 1991; Buffiere *et al.*, 1998; Jeyaseelan, 1997; Wu *et al.*, 1998). Similar in form to the Monod equation is the Michaelis-Menten equation, which has also been used to model acetoclastic methanogenesis (Kasper and Wuhmann, 1978; Ahring and Westermann, 1987; Lin *et al.*, 1989). Both the Monod and Michaelis-Menten rate equations predict that the rate of acetoclastic methanogenesis will reach a maximum when the acetic acid (HAc) concentration is high, and that this maximum will be proportional to the acetoclastic methanogenic biomass concentration (Z_{am}).

High concentrations of various anaerobic digestion products such as acetic acid, ammonia, and undissociated hydrogen sulfide inhibit methane gas production, while other contaminants, such as 3-ethylphenol, also have an inhibitory effect. To include acetic acid inhibition, Andrews and Graef (1971) and Moletta *et al.* (1986) modified the Monod equation with an uncompetitive inhibition term for acetic acid:

$$\text{rate}_{\text{methanogenesis}} = \frac{\mu_{\max} Z_{am}}{Y_{am} \left(1 + \frac{K_s}{[\text{HAc}]} + \frac{[\text{HAc}]}{K_{\text{HAc}}} \right)} \quad (2.20)$$

where K_{HAc} is the acetic acid inhibition constant (mgHAc/L).

Fox and Suidan (1990) used Eq 2.20 to describe acetic acid inhibition and 3-ethylphenol inhibition, when 3-ethylphenol was fed to the system. Hill and Barth (1977) used a similar modified Monod equation for inhibition by high concentrations of both acetic acid and ammonia (NH_3):

$$\text{rate}_{\text{methanogenesis}} = \frac{\mu_{\max} Z_{\text{am}}}{Y_{\text{am}} \left(1 + \frac{K_S}{[\text{HAc}]} + \frac{[\text{HAc}]}{K_{\text{HAc}}} + \frac{[\text{NH}_3]}{K_{\text{NH}_3}} \right)} \quad (2.21)$$

where K_{NH_3} is the ammonia inhibition constant (mgN/L).

These modifications were necessary since the feed to the bioreactor consisted of raw animal wastes, which were high in nitrogen (protein), and would result in the production of high concentrations of ammonia. Twenty years later, Kiely *et al.* (1997) used a model identical in form to the model of Hill and Barth (1977) to model the anaerobic digestion of the organic fraction of municipal solid waste (OFMSW) and primary sewage sludge (PSS). The only differences were in the values for the kinetic constants (μ_{\max} , K_S , K_{HAc} and K_{NH_3}), which can be justified since the two systems were operating at different temperatures: 25°C and 37°C for Hill and Barth (1977) and Kiely *et al.* (1997) respectively.

From the discussions above, the Monod-type expression, with or without inhibition terms, is widely used for kinetic modelling of acetoclastic methanogenesis. This is not unexpected since the substrate acetic acid is a soluble one and Monod kinetics was originally developed on soluble substrates (Monod, 1949). Thus, in this investigation, for those situations where acetoclastic methanogenesis is rate limiting, the Monod formulation can be implemented with confidence. However, it is highly unlikely that for the PSS being investigated as substrate under stable operating conditions, that acetoclastic methanogenesis will ever be rate limiting. More probable is that hydrolysis will be the rate-limiting step (see below).

2.2.7.2 Hydrolysis

Hydrolysis is defined as the extra cellular enzymatic breakdown of polymers (particulate) into monomers and dimers (soluble), which enter the subsequent acidogenesis reactions. Because particulate material cannot pass through the bacterial cell wall, the bacteria form a layer over the surface of the particle, and then secrete enzymes, which hydrolyze the polymers to smaller units that can be taken up.

One of the aims of this study is to select a rate equation to describe the rate of hydrolysis under a wide range of operating conditions. Temperature, pH, acidogenic biomass concentration, particle size and the type of particulate organic have all been identified to affect the rate of hydrolysis. To date, although the rate of hydrolysis is affected by all of these factors, the most common rate equation used to describe this process is the simple first order equation with respect to the total particulate COD (S_p) concentration:

$$\text{rate}_{\text{hydrolysis}} = k_h [S_p] \quad (2.22)$$

where k_h is the first order hydrolysis rate constant (d^{-1}) and S_p is the sum of both biodegradable (S_{bp}) and unbiodegradable (S_{up}) particulate components.

Since this is a simplification of the hydrolysis mechanism, each researcher who has implemented it has calibrated the model with a new value of k_h , giving rise to extensive tables of values (Henze and Harremoës, 1983; Bryers, 1985; Pavlostathis and GiraldoGomez, 1991). Kinetic studies for different substrates give different values as well, with substrates used ranging from primary domestic sludge (Eastman and Ferguson, 1981), to organic solids

Chapter 2: Background

(Gujer and Zehnder, 1983; Bryers, 1985), to wastewater (Henze and Harremoës, 1983).

Ray *et al.* (1989) identified two fractions of waste activated sludge that were hydrolyzed at different rates, one of which degraded at a rate that was two orders of magnitude greater. Two first order rate equations were used in this model, with appropriately adjusted first order rate constants. Other variations in the first order models include a product inhibition term, where high concentrations of total soluble COD (S_s) inhibit the hydrolysis of the particulate COD (Barthakur *et al.*, 1991):

$$\text{rate}_{\text{hydrolysis}} = k_h ([S_p] - [S_s]) \quad (2.23)$$

In all applications of the first order rate equation above, the hydrolysis rate was formulated as first order with respect to the total particulate COD (S_p). No differentiation was made between biodegradable (S_{bp}) and unbiodegradable (S_{up}) fractions. For pure substrate (such as starch, Zhang and Noike, 1994) this omission is reasonable, since the substrate is known and defined. However, for waste sludges, such as PSS, a S_{up} fraction is virtually inevitable (WRC, 1984) and would need to be considered since by definition, this fraction would not participate in the hydrolysis reaction. To accommodate this, Shimizu *et al.* (1993) suggested a similar expression to the above, but in which the rate of hydrolysis is dependent on the concentration of biodegradable particulate organics (S_{bp}) only, with the unbiodegradable particulate fraction (S_{up}) subtracted from the total particulate concentration (S_p):

$$\text{rate}_{\text{hydrolysis}} = k_h (S_p - S_{up}) = k_h \cdot S_{bp} \quad (2.24)$$

This development constitutes a significant, logical advance. However, in all of the above models, the rate equation used suggests that the rate of hydrolysis would increase linearly to infinity as the concentration of the total or biodegradable particulate organics respectively increase to infinity. However, it would seem logical that there should be some limitation on the maximum hydrolysis rate. Further, since the hydrolysis process is mediated by the acidogenic biomass, it would seem that the rate should be linked to the concentration of this biomass in some fashion.

To address these deficiencies, in contrast to the simplified hydrolysis rate models, Jain *et al.* (1992) developed a model for the hydrolysis of cow dung, where the rate of hydrolysis was first order with respect to the bulk enzyme concentration (C_{be}), rather than the biodegradable particulate COD concentration:

$$\text{rate}_{\text{hydrolysis}} = k_h \cdot C_{be} \quad (2.25)$$

In Eq 2.25, the bulk enzyme concentration was calculated from the rate of acidogenic biomass (Z_{ad}) growth on soluble substrate when the substrate concentration is limiting (Eq 2.26), the rate of enzyme production from microorganisms (Eq 2.27), and the rate of mass transfer of enzymes to the bulk liquid (Eq 2.28):

$$r_X = \frac{\mu_{\max} \cdot Z_{ad} \cdot S_{bs}}{K_S} \quad (2.26)$$

$$r_{me} = Y_{xe} r_X - k_L a (C_{me} - C_{be}) \quad (2.27)$$

Chapter 2: Background

$$r_{be} = k_L a (C_{me} - C_{be}) - b_{ad} C_{be} \quad (2.28)$$

where Y_{xe} is the enzyme yield per unit microbe, $k_L a$ is the mass transfer coefficient for enzymes in water, C_{me} is the enzyme concentration in the film surrounding the microbe, and b_{ad} is the cell death rate.

This rate equation allowed for the accurate prediction of the experimental data available, but recalibration of all eight of the kinetic constants was required before this model could be successfully applied to a second set of experimental data. Thus, modelling of hydrolysis in this instance became a curve fitting exercise, which makes the formulation impractical.

Eliosov and Argaman (1995) included the acidogen active biomass concentration in the first order specific rate equation for the hydrolysis of suspended solids in activated sludge systems, with an adjusted kinetic constant (k'_h):

$$\text{rate}_{\text{hydrolysis}} = k'_h \cdot S_{bp} \cdot Z_{ad} \quad (2.29)$$

However, again there is no upper limit to the rate of hydrolysis in this model. In contrast, Hill and Barth (1977) related the rate of disappearance of particulate volatile matter from animal waste to the growth of acidogenic biomass, which were in turn inhibited by the volatile fatty acid concentration (VFA) in the system:

$$\text{rate}_{\text{hydrolysis}} = \frac{\mu_{\max} \cdot Z_{ad}}{YXSO \left(1 + \frac{K_S}{S_{bs}} + \frac{S_{VFA}}{K_{HAc}} \right)} CF \quad (2.30)$$

where $YXSO$ is a yield coefficient, and CF is a conversion factor.

This rate equation does not take into account the biodegradable particulate organic substrate concentration at all, but does restrict the maximum rate of hydrolysis. Kiely *et al.* (1997) used an identical rate formulation to model the hydrolysis of OFMSW and PSS.

Eqs 2.24 to 2.30 quantify the rate of hydrolysis as a function of either the biodegradable particulate substrate or the activity of the biomass responsible for the secretion of the enzymes, or both.

For hydrolysis of PSS during the activated sludge process, Dold *et al.* (1980) modelled the rate of hydrolysis as proportional to the ratio of the biodegradable particulate COD concentration to the active biomass concentration, based on Levenspiel's active site surface reaction kinetic theory (Levenspiel, 1972). This theory was derived for reactions taking place on the surface of catalyst particles (Dold *et al.*, 1980 accepted biomass as being similar to a catalyst) and includes the adsorption of the reactant on the catalyst particle surface, where it reacts, followed by desorption of the reaction products. Any of these three steps could be limiting to the overall reaction. Levenspiel modelled the rate of the reaction itself in terms of the number of adsorption sites that are saturated, expressed as the parameter reactant concentration per unit area.

Similarly for the particulate (slowly) biodegradable substrate utilization concept of Dold *et al.* (1980): The bacteria attach via active sites onto the organic particle surface (termed adsorption), where they secrete enzymes, which hydrolyze the particle. The bacteria use the

products from the hydrolysis reaction for growth. Dold *et al.* (1980) modelled the adsorption process separately via mass transfer principles, but Henze *et al.* (1987) excluded this in subsequent developments of the model, as this process is seldom rate limiting and hence of little consequence.

Dold *et al.* (1980) could assume the growth step as being rapid, and therefore never rate limiting. Accordingly, Dold *et al.* (1986) reduced these two steps to a single hydrolysis process. For the hydrolysis, Dold *et al.* (1986) followed the formulation of Levenspiel with a planar surface and formulated the hydrolysis rate to depend on the concentration of both the active bacteria and the biodegradable particulate organics to active bacteria ratio (Eq 2.31). When either the bacteria concentration or the ratio is low, they will limit the overall reaction rate. However, when the ratio is high, the specific reaction rate reaches a maximum:

$$\text{rate}_{\text{hydrolysis}} = \frac{k_{\text{max}} \left(\frac{S_{\text{bp}}}{Z_{\text{ad}}} \right) Z_{\text{ad}}}{K_s + \left(\frac{S_{\text{bp}}}{Z_{\text{ad}}} \right)} \quad (2.31)$$

For this formulation, only two kinetic constants need to be calibrated for constant pH and temperature. Conceptually, Eq 2.31 seems to be the most appropriate form of the hydrolysis rate equation, as it includes both the substrate and the biomass. Further, although not applied in anaerobic digestion, the formulation has been widely applied to successfully simulate the behaviour of a wide range of activated sludge systems (Henze *et al.*, 1987; 1995) treating the same organics as found in PSS, the substrate under investigation here for anaerobic digestion.

From the discussions above, it is evident that a number of mathematical formulations have been proposed for hydrolysis of particulate biodegradable organics, ranging from simple first order, through enzyme concentration modelling, to surface reaction theory.

Chapter 4 describes an evaluation of the various hydrolysis rate formulations under methanogenic conditions, so that the rate formulation that most accurately predicts the PSS hydrolysis rate under all measured conditions can be determined.

2.2.8 Summary

Well-established reaction schemes are available for methanogenic anaerobic digestion, and have formed the basis for modelling these systems. In the anaerobic digestion of the biodegradable particulate organic substrate PSS under stable methanogenic conditions, the hydrolysis process mediated by the generic group acidogens invariably is the rate-limiting step. This implies that the kinetics of only this process are required to formulate a simplified model for these types of systems, with stoichiometry adequate for the subsequent processes. For the hydrolysis process, a variety of kinetic formulations have been developed or appear suitable. These formulations require evaluation, one objective of this investigation. In evaluating the formulations, pH effects need to be taken into account, as the possibility exists that pH has an influence on the PSS hydrolysis rate. The effect of pH on hydrolysis also will be investigated.

2.3 Influence of Methanogenesis and SRT on the Hydrolysis of PSS

In the anaerobic digestion of PSS, the review on modelling methanogenic systems above has indicated that the hydrolysis process is the rate-limiting step under stable methanogenic conditions. One of the most important factors influencing the hydrolysis of PSS is the solids retention time (SRT, R_s), since this determines the concentrations of both the hydrolysis substrate, the biodegradable particulates (S_{bp}), and the biomass group mediating the process, the acidogens (Z_{ad}).

Several studies have evaluated the effects of SRT on the rate of hydrolysis of particulate organic matter, mostly in completely mixed systems where the hydraulic retention time equals the SRT. By using completely mixed systems, the biological processes dominate, and there is more control of operational parameters such as solids retention time. Three studies will be discussed here in more detail. These three studies have been selected since they include methanogenic digesters that have been operated over a wide range of retention times, including HRT (and SRT) when methanogenesis fails. For two of the three studies, the resultant acidogenic conditions were investigated in depth, allowing for a direct comparison between methanogenic and acidogenic hydrolysis.

O'Rourke (1968) studied the kinetics of anaerobic digestion of PSS as a function of temperature and SRT. Completely mixed, laboratory scale anaerobic digesters fed PSS at 28.4gCOD/L were operated at temperatures of 35, 25, 20 and 15°C. For each temperature, the hydraulic retention time (= SRT) was reduced from 60d to 30d and then further (see Table 2.1). At each retention time, the systems were allowed to reach a steady state of operation, and then analyzed for total volatile solids, pH, alkalinity, total COD, ammonia and organic nitrogen, total volatile acids, cellulose and lipids. The lipids and volatile acids were analyzed further, so that the major species for each of these groups were identified.

For this study, the systems operated by O'Rourke (1968) at 35°C are of interest, and will be discussed further. At 35°C, the minimum SRT for which a stable methanogenic population was maintained was 7.5 days (Table 2.2) (at 25°C, the minimum SRT was 15d, and at 20°C, the minimum SRT was 30d). At this SRT, the intermediate soluble COD (volatile acids) concentration was negligible (140mgCOD/L), indicating a healthy balance between the hydrolysis process and the subsequent methanogenic process. However, at a SRT of 5 days, the volatile acids concentration increased significantly (2530mgCOD/L as HAc), indicating that the methanogenic biomass was no longer stable.

Table 2.1: Steady states measured for varying hydraulic retention times and temperatures from O'Rourke (1968)

T (°C)	Retention time (d)							
	60	30	15	10	7.5	5	3.75	2.5
35	X	X	X	X	X	X	X	X
25	X	X	X	X	X	X	X	
20	X	X	X	X	X	X	X	
15	X	X	X	X	X	X		

Table 2.2: Average steady state concentrations for the measured reactor parameters for varying hydraulic retention times at 35°C from O'Rourke (1968)

Measured Parameter (in gCOD/L)	Retention time (d)								
	Feed	2.5	3.75	5	7.5	10	15	30	60
Total COD	28.4	25.4	24.2	20.9	11.4	11.7	11.8	11.8	10.3
Lipids	12.6	12.6	13.0	12.2	5.05	4.66	4.07	4.45	3.52
Cellulose	4.47	0.48	0.43	0.42	0.41	0.34	0.44	0.36	0.33
Protein	6.40	4.40	4.32	4.27	4.32	4.33	4.35	3.78	3.67
Volatile Acids	1.02	4.64	4.69	2.53	0.14	0.09	0.06	0.06	0.03
*Alkalinity		5.2	4.9	3.6	1.8	1.6	1.8	2.0	2.3
pH Range		7.1 - 7.4	6.9 - 7.3	6.8 - 7.2	6.9 - 7.3	6.8 - 7.3	6.9 - 7.3	7.0 - 7.4	7.0 - 7.4
**Gas Production		167	215	246	496	523	513	521	515
***Gas Composition		34.5	40.7	48.0	62.2	62.7	64.3	67.2	67.5
COD Mass Balance		99.9	101.1	95.1	99.7	100.9	101.6	105.3	99.4

*gCaCO₃/L; ** mL per gram biodegradable COD added per day; *** %CH₄

For SRT's with stable methanogenesis (SRT \geq 7.5d), with the change in SRT, the relative gas composition was constant and independent of SRT, % total COD removed did not vary significantly, effluent VFA were consistently negligible (<140mgCOD/L), lipid removal increased slightly with increase in SRT and maximum COD removal was 63.7% at SRT = 60d which would indicate an unbiodegradable fraction in the PSS.

From Table 2.2, once the methanogenic population became unstable (SRT < 7.5d), several measured parameters showed significant changes from the systems in which the methanogenic population was stable (SRT \geq 7.5d). As noted above, the VFA concentration increased significantly. The gas composition was measured within a narrow range for the stable methanogenic systems (62 – 67% CH₄), but this composition dropped once methanogenesis failed (48.0, 40.7 and 34.5 for the 5, 3.75 and 2.5d retention times). Also, the gas produced was constantly measured at around 500mL per gram biodegradable COD added, but this volume dropped to less than half once methanogenesis failed. Most significantly, the total COD concentration increased once methanogenesis failed, indicating that the hydrolysis rate is directly affected by the stability of the methanogenic population.

The three major components of the particulate COD are cellulose, proteins and lipids, Figure 2.1. From Table 2.2, the residual cellulose and protein concentrations did not change significantly with reduced SRT, indicating that the presence of the methanogenic population does not influence the rates of hydrolysis of these individual components. However, the residual lipids concentration (Table 2.2) increased significantly once methanogenesis failed, with no lipids hydrolysis taking place in the acidogenic systems. This is illustrated in Figure 2.2, where the total lipids concentration remains unchanged below the SRT = 7.5d (acidogenic systems). The concentrations of the various lipid hydrolysis products, selected long chain fatty acids (LCFA's), are also shown in Figure 2.2. Palmitic acid (C16) has the highest concentration in the feed (PSS), and this concentration does not change under acidogenic conditions. However, the oleic acid concentration decreases while the stearic acid

concentration increases under acidogenic conditions. Both the oleic and stearic acids contain 18 carbon atoms per molecule, with oleic acid being unsaturated, while the stearic acid contains only saturated carbon bonds. It is possible that the changes in the concentrations of these two species is due to the saturation of the oleic acid to form stearic acid under acidogenic conditions, although this cannot be verified from the data.

Whatever the mechanism, what is directly evident is that methanogenesis has a direct influence on lipid hydrolysis. The influence of methanogenesis on lipid hydrolysis also was noted by Ghosh *et al.* (1995) who operated a two-phase anaerobic digestion system for WAS, in which the hydrolysis/acidogenesis took place in the first stage, while the methanogenesis took place in the second stage. They found that only 9.8% lipids conversion took place in the acidogenic phase, while 70.8% conversion took place in the methanogenic phase. Protein conversions were similar in both phases (35.8 and 39.4% in the acidogenic and methanogenic phases respectively).

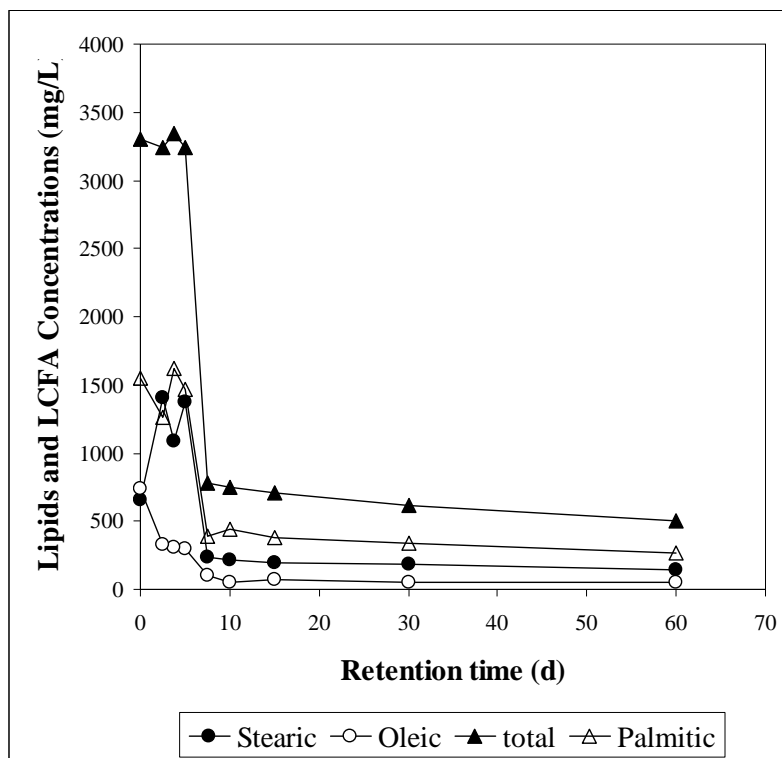


Figure 2.2: Total lipids concentration and individual LCFA concentrations for each steady state retention time from O'Rourke (1968) (feed = 0d)

The inhibition of lipid hydrolysis in the absence of methanogenesis possibly is via the VFA or the dissolved hydrogen concentration. Through end-product inhibition, increased VFA concentrations in the absence of methanogenesis (Table 2.2) possibly would result in inhibition of β -oxidation, leading to accumulation of LCFA, which would in turn inhibit lipid hydrolysis. For the dissolved hydrogen concentration, inhibition of lipid hydrolysis is probably as described in Section 2.2.3 above: In the absence of methanogenesis, dissolved hydrogen concentrations would become elevated inhibiting NADH_2 dehydrogenation (Eq 2.4), whose concentration in turn increases, inhibiting β -oxidation. This causes LCFA concentrations to increase, inhibiting lipid hydrolysis. However, in the absence of substantive

direct evidence, such mechanisms are speculative. Of importance is the apparent direct link between methanogenesis and the PSS hydrolysis rate.

From the above, the rate of hydrolysis of PSS is dependent on the stability of the methanogenic population, which in turn is dependent on the SRT. In the case of O'Rourke (1968), the minimum SRT was around 7.5d at 35°C to maintain a stable methanogenic population. Also, the maximum COD removal was 63.7% of the total feed COD at a retention time of 60d; the author argues that the residual COD is essentially unbiodegradable.

Izzett *et al.* (1992) studied the effects of thermal pretreatment on the anaerobic digestion of a mixture of PSS and humus sludge (40gCOD/L). The completely mixed laboratory scale digesters were operated at 37°C, and retention times (HRT = SRT) of 20, 15, 12, 10 and 7d, with steady state methanogenic operation at each SRT. However, when the SRT was reduced to 4d, the methanogenic population became unstable, resulting in an increase in the VFA concentration, and a decrease in the digester pH and methane production. The steady state data is presented in more detail in Chapter 4, Section 4.9.2, Tables 4.23 and 4.24. From the data of Izzett *et al.* (1992), increase in SRT from 7 to 20d increased total COD removal from 45 to 55%, in contrast to the observations of O'Rourke (1968) above. Clearly, this influence of SRT on hydrolysis requires further investigation and is one of the objectives of this research. Of importance is that the methanogenic population was stable at a 7d retention time with a 40gCOD/L feed concentration, which is similar to the results from O'Rourke (1968) discussed above, despite the significantly higher feed concentration.

Miron *et al.* (2000) studied the effects of SRT (HRT) on hydrolysis and acidification of lipids, proteins and carbohydrates present in PSS (30.8gCOD/L) in CSTR systems at 25°C. The aim of the investigation was to find the optimum SRT for the treatment of domestic sewage in a single or two-step UASB. The systems were mixed at 100rpm for 20 seconds every 20 minutes to simulate a sludge segment of a UASB reactor, and were operated at SRTs (HRT) of 3, 5, 8, 10 and 15d.

For a SRT of less than 10 days, acidogenic conditions prevailed, indicated by negligible gas production, while for longer SRTs (≥ 10 d) methanogenic conditions prevailed. From O'Rourke (1968) at 25°C, the methanogenic population was stable at 15d, but failed at 10d. The feed COD concentrations were similar, 28.4 and 30.8gCOD/L for O'Rourke (1968) and Miron *et al.* (2000) respectively, with the only major difference between the two studies being the mixing conditions in the digester and the feed source.

For the acidogenic systems (<10d), for the 3-day system the hydrolysis conversion of the lipids increased compared to the feed, but did not increase further with an increase in SRT. The authors proposed that either the system was inhibited by the LCFAs produced, or by physical hindrance due to adsorption. Similarly, protein hydrolysis did not increase with an increase in SRT, and the authors proposed that this was due to lipid inhibition or due to the low pH. Carbohydrate hydrolysis increased with an increase in SRT, regardless of whether acidogenic conditions or methanogenic conditions prevailed. Further, under methanogenic conditions, lipid and protein hydrolysis increased significantly compared with acidogenic conditions, with a total particulate COD conversion of approximately 60%, compared to 20% under acidogenic conditions.

The results of the three studies discussed above indicate that methanogenesis has a significant influence on the rate of hydrolysis of PSS. This would appear to be related to hydrolysis of particularly the lipid fraction, which does not seem to be hydrolyzed to any significant degree

under acidogenic conditions. Possible mechanisms for the inhibition of lipid hydrolysis have been identified, but these are largely speculative. What is imperative is that the methanogenic biomass population be present and stable in the system for maximum PSS solids conversion. The parameter with the greatest influence on the presence of methanogenesis is SRT, and this needs to be maintained above a minimum value.

However, from the data of O'Rourke (1968), once SRT is sufficiently long and methanogenic conditions are established, there would seem to be little benefit in increasing the SRT in the digester further, since the total COD concentration removed is not increased significantly with an increase in SRT from 10 to 30d. This is in contrast to the data of Izzett *et al.* (1992), which suggests that increasing SRT increases PSS and humus sludge hydrolysis even under stable methanogenic conditions. Clearly, this aspect requires further investigation (Chapter 4).

2.4 Influence of Acidogenesis and SRT on the Hydrolysis of PSS

From Section 2.3 above, it appears that methanogenesis has a significant effect on the PSS hydrolysis. However, in the absence of methanogenesis, the soluble organic compounds produced directly during sequential hydrolysis then acidogenesis have been widely used to augment BNR activated sludge systems (Pitman *et al.*, 1983; Barnard, 1984; Brinch *et al.*, 1994; Andreasen *et al.*, 1997; Banister and Pretorius, 1998). For this reason, there is considerable interest in hydrolysis/acidogenesis of PSS under acidogenic conditions, and several studies have been performed on purely acidogenic systems. However, the principle aim of these studies has been to develop empirical guidelines to maximize the production of soluble COD, and not on modelling the PSS hydrolysis. Relevant aspects of the results of these studies are discussed further in this section.

Eastman and Ferguson (1981) studied the acidogenic hydrolysis of PSS in completely mixed, continuously fed digesters at 35°C. Six steady state operations were analyzed from systems operated at different hydraulic retention times, seeded with different sludges, and with the addition of NaOH to the feed solution of some of the digesters (see Table 2.3). Additionally, four batch tests were conducted to determine the maximum soluble COD conversion of the PSS before the onset of methanogenesis. Three further batch tests evaluated the effect of feed concentration on the concentration and composition of the soluble organic produced.

From Table 2.3, for all systems studied, methanogenic activity is negligible ($< 0.7\text{gCOD/L}$ feed of methane produced for feed = 52gCOD/L). Steady state numbers 3 and 4 are duplicate experiments except that they were seeded with different seed sludges. From the VFA and soluble COD measurements, the two systems were operating near identically, indicating that the acidogenic bacteria were present in the PSS, and that this biomass operated similarly regardless of the source. Also, the gas production for these two systems was identically negligible, indicating that any methanogens in the AD seed sludge were no longer present. The mechanism responsible for their inactivity probably is a combination of pH inhibition and washout at the comparatively short SRTs.

Table 2.3: Steady state operating data from Eastman and Ferguson (1981) for continuous fed acidogenic systems (Feed total COD = 52.0g/L)

S.S. No	R _h (h)	pH	Seed sludge	VFA (g/L)	Sol. COD (g/L)	VFA**/sol. COD ratio (gCOD/gCOD)	Carbo	Nitro	% CH ₄	Gas Prod. (gCOD/L feed)
	Feed	5.2		1.91	4.78	42.6	0.69	1.52		
1	9	5.21	Acido	5.34	6.22	91.6	0.11	0.34	16	0.06
2	18	5.20	PSS	6.48	7.07	97.8	0.13	0.31	19	0.14
3	36	5.13	PSS	7.83	8.37	99.8	0.14	0.31	19	0.21
4	36	5.15	AD	7.48	8.09	98.6	0.12	0.26	21	0.21
5	72	5.13	PSS	8.4	9.24	97.0	0.14	0.29	20	0.28
6	36	5.85*	AD	8.54	10.07	90.5	0.11	0.30	23	0.3
7	36	6.67*	AD	10.04	11.70	91.5	0.12	0.32	45	0.68

Acido – after 18h retention time steady state (steady state number 2); PSS – feed sludge held at 35°C for 3 days; AD – active methanogenic sludge; *NaOH addition; Carbo – soluble carbohydrates; Nitro – soluble organic nitrogen material (not FSA); **VFA assumed to be acetic acid for COD calculation

The VFA/soluble COD ratio shows that for all of the acidogenic systems, the majority of the soluble COD was made up of VFA. This is also shown by the relatively low concentrations of the soluble carbohydrates and soluble nitrogenous material. Clearly, acidogenesis of the hydrolysis products had taken place almost to completion, even at the extremely low SRTs of 9h. This would indicate hydrolysis as the rate-limiting step in the acidogenic systems, in agreement with the methanogenic systems. However, contrary to the observations of O'Rourke (1968) on methanogenic systems, the data of Eastman and Ferguson (1981) indicate SRT has a significant influence on the hydrolysis in acidogenic systems, with VFA concentrations (and hence hydrolysis) increasing with SRT.

The results of batch tests conducted by Eastman and Ferguson (1981) show that the final concentrations of soluble products was linearly dependent on the initial COD concentration, indicating that the rate of hydrolysis under acidogenic conditions is dependent on the feed COD concentration. However, the composition of the soluble products was not the same for all systems. The fractions of acetic acid and propionic acid decreased with an increase in the feed COD concentration, but were still the major components, while the longer chain fatty acids (butyric, valeric, caproic) show a reciprocal increase with an increase in the feed concentration.

In agreement with the data of O'Rourke (1968), no significant lipid hydrolysis took place in the acidogenic systems. The maximum conversion of the carbohydrates (mainly cellulose) and proteins was 70% and 55% respectively after 14 days batch operation.

Eastman and Ferguson (1981) developed models to describe their acidogenic systems. The results of the modelling exercise showed that a first order rate equation gave an accurate estimate of the rate of hydrolysis for each SRT. The method for calculating the first order rate constant (k_h) was independent of the effluent biodegradable particulate COD concentration, but rather k_h was calculated from the soluble COD production, since this was the focus of the investigation. Two PSS unbiodegradable particulate COD fractions are reported; 70% for stored sludge and 60% for fresh sludge. These differences in the unbiodegradable particulate COD fraction highlight the inconsistencies in the literature in defining parameters such as the

unbiodegradable particulate COD fraction: For this study, the unbiodegradable particulate COD fraction will be accepted as the ratio between the unbiodegradable particulate COD concentration and the total feed COD concentration.

Lilley *et al.* (1991) studied acid fermentation of PSS in batch, single and in-series completely mixed continuous reactor systems, and found that the principal VFA produced were acetic acid and propionic acid, and that this production increased with SRT, but at a declining rate. In addition, an equal COD concentration of non-VFA soluble COD was generated, in contrast to Eastman and Ferguson (1981) above. Similarly to Eastman and Ferguson (1981), Lilley *et al.* (1991) found that the VFA production followed first order type kinetics, which they modelled via a rate proportional to the potential VFA production remaining in the PSS. A maximum VFA generation potential of 17% (on a COD basis) was proposed, which if the non-VFA soluble COD was included, would yield a maximum PSS hydrolysis conversion of 34% under acidogenic conditions. This is substantially less than the maximum of 64% observed under methanogenic conditions by O'Rourke (1968), see Section 2.3.

Elefsiniotis and Oldham (1994) studied the effects of SRT on acidogenesis of PSS at ambient temperatures (18 – 22°C). Two systems were operated in parallel: a completely mixed digester with a clarifier for sludge separation and recycle, and a UASB reactor with internal sludge retention. The feed sludge was diluted to a total solids concentration of 4000mgTS/L for each sludge batch (each batch used for 10 days). The systems were seeded with active acidogenic sludge, and the hydraulic retention time (HRT) was set at 12 hours for all systems, while the SRT was increased from 5 to 10, 15 and 20 days. The two system configurations performed similarly under all conditions, and the results reported here are for the completely mixed digester with a clarifier, Table 2.4.

Table 2.4: Steady state operating data from Elefsiniotis and Oldham (1994) for continuous completely mixed digester with clarifier (Feed TS = 4000mg/L)

R_s (d)	pH	net VFA conc. (mgHAc/L)	Spec. VFA prod. rate (mgVFA/mgVSS.d)	Spec. hydrolysis rate (mgCOD/mgVSS.d)	% VSS Red.	% Protein Red.	VFA/sol. COD ratio (gCOD/gCOD)
5	5.6	140	0.053	0.184	62.8	38.7	42.8
10	5.0	520	0.101	0.187	63.1	42.9	72.3
15	5.2	575	0.125	0.200	67.1	51.2	85.4
20	5.2	590	0.119	0.184	65.6	54.1	90.7

The results show a significant increase in the net VFA production (measured effluent minus feed) and specific VFA production rates when the SRT was increased from 5 to 10 days, in agreement with Eastman and Ferguson (1981) and Lilley *et al.* (1991). However, the increase became less marked when the SRT was increased further above 10d. The specific hydrolysis rate expressed in terms of VSS did not vary significantly for the four steady states. The consistency in the specific rate of hydrolysis probably is due to the decrease in the VSS concentration with an increase in the SRT, since the %VSS reduction increases with an increase in the SRT – the residual feed PSS contributes to the VSS and therefore influences the calculated specific rate. In contrast to Eastman and Ferguson (1981) who reported a VFA: soluble COD ratio of greater than 90% for all retention times, for this study the variation in the ratio was far greater, increasing from 43 to 91% with increase in SRT. The major difference between these two studies was the operating temperatures (35 and 20°C for

Chapter 2: Background

Eastman and Ferguson (1981) and Elefsiniotis and Oldham (1993) respectively), which would have a major effect on the growth rates of the various biological groups. The majority of the VFA were acetic acid, followed by propionic acid, but these fractions decrease with an increase in the SRT, consistent with the observations of Eastman and Ferguson (1981) and Lilley *et al.* (1991).

Skalsky and Daigger (1995) conducted a series of bench scale tests in 4L stirrer reactors. Digesters were operated at a SRT (it is not certain whether this is different to the HRT) of 2, 3, 4, 5 and 6 days at 20°C and a feed TS concentration of 2.6%. The results showed similar VFA production for the 2, 3 and 4 day SRT of around 0.2 gVFA/ gfeed VS, while this value changed to 0.26 and 0.24 for the 5 and 6 day systems. From these results, in contrast to the observations of previous researchers, there is no apparent correlation between the SRT and the VFA production. A second set of experiments examined the effect of the feed solids concentration on the VFA production (T = 20°C; SRT = 2d). The feed TS concentration was diluted from 2.58 to 1.29, 0.86 and 0.43%. The resulting VFA production per feed VS increased with a decrease in the feed TS concentration (0.12, 0.16, 0.20 and 0.22 gVFA /g feed VS respectively), and the authors suggest this is caused by mass transfer (lower solids = better mixing) and product inhibition effects, although actual values for the product concentrations are not reported. When two systems were operated at different temperatures (14 and 20°C) (feed TS concentration = 1%, SRT = 2d), the lower temperature resulted in a VFA production approximately 42% less than the 20°C system. Unfortunately, there was no consistency between the performance of replicate experiments, and this was possibly due to insufficient analysis of the feed, which possibly changed during storage. This highlights the importance of feed characterization in investigations into anaerobic digestion of PSS, and is one of the aspects specifically addresses in this research.

Hatziconstantinou *et al.* (1996) conducted batch and continuous bench scale experiments (T < 20°C) to determine the factors affecting the production of soluble organics and the effect of these soluble organics on the denitrification process. Once again, the reported values show significant variations. The maximum soluble organics production per sludge initial VSS varied from 0.090 to 0.294 g sol COD/ g feed VSS. The soluble COD produced as a fraction of the feed total COD ranged from 4.8 to 22.4%, with a mean of 10.5%, for batch tests with a retention time ranging from 3 to 13 days. Continuous experiments at a 2-day solids and hydraulic retention time produced 5% soluble COD as a fraction of the feed total COD. However, for the 13 days for which the digesters were operated, the feed total COD concentration varied from 4.5 to more than 10 gCOD/L, and thus the systems were never able to reach a steady state of operation.

Andreasen *et al.* (1997) studied the full-scale application of sludge acidogenesis for augmenting BNR processes. Although no operating data other than process temperatures were reported for the acidogenic digesters, two digesters fed PSS were operated at 20°C, and gave soluble organic conversions of 16 and 9% soluble COD production/ total feed COD concentration, while a third was fed activated sludge at 8 – 17°C, and gave a soluble organics conversion of only 2.5%. It is not clear whether the difference in the soluble COD conversions is due to the different sludges, or to the difference in temperature between the two systems.

Banerjee *et al.* (1998) investigated the effects of wastewater composition, hydraulic retention time and temperature on VFA production. Systems fed a 1:1 ratio of starch-rich wastewater from a potato-processing factory and PSS were compared to systems fed PSS only. The systems consisted of a completely mixed continuous fed digester and a clarifier with sludge

recycle, for a SRT of 7 days. Comparative steady state operations were reported at increasing HRT, and then at fixed HRT and increasing temperatures (Table 2.5).

Table 2.5: Steady state operating data from Banerjee *et al.* (1998) for continuous completely mixed digester with clarifier fed PSS only (Feed TS = 5000mg/L)

R _h (h)	T (°C)	VSS (mg/L)	VFA specific rate (mgVFA/mgVSS.d)	Sol. COD specific rate (mgCOD/mgVSS.d)	% VSS removal
18	22	12917	0.028	0.041	34
30	22	20062	0.013	0.018	66
30	30	12065	0.014	0.020	43
30	35	6920	0.008	0.019	50

The effluent was analyzed for acetic acid, propionic acid, isobutyric acid, n-butyric acid, isovaleric acid and n-valeric acid. Acetic acid was always the major component (63 – 76%), with propionic acid as the second highest fraction, in agreement with observations above. For all of the systems operated, the VFA and soluble COD production in the system fed a blend of starch-rich waste and PSS was higher than for the system fed PSS only. This is probably due to the high overall biodegradability of the starch-rich fraction, rather than to an increase in the rate of hydrolysis of the PSS in the presence of the starch, and again highlights the importance of feed characterization. From Table 2.3, trends can be observed for the effect of temperature and HRT on the specific VFA production rate and specific soluble COD production rate. At all temperatures and HRT, the soluble COD specific production rates are significantly higher than the VFA specific production rates, indicating significant production of a non-VFA soluble COD, in agreement with the observations of Lilley *et al.* (1991) and Elefsiniotis and Oldham (1994) above.

However, the most important trend is the decrease in VSS concentration with an increase in temperature. The authors report a decrease in the efficiency of the clarifiers with an increase in temperature, so that the reported SRT of 7 days must be uncertain. Since acidogenesis is a biologically mediated process, and mesophilic bacteria experience an Arrhenius-type relationship with temperature, the production of soluble COD would be expected to increase with an increase in temperature, unless there was some form of product inhibition. This is not apparent since the %VSS destruction as calculated by the authors, does not show any correlation with temperature, and this would be expected to increase with an increase in temperature.

Hence, use of the parameter VSS in expressing specific rates for hydrolysis of particulate organics including PSS has severe deficiencies, since the particulate organics from the feed contribute to the VSS. An alternative parameter is clearly required, and is proposed in this investigation.

In summary, from the review above, it is evident that the absence of methanogenesis (i.e. acidogenic conditions) has a significant effect on the PSS hydrolysis, both on the rate and on the extent to which this occurs. This has implications for comparisons between anaerobic digestion systems, in that care needs to be taken to correctly establish the state of the digester before comparison. Also arising from the review, is the importance of feed characterization in anaerobic digestion studies, and this will form an important part of this research (Chapters 4 to 7).

For acidogenic anaerobic digestion, there is considerable variation in observations on the effects of physical constraints such as SRT on the hydrolysis and on production of non-VFA soluble COD, and these aspects require further investigation (Chapter 5 and 6).

In terms of modelling these systems, developed models are largely empirical, e.g. Lilley *et al.* (1991). Since the hydrolysis process should be similar to that under methanogenic conditions, in that the same bacterial consortium mediate the process on the same substrate (though rates may differ), a common hydrolysis model for both methanogenic and acidogenic anaerobic digestion would seem the most appropriate. This is specifically addressed in this research.

2.5 Biological Sulfate Reduction

2.5.1 Biological sulfate reduction processes

The reduction of sulfate to sulfide takes place according to Eq.2.32:



The 8 moles of electrons required to reduce 1 mole of sulfate are obtained from an organic electron donor. For simple known organics, such as VFA, ethanol and producer gas, taking into account the biomass yield, theoretical molar ratios of the organic substrate to be blended with the sulfate can be calculated, so that sulfate conversion is maximized, and residual organic substrate is minimized. For more complex substrates such as PSS, the molecular formula for the particulates is not known, and rather the total COD is measured. One mole of sulfate requires 8 electrons, Eq 2.32. This is equivalent to:



Therefore, 1 mole sulfate (96g/mol) requires 2 moles oxygen (32g/mol), or 96g sulfate require 64g COD. Therefore, a minimum chemical (excluding biomass yield) COD:SO₄ ratio of 0.67 gCOD/gSO₄ is required.

Biological sulfate reduction is thermodynamically and kinetically favourable over methanogenesis for common substrates (e.g. Kristjansson *et al.*, 1982; Kristjansson and Schönheit, 1983; Nedwell and Reynolds, 1996; Pareek *et al.*, 1998), and sulfate-reducing biomass is more tolerant of the toxic sulfide produced by sulfate-reduction than methanogens (e.g. Maillecheruvu and Parkin, 1996). The sulfate-reducing biomass is less substrate specific (methanogens grow on acetate and hydrogen only, Zeikus, 1977), and utilizes longer chain fatty acids (> C₂) and dissolved hydrogen preferentially to the acetate.

Reis *et al.* (1991) operated a two-stage acidogenic-methanogenic process for the treatment of distillery wastewaters (cane sugar molasses slops) containing sulfate at a minimum concentration of 3gSO₄/L. The aim of the investigation was to maximize acetic acid production and sulfate reduction in the acidogenic phase; then with complete sulfide removal between stages, the methanogenic biomass in the second stage would have a sulfate- and sulfide-free acetic acid feed for maximum methanogenic activity. The feed was similar in composition to the studies of Mosey, (1983), Costello *et al.* (1991) and Sam-Soon *et al.* (1991), who investigated the effects of increased concentrations of dissolved hydrogen on the products of glucose fermentation, and found increased dissolved hydrogen concentrations favoured the production of VFA other than acetic acid, see Section 2.2.3. Reis *et al.* (1991) found increased sulfate reduction correlated with increased production of acetic acid as the

final VFA product. The authors suggested that acetic acid was the major organic product in the presence of sulfate reduction, when the more complex organics were used as substrate.

Based on the discussion in Section 2.2.3, in order to produce acetic acid as the major product of glucose degradation, the dissolved hydrogen concentration needs to be maintained below the limiting thermodynamic concentration. If the same basis applies for the acidogenic stage of the Reis *et al.* (1991) systems, the sulfate-reducing biomass must be responsible for the utilization of the dissolved hydrogen (hydrogenotrophic methanogenic biomass was not present in the acidogenic phase digester), causing the dissolved hydrogen concentration to be low, and hence acetic acid to be produced.

Sam-soon *et al.* (1987) hypothesized that for pellet formation, plug flow regimes were necessary where regions of high and low dissolved hydrogen existed. The hypothesis was based on experimental results obtained from the treatment of apple juice concentrate (mainly sugars) in a UASB reactor. Russo and Dold (1989) operated a UASB reactor treating paper plant effluent that contained 4500mgCOD/L and 250mgSO₄/L. They found that limited pellet formation occurred, and proposed that since 45% of the feed COD was acetic and propionic acid leaving little substrate for hydrogen production, and the sulfate content of the feed resulted in hydrogenotrophic sulfate reduction at the base of the UASB reactor, this resulted in a low dissolved hydrogen concentration, and hence limited pelletization. Sam-soon *et al.* (1991) also studied the effects of sulfate on the pellet formation in a UASB reactor fed glucose and sulfate, and similarly found a reduction in the pellet formation with an increase in the influent sulfate concentration.

From the discussions above, it would appear that the hydrogenotrophic sulfate-reducing biomass may be capable of reducing the dissolved hydrogen concentration to below the thermodynamic or other limits at which the dissolved hydrogen becomes inhibitory. If this is true, then sulfate reduction in digesters fed PSS could similarly reduce the dissolved hydrogen concentration, so that dissolved hydrogen inhibition of β -oxidation of LCFA does not occur, which in turn would keep LCFA concentrations below levels that cause lipid hydrolysis inhibition (see Sections 2.2.3 and 2.3 above). Thus, biological sulfate reduction may have an effect on PSS hydrolysis that is similar to that noted above for methanogenesis, i.e. the hydrolysis rate is increased compared with acidogenic systems.

2.5.2 Biological sulfate reduction with PSS as substrate

PSS has been identified as an economically and practically feasible carbon and electron source for the biological reduction of sulfate in the treatment of sulfate-rich wastes such as AMD (Whittington-Jones, 2000). In this process, necessarily the PSS would need to undergo hydrolysis (and acidogenesis) to generate the substrates required for the sulfate reduction. Thus, hydrolysis of PSS under sulfate reducing conditions is of considerable interest, and is to be investigated in this research (Chapter 7).

A particularly intriguing observation arising from the review of methanogenic and acidogenic anaerobic digestion above is that the presence of methanogenesis significantly increases the rate and extent of PSS hydrolysis. It is of interest whether the presence of sulfate reduction causes a similar increase in the rate and extent of PSS hydrolysis, and hence whether PSS hydrolysis is similar under sulfate-reducing conditions as under methanogenic conditions. In terms of the discussion above, if the dissolved hydrogen concentration does play a regulatory or inhibitory role in the hydrolysis process under acidogenic conditions, which is not apparent under stable methanogenic conditions due to the lower hydrogen concentrations, then sulfate

reduction may similarly reduce hydrogen concentrations (hydrogen is a potential substrate in sulfate reduction), causing higher PSS hydrolysis rates. Also, sulfate reduction may reduce the VFA concentrations leading to higher hydrolysis rates than under acidogenic conditions. In this section, relevant research on biological sulfate reduction is reviewed.

Initial studies on biological sulfate reduction aimed at identifying and quantifying the effects of sulfide on the methane production in anaerobic digesters, and not on the effect of sulfate reduction on the hydrolysis, since the digesters were being operated to maximize methanogenesis. Rudolfs and Amberg (1952a) studied the effects of sulfide on the anaerobic digestion of a mixture of white water concentrates and ripe sewage sludge. Total sulfide (S_T) concentrations less than 200 ppm retarded methane formation, while higher concentrations were toxic to the methane-producing bacteria (MPB). However, sulfide concentrations of up to 300 ppm had no effect on the hydrolysis of the particulate organic matter. They concluded that the high sulfide concentrations would lead to an accumulation of the volatile fatty acids, and ultimately failure of the digester.

Rudolfs and Amberg (1952b) discussed ways of alleviating the effects of the dissolved sulfide species. They concluded that sulfate removal from the feed liquor was not feasible, while precipitation of the sulfide by ferric chloride did not reduce the sulfide concentration sufficiently. A two-stage process in which hydrolysis and sulfate reduction took place in the first, with stripping of the sulfide and methane production in the second, also failed. This was because sulfate reduction was incomplete in the first stage, and the sulfide produced in the second stage was sufficient to retard methane production. Yeast extract addition and purging with a CO_2/N_2 mixture in a single stage reactor however did allow for sufficient removal of the sulfide to allow for increased organic loading rates and methane production rates.

Aulenbach and Heukelekian (1955) studied the effects of various sulfur compounds (sulfite, sulfide, sulfide salts, cystine and methionine) to isolate the compounds affecting anaerobic digestion. It was determined that sulfite and sulfide inhibited methanogenesis, but at lower sulfide concentrations than Rudolfs and Amberg (1952b) (50 ppm - retardation; 100 ppm - complete inhibition). The common hypothesis was that the undissociated hydrogen sulfide (H_2S) is inhibitory to methanogenesis, and these variations in toxicity of the total sulfide concentration are due to variations in the operating pH of the digesters (changing H_2S species concentrations). Once again, the hydrolysis step was less affected by the presence of the sulfide and sulfite than the methane production step, leading to an accumulation of volatile fatty acids (methanogenesis failure).

Lawrence *et al.* (1966) further investigated the effects of various concentrations of soluble and insoluble sulfide. Acid-base equilibria and vapour-liquid equilibria were included in a mathematical model, but this model was not used to isolate the sulfide species causing inhibition of methane production. Results showed that iron sulfide precipitates removed the toxic sulfides, while the precipitate was not toxic itself, up to concentrations of 400 ppm of sulfide.

These studies were aimed at determining the effects of sulfate reduction on the methanogenic anaerobic digestion of solid wastewater, so that the inhibitory effects of the reduced sulfur species could be eliminated. In contrast, Butlin *et al.* (1956) attempted to produce sulfide and elemental sulfur from the anaerobic digestion of primary sewage sludge with simultaneous sulfate reduction. This was to be done without jeopardizing the production of methane, which was being used for heating of the existing treatment plant. They found that pure strains of sulfate-reducing bacteria (SRB) could not hydrolyze the particulate organic feed themselves

and that high biomass concentrations were needed before significant sulfate reduction could take place. Finally, methane production was impossible in the sulfate reducing system, where sulfide inhibition was predominant.

Ueki *et al.* (1988) stated that in nutritionally rich environments, such as anaerobic digester slurry of cattle wastes, sulfate reduction does not compete with methanogenesis for the energy source (VFA), even when the SRB are not sulfate limited. Fukui *et al.* (2000) studied the *in situ* substrates for sulfate reduction and methane production in municipal anaerobic sewage digesters with different levels of sulfate, but failed to measure the effects on the rate of hydrolysis of the sewage sludge.

The first study on the effects of sulfur species on hydrolysis of particulate organic matter was undertaken by Khan and Trottier (1978). Specifically, the hydrolysis of cellulose in sewage sludge was investigated. They found that a sulfur source of 1.5 to 1.7 mmol/L sulfur from sulfate, sulfite, thiosulfate, sulfide or amino sulfur (cysteine or methionine) was essential for the degradation of cellulose to methane, and that sulfur appeared to be an essential nutrient for the mixed culture present in sewage sludge. However, higher concentrations (1.75 mmol/L as S) of either sulfite or undissociated hydrogen sulfide (H₂S) inhibited methane production, while sulfate was not inhibitory. Therefore, low concentrations of sulfur in sewage sludge digestion are essential for the degradation of cellulose.

Kim *et al.* (1997) studied the degradation of cellulose and lignocellulose material in simulated landfill column reactors under sulfate-reducing and methane-producing conditions. Sulfate-reducing conditions (1000 mg/L SO₄²⁻ in the feed) suppressed methane production, and increased the rate of hydrolysis of cellulosic and hemicellulosic material (filter paper and newspaper), in both continuous and batch experiments. Pareek *et al.* (1998) continued the study of enhanced hydrolysis of lignocellulosic materials (office paper and newspaper) under sulfate-reducing and methane-producing conditions. Under sulfate-reducing conditions (1000 mg/L SO₄²⁻), more than twice the hydrolysis of the lignocellulosic materials took place than with methanogenic conditions. However, the hydrolysis conversion was dependent on the lignin content of the substrate, where more lignin resulted in lower conversion.

Whittington-Jones (2000) compared laboratory-scale single-stage and multiple-stage falling sludge bed reactors under sulfate reducing and non-sulfate reducing conditions (feed PSS COD = 2gCOD/L; 2gSO₄/L) and implied higher PSS hydrolysis rates under sulfate-reducing conditions. The HRT in all four systems was maintained at 2d, and the temperature at 22 - 25°C; SRTs were not known. The systems were operated for 14d before steady state was accepted; however, after 39d of operation, the systems showed neither stability nor steady state. For example, the total particulate COD concentration in the sludge bed of the first stage of the multiple stage non-sulfate reducing system increased from 6862 to 24027mgCOD/L over the 39d period during which the system was operated. Also, methane production was not reported, and it is not clear whether the non-sulfate systems were operating under stable methanogenic or acidogenic conditions. It is therefore difficult to directly quantitatively compare the PSS hydrolysis rates under the sulfate and non-sulfate-reducing conditions based on the reported operation of these systems, and to unequivocally determine whether the non-sulfate reducing system was completely or partially methanogenic or acidogenic. This study does however indicate that sulfate reduction may have an influence on the performance of these types of systems, since the nature of the sludge beds was visibly different.

Whittington-Jones (2000) further reported the operation of a pilot-scale (23m³) falling sludge bed reactor and found that PSS should serve as a substrate for sulfate reduction.

Unfortunately, all reported values for the operation of the reactor were based on a COD:SO₄ utilisation ratio of 2gCOD:1gSO₄, which is significantly higher than the stoichiometric ratio of 0.67gCOD:gSO₄ calculated above. Thus, no firm conclusions on PSS hydrolysis rates can be extracted from the operating data.

Whittington-Jones (2000) and Molwantwa *et al.* (2004) conducted batch tests to determine the effects of sulfate reduction on the rate of PSS hydrolysis when compared to non-sulfate reducing systems. Although the results of these batch tests indicate an increase in the soluble carbohydrate concentration under sulfide-rich and sulfate-reducing conditions, methanogenic conditions were not confirmed, and it is possible that the control experiment was in fact operating under acidogenic conditions. Thus, it is difficult to extract comparative kinetic data from these results. Further, initial concentrations of biomass in the tests are not known, so that specific rates cannot be quantified.

These studies highlight that the difficulty with interpreting hydrolysis rate data from a system with internal sludge retention (i.e. SRT uncoupled from HRT) is in quantifying the SRT, in establishing a steady state of operation without sludge accumulation, and in quantifying the various effluent particulate organic fractions, which include the unbiodegradable substrate, the residual biodegradable substrate, and the biomass generated, aspects that would need to be addressed in this study.

Equally difficult is to analyse the results from batch tests, since these depend on the initial concentrations of the feed (can be quantified) and active biomass (difficult to quantify), but also on the lag phases which result from the shocks to the biomass caused by the batch addition of the feed and other media.

Accordingly, in this study, the rates and kinetics of PSS hydrolysis will be investigated under continuously fed, completely mixed conditions, where steady state conditions can be verified, and system stability can be monitored. Also, methanogenic conditions will be verified, so that a direct comparison of the hydrolysis rates can be made between systems with and without sulfate reduction.

In summary from the review above, in biological sulfate reduction with PSS as substrate, the PSS requires hydrolysis to generate the substrates required for the sulfate reduction process, namely VFA and hydrogen. The same generic consortium of bacteria, the acidogens, with the same substrate, PSS, mediates this hydrolysis step as under methanogenic and acidogenic conditions. Very little quantitative information exists in the literature on the rate of hydrolysis under sulfate reducing conditions, and how this rate compares with that under methanogenic and acidogenic conditions. Kinetic studies would suggest that the PSS hydrolysis rate is increased under sulfate-reducing conditions. Studies on hydrolysis of lignocellulose materials would tend to support this. However, direct comparisons of rates under the different conditions are severely limited, and this requires more intense investigation (Chapter 7). Further, no quantitative models exist to describe the PSS hydrolysis under sulfate-reducing conditions. Both deficiencies are addressed directly in this research.

2.6 Closure

In this chapter, the relevant literature on PSS hydrolysis under methanogenic, acidogenic and sulfate-reducing conditions has been reviewed, to highlight deficiencies in existing knowledge, and hence to receive attention in this research. Under all three conditions, the PSS hydrolysis and subsequent acidogenesis processes are common and generate the

Chapter 2: Background

substrates required, namely VFA and possibly hydrogen, in the subsequent processes; for direct discharge to downstream BNR systems in acidogenesis, for methane production in methanogenesis and for sulfate reduction in biological sulfate reduction. The PSS hydrolysis is usually rate limiting and the hydrolysis largely determines the rate at and extent to which the subsequent processes occur. Therefore, a quantitative model describing this process under all three conditions would provide a beneficial tool for design, operation and control of these systems; development of such a model is one of the main aims in this research. Since the hydrolysis process is common to all three conditions, a single unified hydrolysis model would appear to be indicated. This also will facilitate comparison of the PSS hydrolysis under the three conditions, to identify and quantify possibly effects of the conditions on the hydrolysis rate.

In such a study, exact control and operation of any anaerobic digestion system is essential, so that the prevailing conditions are unequivocally defined. This requirement of attention to detail will be carefully adhered to in this study.

Chapter 3

Materials and Methods

3.1 Introduction

As described in Chapter 1, this investigation aims to quantify the rate of hydrolysis of primary sewage sludge (PSS) under anaerobic conditions, and to evaluate the effect of various operating conditions on this hydrolysis rate. Operating conditions to be examined include hydraulic retention time, feed COD concentration, pH, and methanogenic versus acidogenic versus sulfidogenic conditions. To collect the required experimental data, a variety of anaerobic digesters were operated at laboratory scale and their response monitored. The experimental programs for the methanogenic, acidogenic and sulfate-reducing systems are described in more detail in Chapters 4, 5 and 7 respectively. In this chapter, the experimental and analytical methods used to operate the systems and collect the experimental data are described.

3.2 Feed Sludge

3.2.1 Feed Collection and storage

The PSS was collected from the primary settling tanks at the Athlone Wastewater Treatment Works (City of Cape Town, South Africa). This works treats municipal wastewater principally of domestic origin, but with a significant mixed industrial component. At the works, the PSS is pumped from the bottom (underflow) of the primary settling tanks via a pump house to further treatment (anaerobic digesters). The PSS was collected at a sampling point in the pump house.

The PSS was collected in batches using a number of 25L plastic drums, which were transported, back to the laboratory at UCT. In the laboratory, these drums were emptied into a 400L stainless steel tank. The contents of the tank were mixed vigorously to ensure a homogenous sludge, which was decanted back into the 25L drums for storage. The sludge in the 25L drums was decanted further into 1.1L plastic bottles. While emptying the PSS from the 25L drums into the 1.1L bottles, the sludge was passed through a square aperture mesh (6.7 x 6.7mm) to remove large particles such as rags, cigarette butts, seeds and other debris, but without removing a significant fraction of the solids and thereby changing the nature of the sludge. The sludge in the 1.1L bottles was used to prepare the feed for the digesters.

The 25L drums and the 1.1L bottles were stored in a cold room at 4°C. The composition of the sludge changed during storage, with some solubilisation taking place. This was monitored regularly so that the feed characteristics on any given day could be determined. This is discussed in more detail in Appendix A.

3.2.2 Feed preparation

Feeds were prepared using the PSS stored in the 1.1L bottles. All feeds were prepared by weighing a mass of PSS and then adding water until a desired final mass of diluted sludge was obtained. The decision to use weighed masses instead of volumes was due to the difficulties involved in measuring an accurate volume of undiluted sludge: the bottle in which the sludge was being stored was shaken vigorously to re-homogenize the contents. This led to air entrapment, which was difficult to expel once the sludge had been poured into a volumetric flask, influencing the measured volume. When the volumetric flask was agitated to facilitate the expulsion of the trapped air bubbles, a foam layer formed on the surface of the sludge, making it difficult to measure the volume accurately. Also, standing to allow air expulsion caused settling of the solids, and before the correct representative volume of sludge could be removed, the contents needed to be shaken so that the concentration and nature of the feed sludge would not be changed by removing a non-representative volume, leading to re-entrainment of the air.

A hydrometer was used in an attempt to measure the relative sludge density, but the viscosity of the sludge was so high that the hydrometer stayed in its initial position and did not assume a depth relative to the density of the sludge. In a second attempt, the sludge was first diluted by varying amounts before the hydrometer was inserted; the relative densities of the variously diluted sludges differed by less than 2g/1000g. These differences between the density of the sludge and the water were therefore insignificant, so that the density of the feed sludge could be accepted to be equal to that of water (1000g/L).

The advantages of weighing the sludge for dilution were significant. Firstly, there was more flexibility in the final concentration of the diluted sludge, since any mass of sludge could be mixed with any mass of water, rather than being limited to the relative volumes of the volumetric flasks. Secondly, the temperature of the sludge was 4°C when removed from storage, and since the digesters were operated at 35°C, warm or hot water was used to dilute the feed to give a final temperature of around 35°C, in order to prevent temperature shocks to the system. These temperature differences would have induced errors if volumes instead of masses were being measured. Thirdly, the use of an electronic scale allowed for greater accuracy and consistency in the feed preparation. Feed dilutions for each steady state operation are given in Appendix B.

3.2.3 Feed characterization

The PSS was analyzed regularly for total and soluble COD, TKN and FSA (free and saline ammonia), total and soluble P, total VFA, H₂CO₃* alkalinity and pH. Additionally, for each feed batch, an elemental analysis was performed to determine the C_xH_yO_zN_a ratio of the sludge. These latter analyses formed part of a parallel research contract (K5/1338).

For PSS analysis, the sludge initially was diluted by adding an equal mass of water to the sludge, and then further using volumetric dilutions. Once the final dilution had been made, a 500mL sample was blended in an electric blender (Braun MX 2050) for ± 30 seconds. This solution was then analyzed for total COD, TKN and total P. The accepted dilution was based on the COD measurement, with a final concentration around 500mgCOD/L targeted (normally 100 times dilution). This dilution also was acceptable for the TKN and total P analyses.

The soluble COD, FSA, soluble P, VFA and H₂CO₃* alkalinity were measured on filtered PSS. A sample was prepared by adding a flocculent (polyelectrolyte) to a 50mL PSS sample,

and then shaking vigorously for a few seconds. The sample then was centrifuged for 20 minutes at 3500rpm. The 'clear' supernatant was filtered through a glass fibre filter paper (S&S GF/C) followed by a 0.45 μ m membrane filter (S&S ME 25/21), and the filtrate diluted as required for the relevant analyses. The results and trends from these analyses are shown in Appendix A.

3.3 Digester Design and Operation

3.3.1 Digester design

The digesters were constructed from Perspex cylinders (300mm diameter) fitted with Perspex base-plates and lids, so that the contents could be monitored. The digesters were completely sealed so that all gas produced could be collected. The digesters were completely mixed by a lid-mounted motor turning a shaft fitted with a six-bladed impeller. The motor (0.25kW) was fitted with a speed regulator, so that the agitation inside the digester could be increased or decreased where necessary. The impeller, mounted on the shaft, was suspended about 10mm from the bottom of the digester. The impeller shaft was mounted in a bearing housing through the lid of the digester. The housing contained two bearings to hold the shaft in place, and was filled with oil, with a lip-seal on each end to ensure that neither the oil nor the digester gas escaped. The motor was coupled to the shaft using a nylon and brass coupler, so that any misalignment between the motor and the two bearings could be tolerated. A bronze deflector plate was fitted to the shaft on the inside of the digester lid to prevent the sludge and any foam from reaching the oil seals.

Six digesters were used, two of which had a working volume of 16L, and the other four had a working volume of 20L. The headspace varied between the digesters, but was around 2L.

3.3.2 Digester control

The temperature of the digesters was controlled to 35°C using heating coils wrapped around the outside walls, and a thermocouple suspended through the lid into the sludge, connected to a temperature controller. The temperature controller switched the heating coils on and off with a sufficiently high frequency (every few seconds) that the temperature of the digester contents did not fluctuate significantly (< 0.1°C).

Four pH control systems were available, and split over four of the six digesters. The pH probe was suspended through the digester lid and immersed 2 - 3cm below the sludge surface. The pH controller could be selected to add either acid or base, and a 1M HCl or NaOH solution was dosed respectively. Due to the digester size, mixing regime and acid/base concentration, as well as fouling of the pH probe, there was a significant lag between the addition of either the acid or the base and the registered change in pH. This resulted in overdosing of the acid/base. To prevent significant overdosing, the dosing pump was connected to a timer that only allowed dosing for 10 seconds every minute. This allowed the pH controller sufficient time to register the previous addition and determine whether a further addition was necessary.

3.3.3 Feeding and sampling

As discussed above, the feed was prepared by weighing the required mass of PSS and adding the required mass of warm or hot water. The digesters were fed either once or twice daily, depending on the hydraulic retention time of the system (O'Rourke, 1968). For systems operating at a 10-day retention time or less, it was decided to feed twice a day to minimize shocks to the system. Continuous pumping of PSS on a laboratory scale is problematic since

the volumes pumped are small, resulting in low velocities in the feed tubes, and since the solids concentrations are often high, the result is settling of the solids in the tubes and eventually blocking of the flow.

For sulfate-reducing systems, a super-saturated stock solution of Na_2SO_4 at 295.73 g/L (10mL in 1L = 2g SO_4 /L) was prepared and continuously stirred to prevent recrystallization. The required volume of this solution was added directly into the digester when feeding.

Prior to feeding, the gas volumes (see below) were recorded and the gas collection bags (for gas composition analysis) were changed. The pH was measured *in situ* to minimize errors due to CO_2 and H_2S expulsion. A volume of the digester sludge, greater than the feed volume, was removed from the valve at the bottom of the digester. The mixing was stopped while the sludge was being removed to minimize the dissolution of O_2 into the digester sludge.

Samples for analyses on the solids fraction were taken immediately from this waste sludge before the solids could settle. The required prepared feed volume was then added to the digester through the feeding port in the digester lid. The waste sludge was then used to refill the digester to the correct operating volume. The headspace was then purged with nitrogen gas (99.999% N_2) to remove air (oxygen), and the digester resealed. The time that the digester remained unsealed was minimized to less than 30 seconds. Once resealed, mixing was resumed and the remaining samples were taken from the waste sludge.

3.4 Mass Balances

Information was collected from all systems so that mass balances could be performed on all of the major species: COD, C, N, P and S. As a rule, a recovery of between 95 and 105% for all components would be considered excellent for biological systems. Realistically, 90 to 110% recovery would be acceptable for systems where measurements are required in three phases (solid, liquid and gas). Obviously, since the different biological systems (methanogenic, acidogenic and sulfidogenic) generated different products, the required measurements for the mass balances for the three types of systems differed, and these are described below.

3.4.1 Methanogenic systems

Table 3.1 lists the measurements on the feed, effluent and gas required for the mass balance calculation for the methanogenic systems. Total and soluble COD were measured for the feed and effluent, and by difference the feed and effluent particulate COD concentrations could be calculated. The total gas production was measured for each feed cycle, and by measuring the CH_4/CO_2 ratio of the collected gas, the overall methane production was calculated. A COD mass balance was therefore calculated for each steady state.

However, when operating systems with a dilute feed ($\sim 2\text{gCOD/L}$), the volume of gas produced was too small for a sample to be collected for CH_4/CO_2 analysis for each feed cycle ($<500\text{mL}$ per cycle collected in 10L bags). Since the headspace was purged with nitrogen gas after feeding, when analysed, the gas consisted of (for example) 95% N_2 , 4.0% CH_4 and 0.9% CO_2 (vol). The gas chromatograph used to analyze the gas composition was calibrated using three different mixtures of N_2 : O_2 : CH_4 : CO_2 , but the minimum concentration for CH_4 was 3.0% (vol) and CO_2 was 3.4% (vol), see Table 3.4. Therefore, the CO_2 measurement of 0.9% may be inaccurate, since it lies outside the calibration range of the analytical equipment. More importantly, in order to calculate the methane production, the ratio between the CH_4 and CO_2 measurements is required, and since there is reduced confidence in the CO_2

measurement, there is correspondingly reduced confidence in the methane production calculation. This value is used directly in the calculation of the COD balance for methanogenic systems (see Chapter 4 and Appendix B).

The carbon balance was not required for this study, but data was collected for Sötemann (2005). However, the digesters were analysed for all compounds containing carbon in order to facilitate this calculation. Similarly, by measuring the feed and effluent TKN (N) and total P concentrations, a mass balance could be calculated for each of these species (Sötemann, 2005).

Table 3.1: List of analyses required for the methanogenic digester feed and effluent (liquid and gas) in order to perform species balances on the system

Compound analyses required		
	In	Out
COD balance	particulate COD, soluble COD	particulate COD, soluble COD, CH ₄
C balance	C component of sludge, VFA (as HAc), soluble COD (as glucose), H ₂ CO ₃ * alkalinity	C component of sludge, VFA (as HAc), soluble COD (as glucose), H ₂ CO ₃ * alkalinity, CO ₂ , CH ₄
N balance	TKN	TKN
P balance	total P	total P

3.4.2 Acidogenic systems

The acidogenic system mass balances were simpler to calculate since the influent COD, TKN and total P were conserved in the effluent, and the gas consisted of CO₂ only. VFA and alkalinity measurements could not be performed on these systems because the analytical method applied (see Section 3.5.5) requires that the VFA concentration is less than half the H₂CO₃* alkalinity concentration, and in these systems, this criterion was not met.

3.4.3 Sulfidogenic systems

It was not possible to perform a carbon balance on the sulfidogenic systems because the sulfur in the sample interfered with the analysis of the sludge C. Also, because of the low gas production, it was not possible to measure the CO₂ composition and therefore production. Similarly, the H₂S production could not be measured, and therefore a sulfur balance was not possible since the loss of COD in the form of H₂S(g) could not be quantified. This meant that a COD balance was also not possible. Therefore, only the TKN and total P balances were calculated for these systems.

Table 3.2: List of analyses required for the acidogenic digester feed and effluent (liquid and gas) in order to perform species balances on the system

Compound analyses required		
	In	Out
COD balance	particulate COD, soluble COD	particulate COD, soluble COD,
C balance	C component of sludge, VFA (as HAc), soluble COD (as glucose), H ₂ CO ₃ * alkalinity	C component of sludge, VFA (as HAc), soluble COD (as glucose), H ₂ CO ₃ * alkalinity, CO ₂
N balance	TKN	TKN
P balance	total P	total P

Table 3.3: List of analyses required for the sulfidogenic digester feed and effluent (liquid and gas) in order to perform species balances on the system

Compound analyses required		
	In	Out
COD balance	particulate COD, soluble COD	particulate COD, soluble COD, aqueous sulfide, H ₂ S
C balance	C component of sludge, VFA (as HAc), soluble COD (as glucose), H ₂ CO ₃ * alkalinity	C component of sludge, VFA (as HAc), soluble COD (as glucose), H ₂ CO ₃ * alkalinity, CO ₂
N balance	TKN	TKN
P balance	total P	total P
S balance	Na ₂ SO ₄ , SO ₄ ²⁻ in feed sludge	SO ₄ ²⁻ , S _T , H ₂ S

3.5 Analytical Methods

3.5.1 Particulate samples preparation

The particulate and soluble samples were collected immediately when waste sludge was removed from the digester so that the solids did not settle in the waste container. A sample (>100mL) was collected in a 100mL volumetric flask and allowed to cool to room temperature. Once cool, the solution was shaken vigorously to resuspend the solids, and the volume adjusted to 100mL by removing the excess solution. Depending on the necessary dilution, the sample was diluted using serial dilutions until a final 500mL diluted solution was obtained. This solution was blended in an electric food blender (Braun Model MX 2050) for 30 seconds to macerate any large particles. Samples were taken from this solution and analysed for COD, TKN and total P.

For sulfidogenic systems, 6 drops of 10M NaOH were added to the 100mL volumetric flask. This served to increase the pH of the solution sufficiently so that the H₂S(g) was no longer able to escape. The rest of the sample preparation was identical to the methanogenic and acidogenic systems.

3.5.2 Soluble sample preparation

Unless the sample was being collected for a specific measurement such as total aqueous sulfide (S_T) (see below), the soluble samples were collected in 50mL centrifuge tubes. Polyelectrolyte was added to the sample and the solution shaken vigorously for a few seconds. The solution cleared immediately, with the solids floating on the liquid surface. These samples were centrifuged for 20 minutes at 3500rpm. The clear supernatant was vacuum filtered through a layered glass fibre (S&S GF 52) and 0.45µm membrane (S&S ME 25/21 ST) filter (glass fibre filter paper on top of the membrane filter paper). The filtrate was then analysed for soluble organic COD, VFA and alkalinity, FSA and soluble P.

3.5.3 COD and aqueous sulfide

For acidogenic and methanogenic systems, the total and soluble organic COD was measured directly, and the particulate COD calculated by the difference between these measurements. However, for sulfidogenic systems, the measured soluble COD consisted of an organic

fraction and an aqueous total sulfide (S_T) fraction, and the concentrations of the two fractions needed to be independently determined: 3 drops of 10M NaOH were added to the 50mL sample to increase the pH of the solution and prevent the loss of $H_2S(g)$. The soluble COD measured on this sample is the sum of the soluble organic COD and the total sulfide. In a second sample, excess $ZnSO_4$ was added to precipitate the aqueous sulfide as ZnS . Three drops of 10M NaOH were then added to increase the pH so that the residual Zn^{2+} would precipitate as $Zn(OH)_2$. The solution was filtered through a $0.45\mu m$ membrane filter under vacuum, and the COD of the resultant filtrate measured. This gave the soluble organic COD. The difference between this measurement (soluble organic COD) and the total soluble COD measurement above was due to the aqueous sulfide, and this concentration was calculated by difference.

The COD was measured according to Standard Methods (1985) (open reflux method, 508A).

3.5.4 Gas volumes and composition

A novel water displacement gas flow meter was developed in association with E.W. Randall, Department of Chemical Engineering, UCT. The flow meter gives a consistent and accurate measurement of the volume of gas produced. The consistency can be seen by the number of gas units produced per day over a steady state period (see Appendix B for details), while the accuracy is verified by the mass balance calculations in Chapter 4.

Each meter was calibrated by the addition of water from a burette (Metrohm L485) and over ten measurements, the standard deviation was around 1% of the mean volume per unit ($47.3 \pm 0.4\text{mL/unit}$).

Once the gas had passed through the gas meter, it was collected in 10L impermeable Tedlar gasbags. These were sent to an external laboratory (Scientific Services, Cape Metropolitan Council) where they were analysed for N_2 , O_2 , CO_2 and CH_4 (as % vol.) using a gas chromatograph: Varian 3300 with a stainless steel column, $500 \times 2.2\text{mm}$, $\frac{1}{8}$ ", and a 60180 mesh molecular sieve 13X. The carrier gas was helium, the thermal conductivity detector at 120°C , and the oven temperature at 40°C ramped to 170°C at 40°C/min , and held at 170°C for 3min. The gas chromatograph was calibrated with three gas mixtures (Table 3.4).

Table 3.4: Standard gas compositions (% vol) used to calibrate the gas chromatograph

Gas	Standard 1	Standard 2	Standard 3
CO_2	35.9	30.4	3.4
O_2	1.3	10.2	20.3
N_2	2.2	19.7	73.3
CH_4	60.6	39.7	3.0

3.5.5 VFA and Alkalinity

The total volatile fatty acid (VFA) concentration (acetic, propionic, butyric and other acids with a pK_a around 4.7) and carbonate ($H_2CO_3^*$) alkalinity were measured using the 5-point titration method of Moosbrugger *et al.* (1992). The method compensates for the presence of FSA, PO_4 and sulfide weak acid/bases, provided the total species concentrations of these weak acid/bases are known. However, the values reported in Appendix B were calculated with the FSA, PO_4 and total sulfide species concentrations as zero. Stored samples were analysed for these total species concentrations in batches only at the end of a steady state

period. The VFA and alkalinity titrations were performed daily, or more regularly than other measurements on the system, and were used as an indicator of digester stability. Therefore, at the time the total species concentrations of the other weak acid/bases were not available and were assumed equal to zero in the calculations. However, once the total species concentrations of the other species were available from measurement, the VFA and alkalinity concentrations would need to be recalculated. This calculation showed that the carbonate alkalinity dominates the titration compared with the other combined species concentrations, and the inclusion of the latter concentrations in the calculation procedure did not change the values of the carbonate alkalinity and VFA significantly. It was therefore decided to ignore these species in the calculation procedure.

As a rule, a VFA concentration of < 50mg/L as HAc was considered to be sufficiently low for the digester to be considered stable.

3.5.6 Sulfate

The sulfate was measured using the turbidimetric method described in Standard Methods (1985, Method 426C). However, due to the presence of significant organics in the samples that interfere with the test method, a novel sample pre-treatment procedure had to be developed. The sample was pretreated by adding excess zinc acetate to remove the sulfide as ZnS. Any sulfide in the sample would be oxidized to sulfate during the pretreatment, and sulfide removal was thus necessary. Three drops of 10M NaOH were added to increase the pH and thereby precipitate any excess Zn^{2+} as $Zn(OH)_2$. The slurry was filtered through a 0.45 μ m membrane filter under vacuum, and a 5, 10 or 20mL volume (depending on the sample concentration) of the filtrate dried in a platinum crucible at 105°C. Once dry, a half-teaspoon of Na_2CO_3 powder was added, and the crucible heated over a Bunsen burner until the Na_2CO_3 melted and the soluble organics were completely oxidized to CO_2 . The crucible was allowed to cool before the residual salt was dissolved in a 50% HCl solution. This solution was poured into a volumetric flask, a drop of phenolphthalein indicator was added, and the solution neutralized to the pink end point with 10M NaOH. This solution was diluted further as the sample for the turbidimetric method (final concentration between 10 and 40mgSO₄/L).

The development of the carbonate fusion pretreatment of the sulfate samples was essential due to the interference of the soluble organic matter in the sample. The method development is described in more detail elsewhere (see Appendix D).

3.5.7 Suspended solids

Suspended solids concentrations were measured by allowing the waste sludge from the digester to stand for 30 minutes in a 500mL-measuring cylinder. After 30 minutes, a 5 or 10mL sample (depending on the solids concentration) was removed from approximately 8cm below the liquid surface. This was well above the height of the solids bed in the cylinder. The sample was diluted to within the COD measurement range (~ 500mgCOD/L), and the COD measured. From separate measurements of the soluble COD, the suspended solids COD concentration could be calculated. For sulfidogenic systems, 10M NaOH was added to the sample immediately after sampling from the measuring cylinder to retain the sulfides in the system. The soluble COD (sulfides included) was measured from this system as well, since some sulfides would have left the system during the 30 minutes settling time. The difference between the total (+ sulfides) and soluble (+ sulfides) COD was equal to the suspended solids COD concentration.

3.5.8 TKN and FSA

The TKN and FSA concentrations were measured using the micro-distillation method (Standard Methods, 1985, Semi-micro Kjeldahl method, 420B).

3.5.9 Total and soluble P

The total and soluble P were measured using the persulfate digestion method (Standard Methods, 1985, Method 424C III) and the molybdate-vanadate colorimetric method (Standard Methods, 1985, Vanadomolybdophosphoric acid colorimetric method). The persulfate digestion of the total P samples required modification of the digestion acid mixture (De Haas, 1998), due to the high organic concentrations.

3.6 Closure

This chapter describes the experimental and analytical methods applied to gather data at laboratory scale on anaerobic digestion of PSS under methanogenic, acidogenic and sulfate-reducing conditions. The experimental data generated and its analysis are described in detail in the chapters that follow; Chapter 4 describes methanogenic systems, Chapter 5 describes acidogenic systems, Chapter 6 describes the effects of operating pH on methanogenic and acidogenic systems, and Chapter 7 describes sulfate-reducing conditions.

Chapter 3: Materials and Methods

Chapter 4

Methanogenic Systems

4.1 Introduction

The main aim of this part of the investigation was to develop a mathematical model framework in terms of which the rate of hydrolysis of PSS under steady state methanogenic conditions could be determined. This then would allow the effect of various conditions on the hydrolysis rate to be quantified. To achieve this aim, experimental data was collected from anaerobic digesters operating under methanogenic conditions at varying feed COD concentrations and hydraulic retention times. A mathematical model was developed to determine the rate of hydrolysis for each steady state operating condition. Then, the various hydrolysis formulations described in Chapter 2 were tested against the experimental data to determine which formulation would be most appropriate to model the rate of hydrolysis under methanogenic operating conditions. With this calibrated model, the rate of hydrolysis observed under different operating conditions (acidogenic or sulfate-reducing) could be compared to the expected rate under methanogenic conditions (predicted from the model), and any differences in these rates could be quantified.

In this study, methanogenic systems refer to anaerobic digesters fed PSS only and operated with a steady state VFA concentration that is negligible (as a rule $< 50\text{mg/L}$ as HAc). In these systems, there is no accumulation of soluble products from hydrolysis since the methanogenic biomass is in sufficient numbers to utilize all the biodegradable soluble intermediates produced. There was no pH control on the systems, and the systems were allowed to reach a stable operating pH at each steady state.

4.2 Experimental Program

Steady state methanogenic digesters were operated under a range of feed COD concentrations that would be expected during 'normal' operation of methanogenic anaerobic digesters ($40\text{gCOD/L} - 2\text{gCOD/L}$) (see Table 4.1). At each feed COD concentration, the hydraulic retention time was decreased until the methanogenic condition became unstable, that is the methanogens 'washed out' of the system or the system 'failed', leading to an increase in the VFA and soluble COD concentrations, and a decrease in the pH and gas production.

Table 4.1 lists the hydraulic retention times for which stable methanogenic operation was obtained and a steady state of operation analysed for each feed COD concentration. The numbers in Table 4.1 refer to the steady state numbers in Appendix B. In this appendix, each steady state is described in more detail, and the mean and standard deviations are reported for each measured steady state parameter. Also, daily measurements of VFA, alkalinity, pH and

gas production are plotted for the entire period of each experiment. For each steady state period, the measured values for all of the daily analyses are tabulated, for example Table B.6.

Table 4.1: Steady states measured for varying hydraulic retention times and feed COD concentrations

Feed COD Concentration (gCOD/L)	Hydraulic Retention Time (d)							
	60	20	15	10	8	6.67	5.71	5
40			10; 11	12	21	23	28	
25		3	4	1	2	7	8	9
13			5	13	14	24	31	
9	17							
2				25	26			

The systems were seeded with methanogenic sludge initially from the anaerobic digesters at the Athlone Wastewater Treatment Works (City of Cape Town, South Africa) and subsequently from the waste sludge collected from the stable laboratory systems. This seed sludge was kept at room temperature until required, and generally responded immediately to a 20-day retention time at 35°C. The feed volumes were increased incrementally from one steady state operation to the next to minimize shock loads on the system. Generally, the VFA concentration did not increase during the transient phase, and the gas production stabilized during the first retention time of the new steady state of operation.

For systems that were freshly reseeded, the system was operated for 3 retention times before the steady state operation was analysed in more detail. The pH and volumetric gas production were measured either once or twice daily depending on the number of times per day that the digester was fed, while the VFA and alkalinity were measured daily or every second day. For systems following a previous steady state operation, on changing the system operation, the changes in the measured parameters were generally small, except for the gas production, and these systems were operated for between 1.5 and 2 retention times before the steady state was analysed in more detail.

4.3 Mathematical Model

In order to interpret the results obtained for each of the steady states listed in Table 4.1, a ‘simple’ mathematical model was developed. The model includes only biological processes, consisting of two biomass groups, the acidogens and acetoclastic methanogens, and three biological reactions: hydrolysis, acidogenesis and acetoclastic methanogenesis. At this stage, the chemical precipitation, weak acid/base and vapour/liquid equilibria are ignored so as not to overcomplicate the calculations. These equilibria will be included in the future in a more extensive modelling exercise, but do not form part of the objectives of this study.

4.3.1 Model structure

Hydrolysis is mediated by the acidogen organism group and is defined here as the extra cellular enzymatic breakdown of polymers (particulate) into monomers and dimers (soluble), which enter the subsequent acidogenesis reactions. For this model, recognizing that carbohydrates, protein and lipid measurements are unlikely to be routinely available (and were not available in this investigation) and indeed are difficult to do, the hydrolysis of each the three major organic components of PSS (carbohydrates, lipids and proteins) are grouped into a single reaction, acting on a generic organic material representing sewage sludge. The

products of hydrolysis (simple sugars, amino acids and long-chain fatty acids) are represented by a single compound (the idealized intermediate glucose), which is converted to acetic acid via acidogenesis, mediated by the acidogens. The acidogenic processes acting on 'glucose' to convert it to VFA's are not rate limiting under stable digester operating conditions. Accordingly, in the model application here, accumulation of 'glucose' will not occur. This implies that the 'glucose' merely acts as an intermediate, which is acidified to VFA as soon as it is produced. Under stable digester operation, the net result of this simplified scheme is the same as that for the complex schemes with hydrolysis of each component taking place. Acetoclastic methanogenic bacteria then use the acetic acid to form methane. This is illustrated in Figure 4.1.

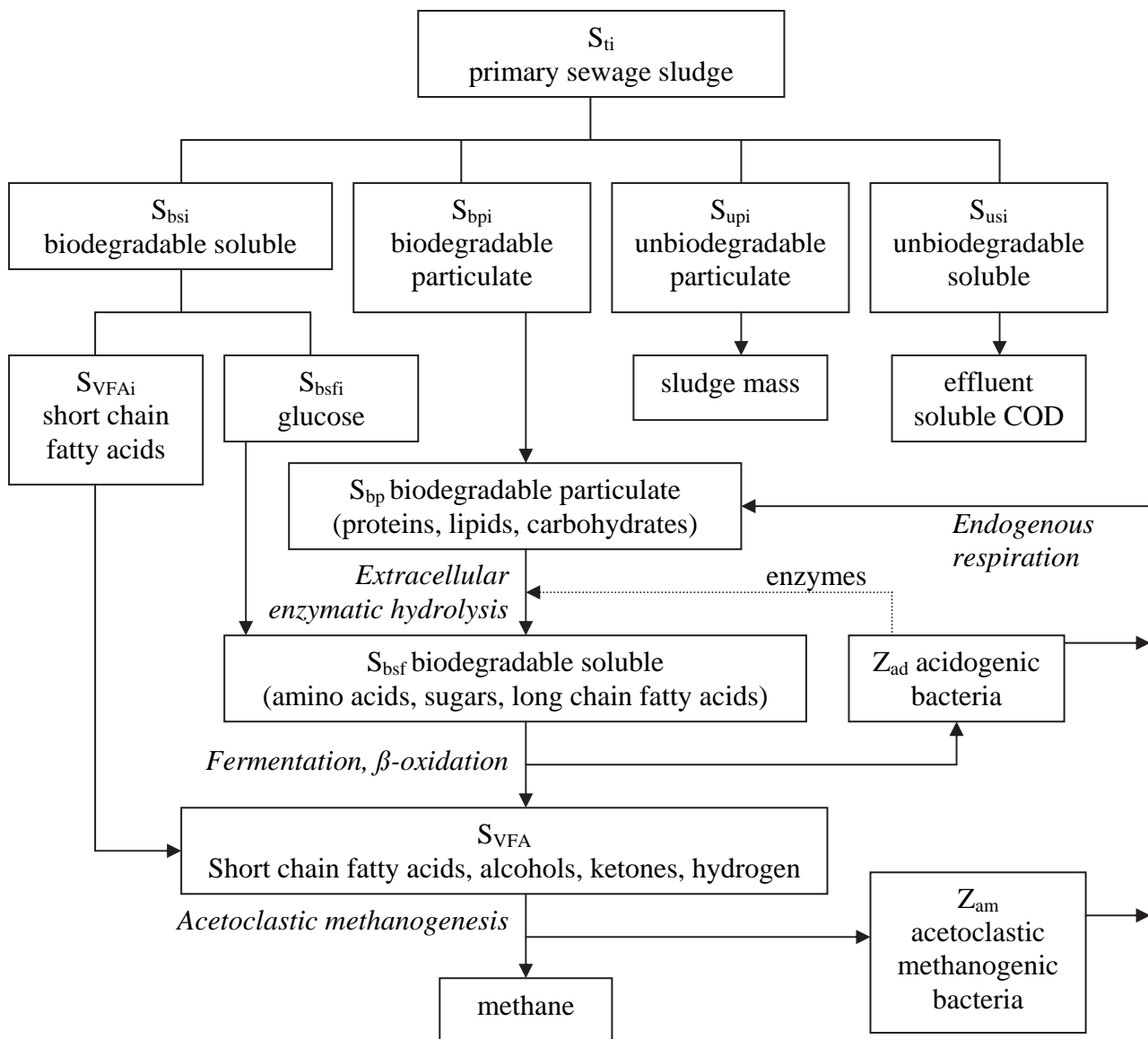


Figure 4.1: Schematic diagram (in units of COD) of the bulk processes involved in the anaerobic digestion of primary sewage sludge as used in the model

4.3.2 Model assumptions

The model is based on the following assumptions:

- The PSS total COD (S_{ti}) consists of an unbiodegradable particulate fraction (S_{upi}), biodegradable particulate fraction (S_{bpi}), unbiodegradable soluble fraction (S_{usi}), biodegradable soluble non-VFA (fermentable) fraction (S_{bsfi}) and volatile fatty acids (S_{VFai})

$$S_{ti} = S_{upi} + S_{bpi} + S_{usi} + S_{bsfi} + S_{VFai} \quad (4.1)$$

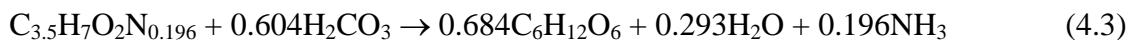
- Under stable operating conditions, three organism groups act on the biodegradable COD, namely acidogens (Z_{ad}), acetoclastic methanogens (Z_{am}) and hydrogenotrophic methanogens (Z_{hm})
- Hydrogenotrophic methanogenic biomass (Z_{hm}) is considered negligible compared with the other active organism biomasses
- The effluent total COD (S_t) for methanogenic systems consists of the unbiodegradable particulate fraction (S_{up}), biodegradable particulate fraction (S_{bp}), unbiodegradable soluble fraction (S_{us}) and the acidogenic and acetoclastic methanogenic biomasses (Z_{ad} and Z_{am})

$$S_t = S_{up} + S_{bp} + S_{us} + Z_{ad} + Z_{am} \quad (4.2)$$

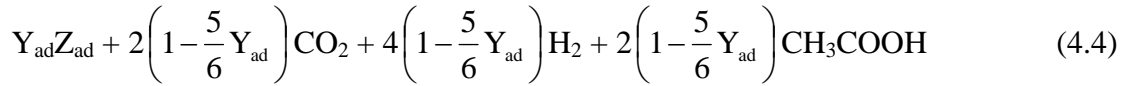
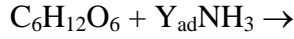
- Active acidogenic and methanogenic biomass concentrations in the influent are negligible ($Z_{adi} = Z_{ami} = 0$)
- Acidogenic biomass grows according to Monod kinetics, using hydrolysis products as organic substrate
- Acetoclastic methanogenic biomass grows according to Monod kinetics, using acidogenesis products (acetate) as organic substrate
- Endogenous respiration of acidogenic and methanogenic biomass forms biodegradable particulate COD; endogenous residue formation is considered negligible
- Effluent soluble biodegradable COD and VFA concentrations are negligible under stable methanogenic conditions ($S_{bsf} = S_{VFA} = 0$)
- PSS hydrolysis is the rate limiting process under stable methanogenic digester operation

4.3.3 Reaction stoichiometry

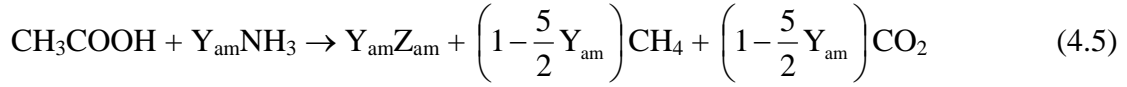
For the purpose of mass balances, as noted above, the soluble fermentable biodegradable COD (S_{bsf}) was given the molecular formula of the idealised organic ‘glucose’, while the short chain fatty acids (S_{VFA}) were assumed to be acetic acid only, which is the dominant VFA intermediate under stable digester operation. The molecular formulae for the PSS generic particulate organics and the biomass were taken from Sötemann *et al.* (2004) as $C_{3.5}H_7O_2N_{0.196}$ and $C_5H_7O_2N$ respectively. Therefore, for hydrolysis:



For acidogenesis, recognising the yield for acidogens as Y_{ad} , then:



For acetoclastic methanogenesis, with biomass yield Y_{am} :



4.3.4 Mass balances

In order to determine the rates of hydrolysis, acidogenesis and methanogenesis, mass balances were developed for the major groups of substrates and products (Q = volumetric flow rate, L/day; V = reactor volume, L; b = relevant organism specific endogenous respiration rate constant, d^{-1}).

4.3.4.1 Biodegradable particulate COD (S_{bp}) mass balance:

$$dS_{bp} \cdot V = Q \cdot S_{bpi} \cdot dt - Q \cdot S_{bp} \cdot dt - V \cdot \text{rate}_{\text{hydrolysis}} \cdot dt + V \cdot b_{ad} \cdot Z_{ad} \cdot dt + V \cdot b_{am} \cdot Z_{am} \cdot dt \quad (4.6)$$

$$\text{Rearranging: } \frac{dS_{bp}}{dt} = \frac{Q}{V} (S_{bpi} - S_{bp}) - \text{rate}_{\text{hydrolysis}} + b_{ad} \cdot Z_{ad} + b_{am} \cdot Z_{am} \quad (4.7)$$

$$\text{At steady state: } \text{rate}_{\text{hydrolysis}} = \frac{Q}{V} (S_{bpi} - S_{bp}) + b_{ad} \cdot Z_{ad} + b_{am} \cdot Z_{am} \quad (4.8)$$

4.3.4.2 Biodegradable fermentable soluble COD (S_{bsf}) mass balance:

$$dS_{bsf} \cdot V = Q \cdot S_{bsfi} \cdot dt - Q \cdot S_{bsf} \cdot dt + V \cdot \text{rate}_{\text{hydrolysis}} \cdot dt - V \cdot \text{rate}_{\text{acidogenesis}} \cdot dt \quad (4.9)$$

$$\text{Rearranging: } \frac{dS_{bsf}}{dt} = \frac{Q}{V} (S_{bsfi} - S_{bsf}) + \text{rate}_{\text{hydrolysis}} - \text{rate}_{\text{acidogenesis}} \quad (4.10)$$

$$\text{At steady state: } \text{rate}_{\text{acidogenesis}} = \text{rate}_{\text{hydrolysis}} + \frac{Q}{V} (S_{bsfi}) \quad (4.11)$$

4.3.4.3 Volatile fatty acid COD (S_{VFA}) mass balance:

$$dS_{VFA} \cdot V = Q \cdot S_{VFai} \cdot dt - Q \cdot S_{VFA} \cdot dt + 2\left(1 - \frac{5}{6}Y_{ad}\right) \cdot V \cdot \text{rate}_{\text{acidogenesis}} \cdot dt - V \cdot \text{rate}_{\text{methanogenesis}} \cdot dt \quad (4.12)$$

Rearranging:

$$\frac{dS_{VFA}}{dt} = \frac{Q}{V} (S_{VFai} - S_{VFA}) + 2\left(1 - \frac{5}{6}Y_{ad}\right) \cdot \text{rate}_{\text{acidogenesis}} - \text{rate}_{\text{methanogenesis}} \quad (4.13)$$

At steady state:

$$\text{rate}_{\text{methanogenesis}} = \frac{Q}{V}(S_{\text{VFAl}}) + 2\left(1 - \frac{5}{6}Y_{\text{ad}}\right)\left(\frac{Q}{V}(\text{rate}_{\text{acidogenesis}})\right) \quad (4.14)$$

4.3.4.4 Acidogenic biomass COD (Z_{ad}) mass balance:

$$dZ_{\text{ad}} \cdot V = Q \cdot Z_{\text{adi}} \cdot dt - Q \cdot Z_{\text{ad}} \cdot dt + Y_{\text{ad}} \cdot \text{rate}_{\text{acidogenesis}} \cdot V \cdot dt - b_{\text{ad}} \cdot Z_{\text{ad}} \cdot V \cdot dt \quad (4.15)$$

$$\text{Rearranging: } \frac{dZ_{\text{ad}}}{dt} = \frac{Q}{V}(Z_{\text{adi}} - Z_{\text{ad}}) + Y_{\text{ad}} \cdot \text{rate}_{\text{acidogenesis}} - b_{\text{ad}} \cdot Z_{\text{ad}} \quad (4.16)$$

$$\text{At steady state: } Z_{\text{ad}} = \frac{Y_{\text{ad}} \cdot \text{rate}_{\text{acidogenesis}} \cdot R_{\text{h}}}{(1 + b_{\text{ad}} \cdot R_{\text{h}})} \quad (4.17)$$

4.3.4.5 Methanogenic biomass COD (Z_{am}) mass balance:

$$dZ_{\text{am}} \cdot V = Q \cdot Z_{\text{ami}} \cdot dt - Q \cdot Z_{\text{am}} \cdot dt + Y_{\text{am}} \cdot \text{rate}_{\text{methanogenesis}} \cdot V \cdot dt - b_{\text{am}} \cdot Z_{\text{am}} \cdot V \cdot dt \quad (4.18)$$

$$\text{Rearranging: } \frac{dZ_{\text{am}}}{dt} = \frac{Q}{V}(Z_{\text{ami}} - Z_{\text{am}}) + Y_{\text{am}} \cdot \text{rate}_{\text{methanogenesis}} - b_{\text{am}} \cdot Z_{\text{am}} \quad (4.19)$$

$$\text{At steady state: } Z_{\text{am}} = \frac{Y_{\text{am}} \cdot \text{rate}_{\text{methanogenesis}} \cdot R_{\text{h}}}{(1 + b_{\text{am}} \cdot R_{\text{h}})} \quad (4.20)$$

Therefore, if equations 4.8, 4.11, 4.14, 4.17 and 4.20 can be solved simultaneously for each methanogenic steady state, the rate of hydrolysis can be calculated for each steady state, and the effects of the feed COD concentration and hydraulic retention time on the rate can be determined. However, these calculations require that the concentrations of each organic fraction in Eqs 4.1 and 4.2 be quantified. Section 4.5 describes these calculations, based on the results of the steady state analyses described in Section 4.4 below.

4.4 Experimental Results

Table 4.1 above lists the steady state numbers for each of the methanogenic steady states analysed at varying hydraulic retention times and feed COD concentrations. In this section, the results from these steady states are discussed in more detail. These results include COD mass balances, methane production rates, pH, VFA, alkalinity concentrations and gas composition. Chapter 3 describes the methods used to calculate mass balances for total N and total P, and Appendix B describes a sample calculation for the N and P mass balances. However, these results are not discussed further in this study, but form part on a parallel study by Sötemann (2004), and will be discussed in more detail in this parallel study. This information, however, is available in the steady state analyses in Appendix B.

4.4.1 COD mass balance

For each steady state of operation, a COD balance was calculated based on the feed COD concentration and the effluent COD concentration and methane production (see Appendix B for sample calculation). These values are shown in Table 4.2. With the exception of one steady state (10d retention time at 2gCOD/L feed), all the values are within the acceptable range (90 – 110% recovery) for particulate fed systems, and only 3 systems have a COD recovery outside the generally acceptable range of 95 – 105% recovery for biological

systems. These good COD recoveries strongly suggest that the methods used to analyse the various parameters are accurate and consistent, and allows for further analysis of the measured parameters with confidence.

From Table 4.2, the COD recoveries for the systems fed at 2gCOD/L were considerably lower (88 and 92%) than for the other systems (96 – 110%), with the 10-day retention time marginally outside the acceptable range (as defined above).

Table 4.2: Steady states measured for varying hydraulic retention times and feed COD concentrations (numbers are calculated COD mass balances)

Feed COD Concentration (gCOD/L)	Hydraulic Retention Time (d)							
	60	20	15	10	8	6.67	5.71	5
40			103.4	103.4	102.7	100.9	103.3	
25		96.0	98.6	110.3	99.6	102.6	101.4	96.0
13			100.1	97.2	98.8	100.9	104.5	
9	100.0							
2				88.4	91.9			

The explanation for this is that for these systems, due to the low influent feed concentration, the volume of gas produced per feed cycle was relatively small compared to the headspace of the digester. In order to drive the volumetric gas measurement equipment, the pressure in the digester headspace is required to increase by approximately 20mm H₂O. To achieve this increase, the amount of gas in the headspace needs to increase. (For an ideal gas, P.V. = n.R.T, and for a constant volume, V, R (Gas constant) and temperature, T, the number of moles, n, must increase to increase the total pressure, P). For operation at higher feed concentrations, this volume is small compared to the total volume of gas produced per feed cycle. However, for the systems fed 2gCOD/L, this volume becomes significant, and the volume of gas produced per feed cycle is under-estimated.

A second source of error, as discussed in Chapter 3, is due to the gasbags used to capture the gas for composition analysis that were 10L in volume, and therefore only one sample was taken for each steady state in order to have sufficient gas for analysis. The results of the analysis showed that the methane and carbon dioxide partial pressures were in the low region of the GC calibration range, and hence the errors in the calculated gas composition due to the analytical errors were possibly also significant.

4.4.2 Minimum retention times

Table 4.1 shows that systems fed with 40 and 13gCOD/L were operated stably down to retention times of 5.71 days, and the system fed with 26gCOD/L was operated down to a 5-day retention time, well below the 7.5d minimum from O'Rourke (1968) and 7d from Izzett *et al.* (1992) (see Chapter 2). The system fed with 2gCOD/L failed below an 8-day retention time. When the retention times in these systems were reduced below the lowest values reported in Table 4.2, the systems immediately showed signs of becoming unstable; decrease in gas production, increased VFA concentration and decrease in the measured reactor pH. Clearly, the methanogenic biomass cannot sustain a stable population at retention times shorter than 5 days, but the systems fed with 2gCOD/L were unable to operate stably at a retention time shorter than 8 days. One of the possible explanations for this is the steady state pH of the system, and this is discussed further in Section 4.4.4 below.

4.4.3 Methane production

Methane production is a good indication of the stability of the system, since methane is the end product of the anaerobic digestion process. Any inconsistencies in the COD mass balances reported in Table 4.2 could be related to inconsistencies either in the COD measurements or the methane gas measurements or both. If these inconsistencies are related to the methane gas measurements, while the effluent OCD measurements remain consistent, further analyses based on the COD measurements can be performed with greater confidence. Table 4.3 lists the mass of methane produced per day for each of the steady states. The mass of methane produced per day increases with reduced retention times, and increases with increasing feed COD concentrations at each retention time, i.e. a correlation between the mass of methane produced per day and the organic loading rate.

Table 4.3: Mass of methane produced (gCH₄ as COD/d) for each methanogenic steady state system

Feed COD Concentration (gCOD/L)	Hydraulic Retention Time (d)							
	60	20	15	10	8	6.67	5.71	5
40			32.3; 30.6	46.1	51.6	60.4	80.7	
25		14.4	20.5	28.4	29.1	31.0	35.2	36.1
13			10.5	13.3	17.0	23.3	24.6	
9	2.1							
2				1.6	2.2			

To evaluate this correlation further, the mass of methane produced per day was compared to the total mass of feed COD added per day. Table 4.4 lists the mass of methane produced per day per mass of feed COD added per day. There is no general trend in the data, although the 60-day retention time system produced more methane per mass of feed COD than the other steady state systems, which is expected since this system exhausts the methane production potential of the feed COD (only unbiodegradable COD remains) (see Section 4.5). For the data set, the mean mass CH₄ as COD/mass COD in the feed is 0.56 ± 0.063 , and displays a normal distribution, excluding one point (10-day retention time, 2gCOD/L feed concentration, 0.41 gCH₄ as COD/gCOD in feed) as a statistical outlier (ratio = $0.41 < \text{mean} - 1.96 \times \text{S.D.}$ i.e. an outlier at the 95% confidence interval). For this steady state system, the COD mass balance was 88.4%, considerably lower than the other steady state systems, indicating that the error in the mass balance calculation lies in the measurement of the methane production.

Table 4.4: Methane mass production per mass of total feed to the system (gCH₄ as COD/gCODin) for each methanogenic steady state

Feed COD Concentration (gCOD/L)	Hydraulic Retention Time (d)							
	60	20	15	10	8	6.67	5.71	5
40			0.61; 0.58	0.58	0.59	0.58	0.56	
25		0.55	0.59	0.68	0.56	0.52	0.50	0.45
13			0.58	0.50	0.51	0.57	0.53	
9	0.64							
2				0.41	0.45			

To evaluate this further, the mass of methane produced per mass of COD reduced in the systems is listed in Table 4.5. In order to show consistency in the analytical procedures for a stable system, the mass of methane produced per mass of COD consumed should be equal. Table 4.5 lists this ratio, and shows that for the majority of the systems, the mass of methane produced was equal to the mass of total COD reduced (1.02 ± 0.058 gCOD/gCOD). This data shows a normal distribution, with two data points lying outside the 95% confidence interval (10-day retention time, 2gCOD/L feed concentration, 0.77gCH₄ as COD produced/g total COD reduced; 8-day retention time, 2gCOD/L feed concentration, 0.83gCH₄ as COD produced/g total COD reduced). For each of these systems, the total methane production was clearly not being analysed correctly, and this verifies the concerns discussed in Chapter 3, Section 3.4.1, where the total volume of gas produced per day was too small compared to the digester headspace and the volume of the gas bags used to collect the sample.

For one other steady state system (10-day retention time, 25gCOD/L feed concentration, 1.18gCH₄ as COD produced/g total COD reduced), the gCH₄ as COD produced/g total COD reduced is larger than the other systems. The gas composition for this steady state was not measured in this system because the analytical procedures were not available at the time of the steady state of operation, and the gas composition was assumed to be equal to the analysed composition of a digester operating in a similar mode (8-day retention time, 25gCOD/L feed concentration). Clearly, this assumption is not valid, since for this system, Table 4.2 shows a COD mass balance of 110.3%, which is significantly higher than the recoveries of any of the other steady state systems. For this system, and the two systems fed 2gCOD/L, the gas measurements show inconsistencies and inaccuracies, but it is assumed that the feed and effluent COD measurements are correct. These will be included in the data set for further analysis below.

Table 4.5: Mass methane produced per mass influent reduced (gCH₄ as COD/gCOD reduced) for each steady state system

Feed COD Concentration (gCOD/L)	Hydraulic Retention Time (d)							
	60	20	15	10	8	6.67	5.71	5
40			1.05; 1.01	1.06	1.05	1.02	1.06	
25		0.93	0.98	1.18	0.99	1.05	1.03	0.92
13			1.00	0.95	0.98	1.02	1.09	
9	1.01							
2				0.77	0.83			

The results listed in Tables 4.2 to 4.5 indicate that the procedures and analytical methods used to operate and analyse the steady state methanogenic systems were consistent and accurate, especially the COD measurements, and from Table 4.5, the methane produced for the majority of the steady state systems can be used to check the validity of a modelling exercise based on the feed and effluent total and soluble COD measurements.

4.4.4 pH

Table 4.6 lists the measured steady state operating pH values for each methanogenic system. The steady state operating pH ranged from 6.38 to 7.12, and showed no trends with changing retention time, except between the shorter retention times, where the pH decreased sharply with a decrease in the retention time. As mentioned above, a further decrease in retention time from this point resulted in digester instability, and the decrease in the pH between the

two shortest retention times for each feed COD concentration is possibly indicative of the impending failure. However, the systems fed 2gCOD/L were unable to operate stably at retention times shorter than 8 days, while for all the other feed COD concentrations, stable operation at shorter retention times (down to 5d) was possible. For the shortest stable retention time for the system fed 2gCOD/L, the operating pH was 6.38, and it is possible that pH inhibition of the methanogenic population is occurring. Chapter 6 discusses this further.

Table 4.6: Steady state operating pH for methanogenic systems

Feed COD Concentration (gCOD/L)	Hydraulic Retention Time (d)							
	60	20	15	10	8	6.67	5.71	5
40			6.98; 7.12	6.92	6.90	6.83	6.75	
25		6.89	6.85	7.00	6.80	6.86	6.93	6.78
13			6.80	6.69	6.78	6.57	6.45	
9	6.74							
2				6.59	6.38			

4.4.5 VFA and Alkalinity

Tables 4.7 and 4.8 list the VFA and alkalinity concentrations measured for each of the steady state systems. The requirement for a stable methanogenic system as stated in the introduction to this chapter is a VFA concentration of 50mgHAc/L or less. Table 4.7 lists the effluent VFA concentration for each steady state, and shows that this requirement was met for all but one of the steady state systems (5-day retention time, feed concentration of 25gCOD/L); the exceptional steady state was included in the data set for methanogenic systems since the changes in the measured values for the rest of the analyses for this steady state was insignificant compared to when digester failure was observed (acidogenic systems).

Table 4.7: Effluent VFA concentrations (mgHAc/L)

Feed COD Concentration (gCOD/L)	Hydraulic Retention Time (d)							
	60	20	15	10	8	6.67	5.71	5
40			28;35	27	22	12	26	
25		11	17	24	21	19	32	87
13			6	8	7	5	19	
9	5							
2				0	10			

The effluent alkalinity concentration decreased with a decrease in the retention time for each feed COD concentration (Table 4.8). This observation will be analysed further when developing and calibrating the more extensive mathematical model that includes acid/base and vapour/liquid equilibria. The carbonate alkalinity concentration, digester pH and carbon dioxide partial pressure in the digester headspace are interdependent, and by measuring these three parameters independently, their interdependency can be calibrated. Gas composition measurements are discussed below.

Table 4.8: Effluent alkalinity concentrations (mgCaCO₃/L)

Feed COD Concentration (gCOD/L)	Hydraulic Retention Time (d)							
	60	20	15	10	8	6.67	5.71	5
40			2446; 2491	2362	1868	1821	1612	
25		1577	1539	2424	1394	1504	1463	1359
13			845	854	863	789	564	
9	775							
2				170	144			

4.4.6 Gas composition

Table 4.7 lists the methane composition (%vol) of the total gas produced by the methanogenic digesters for each steady state of operation. The gas produced consists of methane and carbon dioxide only, and therefore by difference, the carbon dioxide composition (%vol) can be calculated.

Table 4.9: Methane composition (%vol)

Feed COD Concentration (gCOD/L)	Hydraulic Retention Time (d)							
	60	20	15	10	8	6.67	5.71	5
40			61.40;61.17	62.73	58.85	59.23	63.76	
25		63.11	63.08		63.24	60.98	61.67	61.23
13			63.26	60.98	63.06	60.95	65.70	
9	66.51							
2				53.2	59.3			

The methane composition (%vol) of the total gas produced in the steady state systems ranged from 53.2% to 66.5%, but showed no correlation with changing retention time and feed COD concentration. As discussed above, these compositions are dependent on the carbonate alkalinity concentration and digester operating pH, but this will be evaluated further in a parallel study where a mathematical model will be developed including physical processes such as weak acid/base and vapour/liquid equilibria.

The experimental results obtained from the operation of the anaerobic digesters under methanogenic conditions listed in Tables 4.2 to 4.9 show consistency in the experimental data, and allow further analysis of this data with confidence. Further, the results show that the systems were operating under stable and consistent conditions, allowing for comparisons to be made between the steady state systems. However, due to the complex nature of the degradation processes, it is not possible to calculate the rate of hydrolysis for each steady state system from the experimental results, and therefore a mathematical model framework is required to isolate the concentrations of the critical parameters taking part in the hydrolysis process, such as the biodegradable particulate COD concentration of the feed (S_{bpi}) and the effluent (S_{bp}) and the acidogenic biomass concentration (Z_{ad}). The following section describes the algorithms used to calculate the concentrations of these parameters based on the measurements made for each steady state system described above.

4.5 Rate of Hydrolysis Calculation

From Eq 4.1, the feed total COD consists of five components:

$$S_{ti} = S_{upi} + S_{bpi} + S_{usi} + S_{bsfi} + S_{VFai} \quad (4.21)$$

From Eq 4.2, the effluent total COD also consists of five components:

$$S_t = S_{upi} + S_{bp} + S_{us} + Z_{ad} + Z_{am} \quad (4.22)$$

For the feed and effluent, the total COD and soluble COD concentrations were measured. The individual species concentrations were determined as follows, based largely on the assumptions listed in Section 4.3.2.

The effluent soluble COD concentration was measured for each steady state of operation. However, it could be reasonably assumed that the fermentable soluble COD (S_{bsf}) and VFA (S_{VFA}) concentrations in the effluent were negligible, an assumption substantiated by experimental measurement of VFA concentrations (Table 4.7) and the definition of stable methanogenic operation ($< 50\text{mgHAc/L}$). Therefore, the measured effluent soluble COD was essentially unbiodegradable (S_{us}). By definition and accepting negligible generation of unbiodegradable soluble COD in the reactor, the effluent unbiodegradable soluble COD (S_{us}) was equal to the feed unbiodegradable soluble COD concentration (S_{usi}) (see Table 4.10).

Lilley *et al.* (1992) studied the acid fermentation of PSS (to generate substrates favourable for downstream biological nutrient removal), and found that a non-VFA soluble COD concentration was generated in equal concentration to the VFA (as COD) concentration, i.e. the two concentrations were equal ($S_{bsf} = S_{VFA}$) (see Table 4.10). This was verified in this study in which the VFA and soluble COD ($< 0.45\mu\text{m}$) concentrations in ‘fresh’ PSS were measured, as well as the changes in concentrations with time under storage at 4°C . In both cases, the soluble COD concentrations were approximately twice the VFA COD concentrations (i.e. $S_{bsfi} = S_{VFai}$), in agreement with the observations of Lilley *et al.* (1992) (Appendix A). However, it should be noted that Lilley *et al.* (1992) measured the VFA species (acetate, propionate, butyrate) individually with a GC, while in this study the total VFA concentration was determined by the 5-point titration method, which is less accurate when the VFA concentration (mg/L as HAc) is more than half the carbonate alkalinity (mg/L as CaCO_3), which for the feed was always the case (see Chapter 3).

Thus, in the influent it can be reasonably accepted that $S_{bsfi} = S_{VFai}$. In terms of the influent characterisation, the influent soluble COD (S_{si}) is made up of three fractions, S_{usi} , S_{bsfi} and S_{VFai} . With S_{usi} known from effluent soluble COD measurement (see above) and accepting $S_{bsfi} = S_{VFai}$, all the influent soluble COD fractions can be quantified.

For the feed total COD measurement, with the soluble fractions determined, only the particulate COD fractions, biodegradable (S_{bpi}) and unbiodegradable (S_{upi}), remain. Similarly for the effluent, the effluent soluble COD ($= S_{usi}$) has been determined, and thus from the effluent total COD measurement, only the four particulate fractions need to be determined, S_{bp} and S_{up} and the biomass concentrations (Z_{ad} and Z_{am}). Since the unbiodegradable particulate COD concentration of the feed and effluent are equal ($S_{upi} = S_{up}$), there are five unknowns (S_{bpi} , S_{bp} , S_{upi} , Z_{am} and Z_{ad}) and only two measurements.

In order to calculate the rate of hydrolysis for each steady state, the feed and effluent biodegradable particulate COD concentrations (S_{bpi} and S_{bp} respectively) are required. With the rate of hydrolysis (rate_{hydrolysis}, Eq 4.8) calculated, the rates of acidogenesis (rate_{acidogenesis},

Eq 4.11) and methanogenesis ($\text{rate}_{\text{methanogenesis}}$, Eq 4.14) can be calculated, and hence the concentrations of the acidogenic (Z_{ad} , Eq 4.17) and methanogenic (Z_{am} , Eq 4.20) biomass concentrations can be calculated.

These calculations require that the influent and effluent unbiodegradable and biodegradable particulate COD fractions (S_{upi} and S_{bpi} , and S_{up} and S_{bp}) are known. Remembering that $S_{\text{upi}} = S_{\text{up}}$, and that $S_{\text{bpi}} = S_{\text{ti}} - S_{\text{upi}} - S_{\text{si}}$ and $S_{\text{bp}} = S_{\text{t}} - S_{\text{upi}} - S_{\text{usi}} - Z_{\text{ad}} - Z_{\text{am}}$, where S_{ti} , S_{si} and S_{t} are available from measurement, and S_{usi} is known from above and Z_{ad} and Z_{am} can be calculated, essentially one unknown remains, $S_{\text{upi}} = S_{\text{up}}$. If a value for this parameter is known, then through iterative procedures all other parameters can be calculated. The following algorithm was used to determine these concentrations for all of the steady state operating conditions, and the final values are shown in Table 4.10.

As a start, the unbiodegradable particulate fraction of the feed was set at 30% of the total feed concentration. From this value, and the measured influent total (S_{ti}) and soluble (S_{si}) COD concentrations, the feed biodegradable COD concentration (S_{bpi}) was calculated ($S_{\text{bpi}} = S_{\text{ti}} - S_{\text{upi}} - S_{\text{si}}$). By initially assuming that the biomass concentrations were negligible (as a starting point in the calculation), the effluent biodegradable COD concentration could be calculated from the measured effluent total (S_{t}) and soluble (S_{s}) COD concentrations ($S_{\text{bp}} = S_{\text{t}} - S_{\text{upi}} - S_{\text{s}}$). Further, Eq 4.8 could be simplified as follows:

$$\text{rate}_{\text{hydrolysis}} = \frac{Q}{V} (S_{\text{bpi}} - S_{\text{bp}}) + b_{\text{ad}} \cdot Z_{\text{ad}} + b_{\text{am}} \cdot Z_{\text{am}} \sim \frac{Q}{V} (S_{\text{bpi}} - S_{\text{bp}}) \quad (4.23)$$

Thus, from the initial values of the influent and effluent biodegradable particulate COD concentrations, an initial rate of hydrolysis was calculated. From this initial rate, the rates of acidogenesis and methanogenesis were calculated from Eqs 4.11 and 4.14. From these initial rates, the acidogenic and methanogenic biomass concentrations were calculated from Eqs 4.17 and 4.20 respectively, enabling an improved estimate for S_{bp} ($= S_{\text{t}} - S_{\text{upi}} - S_{\text{s}} - Z_{\text{ad}} - Z_{\text{am}}$) to be calculated. This improved S_{bp} and the biomass concentrations were substituted into Eq 4.8, and a modified rate of hydrolysis was calculated. This calculation was iterated until the calculated values converged.

However, the calculation was based on an estimated 30% feed unbiodegradable particulate COD fraction. Clearly, the magnitude of this fraction has a significant influence on the calculation and needs to be experimentally determined. To determine this fraction, a 60-day retention time methanogenic anaerobic digester was operated until steady state (180 days, Steady state No 17, Appendix B). O'Rourke (1968) similarly operated a digester at a 60-day retention time, and argued that any particulate COD that was not digested in 60 days could be considered unbiodegradable. Therefore, for this steady state, the unbiodegradable particulate fraction of the feed was varied in the calculation above until the calculated effluent biodegradable particulate COD concentration for the 60-day retention time system was very small (0.0000780 mgCOD/L). The resultant unbiodegradable particulate fraction of the feed was 33.45% of the total influent COD. This value is slightly lower than the value (36%) determined by O'Rourke (1968). However, when determining the unbiodegradable fraction of the total influent COD, O'Rourke (1968) did not account for the acidogenic and methanogenic biomass concentrations, and therefore a higher value for the unbiodegradable fraction is likely.

Chapter 4: Methanogenic Systems

The results of the iterative calculation are listed in Table 4.10, while the calculated rates of hydrolysis for each feed COD concentration and hydraulic retention time are shown in Figure 4.2.

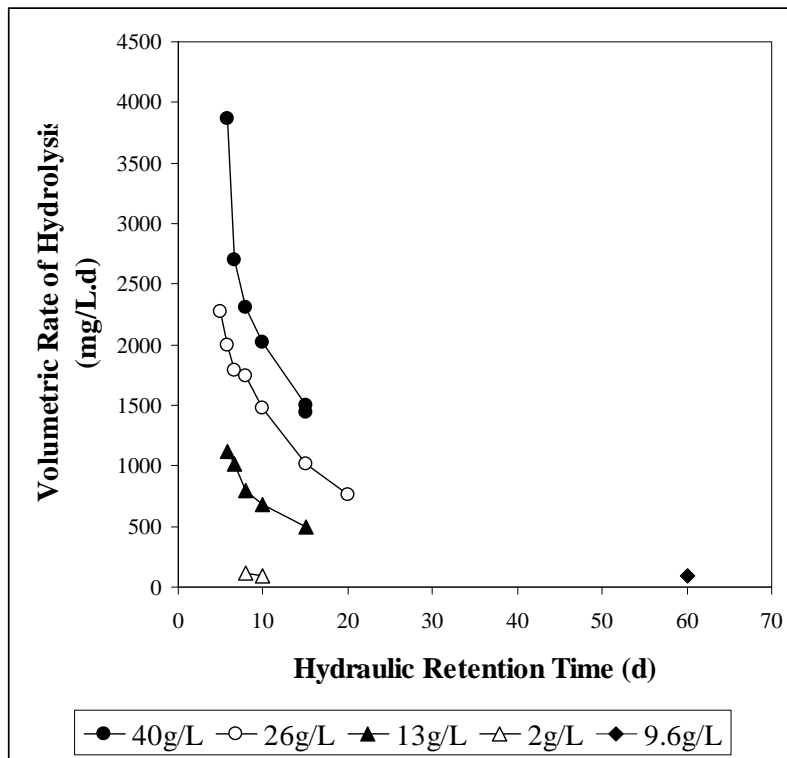


Figure 4.2: Calculated volumetric rate of hydrolysis ($\text{rate}_{\text{hydrolysis}}$) for each feed COD concentration at each hydraulic retention time

Table 4.10: Measured and calculated values of the various components of the feed and effluent COD measurements, and the calculated rates of hydrolysis for each steady state (Concentrations in mgCOD/L.; rates in mgCOD/L.d)

Steady state no.	Retention Time (d)	Measured (mgCOD/L)				Influent				Effluent				Hydrolysis Rate (mgCOD/L.d)	
		Total Feed (S _{fi})	Soluble Feed (S _{si})	Total Effluent (S _t)	Soluble Effluent (S _s)	S _{upi}	S _{bpi}	S _{usi}	S _{bsfi}	S _{VFAi}	S _{up}	S _{bp}	S _{us}		Z _{ad}
28	5.71	41441	2582	19737	295	24998	295	1144	1144	13861	3394	295	1690	498	3868
23	6.67	34818	4398	14984	207	18775	207	2096	2096	11645	1262	207	1416	453	2702
21	8	34818	3828	15094	205	19345	205	1812	1812	11645	1442	205	1371	431	2310
12	10	39810	4436	18085	256	22059	256	2090	2090	13315	2649	256	1415	450	2016
10	15	39790	3521	16792	250	22961	250	1635	1635	13308	1476	250	1343	414	1503
11	15	39790	3990	17167	299	22491	299	1846	1846	13308	1843	299	1307	410	1446
9	5	24881	2694	12610	301	13865	301	1196	1196	8322	2759	301	934	294	2270
8	5.71	24960	2503	12729	205	14109	205	1149	1149	8348	2977	205	912	286	1996
7	6.67	24881	2027	12595	200	14532	200	914	914	8322	2890	200	907	277	1794
2	8	25953	2675	11299	168	14598	168	1253	1253	8680	1107	168	1025	319	1740
1	10	25953	2331	10849	178	14942	178	1076	1076	8680	672	178	1010	309	1480
4	15	25953	2647	10212	157	14625	157	1245	1245	8680	178	157	912	285	1012
3	20	25953	2326	10525	179	14947	179	1073	1073	8680	617	179	801	248	758
31	5.71	13186	956	6757	120	7819	120	418	418	4410	1584	120	494	148	1117
24	6.67	13579	1845	5944	96	7192	96	875	875	4542	591	96	540	175	1019
14	8	13270	1525	6299	104	7307	104	710	710	4438	1124	104	479	153	798
13	10	13270	1174	6249	108	7657	108	533	533	4438	1092	108	467	144	681
5	15	13618	1432	5751	97	7631	97	668	668	4555	504	97	453	143	499
17	60	9810	1204	3590	88	5325	88	558	558	3281	0.0000780	88	166	55	98
26	8	1950	284	892	51	1014	51	116	116	652	93	51	72	23	119
25	10	1950	254	905	32	1043	32	111	111	652	132	32	67	22	95

$$S_{upi} = 0.3345 \times S_{fi}$$

4.6 Hydrolysis Rate Formulations

Chapter 2 discusses the various rate formulations that have been used in the literature to model and predict the rate of anaerobic hydrolysis. The following sections seek to select the rate equation that most accurately predicts the rate of hydrolysis for all of the operating conditions for which steady state methanogenic operating data was obtained. The rate equations that will be evaluated are the first order, first order specific, Monod and surface reaction kinetics.

4.6.1 First order kinetics

The mostly commonly used hydrolysis rate equation and the first to be evaluated is the first order rate equation with respect to the biodegradable particulate COD concentration (S_{bp}):

$$\text{rate}_{\text{hydrolysis}} = k_h \cdot S_{bp} \quad (4.24)$$

Since both the rate of hydrolysis ($\text{rate}_{\text{hydrolysis}}$) and the biodegradable particulate COD concentration are known for each steady state operating condition (Table 4.10), the value for the first order rate constant (k_h) can be calculated by dividing the rate of hydrolysis ($\text{rate}_{\text{hydrolysis}}$) by the biodegradable particulate COD concentration (S_{bp}) (Table 4.11). These values range from 0.62 to 5.67 (Figure 4.3).

The calculated values for the first order rate constant (k_h) were plotted on a transformed rank probit plot, Fig 4.4 (see Muller *et al.*, 2003 for details on the construction and interpretation of these plots).

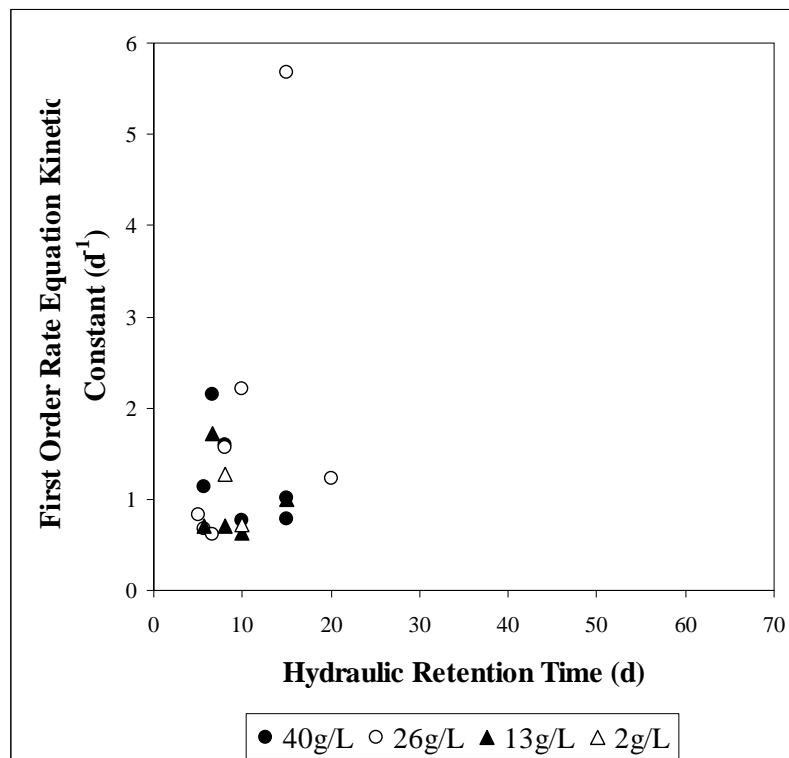


Figure 4.3: Calculated value for the first order rate constant (k_h) for each feed COD concentration at each hydraulic retention time

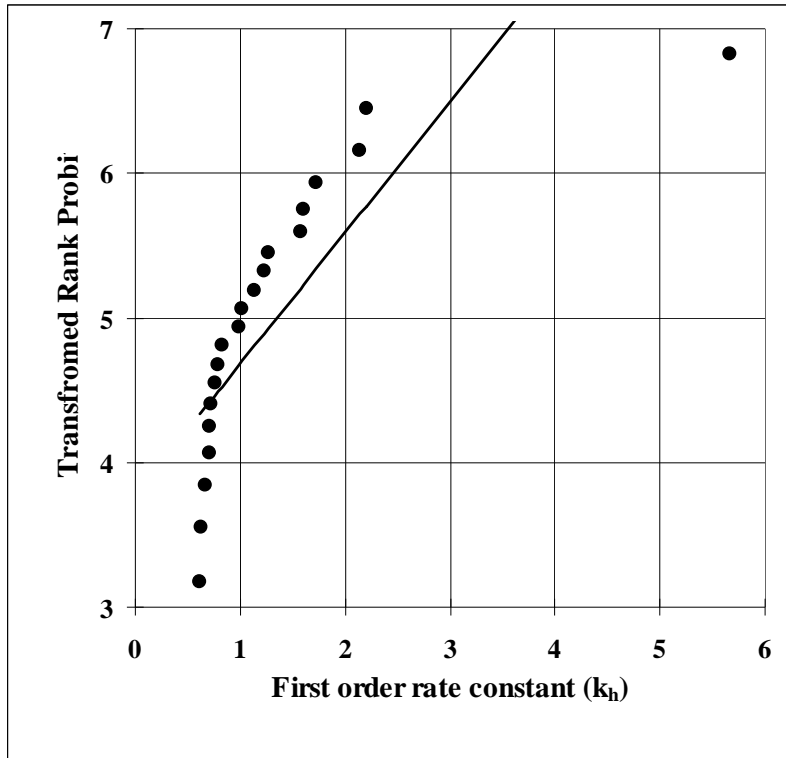


Figure 4.4: Transformed rank probit plot of the first order rate constant including all data points ($k_h = 1.005 \pm 1.102d^{-1}$)

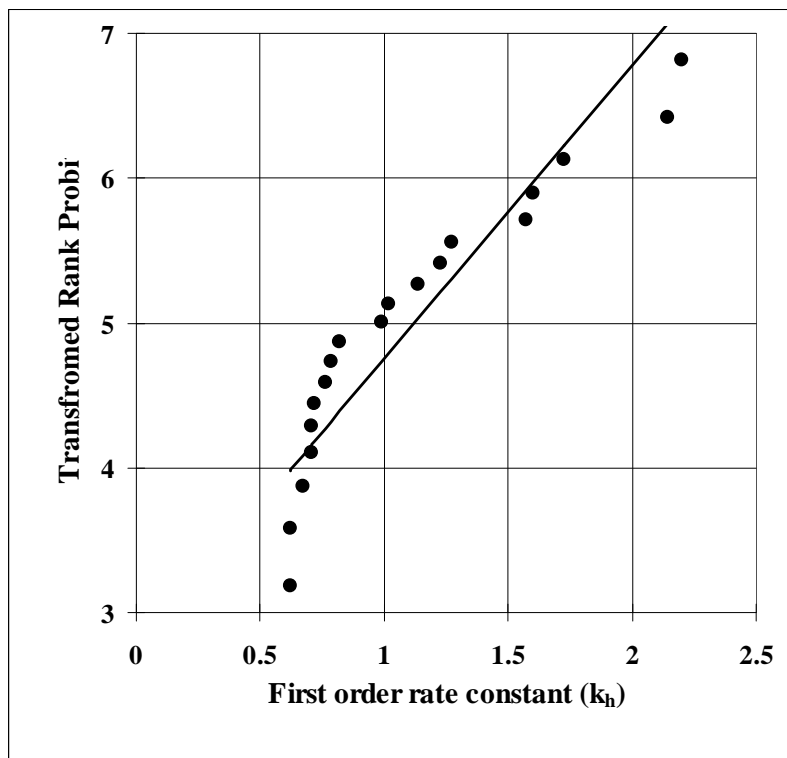


Figure 4.5: Transformed rank probit plot of the first order rate constant ignoring outliers ($k_h = 0.992 \pm 0.492d^{-1}$)

From Figure 4.4, the calculated value of $k_h = 5.67d^{-1}$ is a statistical outlier ($k_h = 5.67 > \text{mean} + 1.96 \times \text{SD}$, i.e. an outlier at the 95% confidence interval), and has been excluded from the data set in Figure 4.5. For the revised data set, the mean and standard deviation are calculated to be $0.992 \pm 0.492d^{-1}$. The standard deviation is large relative to the mean (coefficient of variation = 0.496), suggesting considerable scatter in the data. This would suggest that it would seem unlikely that the first order rate equation would predict the rate of hydrolysis for each of the steady state operating points in Figure 4.2 with sufficient accuracy. To evaluate this, the mean value of $k_h = 0.992d^{-1}$ was used in the first order rate equation to predict the effluent COD concentration for all methanogenic systems operated, which then could be compared with the measured value. To do this, the mass balance equation, Eq 4.6, was rewritten with a first order rate formulation defining the rate of hydrolysis:

$$dS_{bp} \cdot V = Q \cdot S_{bpi} \cdot dt - Q \cdot S_{bp} \cdot dt - V \cdot k_h \cdot S_{bp} \cdot dt + V \cdot b_{ad} \cdot Z_{ad} \cdot dt + V \cdot b_{am} \cdot Z_{am} \cdot dt \quad (4.25)$$

Rearranging:
$$\frac{dS_{bp}}{dt} = \frac{S_{bpi} - S_{bp}}{R_h} - k_h \cdot S_{bp} + b_{ad} Z_{ad} + b_{am} Z_{am} \quad (4.26)$$

At steady state:
$$S_{bp} = \frac{S_{bpi} + b_{ad} Z_{ad} R_h + b_{am} Z_{am} R_h}{1 + k_h R_h} \quad (4.27)$$

Initially, the biomass concentrations (Z_{ad} and Z_{am}) were neglected, and an initial biodegradable particulate COD concentration (S_{bp}) was calculated for each steady state:

$$S_{bp} = \frac{S_{bpi}}{1 + k_h R_h} \quad (4.28)$$

From this S_{bp} value and the mean $k_h = 0.992d^{-1}$, the rate of hydrolysis was calculated via Eq 4.24. From this rate, the rates of acidogenesis and methanogenesis were calculated from Eqs 4.11 and 4.14 respectively, and then the respective biomass concentrations from Eqs 4.17 and 4.20. These biomass concentrations were substituted into Eq 4.27, and a revised biodegradable particulate COD concentration calculated. This algorithm was iterated until the values converged. These values are listed in Table 4.11 for each steady state.

Figure 4.6 shows the predicted (from the first order rate equation) rate of hydrolysis compared with the calculated (from the operating data) rate of hydrolysis for each feed COD concentration and hydraulic retention time. Figure 4.6 shows that the first order rate equation is able to predict the “observed” rate of hydrolysis for each of the steady state operating points remarkably accurately. In fact, when the predicted rate of hydrolysis is plotted against the calculated rate of hydrolysis (Figure 4.7), the good predictions of the first order rate equation are reaffirmed.

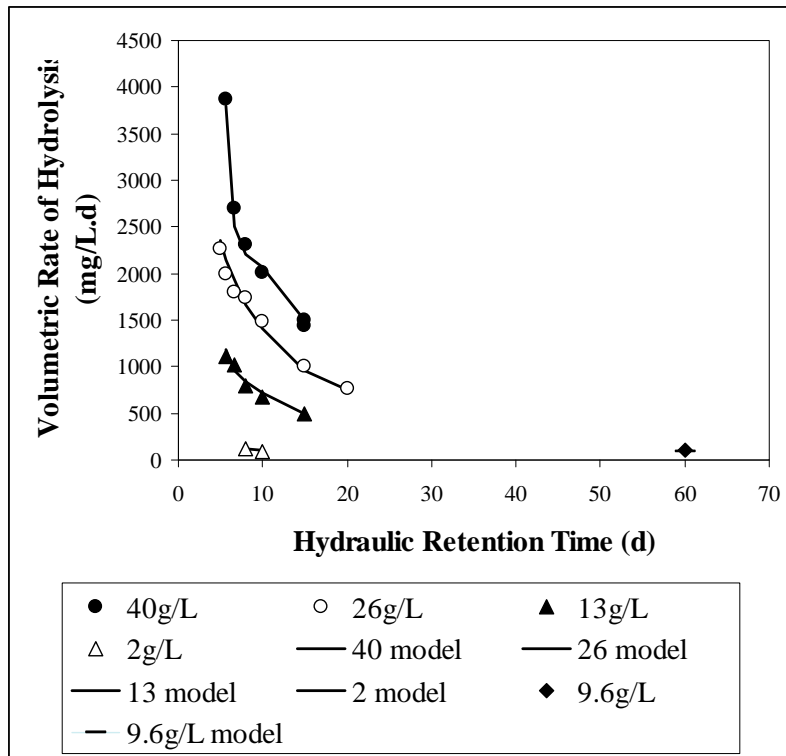


Figure 4.6: Calculated and predicted rate of hydrolysis for each feed COD concentration at each hydraulic retention time

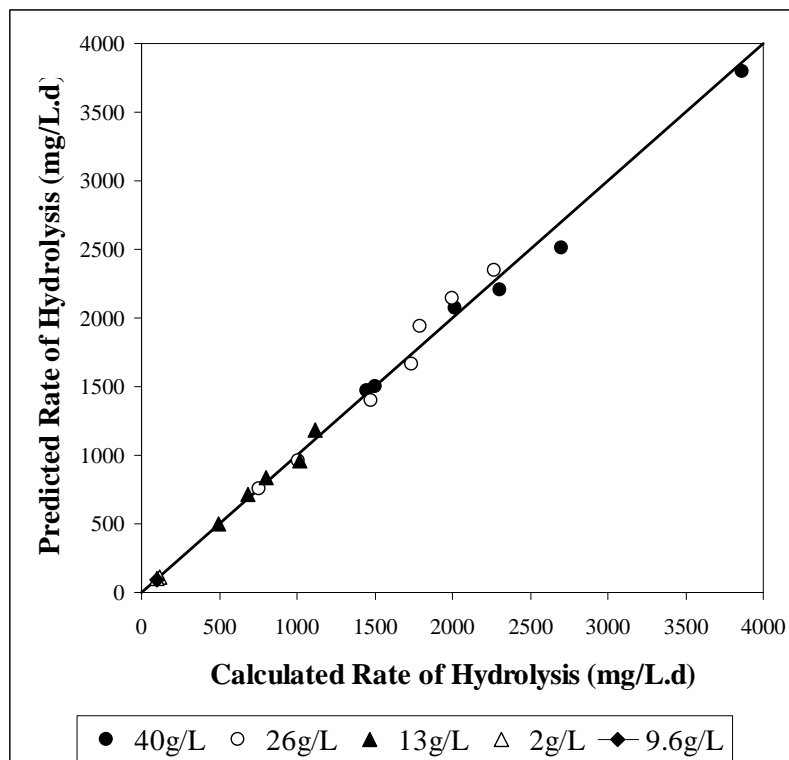


Figure 4.7: Predicted rate of hydrolysis versus the calculated rate of hydrolysis for each feed COD concentration and hydraulic retention time

The first order rate equation also was used to predict the effluent total COD concentration for each steady state operating point, and the predicted values were compared with the measured values, see Figure 4.8; close correlation was obtained. Thus, it can be concluded that the model, based on a first order rate equation to predict the rate of PSS hydrolysis, is able to accurately predict the effluent COD concentration from laboratory scale anaerobic digesters fed PSS, based only on the operating parameters and the feed characteristics.

This is a significant result, because it implies that the experimental data is consistent, and allows for the other hydrolysis rate formulations to be evaluated against the relatively simple first order rate equation.

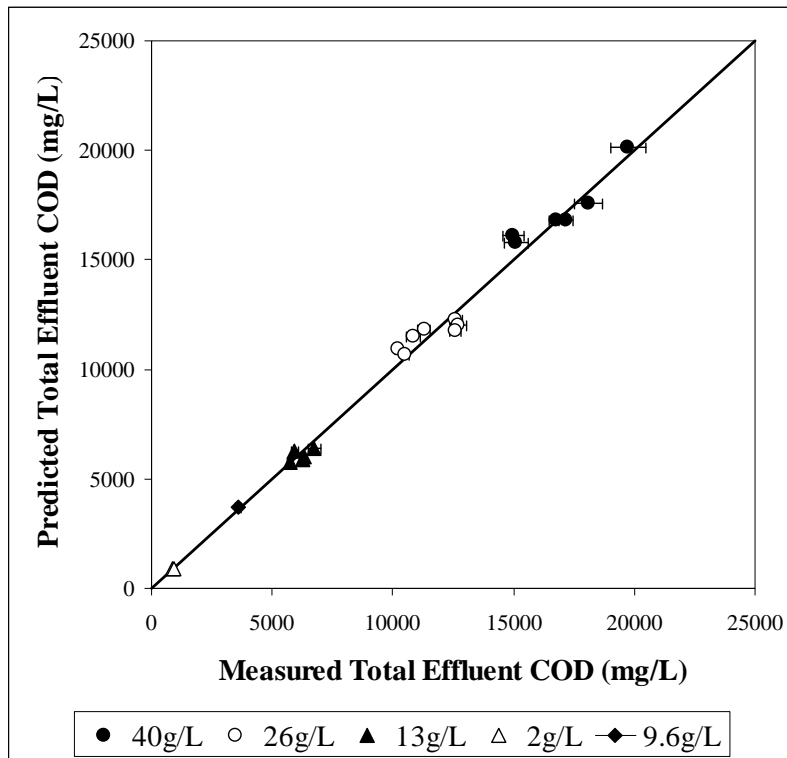


Figure 4.8: Predicted total effluent COD concentration versus measured total effluent COD concentration for each feed COD concentration and hydraulic retention time

Table 4.11: Measured and calculated values of the various components of the feed and effluent COD measurements, and the comparative calculated values predicted by a first order rate equation for PSS hydrolysis (Concentrations in mgCOD/L; rates in mgCOD/L.d)

Steady state no.	Retention Time (d)	Measurements (mgCOD/L)				Calculated from experimental data				First order kinetics			
		Total Feed	Soluble Feed	Total Effluent	Soluble Effluent	S _{bp} i	S _{bp}	Z _{ad}	Rate of hydrolysis	k _h	S _{bp}	Rate of hydrolysis	Total Effluent
		28	41441	2582	19737	295	24998	3394	1690	3868	1.140	3824	3792
23	34818	4398	14984	207	18775	1262	1416	2702	2.141	2528	2507	16134	
21	34818	3828	15094	205	19345	1442	1371	2310	1.602	2228	2209	15810	
12	39810	4436	18085	256	22059	2649	1415	2016	0.761	2091	2073	17574	
10	39790	3521	16792	250	22961	1476	1343	1503	1.018	1514	1501	16827	
11	39790	3990	17167	299	22491	1843	1307	1446	0.785	1483	1471	16834	
9	24881	2694	12610	301	13865	2759	934	2270	0.823	2370	2350	12258	
8	24960	2503	12729	205	14109	2977	912	1996	0.670	2160	2142	11989	
7	24881	2027	12595	200	14532	2890	907	1794	0.621	1954	1938	11745	
2	25953	2675	11299	168	14598	1107	1025	1740	1.572	1681	1666	11822	
1	25953	2331	10849	178	14942	672	1010	1480	2.202	1415	1403	11530	
4	25953	2647	10212	157	14625	178	912	1012	5.671	965	957	10940	
3	25953	2326	10525	179	14947	617	801	758	1.229	757	751	10656	
31	13186	956	6757	120	7819	1584	494	1117	0.705	1196	1186	6406	
24	13579	1845	5944	96	7192	591	540	1019	1.724	969	961	6287	
14	13270	1525	6299	104	7307	1124	479	798	0.710	842	834	6041	
13	13270	1174	6249	108	7657	1092	467	681	0.624	725	719	5913	
5	13618	1432	5751	97	7631	504	453	499	0.992	504	499	5751	
17	9810	1204	3590	88	5325	0.0000780	166	98	n.a.*	97	96	3683	
26	1950	284	892	51	1014	93	72	119	1.272	117	116	913	
25	1950	254	905	32	1043	132	67	95	0.719	99	98	875	

*the calculated value for k_h for the 60-day retention time system is not considered since the value is much larger than the other calculated values since the value for the biodegradable COD concentration is made small

4.6.2 First order specific kinetics

The first order specific rate equation models the rate of hydrolysis as being proportional to the product of the biodegradable particulate COD concentration (S_{bp}) and the acidogenic biomass (Z_{ad}) concentration:

$$\text{rate}_{\text{hydrolysis}} = k'_h \cdot S_{bp} \cdot Z_{ad} \quad (4.29)$$

Conceptually, this form of rate equation is superior to the first order rate equation since the rate of hydrolysis is dependent on the acidogenic biomass concentration, which is the biological organism group mediating the hydrolysis process. Therefore, in a system where the solids retention time is greater than the hydraulic retention time, the increased acidogenic biomass concentration would mean an increased rate of hydrolysis, and Eq 4.29 would be able to predict this.

For each steady state of operation, the values for the rate of hydrolysis, the biodegradable particulate COD concentration and the acidogenic biomass concentration have been calculated (Table 4.10) and therefore the value of the first order specific rate constant (k'_h) can be calculated (see Table 4.12):

$$k'_h = \frac{\text{rate}_{\text{hydrolysis}}}{S_{bp} \cdot Z_{ad}} \quad (4.30)$$

The calculated values of the first order specific rate constant range from 0.00054 to 0.01764 L/mg Z_{ad} .d (Figure 4.9). However, the values calculated for the two systems fed 2gCOD/L were identified as statistical outliers ($>$ mean + 1.96 x SD, i.e. at 95% confidence interval), and therefore removed from the data set (Figure 4.10), to give a mean and standard deviation of $k'_h = 0.00138 \pm 0.00131$ L/mg Z_{ad} as COD.d. Once again, as for the first order rate constant, the standard deviation is relatively large compared to the mean (coefficient of variation = 0.949), suggesting significant scatter in the values. Further, the values are not normally distributed, but exhibit skew to the right.

By substituting the first order specific rate equation into the mass balance equation, Eq 4.6, the biodegradable particulate COD concentration (S_{bp}) can be predicted:

$$dS_{bp} \cdot V = Q \cdot S_{bpi} \cdot dt - Q \cdot S_{bp} \cdot dt - V \cdot k'_h \cdot S_{bp} \cdot Z_{ad} \cdot dt + V \cdot b_{ad} \cdot Z_{ad} \cdot dt + V \cdot b_{am} \cdot Z_{am} \cdot dt \quad (4.31)$$

Rearranging:
$$\frac{S_{bp}}{dt} = \frac{S_{bpi} - S_{bp}}{R_h} - k'_h \cdot S_{bp} \cdot Z_{ad} + b_{ad} Z_{ad} + b_{am} Z_{am} \quad (4.32)$$

At steady state:
$$S_{bp} = \frac{S_{bpi} + b_{ad} Z_{ad} R_h + b_{am} Z_{am} R_h}{1 + k'_h \cdot Z_{ad} R_h} \quad (4.33)$$

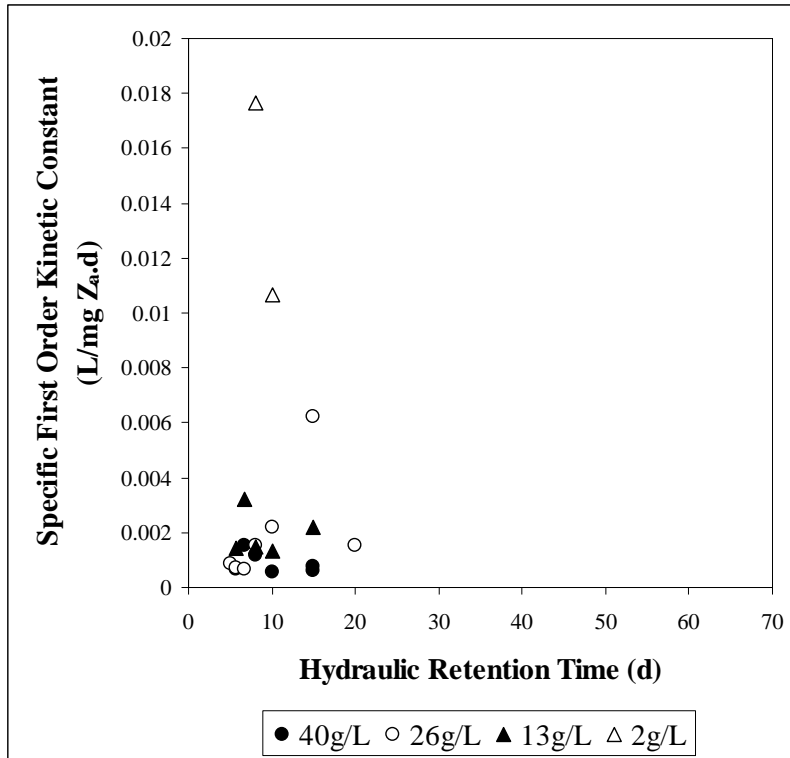


Figure 4.9: Calculated value of the first order specific rate constant for each feed COD concentration at each hydraulic retention time

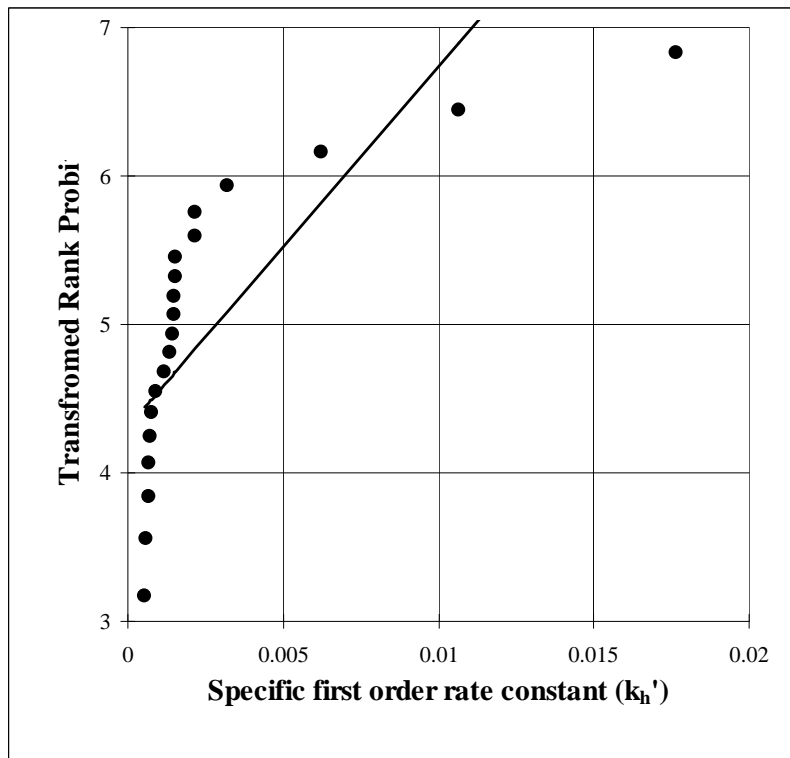


Figure 4.10: Transformed rank probit plot of the first order specific rate including all data points
 ($k_h' = 0.00145 \pm 0.00412d^{-1}$)

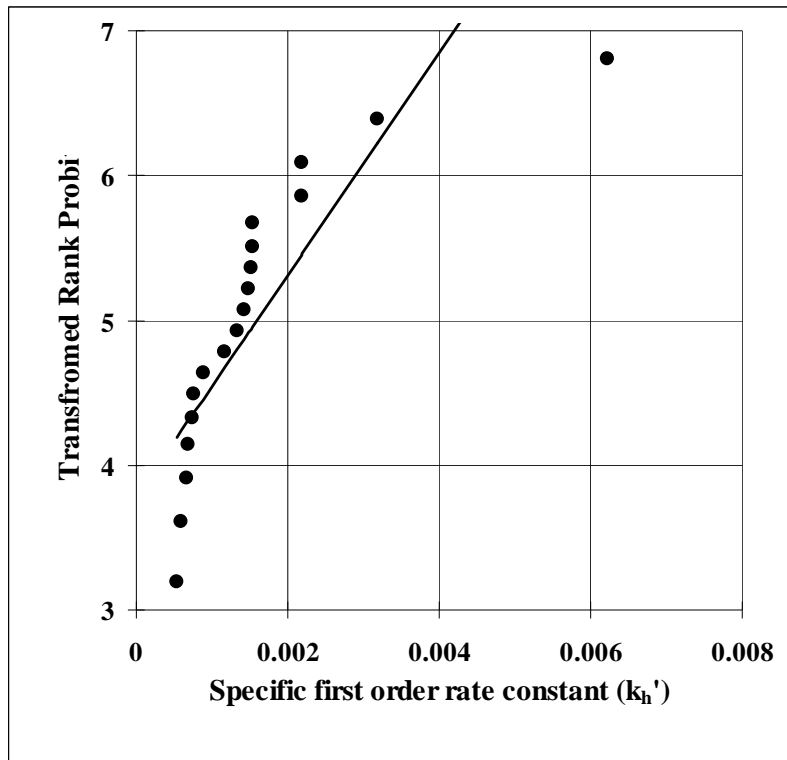


Figure 4.11: Transformed rank probit plot of the first order specific rate constant ignoring two statistical outliers ($k_h' = 0.00138 \pm 0.00131d^{-1}$)

In order to initiate the calculation, the acidogenic biomass concentration was set at an arbitrary value (500 mgCOD/L), and Eq 4.33 simplified by excluding the acetoclastic methanogenic biomass (Z_{am}):

$$S_{bp} = \frac{S_{bpi} + b_{ad}Z_{ad}R_h}{1 + k_h' \cdot Z_{ad}R_h} \quad (4.34)$$

From this initial calculated value for the biodegradable particulate COD concentration, the mean value for the first order specific rate constant, and the assumed value of the acidogenic biomass concentration, an initial rate of hydrolysis was calculated for each steady state system. From this rate, the rates of acidogenesis and methanogenesis were calculated from Eqs 4.11 and 4.14 respectively, and the acidogenic and methanogenic biomass concentrations from Eqs 4.17 and 4.20 respectively. These values were then substituted into Eq 4.33, and a revised biodegradable particulate COD concentration calculated. This algorithm was iterated until the values converged (Table 4.12).

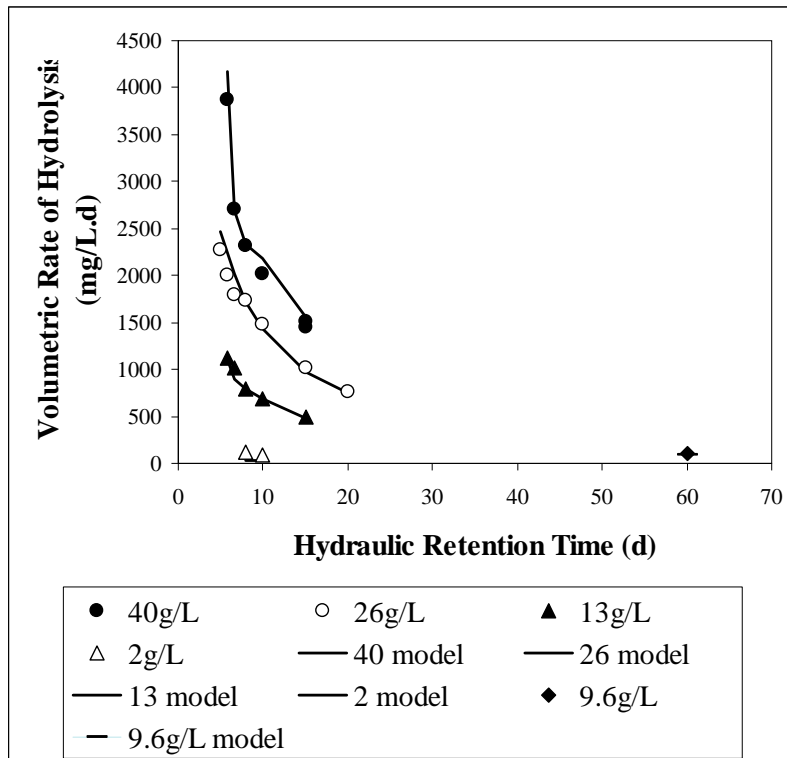


Figure 4.12: Calculated and predicted rate of hydrolysis for each feed COD concentration at each hydraulic retention time

Figure 4.12 shows the predicted (from the first order specific rate equation) rate of hydrolysis compared with the calculated (from the operating data) rate of hydrolysis for each feed COD concentration and hydraulic retention time.

From Figure 4.12, the first order specific rate equation is able to predict the “observed” rate of hydrolysis for each of the steady state operating points, except for the two systems fed 2gCOD/L, for which the calculated first order specific rate constants were statistical outliers. When the predicted rate of hydrolysis is plotted against the calculated rate of hydrolysis (Figure 4.13), the good predictions of the first order specific rate equation are reaffirmed for all systems, except the two operating with a 2gCOD/L feed concentration.

The first order specific kinetics with the mean specific rate constant were also used to predict the effluent COD concentration for all steady state operating points; predicted values are shown plotted against measured values in Figure 4.14. From Figure 4.14, close correlation is obtained, except for the predicted values for the 2gCOD/L systems, which are significantly higher than the measured total effluent COD concentrations (by 176 and 167% COD recovery for the 8 and 10-day retention time systems respectively).

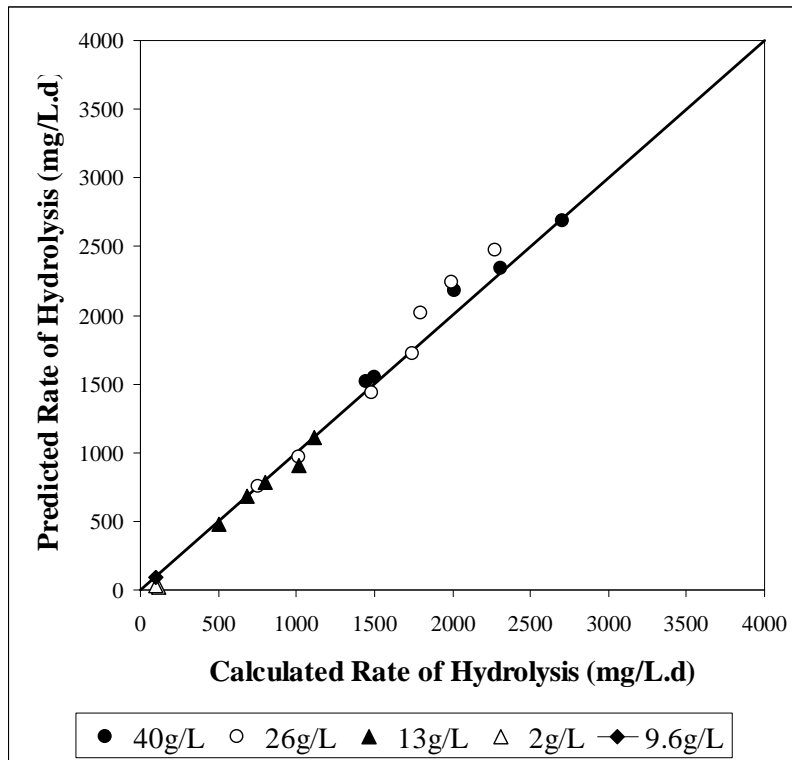


Figure 4.13: Predicted rate of hydrolysis versus the calculated rate of hydrolysis for each feed COD concentration and hydraulic retention time

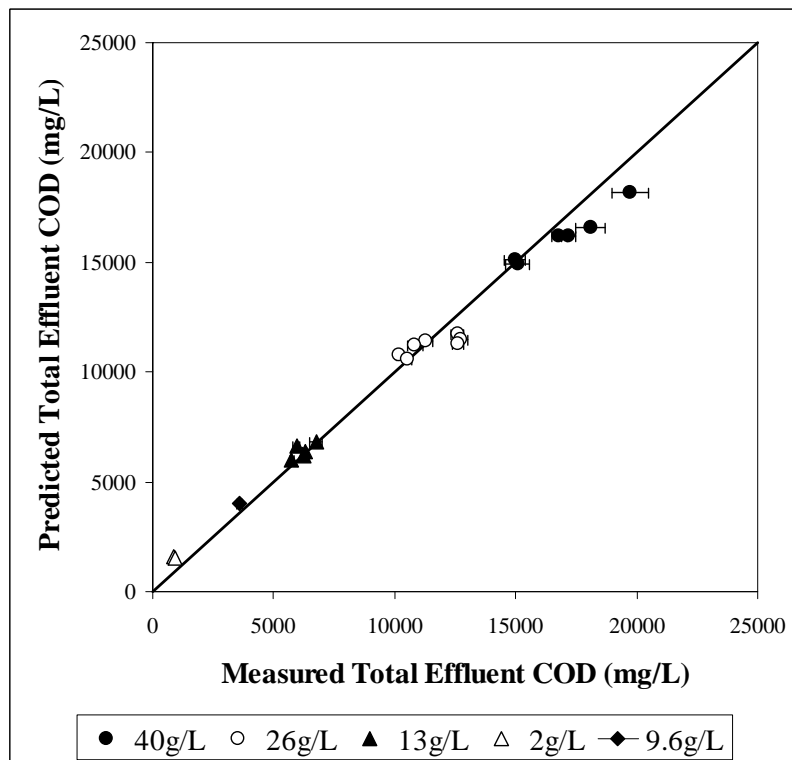


Figure 4.14: Predicted total effluent COD concentration versus measured total effluent COD concentration for each feed COD concentration and hydraulic retention time

Table 4.12: Measured and calculated values of the various components of the feed and effluent COD measurements, and the comparative calculated values predicted by a first order specific rate equation for PSS hydrolysis (Concentrations in mgCOD/L; rates in mgCOD/L.d)

Steady state no.	Retention Time (d)	Measurements (mgCOD/L)				Calculated from experimental data					First order specific kinetics		
		Total Feed	Soluble Feed	Total Effluent	Soluble Effluent	S _{bp}	Z _a	Rate of hydrolysis	k _h	S _{bp}	Rate of hydrolysis	Total Effluent	
28	5.71	41441	2582	19737	295	24998	3394	1690	3868	0.00067	1664	4178	18170
23	6.67	34818	4398	14984	207	18775	1262	1416	2702	0.00151	1380	2684	15091
21	8	34818	3828	15094	205	19345	1442	1371	2310	0.00117	1222	2338	14893
12	10	39810	4436	18085	256	22059	2649	1415	2016	0.00054	1039	2182	16610
10	15	39790	3521	16792	250	22961	1476	1343	1503	0.00076	812	1550	16177
11	15	39790	3990	17167	299	22491	1843	1307	1446	0.00060	804	1518	16205
9	5	24881	2694	12610	301	13865	2759	934	2270	0.00088	1774	2471	11720
8	5.71	24960	2503	12729	205	14109	2977	912	1996	0.00073	1600	2242	11482
7	6.67	24881	2027	12595	200	14532	2890	907	1794	0.00068	1444	2016	11282
2	8	25953	2675	11299	168	14598	1107	1025	1740	0.00153	1228	1725	11410
1	10	25953	2331	10849	178	14942	672	1010	1480	0.00218	1059	1440	11204
4	15	25953	2647	10212	157	14625	178	912	1012	0.00622	801	968	10788
3	20	25953	2326	10525	179	14947	617	801	758	0.00154	686	755	10589
31	5.71	13186	956	6757	120	7819	1584	494	1117	0.00143	1636	1108	6803
24	6.67	13579	1845	5944	96	7192	591	540	1019	0.00319	1346	903	6630
14	8	13270	1525	6299	104	7307	1124	479	798	0.00148	1204	788	6372
13	10	13270	1174	6249	108	7657	1092	467	681	0.00134	1056	685	6216
5	15	13618	1432	5751	97	7631	504	453	499	0.00219	795	479	6021
17	60	9810	1204	3590	88	5325	0.0000780	166	98	*n.a.	422	90	3997
26	8	1950	284	892	51	1014	93	72	119	0.01764	832	24	1566
25	10	1950	254	905	32	1043	132	67	95	0.01067	797	26	1514

* once again, the calculated value for the 60-day retention time system is not considered

4.6.3 Monod kinetics

The Monod equation is probably the most extensively used rate formulation to predict the growth of bacteria. However, no examples could be found in the literature of the application of this formulation to model the rate of hydrolysis. This application will be evaluated. For Monod kinetics:

$$\text{rate}_{\text{hydrolysis}} = \frac{\mu_{\text{max}} \cdot S_{\text{bp}} \cdot Z_{\text{ad}}}{Y_{\text{ad}} (K_S + S_{\text{bp}})} \quad (4.35)$$

Eq 4.35 can be linearised:

$$\frac{Z_{\text{ad}}}{Y_{\text{ad}} \cdot \text{rate}_{\text{hydrolysis}}} = \frac{K_S}{\mu_{\text{max}} \cdot S_{\text{bp}}} + \frac{1}{\mu_{\text{max}}} \quad (4.36)$$

Therefore, by plotting $\frac{Z_{\text{ad}}}{Y_{\text{ad}} \cdot \text{rate}_{\text{hydrolysis}}}$ against $\frac{1}{S_{\text{bp}}}$, the values for the kinetic constants μ_{max} and K_S can be calculated from the slope = $\frac{K_S}{\mu_{\text{max}}}$ and y-intercept = $\frac{1}{\mu_{\text{max}}}$. Figure 4.15 shows this plot, with the linear regression straight line fitted to the data and the linear regression line equation.

Figure 4.15 shows that the linear regression to the linearised Monod equation does not give a good correlation with the experimental data ($R^2 = 0.0357$), and therefore the values for the two derived kinetic constants ($\mu_{\text{max}} = 0.142\text{d}^{-1}$ and $K_S = 20.2\text{mgCOD/L}$) would not be expected to accurately predict the rate of hydrolysis under all of the steady state operating conditions.

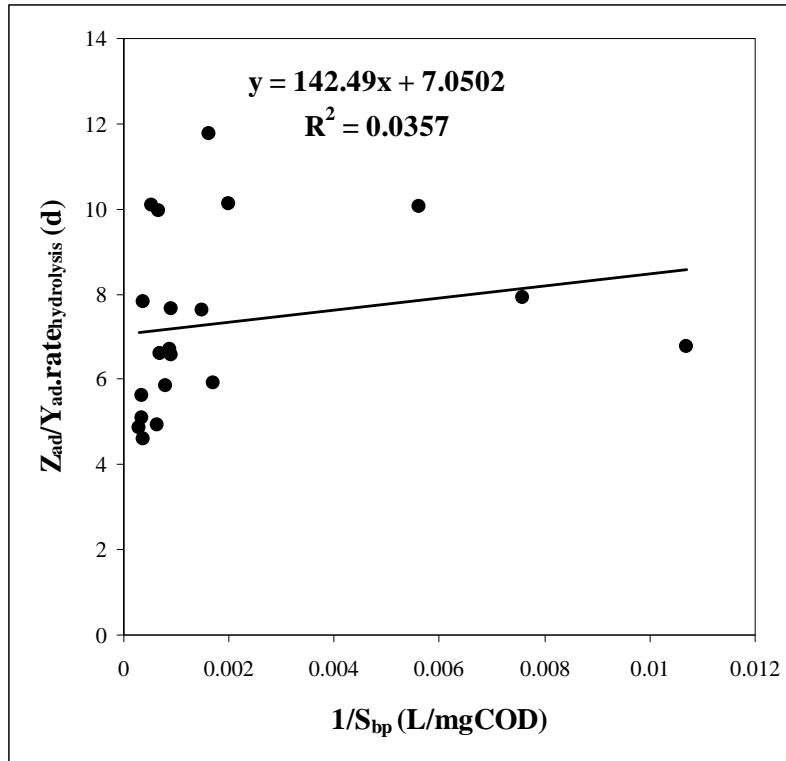


Figure 4.15: Linearised Monod equation plot for calculation of μ_{max} and K_S from the slope and y-intercept ($\mu_{max} = 0.142d^{-1}$ and $K_S = 20.2mgCOD/L$)

By substituting Eq 4.35 into the mass balance equation, Eq 4.6:

$$dS_{bp} \cdot V = Q \cdot S_{bpi} \cdot dt - Q \cdot S_{bp} \cdot dt - V \cdot \frac{\mu_{max} \cdot S_{bp} \cdot Z_{ad}}{Y_{ad} (K_S + S_{bp})} \cdot dt + V \cdot b_{ad} \cdot Z_{ad} \cdot dt + V \cdot b_{am} \cdot Z_{am} \cdot dt \quad (4.37)$$

Rearranging:
$$\frac{dS_{bp}}{dt} = \frac{S_{bpi} - S_{bp}}{R_h} - \frac{\mu_{max} \cdot S_{bp} \cdot Z_{ad}}{Y_{ad} (K_S + S_{bp})} + b_{ad} \cdot Z_{ad} + b_{am} \cdot Z_{am} \quad (4.38)$$

At steady state:
$$Y_{ad} \cdot S_{bp}^2 + (Y_{ad} \cdot K_S + \mu_{max} \cdot Z_{ad} \cdot R_h - Y_{ad} \cdot N) \cdot S_{bp} - Y_{ad} \cdot K_S \cdot N = 0 \quad (4.39)$$

where:
$$N = S_{bpi} + b_{ad} \cdot Z_{ad} \cdot R_h + b_{am} \cdot Z_{am} \cdot R_h \quad (4.40)$$

Therefore, to calculate S_{bp} , the roots of Eq 4.39 need to be calculated from:

$$S_{bp} = \frac{-b \pm \sqrt{b^2 - 4ac}}{2a} \quad (4.41)$$

where $a = Y_{ad}$ (4.42)

$$b = Y_{ad} \cdot K_S + \mu_{max} \cdot Z_{ad} \cdot R_h - Y_{ad} \cdot N \quad (4.43)$$

$$c = -Y_{ad} \cdot K_S \cdot N \quad (4.44)$$

Taking only the addition option in Eq 4.41 (subtraction option gives the nonsensical negative concentration), the value of S_{bp} was calculated for each feed COD concentration and hydraulic retention time (Table 4.13). From this calculated value, and the kinetic constants (μ_{max} and K_S) calculated from Figure 4.15, and assuming an initial acidogenic biomass concentration, an initial rate of hydrolysis was calculated from Eq 4.35. From this rate, the rates of acidogenesis and methanogenesis were calculated from Eqs 4.11 and 4.14 respectively. Further, the acidogenic and methanogenic biomass concentrations were calculated from Eqs 4.17 and 4.20 respectively. The calculated values of the acidogenic and methanogenic biomass concentrations were then substituted into Eq 4.41, and the algorithm iterated until the values converged (Table 4.13).

The rate of hydrolysis predicted by the Monod kinetics for all the steady state systems are compared with the “observed” value in Figure 4.16. Figure 4.16 shows that at the longer retention times (> 8 days), the model is able to accurately predict the calculated rate of hydrolysis, but at the shorter retention times (< 8 days), the predicted rates are considerably lower than the calculated rates, and the model is no longer able to predict the rate of hydrolysis. This result is confirmed in Figure 4.17, where the predicted and “observed” rates are compared, several data points deviate significantly from the diagonal (1:1 correspondence) line, meaning that the calculated and predicted rates are not equal. The result of the inaccurate hydrolysis rate prediction is that the predicted effluent total COD concentration is higher than the measured effluent total COD concentration for a number of steady states (particularly those at shorter retention times), as shown in Figure 4.18. Clearly, the kinetic constants (μ_{max} and K_S) calculated from the experimental data do not fit the entire data set, and revised constants may increase the accuracy of the predicted values. This is discussed further in Section 4.6.5.

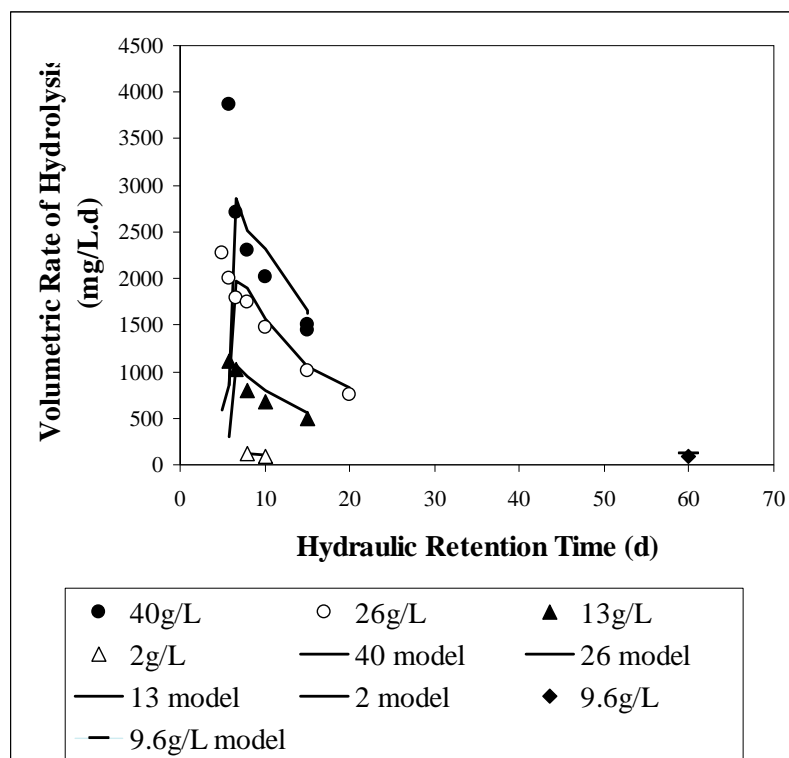


Figure 4.16: Calculated and predicted rate of hydrolysis for each feed COD concentration at each hydraulic retention time

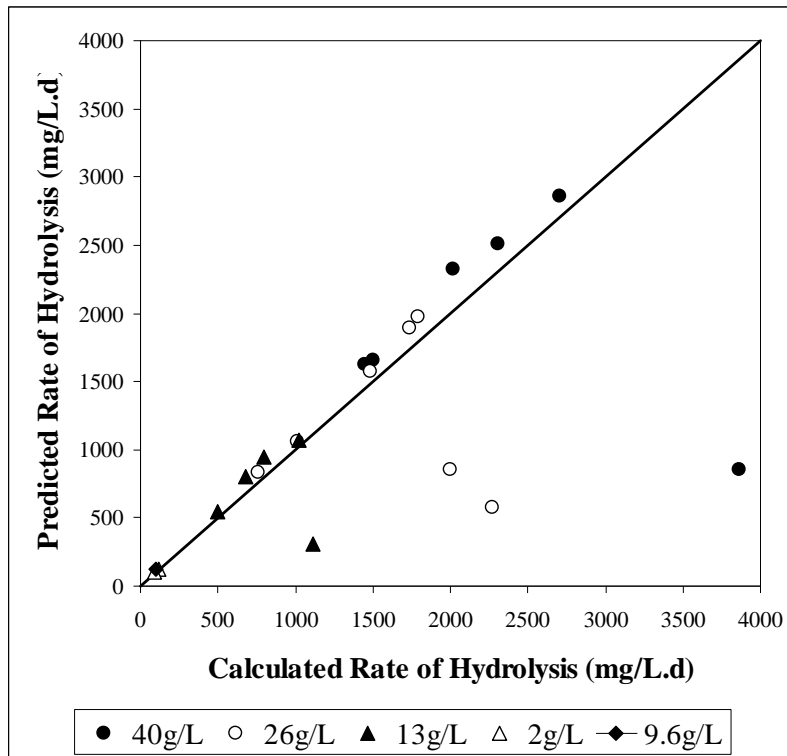


Figure 4.17: Predicted rate of hydrolysis versus the calculated rate of hydrolysis for each feed COD concentration and hydraulic retention time

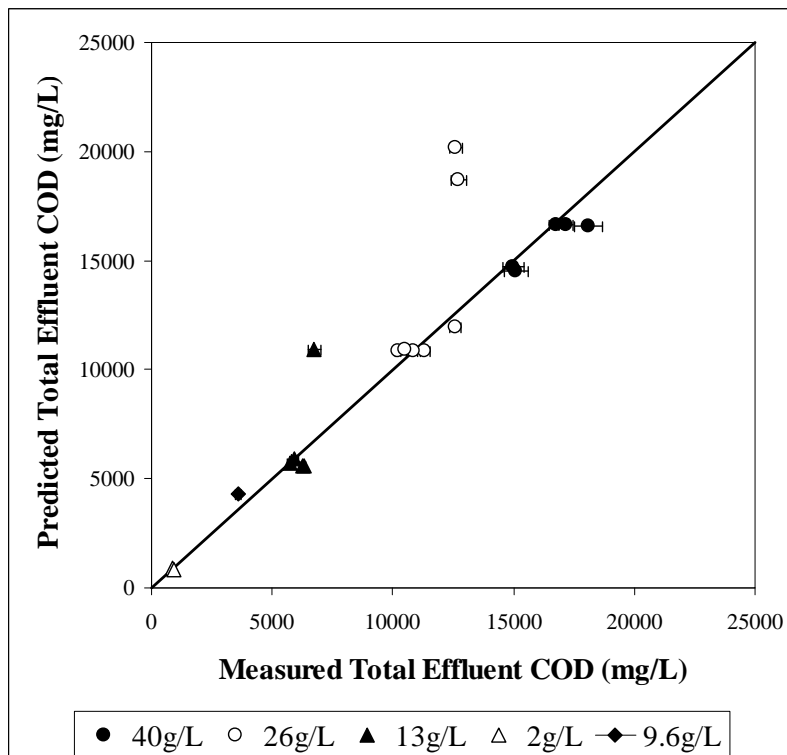


Figure 4.18: Predicted total effluent COD concentration versus measured total effluent COD concentration for each feed COD concentration and hydraulic retention time

Table 4.13: Measured and calculated values of the various components of the feed and effluent COD measurements, and the comparative calculated values predicted by a Monod rate equation for PSS hydrolysis (Concentrations in mgCOD/L; rates in mgCOD/L.d)

Steady state no.	Retention Time (d)	Measurements (mgCOD/L)					Calculated from experimental data					Monod kinetics		
		Total Feed	Soluble Feed	Total Effluent	Soluble Effluent	S _{bp}	S _{bp}	Z _{ad}	Rate of hydrolysis	S _{bp}	Rate of hydrolysis	Total Effluent		
28	5.71	41441	2582	19737	295	24998	3394	1690	3868	20299	852	35183		
23	6.67	34818	4398	14984	207	18775	1262	1416	2702	407	2855	14744		
21	8	34818	3828	15094	205	19345	1442	1371	2310	85	2510	14496		
12	10	39810	4436	18085	256	22059	2649	1415	2016	37	2321	16566		
10	15	39790	3521	16792	250	22961	1476	1343	1503	16	1653	16643		
11	15	39790	3990	17167	299	22491	1843	1307	1446	16	1621	16669		
9	5	24881	2694	12610	301	13865	2759	934	2270	11068	580	20204		
8	5.71	24960	2503	12729	205	14109	2977	912	1996	9415	851	18697		
7	6.67	24881	2027	12595	200	14532	2890	907	1794	1802	1975	11961		
2	8	25953	2675	11299	168	14598	1107	1025	1740	88	1890	10848		
1	10	25953	2331	10849	178	14942	672	1010	1480	39	1568	10845		
4	15	25953	2647	10212	157	14625	178	912	1012	16	1054	10840		
3	20	25953	2326	10525	179	14947	617	801	758	10	829	10919		
31	5.71	13186	956	6757	120	7819	1584	494	1117	6122	308	10916		
24	6.67	13579	1845	5944	96	7192	591	540	1019	327	1067	5908		
14	8	13270	1525	6299	104	7307	1124	479	798	84	942	5591		
13	10	13270	1174	6249	108	7657	1092	467	681	39	802	5579		
5	15	13618	1432	5751	97	7631	504	453	499	16	550	5706		
17	60	9810	1204	3590	88	5325	0.0000780	166	98	2	127	4322		
26	8	1950	284	892	51	1014	93	72	119	75	123	907		
25	10	1950	254	905	32	1043	132	67	95	36	106	858		

4.6.4 Surface reaction kinetics

The surface reaction or Contois kinetic theory, as described in Chapter 2, is based on the particulate organic substrate having a number of active sites for biological attack, and the overall rate of hydrolysis of the particle is dependent on the number of bacteria attached to the active sites. Once the active sites are saturated by acidogenic biomass, the rate of hydrolysis reaches a maximum:

$$\text{rate}_{\text{hydrolysis}} = \frac{k_{\text{max}} \left(\frac{S_{\text{bp}}}{Z_{\text{ad}}} \right)}{\left(K_{\text{S}} + \frac{S_{\text{bp}}}{Z_{\text{ad}}} \right)} Z_{\text{ad}} \quad (4.45)$$

Similarly to the Monod kinetics, this equation can also be linearized:

$$\frac{Z_{\text{ad}}}{\text{rate}_{\text{hydrolysis}}} = \frac{K_{\text{S}}}{k_{\text{max}}} \frac{Z_{\text{ad}}}{S_{\text{bp}}} + \frac{1}{k_{\text{max}}} \quad (4.46)$$

Therefore, by plotting $\frac{Z_{\text{ad}}}{\text{rate}_{\text{hydrolysis}}}$ against $\frac{Z_{\text{ad}}}{S_{\text{bp}}}$, the values for the kinetic constants k_{max} and K_{S}

can be calculated from the slope = $\frac{K_{\text{S}}}{k_{\text{max}}}$ and y-intercept = $\frac{1}{k_{\text{max}}}$. To generate the plot, Z_{ad} ,

$\text{rate}_{\text{hydrolysis}}$ and S_{bp} for each steady state are available from the previous kinetic formulation evaluations (Table 4.10). Figure 4.19 shows this plot with the linear regression straight line and the regression equation. As for the Monod plot, the low value of the correlation coefficient ($R^2 = 0.2006$) suggests that the straight line is not representative of the entire data set, and in fact one data point lies well away from the group (5.11, 0.90). The predicted values for the kinetic constants ($k_{\text{max}} = 1.72 \text{mgCOD/mgZ}_{\text{ad}}$ as COD.d and $K_{\text{S}} = 0.139 \text{mgCOD/mgZ}_{\text{ad}}$ as COD) would not be expected to accurately predict the rate of hydrolysis for all operating conditions.

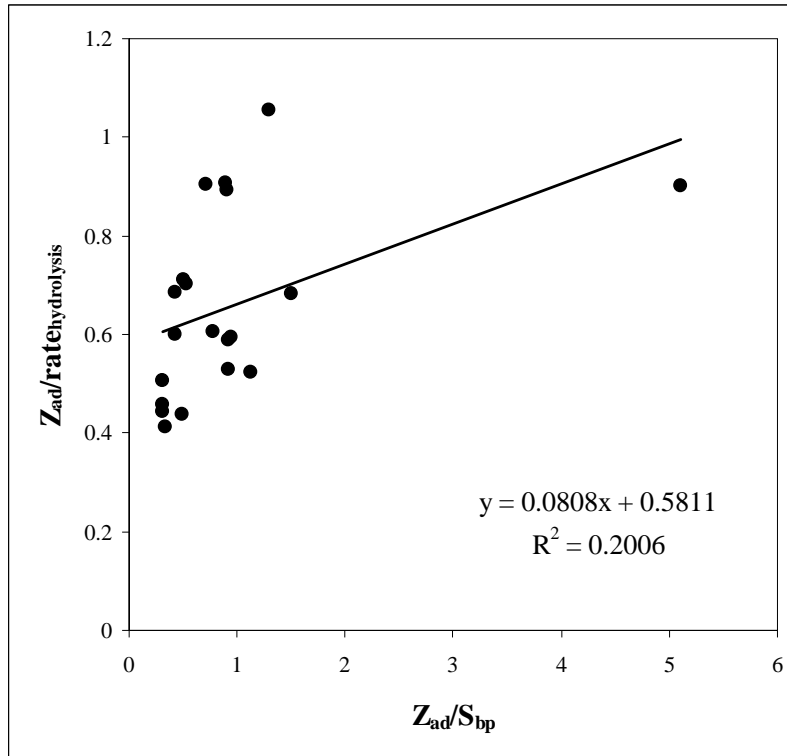


Figure 4.19: Linearised surface reaction kinetics plot for the calculation of k_{max} and K_S from the slope and y-intercept ($k_{max} = 1.72\text{mgCOD}/\text{mgZ}_{ad}\cdot\text{d}$ and $K_S = 0.139\text{mgCOD}/\text{mgZ}_{ad}$)

By substituting Eq 4.45 into the mass balance equation, Eq 4.6:

$$dS_{bp} \cdot V = Q \cdot S_{bpi} \cdot dt - Q \cdot S_{bp} \cdot dt - V \cdot \frac{k_{max} \cdot \left(\frac{S_{bp}}{Z_{ad}}\right)}{K_S + \left(\frac{S_{bp}}{Z_{ad}}\right)} Z_{ad} \cdot dt + V \cdot b_{ad} \cdot Z_{ad} \cdot dt + V \cdot b_{am} \cdot Z_{am} \cdot dt \quad (4.47)$$

Rearranging:
$$\frac{dS_{bp}}{dt} = \frac{S_{bpi} - S_{bp}}{R_h} - \frac{k_{max} \cdot S_{bp} \cdot Z_{ad}}{K_S \cdot Z_{ad} + S_{bp}} + b_{ad} \cdot Z_{ad} + b_{am} \cdot Z_{am} \quad (4.48)$$

At steady state:
$$S_{bp}^2 + (K_S \cdot Z_{ad} + k_{max} \cdot Z_{ad} \cdot R_h - N) \cdot S_{bp} - N \cdot K_S \cdot Z_{ad} = 0 \quad (4.49)$$

where:
$$N = S_{bpi} + b_{ad} \cdot Z_{ad} \cdot R_h + b_{am} \cdot Z_{am} \cdot R_h \quad (4.50)$$

Therefore, to calculate S_{bp} , the roots of Eq 4.49 need to be calculated from:

$$S_{bp} = \frac{-b \pm \sqrt{b^2 - 4ac}}{2a} \quad (4.51)$$

where $a = 1$ (4.52)

$$b = K_S \cdot Z_{ad} + k_{max} \cdot Z_{ad} \cdot R_h - N \quad (4.53)$$

$$c = -N \cdot K_S \cdot Z_{ad} \quad (4.54)$$

Taking only the addition option in Eq 4.51 (subtraction option gives the nonsensical negative concentration), the value of S_{bp} was calculated for each feed COD concentration and hydraulic retention time (Table 4.14). From this calculated value, and the kinetic constants (k_{max} and K_S) calculated from Figure 4.19, and assuming an initial acidogenic biomass concentration, an initial rate of hydrolysis was calculated from Eq 4.45. From this rate, the rates of acidogenesis and methanogenesis were calculated from Eqs 4.11 and 4.14 respectively. Further, the acidogenic and methanogenic biomass concentrations were calculated from Eqs 4.17 and 4.20 respectively. The calculated values of the acidogenic and methanogenic biomass concentrations were then substituted into Eq 4.49, and the algorithm iterated until the values converged (Table 4.14).

The rate of hydrolysis predicted with the surface reaction kinetics for all steady state systems are compared with the “observed” values in Figure 4.20. As with the Monod kinetics in Section 4.6.3, the surface reaction kinetics model is able to predict the rate of hydrolysis accurately for the longer retention times, but the predicted rate is significantly lower than the calculated rate at retention times less than 10 days. This result is confirmed in Figure 4.21 where predicted and “observed” rates are compared; many of the data points lie below the diagonal (1:1 correspondence) line, which means that for these points the predicted rate is lower than the calculated rate. This would imply that the predicted effluent total COD concentration would be higher than the measured effluent total COD concentration for these data points, and Figure 4.22 demonstrates this. Clearly, the surface reaction rate kinetics with the kinetic constants (k_{max} and K_S) calculated from all the experimental data does not predict the rate of hydrolysis under all operating conditions.

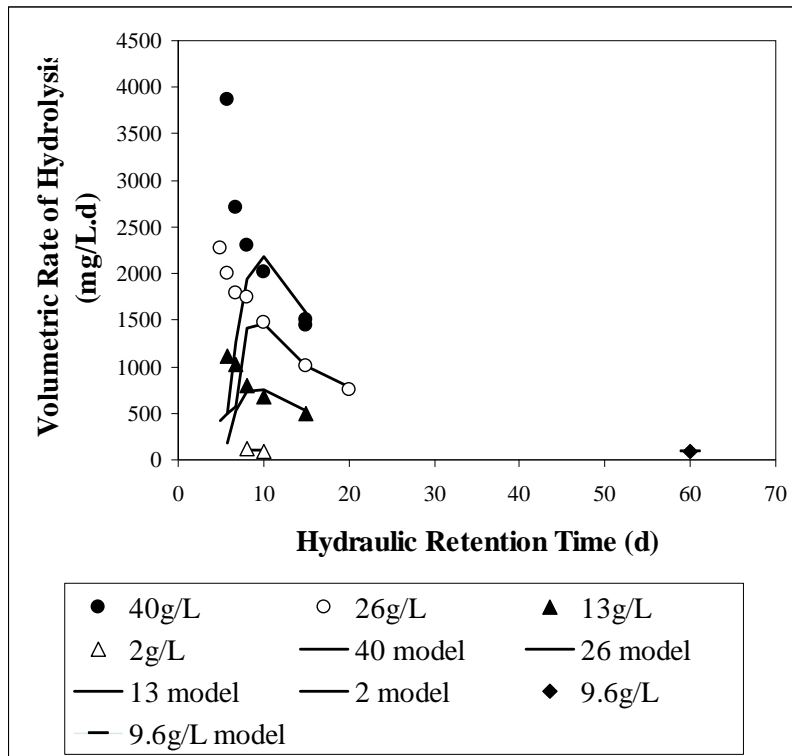


Figure 4.20: Calculated and predicted rate of hydrolysis for each feed COD concentration at each hydraulic retention time

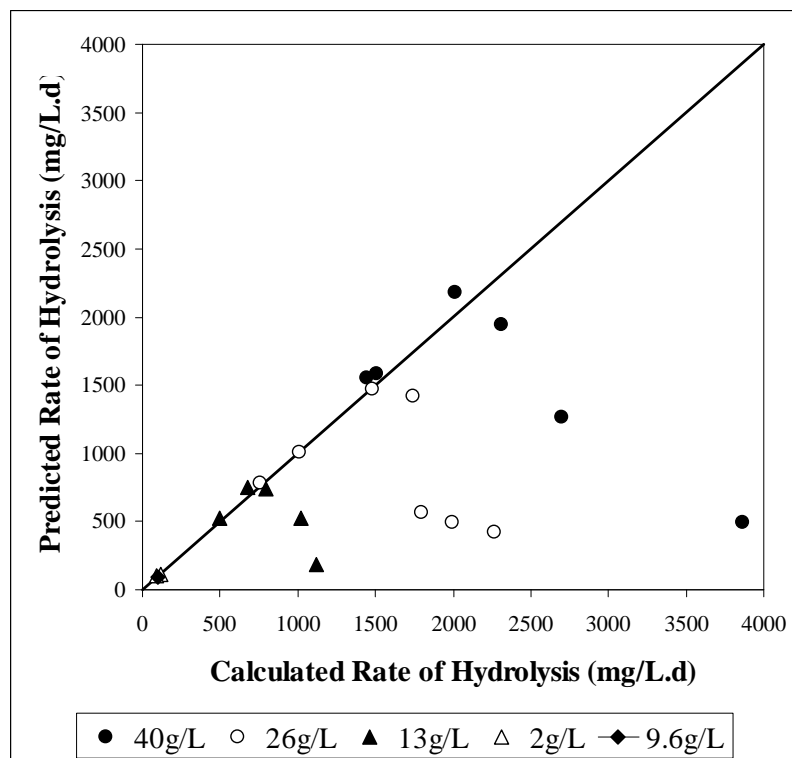


Figure 4.21: Predicted rate of hydrolysis versus the calculated rate of hydrolysis for each feed COD concentration and hydraulic retention time

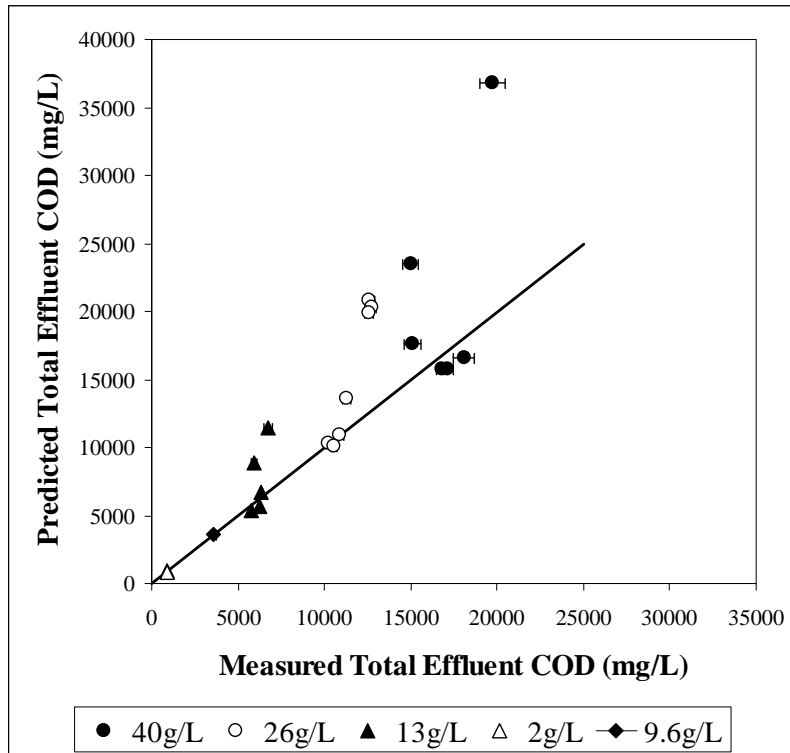


Figure 4.22: Predicted total effluent COD concentration versus measured total effluent COD concentration for each feed COD concentration and hydraulic retention time

Table 4.14: Measured and calculated values of the various components of the feed and effluent COD measurements, and the comparative calculated values predicted by the surface reaction rate equation for PSS hydrolysis (Concentrations in mgCOD/L; rates in mgCOD/L.d)

Steady state no.	Retention Time (d)	Measurements (mgCOD/L)				Calculated from experimental data				Surface reaction kinetics		
		Total Feed	Soluble Feed	Total Effluent	Soluble Effluent	S _{bp}	Z _{ad}	Rate of hydrolysis	S _{bp}	Rate of hydrolysis	Total Effluent	
28	5.71	41441	2582	19737	295	24998	3394	1690	3868	22245	498	36807
23	6.67	34818	4398	14984	207	18775	1262	1416	2702	10638	1261	23498
21	8	34818	3828	15094	205	19345	1442	1371	2310	4279	1945	17679
12	10	39810	4436	18085	256	22059	2649	1415	2016	1058	2180	16627
10	15	39790	3521	16792	250	22961	1476	1343	1503	368	1581	15766
11	15	39790	3990	17167	299	22491	1843	1307	1446	354	1550	15788
9	5	24881	2694	12610	301	13865	2759	934	2270	11821	423	20797
8	5.71	24960	2503	12729	205	14109	2977	912	1996	11359	497	20319
7	6.67	24881	2027	12595	200	14532	2890	907	1794	10885	565	19855
2	8	25953	2675	11299	168	14598	1107	1025	1740	3619	1417	13589
1	10	25953	2331	10849	178	14942	672	1010	1480	796	1467	10962
4	15	25953	2647	10212	157	14625	178	912	1012	229	1008	10259
3	20	25953	2326	10525	179	14947	617	801	758	141	784	10081
31	5.71	13186	956	6757	120	7819	1584	494	1117	6814	182	11493
24	6.67	13579	1845	5944	96	7192	591	540	1019	3821	522	8877
14	8	13270	1525	6299	104	7307	1124	479	798	1538	745	6676
13	10	13270	1174	6249	108	7657	1092	467	681	413	751	5627
5	15	13618	1432	5751	97	7631	504	453	499	119	526	5395
17	60	9810	1204	3590	88	5325	0.0000780	166	98	12	97	3602
26	8	1950	284	892	51	1014	93	72	119	171	109	963
25	10	1950	254	905	32	1043	132	67	95	48	103	828

4.6.5 Revised data for kinetic constant determination

The Monod kinetics and surface reaction kinetics from Sections 4.6.3 and 4.6.4 were both not able to accurately predict the rate of hydrolysis under all operating conditions, particularly at the lower retention times.

For both forms of kinetics, all of the experimental data points (except the 60-day retention time) were used to calculate the values for the kinetic constants, and Figure 4.15 (for the Monod kinetics) and Figure 4.19 (for surface reaction kinetics) show that a number of data points lie outside the group containing the majority of the data points. Since linear regression was fitted to all these data points, the ‘outliers’ probably exert disproportional weighting and skew the linear regression. Thus, the values for the kinetic constants determined from the linear regression statistics may not be representative of the majority of the experimental data points.

From consideration of the effluent biodegradable particulate COD concentrations (Table 4.10), it can be argued that the longer retention times (> 10 days) are more useful for calculating the unbiodegradable particulate COD concentration, since the residual effluent biodegradable particulate COD concentration is relatively small. In contrast, at the shorter retention times, the residual biodegradable particulate COD concentration is higher, and the system behaviour is hydrolysis rate limited, rather than substrate limited. It is therefore at these shorter retention times that the most useful information regarding the rate of hydrolysis can be extracted. This would suggest that the calculation of the kinetic constants should be limited to these data points only. With this restriction, it is possible that kinetic constants derived for the Monod kinetics and surface reaction kinetics would enable prediction of the rate of hydrolysis at the shorter as well as the longer retention times. This is evaluated below.

4.6.5.1 Revised Monod kinetics

The data in Figure 4.15 has been replotted in Figure 4.23, but with the fitted linear regression restricted to the data points corresponding to the lower retention times only. These selected data points are shown in Table 4.15. One of the selected data points (6.67-day retention time, 13gCOD/L feed concentration), even though belonging to the ‘shorter’ retention time group, was excluded because it significantly skewed the linear regression.

Table 4.15: Steady state data points (values are steady state numbers from Appendix B) used to calculate the values of the revised Monod kinetics constants

Feed COD Concentration (gCOD/L)	Hydraulic Retention Time (d)							
	60	20	15	10	8	6.67	5.71	5
40					21	23	28	
25					2	7	8	9
13					14		31	
9								
2								

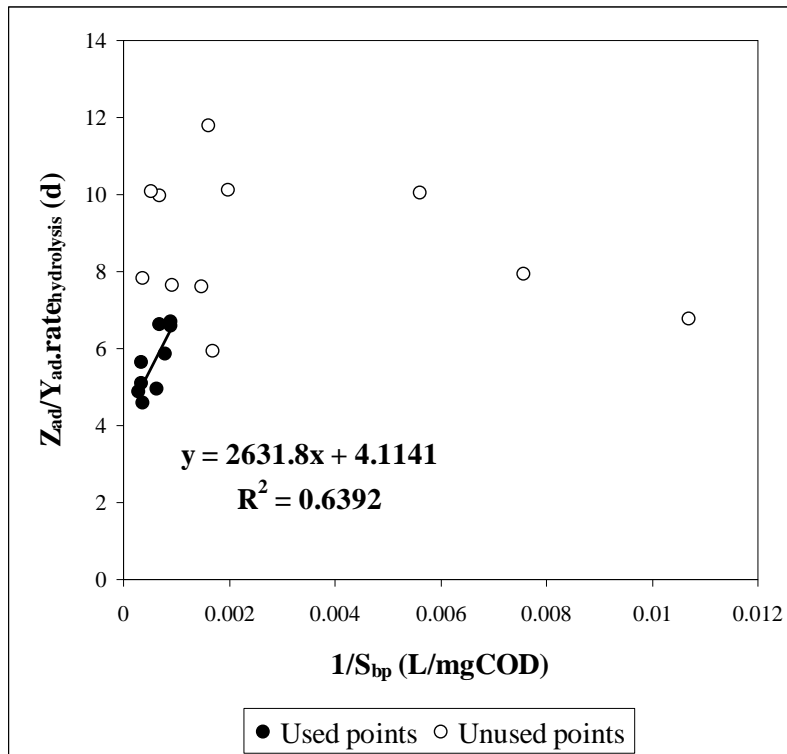


Figure 4.23: Linearised Monod equation plot on the revised ‘shorter’ retention time data set for the calculation of μ_{\max} and K_S from the slope and y-intercept
(new $\mu_{\max} = 0.243\text{d}^{-1}$ and $K_S = 640\text{mgCOD/L}$)

From the regression analysis, the value for μ_{\max} increased from 0.142 to 0.243d^{-1} and K_S increased from 20.2 to 640mgCOD/L . These changes represent an increase in the maximum specific rate of hydrolysis of 71%, but the increase in the half-saturation constant (K_S) means that the maximum rate will only be reached at significantly higher biodegradable particulate COD concentrations, above about 1280mgCOD/L ($2 \times K_S$). The predicted rate of hydrolysis using Monod kinetics and the revised values for the kinetic constants (μ_{\max} and K_S) are shown in Figure 4.24 together with the corresponding “observed” values.

From Figure 4.24, the revised values for the kinetic constants in the Monod formulation are able to predict the rate of hydrolysis with greater accuracy than the initial values (Figure 4.15), even at the low retention times. Of equal importance is that the predicted rates at the longer retention times have remained accurate, so that this set of kinetic constants can be used for all hydraulic retention times and feed COD concentrations. Predicted versus “observed” hydrolysis rates are shown in Figure 4.25, where all the data points lie close to the diagonal (1:1 correspondence), meaning that the predicted rates of hydrolysis are close to the calculated rates. This is again reflected in the predicted versus measured total effluent COD concentrations (Figure 4.26), where the model is now able to reasonably accurately predict the effluent total COD concentration at all operating conditions.

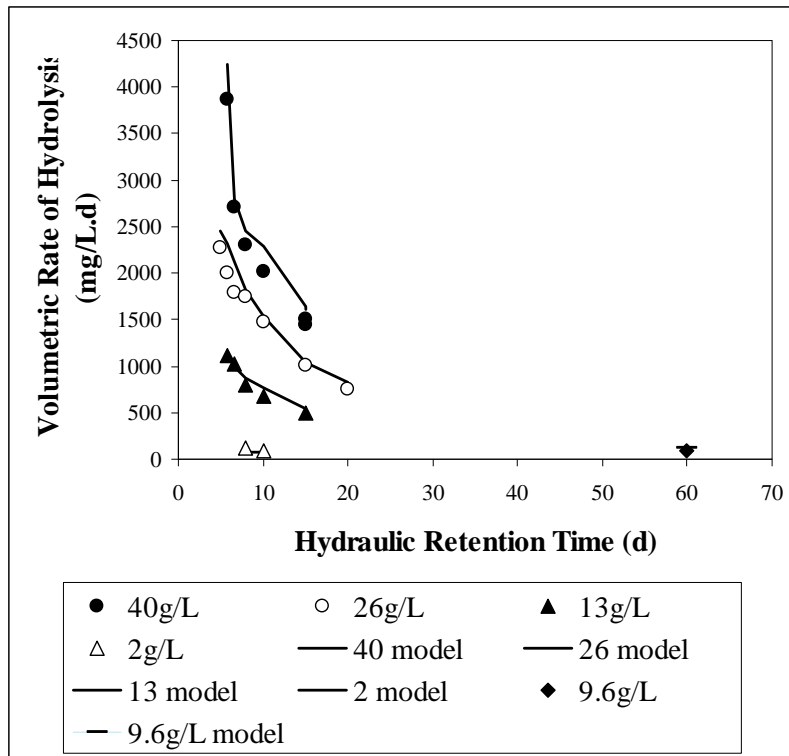


Figure 4.24: Calculated and predicted rate of hydrolysis for each feed COD concentration at each hydraulic retention time

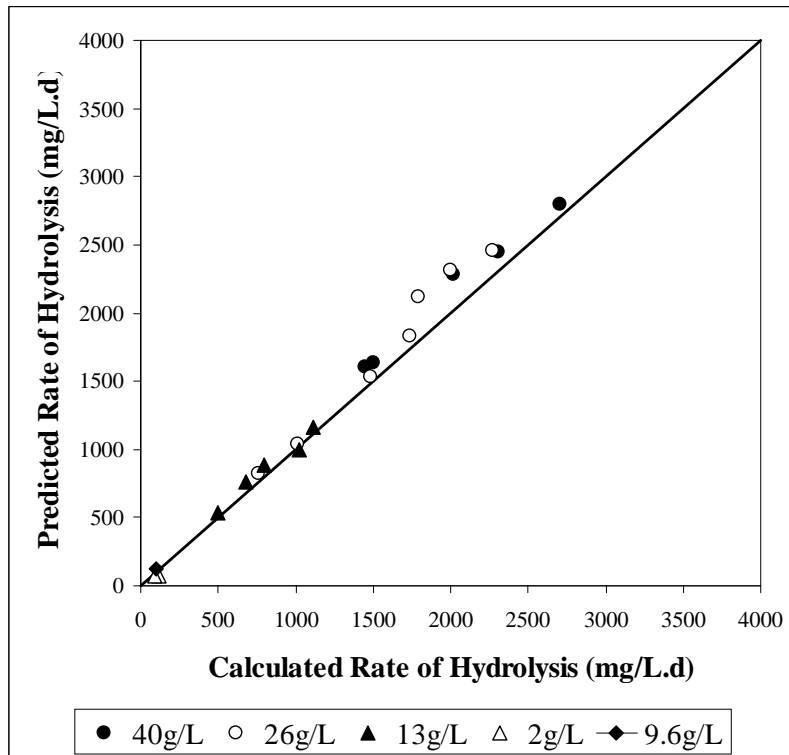


Figure 4.25: Predicted rate of hydrolysis versus the calculated rate of hydrolysis for each feed COD concentration and hydraulic retention time

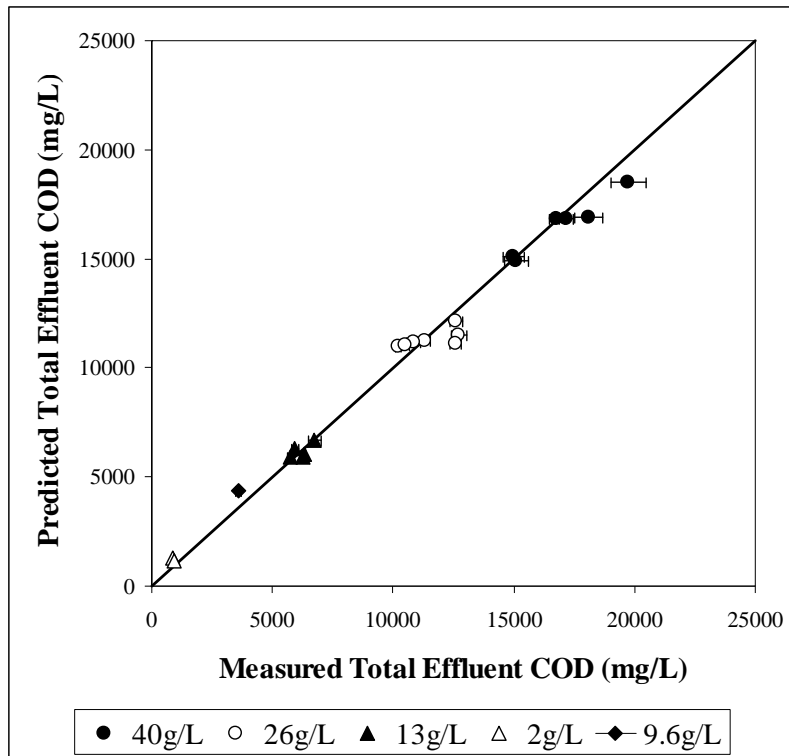


Figure 4.26: Predicted total effluent COD concentration versus measured total effluent COD concentration for each feed COD concentration and hydraulic retention time

Table 4.16: Measured and calculated values of the various components of the feed and effluent COD measurements, and the comparative calculated values predicted by the Monod equation with revised values for the kinetic constants (Concentrations in mgCOD/L; rates in mgCOD/L.d)

Steady state no.	Retention Time (d)	Measurements (mgCOD/L)					Calculated from experimental data					Monod kinetics		
		Total Feed	Soluble Feed	Total Effluent	Soluble Effluent	S _{bp}	S _{bp}	Z _{ad}	Rate of hydrolysis	S _{bp}	Rate of hydrolysis	Total Effluent		
28	5.71	41441	2582	19737	295	24998	3394	1690	3868	1408	4246	18497		
23	6.67	34818	4398	14984	207	18775	1262	1416	2702	797	2794	15088		
21	8	34818	3828	15094	205	19345	1442	1371	2310	569	2447	14923		
12	10	39810	4436	18085	256	22059	2649	1415	2016	387	2284	16875		
10	15	39790	3521	16792	250	22961	1476	1343	1503	222	1639	16823		
11	15	39790	3990	17167	299	22491	1843	1307	1446	219	1607	16847		
9	5	24881	2694	12610	301	13865	2759	934	2270	1916	2453	12116		
8	5.71	24960	2503	12729	205	14109	2977	912	1996	1256	2317	11490		
7	6.67	24881	2027	12595	200	14532	2890	907	1794	882	2117	11149		
2	8	25953	2675	11299	168	14598	1107	1025	1740	576	1827	11278		
1	10	25953	2331	10849	178	14942	672	1010	1480	399	1531	11163		
4	15	25953	2647	10212	157	14625	178	912	1012	218	1040	11018		
3	20	25953	2326	10525	179	14947	617	801	758	153	821	11044		
31	5.71	13186	956	6757	120	7819	1584	494	1117	1344	1166	6695		
24	6.67	13579	1845	5944	96	7192	591	540	1019	768	999	6297		
14	8	13270	1525	6299	104	7307	1124	479	798	561	880	6012		
13	10	13270	1174	6249	108	7657	1092	467	681	400	764	5896		
5	15	13618	1432	5751	97	7631	504	453	499	217	535	5883		
17	60	9810	1204	3590	88	5325	0.0000780	166	98	44	126	4357		
26	8	1950	284	892	51	1014	93	72	119	475	71	1261		
25	10	1950	254	905	32	1043	132	67	95	355	73	1139		

4.6.5.2 Revised surface reaction kinetics

Following the success in the revision of the Monod kinetic constants above, the surface reaction kinetics were also re-evaluated. Again, determination of constants was restricted to the shorter retention times. The steady states in Table 4.17 were used to determine the revised values for the surface reaction kinetic constants. The data set from Table 4.15, used to determine the revised Monod kinetic constants, was reduced by visually identifying outlying data points in the linearised surface reaction kinetics plot in Figure 4.27. Once the data set had been selected, the kinetic constants were calculated from the slope and intercept of the linear regression line fitted to the selected data, Figure 4.27. This gave revised values for k_{max} of 11.2mgCOD/mgZ_{ad} as COD.d and $K_S = 13.0$ mgCOD/mgZ_{ad} as COD)

Table 4.17: Steady state data points (values refer to steady state numbers in Appendix B) used to calculate the values of the revised Monod kinetics constants

Feed COD Concentration (gCOD/L)	Hydraulic Retention Time (d)							
	60	20	15	10	8	6.67	5.71	5
40								
25						7	8	9
13					14		31	
9								
2								

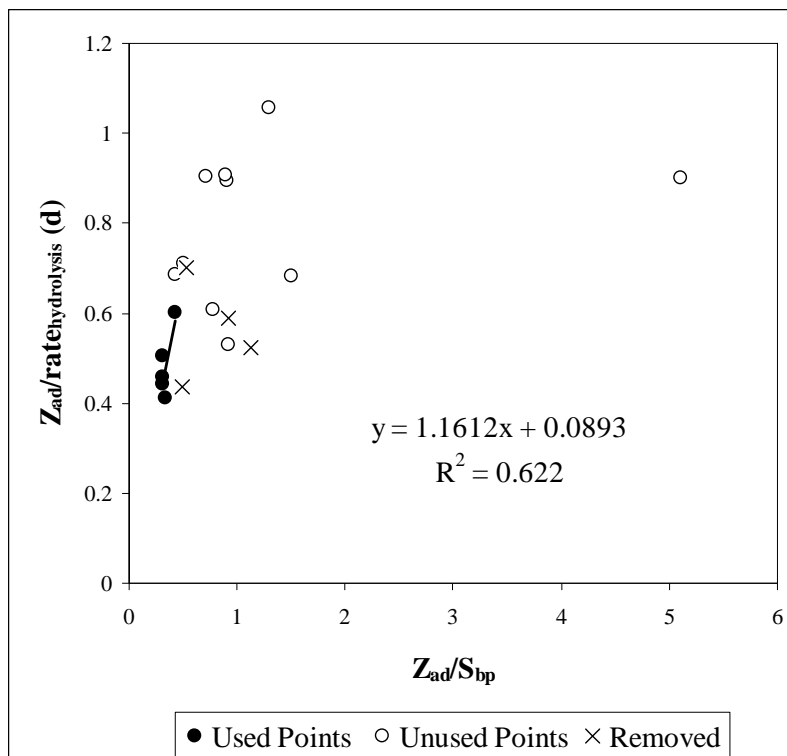


Figure 4.27: Linearised surface reaction kinetics plot for the calculation of the revised k_{max} and K_S from the slope and y-intercept ($k_{max} = 11.2$ mgCOD/mgZ_{ad}.d and $K_S = 13.0$ mgCOD/mgZ_{ad})

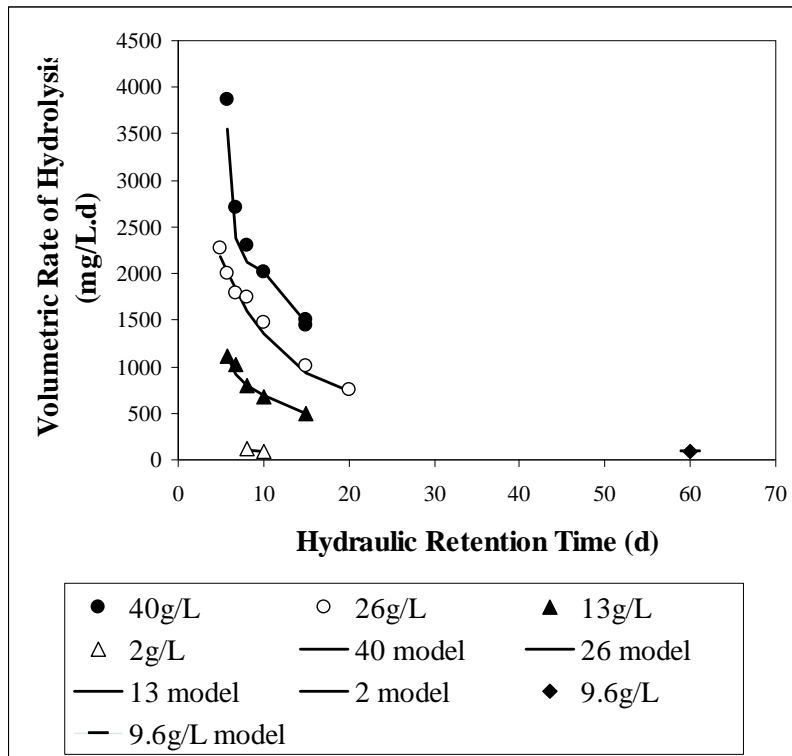


Figure 4.28: Calculated and predicted rate of hydrolysis for each feed COD concentration at each hydraulic retention time

Figure 4.28 shows the hydrolysis rates predicted with the revised values for the surface reaction kinetic constants (k_{\max} and K_S) together with the “observed” values; the model accurately predicts the rate of hydrolysis under all operating conditions, including the shorter hydraulic retention times. Of equal importance is that the model accurately predicts the rate of hydrolysis at the longer retention times, even though the kinetic constants were calibrated using the shorter retention time data only. Therefore, the hypothesis that the shorter retention times have more value in determining the magnitude of the kinetic constants is substantiated.

Figure 4.29 shows the predicted versus “observed” rates of hydrolysis for all steady state systems; the data points lie close to the diagonal (1:1 correspondence), meaning that the predictions are accurate. Similarly, the predicted and measured effluent total COD concentrations show close correlation, Figure 4.30. This illustrates that the model based on surface reaction kinetics, using the revised values for the kinetic constants, can accurately predict the effluent total COD concentration for laboratory-scale methanogenic anaerobic digesters.

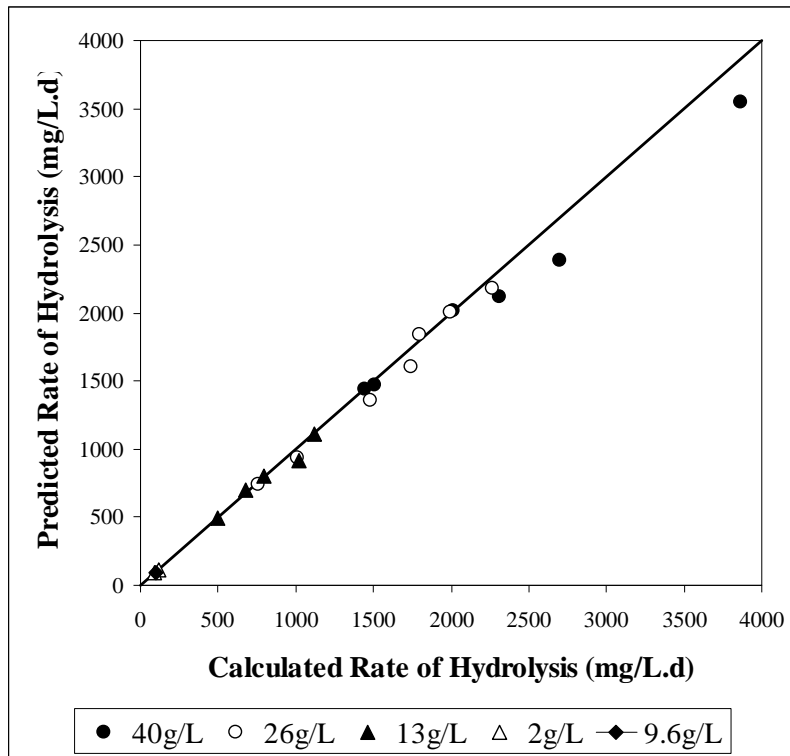


Figure 4.29: Predicted rate of hydrolysis versus the calculated rate of hydrolysis for each feed COD concentration and hydraulic retention time

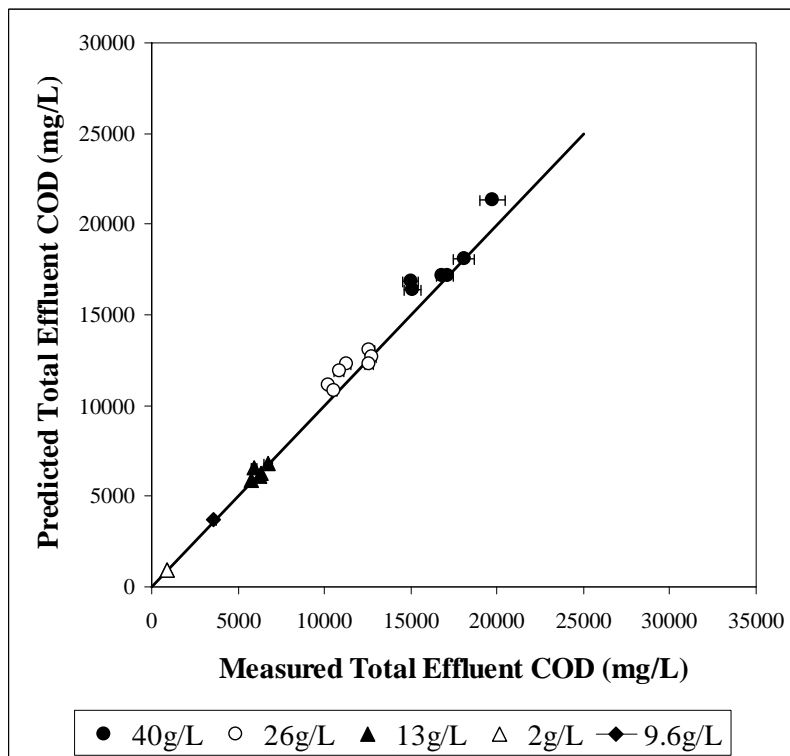


Figure 4.30: Predicted total effluent COD concentration versus measured total effluent COD concentration for each feed COD concentration and hydraulic retention time

Table 4.18: Measured and calculated values of the various components of the feed and effluent COD measurements, and the comparative calculated values predicted by the surface reaction kinetics with revised values for the kinetic constants (Concentrations in mgCOD/L; rates in mgCOD/L.d)

Steady state no.	Retention Time (d)	Measurements (mgCOD/L)				Calculated from experimental data				Surface reaction kinetics		
		Total Feed	Soluble Feed	Total Effluent	Soluble Effluent	S _{bp1}	S _{bp}	Z _{ad}	Rate of hydrolysis	S _{bp}	Rate of hydrolysis	Total Effluent
28	5.71	41441	2582	19737	295	24998	3394	1690	3868	1408	4246	18497
23	6.67	34818	4398	14984	207	18775	1262	1416	2702	797	2794	15088
21	8	34818	3828	15094	205	19345	1442	1371	2310	569	2447	14923
12	10	39810	4436	18085	256	22059	2649	1415	2016	387	2284	16875
10	15	39790	3521	16792	250	22961	1476	1343	1503	222	1639	16823
11	15	39790	3990	17167	299	22491	1843	1307	1446	219	1607	16847
9	5	24881	2694	12610	301	13865	2759	934	2270	1916	2453	12116
8	5.71	24960	2503	12729	205	14109	2977	912	1996	1256	2317	11490
7	6.67	24881	2027	12595	200	14532	2890	907	1794	882	2117	11149
2	8	25953	2675	11299	168	14598	1107	1025	1740	576	1827	11278
1	10	25953	2331	10849	178	14942	672	1010	1480	399	1531	11163
4	15	25953	2647	10212	157	14625	178	912	1012	218	1040	11018
3	20	25953	2326	10525	179	14947	617	801	758	153	821	11044
31	5.71	13186	956	6757	120	7819	1584	494	1117	1344	1166	6695
24	6.67	13579	1845	5944	96	7192	591	540	1019	768	999	6297
14	8	13270	1525	6299	104	7307	1124	479	798	561	880	6012
13	10	13270	1174	6249	108	7657	1092	467	681	400	764	5896
5	15	13618	1432	5751	97	7631	504	453	499	217	535	5883
17	60	9810	1204	3590	88	5325	0.0000780	166	98	44	126	4357
26	8	1950	284	892	51	1014	93	72	119	475	71	1261
25	10	1950	254	905	32	1043	132	67	95	355	73	1139

4.7 Hydrolysis Rate Equation Selection

Section 4.6 evaluated the various forms of hydrolysis rate formulations in predicting the rate of hydrolysis at varying feed COD concentrations and hydraulic retention times. For each rate formulation, the kinetic constants were calibrated so that the rate equation was able to accurately predict the rate of hydrolysis over the range of operating conditions. It is therefore necessary to compare the predictions of all of the rate formulations, in order to select the most appropriate rate equation to be used for further modelling.

To summarise, the four different rate equations and the values of the kinetic constants are:

$$\text{First order kinetics:} \quad \text{rate}_{\text{hydrolysis}} = k_h \cdot S_{\text{bp}} \quad (4.55)$$

where $k_h = 0.992 \pm 0.492 \text{d}^{-1}$

$$\text{First order specific kinetics:} \quad \text{rate}_{\text{hydrolysis}} = k'_h \cdot S_{\text{bp}} \cdot Z_{\text{ad}} \quad (4.56)$$

where $k'_h = 0.00138 \pm 0.00131 \text{ L/mgZ}_{\text{ad}} \text{ as COD.d}$

$$\text{Monod kinetics:} \quad \text{rate}_{\text{hydrolysis}} = \frac{\mu_{\text{max}} \cdot S_{\text{bp}} \cdot Z_{\text{ad}}}{Y_{\text{ad}} (K_S + S_{\text{bp}})} \quad (4.57)$$

where $\mu_{\text{max}} = 0.243 \text{d}^{-1}$ and $K_S = 640 \text{mgCOD/L}$

$$\text{Surface reaction kinetics:} \quad \text{rate}_{\text{hydrolysis}} = \frac{k_{\text{max}} \left(\frac{S_{\text{bp}}}{Z_{\text{ad}}} \right)}{\left(K_S + \frac{S_{\text{bp}}}{Z_{\text{ad}}} \right)} Z_{\text{ad}} \quad (4.58)$$

where $k_{\text{max}} = 11.2 \text{mgCOD/mgZ}_{\text{ad}} \text{ as COD.d}$ and $K_S = 13.0 \text{mgCOD/mgZ}_{\text{ad}} \text{ as COD}$

Conceptually, first order kinetics (Eq 4.55) oversimplify the mechanism of hydrolysis, by predicting the rate as being proportional only to the biodegradable particulate COD concentration. However, surprisingly, first order kinetics are able to predict the rate of hydrolysis with good accuracy (Figures 4.6 to 4.8). First order specific kinetics include the acidogenic biomass concentration in the rate equation, and since this biomass group is directly responsible for the hydrolysis process, intuitively this would seem to be a superior form of rate equation. Monod kinetics and surface reaction kinetics similarly include acidogen biomass in the formulation, but additionally incorporate a maximum rate of hydrolysis under conditions of high substrate and substrate/biomass concentrations respectively. In evaluating the various formulations, the difficulty is defining a specific parameter that can be used to quantify the prediction capabilities of the rate equations. For example, the percentage error between the predicted and calculated volumetric rates of hydrolysis can be calculated, see Table 4.20, which lists the calculated and predicted rates of hydrolysis for each of the rate formulations and the percentage errors.

If these mean percentage errors and standard deviations are used to select the most suitable form of the rate equation, then the first order and surface reaction kinetics are the most

suitable, because these have significantly smaller mean percentage errors and standard deviations (Table 4.20) than the other two formulations. From Table 4.20, the first order specific kinetics would appear to be the least suitable, especially at low feed COD concentrations, where the percentage error is greater than 70% for both steady states; similarly for the Monod kinetics. Thus, based on this assessment, either the first order kinetics or surface reaction kinetics would be the most suitable choice of rate equation to predict the rate of hydrolysis.

The methane production rate is another parameter that can be used to determine the most appropriate formulation for the hydrolysis rate. The measured rates are presented in Table 4.3, and Table 4.19 compares the errors between the measured rates and the rates predicted by the mathematical models containing each of the hydrolysis rate formulations.

Table 4.19 shows that the four rate formulations evaluated in this study (first order, first order specific, Monod and surface reaction kinetics) predict the methane production rates equally well (mean absolute errors of 4.35, 3.47, 4.38 and 5.46% for the first order, first order specific, Monod and surface reaction formulations respectively, with similar standard deviations) and clearly the methane production rate is less sensitive to the hydrolysis rate formulation than the measured effluent total and soluble COD concentrations, and is thus of less value in evaluating the various rate formulations.

Based on the results from Table 4.20, the first order and surface reaction kinetics most accurately predict the rate of hydrolysis for all of the steady state systems measured. However, if Eq 4.58 is rearranged in terms of the specific rate of hydrolysis:

$$\frac{\text{rate}_{\text{hydrolysis}}}{Z_{\text{ad}}} = \frac{k_{\text{max}} \left(\frac{S_{\text{bp}}}{Z_{\text{ad}}} \right)}{\left(K_s + \frac{S_{\text{bp}}}{Z_{\text{ad}}} \right)} \quad (4.59)$$

For Eq 4.59, the values for the rate of hydrolysis ($\text{rate}_{\text{hydrolysis}}$), S_{bp} and Z_{ad} can be calculated for each of the steady state data points by following the procedures detailed earlier. By calculating the ratios of $S_{\text{bp}}/Z_{\text{ad}}$, then for Eq 4.59, it is possible to construct a Monod type plot of the specific hydrolysis rate versus $S_{\text{bp}}/Z_{\text{ad}}$, Figure 4.31, using the k_{max} and K_s values determined above.

Table 4.19: Measured methane production rates (gCH₄ as COD/d) and comparisons with the predicted methane production rates for models evaluating the various hydrolysis rate formulations (first order, first order specific, Monod and surface reaction kinetics)

Steady state no.	R _h (d)	Measured methane production (gCH ₄ as COD/d)	Absolute % error between measured and predicted methane production rates			
			First order	First order specific	Monod	Surface reaction
28	5.71	80.7	7.55	0.93	0.49	12.86
23	6.67	60.4	7.20	2.02	2.00	10.80
21	8	51.6	7.91	3.46	3.61	10.87
12	10	46.1	3.53	0.65	0.50	5.86
10	15	32.3	5.16	2.48	5.15	6.64
11	15	30.6	0.07	2.82	0.02	1.45
9	5	36.1	11.89	16.67	13.15	5.06
8	5.71	35.2	3.18	7.21	7.15	2.16
7	6.67	31	1.70	5.28	6.32	2.81
2	8	29.1	2.88	0.05	0.86	6.07
1	10	28.4	no gas composition measurement			
4	15	20.5	2.31	1.32	2.82	3.79
3	20	14.4	6.22	6.69	3.53	5.04
31	5.71	24.6	3.53	9.19	7.66	8.95
24	6.67	23.3	6.11	10.52	6.24	9.67
14	8	17	6.31	1.44	6.74	2.92
13	10	13.3	10.63	6.07	10.88	7.78
5	15	10.5	0.05	3.48	1.73	1.55
17	60	2.1	2.75	7.72	13.44	3.06
26	8	2.2	errors in gas composition measurement due to low			
25	10	1.6	gas production rates (see discussion)			
mean absolute error			4.35	3.47	4.38	5.46
standard deviation			3.227	4.158	4.090	3.415

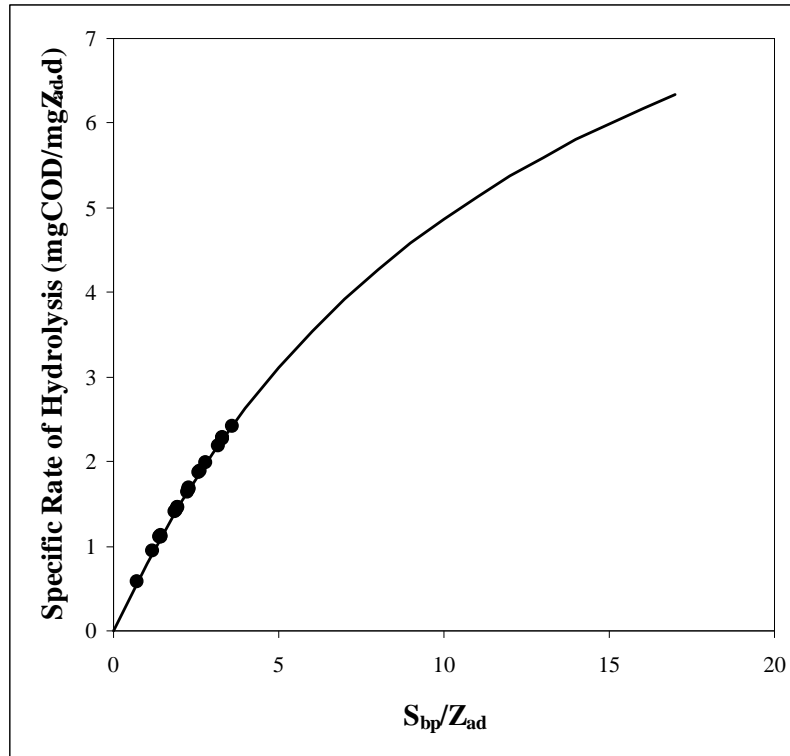


Figure 4.31: Plot of the specific rate of hydrolysis versus the saturation ratio showing that the systems are operating in the substrate-limiting region of the graph

Since $K_S = 13.0 \text{ mgCOD/mgZ}_{ad}$ as COD, and the maximum value calculated for (S_{bp}/Z_{ad}) for the various operating conditions is $3.59 \text{ mgCOD/mgZ}_{ad}$ as COD, the system is operating in the region where it is substrate limited. In this region, $K_S \gg (S_{bp}/Z_{ad})$, and Eq 4.59 can be simplified as follows:

$$\frac{\text{rate}_{\text{hydrolysis}}}{Z_{ad}} = \frac{k_{\max} \left(\frac{S_{bp}}{Z_{ad}} \right)}{K_S} \quad (4.60)$$

Simplifying:
$$\text{rate}_{\text{hydrolysis}} = \frac{k_{\max}}{K_S} S_{bp} = k_h^* \cdot S_{bp} \quad (4.61)$$

The value of k_h^* calculated from the ratio of k_{\max} and K_S is $(11.19/13.00 = 0.861 \text{ d}^{-1})$, which is almost identical to the value determined for the first order kinetic constant in Section 4.6.1 ($k_h = 0.992 \pm 0.492 \text{ d}^{-1}$). Therefore, the surface reaction kinetics are operating in the first order range of the rate formulation, and under these conditions, the rate formulations would be expected to predict similar rates of hydrolysis. Either of these rate formulations can be used to predict the rate of hydrolysis for methanogenic systems in this study, but since the first order kinetics are identified as oversimplifying the hydrolysis process, the surface reaction kinetics are identified as being the most appropriate and accurate form of hydrolysis rate kinetics. However, due to the accuracy and simplicity, the first order kinetic formulation will be used in all subsequent evaluations for acidogenic (Chapter 5) and sulfate-reducing (Chapter 7) systems in this study.

Table 4.20: Comparison of the calculated rate of hydrolysis (mgCOD/L.d) from experimental data and the rates predicted from the four rate equations tested with percentage error in the predicted rate (mean percentage error with standard deviation)

R_h (d)	Feed COD concentration (gCOD/L)	Calculated Rate (mgCOD/L.d)	First order kinetics		First order specific kinetics		Monod kinetics		Surface reaction kinetics	
			Rate	% error	Rate	% error	Rate	% error	Rate	% error
5.71	41.44	3868	3792	1.98	4178	8.00	4246	9.76	3550	8.23
6.67	34.82	2702	2507	7.20	2684	0.67	2794	3.43	2384	11.75
8	34.82	2310	2209	4.37	2338	1.23	2447	5.95	2123	8.10
10	39.81	2016	2073	2.86	2182	8.26	2284	13.32	2013	0.15
15	39.79	1503	1501	0.17	1550	3.08	1639	9.00	1474	1.97
15	39.79	1446	1471	1.73	1518	5.01	1607	11.11	1445	0.09
5	24.88	2270	2350	3.50	2471	8.85	2453	8.05	2176	4.17
5.71	24.96	1996	2142	7.32	2242	12.34	2317	16.07	2010	0.69
6.67	24.88	1794	1938	8.02	2016	12.39	2117	18.05	1839	2.53
8	25.95	1740	1666	4.24	1725	0.90	1827	4.99	1601	7.99
10	25.95	1480	1403	5.19	1440	2.70	1531	3.43	1361	8.00
15	25.95	1012	957	5.42	968	4.29	1040	2.78	940	7.11
20	25.95	758	751	0.98	755	0.48	821	8.26	741	2.25
5.71	13.19	1117	1186	6.21	1108	0.82	1166	4.42	1111	0.51
6.67	13.58	1019	961	5.70	903	11.39	999	1.91	914	10.29
8	13.27	798	834	4.56	788	1.29	880	10.22	802	0.49
10	13.27	681	719	5.56	685	0.54	764	12.16	698	2.43
15	13.62	499	499	0.00	479	4.07	535	7.19	490	1.79
60	9.81	98	96	1.79	90	7.83	126	28.97	95	2.17
8	1.95	119	116	2.53	24	79.92	71	40.62	111	6.28
10	1.95	95	98	3.59	26	72.59	73	23.11	95	0.58
mean % error \pm SD			4.36 \pm 2.24		11.75 \pm 21.85		11.56 \pm 9.56		4.17 \pm 3.73	

4.8 Unbiodegradable Particulate COD Fraction

Section 4.5 describes the algorithm used to calculate the rate of hydrolysis for each steady state system from the results of the experimental measurements of the total and soluble feed and effluent COD. The algorithm initially assumed a particulate unbiodegradable COD fraction of the total influent COD of 30%, and this value is refined based on the effluent total and soluble COD measurements for a digester operated at a 60-day retention time. The total particulate COD in the effluent from this 60-day retention time digester was assumed to consist of unbiodegradable particulate COD (S_{up}) and acidogenic (Z_{ad}) and methanogenic (Z_{am}) biomass only; any particulate organic matter remaining is considered unbiodegradable, inferring that the biodegradable particulate COD concentration (S_{bp}) concentration was zero. The unbiodegradable particulate COD fraction was then varied in the algorithm until the biodegradable particulate COD (S_{bp}) concentration was small (0.0000780mgCOD/L), and the final value of the unbiodegradable particulate COD fraction was 33.45%.

Based on this calculated value, the various formulations for the rate of hydrolysis were evaluated, and a first order rate formulation was chosen for further modelling of the rate of hydrolysis of PSS in this investigation. In this section, the unbiodegradable particulate COD fraction is re-evaluated within the model structure to find the unbiodegradable particulate COD fraction for which the first order formulation for the rate of hydrolysis predicts the “observed” rate based on the measured data with the greatest accuracy. .

The absolute % error between the “observed” rate of hydrolysis and the rate predicted by the first order rate formulation was calculated previously for each of the steady state operating systems in Section 4.7 (Table 4.20). The mean and standard deviation of these absolute error values was calculated, and from these two values, the coefficient of variation was calculated (coefficient of variation = standard deviation/mean). For an unbiodegradable particulate COD fraction of 33.45%, the mean absolute error and standard deviation is $4.36 \pm 2.24\%$ (Table 4.20) (Coefficient of variation = 0.538). The unbiodegradable particulate COD fraction was then varied between 32 and 35%, and the coefficient of variation calculated for each point (Figure 4.32). Figure 4.32 shows a distinct minimum coefficient of variation (0.515) when the unbiodegradable particulate COD fraction is 33.3% (compared to 0.538 at 33.45%). However, this difference in the unbiodegradable particulate COD fraction is insignificant, and the value of 33.45% will be used for all further analyses in this study.

Further, when using an unbiodegradable COD fraction of 33.45% of the total feed COD, and a value of $k_h = 0.992d^{-1}$ for the first order hydrolysis rate formulation, the calculated biodegradable particulate COD concentration for the 60-day retention time system was predicted as 97mgCOD/L. This value represents 2.70% of the measured total effluent COD from the digester, which is insignificant, and substantiates the reasoning that the effluent particulate COD for a 60-day retention time is unbiodegradable.

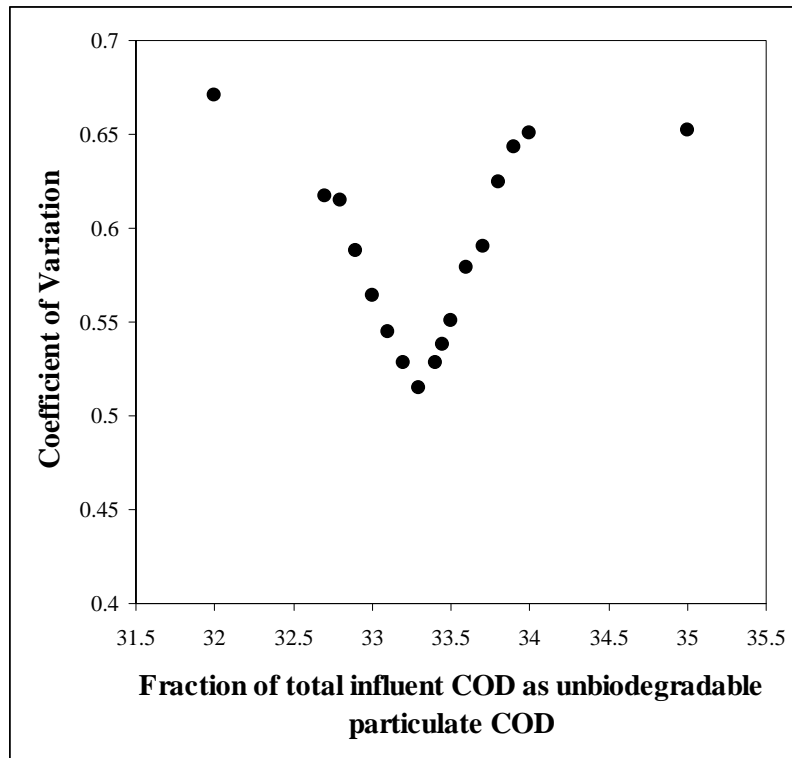


Figure 4.32: Coefficient of variation of the absolute % error between the “observed” and predicted rate of hydrolysis as a function of the unbiodegradable particulate COD fraction

4.9 Model Validation

The model developed in this chapter is able to accurately predict the experimental data that was used to calibrate the model. The experimental data used to calibrate the model was collected from systems that were operated under identical conditions, fed PSS from the same source, and had a direct influence on the values of the kinetic constants and the unbiodegradable particulate COD fraction. Other data has been obtained from two separate studies on the anaerobic digestion of solid wastes, and the model will be tested on this data.

4.9.1 Data set of O’Rourke (1968)

O’Rourke (1968) studied the kinetics of anaerobic waste treatment at reduced temperatures, since at the time, most anaerobic digestion systems were operated at 35°C, and little was known about the performance of the systems at reduced temperatures. In order to determine the changes in the kinetics of anaerobic treatment at the reduced temperatures, digesters were operated at a feed PSS concentration of 28.4 gCOD/L, at 35, 25, 20 and 15°C, and at hydraulic retention times from 60 days to as little as 2.75 days. For the evaluation here, only the systems operated at 35°C are considered, and are presented in more detail in Table 4.21.

Table 4.21 shows that systems were operated at retention times of 60, 30, 15, 10, 7.5, 5, 3.75 and 2.5 days. At the shorter retention times, alkalinity was added to the feed to maintain an operating pH in the range of 6.8 – 7.3, evidenced by the significant increase in the alkalinity for the three systems operating at retention times of 5 days and less. For these three systems, the volatile acids (VFA’s) increased from around 100mgCOD/L to over 1000mgCOD/L, indicating that the methanogenic population was no longer stable in the system, resulting in

an accumulation of soluble products. At the same time, the lipids concentration increased significantly, suggesting that the methanogenic population are somehow related to the hydrolysis of lipids. This is a phenomenon that has been reported in greater detail by Rollon-Pelenzuela (1999) (see Chapter 2). The cellulose and protein concentrations do not follow the same trend, and these are digested to a similar degree in all of the systems. A COD balance was calculated for each of the steady states, and the results show COD recoveries (95 – 105%) within the range defined as excellent for these systems (95 – 105%).

Table 4.22 and Figure 4.33 show the results of applying the first order kinetics based model to the data of O'Rourke (1968), with k_h as determined above ($0.992d^{-1}$). For the four systems with a retention time of 7 days or longer, the model is able to accurately predict the rate of hydrolysis (< 7% error in predicted rate), while at the shorter retention times, the model predicts a higher rate of hydrolysis than the experimental data indicates. This may be related to the reduced conversion of the lipids fraction at the shorter retention times, since from Table 4.21, there is no significant increase in the concentrations of the cellulose or the proteins. At the same time, the methanogens were unable to utilize all of the VFA produced, but it is unclear whether the methanogens influence the rate of hydrolysis of lipids, or whether the lipids inhibit the methanogenic activity, or both or either are inhibited by the VFA's and dissolved hydrogen gas. Clearly, the absence of a stable methanogenic population influences the rate of hydrolysis of PSS.

The ability of the model to accurately predict the behaviour of a completely independent data set under methanogenic conditions provides substantive support validating the model developed here. The model should provide a good platform for a more comprehensive model, including chemical and physical processes as well as the biological processes.

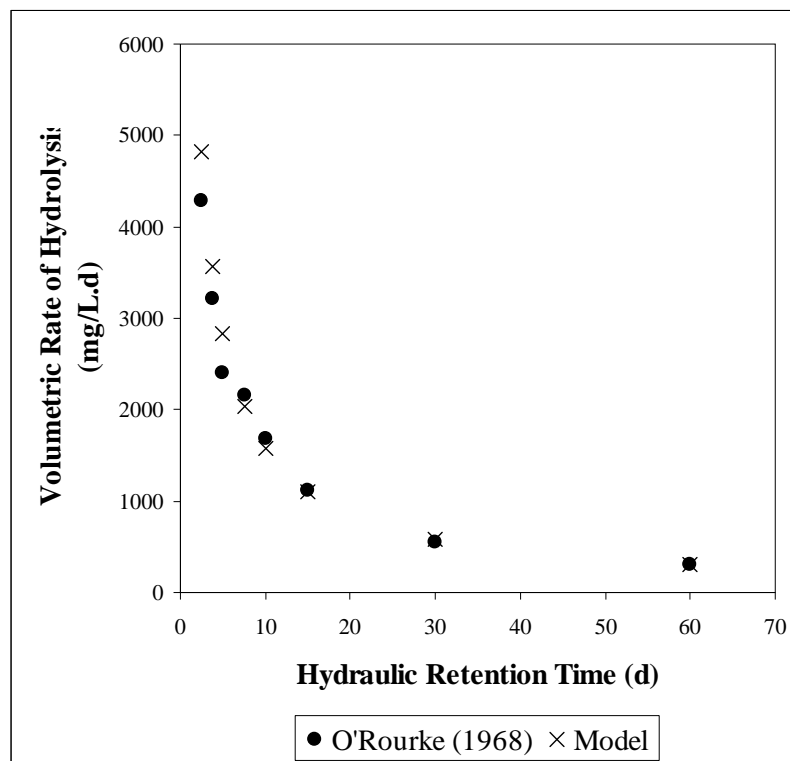


Figure 4.33: Calculated (from experimental data) and predicted (first order kinetics) rate of hydrolysis for each hydraulic retention time for the data of O'Rourke (1968)

Table 4.21: Experimental data from O'Rourke (1968) with COD mass balances calculated in this study

R_h (d)	Volatile solids	Total COD	Lipids	Cellulose	Protein	Volatile acids	Alkalinity	pH Range	Gas Production (mLCH₄/gCOD biodegradable added)	% COD Balance
Feed	18.4	28.4	12.6	4.47	6.40	1.02				
60	6.6	10.3	3.52	0.33	3.67	0.03	2.3	7.0 – 7.4	347	99.4
30	7.1	11.8	4.45	0.36	3.78	0.06	2.0	7.0 – 7.4	350	105.3
15	7.2	11.8	4.07	0.44	4.35	0.06	1.8	6.9 – 7.3	330	101.6
10	8.1	11.7	4.66	0.34	4.33	0.09	1.6	6.8 – 7.3	328	100.9
7.5	8.3	12.4	5.05	0.41	4.32	0.14	1.8	6.9 – 7.3	308	99.7
5	13.8	20.9	12.2	0.42	4.27	2.53	3.6	6.8 – 7.2	118	95.1
3.75	15	24.2	13.0	0.43	4.32	4.69	4.9	6.9 – 7.3	87.5	101.1
2.5	15.2	25.4	12.6	0.43	4.40	4.64	5.2	7.1 – 7.4	34.5	99.9

Table 4.22: Model calculated values for the various species from the data of O'Rourke (1968) with the model prediction of the rate of hydrolysis and the associated percent error (Total feed concentration = 28400 mgCOD/L, soluble feed concentration = 2040 mgCOD/L)

R_h (d)	Influent						Effluent						Model Prediction			
	S_{npi} (33.44%)	S_{bpi}	S_{nsi}	S_{bsfi}	S_{VFAi}	Measured total COD	Measured soluble COD	S_{bp}	S_{ns}	S_{bsf}	S_{VFA}	Rate of hydrolysis	S_{bp}	Rate of hydrolysis	% Error in Rate	Effluent total COD
60	9499	16861	227	906	906	10300	60	88	60	0	0	306	304	302	1.3	10509
30	9499	16861	227	906	906	11800	120	1255	120	0	0	557	586	581	-4.3	11168
15	9499	16861	227	906	906	11800	120	907	120	0	0	1115	1109	1101	1.3	11987
10	9499	16861	227	906	906	11700	180	550	180	0	0	1690	1595	1582	6.4	12657
7.5	9499	16861	227	906	906	12400	280	1096	227	26.4	26.4	2163	2049	2033	6.0	13214
5	9499	16861	227	906	906	20900	5060	5087	227	2416.4	2416.4	2405	2853	2830	-17.7	18111
3.75	9499	16861	227	906	906	24200	9380	4852	227	4576.4	4576.4	3222	3589	3560	-10.5	22987
2.5	9499	16861	227	906	906	25400	9280	6185	227	4526.4	4526.4	4288	4860	4821	-12.4	24129

4.9.2 Data set of Izzett *et al.* (1992)

Izzett *et al.* (1992) studied the effects of thermal pre-treatment on the anaerobic digestion of a mixture of primary and humus sludge. The mixture ratio of the two sludges was not reported. The sludge was digested in 14L digesters under methanogenic conditions. The systems were operated at 37°C, completely mixed and were not pH controlled. The digesters were batch fed once or twice daily depending on the volume of sludge being fed per batch, and operated at steady state retention times of 20, 15, 12, 10 and 7 days. When the systems were operated at a 4-day retention time, methanogenesis 'failed'. The feed and effluent were analysed so that COD, N and P balances could be calculated. The measured data and results of the COD analyses are reported in Table 4.23.

The feed sludge was collected every 14 days and stored at 4°C to minimise the effects of storage. Each system was operated for three retention times, and for the longer retention times, several batches of feed sludge were required before a steady state of operation was achieved. Analysis of the data showed that the second of the three feed batches used for the 15-day retention time differed considerably from the other two, so that reliable steady state operation was not possible.

Applying the first order hydrolysis kinetics based model developed in this chapter to the data of Izzett *et al.* (1992) in Table, 4.23, the predicted effluent total COD concentrations and rates of hydrolysis can be compared to the measured and values calculated from the experimental data in Table 4.24. The predicted rates of hydrolysis for all of the retention times of the Izzett *et al.* (1992) data set (Table 4.16) are greater than the rates calculated from the first order model calibrated on the experimental data from this study. Consequently, the predicted effluent total COD concentrations are consistently less than the measured effluent COD concentrations. Clearly, the model is unable to accurately predict the rate of hydrolysis of the mixture of PSS and humus sludge used as feed by Izzett *et al.* (1992). It is not clear whether the differences in the rates are due to the different sources of PSS, or whether the humus sludge digests at a significantly lower rate and therefore reduces the overall rate of hydrolysis of the combined sludge. This is an area that requires further investigation.

Table 4.23: Experimental data from Izzett *et al.* (1992) with COD mass balances calculated in this study

R_h (d)	Feed				Effluent				Gas Production (L/d)	% CH ₄	% COD Balance
	Total COD (g/L)	VFA (mgHAc/L)	Alkalinity (mgCaCO ₃ /L)	pH	Total COD (g/L)	VFA (mgHAc/L)	Alkalinity (mgCaCO ₃ /L)	pH			
20	42.595	2249	56	5.28	19.005	23	2066	7.15	11.053	63.3	107.3
12	39.222	2872	90	5.20	18.678	28	2072	7.20	16.696	63.3	109.1
10	40.721	1961	81	5.34	20.521	28	1951	7.11	20.070	62.1	108.6
7	43.286	1871	80	5.35	23.637	50	1882	7.12	27.932	63.2	108.4

Table 4.24: Model calculated values for the various species from the data of Izzett *et al.* (1992) with the model prediction of the rate of hydrolysis and the associated percent error (Concentrations in mgCOD/L; Rates in mgCOD/L.d)

R_h (d)	Influent										Effluent					Model Prediction	
	S_{bpi} (33.44%)	S_{hsi}	S_{bsfi}	S_{VFAl}	Measured total COD	Measured soluble COD	S_{bp}	S_{ns}	S_{bsf}	S_{VFAs}	Rate of hydrolysis	S_{bp}	Rate of hydrolysis	% Error in Rate	Effluent total COD		
20	14247	23510	341	2249	19005	60	2842	341	0	1096	1193	1183	-7.9	17466			
12	13118	20046	314	2872	18678	120	3628	314	0	1433	1620	1607	-12.1	16830			
10	13620	22853	326	1961	20521	120	4842	326	0	1870	2165	2147	-14.8	18068			
7	14478	24720	346	1871	23637	180	6967	346	0	2610	3189	3164	-21.2	20203			

4.10 Conclusions and Future Work

A simple mathematical model, involving biological processes only, was developed to predict the rate of hydrolysis of PSS under anaerobic conditions. The model was calibrated on experimental data obtained from operating anaerobic digesters at varying feed COD concentrations (2 – 40g/L) and hydraulic retention times. The experimental results show that stable methanogenic systems can be operated at retention times as low as 5 days, but at reduced feed COD concentrations (2gCOD/L), the operating pH and alkalinity concentrations were low, and the methanogenic biomass possibly became pH inhibited.

The rate of hydrolysis was calculated for each of the 21 steady states measured in the experimental study, and various rate formulations were tested in order to select the rate equation that was able to predict the rate of hydrolysis under all of the operating conditions. Four equations were tested (first order, first order specific, Monod and surface reaction kinetics), with the first order and surface reaction kinetics most accurately predicting the rate of hydrolysis under all of the operating conditions. However, due to the operating conditions, the surface reaction kinetics equation could be simplified to resemble first order kinetics, which a calculated kinetic constant within the range of values calculated for the first order kinetics.

For a steady state model predicting the performance of completely mixed digesters, first order kinetics for the rate of hydrolysis are adequate. However, when solids retention is present in the experimental system, and the biomass concentration is increased, surface reaction kinetics would be, conceptually, a superior choice since the acidogenic biomass concentration is included in the rate equation directly.

The mathematical model was then used to predict the results from two other anaerobic digestion studies. The first study (O'Rourke, 1968) tested the performance of anaerobic digesters fed PSS at different temperatures, and for the systems operated at 35°C, the model was able to accurately predict the rate of hydrolysis and effluent total COD concentration for all hydraulic retention times operating under methanogenic conditions. However, for the second study, anaerobic digesters were fed a mixture of PSS and humus sludge at 37°C, and the model predicted a greater rate of hydrolysis, and therefore a lower effluent total COD concentration for each steady state hydraulic retention time.

The model developed in this chapter is able to accurately predict the performance of anaerobic digesters fed PSS only, and operated under methanogenic conditions at 35°C. The model is unable to accurately predict the rate of hydrolysis when methanogenic conditions are not maintained. The model was calibrated on systems fed PSS only, and for mixtures of PSS and other sludges (waste activated and humus sludge), the rates of hydrolysis of the individual sludges and the combined sludges needs to be determined.

As mentioned before, the model developed in this chapter forms part of a larger modelling exercise, and the larger model will be validated on the experimental results from this study. Specifically, the pH, alkalinity and gas composition measured in this study is important to the modelling exercise, where acid/base, solids/liquid and vapour/liquid equilibria are included. The model developed here also forms a basis for comparison between the methanogenic systems in this chapter and the acidogenic and sulfidogenic systems studied and presented in Chapters 5, 6 and 7.

Chapter 4: Methanogenic Systems

Chapter 5

Acidogenic Systems

5.1 Introduction

Acidogenic systems refer to anaerobic digestion of complex organic matter (normally sludges) where the acidogenic biomass only is present (no subsequent methanogenesis or sulfidogenesis). The products of these systems include soluble readily biodegradable COD, mostly VFA's such as acetic acid. Acidogenic systems have been operated mainly to produce readily biodegradable organic substrates to augment downstream BNR activated sludge systems in sewage treatment (e.g. Venter *et al.*, 1977; Eastman and Ferguson, 1982; Pitman *et al.*, 1983, Barnard, 1984; Lilley *et al.*, 1991; Elefsiniotis and Oldham, 1993; Brinch *et al.*, 1994; Skalsky and Daigger, 1995; Hatziconstantinou *et al.*, 1996, Andreasen *et al.*, 1997; Banerjee *et al.*, 1998; Banister and Pretorius, 1998).

In these studies, mainly net production of VFA and soluble COD are reported, as well as factors influencing VS reduction efficiencies (see Chapter 2, Section 2.4), but a structured modelling approach to determine the rate of hydrolysis of the particulate substrate or the soluble COD and VFA production rates based on the feed characteristics and digester operating conditions are not reported. Such a structured modelling approach will be beneficial as an aid in the design, operation and control of acidogenic systems. Also, it will be of use for the proposed implementation in a two-stage system of acidogenesis of PSS (first stage) to produce substrates favourable for subsequent external sulfate reduction (second stage) (Rose *et al.*, 2002; see Chapter 7).

The aim of this chapter is to develop such a modelling approach based on the framework for the modelling of anaerobic digestion of PSS established in Chapter 4. This will enable determination of the rate of hydrolysis of PSS under acidogenic conditions, and comparison of this rate with the rate of hydrolysis of PSS under methanogenic conditions, as determined in Chapter 4. To achieve this aim, experimental data was collected from anaerobic digesters operating under acidogenic conditions at varying feed COD concentrations and hydraulic retention times. The mathematical model developed in Chapter 4 was modified to exclude the methanogenic processes, and then applied to determine the rate of hydrolysis of PSS under acidogenic conditions. This rate was then compared with the hydrolysis rate under methanogenic conditions.

5.2 Experimental Program

Steady state acidogenic digesters were operated at laboratory-scale over a range of feed COD concentrations and hydraulic retention times. In Chapter 4, the completely-mixed anaerobic

digesters were operated under methanogenic conditions at varying feed concentrations (40gCOD/L – 2gCOD/L), and for each feed concentration, the hydraulic retention time was reduced until the methanogenic biomass became unstable. This instability led to an increase in the effluent VFA concentration, a reduction in the effluent alkalinity, a decrease in gas production, and a decrease in the digester pH. Once this instability was observed, usually by the associated changes in all four parameters simultaneously, the retention times in these systems were reduced to 3.33 days to ensure that all of the methanogenic biomass was washed out, and hence acidogenic conditions established. A retention time of 3.33d was selected because the increments in the feed volume per feed cycle would be consistent, i.e. 3, 2 and 1L for the 3.33, 5 and 10d retention times. Izzett *et al.* (1992) was unable to maintain a stable methanogenic population at a 4d retention time (see Chapter 2, Section 2.3). Each digester was allowed to reach a steady state of operation at these reduced retention times (initially more than 3 retention times), before the system was analysed in more detail. The feed rate was then decreased/ retention time increased to a 5-day retention time. Once again, the steady state was analysed. Thereafter, the retention time increased to a 10-day retention time and the steady state analysed. No methanogenesis was observed, indicated by a low gas production, even at the longer retention times.

For each feed COD concentration, Table 5.1 lists the hydraulic retention times for which steady state acidogenic systems were analysed. The numbers in Table 5.1 refer to the steady state numbers, and in Appendix B, each steady state is described in more detail, and the mean and standard deviations reported for each measured steady state parameter. Also, in Appendix B, daily measurements of pH and gas production are plotted for the entire period of that experiment and for each steady state period, the measured values for all of the daily analyses are tabulated. Digester operational procedures, sampling and sample analysis were as described in Chapter 4.

Table 5.1: Acidogenic steady states measured for varying hydraulic retention times and feed COD concentrations; numbers refer to steady state index, detailed results in Appendix B

Feed COD Concentration (gCOD/L)	Hydraulic Retention Time (d)		
	10	5	3.33
40		30	29
13	38	33	32
2	39	35	34

5.3 Mathematical Model

In order to interpret the results obtained for each of the acidogenic steady states listed in Table 5.1, the mathematical model developed for methanogenic systems in Chapter 4 was modified to represent the changes in the digester between the methanogenic and acidogenic conditions.

5.3.1 Model structure

The main difference between the model structure used for the methanogenic model (Figure 4.1) and the acidogenic model (Figure 5.1) is the absence of the methanogenic biomass groups with associated VFA and H₂ consumption and CO₂ and methane production. This omission results in more organic species leaving the system as soluble COD: for acidogenic

systems the effluent total soluble COD concentration consists of unbiodegradable soluble COD (S_{us}), biodegradable fermentable soluble COD (S_{bsf}) and VFA's (S_{VFA}) (Figure 5.1), whereas in methanogenic systems, the effluent soluble COD consisted of unbiodegradable soluble COD only (Figure 4.1). For the effluent particulate COD, in both types of systems, this is made up of unbiodegradable particulates (S_{up}), residual biodegradable particulates (S_{bp}), and biomass (Z). However, whereas for the methanogenic systems, the biomass comprises acidogenic (Z_{ad}) and methanogenic (Z_{am}) groups, for the acidogenic systems as noted above it comprises the acidogenic group (Z_{ad}) only.

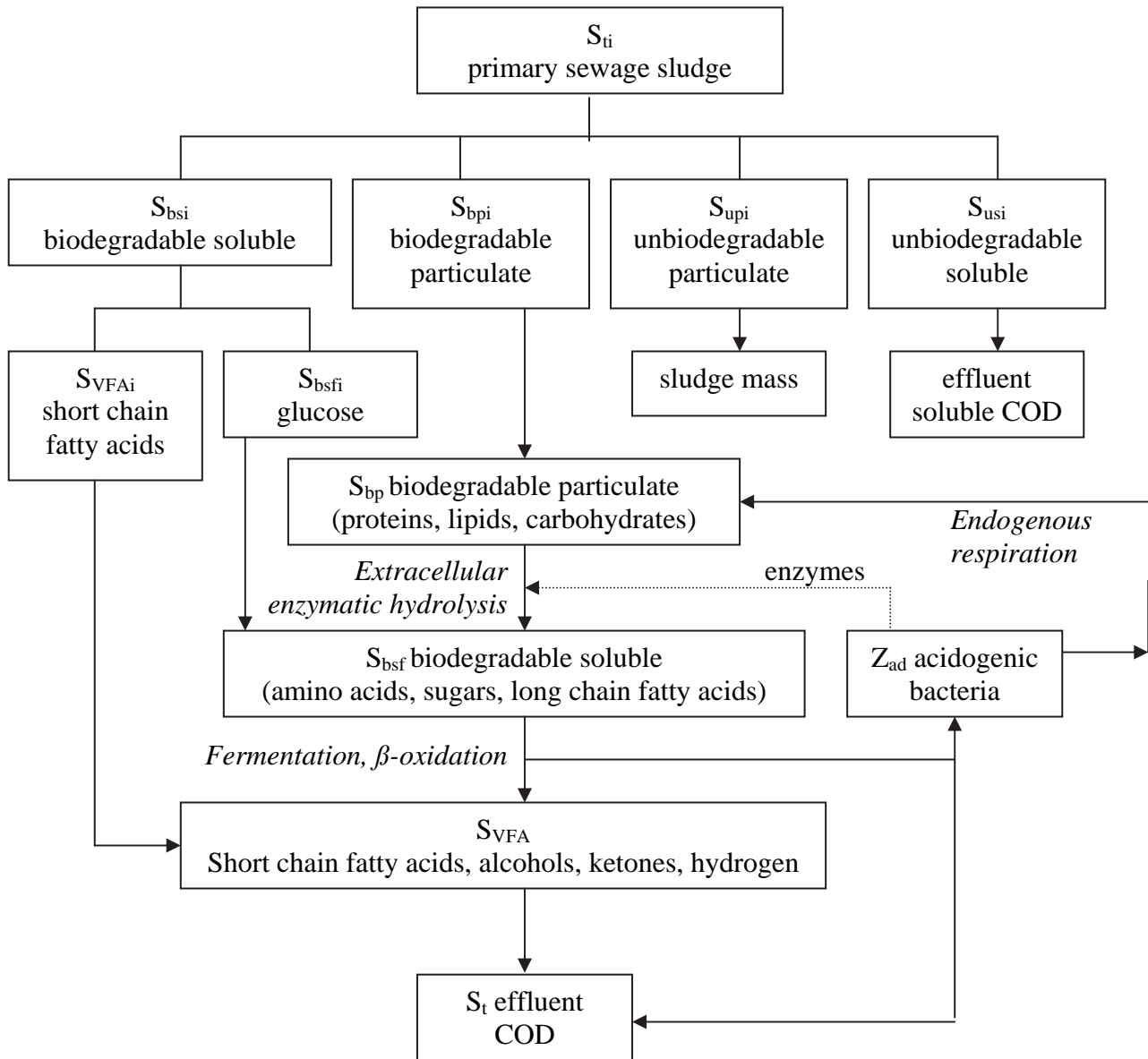


Figure 5.1: Schematic diagram (in units of COD) of the bulk processes involved in the anaerobic digestion of primary sewage sludge under acidogenic conditions (modified from Figure 4.1)

5.3.2 Model assumptions

The acidogenic model was based on the following assumptions:

- As for the methanogenic model (Chapter 4), the PSS total COD (S_{ti}) consists of an unbiodegradable particulate fraction (S_{upi}), biodegradable particulate fraction (S_{bpi}), unbiodegradable soluble fraction (S_{usi}), biodegradable soluble non-VFA fraction (S_{bsfi}) and volatile fatty acids (S_{VFai})

$$S_{ti} = S_{upi} + S_{bpi} + S_{usi} + S_{bsfi} + S_{VFai} \quad (5.1)$$

- Under stable operating conditions, only one group of organisms act on the biodegradable COD, namely acidogens (Z_{ad})
- The effluent total COD (S_t) for acidogenic systems consists of the unbiodegradable particulate fraction (S_{up}), biodegradable particulate fraction (S_{bp}), unbiodegradable soluble fraction (S_{us}), biodegradable fermentable soluble fraction (S_{bsf}), volatile fatty acids (S_{VFA}) and the acidogenic biomasses (Z_{ad})

$$S_t = S_{up} + S_{bp} + S_{us} + S_{bsf} + S_{VFA} + Z_{ad} \quad (5.2)$$

- Active acidogenic biomass concentration in the influent is negligible ($Z_{adi} = 0$)
- Acidogenic biomass grows according to Monod kinetics, using hydrolysis products as organic substrate
- Endogenous respiration of acidogenic biomass forms biodegradable particulate COD; endogenous residue formation is considered negligible
- Effluent soluble biodegradable and VFA concentrations are produced in a net 1: 1 COD ratio (Lilley *et al.*, 1992)

5.3.3 Reaction stoichiometry

The reaction stoichiometry does not change from the methanogenic model developed in Chapter 4, and was used directly in this acidogenic model.

5.3.4 Mass balances

Following the procedures developed in Chapter 4, in order to determine the rate of hydrolysis, mass balances were developed for the biodegradable particulate COD and acidogen biomass concentrations (Q = volumetric flow rate, L/day; V = reactor volume, L; b = relevant organism specific endogenous respiration rate constant, d^{-1}). For the biodegradable particulate COD (S_{bp}):

$$dS_{bp} \cdot V = Q \cdot S_{bpi} \cdot dt - Q \cdot S_{bp} \cdot dt - V \cdot \text{rate}_{\text{hydrolysis}} \cdot dt + V \cdot b_{ad} \cdot Z_{ad} \cdot dt \quad (5.3)$$

Rearranging:
$$\frac{dS_{bp}}{dt} = \frac{Q}{V} (S_{bpi} - S_{bp}) - \text{rate}_{\text{hydrolysis}} + b_{ad} \cdot Z_{ad} \quad (5.4)$$

$$\text{At steady state:} \quad \text{rate}_{\text{hydrolysis}} = \frac{Q}{V}(S_{\text{bpi}} - S_{\text{bp}}) + b_{\text{ad}} \cdot Z_{\text{ad}} \quad (5.5)$$

For the acidogenic biomass (Z_{ad}):

$$dZ_{\text{ad}} \cdot V = Q \cdot Z_{\text{adi}} \cdot dt - Q \cdot Z_{\text{ad}} \cdot dt + Y_{\text{ad}} \cdot \text{rate}_{\text{acidogenesis}} \cdot V \cdot dt - b_{\text{ad}} \cdot Z_{\text{ad}} \cdot V \cdot dt \quad (5.6)$$

$$\text{Rearranging:} \quad \frac{dZ_{\text{ad}}}{dt} = \frac{Q}{V}(Z_{\text{adi}} - Z_{\text{ad}}) + Y_{\text{ad}} \cdot \text{rate}_{\text{acidogenesis}} - b_{\text{ad}} \cdot Z_{\text{ad}} \quad (5.7)$$

$$\text{At steady state:} \quad Z_{\text{ad}} = \frac{Y_{\text{ad}} \cdot \text{rate}_{\text{acidogenesis}} \cdot R_{\text{h}}}{(1 + b_{\text{ad}} \cdot R_{\text{h}})} \quad (5.8)$$

In order to simulate the 1:1 ratio between the soluble biodegradable COD (S_{bsf}) and VFA COD (S_{VFA}) concentrations, the rate of acidogenesis was accepted to be half the rate of hydrolysis, so that for 2g soluble COD produced by hydrolysis, 1g is acidified to VFA as COD in acidogenesis. This ratio was measured and ranged from 1.7 to 2.0 g total sol COD/g VFA COD (i.e. a 1:1 ratio between S_{bsf} and S_{VFA}) (Appendix A), in agreement with the observations of Venter *et al.* (1977) and Lilley *et al.* (1991), but in contrast with other studies which have shown that up to 90% of the total soluble COD may be in the form of VFA's (Eastman and Ferguson, 1981; Elefsiniotis and Oldham, 1994) (see Chapter 2, Section 2.4 for details). In application of the equations above to the experimental data, the value for this ratio affects the rate of acidogenesis, which in turn affects the acidogenic biomass concentration, which in turn affects the rate of hydrolysis through the endogenous respiration term ($b_{\text{ad}} \cdot Z_{\text{ad}}$) in the hydrolysis rate equation (Eq 5.5). However, the term $b_{\text{ad}} \cdot Z_{\text{ad}}$ in Eq 5.5 is around 1% of the total rate ($\text{rate}_{\text{hydrolysis}}$), which can be ignored, and therefore the exact value of the sol COD: VFA COD ratio chosen for the acidogenesis rate is not of any importance in this modelling exercise. However, the value for this ratio would affect the effluent pH, and any possible downstream processes, and would need to be taken into account when these are considered, but do not form part of this study.

Therefore, by solving Equations 5.5 and 5.8 simultaneously for each steady state, the rate of hydrolysis could be calculated. These rates require that the concentration of each organic species in Eqs 5.1 and 5.2 be quantified, see below.

5.4 Experimental Results

For each steady state of operation, a COD balance was calculated based on the feed total COD concentration and the effluent total COD concentration. These values are shown in Table 5.2. As for the methanogenic systems (Table 4.2), the COD recoveries are excellent, and hence further analysis of the results can be performed with confidence.

The operating pH in all of these systems was around 5.0 as expected, which is well below the pH limit for the methanogens of between 6.0 and 6.5 (see Chapter 6). Also, since no CH_4 gas production was taken into account in the COD mass balance calculations, and the balances were close to 100%, implies that the amount of CH_4 produced was negligible, indicating that acidogenic conditions existed. This was substantiated by measurement of negligible gas production. Thus, truly acidogenic conditions prevailed in all systems, enabling development and correct calibration of the acidogenic model.

Table 5.2: COD recoveries (%) for the steady state acidogenic systems listed in Table 5.1

Feed COD Concentration (gCOD/L)	Hydraulic Retention Time (d)		
	10	5	3.33
40		95.5	92.6
13	97.8	97.8	96.6
2	96.6	95.6	102.2

5.5 Rate of Hydrolysis Calculation

From Eq 5.1, the feed total COD consists of five components:

$$S_{ti} = S_{upi} + S_{bpi} + S_{usi} + S_{bsfi} + S_{VFai} \quad (5.9)$$

From Eq 5.2, the effluent total COD also consists of five components:

$$S_t = S_{up} + S_{bp} + S_{us} + S_{bsf} + S_{VFA} + Z_{ad} \quad (5.10)$$

The feed particulate COD concentration ($S_{upi} + S_{bpi}$) could be calculated directly from the measured feed total and soluble COD concentrations. Using the same unbiodegradable particulate COD fraction as for the methanogenic systems in Chapter 4 of 33.45% (same PSS feed used for both types of systems), the feed biodegradable particulate COD concentration could be calculated (S_{bpi} , see Chapter 4). By initially accepting that the acidogenic biomass concentration (Z_{ad}) was equal to zero, the effluent particulate COD concentration ($S_{up} + S_{bp}$) could also be calculated from the measured total and soluble COD concentrations. Accepting that the effluent unbiodegradable particulate COD concentration was equal to that in the influent ($S_{up} = S_{upi}$), then the effluent biodegradable particulate COD (S_{bp}) could be calculated. From this S_{bp} , an initial PSS hydrolysis rate ($\text{rate}_{\text{hydrolysis}}$) could be calculated via Eq 5.5. This initial rate of hydrolysis was used to calculate an initial rate of acidogenesis at half the hydrolysis rate. This in turn was used to calculate an initial acidogenic biomass concentration via Eq 5.8. This concentration was substituted into Eq 5.5, and a revised rate of hydrolysis calculated. This procedure was iterated until the values converged. Resultant data are listed in Table 5.3, and Figure 5.2 shows the calculated rates of hydrolysis for each steady state at varying feed COD concentrations and hydraulic retention times.

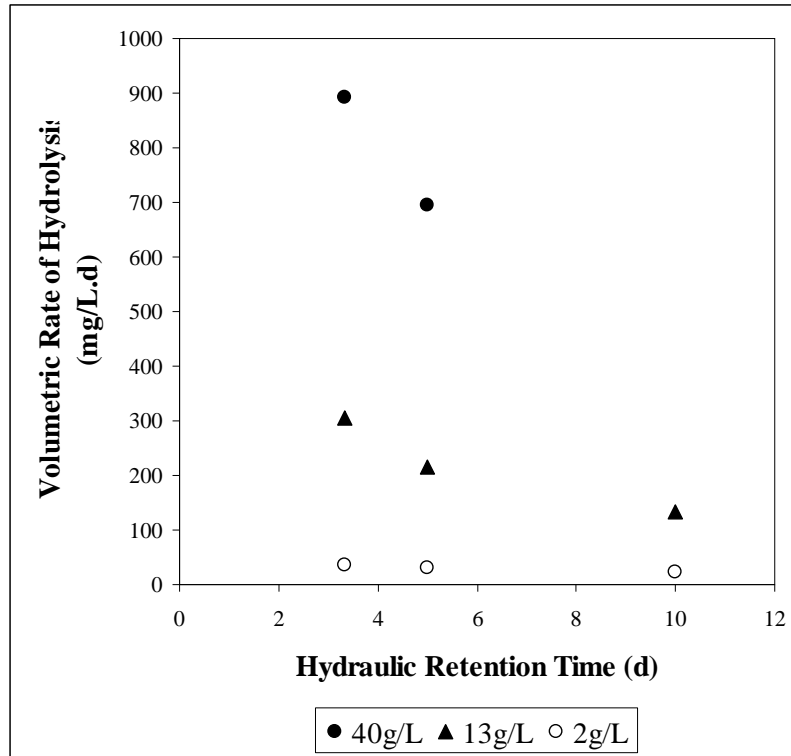


Figure 5.2: Calculated rate of hydrolysis for each feed COD concentration at each hydraulic retention time for acidogenic systems

Table 5.3: Measured and calculated values of the various components of the feed and effluent COD measurements, and the calculated rates of hydrolysis for each steady state (Concentrations in mgCOD/L; rates in mgCOD/L.d)

Steady state no.	Retention Time (d)	Measurements (mgCOD/L)				Determined parameters (mgCOD/L)						Rates (mgCOD/L.d)			
		Influent		Effluent		Influent			Effluent						
		Total Feed (S_{ti})	Soluble Feed	Total Effluent (S_t)	Soluble Effluent	S_{upi}	S_{bpi}	S_{usi}	S_{bsfi}	S_{up}	S_{bp}		S_{us}	S_{bsf}	Z_{ad}
30	5	42030	4416	39889	7738	14058	23556	336	2040	14058	17881	336	3701	213	1144
29	3.33	41206	3901	37992	6739	13782	23523	330	1786	13782	17221	330	3205	250	1901
32	3.33	13186	1248	12676	2219	4410	7527	105	571	4410	5986	105	1057	61	465
33	5	13186	1382	12823	2405	4410	7394	105	638	4410	5954	105	1150	54	290
38	10	13186	1467	12782	2732	4410	7309	105	681	4410	5584	105	1313	56	175
39	10	2017	224	1934	434	675	1118	16	104	675	815	16	209	10	31
34	3.33	2013	192	2053	306	673	1148	16	88	673	1071	16	145	3	23
35	5	2011	211	1915	359	673	1127	16	98	673	871	16	171	12	52

$$S_{upi} = 0.3345 \times S_{ti}$$

Table 5.4: Comparison of the calculated PSS rates of hydrolysis under acidogenic conditions with the rates predicted by the model developed for methanogenic conditions, with constants calibrated for methanogenic conditions
(Concentrations in mgCOD/L; rates in mgCOD/L.d)

Steady state no.	Retention Time (d)	Total Feed (S_{fi})	Soluble Feed	Total Effluent (S_t)	Soluble Effluent	S_{bpi}	S_{bp}	Z_{ad}	% S_{bp} Conversion	Methanogenic Model prediction			
										Rate of hydrolysis	S_{bp}	Z_{ad}	Rate of hydrolysis
30	5	42030	4416	39889	7738	23556	17881	213	24.09	1144	3979	734	3946
29	3.33	41206	3901	37992	6739	23523	17221	250	26.79	1901	5486	716	5440
32	3.33	13186	1248	12676	2219	7527	5986	61	20.48	465	1756	229	1741
33	5	13186	1382	12823	2405	7394	5954	54	19.48	290	1249	230	1238
38	10	13186	1467	12782	2732	7309	5584	56	23.60	175	678	214	672
39	10	2017	224	1934	434	1118	815	10	27.08	31	104	33	103
34	3.33	2013	192	2053	306	1148	1071	3	6.76	23	268	35	266
35	5	2011	211	1915	359	1127	871	12	22.71	52	190	35	189

5.6 Comparison of Rates of Hydrolysis of PSS under Methanogenic and Acidogenic conditions

In order to compare the calculated rates of PSS hydrolysis for each steady state in Table 5.3 for acidogenic systems with those for the methanogenic systems in Chapter 4 (Table 4.10), the mathematical model developed above was applied to the acidogenic systems' operating data in Table 5.3, but with the hydrolysis first order rate constant calibrated in application to the methanogenic systems ($k_h = 0.992d^{-1}$). For all acidogenic systems, the mathematical model predicted a rate of hydrolysis that is many times higher than the calculated rate (Table 5.4). Clearly, the PSS hydrolysis process is substantially slower under acidogenic conditions than under methanogenic conditions (as noted for O'Rourke, 1968 and Miron *et al.*, 2000, see Chapter 2, Section 2.3). As to a reason for the slower rate, there is insufficient information in this study to determine whether the process is inhibited by the products of hydrolysis (VFA, long-chain fatty acids, low pH) or by the increased concentrations of the substrates of hydrolysis (such as lipids). This is an area that requires further investigation, specifically measuring the lipids and long-chain fatty acid concentrations, as well as controlling the VFA concentration by external addition, in order to isolate the parameters that cause the hydrolysis rate to be substantially lower under acidogenic conditions than under methanogenic conditions.

The consequence of the reduced hydrolysis rate under acidogenic conditions is the reduced conversion of the biodegradable particulate COD (S_{bp}). Figure 5.3 compares this conversion for the methanogenic systems reported in Chapter 4 with the results of the acidogenic systems operated in this chapter. Also included are the conversions for the acidogenic and methanogenic systems operated by O'Rourke (1968). Figure 5.3 shows that for the systems operated in this investigation under methanogenic conditions, the biodegradable particulate COD conversion exceeds 78% at all retention times, and for methanogenic systems operating with a retention time of greater than 10 days, the biodegradable particulate COD conversion is greater than 90%. Similarly for the results of O'Rourke (1968), where for "true" methanogenic conditions, the biodegradable particulate COD conversion is greater than 90%. However, for the O'Rourke (1968) data, as soon as methanogenesis is incomplete, the conversion decreases, and for the fully acidogenic systems (no methanogenesis), the conversion is less than 15%. Near identical results have been obtained in this study: for all the acidogenic systems in this study (all fully acidogenic), the biodegradable particulate COD conversion was between 10 and 21%, even at the 10-day retention times, substantiating that the rate of hydrolysis is significantly reduced compared with methanogenic conditions.

Clearly, the data presented in this study, and substantiated by the observations of O'Rourke (1968) unequivocally indicates that the presence of methanogenesis substantially increases the rate of PSS hydrolysis, or conversely, the absence of methanogenesis and conditions created by acidogenesis substantially reduces the rate of PSS hydrolysis.

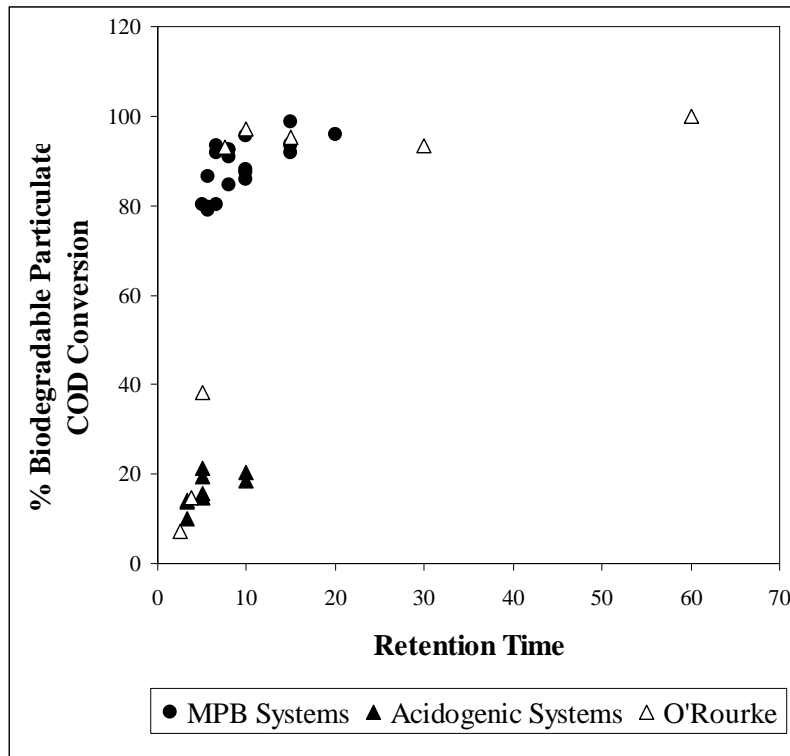


Figure 5.3: Particulate COD conversions for methanogenic systems (this study, Chapter 4), acidogenic systems (this study, Chapter 5) and the results from O'Rourke (1968)

5.7 Calibration of Model for Acidogenic Systems

In an attempt to predict the performance of acidogenic systems, the first order kinetic constant (k_h , Eq 4.24) was calculated for each acidogenic steady state of operation, based on the calculated effluent biodegradable particulate COD concentration (S_{bp}) and the volumetric rate of hydrolysis ($rate_{hydrolysis}$) listed in Table 5.4:

$$k_h = \frac{rate_{hydrolysis}}{S_{bp}} \quad (5.11)$$

The calculated k_h values are plotted as a function of retention time in Figure 5.4. Figure 5.4 shows that the k_h values for the acidogenic systems range from 0.022 to 0.110d⁻¹ (0.054 ± 0.027d⁻¹). As expected from the above, these k_h values are significantly lower than the $k_h = 0.992d^{-1}$ for methanogenic systems. Further, from Figure 5.4, a definite trend in the k_h with retention time is evident, with k_h decreasing as the retention time increases, especially for the systems fed 40 and 13gCOD/L. The value of k_h calculated for the system fed with 2gCOD/L at retention time 3.33d appears to be the exception to this trend. This would indicate that the accumulation of an acidogenesis end product probably is the cause for the inhibition of the PSS hydrolysis rate – from Figure 5.3, for the acidogenic systems, as the retention time increases, the % biodegradable particulate COD conversion increases, implying increased end product accumulation. However, if this is true, it would be expected that the inhibition would be more marked at the higher feed concentrations (lower k_h values) since these would result in higher acidogenesis end product concentrations, but this is clearly not the case. These contradictory observations indicate that suppression of the PSS hydrolysis rate under acidogenic conditions is more complex than a simple end product (e.g. VFA) inhibition.

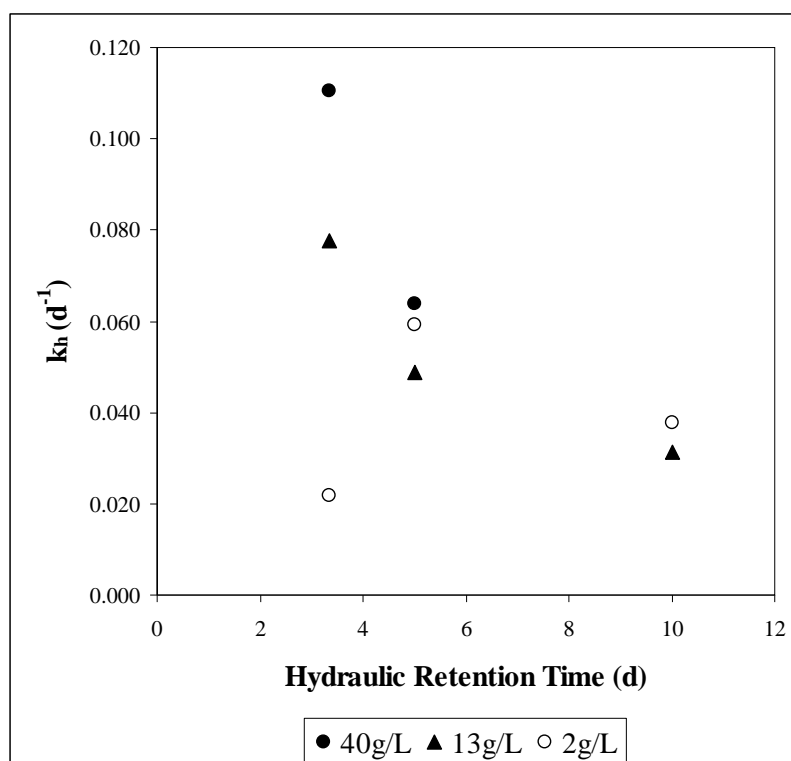


Figure 5.4: Calculated values of the first order kinetic constant (k_h) for each feed COD concentration and retention time for acidogenic systems

Using the mean acidogenic system value of $k_h = 0.054d^{-1}$, the effluent biodegradable particulate COD concentration (S_{bp}) was predicted with Eq 5.12, modified appropriately from Eq 4.27:

$$S_{bp} = \frac{S_{bpi} + b_{ad}Z_{ad}R_h}{1 + k_h R_h} \quad (5.12)$$

The calculated S_{bp} concentration was then substituted into the re-arranged Eq 5.11, and the rate of hydrolysis ($rate_{hydrolysis}$) calculated for each steady state of operation. In Figure 5.5, the predicted hydrolysis rates from Eq 5.11 and 5.12 are compared with the calculated hydrolysis rates in Table 5.4.

Figure 5.5 shows that a first order rate equation with a single value for the specific rate constant ($k_h = 0.054d^{-1}$, as the mean constant for the operated systems) does not accurately predict the rate of PSS hydrolysis for each feed COD concentrations and hydraulic retention time: The predicted rates differ from the calculated rates by as much as 38%. This is as expected due to the observed influence of the retention time on the value of k_h (see Figure 5.4), speculated above to be possibly due to the different concentrations of inhibitory substances present in the systems at each steady state arising from differences in the feed concentration, as well as differences in the conversion or production of these substances. Clearly, more detailed understanding of the inhibition mechanisms involved in acidogenic systems is required before a model can be developed that accurately predicts the rate of hydrolysis of PSS under acidogenic conditions.

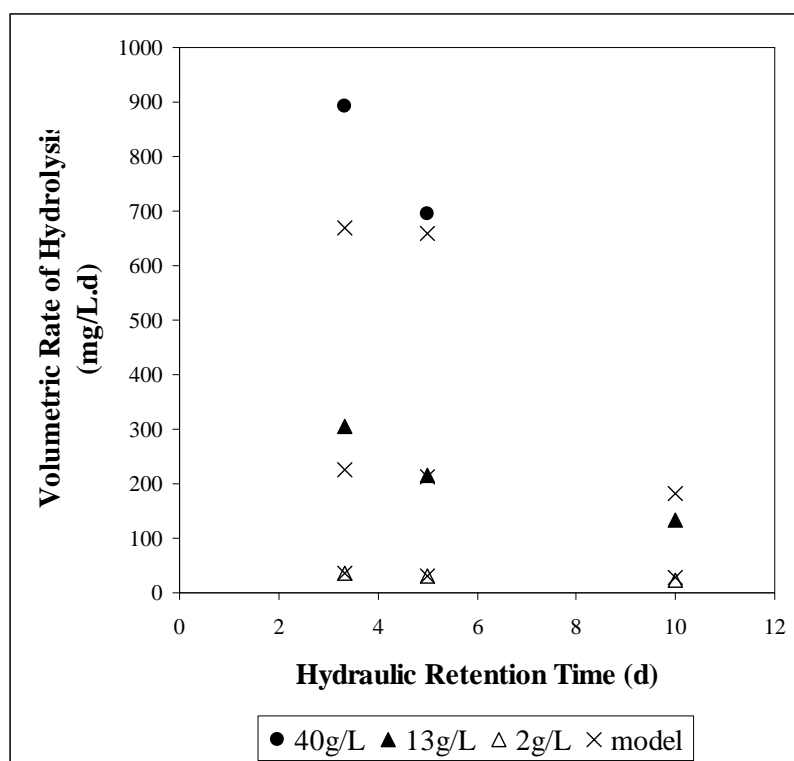


Figure 5.5: Comparison of the calculated and predicted hydrolysis rates for acidogenic systems using a first order rate formulation ($k_h = 0.054d^{-1}$)

In the interim, an empirical relationship can be developed relating the value for k_h to the retention time by excluding two data points in Figure 5.4 ((3.33, 0.022) and (3.33, 0.110)), and plotting a linear regression straight line through the remaining data points (see Figure 5.6). The resultant regression equation expresses the first order kinetic constant (k_h) as a function of the retention time (R_h):

$$k_h = 0.0883 - 0.0055.R_h \quad (5.13)$$

Recalculating the hydrolysis rates for the acidogenic systems by following the procedures above, but with the k_h value determined via Eq 5.13, the predicted and calculated (Table 5.5) hydrolysis rates are compared in Figure 5.7; a significantly improved correlation was obtained.

The mean absolute percent errors between the calculated hydrolysis rates and the rates predicted by (i) the first order formulation with a single value for the first order constant ($k_h = 0.054d^{-1}$) and (ii) the first order formulation with a first order constant dependent on the hydraulic retention time ($k_h = 0.0883 - 0.0055.R_h d^{-1}$) are $27.12 \pm 35.96\%$ and $8.35 \pm 56.14\%$ respectively. Therefore, by varying the first order kinetic constant with retention time (Eq 5.13), the predicted rate of hydrolysis under acidogenic conditions can be calculated with significantly improved and acceptable accuracy, particularly at retention times greater than 3.33d. Since acidogenic systems have typically been operated with solids retention times in excess of 3.33d (e.g. 5, 10 and 20 days, Elefsiniotis and Oldham, 1994; 2, 3, 4, 5 and 6d, Skalsky and Daigger, 1995; 7d, Banerjee *et al.*, 1998), the proposed model in which k_h is linked to R_h provides an acceptably accurate estimate of the acidogenic rate.

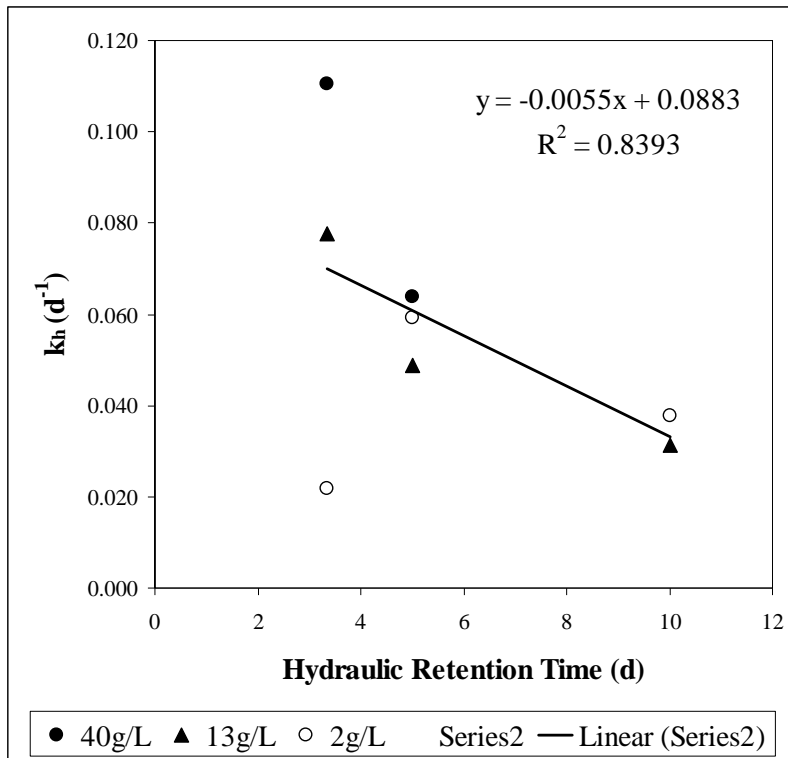


Figure 5.6: Calculated values of the first order kinetic constant (k_h) and linear regression line and line equation ignoring two data points (3.33, 0.022; 3.33, 0.110)

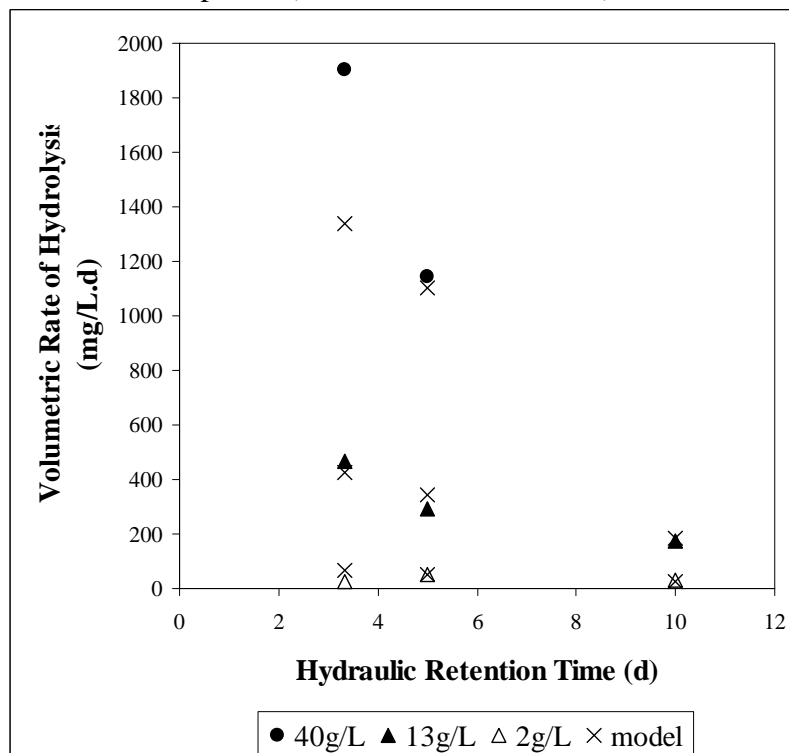


Figure 5.7: Comparison of the calculated and predicted hydrolysis rates for acidogenic systems using the first order rate formulation with the rate constant calculated from $k_h = 0.0883 - 0.0055.R_h$ (d^{-1})

Table 5.5: Comparison of the calculated PSS rates of hydrolysis under acidogenic conditions with the rates predicted by a first order rate formulation with a single k_h value ($0.054d^{-1}$) and with a value dependent on the retention time ($k_h = 0.0883 - 0.0055R_h$) (Concentrations in mgCOD/L; rates in mgCOD/L.d)

Steady state no.	Retention Time (d)	Measurements (mgCOD/L)				Calculated		Predicted ($k_h = 0.054d^{-1}$)			Predicted ($k_h = 0.0883 - 0.0055R_h$)			
		Total Feed (S_{fi})	Soluble Feed	Total Effluent (S_t)	Soluble Effluent	Rate	k_h (d^{-1})	S_{pb}	Rate	Abs % error	k_h	S_{pb}	Rate	Abs % error
30	5	42030	4416	39889	7738	1144	0.064	18580	1003	12.32	0.061	18097	1100	3.81
29	3.33	41206	3901	37992	6739	1901	0.110	19952	1077	43.33	0.070	19093	1336	29.71
32	3.33	13186	1248	12676	2219	465	0.078	6385	345	25.88	0.070	6110	427	8.06
33	5	13186	1382	12823	2405	290	0.049	5832	315	8.48	0.061	5680	345	19.00
38	10	13186	1467	12782	2732	175	0.031	4768	257	47.30	0.033	5501	183	4.82
39	10	2017	224	1934	434	31	0.038	730	39	28.37	0.033	842	28	8.65
34	3.33	2013	192	2053	306	23	0.022	974	53	124.60	0.070	932	65	178.59
35	5	2011	211	1915	359	52	0.059	889	48	6.98	0.061	866	53	2.05

5.8 Closure

Literature studies have indicated that the rate of PSS hydrolysis under acidogenic conditions is significantly reduced compared with methanogenic conditions, apparently because lipids are not hydrolysed under acidogenic conditions. In this study, similar reduction in PSS hydrolysis rate under acidogenic conditions compared with methanogenic conditions has been obtained, although lipids were not measured specifically.

The mathematical model developed in Chapter 4 for PSS sludge hydrolysis in methanogenic systems has been modified for acidogenic conditions. With a first order formulation and a modified first order kinetic constant that is dependent on the retention time, the model is able to accurately predict the observed rate of hydrolysis under acidogenic conditions for nearly all of the operating conditions. This constitutes a significant advance, since no structured mathematical models exist for acidogenic systems.

However, the mechanism for the inhibition of the hydrolysis rate under acidogenic conditions compared with methanogenic conditions is not well understood, and therefore this mechanism cannot be included directly in a structured mathematical model. This is an area that requires further investigation.

Chapter 6

Effect of pH on the Rate of Hydrolysis under Methanogenic and Acidogenic Conditions

6.1 Introduction

Chapters 4 and 5 describe measurement and calculation of the rate of hydrolysis of PSS under methanogenic and acidogenic conditions respectively over a range of feed concentrations and reactor retention times. For these various systems, the pH was allowed to reach a steady state operating pH. These pH values ranged from 6.3 to 7.2 for methanogenic systems, and from 4.7 to 5.4 for acidogenic systems. Figure 5.3 demonstrated that there is a significant difference in the rate of hydrolysis between the methanogenic and acidogenic systems, shown by the significant differences in the substrate conversions by the hydrolysis process (S_{bp}) between the two types of systems. The data from O'Rourke (1968) was also included in the analyses in Chapters 4 and 5. O'Rourke (1968) collected this data from digesters in which the pH was controlled to between 6.9 and 7.4. Under these conditions, the rates of hydrolysis under methanogenic conditions were similar to those measured in the corresponding systems operated in this study, while for the acidogenic systems, the rates of hydrolysis (calculations not shown) were significantly higher than those measured in this study in which the pH was not controlled. In this Chapter, the effects of pH on the methanogenic and acidogenic systems will be investigated under overlapping pH conditions, to more clearly elucidate the effects of pH on the two types of systems.

6.2 Experimental Program

To examine the effects of pH on the PSS hydrolysis rates under methanogenic and acidogenic conditions, a series of laboratory-scale anaerobic digesters were operated under these two conditions, and the pH controlled over a range of values (see Table 6.1). All systems were operated at a feed COD concentration of 2gCOD/L, governed by the comparative study on the sulfate-reducing systems (Chapter 7). The methanogenic systems were operated at an 8-day retention time, while the acidogenic systems were operated at a 5-day retention time. These retention times were chosen to ensure either stable methanogenic or acidogenic conditions; in this study, it was not possible to operate a stable methanogenic digester fed 2gCOD/L at a 5-day retention time, while these systems were stable at an 8-day retention time. For both types of systems, the pH was controlled to selected values by external dosing strong acid or base, and the behaviour monitored. For the methanogenic systems, the pH was

controlled to 7.5 by an automated pH controller (Chapter 3, Section 3.3.2), which added small aliquots of 1M NaOH. Once steady state of operation was observed, this was analysed in more detail. Then, the pH was decreased stepwise to 7, and again to 6.5, analysing the system steady state behaviour at each pH point. These pH conditions were controlled by the addition of 1M NaOH only, since the steady state operating pH was around 6.4 (steady state number 26). When the pH was decreased below the natural pH (6.4) to 6 by the addition of 1M HCl, the methanogenic biomass population became unstable, the effluent VFA concentration increased, the gas production decreased, indicating methanogenic system failure was observed. This system was then reseeded and the pH controlled to 7.5 until steady state was reached, after which the pH was increased to 8 and the steady state monitored. The experimental pH range covered the range of operating pH values where ‘normal’ anaerobic digesters (and possible sulfate-reducing systems, Chapter 7) would operate.

For the acidogenic systems, the steady state operation of 2gCOD/L feed concentration and a 5-day retention time (steady state number 35) was used as the starting point for the series of experiments, with an uncontrolled steady state pH of 5.05. The pH of the system was increased stepwise to 6, 7 and 8 by the addition of 1M NaOH, analyzing the steady state condition at each pH point. This series of results could be compared to those obtained for the corresponding methanogenic systems.

Table 6.1: Steady states measured for methanogenic and acidogenic systems fed 2gCOD/L at varying controlled pH conditions; number in table refer to the steady state number (Appendix B)

Biological systems	System pH					
	5	6	6.5	7	7.5	8
Methanogenic			27	19	18;37	44
Acidogenic	35	40		43		45

6.3 Mathematical Model

The mathematical models and calculation algorithms developed in Chapters 4 and 5 were used to calculate the rates of hydrolysis for the pH controlled methanogenic and acidogenic systems respectively for each of the steady states listed in Table 6.1.

6.4 Experimental Results

For each steady state of operation, a COD balance was calculated based on the feed COD concentration and the effluent COD concentration and methane production (where applicable), see Chapters 4 and 5 respectively. These values are listed in Table 6.2. Table 6.2 shows that for the majority of the steady state periods measured, the COD recoveries were excellent, but for the two systems operated at a pH of 8, the recoveries were comparatively low. The same observation was made for the methanogenic systems reported in Chapter 4, Table 4.2, where for the two systems fed at 2gCOD/L, the COD recoveries were low. This is discussed in more detail in Chapter 3, Section 3.3.1.

Table 6.2 shows that the controlled pH of 6.5 was the minimum pH which maintained methanogenic operation, while a steady state pH of 6.38 was measured for an uncontrolled system. When the pH was decreased to 6 by the addition of 1M HCl, the methanogenic biomass failed. This is illustrated in Figure 6.1.

Table 6.2: Calculated % COD mass balances for each of the steady states in Table 6.1

Biological systems	System pH					
	5	6	6.5	7	7.5	8
Methanogenic			91.3	95.8	99.9;99.2	88.2
Acidogenic	95.6	96.9		95.9		92.5

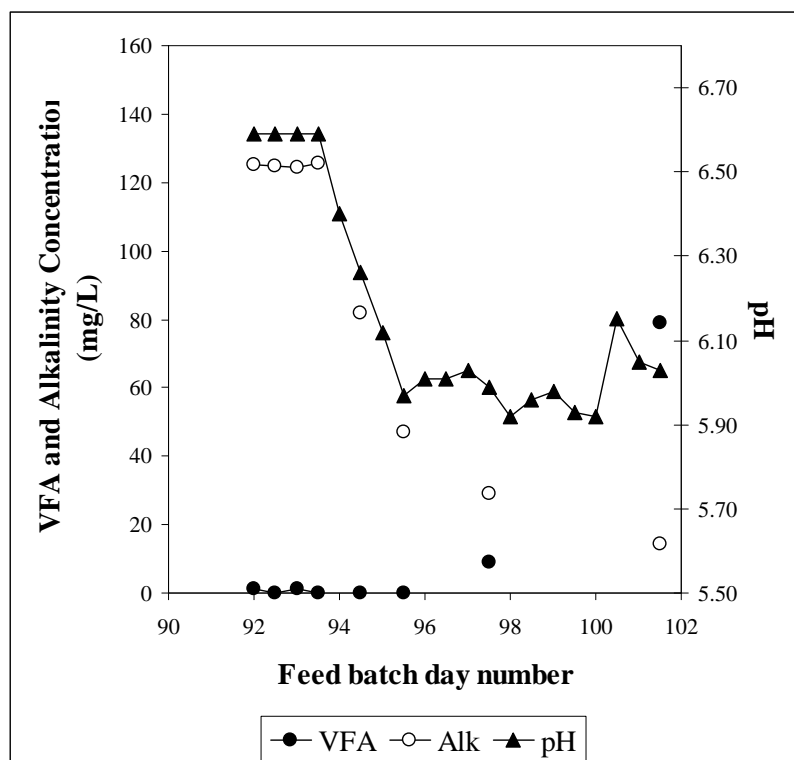


Figure 6.1: Transient values showing the failure of methanogenesis, indicated by the decrease in the alkalinity (mg/L as CaCO_3) and increase in the VFA concentration (mg/L as HAc) when the pH was decreased from 6.6 to around 6

Figure 6.1 shows that as the pH of the system decreased, the alkalinity correspondingly decreased as expected. However, after 2 days, the pH was kept constant, but the alkalinity continued to decrease. Correspondingly the effluent VFA concentration started to increase from a value of $< 3\text{mg/L}$ as HAc. After 6 days (< 1 retention time), the effluent VFA concentration had reached 78mg/L as HAc, with the trend showing an ever-increasing VFA concentration, suggesting that the methanogenic biomass had become unstable. The VFA concentration increase corresponded to a steady decrease in the volumetric gas production, from 12 units per feed cycle at a pH of 6.5, to 1 unit per feed cycle when the experiment was terminated. The methanogenic system could therefore not be operated at a pH of less than 6.5, where the control decrement in pH was 0.5 units. In contrast, the observed steady state pH in the corresponding uncontrolled pH system was 6.38 (Steady state number 25, Chapter 4). This indicated that for the conditions imposed, the minimum pH for stable methanogenic system operation lay between 6.38 and 6.0. Accordingly, the lower pH limit for the pH investigation on the methanogenic systems was accepted to be 6.5.

6.5 Rate of Hydrolysis Calculation

For each of the steady states analysed in Table 6.2, a rate of hydrolysis was calculated based on the procedures set out in Chapters 4 and 5 for methanogenic and acidogenic systems respectively (Figure 6.2).

6.5.1 Methanogenic Systems

From Figure 6.2, the rates calculated for the methanogenic systems vary over a relatively narrow range, between 119 and 140 mgCOD/L.d. Further, the operating pH does not appear to have had a significant influence on the calculated hydrolysis rate, with possibly only a small increase in the rate with increase in pH. To evaluate whether this small increase could be ascribed to the pH increase or was due to differences in the system conditions, the hydrolysis rates for each steady state were predicted by the first order methanogenic model derived in Chapter 4, with the average value for the first order rate constant determined for the uncontrolled pH methanogenic systems ($k_h = 0.992d^{-1}$). The predicted hydrolysis rates range from 115 to 130 mgCOD/L.d, which corresponds closely to the range of calculated hydrolysis rates above. Further, for each steady state pH controlled methanogenic system, the predicted and calculated hydrolysis rates correspond reasonably closely, Figure 6.2. Thus, since the model applied was calibrated on data in which the operating pH was not controlled, and since the predicted hydrolysis rates are in the same range as and correspond reasonably with the calculated rates, it would appear that the effect of pH on the rate of hydrolysis in stable methanogenic systems is not of major significance, and can be excluded from the steady state based model. In stable methanogenic systems throughout this study the biodegradable particulate COD conversions have been greater than 78% (Chapter 5, Figure 5.3), and typically greater than 90%. Such significant biodegradable particulate COD conversion would tend to mask any increase in the hydrolysis rate with increasing pH.

For all systems, the pH does have a significant impact on the methanogenesis failure. Prediction of this failure would require application of a dynamic kinetic based model, and is beyond the scope of this research.

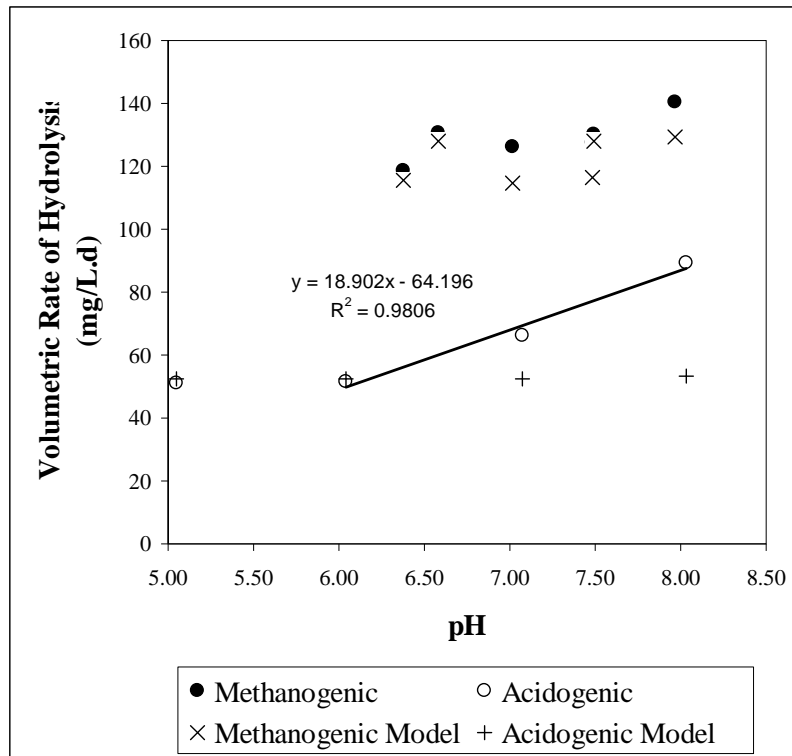


Figure 6.2: Calculated rate of hydrolysis for methanogenic and acidogenic systems at varying pH conditions, and the comparative rate predicted by the methanogenic and acidogenic models, including the regression line indicating the linear increase in the rate of hydrolysis with an increase in pH for acidogenic systems

6.5.2 Acidogenic Systems

For the acidogenic systems, from Figure 6.2, at all pH values the rate of hydrolysis is lower than the rate in the corresponding methanogenic systems. Further, there is no change in the calculated rate of hydrolysis when the pH is increased from 5 to 6 (51mgCOD/L.d for both systems), but when increased from 6 to 7 and then 8, there is a distinct increase in the calculated rate of hydrolysis (51, 66 and 89mgCOD/L.d for the systems at pH 6, 7 and 8 respectively). For the systems operated at a pH of 5 and 6, the calculated hydrolysis rate (51mgCOD/L.d for both systems) corresponds closely with the rate predicted by the first order rate equation (53 and 52mgCOD/L.d for systems operating at pH 5 and 6 respectively) from Chapter 5, with the average value for the first order rate constant from the acidogenic systems where the pH was not controlled (pH = 4.71 – 5.37) ($k_h = 0.0883 - 0.0055.R_h d^{-1}$, Eq 5.13). This implies that there is no pH effect for acidogenic systems operating at a pH of less than 6. However, Figure 6.2 demonstrates that the calculated rates increase linearly ($R^2 = 0.9806$) when the pH is increased from 6 to 8. To accommodate the influence of pH on the rate of hydrolysis in the model, the value for the first order rate constant (k_h) would need to be changed in some fashion with pH. For the acidogenic systems in this study with $pH \geq 6$, the calculated values for k_h are plotted versus pH in Figure 6.3, together with a linear regression line fitted to the experimental data.

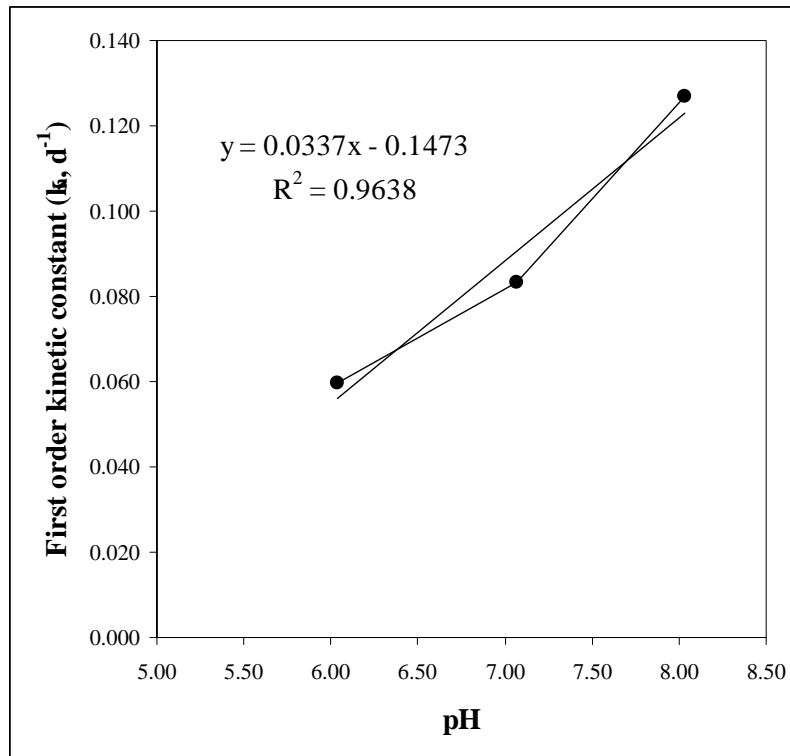


Figure 6.3: Calculated first order kinetic constants for the acidogenic systems at pH values greater than 6, including the regression line indicating the linear increase in the value of the first order kinetic constant with an increase in pH

From Figure 6.3, a linear increase in the value of the first order kinetic constant (k_h) with pH would seem reasonable for the pH range between 6 and 8. In this pH range, the value of the first order kinetic constant can be calculated as a function of the system retention time and pH from Eq 6.1:

$$k_h = (0.0883 - 0.055.R_h) + 0.06 \left(\frac{\text{pH} - \text{pH}_{\text{LL}}}{\text{pH}_{\text{UL}} - \text{pH}_{\text{LL}}} \right) \quad (6.1)$$

where pH is the digester operating pH, pH_{LL} is the lower limit for the pH range in which this function holds (6.04), pH_{UL} is the upper limit for the pH range in which this function holds (8.0), and the term $0.06 \left(\frac{\text{pH} - \text{pH}_{\text{LL}}}{\text{pH}_{\text{UL}} - \text{pH}_{\text{LL}}} \right)$ is a more elegant expression for the linear increase in k_h with pH.

Thus, for acidogenic systems, Eq 6.1 can be applied for elevated pH systems to determine the value of k_h for the selected pH in the range of 6 to 8. Below pH 6, the value of k_h is determined from Eq 5.13. To evaluate the predictions with Eq 6.1, the hydrolysis rates for the acidogenic systems were predicted using the procedures set out in Chapter 5, but with the influence of pH and retention time on the k_h value included via Eq 6.1, and the predicted values compared with the calculated values, see Figure 6.4.

From Figure 6.4, when applying Eq 6.1 in the mathematical model developed in Chapter 5 for acidogenic systems, the model is able to accurately predict the rate of hydrolysis for the pH-controlled systems.

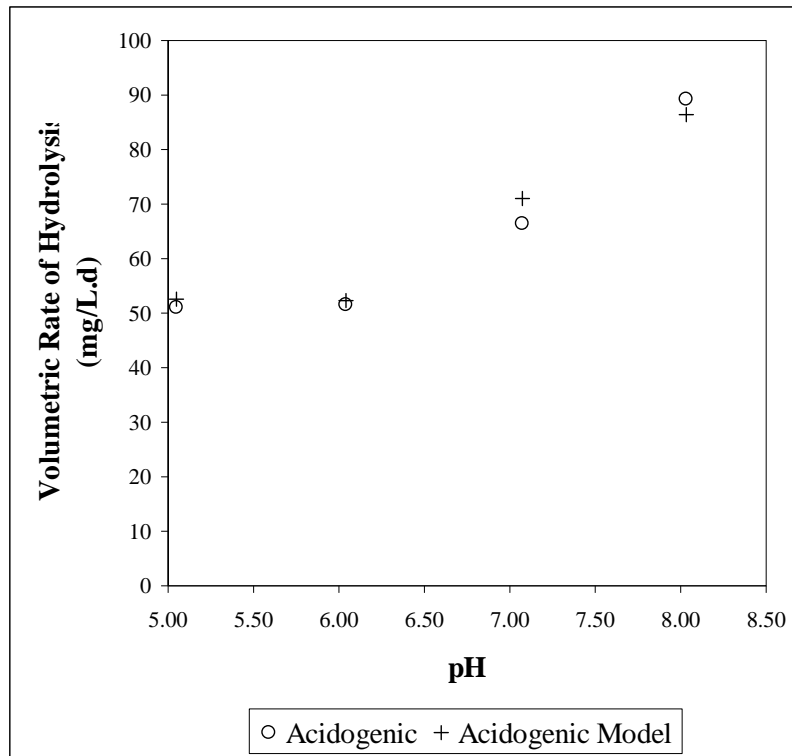


Figure 6.4: Comparison of the calculated hydrolysis rates for the acidogenic systems and the rates predicted by the acidogenic model using Eq 6.1 to determine the value of k_h for system $\text{pH} > 6$

6.6 Closure

In this chapter, the influence of pH on the rate of PSS hydrolysis in anaerobic digestion systems under both methanogenic and acidogenic conditions has been investigated. For the methanogenic conditions here, the effect of pH on the PSS hydrolysis is small, and can be neglected. However, in methanogenic systems with reduced PSS hydrolysis (for whatever reason), the effect of pH may not be negligible, and would need to be taken into account.

For the acidogenic systems here, for all pH values in the range investigated (5 to 8), the rate of PSS hydrolysis was lower than the rate in the corresponding methanogenic systems. With $\text{pH} \leq 6$, no pH effect on PSS hydrolysis was noted. However, for $\text{pH} > 6$, an increase in pH resulted in a corresponding increase in PSS hydrolysis. This was taken into account in the first order rate expression for the PSS hydrolysis, by modifying the value for the first order rate constant through a linear relationship with pH. With this modification, the first order model is able to accurately predict the observed rate of hydrolysis for all the acidogenic systems operated.

Table 6.3: Measured and calculated values of the various components of the feed and effluent COD measurements, and the calculated rates of hydrolysis for each steady state (Concentrations in mgCOD/L; rates in mgCOD/L.d)

Steady state no.	Retention Time (d)	Measurements (mgCOD/L)		Calculated from experimental data										% Solids Conversion	
		Total Feed (S _{fi})	Soluble Feed	Total Effluent (S _f)	Soluble Effluent	S _{upi}	S _{ppi}	S _{usi}	S _{bsfi}	S _{up}	S _{bp}	S _{us}	S _{bsf}		Z _{ad}
Methanogenic systems															
26	8	1950	284	892	51	1014	51	116	652	93	51	0	72	119	91
27	8	2017	219	913	27	1124	27	96	675	110	27	0	77	131	90
19	8	1950	293	815	35	1004	35	129	652	26	35	0	77	126	97
18	8	1950	280	827	43	1017	43	119	652	30	43	0	77	127	97
37	8	2017	221	921	33	1121	33	94	675	113	33	0	77	130	90
44	8	2017	208	866	38	1135	38	85	675	47	38	0	82	140	96
Acidogenic systems															
35	5	2011	211	1915	359	1127	16	98	673	874	359	171	9	51	22
40	5	2011	220	1969	424	1118	16	102	673	863	424	204	10	51	23
43	5	2011	211	1914	431	1127	16	97	673	798	431	207	12	66	29
45	5	2011	193	1846	454	1145	16	88	673	703	454	219	17	89	39

Table 6.4: Comparison between the calculated rates and predicted rate (First order) for the methanogenic systems

Steady state no.	pH	Measurements (mgCOD/L)				Calculated from experimental data				Calculated using the first order hydrolysis rate formulation ($k_H = 0.992d^{-1}$)			
		Total Feed (S_{fi})	Soluble Feed	Total Effluent (S_t)	Soluble Effluent	S_{bpi}	S_{bp}	Z_{ad}	Rate of hydrolysis	S_{bp}	Rate of hydrolysis	Z_{ad}	% Error in Predicted Rate
26	6.38	1950	284	892	51	1014	93	72	119	117	116	70	2.63
27	6.58	2017	219	913	27	1124	110	77	131	129	128	76	2.00
19	7.02	1950	293	815	35	1004	26	77	126	116	115	71	9.15
18	7.48	1950	280	827	43	1017	30	77	127	117	116	71	8.77
37	7.49	2017	221	921	33	1121	113	77	130	129	128	76	1.62
44	7.97	2017	208	866	38	1135	47	82	140	131	130	76	7.68

Table 6.5: Comparison between the calculated rates and predicted rate for the acidogenic systems using the retention time and pH dependent first order kinetic constant formulation

Steady state no.	pH	Measurements (mgCOD/L)				Calculated from experimental data				Calculated using the modified first order kinetic constant formulation			
		Total Feed (S_{fi})	Soluble Feed	Total Effluent (S_t)	Soluble Effluent	S_{bpi}	S_{bp}	Z_{ad}	Rate of hydrolysis	S_{bp}	Rate of hydrolysis	Z_{ad}	% Error in Predicted Rate
35	5.05	2011	211	1915	359	1127	874	9	51	866	53	10	-3.16
40	6.04	2011	220	1969	424	1118	863	10	51	859	52	10	-1.52
43	7.07	2011	211	1914	431	1127	798	12	66	774	71	13	-7.17
45	8.03	2011	193	1846	454	1145	703	17	89	716	87	16	2.99

Chapter 6: Effect of pH on the Rate of Hydrolysis

Chapter 7

Sulfate-Reducing Systems

7.1 Introduction

PSS treatment in sulfate-reducing anaerobic digestion systems is a novel treatment approach, possible only in situations where sufficient sulfate is available in the PSS stream to remove all biodegradable organic matter and to maintain a balanced sulfate-reducing population. The converse application, where a sulfate-rich wastewater is treated using PSS and sulfate-reducing bacteria, has received some attention. However, in both types of application, far fewer studies have been conducted on sulfate-reducing systems with PSS as feed than on methanogenic and acidogenic systems. As yet, no research has been reported where quantitative rates of PSS hydrolysis have been determined under sulfate-reducing conditions, since the majority of the published research has been simply to establish whether sulfate-reduction with PSS treatment is feasible (Pipes, 1961; Kaufman *et al.*, 1996), or to develop novel bioreactor designs to increase the solids retention time, and therefore solids conversion (Whittington-Jones, 2000; Corbett *et al.*, 2000; Rose *et al.*, 2002). Unfortunately, these studies do not allow the PSS hydrolysis rates to be quantified.

The aim of this chapter is to determine the rate of PSS hydrolysis under sulfate-reducing conditions, to compare the observed rate under sulfate-reducing conditions with the rates of hydrolysis calculated for methanogenic and acidogenic systems in Chapters 4 and 5, and to determine what other factors present in sulfate-reducing systems affect this rate, that would not be present under methanogenic or acidogenic conditions.

To achieve these aims, a series of experiments were conducted in completely mixed anaerobic digesters under sulfate-reducing conditions, in which the systems were operated with excess sulfate. Sulfate-reducing bacteria are expected to out-compete the methanogenic bacteria for soluble organic substrate (Kristjansson *et al.*, 1982; Kristjansson and Schönheit, 1983; Gupta *et al.*, 1994; Colleran *et al.*, 1995), and are less sensitive than the methanogenic bacteria to the sulfide produced in the sulfate reduction reaction (Pipes, 1961; Oude Elferink *et al.*, 1994). Consequently, under conditions of excess sulfate, methanogenesis is not expected to occur.

In this chapter, mostly direct comparisons between equivalent sulfate-reducing systems and methanogenic systems are performed, so that direct comparison between the two systems can be made. As for methanogenic systems, in this study stable sulfate-reducing conditions were accepted to require that the VFA concentration was negligible ($< 50\text{mg/L}$ as HAc).

7.2 Experimental Program

Table 7.1 lists the sulfate-reducing steady states, as well as the corresponding methanogenic system with which the sulfate-reducing system is being compared in this study (where applicable); detailed data are listed in Appendix B. The experiments will be discussed in groups in this chapter (Experiments 1 – 4), where the sulfate-reducing systems are compared to other sulfate-reducing systems and to the corresponding methanogenic system, with a single parameter changed between the steady states in a single experiment.

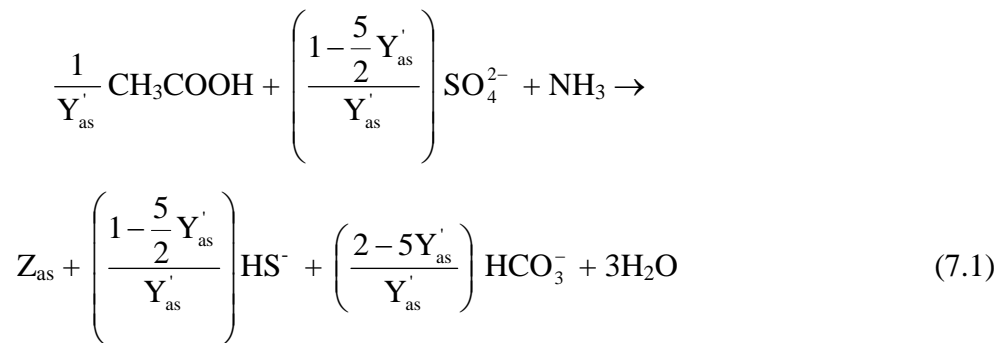
Table 7.1: Sulfate-reducing steady states and corresponding methanogenic systems at various operating conditions (retention times, feed COD and sulfate concentrations, operating pH and sulfide concentrations)

Steady state number	Operating conditions				Comparative steady state number
	R _h (d)	Feed COD (g/L)	Feed SO ₄ (g/L)	Additional factors	
6	10	26	1	Excess COD	1
15	8	13	9.6	All S _t as FeS	14
16	8	13	9.6	No Fe addition	14 and 15
20	8	2	2	pH ~ 7.5	18 and 37
22	8	2	2	pH ~ 7	19
36	8	2	2	pH ~ 6.5	27
41	16	2	2		
42	13.3	2	2		
46	10	1	1		
47	8	2	2	pH ~ 8.3	

7.3 Mathematical Model

The mathematical model developed for methanogenic systems in Chapter 4 was applied to the sulfate-reducing systems in this chapter, except that the methanogenic biomass was replaced with acetoclastic sulfate-reducing biomass (Z_{as}), with different growth constants (metabolic yield constant and cell decay coefficient). The rate of hydrolysis was calculated using the same algorithms as in Chapter 4, with the same feed characterization.

For the sulfate reducing bacteria, only acetate was considered as the soluble organic substrate, consistent with the methanogenic systems model in Chapter 4:



where the metabolic yield and endogenous respiration coefficient for the acetoclastic sulfate-reducing biomass are $Y'_{as} = 0.058\text{gCOD/gCOD}$ and $b_{as} = 0.025\text{d}^{-1}$ respectively (Kalyuzhnyi and Fedorovich, 1998).

7.4 Experimental Results

7.4.1 Experiment 1

7.4.1.1 Aim and experimental method

The aim of this experiment was to determine whether in regular methanogenic anaerobic digestion of PSS, limited sulfate reduction could be achieved without inhibiting the methanogenic processes, and to quantify the effects of the limited sulfate reduction on the rate of hydrolysis.

This experiment compared a methanogenic digester (MPB) (steady state number 1, Table 7.1, Appendix B) and a methanogenic/sulfate-reducing (MPB + SRB) digester (steady state number 6, Table 7.1, Appendix B). Both systems were operated identically under methanogenic conditions at a 10-day retention time and a feed COD concentration of 26g/L, but 1gSO₄/L was added to the feed of the 'MPB + SRB' system. The pH in both systems was controlled to around 7. The systems were allowed to reach a steady state (after 20 days and 38 days for 'MPB' and 'MPB + SRB' respectively), and then analysed in more detail.

7.4.1.2 Results and discussion

The systems were not analysed at exactly the same time since the 'MPB + SRB' system took longer to stabilize, which is why the feed soluble COD concentrations are closely similar but not identical (Table 7.2) (see Appendix A for the changes in feed soluble COD concentration with time). However, these different concentrations are taken into account when calculating the rate of hydrolysis with the algorithms developed in Chapter 4.

In both systems, the volatile fatty acid (VFA's) concentration was negligible (24 and 37mgHAc/L for the 'MPB' and 'MPB + SRB' systems respectively), indicating a balance between the VFA producing acidogens and the VFA utilizing methanogens in 'MPB' and additionally sulfate reducers in 'MPB and SRB'. The effluent sulfate concentration of 34mgSO₄/L in 'MPB + SRB' is artificially inflated due to nitric acid interference in the sulfate measurement (a problem only identified after the steady state data had been collected, but rectified for subsequent experiments), so that 100% sulfate reduction was probable. The soluble COD measured for the 'MPB + SRB' system included aqueous sulfide. However, the concentration was similar to the MPB system, indicating that the aqueous sulfide concentration was low. This is understandable, since the system generated 13.76L of gas per day (CH₄ and CO₂), which at the operating pH of 7.06 would have stripped the sulfide from the system.

Table 7.2: Feed and effluent concentrations and substrate conversions for two comparative 10-day retention time digesters, one operating under methanogenic (MPB) conditions, the other under methanogenic and sulfate reducing (MPB + SRB) conditions

	MPB	MPB + SRB
Feed total COD (g/L)	25.95	25.95
Average feed soluble COD (g/L)	2.33	2.65
Effluent total COD (g/L)	10.85 ± 0.3	10.68 ± 0.3
Effluent soluble organic COD (mg/L)	178 ± 14	157 ± 8
Effluent pH	7.00 ± 0.02	7.06 ± 0.03
Effluent VFA (mgHAc/L)	24 ± 14	37 ± 18
Effluent total alkalinity (mgCaCO₃/L)	2424 ± 127	2534 ± 62
Sulfate addition (mgSO₄/L)	0	1000
Effluent sulfate (mgSO₄/L)	0	34 ± 3
% Total Solids (as COD) Conversion	54.82	54.84
% Biodegradable Particulate COD Conversion	96.4	95.5
% Sulfate conversion		96.6
Methane production (L/day)	10.67*	9.76
Rate of hydrolysis (mgCOD/L.d)	1480	1463

* Based on assumed methane composition, which is questioned in Chapter 4, Section 4.4.3.

Table 7.2 shows that the total solid COD conversions, and more specifically, the biodegradable particulate COD conversions, were near identical for the two systems despite the sulfate reduction 1gSO₄/L in the ‘MPB + SRB’ system. This observation is substantiated by the rates of hydrolysis, which differed by only 1.1% (well within experimental error). From these results, it is clear that for the ‘MPB + SRB’ system operating under similar conditions to the MPB system, the rate of hydrolysis under limited sulfate-reducing methanogenic conditions is closely similar to the rate under purely methanogenic conditions. However, since only 1gSO₄/L was being added to the system (COD: SO₄ = 26:1), and the two systems were nearly identical in operation, closely similar operating performance would be expected. In order to increase the magnitude of any effects of sulfate reduction on the rate of PSS hydrolysis compared with methanogenic anaerobic digestion, the sulfate-reducing systems needed to be operated such that methanogenesis is excluded from the system.

The following experiment (Experiment 2) evaluates the performance of a sulfate-reducing system when the sulfate-reducing biomass is not sulfate limited and hence out-competes the methanogenic biomass for organic substrate, with the result that the methanogenic biomass is not present in the system. This allows for the determination of the effects of sulfate-reduction on the PSS hydrolysis rate when a purely sulfate-reducing system is compared with a purely methanogenic system.

7.4.2 Experiment 2

7.4.2.1 Aim and experimental method

The aim of this experiment was to compare the rate of PSS hydrolysis under purely sulfate-reducing conditions (no methanogenesis, excess sulfate added) with the observed rate under methanogenic conditions. Two sulfate-reducing systems were operated, one under sulfide-free (brought about by the precipitation of the produced sulfide as ferrous sulfide (FeS)) and the other under sulfide-rich (no sulfide removal) conditions. Thus, the experiment consisted of three operating conditions, all at an 8-day retention time, controlled to a pH of around 6.8,

and fed PSS at 13gCOD/L: The first system was methanogenic (MPB; steady state number 14, Table 7.1), while for the other two systems, sulfate was supplemented to the influent at 9.6gSO₄/L (feed COD: SO₄ = 1.38). Ferrous (Fe²⁺) in excess of the sulfide produced was also added to one of the sulfate-reducing systems (SRB 1; steady state number 15, Table 7.1) in the form of soluble ferrous chloride (FeCl₂·4H₂O), to remove all sulfides produced via precipitation. The second sulfate-reducing system (SRB 2; steady state number 16, Table 7.1) did not have ferrous addition, and therefore equilibrium concentrations of aqueous sulfide were present in the system. This allowed for a direct comparison between a methanogenic and two sulfate-reducing systems, one with the effects of sulfide present and one without. The performance of the methanogenic system (MPB) was used as a basis for comparison with and between the two sulfate-reducing systems.

7.4.2.2 Results and discussion

The first sulfate-reducing system (SRB 1) was seeded with waste methanogenic sludge, and fed PSS at 13gCOD/L. The feed sulfate dose was slowly increased from 1gSO₄/L to 9.6gSO₄/L, while ferrous chloride (FeCl₂) addition was concomitantly increased to remove the aqueous sulfide produced as FeS. The system turned black, indicating the presence of metal sulfides, and there was no hydrogen sulfide odour from the digester when opened. This was a good qualitative test for the presence of sulfide, since the H₂S odour can be detected at extremely low concentrations.

The VFA and sulfate concentrations were analysed regularly to determine whether steady state of operation had been reached: A VFA concentration of 50mgHAc/L or less would indicate a steady balance between the hydrolysis process and the methanogenic and sulfate-reducing processes, while the sulfate concentration would indicate whether the sulfate-reducing bacteria had reached a stable concentration in the system. Figure 7.1 shows the concentrations of these two species with time.

Initially, before the addition of the FeCl₂, the methanogenic biomass was unstable, probably due to the presence of sulfide, while the sulfate-reducing biomass concentration was too low to maintain a low VFA concentration, since the systems was not seeded with sulfate reducing biomass. As a consequence, the VFA concentration increased to more than 1000mgHAc/L, while the sulfate concentration was greater than 3500mgSO₄/L. However, from day 60 (Figure 7.1), the sulfate-reducing biomass had reached a sufficiently high concentration to utilize both the VFA and sulfate present, indicated by the reduction in both these concentrations at roughly the same time, and by the equivalent slope of the trends (stoichiometric).

After day 65, the VFA concentration had decreased to below 50mg/L as HAc, and the sulfate concentration ranged from between 450 to 850 mgSO₄/L (91 – 96% conversion). This indicated that the sulfate-reducing biomass concentration had reached a steady state, and that the system was organic substrate limited and not sulfate limited. The system was analysed in more detail to determine the steady state behaviour (Table 7.3).

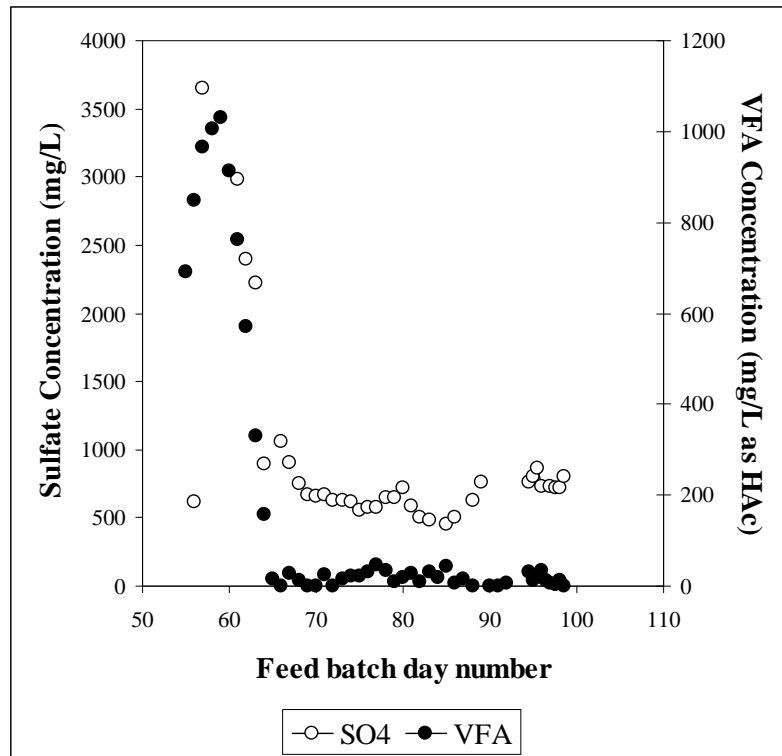


Figure 7.1: Daily measurements of the VFA and sulfate concentration leading up to and including steady state number 15 (steady state from day 90)

Table 7.3: Operating conditions and results of an 8-day retention methanogenic and sulfate-reducing digester without aqueous sulfide present

	MPB	SRB 1
Feed total COD (g/L)	13.27	13.27
Effluent total COD (g/L)	6.30 ± 0.1	*13.00 ± 0.5
Effluent soluble organic COD (mg/L)	104 ± 5	197 ± 19
pH	6.78 ± 0.01	6.87
Sulfate addition (mgSO₄/L)	-	9600
Effluent sulfate (mgSO₄/L)	-	733 ± 35
Effluent Total Organic Particulate COD (mg/L)	6195 ± 86	6165 ± 457
% Sulfate conversion	-	92.2
Methane production (L/day)	6.34	0
Rate of hydrolysis (mgCOD/L.d)	798	805

* Includes ferrous sulfide (FeS) precipitate in the measurement

Table 7.3 shows that the effluent total COD concentration for SRB 1 (13gCOD/L) was much higher than for MPB (6.3gCOD/L), and that the soluble COD concentration was also higher for SRB 1 (197mgCOD/L) than for MPB (104mgCOD/L). The effluent total COD for SRB 1 consists of unbiodegradable particulate COD, biodegradable particulate COD, acidogenic biomass, sulfate-reducing biomass, ferrous sulfide precipitate, unbiodegradable soluble COD and residual ferrous.

$$S_t = S_{up} + S_{bp} + Z_{ad} + Z_{as} + S_{FeS} + S_{us} + S_{Fe} \quad (7.2)$$

Chapter 7: Sulfate-reducing Systems

The residual ferrous contributes to the difference between the soluble COD measurements ($197 - 104 = 93\text{mgCOD/L}$) between the two systems ($S_s = S_{us} + S_{Fe}$), while the ferrous sulfide precipitate is the major contributing factor to the difference in the total COD measurement (Eq 7.2) ($13.0 - 6.3 = 6.7\text{gCOD/L}$). It was not possible to quantify the ferrous sulfide precipitate contribution to the COD directly, since there was no way of separating the particulate fractions in the COD measurement ($S_p = S_{up} + S_{bp} + Z_{ad} + Z_{as} + S_{FeS}$).

However, by knowing the sulfate conversion ($S_{SO_4i} - S_{SO_4} = 9600 - 733 = 8867\text{mgSO}_4/\text{L}$), the sulfide production was calculated ($S_T \text{ produced} = \frac{M_S}{M_{SO_4}}(S_{SO_4i} - S_{SO_4}) = 2956\text{mgS/L}$, where

$M_S (=32\text{g/mol})$ and $M_{SO_4}(=96\text{g/mol})$ are the molar masses of sulfur and sulfate respectively. From this value, the mass of ferrous sulfide precipitate was calculated by assuming all sulfide produced was precipitated as FeS ($M_{Fe} = 55.8\text{g/mol}$) (mass of FeS = $S_T \left(\frac{55.8 + 32}{32} \right) = 8096\text{mgFeS/L}$). Since 1gFeS is equivalent to 0.82gCOD, the mass of FeS is equivalent to 6639mgCOD/L, which represents S_{FeS} in Eq 7.2. By subtracting the FeS COD and soluble COD concentrations from the total COD measurement ($S_t = 13001\text{mgCOD/L}$), the effluent total organic particulate COD concentration could be calculated ($S_{up} + S_{bp} + Z_{ad} + Z_{as} = S_t - S_{FeS} - S_{us} - S_{Fe} = 13001 - 6639 - 197 = 6165\text{mgCOD/L}$). Following the algorithms in Chapter 4, the mathematical model was then used to quantify each of the particulate organic species, so that the rate of hydrolysis could be calculated.

Table 7.3 shows that the calculated particulate COD concentrations for the two systems were virtually identical (within experimental error), while the calculated rates of hydrolysis were also near identical (0.87% difference). Therefore, it can be concluded that under stable sulfate-reducing conditions, the rate of PSS hydrolysis is the same as under methanogenic conditions.

Also, from SRB 1, the total mass of COD utilized to reduce the total mass of sulfate can be calculated. This ratio should be closely constant, since the chemical reaction stoichiometric COD:SO₄ ratio is fixed (= 0.67gCOD/gSO₄). The observed ratio should be slightly higher than the chemical reaction ratio, since the metabolic yield of the acidogenic and sulfate-reducing biomass would increase the mass of COD consumed, while the anabolic sulfate consumption (incorporation of S in biomass) of these biomass groups can be considered negligible. Based on the above calculation calculations and discussions, the COD:SO₄ utilization ratio for this experiment was $\left(\frac{13270 - 6165}{9600 - 733} \right) = 0.80 \text{gCOD/gSO}_4$. Based on the stoichiometric COD utilization for the sulfate reduced, approximately 16% of the COD consumed in the systems is not used for sulfate reduction, but probably for biomass production and maintenance of both the acidogen and sulfate-reducing populations. Noting that the yield values of 0.09 and 0.058 gCOD/gCOD for the acidogens and sulfate-reducers respectively used in the model would give a net biomass yield of about 13%, the observed yield corresponds closely to the theoretical value.

Following the collection of the steady state operating data for SRB 1, the ferrous chloride addition was stopped, while the PSS and sulfate addition continued, along with the pH control, to give SRB 2. Within days, hydrogen sulfide gas was detected in the digester headspace (could be smelled), while the soluble organic COD concentration started to

increase (Figure 7.2). This indicated that the SRB were no longer able to utilize all of the soluble products of hydrolysis, and that the system was no longer 'stable'. At the same time, there was a significant increase in the sulfate concentration, confirming that the sulfate-reducing bacteria were inhibited.

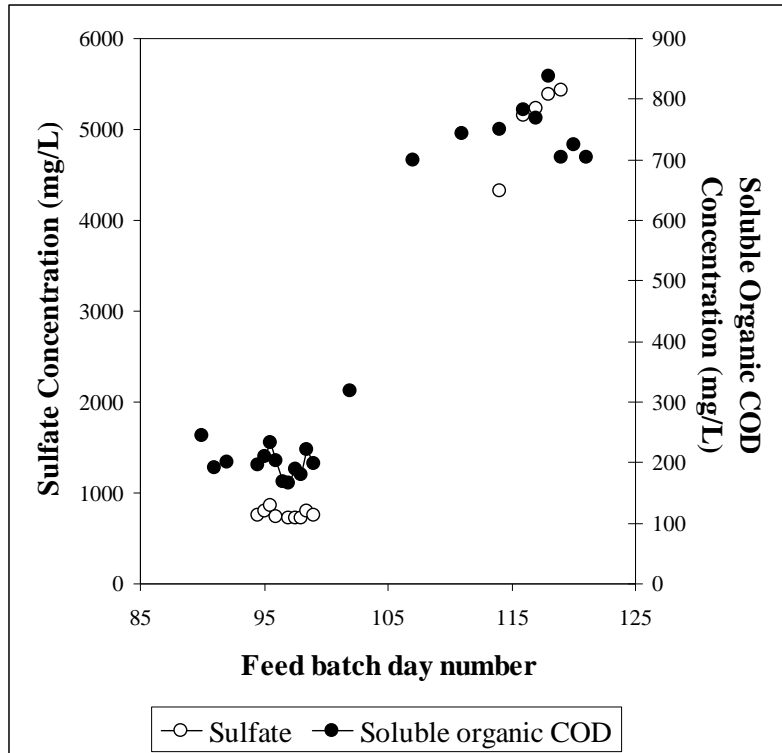


Figure 7.2: Daily measurements of the soluble organic COD and sulfate concentrations following the SRB 1 steady state (steady state ended on day 99)

Further analysis of the digester at this stage showed that the total COD was decreasing, probably due to washout of the ferrous sulfide precipitate. However, it was necessary to terminate this experiment before the system had reached a steady state of operation because the batch of PSS used as feed was coming to an end, and at this stage of the study, it was unclear whether different PSS feed batches would influence the rate of hydrolysis. However, sufficient qualitative data had been collected to enable some interesting observations to be made.

Figure 7.2 shows that the sulfate-reducing bacteria were not stable under the operating conditions for SRB 2, while stable for SRB 1. The only difference between the two systems was the aqueous sulfide concentration (0 and 739mgS/L in SRB 1 and SRB 2 respectively). At the controlled operating pH of around 6.75, more than half of the concentration in SRB 2 would be in the undissociated H₂S form (pK_a ~ 7 for H₂S – HS⁻ equilibrium), which is typically considered to be the sulfide species that is toxic (Koster *et al.*, 1986; McCartney and Oleszkiewicz, 1991). Clearly, this concentration of H₂S was above the tolerance threshold for sulfate-reducing bacteria, but unfortunately the system was not analysed in sufficient detail or at steady state so that further conclusions could be drawn.

7.4.3 Experiment 3

7.4.3.1 Aim and experimental method

The aim of the following series of experiments was to determine the rate of hydrolysis of PSS under stable sulfate reducing conditions, where the systems were neither sulfate limited nor sulfide inhibited, and were allowed to stabilize at a steady state operating pH. These rates of PSS hydrolysis under sulfate-reducing conditions would then be compared with the rates in the comparative methanogenic systems in Chapter 4, to determine if sulfate-reduction has any influence on the hydrolysis rate (The data collected in these systems also could be used to calibrate a more extensive mathematical model than described in Chapter 4 and Section 7.3, where physical processes, as well as biological processes, are included; required modifications to the model would include acid/base, vapour/liquid and solid/liquid equilibria).

To collect operating data that could be used to determine the PSS hydrolysis rates under sulfate-reducing conditions, three steady state systems were operated at varying feed concentrations (COD and SO_4) and hydraulic retention times. Initially, the aim was to operate an extensive range of systems by reducing the hydraulic retention times until the sulfate-reducing bacteria washed out of the system, and the systems failed. However, the time taken to reach a steady state of operation for each sulfate-reducing system was excessively long (up 8 retention times, compared to 2 – 3 retention times for methanogenic systems), which meant that data on only a limited number (3) of steady states could be collected. However, if a link could be established between the three steady states measured here under sulfate-reducing conditions and the extensive data set collected for methanogenic conditions in Chapter 4, then three steady state data points may suffice in concluding whether the rates of hydrolysis are or are not similar under methanogenic and sulfate-reducing conditions: If these rates were found to be similar, more data for a wider range of steady states points would not be necessary. However, if the rates differed significantly, this would require a more extensive investigation.

Of the three steady state sulfate-reducing systems, the first two systems were operated with a feed COD and sulfate concentration of 2g/L, which would ensure that the sulfate-reducing bacteria were never sulfate limited and sulfide would not be inhibitory. These two systems were operated at hydraulic retention times of 16 and 13.3 days respectively. For the third system, the feed COD and sulfate concentrations were halved to 1g/L each, to reduce the sulfide concentration in the digester, to confirm that the first two systems were not sulfide inhibited. All three systems are described in Table 7.4 and in more detail in Appendix B (steady state numbers 41, 42 and 46 respectively).

In operation and analysis of the three sulfate-reducing systems, due cognizance had to be taken of the complexities involved in collecting steady state data under sulfate-reducing conditions, such as sulfide interference in the alkalinity measurements, sulfide quantification in the COD measurements, as well as the inability to measure the sulfide gas and thus calculate either a sulfur mass balance or a COD mass balance.

7.4.3.2 Results and discussion

One of the major differences between the steady state methanogenic and sulfate-reducing systems is that, due to the production of alkalinity (H^+ consumed in sulfate reduction), the steady state operating pH of the sulfate-reducing systems is significantly higher than that for the corresponding methanogenic systems. Chapter 6 quantified the effect of pH on the rate of

hydrolysis of PSS under methanogenic conditions and found that pH in the range 6 – 8 had no influence on the rate of hydrolysis. Based on this result, and that the pH values in the sulfate-reducing systems fell in the 6 – 8 range (Table 7.4), the higher pH values in the sulfate-reducing systems than in the corresponding methanogenic systems would not influence the rate of PSS hydrolysis, i.e. pH could be eliminated as a causative parameter for any observed differences in PSS hydrolysis rates.

Following the algorithms set out in Chapter 4, with modifications in Section 7.3, the volumetric rates of hydrolysis for the three sulfate-reducing systems were calculated, see Table 7.4. If sulfate reduction had no influence on the PSS hydrolysis rate, the calculated rate of PSS hydrolysis for the three sulfate-reducing conditions would be expected to be the same as predicted by the methanogenic model, with a value for the first order rate constant calibrated for methanogenic systems.

Table 7.4: Selected results of the sulfate-reducing systems at varying hydraulic retention times and feed concentrations under steady state pH operating conditions, as well as the calculated and predicted rates of hydrolysis

R_h (d)	Feed COD Concentration (gCOD/L)	Feed Sulfate Concentration (gSO ₄ /L)	pH	Rate of hydrolysis (mgCOD/L.d)	
				Calculated	Predicted
16	2	2	7.64	72	70
13.3	2	2	7.75	86	81
10	1	1	7.92	52	52

Accordingly, for each of the three steady states, the PSS hydrolysis rates were predicted with the first-order based model developed in Chapter 4 (but with the methanogen biomass replaced with the sulfate-reducing biomass, see Section 7.3), with the value for the first order rate constant calibrated for the methanogenic systems in Chapter 4 ($k_h = 0.992d^{-1}$). From Table 7.4, the calculated PSS hydrolysis rates are near identical to the rates predicted by the first order model. Therefore, it can be deduced that sulfate-reducing conditions had no significant influence on the rate of PSS hydrolysis when compared to equivalent methanogenic systems. Further, the sulfate-reducing systems were not sulfide inhibited in this study.

In summary, for sulfate-rich waste streams with a sulfate concentration of 2gSO₄/L or less, biological sulfate-reducing systems with PSS as the electron donor can operate stably without sulfide inhibition, and the rate at which the PSS is degraded is neither enhanced nor reduced compared with equivalent methanogenic conditions. Thus, there would be no benefit in treating PSS under sulfate-reducing conditions compared with the conventional methanogenic conditions, unless the removal of the sulfate component is of equal or greater importance than the digestion of the PSS organic solids. This certainly would be the case for the treatment of AMD using PSS and biological sulfate reduction.

The following set of experiments were to determine the effects of pH on the rate of PSS hydrolysis under sulfate-reducing conditions.

7.4.4 Experiment 4

7.4.4.1 Aim and experimental method

The final series of sulfate reduction experiments were aimed to determine the effects of pH on the rate of PSS hydrolysis under sulfate-reducing conditions. The systems were operated as described above, but with pH controlled to pH values of 6.5, 7, 7.5 and 8.3, to enable comparison with the methanogenic systems operated in Chapter 6. As for the methanogenic systems, the feed COD was 2g/L, while for all but the pH = 8.3 systems, the feed sulfate concentrations were 2g/L. For the pH = 8.3 system, the feed sulfate concentration unintentionally was reduced to 1.6g/L (see Table 7.5); the system was still not sulfate limited. For each selected pH, the digesters were allowed to reach a steady state of operation, and then analysed in more detail, see Table 7.5 and Appendix B for detailed results.

Table 7.5: Selected results of the sulfate-reducing systems at a 8d retention time and constant feed concentrations under varying controlled pH operating conditions, as well as the calculated and predicted rates of hydrolysis

Steady state number	Feed COD Concentration (gCOD/L)	Feed Sulfate Concentration (gSO ₄ /L)	pH	Rate of hydrolysis (mgCOD/L.d)	
				Calculated	Predicted
36	2	2	6.47	127	116
22	2	2	6.99	129	114
20	2	2	7.52	130	115
47	2	1.6	8.27	85	120

7.4.4.2 Results and discussion

Figure 7.3 shows a plot of the total effluent COD concentration versus the digester pH for each of the four steady state systems. The total effluent COD increased almost linearly with an increase in pH. More detailed analysis showed that the increase in the total effluent COD concentration was due to an increase in the soluble COD concentration, not the particulate COD concentration. Further speciation of the soluble COD concentration showed that the soluble organic COD concentration was consistently low for all systems, while the aqueous sulfide concentration showed an increase with an increase in pH similar to the total COD concentration (see Figure 7.3), and thus the observed increase was due to an increase in the dissolved sulfide concentration.

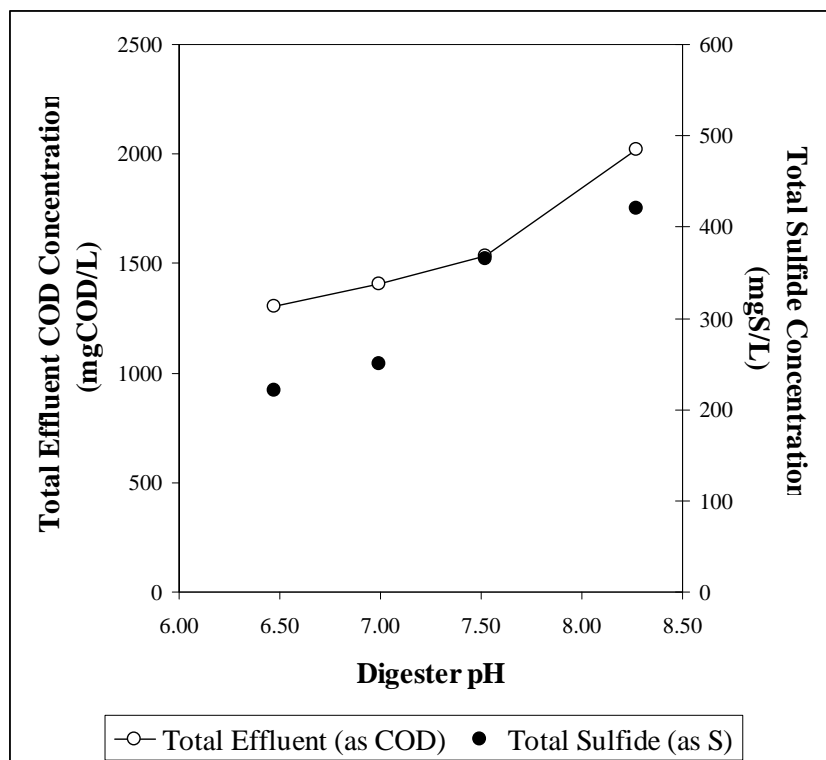


Figure 7.3: Effluent total COD concentrations (mgCOD/L) and total sulfide concentrations (mgS/L) for the four sulfate-reducing systems operated at varying pH's, to show the effect digester pH on the sulfide concentration, and the effect of the aqueous sulfide concentration on the total COD measurement

Thus, the effluent particulate COD concentration remained relatively constant at the four pH values. This would indicate a constant rate of PSS hydrolysis for all digester pH values, since for three of the systems, the feed PSS was common, and the retention time was the same in all four systems. Following the procedures described above, the volumetric rates of PSS hydrolysis were calculated for all four systems, see Table 7.5. The calculated rates of PSS hydrolysis for three of the four systems are near identical (127 – 130mgCOD/L.d), while the fourth system (pH = 8.3) is markedly different (85mgCOD/L.d). That the three systems have the same rate of hydrolysis for the pH range 6.5 – 7.5 substantiates that the pH does not affect the rate of hydrolysis under sulfate-reducing conditions, similar to methanogenic systems as described in Chapter 6. The sulfate-reducing systems operating at pH's 6.5 – 7.5 were fed with PSS feed batch 14; while the system with a pH of 8.3 was fed with feed batch 16. Therefore, it is possible that the different rates of PSS hydrolysis for this system was due to the different feed batch. Since this was the only system for which this batch was used as feed, this could not be verified.. Therefore, there is no evidence based on other operating data to indicate whether the problem with the different rate of hydrolysis is due to the feed batch or not.

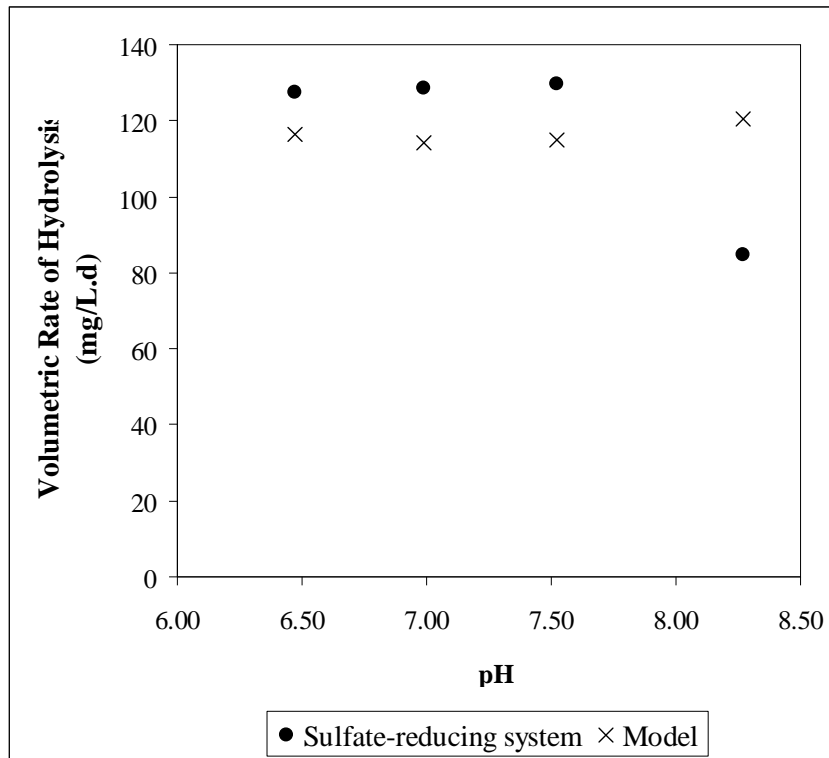


Figure 7.4: Calculated and predicted volumetric hydrolysis rates as a function of the digester pH showing that digester pH has little effect on the observed rate of hydrolysis (pH 8.30 is not consistent with trend, different feed batch)

Table 7.6: Summary of the results from the sulfate-reducing systems (COD concentrations in mgCOD/L; rate in mgCOD/L.d)

Steady state	R _h (d)	pH	Measurements (mg/L)						Calculated				
			Total Feed COD (mgCOD/L)	Soluble Feed COD (mgCOD/L)	Total Effluent COD (mgCOD/L)	Soluble Effluent COD (mgCOD/L)	Soluble Effluent Organic COD (mgCOD/L)	Feed Sulfate Conc. (mgSO ₄ /L)	Effluent Sulfate Conc. (mgSO ₄ /L)	COD:SO ₄ ratio added (gCOD/gSO ₄)	COD:SO ₄ ratio consumed (gCOD/gSO ₄)	Sulfide Conc. (mgS/L)	Rate of Hydrolysis (mgCOD/L.d)
36	8	6.47	1950	278	1304	521	80	2000	436	0.97	0.75	221	127
22	8	6.99	1950	298	1406	655	155	2000	770	0.97	0.98	250	129
20	8	7.52	1950	293	1532	790	61	2000	530	0.97	0.82	365	130
47	8	8.27	1890	203	2020	926	84	1600	47	1.18	0.51	421	85
15	8	6.87	13270	1509	13001	197	197	9600	733	1.38	0.80	0	805
6	10	7.06	25953	2647	10684	157	157	1000	34	25.95	0	0	1463
46	10	7.92	989	102	897	466	42	1000	51	0.99	0.59	212	52
42	13.3	7.75	2013	221	1749	964	129	2000	147	1.01	0.66	418	86
41	16	7.64	2015	207	1697	897	85	2000	no analysis	1.01	0	406	72

7.5 COD:SO₄ Utilization Ratio

Table 7.6 lists the COD:SO₄ utilization ratios for all of the sulfate-reducing steady state systems investigated. The minimum COD:SO₄ ratio excluding biomass metabolic yield is 0.67, see Section 7.4.1.2 above. Taking into account anabolic COD utilization for cell production, the COD:SO₄ utilization ratio should be >0.67. Table 7.6 lists observed values ranging from 0.5 to 0.975. The ratios below 0.67 (steady states 42, 46 and 47) seemed to be due to experimental error. Further investigation showed that these steady states were all collected towards the end of the research program (Steady state numbers 41, 42, 46 and 47 out of 47 total steady states analysed). The sulfate samples collected for steady state number 41 were stored after filtration in glass bottles with screw-on lids, and the inside of the lids contained a rubber seal. Due to analytical demands, the samples were stored before analysis. When the sulfate analyses were performed (after about a week), the results showed significant variation, and no steady state sulfate concentration was obtained. Although not confirmed, the sulfide possibly reacted with the rubber seals, oxidizing back to sulfate, which would be included in the sulfate measurement.

Based on the concerns that the sulfate samples could not be stored before analysis, for the next three steady states (steady state numbers 42, 46 and 47) the samples were pretreated by adding zinc acetate to precipitate the aqueous sulfide, followed by addition of 10M NaOH to precipitate excess zinc, and then filtration through a membrane filter paper (see Chapter 3, Section 3.5.6 and Appendix D). In the analysis for sulfate, this filtrate was placed in a platinum crucible and dried, before the carbonate fusion pretreatment was performed (Chapter 3). Further investigation showed that at this time, the drying was performed in an oven at 180°C, while previously a steam bath had been used. The rapid drying in the oven plus the high temperature caused that the crystals that formed in the crucible developed stresses that, when released, resulted in the crystals, and therefore the contained sulfate, to be expelled from the crucible. Therefore, the sulfate concentration in these systems was being under measured, resulting in the low COD: SO₄ utilization ratios. Accordingly, steady state numbers 41, 42, 46 and 47 were excluded from further analysis.

Based on the systems where the sulfate samples were dried on a steam bath, the mean COD: SO₄ utilization ratio was $0.81 \pm 0.085 \text{gCOD/gSO}_4$. This ratio compares very favourably with the ratio of 0.78gCOD/gSO_4 calculated for the system operated by Enongene (2003). This ratio is of critical importance in operating sulfate-reducing systems with PSS, since it allows for the correct mass of PSS to be blended with the sulfate-rich wastewater, so that the residual sulfate concentration will be below the discharge limit, and excess organics will not be present in the effluent. This ratio was verified in a laboratory scale upflow solids retention sulfate reducing system (see Section 7.7 below).

It is important to note that although the effluent sulfate concentration was being underestimated due to loss of sulfate sample in the 180°C oven, there was still residual sulfate in the systems, and hence the systems were not sulfate limited, and sulfate-reducing conditions were maintained.

7.6 Comparison of Rates of Hydrolysis of PSS under Sulfidogenic, Methanogenic and Acidogenic Conditions

The rates of PSS hydrolysis under sulfidogenic, methanogenic and acidogenic conditions were compared by comparing the conversions of PSS biodegradable particulate COD

calculated in terms of the model framework under the three conditions, see Figure 7.5. Also included are the conversions for the methanogenic and acidogenic systems operated by O'Rourke (1968). Figure 7.5 shows that for the systems operated in this investigation under methanogenic conditions, the biodegradable particulate COD conversion exceeds 78% at all retention times, and for methanogenic systems operating with a retention time greater than 10 days, the biodegradable particulate COD conversion is greater than 90%. Similarly for the O'Rourke (1968) data, where for "true" methanogenic conditions, the biodegradable particulate COD conversion is greater than 90% and lies within the data collected in this investigation. However, for the O'Rourke (1968) data, when methanogenesis is incomplete, the % conversion decreases, and for fully acidogenic systems (no methanogenesis) the conversion is less than 15%. As noted in Chapter 5, near identical results have been obtained in this study: For all the acidogenic systems (all fully acidogenic), the biodegradable particulate COD conversion was between 10 and 21 %, even at the 10 day retention times. Clearly the rate of PSS hydrolysis is significantly reduced in the absence of methanogenesis. In Chapter 6 (Figure 6.4), it was shown that the effect of pH on the rate of PSS hydrolysis under acidogenic conditions is relatively small, and hence this cannot account for the observed difference between acidogenic and methanogenic systems.

For the sulfate reducing systems, for the data collected in this study the biodegradable particulate COD conversions all fall within the equivalent methanogenic conversions for data collected in both this study and by O'Rourke (1968). Clearly, under the conditions which these systems were operated (sulfide not inhibitory), sulfate reduction *per se* does not influence the rate of PSS hydrolysis.

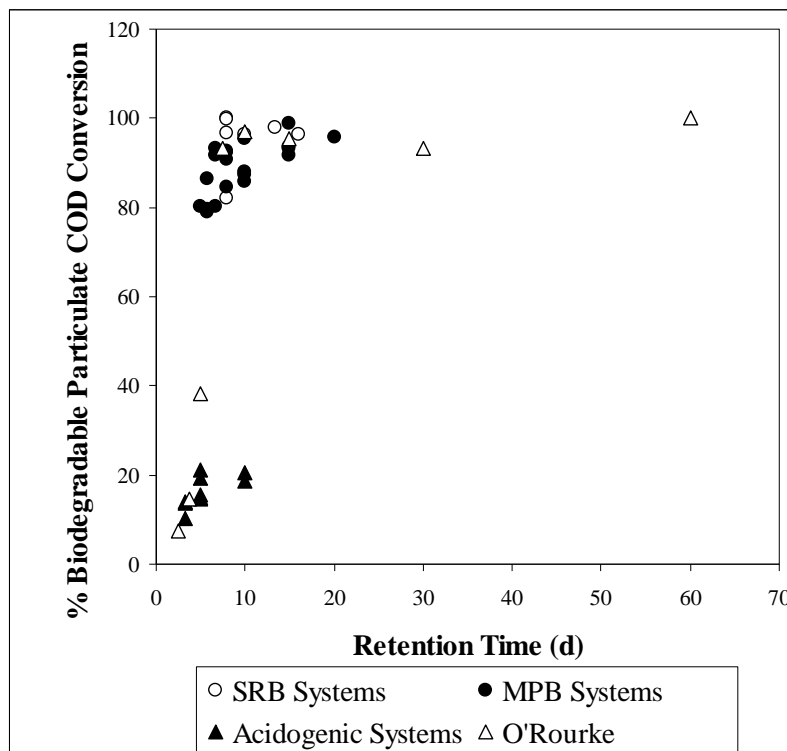


Figure 7.5: Biodegradable particulate COD conversions (as a % of influent PSS biodegradable particulate COD) versus retention time for the methanogenic (Chapter 4), acidogenic (Chapter 5) and sulfate reducing (Chapter 7) systems operated in this study, and the systems operated by O'Rourke (1968)

7.7 Effluent Suspended Solids Concentration

For the treatment of PSS in systems where the solids retention time is uncoupled from the hydraulic retention time due to solids retention by gravity settling (nearly all systems other than a completely mixed digester), the settleability of the sludge is critical for the design of the system, since this would impact the effluent solids concentration which directly affects the solids retention time and effluent quality; a sludge that has reduced settleability would require provision of increased settling zones or result in a lower solids retention time. Therefore, for the methanogenic, acidogenic and sulfate-reducing steady states presented and discussed in this study, the suspended solids concentration was measured, using the method described in detail in Chapter 3, Section 3.5.7.

This method required that the effluent from the digesters was placed in a 500mL-measuring cylinder and allowed to settle for 30min. After the settling time, a sample was drawn from the cylinder approximately 8cm from the liquid surface, which was always above the height of the settled solids zone. This sample was diluted as necessary ($\sim 500\text{mgCOD/L}$), and the total COD (S_t) analysed. From this analysis, and a separate measurement of the soluble COD concentration (S_s), the total suspended solids COD concentration (S_{SS}) was calculated ($S_{SS} = S_t - S_s$). Since for each of the steady state systems analysed the feed COD ranged from 2 to 40gCOD/L, the total effluent COD was different, and hence the absolute values for suspended solids COD concentrations for all systems could not be compared directly. Therefore, the ratio (f_{SS}) between the effluent suspended solids COD concentration and the effluent total particulate COD concentration (already calculated for each of the systems, see Chapter 4 to 7) was calculated for each steady state, and this ratio is plotted in Figure 7.6.

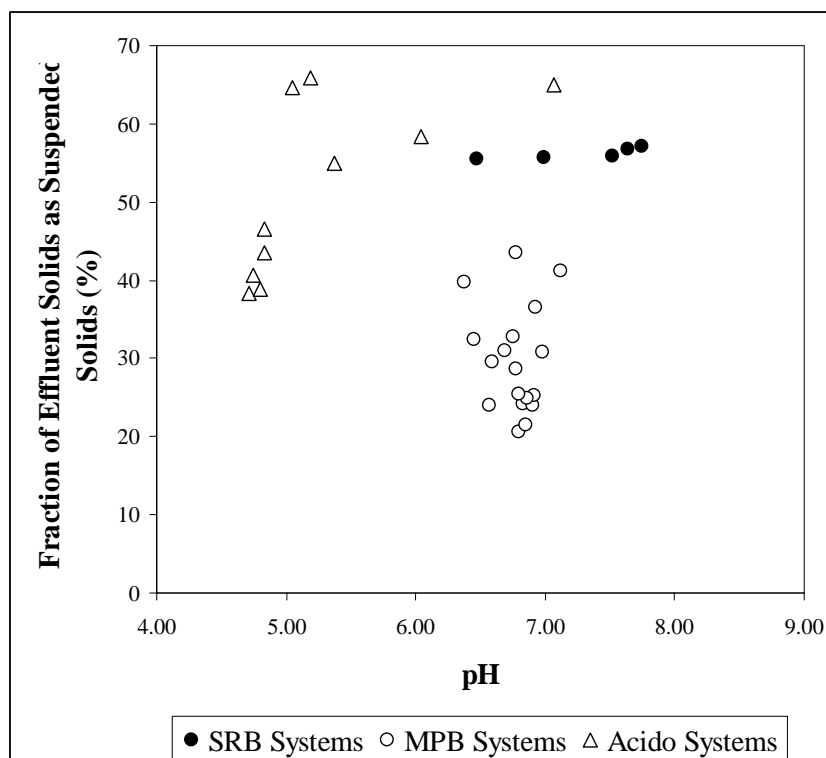


Figure 7.6: Ratio between the effluent suspended solids COD concentration and the effluent total particulate COD concentration (f_{SS}) for methanogenic (MPB), acidogenic (Acido) and sulfate-reducing (SRB) systems as a function of pH

For methanogenic (MPB) systems, (Figure 7.6) there is no correlation between the ratio (f_{SS}) and pH, and f_{SS} ranges between 20.6 and 43.5%, with a mean value of $29.0 \pm 6.7\%$. For the acidogenic systems, there is a significant increase in f_{SS} with an increase in pH. Also, for the systems fed 2gCOD/L, f_{SS} is significantly higher (64.7 and 65.8%) than for the systems fed at 26 and 40gCOD/L ($40.6 \pm 3.1\%$). For the sulfate-reducing systems, there is no significant change in f_{SS} with a change in pH ($55.9 \pm 0.6\%$). The f_{SS} for sulfate-reducing systems is significantly higher than for methanogenic systems ($55.9 \pm 0.6\%$ and $29.0 \pm 6.7\%$ for sulfate-reducing and methanogenic systems respectively), indicating that it would be more difficult to retain the solids in a sulfate-reducing system than in a methanogenic system. Further, for acidogenic systems, reducing the feed COD concentration and increasing the digester pH would result in poorer settling and hence retention of the solids. However, typically, these systems would not be diluted to concentrations as low as 2gCOD/L, and from Chapter 5, the steady state operating pH would be in the region of 5, for which the settleability of the solids is shown to be greater than at higher pH values, and comparable with methanogenic systems.

7.8 Laboratory Scale Sulfate Treatment Process

7.8.1 Conceptual process design

PSS has been identified as a low cost carbon and electron source for biological sulfate reduction in the treatment of acid mine drainage (AMD, Whittington-Jones, 1999; Corbett *et al.*, 2000, Rose *et al.*, 2002, see Chapter 2, Section 2.5.1). The AMD would consist of heavy metals, sulfate (2.4gSO₄/L) and a low pH (2 – 3). The values for sulfate would differ for each source of AMD, and are used for illustration purposes only. A conceptual unit process train to treat AMD of this nature would consist of a number of unit operations in which the various components of AMD are treated individually. Figure 7.7 describes such a conceptual unit process train for the treatment of AMD.

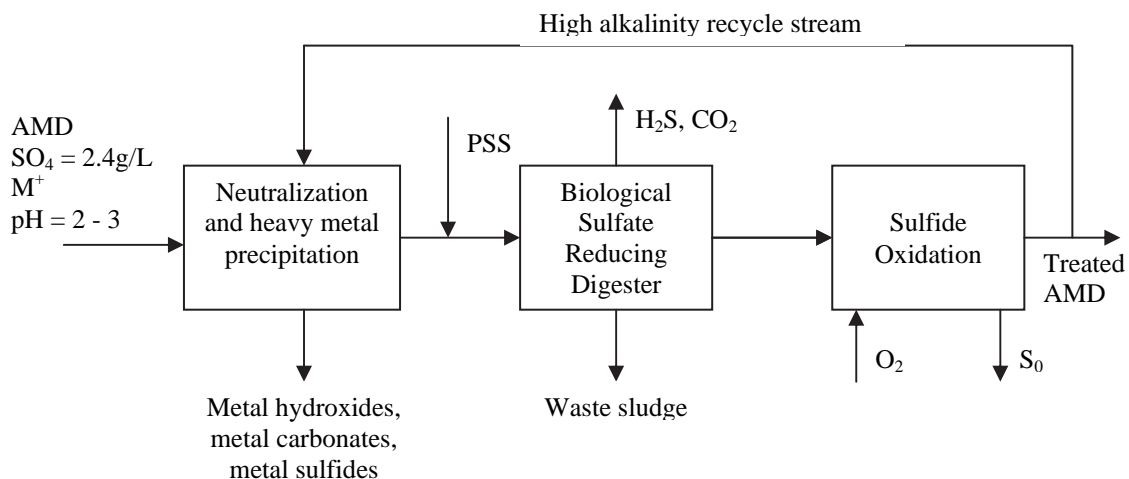


Figure 7.7: Conceptual process from the treatment of AMD using biological sulfate reduction and primary sewage sludge

The central unit operation in the above treatment is the biological sulfate reducing digester, in which the sulfate is reduced to sulfide, some of which leaves the system as hydrogen sulfide gas, but the majority leaves as aqueous sulfide. Similarly, carbon dioxide gas produced is in equilibrium with the dissolved carbonate species, and both the dissolved and gaseous forms leave the sulfate reducing digester. The next step in the process is the sulfide oxidation step,

in which the aqueous sulfide produced in the sulfate-reducing digester is oxidised either chemically or biologically to elemental sulfur. The effluent from this unit operation would contain dissolved carbonate species and residual sulfide, and probably a near neutral pH. This high alkalinity effluent is split and recycled to blend with the raw AMD stream. The increase in pH of the AMD stream when blended with the recycle stream would result in precipitation of the metals as metal carbonates, hydroxides and some metal sulfides. These metal precipitates are settled out of the AMD stream, leaving a neutral pH and metal-free stream. This is blended with PSS and enters the biological sulfate-reducing process. Therefore, using this type of scheme, all of the components of AMD (metals removal, pH neutralization and sulfate reduction) can be treated.

The unit operation of interest to this study is the biological sulfate-reducing digester, but clearly the feed to this unit operation is dependent on the operation and configuration of the overall treatment. For this study, the recycle stream flow rate in the conceptual process is made equal to the AMD flow rate, so that the sulfate concentration entering the sulfate-reducing digester is halved ($1200\text{mgSO}_4/\text{L}$) by dilution. Also, the pH of this stream is near neutral, and probably contains some alkalinity. Based on these assumptions, the feasibility of operation of a biological sulfate-reducing system was evaluated at laboratory scale. For the biological sulfate-reducing system, an upflow configuration was selected, to combine biological reactions and phase separation in a single reactor, similar to the UASB.

7.8.2 Laboratory-scale reactor operation

A laboratory-scale UASB-type reactor was operated to determine the feasibility of using this type of reactor configuration as the biological sulfate-reducing digester in the treatment scheme described in Figure 7.7. The laboratory-scale digester feed consisted of $1200\text{mgSO}_4/\text{L}$, added as dissolved Na_2SO_4 , and alkalinity ($500\text{mgCaCO}_3/\text{L}$) added as NaHCO_3 powder. To this, $1.6\text{gCOD}/\text{L}$ of PSS was added. The feed COD: SO_4 ratio was based on the $0.8\text{gCOD}/\text{gSO}_4$ utilization ratio determined in Section 7.5 ($1200\text{mgSO}_4/\text{L}$ requires $960\text{mgCOD}/\text{L}$ of biodegradable COD), and a total unbiodegradable COD fraction of 40% which is close enough to that determined in Chapter 4 (60% of total COD = $960\text{mgCOD}/\text{L}$; total COD = $1600\text{mgCOD}/\text{L}$). The PSS was macerated for 1min to break up the larger particles, since the feed was to be pumped through a laboratory-scale positive displacement pump, which would be susceptible to blocking by larger particles.

The UASB reactor had a total volume of 10.5L, and a diameter of 10cm. The digester was heated to approximately 35°C with heating wires wrapped around the column to the height of the sludge bed, with a thermocouple situated near the bottom of the column, and controlled by the same temperature controller used for the completely mixed systems (see Chapter 3, Section 3.3.2). The system was seeded with waste sulfate-reducing sludge from the completely mixed sulfate-reducing systems fed PSS, and waste from methanogenic anaerobic digesters being fed waste activated sludge. The seed sludge thus contained acidogenic, methanogenic and sulfate-reducing biomass.

The hydraulic retention time was initially set to above 5d, to allow for the biomass to acclimatise and for the sludge bed to accumulate. The sludge bed volume was allowed to increase from the initial volume of around 2L to between 4.5 and 5L, at which time sludge was wasted from a sample port along the length of the column. The sludge was wasted from the top of the sludge bed, and although not confirmed through measurement, this sludge was thought to consist mainly of unbiodegradable particulate matter.

At regular intervals, the hydraulic retention time was reduced stepwise by increasing the dosing rate of the feed pump. At each dosing rate, the system was allowed to stabilise until the VFA concentration was negligible, and the alkalinity and pH was constant, before the next retention time decrease.

7.8.3 Results

Figure 7.8 plots the daily volume of feed (measured as the volume of effluent collected) fed to the UASB-type system. Based on the 10.5L reactor volume, the hydraulic retention time was calculated from the feed volume, and this is also plotted in Figure 7.8. From Figure 7.8, the system was operated with a hydraulic retention time less than 12h without the sludge bed becoming unstable or fluidising the solids.

The sludge bed initially, was allowed to accumulate until a final volume of 4.5 – 5L was reached. Thereafter, sludge was wasted regularly from the top of the sludge bed (oldest sludge) to maintain a bed volume of approximately 4.5L. The hydraulic retention time in the sludge bed was calculated based on a bed volume of 4.5L, Figure 7.9. From Figure 7.9, the minimum sludge bed hydraulic retention time was 4.8h, and this was maintained for more than 1 week.

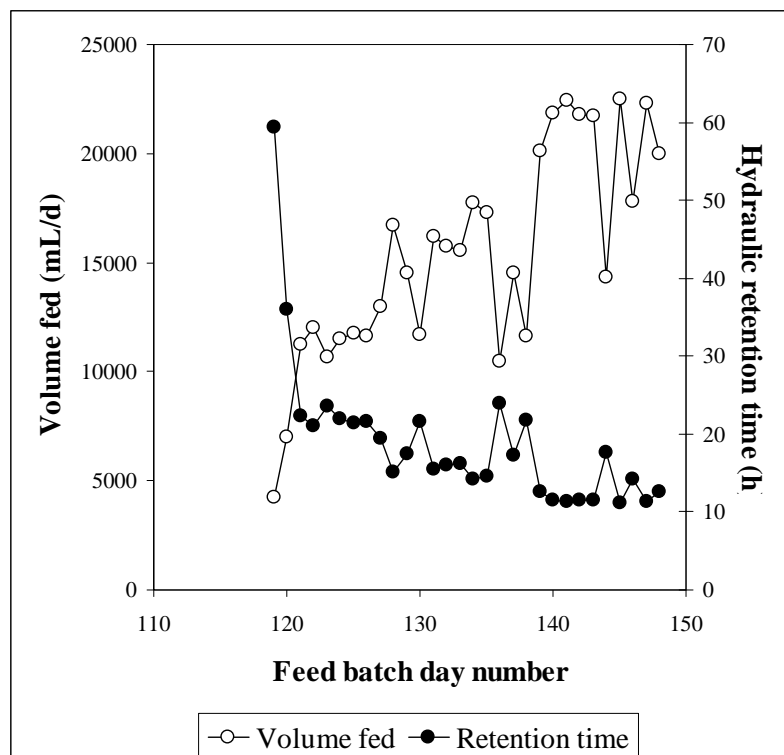


Figure 7.8: Daily feed volume and hydraulic retention time for the UASB-type digester treating the sulfate component of AMD using PSS

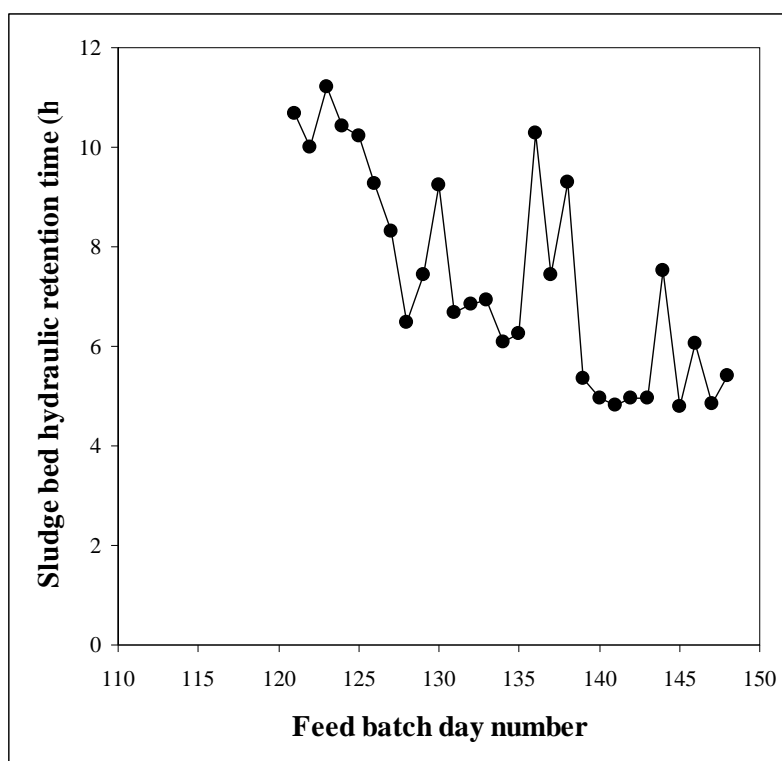


Figure 7.9: Sludge bed hydraulic retention time based on a bed volume of 4.5L (controlled)

Considering that the biodegradable particulate organic substrate and active biomass are in significant concentrations only in the sludge bed, and that the settling zone above the bed contains negligible masses of both substrate and biomass, then the sludge bed volume is the biologically active volume of the system. If the system were designed such that the settling zone volume was small compared with the sludge bed volume, the hydraulic retention time in the system could be reduced to close to 4.8h without negatively affecting the performance of the biological processes or the stability of the sludge bed.

As with the methanogenic and sulfate reducing completely mixed digesters discussed previously for the kinetic studies, an effluent VFA concentration below 50mgHAc/L would constitute a stable digester performance, with a balance existing between the VFA-producing hydrolysis/acidogenesis processes and the VFA-consuming sulfate-reducing processes. Figure 7.10 plots the VFA and alkalinity concentrations in the settling zone of the UASB-type system over 20 days of operation during which the hydraulic retention time was reduced to <12h, and the sludge bed retention time was a low as 4.8h. From Figure 7.10, the VFA concentration was well below the 50mgHAc/L limit, and the alkalinity was constant at $1883 \pm 108\text{mgCaCO}_3/\text{L}$. The constant alkalinity measurement indicates that the substrates were being converted to a constant degree, since the net alkalinity production is a consequence of the overall PSS anaerobic digestion conversion, provided the VFA remain as low as is the case here.

The system was analysed in more detail on two occasions. The particulate COD, soluble organic COD, aqueous sulfide and residual sulfate concentrations were analysed for both the feed and effluent where applicable.

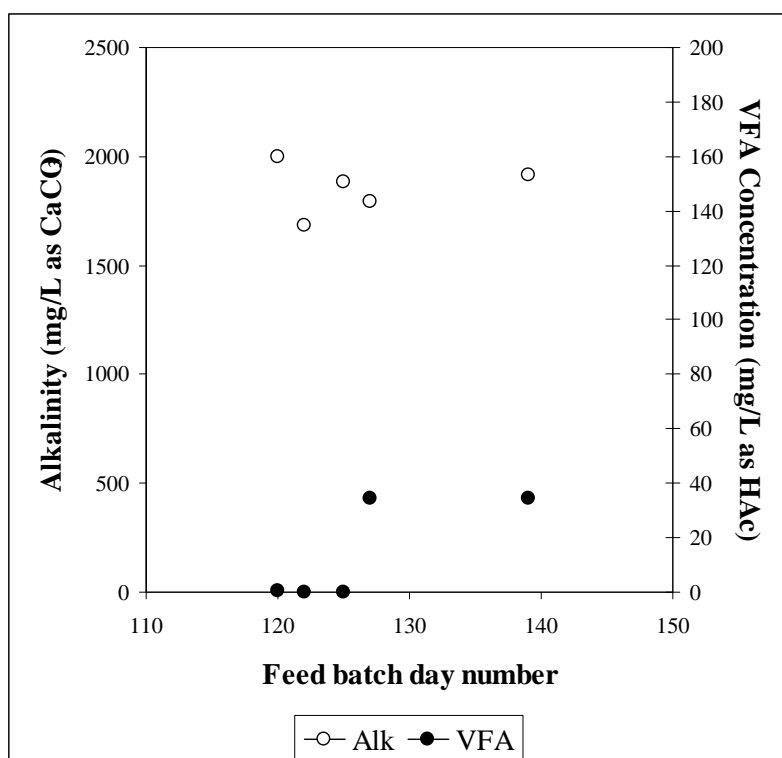


Figure 7.10: Effluent VFA and alkalinity concentrations for the UASB-type digester treating the sulfate component of AMD using PSS

Table 7.7: Summary of the results from the sulfate

	Feed 1	Feed 2	Effl. 1	Effl. 2	Effl. 3
Total COD (mgCOD/L)	1611	1666	837	853	
Soluble organic COD (mgCOD/L)	221	214	56	89	
Particulate COD (mgCOD/L)	1390	1452	248	236	
Aqueous Sulfide (mgS/L)			266	264	
Sulfate (mgSO₄/L)	1200	1200	133	86	71
Sulfate Conversion (%)			88.9	92.8	94.1
VFA (mgHAc/L)	96	88	0	31.9	34.2
Alkalinity (mgCaCO₃/L)	450	680	1883.2	1810.5	1790.5

Table 7.7 lists the results of the analysis of the feed and effluent. The effluent particulate COD concentration was 248 and 236mgCOD/L, while the feed particulate COD concentration was 1421 ± 31 mgCOD/L. Only 17% of the feed particulate COD was leaving the system with the effluent, the remainder being degraded or removed when the system was desludged. Also, the effluent soluble organic COD concentration was low (56 and 89mgCOD/L), suggesting a stable sulfate-reducing biomass. Importantly, the effluent sulfate concentration (86 ± 26 mgSO₄/L) was well below the discharge limit of 250mgSO₄/L (personal communication with P.D. Rose). Therefore, the feed COD: SO₄ ratio of 1.6: 1.2 gCOD/gSO₄ (1.33:1 gCOD/gSO₄) resulted in sufficient sulfate removal without excess COD addition, and is thus confirmed as the appropriate feed blend ratio.

It is important to note that this exercise was only to determine the feasibility of using an up-flow type reactor configuration to treat sulfate-containing water with PSS. The results show

that stable operation and significant removal of sulfate is possible in such a configuration. Also, the effluent from such a system contains very low concentrations of soluble and particulate organic COD. The configuration used in this feasibility study is by no means optimised, nor has the lower hydraulic retention time limit been determined. There is sufficient evidence though to suggest that this configuration has potential for the treatment of the sulfate component of AMD with PSS, and that further evaluation of the system is required.

7.9 Closure

In this chapter, the biological reduction of sulfate with PSS as substrate has been investigated, and the effect of the sulfate reduction on the PSS hydrolysis rate was examined through a series of experiments.

Experiment 1 shows that a sulfate stream containing 1gSO₄/L can be treated successfully in an anaerobic digester operated at a 10-day retention time with a feed COD concentration of 26g/L without causing any negative effects on the behaviour of the digester, or more specifically, the methanogenic processes. In fact, the stability of the digester may be enhanced due to the increase in alkalinity from the sulfide production. An important further observation is that sulfate reduction, at the concentration of sulfate added, had no influence on the rate of PSS hydrolysis. These are important observations for the potential treatment of sulfate rich waste streams in existing methanogenic sludge treatment plants.

The observations from Experiment 2 are of particular relevance for the treatment of sulfate rich wastes with PSS. From the comparison with the methanogenic system, it is clear that in the absence of sulfide, the hydrolysis rates of the particulate organic matter in PSS are not altered when sulfate reduction takes place. The effluent soluble organic COD concentration was negligible in both systems, showing that, in the absence of sulfides, the SRB can use all organic acids produced as substrate when not sulfate limited. The implications of these observations to a SRB process are significant. They indicate that in sulfate reduction and removal with PSS, there is no need for a polishing step to remove unstabilized organic matter, since this can be achieved within the sulfate-reducing digester.

The results from the SRB 2 digester (without ferrous addition) also are important from a kinetic and process design and operation point of view. From the observations, it is clear that aqueous sulfide inhibits the SRB since the effluent SO₄ concentration increased significantly when the ferrous dosing ceased, even though there was residual soluble organic COD present in the system. Unfortunately, it is not clear whether the rate of PSS solubilisation was affected since the system was not allowed to reach steady state, and this aspect requires further investigation.

For systems operating at 2gCOD/L and 2gSO₄/L, no sulfide inhibition effects were observed, and the rate of PSS hydrolysis under sulfate-reducing conditions was near identical to the rate observed for methanogenic systems fed 2gCOD/L, and the mathematical model can predict the digester performance. Further, as for methanogenic systems, the operating pH has no effect on the rate of hydrolysis under sulfate-reducing conditions.

Chapter 7: Sulfate-reducing Systems

Chapter 8

Conclusions

The principle aim in this study was to determine the rate of hydrolysis of primary sewage sludge (PSS) under methanogenic, acidogenic and sulfate-reducing conditions, and the influence of the system physical constraints on the rate. To achieve this aim, a wide ranging comprehensive experimental investigation has been undertaken, with laboratory-scale anaerobic digesters receiving PSS as feed, operated and monitored under carefully controlled and defined conditions. These conditions include methanogenic, acidogenic and sulfate-reducing systems, and the physical constraints of varying solids retention time, feed COD and sulfate concentrations and pH.

8.1 Methanogenic systems

Completely mixed methanogenic anaerobic digesters were operated at hydraulic retention times (= SRT) from 5 to 60d, with feed COD concentrations of 2, 13, 25 and 40gCOD/L at a controlled temperature of 35°C. For each feed COD concentration, the system hydraulic retention time was decreased step-wise until methanogenesis became unstable. Steady states periods were operated and analysed at regular retention time intervals. For these steady states:

- The minimum hydraulic retention time at which stable operation was observed was 5d at a feed COD concentration of 25gCOD/L
- Very good COD mass balances were obtained (mostly within 95 – 105%). The good COD recoveries lend credibility to the experimental data
- Reactor volatile fatty acid (VFA) concentrations were below 50mgHAc/L, and for most steady states considerably less than this

The above two observations indicate that stable methanogenic conditions had been established in all systems, a requirement for further analysis of the data

Based on an understanding of the concepts of the processes operating in the digesters:

- Characterization of the PSS is essential in order to quantify PSS hydrolysis rates correctly
- The influent PSS was characterized to give:

$$S_{ti} = S_{upi} + S_{bpi} + S_{usi} + S_{bsfi} + S_{VFai}$$

Chapter 8: Conclusions

where S_{fi} is the PSS total feed COD concentration, S_{upi} is the unbiodegradable particulate concentration, S_{bpi} is the biodegradable particulate concentration, S_{usi} is the unbiodegradable soluble concentration, S_{bsfi} is the biodegradable soluble non-VFA (fermentable) concentration and S_{VFAi} is the volatile fatty acids concentration.

In terms of the characterization of the PSS above, from the application of mass balance principles, the volumetric rate of PSS hydrolysis ($rate_{hydrolysis}$) was quantified for each steady state of operation (Figure 8.1):

- Consistent trends in the effects of SRT and PSS feed concentration were evident, substantiating data consistency
- For all feed COD concentrations, a decrease in the PSS feed concentration causes a corresponding decrease in $rate_{hydrolysis}$
- From an analysis of the data for the SRT = 60d system, the unbiodegradable particulate COD (S_{upi}) as a fraction of the total PSS COD concentration (S_{fi}) was 33.45%. This closely corresponds with the 36% obtained for data of O'Rourke (1968)

From the literature, various rate formulations for PSS hydrolysis were identified, and evaluated against the measured methanogenic anaerobic digester data. These included (with the appropriate calibrated kinetic constants):

- First order kinetics: $rate_{hydrolysis} = k_h \cdot S_{bp}$ (8.1)

where $k_h = 0.992 \pm 0.492d^{-1}$

- First order specific kinetics: $rate_{hydrolysis} = k'_h \cdot S_{bp} \cdot Z_{ad}$ (8.2)

where $k'_h = 0.00138 \pm 0.00131 \text{ L/mgZ}_{ad} \text{ as COD.d}$

- Monod kinetics: $rate_{hydrolysis} = \frac{\mu_{max} \cdot S_{bp} \cdot Z_{ad}}{Y_{ad} (K_S + S_{bp})}$ (8.3)

where $\mu_{max} = 0.243d^{-1}$ and $K_S = 640\text{mgCOD/L}$

- Surface reaction kinetics: $rate_{hydrolysis} = \frac{k_{max} \left(\frac{S_{bp}}{Z_{ad}} \right)}{\left(K_S + \frac{S_{bp}}{Z_{ad}} \right)} Z_{ad}$ (8.4)

where $k_{max} = 11.2\text{mgCOD/mgZ}_{ad} \text{ as COD.d}$ and $K_S = 13.0\text{mgCOD/mgZ}_{ad} \text{ as COD}$, and where S_{bp} is the biodegradable particulate COD concentration (mgCOD/L) and Z_{ad} is the acidogenic biomass concentration (mgCOD/L).

From an assessment of the fit of predicted to calculated values, it could be concluded that:

- The first order kinetics and surface reaction kinetics most accurately predict the rate of PSS hydrolysis under methanogenic conditions for all hydraulic retention times and feed COD concentrations evaluated.

Chapter 8: Conclusions

- Since first order kinetics are a simplification of the hydrolysis process (the acidogenic biomass is not explicitly included, nor is there an upper limit to the rate), surface reaction kinetics (Eq 8.4) are the most appropriate rate formulation for PSS hydrolysis
- However, due to the simplicity of first order kinetics, and since these kinetics were able to accurately predict the PSS hydrolysis rate under all operating conditions, first order kinetics were used in this study to compare the PSS hydrolysis rates under the different operation conditions
- With the first order kinetics and a first order kinetic constant value of 0.992d^{-1} , and an unbiodegradable particulate COD fraction of 33.45% of the total feed COD concentration, very close correlation was obtained between model predicted and calculated (from experimental data) volumetric rates of PSS hydrolysis under methanogenic conditions for all hydraulic retention times and feed COD concentrations, see Figure 8.1
- The model, as calibrated above, was applied to data collected in the independent study of O'Rourke (1968); close correlation was obtained
- The good fits of the model predictions to the data collected in this and the independent study of O'Rourke (1968) provides powerful evidence validating the model

From an extensive investigation into the effect of pH on methanogenic anaerobic digesters:

- The minimum operating pH for methanogenic systems was determined at 6.38 before methanogenesis failed
- Increase in the operating pH above 6.38 has no effect on the PSS hydrolysis rate (pH = 6.38, 6.5, 7.0, 7.5, 8.0)

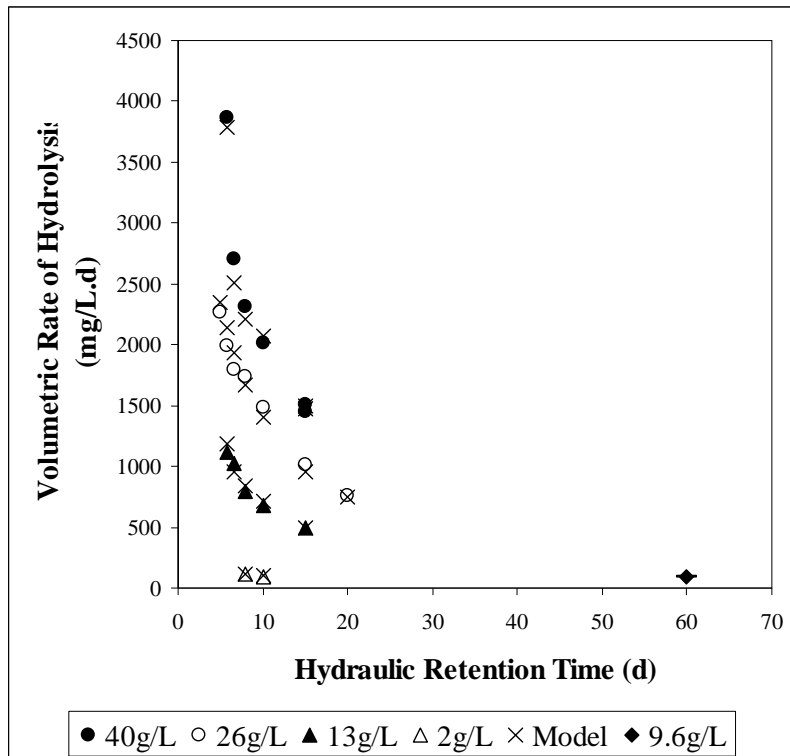


Figure 8.1: Calculated (from experimental data) and predicted (first order kinetics) rate of hydrolysis for each hydraulic retention time at each feed COD concentration

8.2 Acidogenic systems

Acidogenic systems were operated under varying hydraulic retention times (3.33 - 10d) and feed COD concentrations (2 – 40gCOD/L) at a constant temperature of 35°C.

At each retention time and feed concentration, steady state periods were identified and analysed in detail:

- Very good COD mass balances were obtained (92 – 103%). This lends credibility to the experimental data
- Negligible methane gas productions were recorded
- The observations above substantiate the acidogenic condition, i.e. no methanogenesis

For each steady state of operation, the volumetric rate of hydrolysis was calculated:

- For systems fed the same feed COD concentration and operating at the same hydraulic retention time, the volumetric rates of hydrolysis were significantly lower under acidogenic conditions compared with the corresponding methanogenic conditions.

In applying the first order PSS hydrolysis kinetics developed for the methanogenic systems to the acidogenic systems:

Chapter 8: Conclusions

- The value of the first order rate constant had to be decreased significantly, substantiating the lower hydrolysis rate
- The first order kinetic constant for acidogenic conditions is linearly dependent on the hydraulic retention time; the relationship was formulated to give:

$$k_h = 0.0883 - 0.0055.R_h \quad (8.5)$$

where R_h is the retention time (d)

- With the formulation above to calculate the value of the first order kinetic constant under acidogenic conditions (Eq 8.5), the model was able to reasonably accurately predict the rate of PSS hydrolysis under acidogenic conditions

To investigate the influence of pH on PSS hydrolysis under acidogenic conditions, further acidogenic steady state systems were operated at a constant hydraulic retention time (5d) and feed COD concentration (2gCOD/L), but with the digester operating pH controlled, and increased from the minimum pH 5 (steady state pH), to 8 at pH intervals of 1 (5.0, 6.0, 7.0, 8.0).

- The calculated rate of PSS hydrolysis under acidogenic conditions did not change when the pH was increased from 5 to 6
- However, when the pH was increased from 6 to 8, the observed rate of PSS hydrolysis increased linearly
- To include the effect above in the first order kinetics, Eq 8.5 was modified:

$$k_h = (0.0883 - 0.055.R_h) + 0.06 \left(\frac{pH - pH_{LL}}{pH_{UL} - pH_{LL}} \right) \quad (8.6)$$

where $pH_{LL} = 6.04$ and $pH_{UL} = 8.0$.

- With the modification above, first order kinetics was able to accurately predict the volumetric rate of PSS hydrolysis under acidogenic conditions for all operating pH values, see Figure 8.2

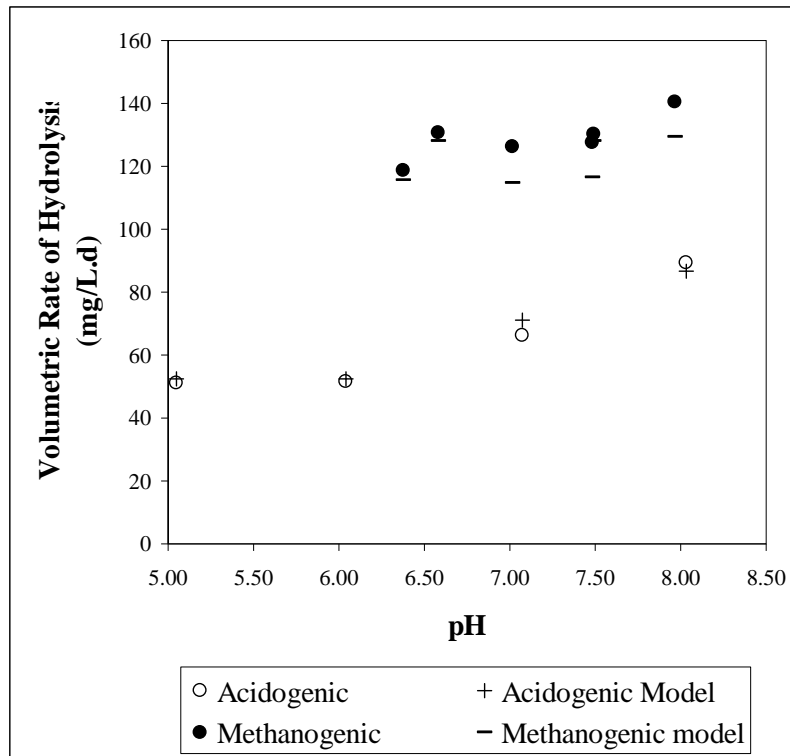


Figure 8.2: Calculated (from experimental data) and predicted (first order kinetics) rate of hydrolysis for methanogenic and acidogenic systems at varying operating pH values

8.3 Sulfate-Reducing systems

To quantify the rate of PSS hydrolysis under sulfate-reducing conditions and compare this rate with that for methanogenic systems, where possible these systems were operated in parallel digesters. Results from the initial experiments with limited sulfate reduction (1gSO₄/L with 26gCOD/L) showed that:

- The sulfate reduction did not influence the PSS hydrolysis rate compared with a parallel purely methanogenic system
- Methanogenesis was maintained in the digester. Therefore, a limited amount of sulfate reduction in methanogenic systems does not inhibit the hydrolysis nor methanogenesis processes, and can be treated in existing methanogenic digesters without jeopardising the process stability.

When the feed sulfate concentration was increased (9.6gSO₄/L with 13gCOD/L):

- No methanogenesis was observed
- Sulfate-reducing biomass outcompete methanogenic biomass for organic substrate
- Under sulfate-reducing conditions with low aqueous sulfide (precipitated with ferrous), the volumetric rate of PSS hydrolysis was the same as for the parallel methanogenic system

Chapter 8: Conclusions

- When the aqueous sulfide was not removed, sulfate reduction was inhibited, but no information regarding the PSS hydrolysis rate was collected
- From the observations above, it can be concluded that aqueous sulfide is inhibitory to sulfate reduction

A range of systems were operated at feed COD concentrations of 2gCOD/L and feed sulfate concentrations of 2gSO₄/L, at varying retention times:

- In all systems, sulfate was slightly in excess and effluent VFA concentrations were low (< 50mgHAc/L), indicating absence of inhibitions. Thus, at lower aqueous sulfide concentrations, sulfate reduction is not inhibited

The first order rate formulation calibrated under methanogenic conditions ($k_h = 0.992d^{-1}$ and 33.45% unbiodegradable particulate COD fraction) was able to adequately predict the rate of PSS hydrolysis under sulfate-reducing conditions.

- The observation above led to the conclusion that the PSS hydrolysis rate is closely similar under methanogenic and sulfate-reducing conditions, i.e. sulfate reduction *per se* does not appear to influence the PSS hydrolysis rate

Further investigation and analysis of the data showed that:

- An operating pH between 6.5 and 7.5 did not affect the rate of PSS hydrolysis under sulfate-reducing conditions
- The mean COD:SO₄ utilisation ratio in the sulfate-reducing systems was 0.8gCOD/gSO₄, similarly to 0.78gCOD/gSO₄ obtained by Enongene (2003). These ratios are significantly higher than the theoretical stoichiometric ratio of 0.67gCOD/gSO₄. However, taking into account COD utilization for the production of acidogen and sulfate-reducing biomasses, the theoretical ratio should be approximately 0.85gCOD/gSO₄, which is very close to the measured values
- The suspended solids concentration was significantly higher for sulfate-reducing systems compared with methanogenic systems, and the operating pH did not affect this concentration
- This has significant implications for sulfate-reducing systems in which solids and hydraulic retention times are uncoupled, as retention of sulfate-reducing biomass and PSS biodegradable particulate substrate may prove problematic

For acidogenic systems, the suspended solids concentration increased with increasing pH.

A feasibility study was conducted using a UASB-type reactor for biological sulfate reduction with PSS as feed. The system was fed PSS at 1.6gCOD/L and sulfate at 1.2gSO₄/L, and operated in an upflow configuration without recycle at hydraulic retention times below 12h, with a sludge bed retention time below 5h:

- The residual sulfate concentration was below 100mgSO₄/L, with negligible soluble organic COD in the effluent, indicating near complete sulfate reduction

- Effluent particulate COD concentration of 200mgCOD/L, indicating successful sludge retention in the system

These results were encouraging, and it can be concluded that:

- This reactor configuration is a feasible option for the treatment of large volumes of sulfate-rich water such as acid mine drainage
- A feed COD:SO₄ ratio of 1.33:1 gCOD:gSO₄ is adequate for the removal of more than 90% of the feed sulfate without significant residual biodegradable organic COD concentrations

8.4 Comparison of PSS Hydrolysis Rate under Methanogenic, Acidogenic and Sulfate Reducing Conditions

The PSS biodegradable particulate COD conversions for the systems operated in this study under methanogenic, acidogenic and sulfate reducing conditions were compared (Chapter 7, Section 7.6), together with the methanogenic and acidogenic systems operated by O'Rourke (1968), see Figure 8.3.

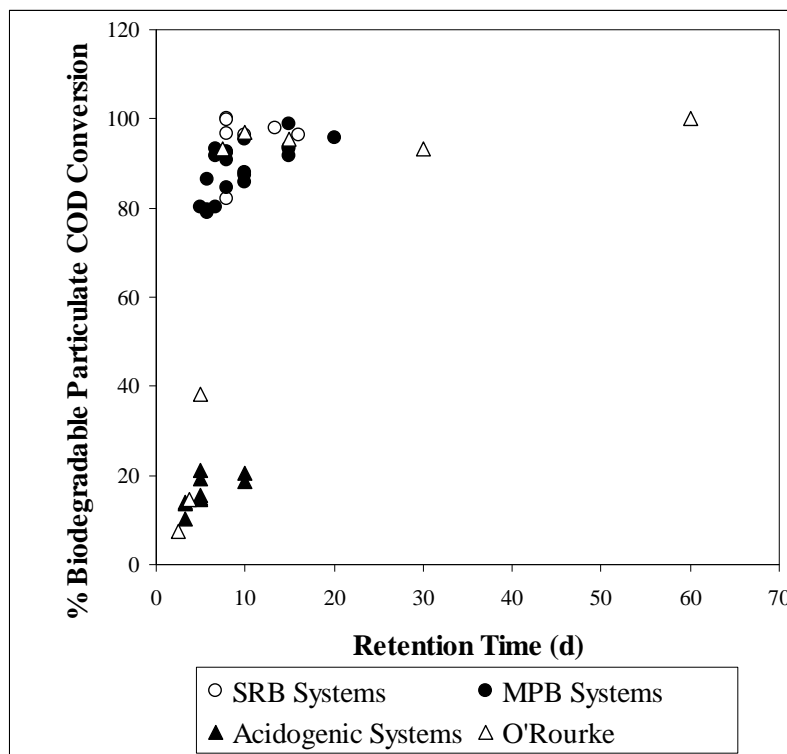


Figure 8.3: Biodegradable particulate COD conversions (as a % of influent PSS biodegradable particulate COD) versus retention time for the methanogenic (Chapter 4), acidogenic (Chapter 5) and sulfate reducing (Chapter 7) systems operated in this study, and the systems operated by O'Rourke (1968)

From Figure 8.3, it could be concluded that:

- The data gathered in this study, and substantiated by the observations of O'Rourke (1968) clearly indicates that the presence of methanogenesis substantially increases the rate of PSS hydrolysis, or conversely, the absence of methanogenesis and conditions created by acidogenesis substantially reduces the rate of PSS hydrolysis
- The effect above is not pH related; the effect of pH on PSS hydrolysis rates under acidogenic conditions is relatively small and could not account for the magnitude of the reduction in PSS hydrolysis rates
- Under the conditions which the sulfate reducing systems were operated (sulfide not inhibitory), sulfate reduction *per se* does not influence the rate of PSS hydrolysis

8.5 Closure

In this investigation, an extensive data set has been collected on anaerobic digestion of PSS under methanogenic, acidogenic and sulfate-reducing conditions, at varying retention times, feed concentrations and pH values. Through a strict attention to detail, the operating conditions for all systems were carefully controlled and completely defined.

To quantify the volumetric rate of PSS hydrolysis in such systems, a logical mathematical framework has been developed in terms of mass balance principles and characterisation of the PSS feed. This framework should provide a useful, common and systematic basis for comparisons of the hydrolysis rates for different systems. Further, a simple unified first order kinetics based model has been developed to describe PSS hydrolysis under methanogenic, acidogenic and sulfate-reducing conditions. This model takes into account the effects of retention time, feed COD concentration and pH, and the model has been validated both on data collected in this study and on data collected in independent studies.

Since PSS hydrolysis is the rate-limiting step in most methanogenic, acidogenic and sulfate-reducing systems, the subsequent processes are essentially stoichiometric. Hence, this simple model should be a valuable tool in the design, operation and control of steady state digestion systems. However, the model cannot take account of digester failure or behaviour under dynamic loading conditions. These will require development of a more extensive dynamic simulation model. In such a model, the evaluation here would suggest that surface reaction (Contois) kinetics is the most suitable for the PSS hydrolysis process. In this study, extensive data on transitions between steady states has been collected, which should prove useful for the calibration and validation of such a model.

In terms of the framework developed above, comparing the rates of PSS hydrolysis under methanogenic, acidogenic and sulfate-reducing conditions, the rates are closely similar under methanogenic and sulfate-reducing conditions, but significantly reduced under acidogenic conditions. This implies that the products of PSS hydrolysis (and subsequent acidogenesis) inhibit the PSS hydrolysis rate. If these products are removed, then PSS hydrolysis remains uninhibited, irrespective of whether the biological process that removes the products is methanogenesis or sulfate reduction.

In revising the literature on the hydrolysis of particulate organic wastes, it appeared that hydrolysis inhibition was linked to the lipids. Possible mechanisms for the inhibition due to VFA and/or hydrogen concentration inhibition of β -oxidation of long-chain fatty acids were proposed. However, these mechanisms are speculative, and require detailed experimental investigation.

Chapter 8: Conclusions

References

1. Ahring, B.K. and Westermann, P. 1987. Kinetics of butyrate and hydrogen metabolism in a thermophilic, anaerobic, butyrate degrading triculture. *Appl. Environ. Microbiol.* **53**(2): 434 – 439.
2. Ahring, B.K. 1994. Status on science and application of thermophilic anaerobic digestion. *Wat. Sci. Tech.* **30**(12): 241 – 249.
3. Andara, A.R. and Estaban, J.M.L. 1999. Kinetic study of the anaerobic digestion of the solid fraction of piggery slurries. *Biomass Bioenergy* **17**: 435 – 443.
4. Andara, A.R. and Estaban, J.M.L. 2002. Transition of particle size fractions in anaerobic digestion of the solid fraction of piggery manure. *Biomass Bioenergy* **23**: 229 – 235.
5. Andreasen, K., Petersen, G., Thomsen, H. and Strube, R. 1997. Reduction of nutrient emission by sludge hydrolysis. *Wat. Sci. Tech.* **35**(10): 79 – 85.
6. Andrews, J.F. and Graef, S.P. 1971. Dynamic modelling and simulation of the anaerobic digestion process. In *Anaerobic Biological Treatment Processes*. R.F. Gould [Ed.] Advances in Chemistry Series, Amer. Chem. Soc., Washington, D.C.
7. Aulenbach, D.B. and Heukelekian, H. 1955. Transformation and effects of reduced sulfur compounds in sludge digestion. *Sewage Ind. Wastes* **27**(10): 1147 – 1159.
8. Banerjee, A., Elefsiniotis, P. and Tuhtar, D. 1998. Effect of HRT and temperature on the acidogenesis of municipal primary sludge and industrial wastewater. *Wat. Sci. Tech.* **38**(8-9): 417 – 423.
9. Banister, S.S. and Pretorius, W.A. 1998. Optimisation of primary sludge acidogenic fermentation for biological nutrient removal. *Water SA* **24**(1): 35 – 41.
10. Barnard, J.L. 1984. Activated primary tanks for phosphate removal. *Water SA* **10**(3): 121 – 126.
11. Barthakur, A., Bora, M. and Singh, H.D. 1991. Kinetic model for substrate utilisation and methane production in the anaerobic digestion of organic feeds. *Biotechnol. Prog.* **17**(4): 369 – 376.
12. Bekker, J.L. 1982. Water use in South Africa and estimated future needs. *Civ. Eng. S. Africa* Dec: 653.
13. Brinch, P.P., Rindel, K. and Kalb, K. 1994. Upgrading to nutrient removal by means

References

- of internal carbon from sludge hydrolysis. *Wat. Sci. Tech.* **29**(12): 31 – 40.
14. Bryers, J.D. 1985. Structural modeling of the anaerobic digestion of biomass particulates. *Biotech. Bioeng.* **27**: 638 – 649.
 15. Buffiere, P., Fonade, C. and Moletta, R. 1998. Mixing and phase hold-ups variations due to gas production in anaerobic fluidised-bed reactors: Influence on reactor performance. *Biotech. Bioeng.* **60**(1): 36 – 43.
 16. Butlin, K.R., Selwyn, S.C. and Wakerley, D.S. 1956. Sulfide production from sulfate-enriched sewage sludges. *J. App. Bacteriol.* **19**(1): 3 – 15.
 17. Christensen, B., Laake, M. and Liene, T. 1996. Treatment of acid mine drainage by sulfate-reducing bacteria: results from a bench scale experiment. *Wat.Res.* **30**(7): 1617 – 1624.
 18. Colleran, E., Finnegan, S. and Lens, P. 1995. Anaerobic treatment of sulfate-containing waste streams. *Antonie van Leeuwenhoek* **67**: 29 – 46.
 19. Corbett, C.J., Whittington-Jones, K., Hart, O.O. and Rose, P.D. 2000. Biological treatment of acid mine drainage wastewaters using a sewage sludge carbon source. Proceeding of the *WISA Biennial Conference*, Sun City, South Africa.
 20. Costello, D.J., Greenfield, P.F. and Lee, P.L. 1991. Dynamic modelling of a single stage high rate anaerobic reactor. *Wat. Res.* **25**(7): 847 – 871.
 21. De Haas, D.W. 1998. The use of simultaneous chemical precipitation in modified activated sludge systems exhibiting biological enhanced phosphate removal. *Ph.D. thesis*, University of Cape Town, South Africa.
 22. Devai, I. and DeLaune, R.D. 1999. Emission of reduced malodorous sulfur gases from wastewater treatment plants. *Wat. Environ. Res.* **71**(2): 203 – 208.
 23. Dold, P.L., Ekama, G.A. and Marais, G.v.R. 1980. A general model for the activated sludge process. *Prog. Wat. Tech.* **12**: 47 – 77.
 24. Dold, P.L. and Marais, G.v.R. 1986. Evaluation of the general activated sludge model proposed by the IAWPRC task group. *Wat. Sci. Tech.* **18**: 63 – 89.
 25. Eastman, J.A. and Ferguson, J.F. 1981. Solubilization of particulate organic carbon during the acid phase of anaerobic digestion. *JWPCF* **53**(3): 352 – 366.
 26. Elefsiniotis, P and Oldham, W.K. 1994. Anaerobic acidogenesis of primary sludge: The role of solids retention time. *Biotech. Bioeng.* **44**: 7 – 13.
 27. Eliosov, B. and Argaman, Y. 1995. Hydrolysis of particulate organics in activated sludge systems. *Wat. Res.* **29**(1): 155 – 163.
 28. Enongene, G.N. 2003. The enzymology of enhanced hydrolysis within the biosulphidogenic Recycling Sludge Bed Reactor (RSBR). *PhD Thesis*, Rhodes University, Grahamstown, South Africa.

References

29. Fox, P. and Suidan, M.T. 1990. Batch tests to determine activity distribution and kinetic parameters for acetate utilisation in expanded bed anaerobic reactors. *App. Environ. Microbiol.* **56**(4) 887 – 894.
30. Fukui, M., Suh, J.-I. and Urushigawa, Y. 2000. *In situ* substrates for sulfidogenesis and methanogenesis in municipal anaerobic sewage digesters with different levels of sulfate. *Wat Res.* **34**(5): 1515 – 1524.
31. Ghosh, S., Buoy, K., Dressel, L., Miller, T., Wilcox, G. and Loos, D. 1995. Pilot- and full-scale two-phase anaerobic digestion of municipal sludge. *Wat. Environ. Res.* **67**(2): 206 – 214.
32. Gujer, W. and Zehnder, A.J.B. 1983. Conversion processes in anaerobic digestion. *Wat. Sci. Tech.* **15**: 127 – 167.
33. Gupta, A.K., Oldham, W.K. and Coleman, P.F. 1985. The effects of temperature, pH and retention time on volatile fatty acid production from primary sludge. Proceedings of *UBC International Conference on New Directions and Research in Waste Treatment and Residuals Management*, Univ. British Columbia, Vancouver, Canada, June.
34. Gupta, A., Flora J.R.V., Gupta, M., Sayles, G.D. and Suidan, M.T. 1994. Methanogenesis and sulfate reduction in chemostats – I. Kinetic studies and experiments.
35. Harper, S.R. and Pohland, F.G. 1986. Recent developments in hydrogen management during anaerobic biological wastewater treatment. *Biotech. Bioeng.* **28**(4): 585 – 602.
36. Hatziconstantinou, G.J., Yannakopolous, P. and Andreadakis, A. 1996. Primary sludge hydrolysis for biological nutrient removal. *Wat. Sci. Tech.* **34**(1-2): 417 – 423.
37. Heynike, J.J.C. 1981. The economic effect of the mineral content present in the Vaal River water on the community of the PWV complex. Report to the Water Research Commission.
38. Henze, M., and Harremöes, P. 1983. Anaerobic treatment of wastewater in fixed film reactors - A literature review. *Wat. Sci. Tech.* **15**: 1 – 101.
39. Henze, M., Grady, C.P.L., Gujer, W., Marais, G.v.R. and Matsuo, T. 1987. *Activated sludge model No. 1*. IAWPRC Scientific and Technical Report No. 1, IAWPRC, London
40. Henze, M., Gujer, W., Mino, T., Matsuo, T., Wentzel, M.C. and Maris, G.v.R. 1995. *Activated sludge model No. 2*. IAWQ Scientific and Technical Report No. 3, IAWQ, London.
41. Hill, D.T., Barth, C.L. 1977. A dynamic model for simulation of animal waste digestion. *JWPCF* **October**: 2129 —2143, Technical Contribution No. 1318.
42. Huang, J.-C., Ray, B.Y. and Huang, Y.-J. 1989. Sludge digestion by anaerobic fluidized beds. I: Lab performance data. *J. Environ. Eng.* **115**(6): 1139 – 1155.
43. Izzett, H.B., Wentzel, M.C. and Ekama, G.A. 1992. The effect of thermophilic heat

References

- treatment on the anaerobic digestibility of primary sludge. Report to the Water Research Commission, W76, Department of Civil Engineering, UCT, Rondebosch, 7701.
44. Jain, S., Lala, A.K., Bhatia, S.K. and Kudchadker, A.P. 1992. Modelling of hydrolysis controlled anaerobic digestion. *J. Chem. Tech. Biotechnol.* **53**: 337 – 344.
 45. Jeyaseelan, S. 1997. A simple mathematical model for anaerobic digestion process. *Wat. Sci. Tech.* **35**(8): 185 – 191.
 46. Kalyuzhnyi, S.V. and Fedorovich, V.V. 1998. Mathematical modelling of competition between sulfate reduction and methanogenesis in anaerobic reactors. *Bioresource Tech.* **9**:187 – 199.
 47. Kasper, H.F. and K. Wuhrmann. 1978. Kinetic parameters and relative turnover of some important catabolic reactions in digesting sludge. *App. Environ. Microbiol.* **36**(1): 1 – 7.
 48. Kaufman, E.N., Little, M.H. and Selvaraj, P.T. 1996. Recycling of FGD gypsum to calcium carbonate and elemental sulfur using mixed sulfate-reducing bacteria with sewage digest as a carbon source. *J. Chem. Tech. Biotechnol.* **66**:365 – 374.
 49. Khan, A.W. and Trottier, T.M. 1978. Effect of sulfur-containing compounds on anaerobic degradation of cellulose to methane by mixed cultures obtained from sewage sludge. *App. Environ. Microbiol.* **35**(6): 1027 – 1034.
 50. Kiely, G., Tayfur, G., Dolan, C. and Tanji, K. 1997. Physical and mathematical modelling of anaerobic digestion of organic wastes. *Wat. Res.* **31**(3): 534 – 540.
 51. Kim, S.K., Matsui, S., Pareek, S., Shimuzu, Y. and Matsuda, T. 1997. Biodegradation of recalcitrant organic matter under sulfate-reducing and methanogenic conditions in the landfill column reactors. *Wat. Sci. Tech.* **36**(6-7): 91 – 98.
 52. Knapp, J.S. and Howell, J.A. 1978. Treatment of primary sewage sludge with enzymes. *Biotech. Bioeng.* **20**: 1221 – 1234.
 53. Kristensen, G.H., Jorgensen, P.E., Strube, R. and Henze, M. 1992. Combined pre-precipitation, biological sludge hydrolysis and nitrogen reduction – A pilot demonstration of integrated nutrient removal. *Wat. Sci. Tech.* **25**(5-6): 1057 – 1066.
 54. Kristjansson, J.K., Schönheit, P. and Thauer, R.K. 1982. Different K_s values for hydrogen of methanogenic bacteria and sulfate reducing bacteria: An explanation for the apparent inhibition of methanogenesis by sulfate. *Arch. Microbiol.* **131**: 278 – 282.
 55. Kristjansson, J.K. and Schönheit, P. 1983. Why do sulfate-reducing bacteria outcompete methanogenic bacteria for substrates? *Oecologia* **60**: 264 – 266.
 56. Lawrence, A.W., McCarty, P.L. and Guerin, F.J.A. 1966. The effects of sulfides on anaerobic treatment. *Air Wat. Int. J.* **10**: 207 – 221.
 57. Levenspiel, O. 1972. Chemical reaction engineering. 2nd Ed. John Wiley, New York, 465 – 469.

References

58. Lilley, I.D., Wentzel, M.C., Loewenthal, R.E., Ekama, G.A. and Marias, G.v.R. 1991. Acid fermentation of primary sludge at 20°C. In Proceedings of 2nd WISA Biennial Conference, Kempton Park, May: 294 – 313.
59. Lin, C.Y., Noike, T., Furumai, H. and Matsumoto, J. 1989. A kinetic study of the methanogenesis process in anaerobic digestion. *Wat. Sci. Tech.* **21**: 175 – 186.
60. Maillacheruvu, K.Y. and Parkin, G.F. 1996. Kinetics of growth, substrate utilization, and sulfide toxicity for propionate, acetate and hydrogen utilisers in anaerobic systems. *Wat. Environ. Res.* **58**(7): 1099 – 1106.
61. Massé, D.I. and Droste, R.L. 2000. Comprehensive model of anaerobic digestion of swine manure slurry in a sequencing batch reactor. *Wat. Res.* **34**(12): 3087 – 3106.
62. McCarty, P.L. and Mosey, FE. 1991. Modelling of anaerobic digestion processes (A discussion of concepts). *Wat. Sci. Tech.* **24**(8): 17 – 33.
63. Miron, Y., Zeeman, G., van Lier, J.B. and Lettinga, G. 2000. The role of sludge retention time in the hydrolysis and acidification of lipids, carbohydrates and proteins during digestion of primary sludge in CSTR systems. *Wat. Res.* **34**(5): 1705 – 1713.
64. Moen, G., Stensel, H.D., Lepistö, R and Ferguson, J. 2001. Effects of solids retention time on the performance of thermophilic and mesophilic digestion. In Proceeding of the Annual Water Environment Federation Conference and Exhibition, Atlanta.
65. Moletta, R.E., Verrier, D. and Albagnac, G. 1986. Dynamic modelling of anaerobic digestion. *Wat. Res.* **20**(4): 427 – 434.
66. Molwantwa, J.B., Whittington-Jones, K.J. and Rose, P.D. 2004. An investigation into the mechanism underlying enhanced hydrolysis of complex carbon in a biosulphidogenic recycling sludge bed reactor (RSBR). Proceeding of the WISA Biennial Conference, Cape Town, South Africa.
67. Monod, J. 1949. The growth of bacterial cultures. Pasteur Institute, Paris.
68. Moosbrugger, R.E., Wentzel, M.C., Ekama, G.A. and Marais, G.v.R. 1992. Simple titration procedures to determine H₂CO₃* alkalinity and short-chain fatty acids in aqueous solutions containing known concentrations of ammonium, phosphate and sulfide weak acid/bases. Report to the Water Research Commission South Africa No. TT 57/92.
69. Mosey, F.E. 1983. Mathematical modelling of the anaerobic digestion process: Regulatory mechanisms for the formation of short-chain volatile fatty acids from glucose. *Wat. Sci. Tech.* **15**: 209 – 232.
70. Muller, A., Wentzel, M.C. and Ekama, G.A. 2003. Measurement of ordinary heterotroph organism anoxic-aerobic activated sludge systems. Report to the Water Research Commission South Africa, W119, Department of Civil Engineering, UCT, Rondebosch, 7701.
71. Musvoto, E.V., Wentzel, M.C., Loewenthal, R.E. and Ekama, G.A. 1997. Kinetic-based model for mixed weak acid/base systems. *Water SA* **23**(4): 311 – 322.

References

72. Musvoto, E.V., Wentzel, M.C., Loewenthal, R.E. and Ekama, G.A. 2000. Integrated chemical, physical and biological processes modeling. Part 1- Development of a kinetic based model for weak acid/base systems. *Wat. Res.* **34**(6): 1857 – 1867.
73. Nedwell, D.B. and Reynolds, P.J. 1996. Treatment of landfill leachate by methanogenic and sulfate-reducing digestion. *Wat. Res.* **30**(1): 21 – 28.
74. O'Rourke, J.T. 1968. Kinetics of anaerobic treatment at reduced temperatures. *Dissertation*, Department of Civil Engineering, Stanford University.
75. Oude Elferink, S.J.W.H., Visser, A., Hulshoff Pol, L.W. and Stams, A.J.M. 1994. Sulfate reduction in methanogenic bioreactors. *FEMS Microbiol. Reviews* **15**: 119 – 136.
76. Palenzuela-Rollon, A. 1999. Anaerobic digestion of fish processing wastewater with special emphasis on hydrolysis of suspended solids. *PhD thesis*, Agricultural University, Wageningen.
77. Pareek, S., Kim, S.K., Matsui, S. and Shimizu, Y. 1998. Hydrolysis of (ligno)cellulosic materials under sulfidogenic and methanogenic conditions. *Wat. Sci. Tech.* **38**(2): 193 – 200.
78. Pauss, A and Guiot, S.R. 1993. Hydrogen monitoring in anaerobic sludge bed reactors at various hydraulic regimes and loading rates. *Wat. Envir. Res.* **65**(3): 276 – 280.
79. Pavlostathi, S.G. and Giraldo-Gomez, E. 1991. Kinetics of anaerobic treatment. *Wat. Sci. Tech.* **24**(8): 35 – 59.
80. Pipes, W.O. 1961. Sludge digestion by sulfate reducing bacteria. In Proceedings of the *15th Industrial Waste Conference* Purdue University, Lafayette, Indiana.
81. Pitman, A.R., Venter, S.L.V. and Nicholls, H.A. 1983. Practical experience with biological P removal plants in Johannesburg. *Wat. Sci. Tech.* **15**: 233 – 259.
82. Ray, B T., Huang, J-C. and Dempsey, B.A. 1989. Sludge digestion by anaerobic fluidised beds. II. Kinetic model. *J. Environ. Eng.* **115**(6): 1156 – 1170.
83. Reis, M.A.M., Lemos, P.C., Martins, M.J., Costa, P.C., Gonçalves, L.M.D. and Carrondo, M.J.T. 1991. Influence of sulfate and operational parameters on volatile fatty acids concentration profile in acidogenic phase. *Bioprocess Eng.* **6**: 145 – 151.
84. Rose, P.D., Corbett, C.J., Whittington-Jones, K. and Hart, O.O. 2002. The Rhodes BioSURE Process[®] Part 1: Biodesalination of mine drainage wastewaters. Report to the Water Research Commission TT 195/02.
85. Rudolfs, W. and Amberg, H.R. 1952a. White water treatment II: Effect of sulfides on digestion. *Sewage Ind. Wastes* **24**(10): 1278 – 1287.
86. Rudolfs, W. and Amberg, H.R. 1952b. White water treatment III: Factors affecting digestion efficiency. *Sewage Ind. Wastes* **24**(11): 1402 – 1409.
87. Russo, S.L. and Dold, P.L. 1989. Sludge character and role of sulfate in a UASB

References

- system treating a paper plant effluent. *Wat. Sci. Tech.* **31**: 121 – 132.
88. Salminen, E.A. and Rantala, J.A. 2002. Semi-continuous anaerobic digestion of solid poultry slaughterhouse waste: effect of hydraulic retention time and loading. *Wat. Res.* **36**: 3175 – 3182.
 89. Sam-Soon, P.A.L.N.S., Loewenthal, R.E., Dold, P.L. and Marais, G.v.R. 1987. Hypothesis for pelletization in the Upflow Anaerobic Sludge Bed reactor. *Water SA* **13**(2): 69 – 80.
 90. Sam-Soon, P.A.L.N.S., Loewenthal, R.E., Wentzel, M.C. and Marais, G.v.R. 1990. Growth of biopellets on glucose in upflow anaerobic sludge bed (UASB) systems. *Water SA* **16**(3): 151 – 164.
 91. Sam-Soon, P.A.L.N.S., Loewenthal, R.E., Wentzel, M.C. and Marais, G.v.R. 1991. Effect of sulfate on pelletization in the UASB system with glucose as substrate. *Water SA* **17**(1): 47 – 56.
 92. Shimizu, T., Kudo, K. and Nasu, Y. 1993. Anaerobic waste activated sludge digestion - A bioconversion mechanism and kinetic model. *Biotech. Bioeng.* **41**(11): 1082 – 1091.
 93. Siegrist, H., Renggli, D. and Gujer, W. 1993. Mathematical modelling of anaerobic mesophilic sewage treatment. *Wat. Sci. Tech.* **27**(2): 25 — 36.
 94. Skalsky, D.S. and Daigger, G.T. 1995. Wastewater solids fermentation for volatile acid production and enhanced biological phosphorous removal. *Wat. Environ. Res.* **67**: 230 – 237.
 95. Sötemann, S.W. 2004. Integrated chemical, physical and biological process modeling of WWT systems. *Ph.D. thesis*, Department of Civil Engineering, University of Cape Town.
 96. *Standard methods for the Examination of Water and Wastewater.* 1985. 19th Edn, American Public Health Association/American Water Works Association/Water Environment Federation, Washington DC, USA.
 97. Thiele, J.H. and Ziekus, J.G. 1988. The anion-exchange substrate shuttle process: A new approach to two-stage biomethanation of organic and toxic wastes. *Biotech. Bioeng.* **31**(4): 521 – 535.
 98. Toerien, D.F. and Maree, J.P. 1987. Reflections on anaerobic process biotechnology and its impact on water utilization in South Africa. *Water SA* **13**: 137 – 144.
 99. Ueki, K., Kotaka, K., Itoh, K. and Ueki, A. 1988. Potential availability of anaerobic treatment with digester slurry of animal waste for the reclamation of acid mine water containing sulfate and heavy metals. *J. Fermentation Tech.* **65**(1): 43 – 50.
 100. Van Rensburg, P., Wentzel, M.C. and Ekama, G.A. 2001. Integrated modeling of the chemical, biological and physical processes in anaerobic digestion of primary sludge. Report to the Water Research Commission, Report No. W113, Civil Engineering Department, UCT, Rondebosch, 7701.

References

101. Vavilin, V.A., Vasiliev, V.B., Rytov, S.V. and Ponomarev, A.V. 1995. Modeling ammonia and hydrogen sulfide inhibition in anaerobic digestion. *Wat. Res.* **29**(3): 827 – 835.
102. Veeken, A., Kalyuzhnyi, S., Scharff, H. and Hamelers, B. 2000. Effect of pH and VFA on hydrolysis of organic solid waste. *J. Environ. Eng.* **126**(12): 1076 – 1081.
103. Venter, S.L.V., Halliday, J. and Pitman, A.R. 1977. Optimization of the Johannesburg Olifantsvlei extended aeration plant for phosphorous removal. *Prog. Wat. Tech.* **10**: 279 – 292.
104. Whiteley, C.G., Burgess, J.E., Melamane, X., Pletschke, B. and Rose, P.D. 2003. The enzymology of sludge solubilisation utilizing sulfate-reducing systems: the properties of lipases. *Wat. Res.* **37**: 289 – 296.
105. Whittington-Jones, K. 2000. Sulfide-enhanced hydrolysis of primary sewage sludge: implications for the bioremediation of acid mine drainage. *Ph.D. Thesis*, Rhodes University, Grahamstown, South Africa.
106. Wu, C., Huang, J. and Jih, C. 1998. Consecutive reaction kinetics involving distributed fraction of methanogens in fluidised-bed reactors. *Biotech. Bioeng.* **57**: 367 – 379.
107. Zeikus, J.G. 1977. The biology of methanogenic bacteria. *Bacteriol. Rev.* **41**: 514 – 541.
108. Zhang, T.C. and Noike, T. 1994. Influence of retention time on reactor performance and bacterial trophic populations in anaerobic digestion processes. *Wat. Res.* **28**(1): 27 – 36.

Appendix A

Feed Characterization

The PSS collection, storage, preparation and characterisation were described in Chapter 3. In the experimental protocol, PSS was collected in batches from the Athlone Wastewater Treatment Plant (Cape Town, South Africa), and stored in a cold room at 4°C. These batches served as feed to the laboratory-scale anaerobic digesters over periods ranging from several weeks to several months. This approach was adopted to minimize the effects of variations in the PSS characteristics on the experiments. However, during storage at 4°C, it became evident that the PSS was undergoing activity causing the PSS characteristics to change with time. Accordingly, the measurements on the PSS feed were analysed in more detail, to track the nature of the changes in the PSS on storage and hence enable the PSS to be correctly characterised for any given day or steady state period. This appendix reports on this analysis.

This appendix describes the PSS feed batches that have been collected and analysed in more detail. The first three feed batches described here (batches 1, 9 and 10) were not used during any of the steady state operating systems described in Chapters 4 to 7. However, these feed batches were analysed in sufficient detail for useful information to be collected on changes in PSS on storage. Feed batches 12 to 16 were used during the steady state operating periods in Chapters 4 to 7, and are also analysed in more detail.

For feed batches 1, 9 and 10, the total COD, soluble COD, VFA and alkalinity were analysed regularly, while for feed batches 12, 13, 14 and 15, the TKN, FSA, total P and soluble P were also analysed, while the VFA and alkalinity was not. The mean and standard deviations were calculated for the total COD, TKN and total P measurements, all of which did not change with storage. For the parameters that did change with time (soluble COD, VFA, FSA and soluble P), the changes with time were modelled using best fit lines, either linear or polynomial, and the equations describing these lines can be used to calculate these concentrations on any day.

Feed batch number 1

This feed was used from October 2001 until February 2002. Figure A.1 shows the plot of the total COD analyses with time (69687 ± 2835 (54)), while Figure A.2 shows the plot of the soluble COD and VFA concentration with time, as well as the ratio between these two concentrations.

Figure A.1 indicates that the total COD concentration did not change discernibly with time. Figure A.2 shows that the soluble COD and VFA (as COD) concentrations increased with time, while the ratio between these two concentrations remained fairly constant (2.039 ± 0.107 (12)).

Appendix A: Feed Characterization

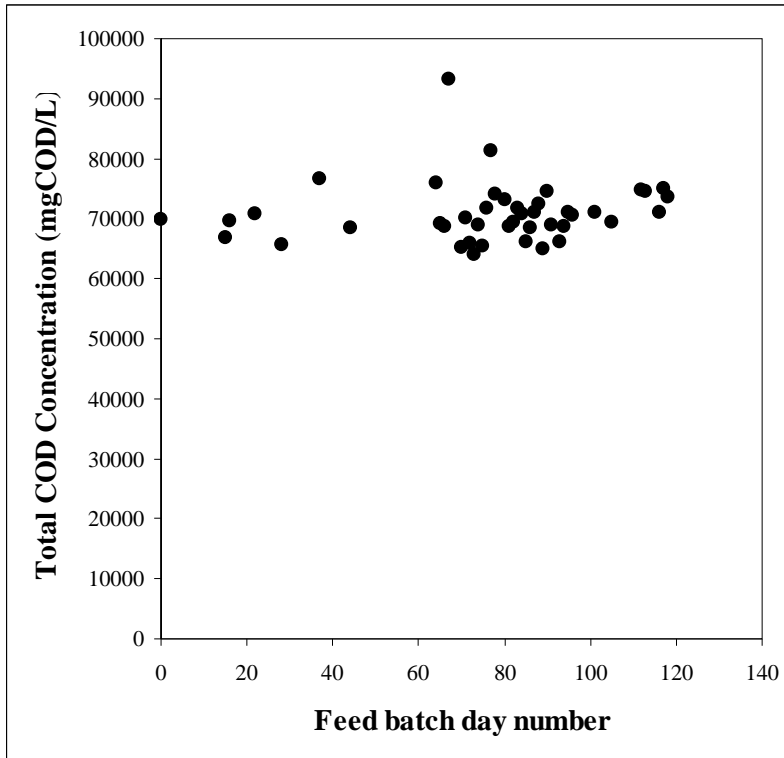


Figure A.1: Daily measurements of the total COD concentration for feed batch F1

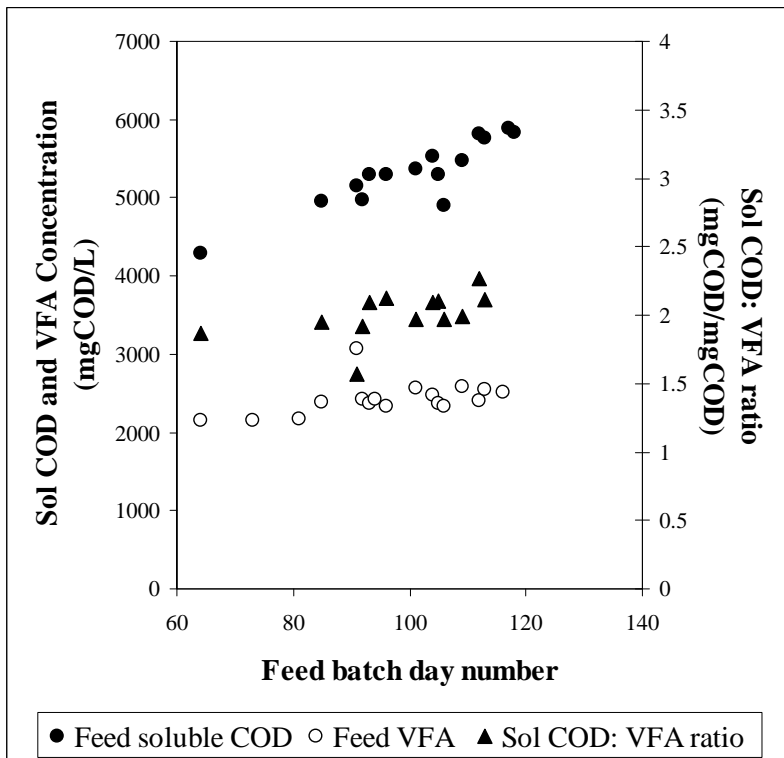


Figure A.2: Daily measurements of the soluble COD and VFA concentrations for feed batch F1

Feed batch number 9

This feed was used from December 2002 until January 2003. Figure A.3 shows the plot of the total COD analyses with time (40431 ± 1331 (24)), while Figure A.4 shows a plot of the soluble COD and VFA concentration with time, as well as the ratio between these two concentrations. (1.777 ± 0.123 (22)). The same behaviour noted for feed batch number 1 is seen here also.

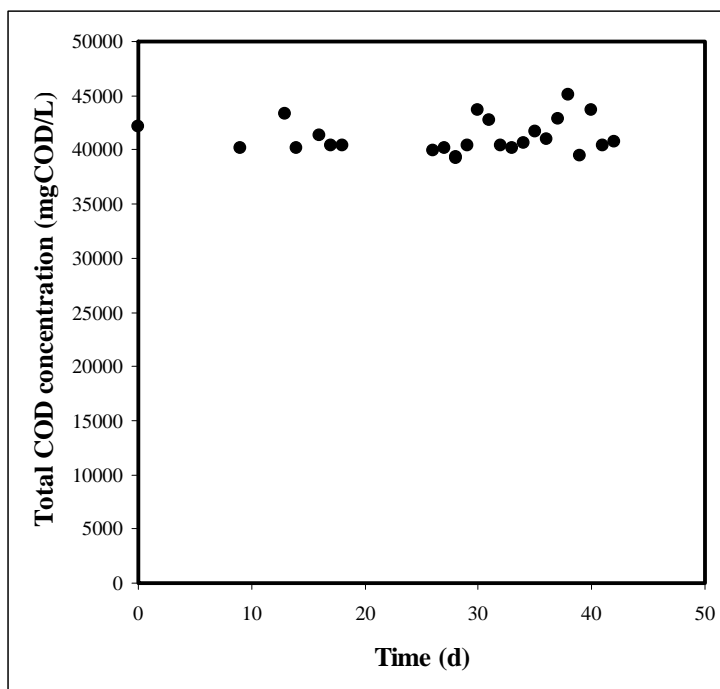


Figure A.3: Daily measurements of the total COD concentration for feed batch F9

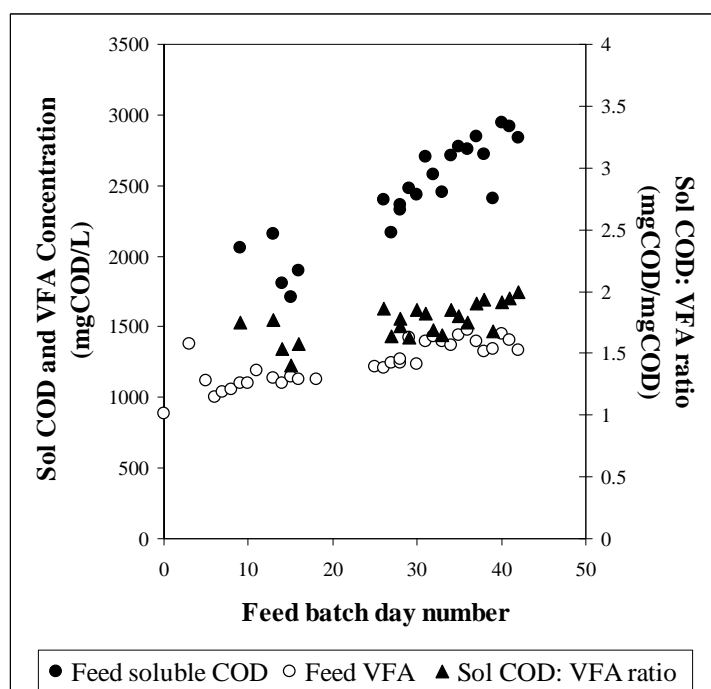


Figure A.4: Daily measurements of the soluble COD and VFA concentrations for feed batch F9

Feed batch number 10

This feed was used from January 2003 until February 2003. Figure A.5 shows a plot of the total COD analyses with time (25662 ± 554 (22)), while Figure A.6 shows a plot of the soluble COD and VFA concentration with time, as well as the ratio between these two concentrations (1.693 ± 0.069 (18)). Again, the observed behaviour is consistent with the previous two feed batches.

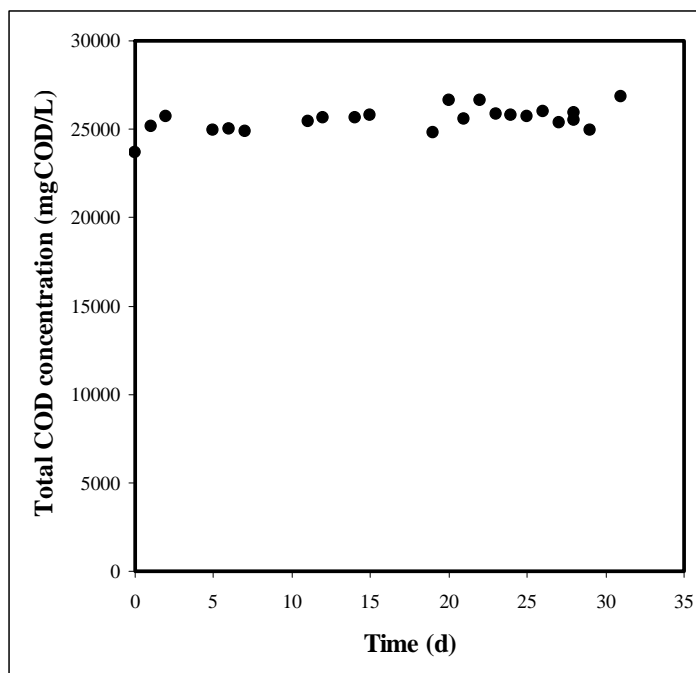


Figure A.5: Daily measurements of the total COD concentration for feed batch F10

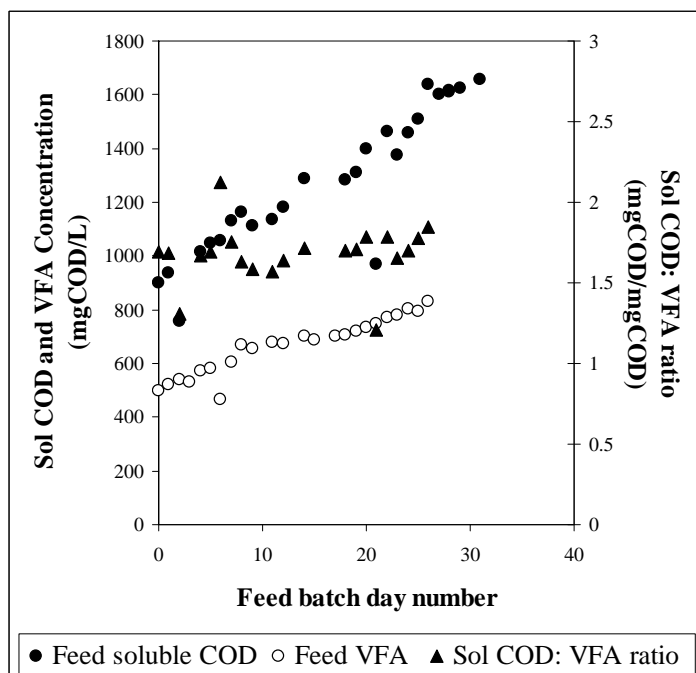


Figure A.6: Daily measurements of the soluble COD and VFA concentrations for feed batch F10

Feed batch number 12

This feed was used from March 2003 until October 2003. Figure A.7 shows a plot of the total COD analyses with time, and the increase in the feed soluble COD concentration with time. Figure A.7 shows that, for this feed batch, there was a linear increase in the feed soluble COD concentration with time. The equation that describes the best-fit linear plot is shown in Figure A.7.

Figures A.8 and A.9 show the daily analyses for the TKN and FSA, and total and soluble P concentrations respectively. Both these figures show that the soluble components (FSA and soluble P) do not show a discernible increase in concentration with time as the soluble COD concentration increases in Figure A.7. For these components, the mean and standard deviations are shown in Table A.1.

Table A.1: Average values and the formula for calculating the time dependent soluble COD concentration for F12

F12 total COD (mg/L)	51905 ± 1354 (19)
F12 soluble COD (mg/L)	13.62 (d) + 4041.1 (Eq A.1)
F12 TKN (mgN/L)	963 ± 98 (11)
F12 FSA (mgN/L)	78 ± 5 (13)
F12 Total P (mgP/L)	251 ± 33 (11)
F12 soluble P (mgP/L)	34 ± 5 (14)

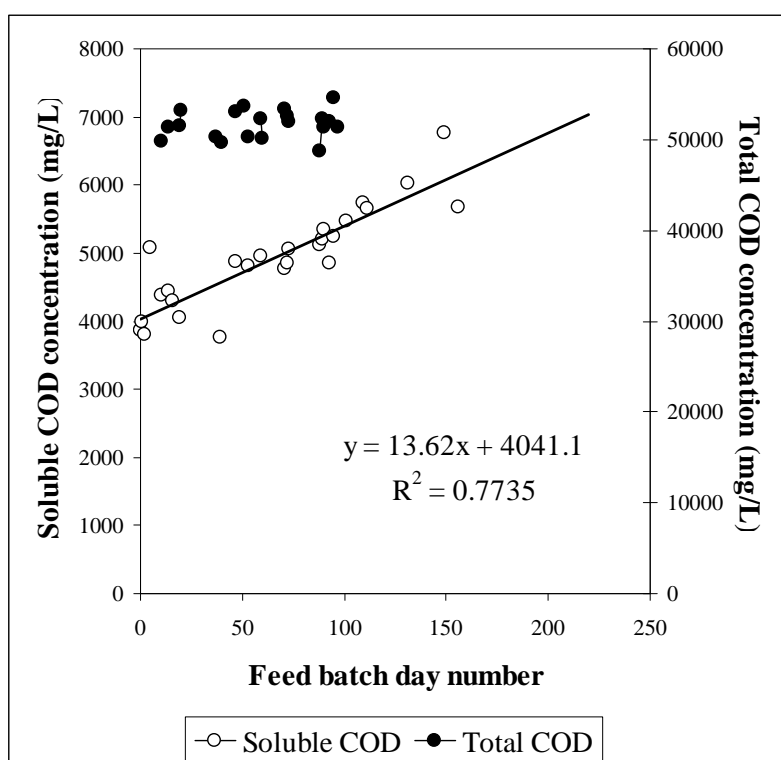


Figure A.7: Daily measurements of the total and soluble COD concentrations for feed batch F12

Appendix A: Feed Characterization

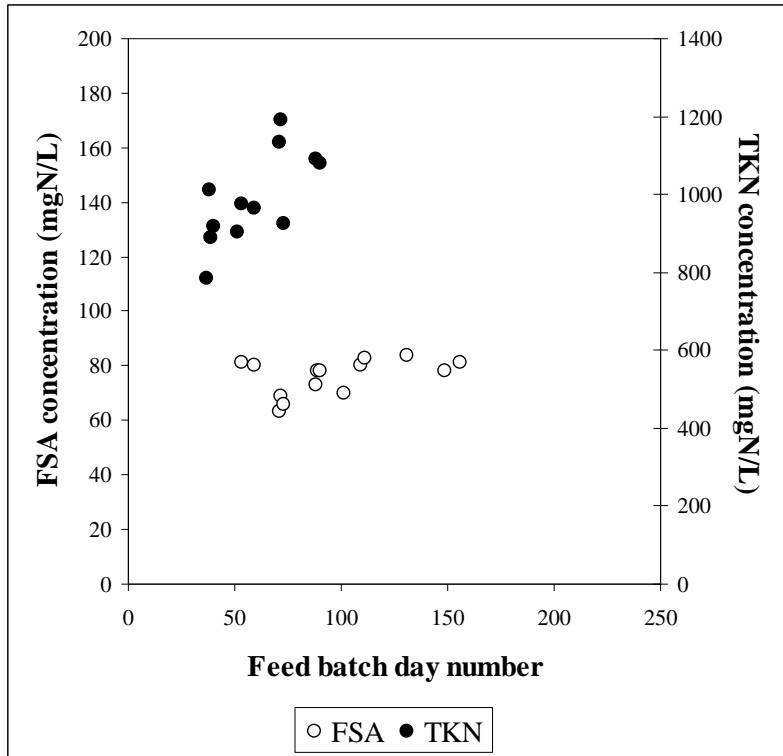


Figure A.8: Daily measurements of the TKN and free and saline ammonia concentrations for feed batch F12

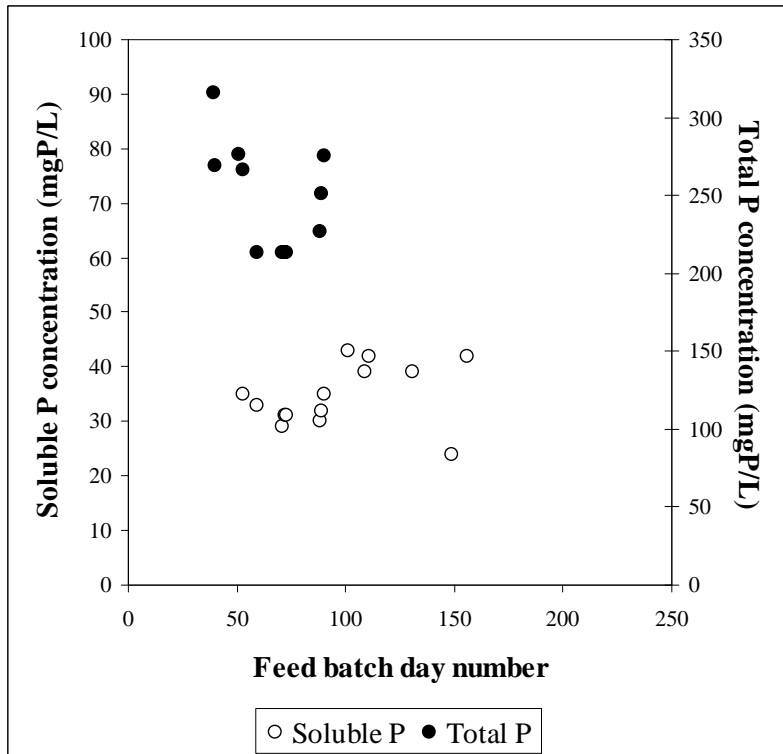


Figure A.9: Daily measurements of the total and soluble P concentrations for feed batch F12

Feed batch number 13

F13 was used from June 2003 until September 2003. Figure A.10 shows a plot of the total COD analyses with time, and the increase in the feed soluble COD concentration with time. In comparison to Figure A.7, Figure A.10 shows that the increase in the feed soluble COD concentration is more accurately described with a second order polynomial. This equation (Eq A.2) is shown in Figure A.10 and Table A.2.

Figures A.11 and A.12 show the daily analyses for the TKN and FSA, and total and soluble P concentrations respectively. Both these figures show that the soluble components (FSA and soluble P) also exhibited a non-linear increase with time, described by Eq A.3 and A.4 respectively.

Table A.2: Average values and the formulae for calculating the time dependent soluble COD, FSA and soluble P concentrations for F13

F13 total COD (mg/L)	44233 ± 1198 (10)
F13 soluble COD (mg/L)	$-0.2236 (d)^2 + 48.451 (d) + 2459.3$ (Eq A.2)
F13 TKN (mgN/L)	1092 ± 48 (9)
F13 FSA (mgN/L)	$-0.0094 (d)^2 + 1.9493 (d) + 141.19$ (Eq A.3)
F13 Total P (mgP/L)	252 ± 37 (9)
F13 soluble P (mgP/L)	$-0.0042 (d)^2 + 0.7187 (d) + 29.246$ (Eq A.4)

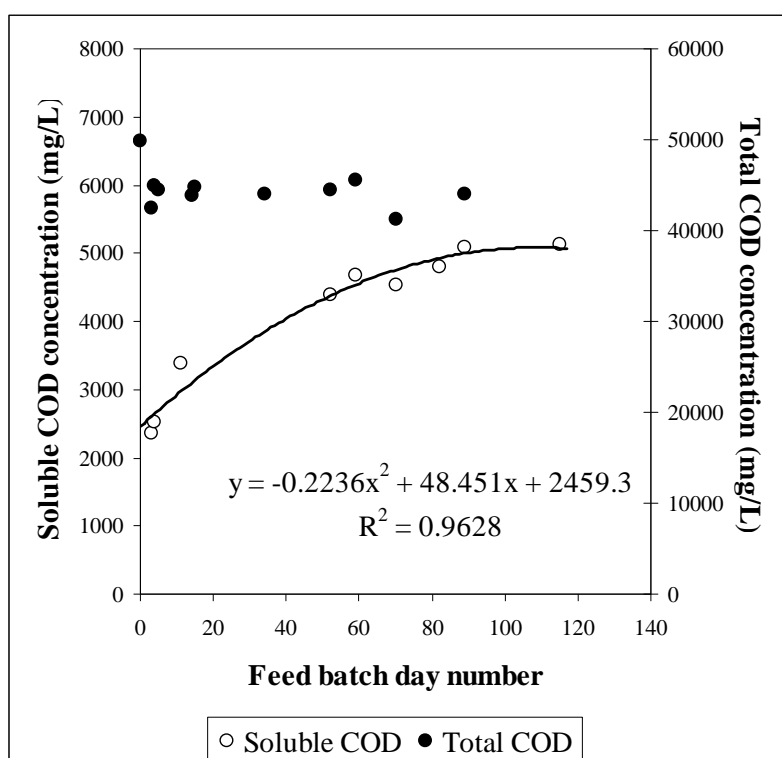


Figure A.10: Daily measurements of the total and soluble COD concentrations for feed batch F13 (trendline ignores data point (34, 6034) not shown)

Appendix A: Feed Characterization

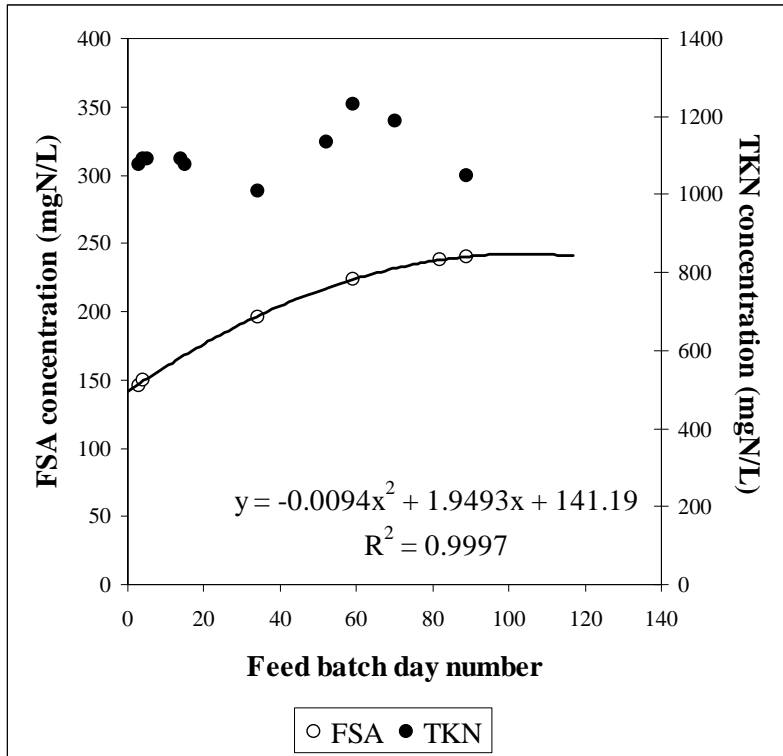


Figure A.11: Daily measurements of the TKN and free and saline ammonia concentrations for feed batch F13 (trend line ignores data points (11, 134) and (52, 168) not shown)

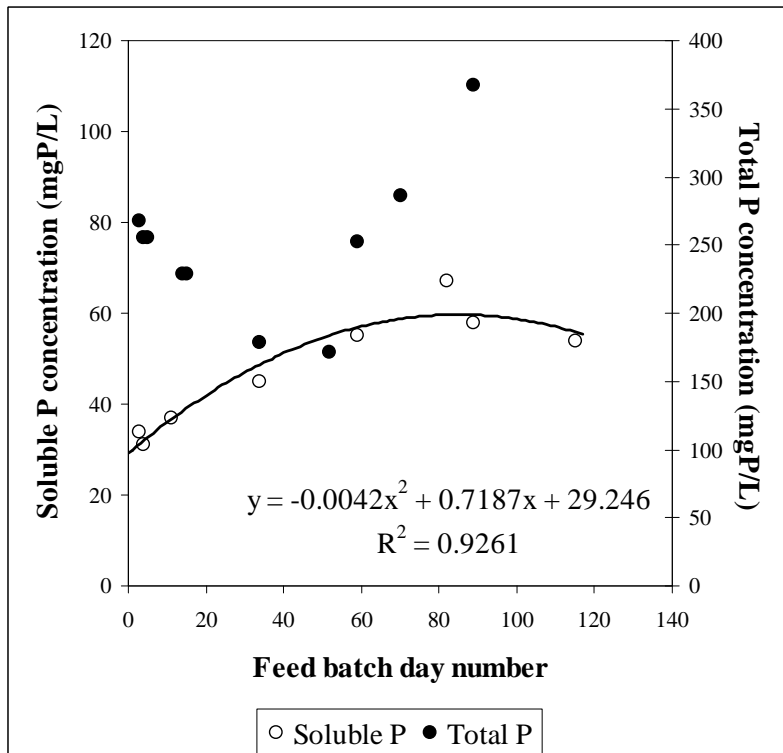


Figure A.12: Daily measurements of the total and soluble P concentrations for feed batch F13 (trendline ignores data point (52,27) not shown)

Feed batch number 14

This feed was used from September 2003 until June 2004. Figure A.13 shows a plot of the total COD analyses with time, and the increase in the feed soluble COD concentration with time. Figure A.13 shows that the increase in the feed soluble COD concentration is more accurately described with a second order polynomial. This equation (Eq A.5) is shown in Figure A.13 and Table A.3.

Figures A.14 and A.15 show the daily analyses for the TKN and FSA, and total and soluble P concentrations respectively. The FSA concentration increased linearly with time (Figure A.14 and Eq. A.6), while the soluble P concentration showed no increase with time.

Table A.3: Average values and the formulae for calculating the time dependent soluble COD and FSA concentration for F14

F14 total COD (mg/L)	34818 ± 1824 (12)
F14 soluble COD (mg/L)	$-0.1298 (d)^2 + 37.136 (d) + 2658.9$ (Eq A.5)
F14 TKN (mgN/L)	770 ± 101 (13)
F14 FSA (mgN/L)	$2.4141 (d) + 18.891$ (Eq A.6)
F14 Total P (mgP/L)	172 ± 38 (13)
F14 soluble P (mgP/L)	48 ± 8 (10)

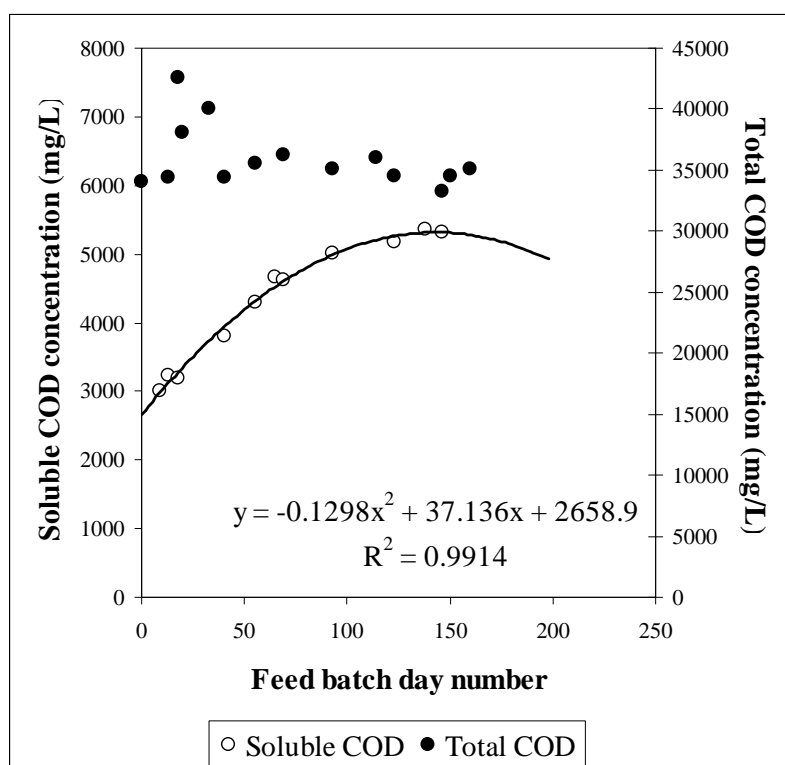


Figure A.13: Daily measurements of the total and soluble COD concentrations for feed batch F14 (trendline ignores data points (114, 4463) and (197, 5525) not shown)

Appendix A: Feed Characterization

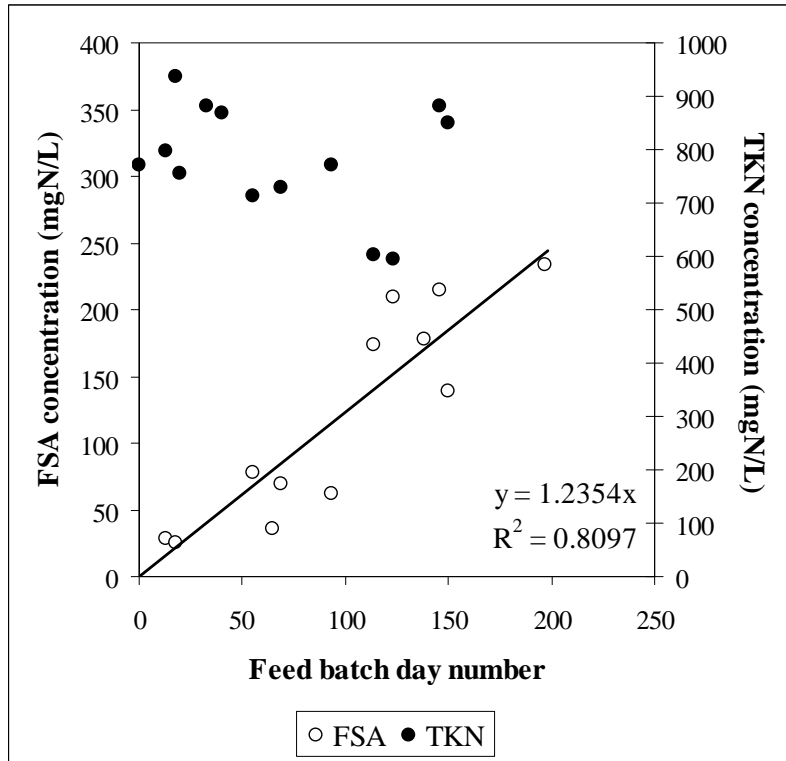


Figure A.14: Daily measurements of the TKN and free and saline ammonia concentrations for feed batch F14 (trendline ignores data point (40, 250) not shown)

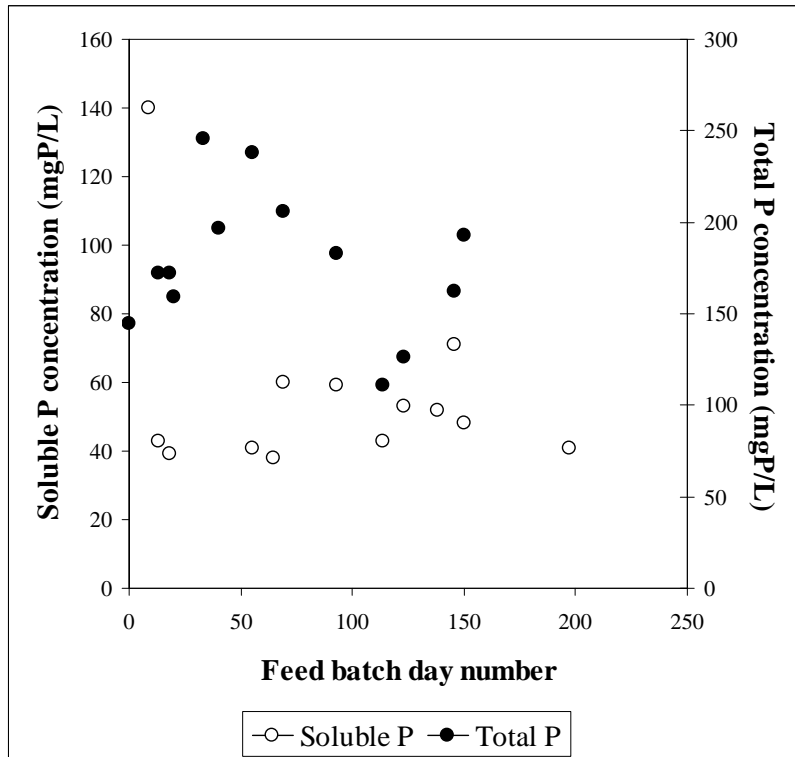


Figure A.15: Daily measurements of the total and soluble P concentrations for feed batch F14

Feed batch number 15

This feed was used from November 2003 until June 2004. Figure A.16 shows a plot of the total COD analyses with time, and the increase in the feed soluble COD concentration with time, described by a second order polynomial. This equation (Eq A.7) is shown in Figure A.16 and Table A.4.

Figures A.17 and A.18 show the daily analyses for the TKN and FSA, and total and soluble P concentrations respectively. The increase in the FSA concentration was again linear (Figure A.17 and Eq A.8) while the soluble P concentration showed no increase with time.

Table A.4: Average values and the formulae for calculating the time dependent soluble COD and FSA concentration for F15

F15 total COD (mg/L)	65929 ± 1107 (10)
F15 soluble COD (mg/L)	$-0.3571 (d)^2 + 81.111 (d) + 2730.8$ (Eq A.7)
F15 TKN (mgN/L)	1260 ± 211 (7)
F15 FSA (mgN/L)	$2.4141 (d) + 18.891$ (Eq A.8)
F15 Total P (mgP/L)	301 ± 16 (7)
F15 soluble P (mgP/L)	59 ± 11 (9)

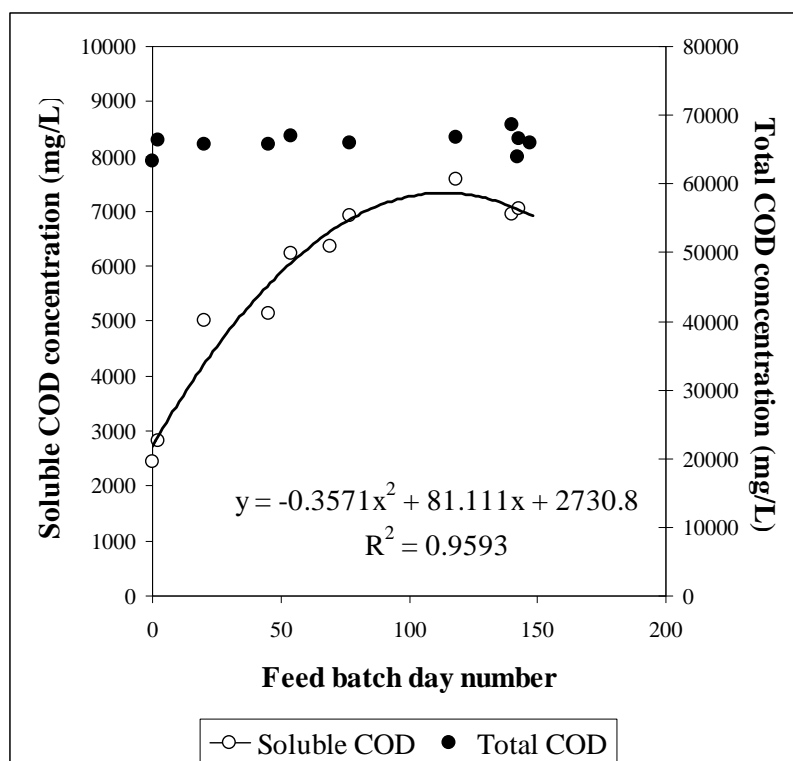


Figure A.16: Daily measurements of the total and soluble COD concentrations for feed batch F15

Appendix A: Feed Characterization

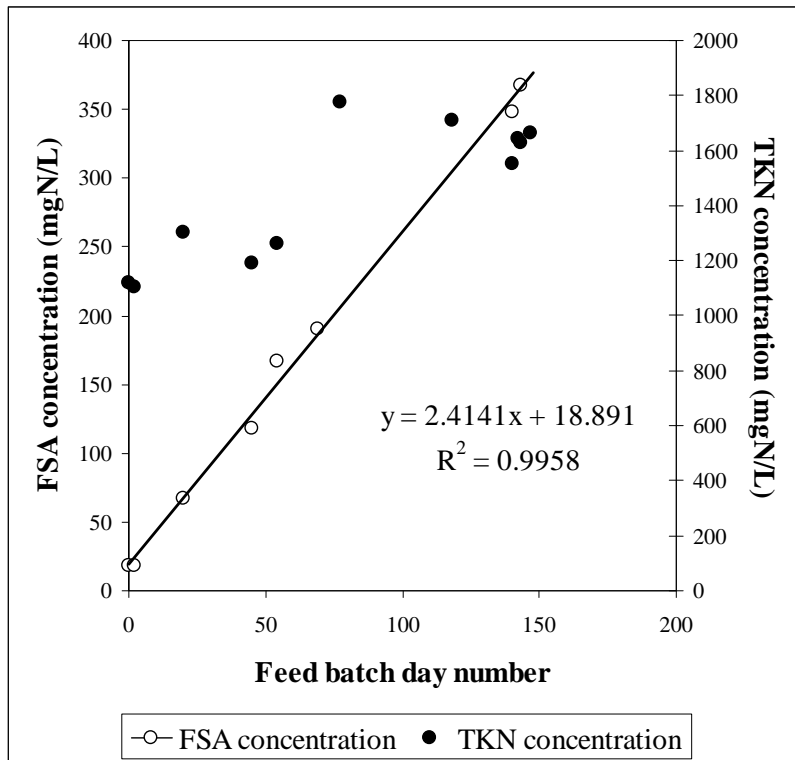


Figure A.17: Daily measurements of the TKN and free and saline ammonia concentrations for feed batch F15 (trendline ignores data points (77, 160) and (118, 140) not shown)

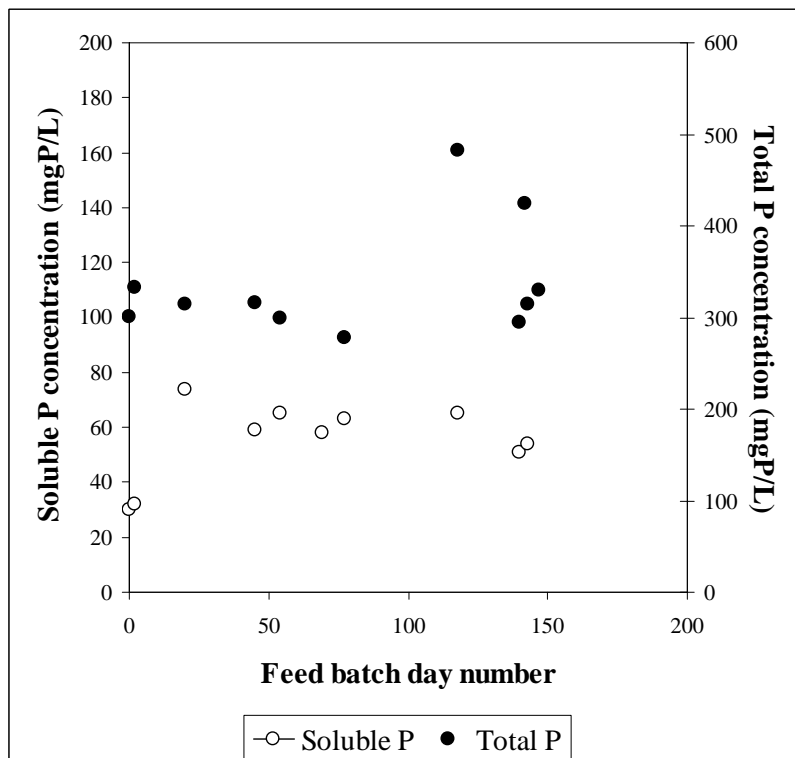


Figure A.18: Daily measurements of the total and soluble P concentrations for feed batch F15

Summary

Several PSS feed batches have been used in this study, and analysis of these feed batches with time shows that under storage at 4°C, the soluble COD concentration increases with time for all batches analysed, while the VFA concentration also increases with time. The ratio between the soluble COD concentration and the VFA concentration is relatively constant between 1.7 and 2, which is similar to the findings of Lilley *et al.* (1992), and this result is used in the model developed in Chapter 4 and modified in Chapter 5. The total COD, TKN and total P concentrations showed neither an increase nor decrease with time, and were chosen to remain constant for the entire time that a PSS feed batch was used as feed. The FSA and soluble P concentrations were expected to follow similar trends to the soluble COD concentration, but this was not always observed.

The changes observed above can be ascribed to PSS hydrolysis taking place in the feed storage containers at 4°C. This hydrolysis is substantiated by the observation that the initial soluble COD concentration for the feed batches was never zero, even when measured as soon as the feed was brought to the laboratory. This indicates that hydrolysis took place in the primary settling tanks, in the pipes from the settling tanks to the pump house collection point, and in the feed drums during transportation from the wastewater treatment plant to the laboratory.

Appendix A: Feed Characterization

Appendix B

Steady State Operating Data

This chapter describes each of the 47 steady state periods analysed in this study in more detail. Table B.1 lists the steady states analysed for the methanogenic systems discussed further in Chapter 4. Table B.2 lists the steady states analysed for the acidogenic systems discussed further in Chapter 5. Table B.3 lists the steady states analysed for the pH controlled methanogenic and acidogenic systems discussed further in Chapter 6, while Table B.4 lists the steady states analysed for the sulfidogenic systems discussed further in Chapter 7.

For each steady state, a COD (except the sulfate-reducing systems), TKN and total P balance has been calculated. The method used to calculate the percent recovery of the feed (for steady state number 2) is as follows:

From Table A.1:

Feed COD concentration: 51905 mgCOD/L

Feed TKN concentration: 963 mgN/L

Feed total P concentration: 251mgP/L

Feed dilution of 1000g F12 up to 2000g with water. Therefore, the above concentrations are diluted twice (Table B.6):

Feed COD concentration: 25953 mgCOD/L

Feed TKN concentration: 482 mgN/L

Feed total P concentration: 126 mgP/L

COD Balance

COD in: 2000mL/d (~2000g/d) at 25953 mgCOD/L = 51.906 gCOD/d

Effluent concentration: 11299 mgCOD/L

Out: 2000ml at 11299 mgCOD/L = 22.598 gCOD/d

Gas volume: 344 units/d at 50.3 mL/unit = 17.303 L/d

at 63.24 %CH₄ (vol) = 10.942 L CH₄/d

at 1 atm and 20°C = $\frac{101.3 \times 10.942}{8.314 \times 293} = 0.455 \text{ mol CH}_4/\text{d}$

at 16g/mol = 7.28 g CH₄/d

at 4gCOD/gCH₄ = 29.121 gCOD/d

Total COD out = 22.598 + 29.121 = 51.719gCOD/d

Appendix B: Steady State Data

$$\% \text{COD recovery} = 100 \times \frac{51.719}{51.906} = 99.640\%$$

TKN Balance

TKN in: 2000mL/d (~2000g/d) at 482 mgN/L = 964 mgN/d

Effluent concentration = 543 mgN/L

Out: 2000ml at 543 mgN/L = 1086 mgN/d

$$\% \text{TKN recovery} = 100 \times \frac{1.086}{0.964} = 112.66\%$$

Total P Balance

Total P in: 2000mL/d (~2000g/d) at 126 mgP/L = 252 mgP/d

Effluent concentration: 130 mgP/L

Out: 2000ml at 130 mgP/L = 260 mgP/d

$$\% \text{P recovery} = 100 \times \frac{260}{252} = 103.17\%$$

Table B.1: Steady state numbers for the methanogenic systems discussed in Chapter 4, to determine the effects of feed COD concentration and hydraulic retention time on the rate of hydrolysis under methanogenic conditions

Feed COD Concentration (gCOD/L)	Hydraulic Retention Time (d)							
	60	20	15	10	8	6.67	5.71	5
40			10;11	12	21	23	28	
25		3	4	1	2	7	8	9
13			5	13	14	24	31	
9	17							
2				25	26			

Table B.2: Steady state numbers for the acidogenic systems discussed in Chapter 5, to determine the effects of feed COD concentration and hydraulic retention time on the rate of hydrolysis under acidogenic conditions

Feed COD Concentration (gCOD/L)	Hydraulic Retention Time (d)		
	10	5	3.33
40		30	29
13	38	33	32
2	39	35	34

Appendix B: Steady State Data

Table B.3: Steady state numbers for the systems discussed in Chapter 6, to determine the effects of pH on the rate of hydrolysis

Biological systems	System pH					
	5	6	6.5	7	7.5	8
Methanogenic			27	19	18;37	44
Acidogenic	35	40		43		45

Table B.4: Steady state numbers for the sulfidogenic systems discussed in Chapter 7, to determine the effects of sulfate reduction on the rate of hydrolysis

Steady state number	Operating conditions				Comparative steady state
	R_h (d)	Feed COD (g/L)	Feed SO_4 (g/L)		
6	10	26	1	Excess COD	1
15	8	13	9.6	All S_t as FeS	14
16	8	13	9.6	No Fe addition	14 and 15
20	8	2	2	pH ~ 7.5	18 and 37
22	8	2	2	pH ~ 7	19
36	8	2	2	pH ~ 6.5	27
41	16	2	2		
42	13.3	2	2		
46	10	1	1		
47	8	2	2	pH ~ 8.3	

Steady state No 1**Table B.5:** Operating conditions for steady state number 1

Feed batch number	F12
Mass of PSS in feed (g)	800
Total Mass of feed (g)	1600
Reactor Volume (L)	16
Retention time (day)	10
Sulfate addition (gSO₄/L)	0
pH	steady state
Biological groups present	Acidogens and methanogens

The digester was seeded with waste from two other methanogenic digesters. The feed volume was incremented by 100g per day until a 10-day retention time. On day 16, the temperature control failed and the digester was operated at 20°C for 12 hours. The system was not fed for 1 day, after which the 10-day retention time was resumed.

Table B.6: Results summary for steady state number 1

Feed total COD (mg/L)	25953
Feed soluble COD (mg/L)	2331
Feed TKN (mgN/L)	482
Feed FSA (mgN/L)	39
Feed Total P (mgP/L)	126
Feed soluble P (mgP/L)	17
Steady state measured after 20 days (2 x R_H)	
Effluent total COD (mg/L)	10849 ± 304 (11)
Effluent soluble COD (mg/L)	178 ± 14 (12)
Effluent VFA (mg/L as HAc)	24 ± 14 (18)
Effluent Alkalinity (mg/L as CaCO₃)	2424 ± 127 (17)
Reactor pH	7.00 ± 0.01 (17)
Gas Produced (units/day)	336 ± 4 (10)
Volume per unit (ml)	50.3 ± 0.2
Gas composition (%CH₄)	Assumed* (63.24)
Methane production (L/day)	10.69
Methane production (gCOD/day)	28.4
Effluent TKN (mgN/L)	518 ± 10 (10)
Effluent FSA (mgN/L)	208 ± 4 (10)
Effluent Total P (mgP/L)	129 ± 15 (10)
Effluent soluble P (mgP/L)	23 ± 2 (10)
COD balance (%)	110.3
TKN balance (%)	107.5
Total P balance (%)	102.4

* Systems for measuring gas compositions were not established at this stage, and compositions from other comparable systems were observed and this composition estimated (equal to steady state number 2)

Appendix B: Steady State Data

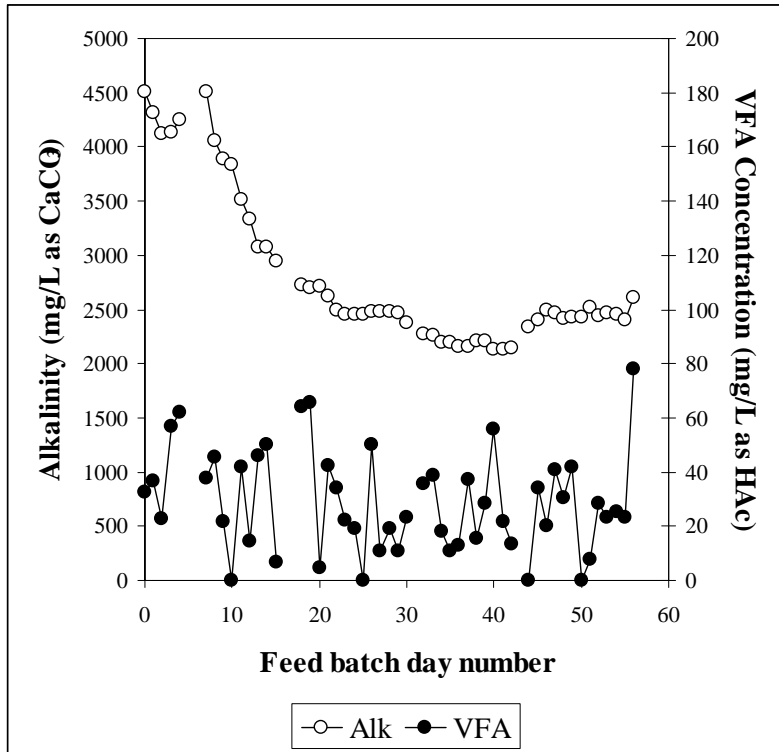


Figure B.1: Daily measurements of the VFA and alkalinity leading up to and including steady state number 1 (steady state from day 37)

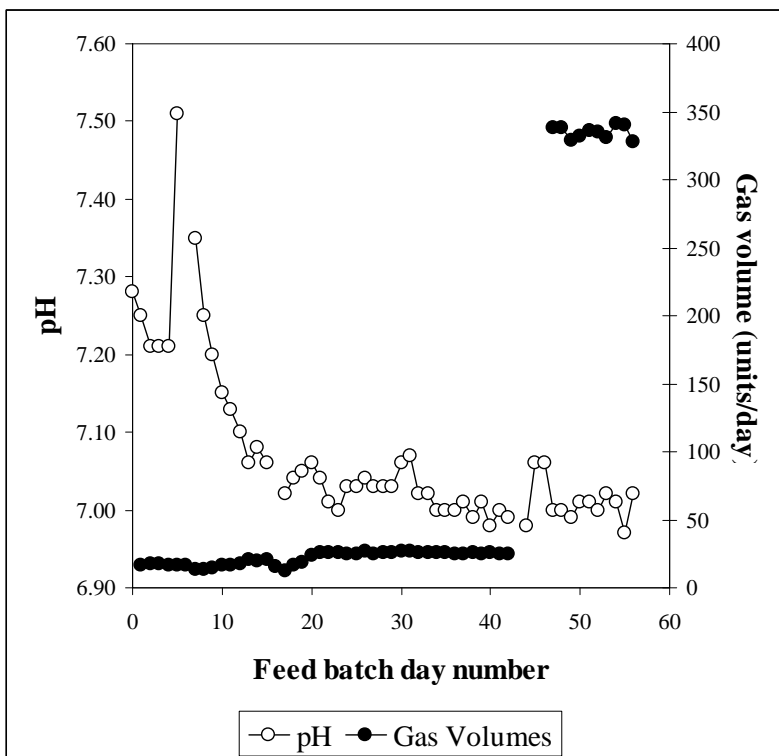


Figure B.2: Daily measurements of the pH and volumetric gas production leading up to and including steady state number 1 (steady state from day 37). First gas volume readings using an old gas meter (~500ml/unit)

Appendix B: Steady State Data

Table B.7: Daily measured data for steady state number 1

Date	Day	Total COD (mgCOD/L)	Soluble COD (mgCOD/L)	VFA (mg/L as HAc)	Alkalinity (mg/L as CaCO ₃)	pH	Gas Volume (Units/day)	TKN (mgN/L)	NH ₃ (mgN/L)	TP (mgP/L)	PO ₄ (mgP/L)
14-Apr	37	10934	186	37.2	2161.2	7.01		460			
15-Apr	38			15.3	2204.3	6.99					
16-Apr	39	10274	161	28.6	2203.2	7.01		501	193	111	23
17-Apr	40	10520	181	55.6	2134.5	6.98			200		23
18-Apr	41	10849	179	21.6	2135.5	7.00		522	207	126	23
19-Apr	42	11042	190	13.6	2149.9	6.99			211		23
20-Apr	43										
21-Apr	44			0	2333.2	6.98					
22-Apr	45			33.9	2407.6	7.06					
23-Apr	46			20.3	2487.5	7.06					
24-Apr	47			40.6	2472.3	7.00	338				
25-Apr	48	10645	197	30.7	2416.8	7.00	338	518	213	147	23
26-Apr	49	10970	175	41.7	2429.2	6.99	329	511	213	132	22
27-Apr	50	10884	191	0	2424.1	7.01	332	504	204	132	23
28-Apr	51	12600	176	8	2513.8	7.01	336	490	207	147	22
29-Apr	52	11414	167	28.4	2437.6	7.00	335	518	203	141	22
30-Apr	53	10261	154	23	2462.8	7.02	331	525	210	126	15
01-May	54			25.1	2455.2	7.01	341				
02-May	55	10645	161	23	2406.7	6.97	340	518	209	113	16
03-May	56	10468	155	77.9	2603.7	7.02	328	518	224	100	15
Mean		10849	178	24	2424	7.00	336	518	208	129	23
S.D.		304	14	14	127	0.01	4	10	4	15	2
Data points		11	12	18	17	17	10	10	10	10	10

Steady state No 2**Table B.8:** Operating conditions for steady state number 2

Feed batch number	F12
Mass of PSS in feed (g)	1000
Total Mass of feed (g)	2000
Reactor Volume (L)	16
Retention time (day)	8
Sulfate addition (gSO₄/L)	0
pH	steady state
Biological groups present	Acidogens and methanogens

This experiment followed directly from steady state number 1 with the same feed dilution. The feed volumes were changed over 4 days with 100g increments, maintaining the dilution ratio and thus the feed concentration.

Table B.9: Results summary for steady state number 2

Feed total COD (mg/L)	25953
Feed soluble COD (mg/L)	2675
Feed TKN (mgN/L)	482
Feed FSA (mgN/L)	39
Feed Total P (mgP/L)	126
Feed soluble P (mgP/L)	17
Steady state measured after 20 days (2.5 x R_h)	
Effluent total COD (mg/L)	11299 ± 266 (11)
Effluent soluble COD (mg/L)	168 ± 4 (9)
Suspended solids (mgCOD/L)	2163
Effluent VFA (mg/L as HAc)	21 ± 11 (11)
Effluent Alkalinity (mg/L as CaCO₃)	1394 ± 26 (10)
Reactor pH	6.80 ± 0.02 (10)
Gas Produced (units/day)	344 ± 3 (10)
Volume per unit (ml)	50.3 ± 0.2
Gas composition (%CH₄)	63.24*
Methane production (L/day)	10.94
Methane production (gCOD/day)	29.1
Effluent TKN (mgN/L)	543 ± 17 (10)
Effluent FSA (mgN/L)	186 ± 9 (10)
Effluent Total P (mgP/L)	130 ± 11 (10)
Effluent soluble P (mgP/L)	19 ± 2 (10)
COD balance (%)	99.6
TKN balance (%)	113.3
Total P balance (%)	103.2

* Average for 5 measurements made

Appendix B: Steady State Data

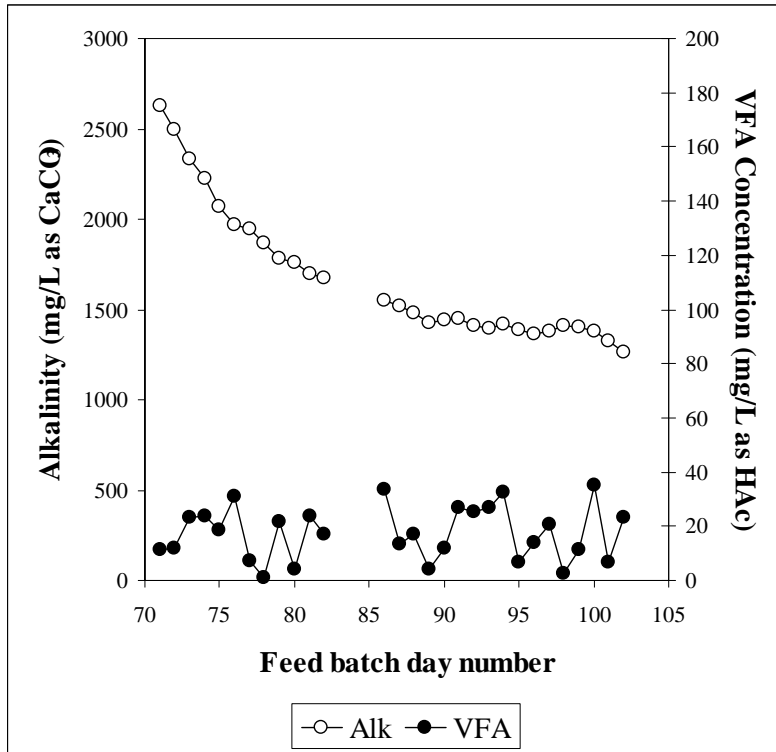


Figure B.3: Daily measurements of the VFA and alkalinity leading up to and including steady state number 2 (steady state from day 92)

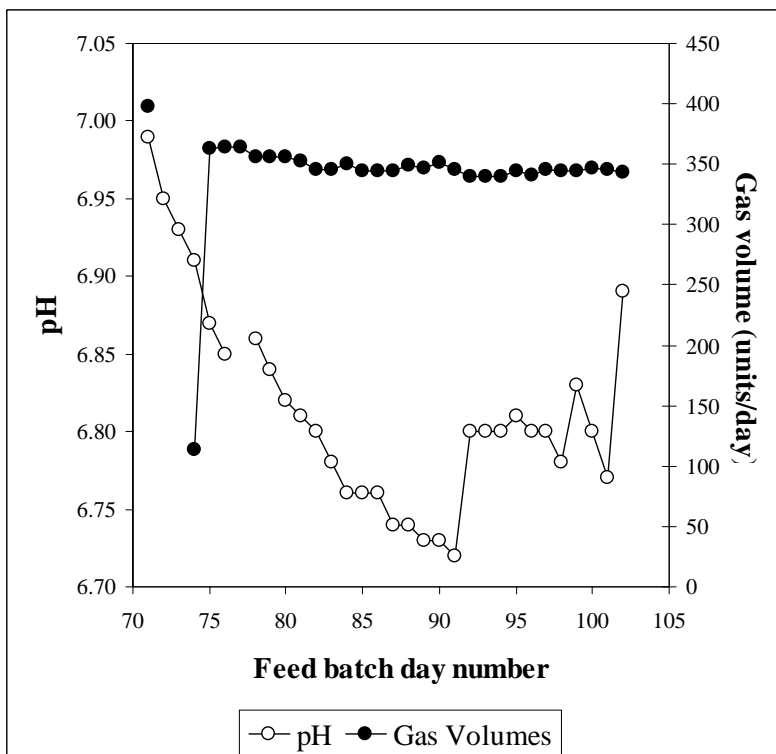


Figure B.4: Daily measurements of the pH and volumetric gas production leading up to and including steady state number 2 (steady state from day 92)

Appendix B: Steady State Data

Table B.10: Daily measured data for steady state number 2

Date	Day	Total COD (mgCOD/L)	Soluble COD (mgCOD/L)	Suspended Solids (mgCOD/L)	VFA (mg/L as HAc)	Alkalinity (mg/L as CaCO ₃)	pH	Gas Volume (Units/day)	TKN (mgN/L)	NH ₃ (mgN/L)	TP (mgP/L)	PO ₄ (mgP/L)
08-Jun	92	10856	163	2526	25.1	1410.5	6.80	340	540	199	108	14
09-Jun	93	11516	158	2256	26.7	1395.7	6.80	340	497	202	111	16
10-Jun	94	11538	183	2330	32.8	1415.3	6.80	340	518	202	120	18
11-Jun	95	11307	165	2551	6.8	1391.3	6.81	344	525	202	120	18
12-Jun	96				13.9	1363.6	6.80	341				
13-Jun	97	10906	167	2671	20.6	1381	6.80	346	553	186	140	20
14-Jun	98	11593	169	2331	2.8	1407.9	6.78	345	546	186	137	19
15-Jun	99	11010	174	2233	11.6	1399.8	6.83	344	553	183	134	19
16-Jun	100	11172	169	2381	35.3	1382.2	6.80	347	553	185	131	20
17-Jun	101	11291	168	2577	6.7	1322.2	6.77	346	546	182	128	20
18-Jun	102	11570	171	2296	23.1	1262.1	6.89	343	539	182	140	20
Mean		11299	168	2331	21	1394	6.80	344	546	186	130	19
S.D.		266	4	124	11	26	0.02	3	12	9	11	1
Data points		10	9	9	11	10	10	11	9	10	10	9

Steady state No 3**Table B.11:** Operating conditions for steady state number 3

Feed batch number	F12
Mass of PSS in feed (g)	500
Total Mass of feed (g)	1000
Reactor Volume (L)	20
Retention time (day)	20
Sulfate addition (gSO₄/L)	0
pH	steady state
Biological groups present	Acidogens and methanogens

This digester was operating stably at a 16-day retention time for 8 days using F11. However, F11 contained an oily scum and was discarded. The system was changed to a 20-day retention time with F12 without digester performance upsets.

Table B.12: Results summary for steady state number 3

Feed total COD (mg/L)	25953
Feed soluble COD (mg/L)	2327
Feed TKN (mgN/L)	482
Feed FSA (mgN/L)	39
Feed Total P (mgP/L)	126
Feed soluble P (mgP/L)	17
Steady state measured after 37 days (1.85 x R_h)	
Effluent total COD (mg/L)	10525 ± 166 (11)
Effluent soluble COD (mg/L)	179 ± 8 (9)
Effluent VFA (mg/L as HAc)	11 ± 7 (17)
Effluent Alkalinity (mg/L as CaCO₃)	1577 ± 20 (17)
Reactor pH	6.89 ± 0.02 (17)
Gas Produced (units/day)	150 ± 4 (9)
Volume per unit (ml)	57.1 ± 0.6
Gas composition (%CH₄)	63.11*
Methane production (L/day)	5.41
Methane production (gCOD/day)	14.4
Effluent TKN (mgN/L)	518 ± 6 (11)
Effluent FSA (mgN/L)	231 ± 6 (12)
Effluent Total P (mgP/L)	138 ± 16 (11)
Effluent soluble P (mgP/L)	22 ± 3 (11)
COD balance (%)	96.0
TKN balance (%)	107.5
Total P balance (%)	109.5

* 3 measurements made. One measurement different from other two, so average of two measurements used for steady state

Appendix B: Steady State Data

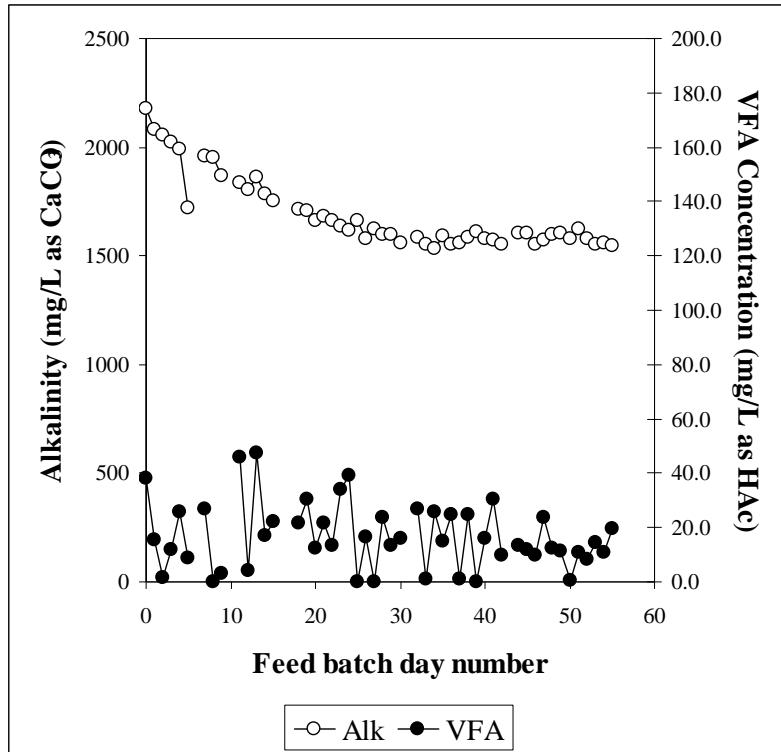


Figure B.5: Daily measurements of the VFA and alkalinity leading up to and including steady state number 3 (steady state from day 37)

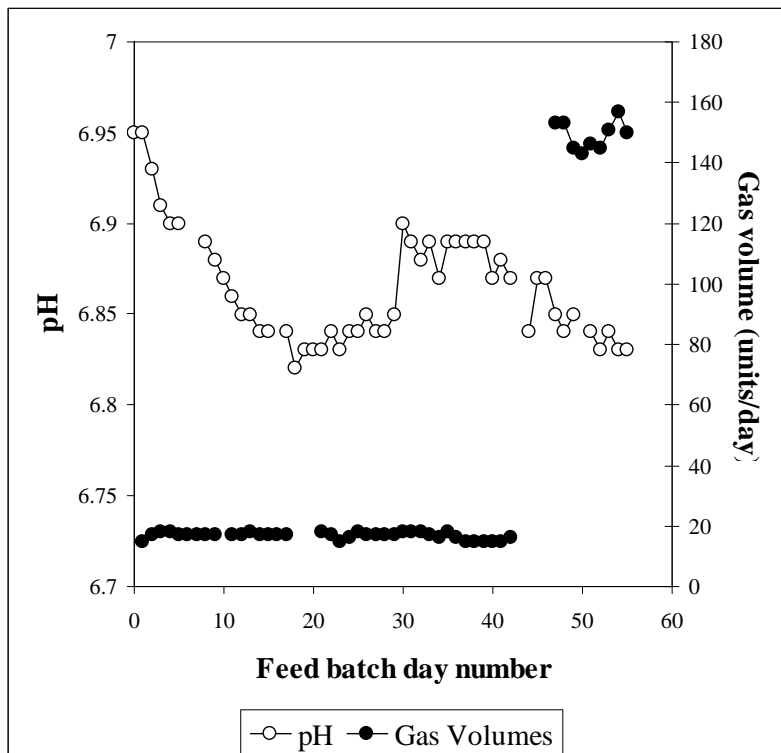


Figure B.6: Daily measurements of the pH and volumetric gas production leading up to and including steady state number 3 (steady state from day 37)

Appendix B: Steady State Data

Table B.13: Daily measured data for steady state number 3

Date	Day	Total COD (mgCOD/L)	Soluble COD (mgCOD/L)	VFA (mg/L as HAc)	Alkalinity (mg/L as CaCO ₃)	pH	Gas Volume (Units/day)	TKN (mgN/L)	NH ₃ (mgN/L)	TP (mgP/L)	PO ₄ (mgP/L)
14-Apr	37	10899	174	1.2	1557.1	6.89		423			
15-Apr	38			24.9	1586.7	6.89					
16-Apr	39	8847	182	0.0	1609	6.89		525	223	125	22
17-Apr	40	10522	185	16.0	1578	6.87		518	228	135	22
18-Apr	41	10525	185	30.5	1570.4	6.88		522	232	147	22
19-Apr	42	10608	173	9.9	1553.2	6.87		525	231	156	22
20-Apr	43										
21-Apr	44			13.3	1602	6.84					
22-Apr	45			12.1	1605.1	6.87					
23-Apr	46			9.7	1554.1	6.87					
24-Apr	47	10578		23.5	1574.7	6.85	153				
25-Apr	48	10588	185	12.6	1594.8	6.84	153	511	238	150	23
26-Apr	49	10909	191	11.2	1602.3	6.85	145	511	231	150	22
27-Apr	50	10369	179	0.4	1577.1		143	508	230	147	22
28-Apr	51	10429	171	10.6	1624.8	6.84	146	511	228	138	22
29-Apr	52	10455	167	8.2	1579	6.83	145	515	220	138	22
30-Apr	53	10043	155	14.6	1554.1	6.84	151	518	238	106	16
01-May	54			10.8	1560.6	6.83	157				
02-May	55	10523		19.4	1544.3	6.83	150	525	239	106	15
Mean		10525	179	11	1577	6.89	150	518	231	138	22
S.D.		166	8	7	20	0.02	4	6	6	16	3
Data points		11	9	17	17	17	9	11	12	11	11

Steady state No 4**Table B.14:** Operating conditions for steady state number 4

Feed batch number	F12
Mass of PSS in feed (g)	667
Total Mass of feed (g)	1334
Reactor Volume (L)	20
Retention time (day)	15
Sulfate addition (gSO₄/L)	0
pH	steady state
Biological groups present	Acidogens and methanogens

This experiment followed directly from steady state number 3 with the same feed dilution. The feed was increased from 1000g to 1334g in a single step, and transient data was collected for the next 12 days (Transient state number 1, Appendix C). On day 68 the gas seals were repaired, and the system was upset. The system was not fed for one day, and fed 1kg the following day, after which normal feeding was resumed.

Table B.15: Results summary for steady state number 4

Feed total COD (mg/L)	25953
Feed soluble COD (mg/L)	2647
Feed TKN (mgN/L)	482
Feed FSA (mgN/L)	39
Feed Total P (mgP/L)	126
Feed soluble P (mgP/L)	17
Steady state measured after 32 days (2.13 x R_h)	
Effluent total COD (mg/L)	10212 ± 131 (10)
Effluent soluble COD (mg/L)	157 ± 4 (9)
Effluent VFA (mg/L as HAc)	17 ± 9 (10)
Effluent Alkalinity (mg/L as CaCO₃)	1539 ± 40 (10)
Reactor pH	6.85 ± 0.03 (9)
Gas Produced (units/day)	214 ± 4 (10)
Volume per unit (ml)	57.1 ± 0.6
Gas composition (%CH₄)	63.08*
Methane production (L/day)	7.71
Methane production (gCOD/day)	20.5
Effluent TKN (mgN/L)	522 ± 6 (8)
Effluent FSA (mgN/L)	212 ± 6 (8)
Effluent Total P (mgP/L)	114 ± 2 (8)
Effluent soluble P (mgP/L)	17 ± 2 (9)
COD balance (%)	98.6
TKN balance (%)	108.3
Total P balance (%)	90.5

*Average of 4 measurements made

Appendix B: Steady State Data

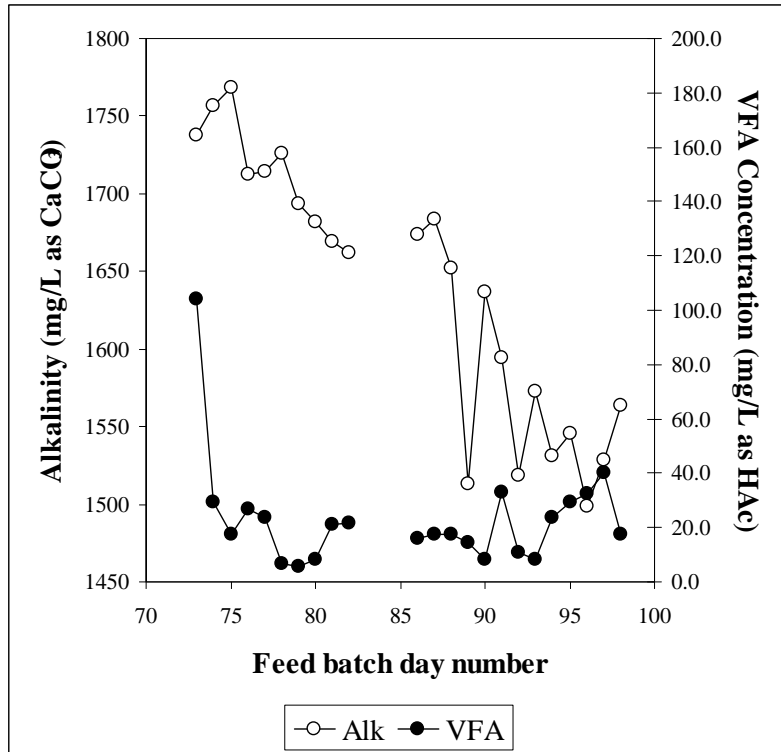


Figure B.7: Daily measurements of the VFA and alkalinity leading up to and including steady state number 4 (steady state from day 88)

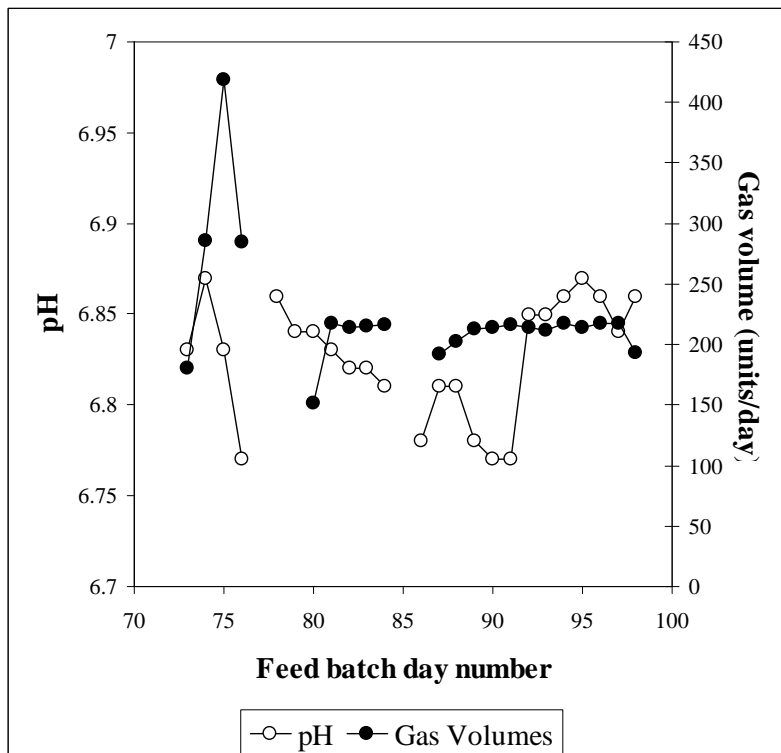


Figure B.8: Daily measurements of the pH and volumetric gas production leading up to and including steady state number 4 (steady state from day 88)

Appendix B: Steady State Data

Table B.16: Daily measured data for steady state number 4

Date	Day	Total COD (mgCOD/L)	Soluble COD (mgCOD/L)	Suspended Solids (mgCOD/L)	VFA (mg/L as HAc)	Alkalinity (mg/L as CaCO ₃)	pH	Gas Volume (Units/day)	TKN (mgN/L)	NH ₃ (mgN/L)	TP (mgP/L)	PO ₄ (mgP/L)
04-Jun	88	10232	164	2221	17.3	1651.8	6.81	203	553	221	111	14
05-Jun	89	10283	155	2257	14.2	1512.8	6.78	213	525	230	114	16
06-Jun	90	10173	161	2177	8.5	1636.6	6.77	214	518	218	114	16
07-Jun	91	10028	156	2178	33.2	1594.4	6.77	216	525		114	
08-Jun	92	10369	174	2265	10.8	1518.4	6.85	214	511	218	111	16
09-Jun	93	10013	155	2195	8.3	1572.3	6.85	212	525	207	111	18
10-Jun	94	9960	165	2288	23.8	1531.2	6.86	217	511	213	114	20
11-Jun	95	10322	157	2195	29.6	1545.8	6.87	214	525	210	117	17
12-Jun	96				32.4	1499.1	6.86	217				
13-Jun	97	10191	159	2165	40	1528.9	6.84	217		206	140	18
14-Jun	98	10235	157	2185	17.5	1563.3	6.86	193	518	203	137	18
Mean		10212	157	2195	17	1539	6.85	214	522	212	114	17
S.D.		131	4	34	9	40	0.03	4	6	6	2	2
Data points		10	9	9	10	10	19	10	8	8	8	9

Steady state No 5**Table B.17:** Operating conditions for steady state number 5

Feed batch number	F12
Mass of PSS in feed (g)	350
Total Mass of feed (g)	1334
Reactor Volume (L)	20
Retention time (day)	15
Sulfate addition (gSO₄/L)	0
pH	steady state
Biological groups present	Acidogens and methanogens

This reactor was seeded with waste methanogenic sludge. The waste sludge was collected from digesters operating with a feed concentration more than double that used for this experiment, hence the observed washout of alkalinity.

Table B.18: Results summary for steady state number 5

Feed total COD (mg/L)	13618
Feed soluble COD (mg/L)	1432
Feed TKN (mgN/L)	253
Feed FSA (mgN/L)	20
Feed Total P (mgP/L)	66
Feed soluble P (mgP/L)	9
Steady state measured after 48 days (3.2 x R_h)	
Effluent total COD (mg/L)	5751 ± 106 (10)
Effluent soluble COD (mg/L)	97 ± 3 (7)
Suspended solids (mgCOD/L)	1362
Effluent VFA (mg/L as HAc)	6 ± 6 (10)
Effluent Alkalinity (mg/L as CaCO₃)	845 ± 22 (11)
Reactor pH	6.80 ± 0.02 (11)
Gas Produced (units/day)	128 ± 2 (12)
Volume per unit (ml)	48.8 ± 0.5
Gas composition (%CH₄)	*63.26
Methane production (L/day)	3.95
Methane production (gCOD/day)	10.5
Effluent TKN (mgN/L)	294 ± 7 (8)
Effluent FSA (mgN/L)	114 ± 3 (8)
Effluent Total P (mgP/L)	79 ± 4 (8)
Effluent soluble P (mgP/L)	13 ± 1 (7)
COD balance (%)	100.1
TKN balance (%)	116.4
Total P balance (%)	120.0

*Average of 7 measurements made

Appendix B: Steady State Data

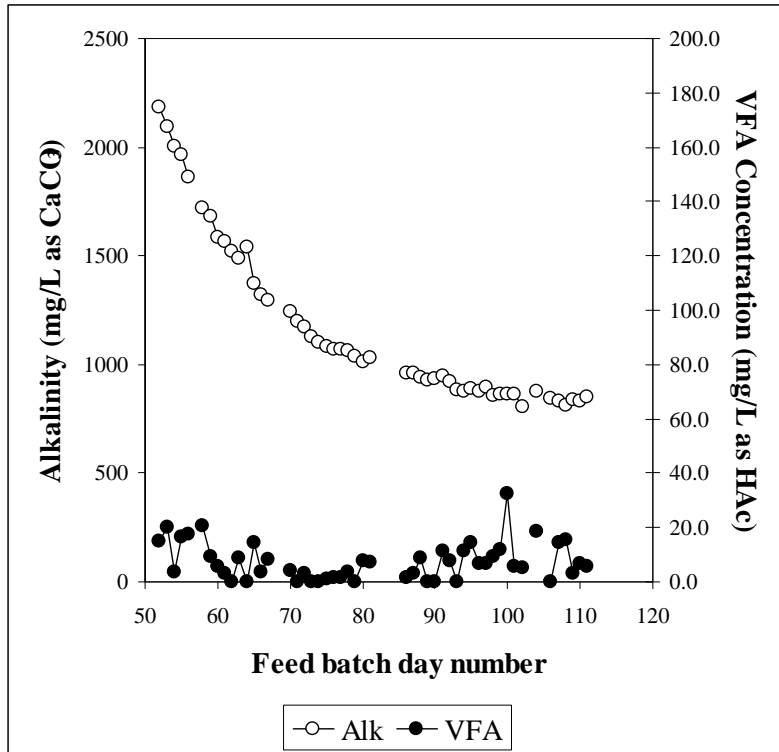


Figure B.9: Daily measurements of the VFA and alkalinity leading up to and including steady state number 5 (steady state from day 99)

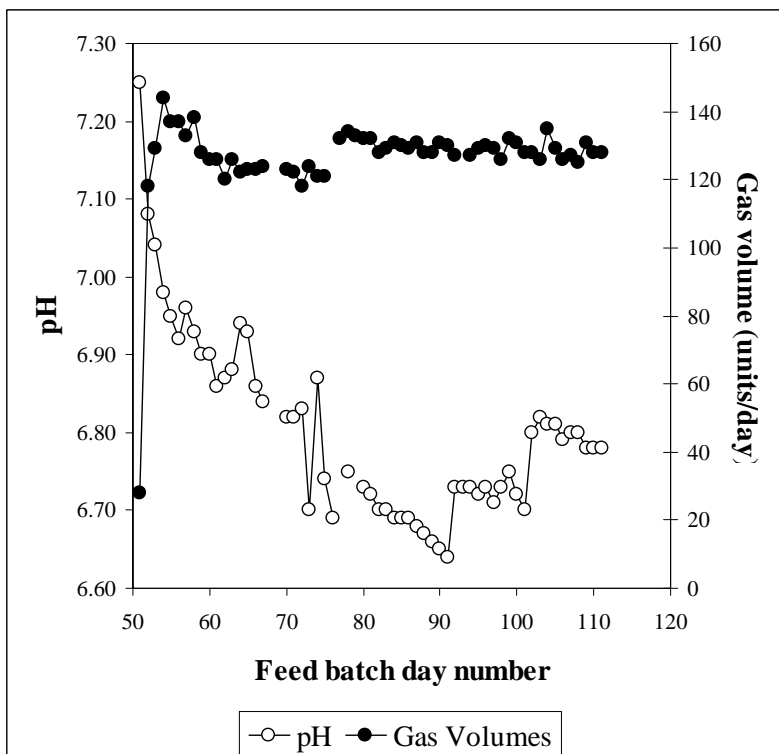


Figure B.10: Daily measurements of the pH and volumetric gas production leading up to and including steady state number 5 (steady state from day 99)

Appendix B: Steady State Data

Table B.19: Daily measured data for steady state number 5

Date	Day	Total COD (mgCOD/L)	Soluble COD (mgCOD/L)	Suspended Solids (mgCOD/L)	VFA (mg/L as HAc)	Alkalinity (mg/L as CaCO ₃)	pH	Gas Volume (Units/day)	TKN (mgN/L)	NH ₃ (mgN/L)	TP (mgP/L)	PO ₄ (mgP/L)
15-Jun	99	5538			11.7	860.8	6.75	132	294		83	
16-Jun	100	5632	110	1632	32.6	865.9	6.72	131	284	108	83	13
17-Jun	101	6204	98	1518	5.8	865.2	6.70	128	280	108	86	13
18-Jun	102	5796			5.1	806.7	6.80	128				
19-Jun	103						6.82	126				
20-Jun	104	5871			18.8	879.1	6.81	135				
21-Jun	105						6.81	129				
22-Jun	106	5829	99	1587	0.0	845.2	6.79	126	315	115	76	11
23-Jun	107	5811	97	1503	14.3	833.1	6.80	127	298	112	79	9
24-Jun	108	5809	95	1422	15.5	810.6	6.80	125	280	116	79	13
25-Jun	109	5706	101	1459	3.1	837.3	6.78	131	298	115	79	13
26-Jun	110	5696	92	1416	6.8	830	6.78	128	294	116	73	15
27-Jun	111	5600	93	1451	5.5	847.7	6.78	128	294	111	67	13
Mean		5751	97	1459	6	845	6.80	128	294	114	79	13
S.D.		106	3	56	6	22	0.02	2	7	3	4	1
Data points		10	7	7	10	11	11	12	8	8	8	7

Steady state No 6**Table B.20:** Operating conditions for steady state number 6

Feed batch number	F12
Mass of PSS in feed (g)	800
Total Mass of feed (g)	1600
Reactor Volume (L)	16
Retention time (day)	10
Sulfate addition (mgSO₄/L)	1000
pH	steady state
Biological groups present	Acidogens, methanogens and sulfate reducers

This reactor was seeded with waste sludge from other methanogenic systems. Once the system had stabilised (VFA < 50mg/L), sulfate was added to the feed. The system was not seeded with sulfate-reducing bacteria; only those present in the seed methanogenic sludge.

Table B.21: Results summary for steady state number 6

Feed total COD (mg/L)	25953
Feed soluble COD (mg/L)	2647
Feed TKN (mgN/L)	482
Feed FSA (mgN/L)	39
Feed Total P (mgP/L)	126
Feed soluble P (mgP/L)	17
Steady state measured after 38 days (3.8 x R_h)	
Effluent total COD (mg/L)	10684 ± 297 (9)
Effluent soluble organic COD (mg/L)	157 ± 8 (10)
Suspended solids (mgCOD/L)	3021
Effluent VFA (mg/L as HAc)	37 ± 18 (11)
Effluent Alkalinity (mg/L as CaCO₃)	2534 ± 62 (11)
Reactor pH	7.06 ± 0.03 (10)
Effluent Sulfate Concentration (mgSO₄/L)	34 ± 3 (10)
Gas Produced (units/day)	291 ± 4 (9)
Volume per unit (ml)	47.3 ± 0.4
Gas composition (%CH₄)	*64.53
Methane production (L/day)	8.88
Methane production (gCOD/day)	23.6
Effluent TKN (mgN/L)	532 ± 19 (8)
Effluent FSA (mgN/L)	207 ± 6 (9)
Effluent Total P (mgP/L)	114 ± 9 (7)
Effluent soluble P (mgP/L)	20 ± 2 (9)
COD balance (%)	98.1
TKN balance (%)	110.5
Total P balance (%)	90.8

*Average of 7 measurements made

Appendix B: Steady State Data

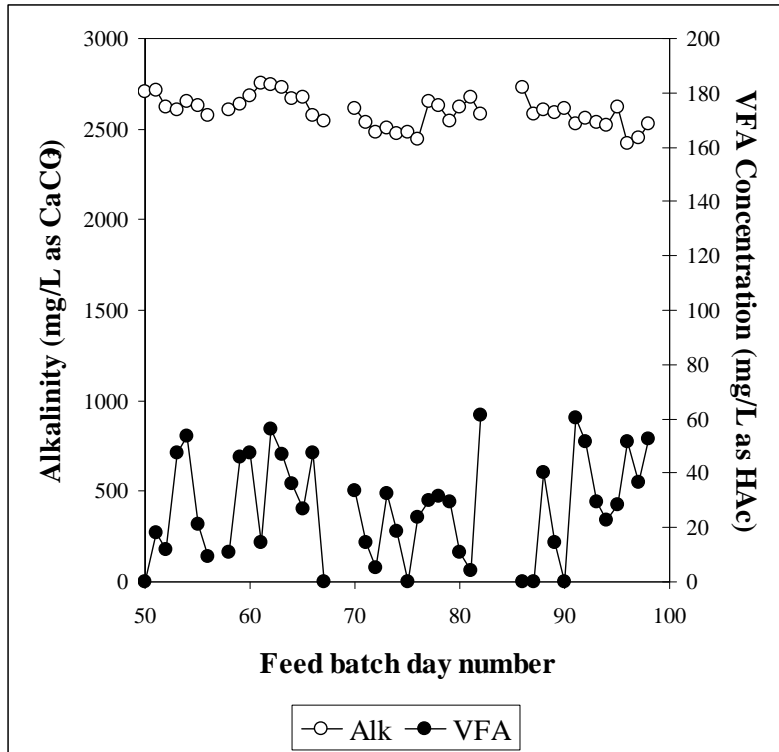


Figure B.11: Daily measurements of the VFA and alkalinity leading up to and including steady state number 6 (steady state from day 88)

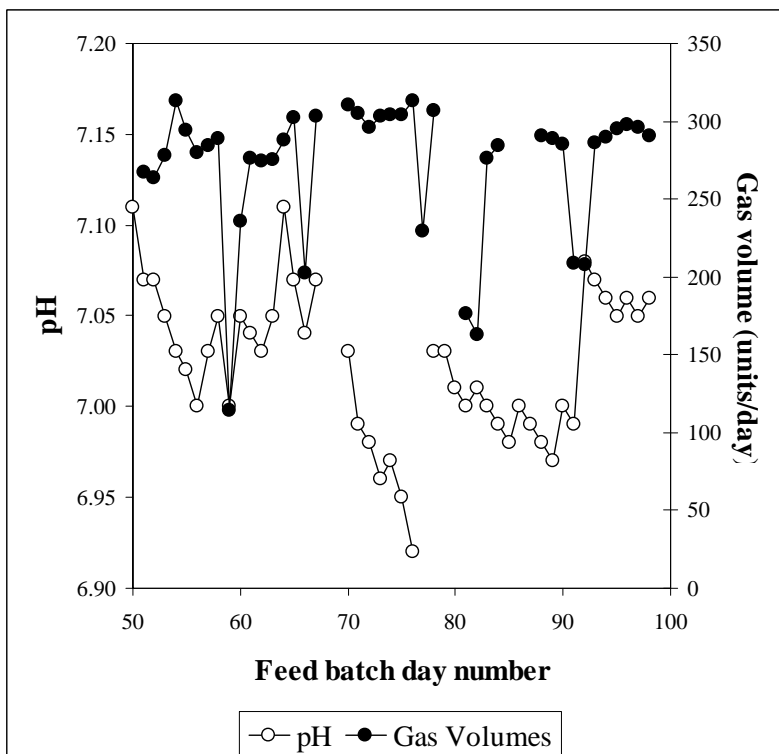


Figure B.12: Daily measurements of the pH and volumetric gas production leading up to and including steady state number 6 (steady state from day 88)

Appendix B: Steady State Data

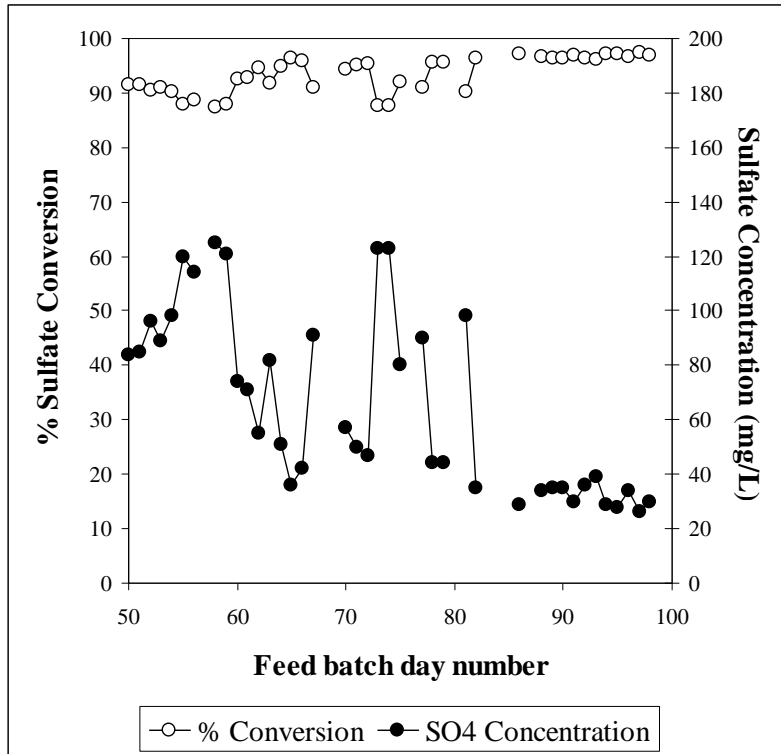


Figure B.13: Daily measurements of the sulfate concentration and sulfate conversion leading up to and including steady state number 6 (steady state from day 88)

Appendix B: Steady State Data

Table B.22: Daily measured data for steady state number 6

Date	Day	Total COD (mgCOD/L)	Soluble COD (mgCOD/L)	Suspended Solids (mgCOD/L)	VFA (mg/L as HA/c)	Alkalinity (mg/L as CaCO ₃)	pH	Gas Volume (Units/day)	SO ₄ (mgSO ₄ /L)	TKN (mgN/L)	NH ₃ (mgN/L)	TP (mgP/L)	PO ₄ (mgP/L)
04-Jun	88	10901	169	3304	40	2604.6	6.98	291	34		213		20
05-Jun	89	10684	144	3410	14.2	2590.1	6.97	289	35	539	210	108	25
06-Jun	90	10745	166	3176	0	2616.6	7.00	285	35	546	210	114	16
07-Jun	91	10264	158	2930	60.2	2530.1	6.99	209	30				
08-Jun	92	10634	155	3219	51.4	2560.6	7.08	208	36	497	202	111	19
09-Jun	93	10580	156	3108	29.3	2534.3	7.07	286	39	518	207	114	22
10-Jun	94	11153	161	3227	22.7	2521.5	7.06	290	29	525	207	120	20
11-Jun	95	11203	151	3173	28.3	2620.9	7.05	295	28	518	213	128	20
12-Jun	96				51.7	2419.3	7.06	298	34				
13-Jun	97	10399	152	3180	36.6	2453.7	7.05	296	26	546	196	153	19
14-Jun	98	11982	170	2949	52.8	2527.8	7.06	291	30	560	199	134	19
Mean		10684	157	3178	37	2534	7.06	291	34	532	207	114	20
S.D.		297	8	138	18	62	0.03	4	3	19	6	9	2
Data points		9	10	10	11	11	10	9	10	8	9	7	9

Steady state No 7**Table B.23:** Operating conditions for steady state number 7

Feed batch number	F13
Mass of PSS in feed (g)	675
Total Mass of feed (g)	1200
Reactor Volume (L)	16
Retention time (day)	6.67
Sulfate addition (gSO₄/L)	0
pH	steady state
Biological groups present	Acidogens and methanogens

This steady state followed directly after steady state number 2. The feed volume was incremented by 100g over 4 days. The system was then fed twice a day to minimise the shock of feeding on the system.

Table B.24: Results summary for steady state number 7

Feed total COD (mg/L)	24881
Feed soluble COD (mg/L)	2038
Feed TKN (mgN/L)	614
Feed FSA (mgN/L)	106
Feed Total P (mgP/L)	142
Feed soluble P (mgP/L)	26
Steady state measured after 12.5 days (1.87 x R_h)	
Effluent total COD (mg/L)	12595 ± 239 (12)
Effluent soluble COD (mg/L)	200 ± 12 (13)
Suspended solids (mgCOD/L)	2924
Effluent VFA (mg/L as HAc)	19 ± 13 (13)
Effluent Alkalinity (mg/L as CaCO₃)	1504 ± 27 (13)
Reactor pH	6.86 ± 0.05 (6)
Gas Produced (units/day)	[190 ± 3 (7)] twice = 380
Volume per unit (ml)	50.3 ± 0.2
Gas composition (%CH₄)	*60.98
Methane production (L/day)	11.66
Methane production (gCOD/day)	31.0
Effluent TKN (mgN/L)	581 ± 28 (13)
Effluent FSA (mgN/L)	196 ± 2 (12)
Effluent Total P (mgP/L)	124 ± 5 (11)
Effluent soluble P (mgP/L)	15 ± 1 (13)
COD balance (%)	102.6
TKN balance (%)	94.6
Total P balance (%)	87.5

*Average of 5 measurements made

Appendix B: Steady State Data

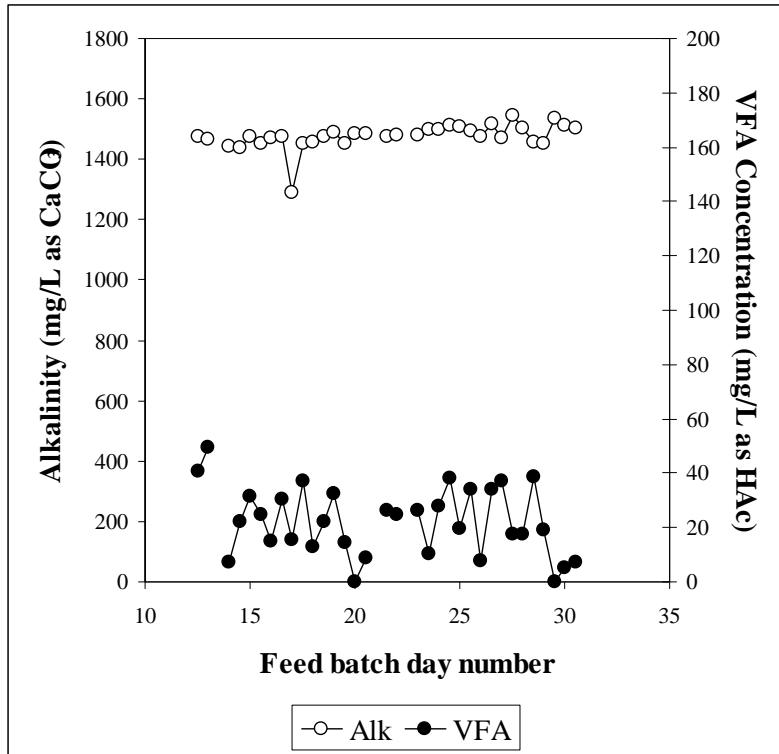


Figure B.14: Daily measurements of the VFA and alkalinity leading up to and including steady state number 7 (steady state from day 24.5)

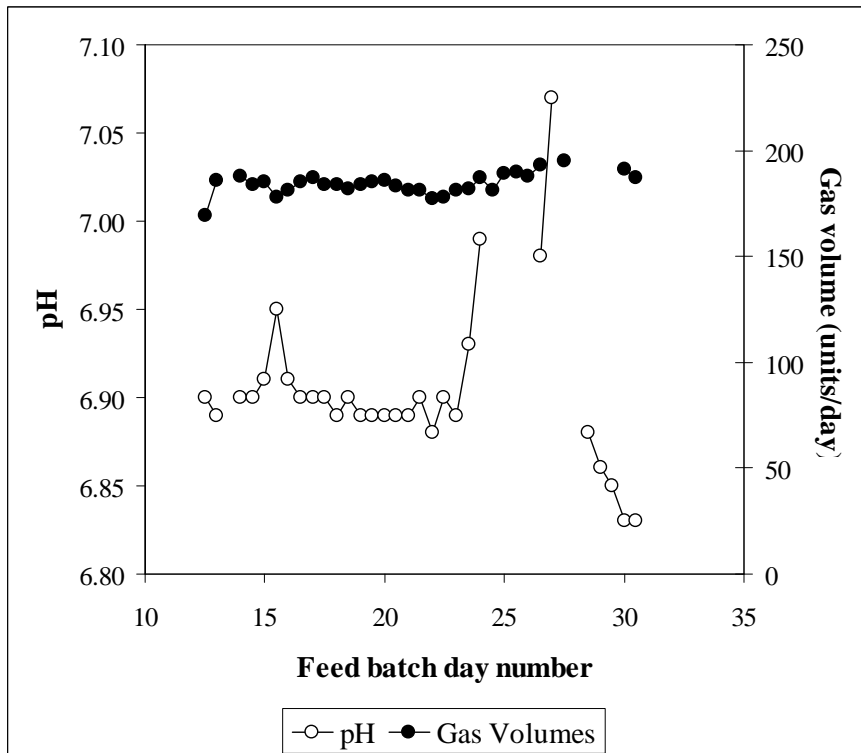


Figure B.15: Daily measurements of the pH and volumetric gas production leading up to and including steady state number 7 (steady state from day 24.5)

Appendix B: Steady State Data

Table B.25: Daily measured data for steady state number 7

Date	Day	Total COD (mgCOD/L)	Soluble COD (mgCOD/L)	Suspended Solids (mgCOD/L)	VFA (mg/L as HA/c)	Alkalinity (mg/L as CaCO ₃)	pH	Gas Volume (Units/day)	TKN (mgN/L)	NH ₃ (mgN/L)	TP (mgP/L)	PO ₄ (mgP/L)
06-Jul	24.5	12452	183	3369	38.1	1510.3		181	546	200	124	16
07-Jul	25	12226	181	3292	19.6	1508.8		189	553	202	130	15
07-Jul	25.5	12632	199	3089	34	1493.3		190	623	200	130	12
08-Jul	26	13453	202	3114	7.7	1475.2		188	630	196	124	15
08-Jul	26.5	12469	201	3151	34.2	1515.8	6.98	193	630	196	111	14
09-Jul	27	13178	200	2993	36.9	1469.1	7.07		581	193	111	15
09-Jul	27.5	12852	214		17.5	1545.7		195	602	196	117	15
10-Jul	28	12730	223		17.6	1503.7			595	196	124	15
10-Jul	28.5	12416	203		38.8	1454.9	6.88		581	196	117	15
11-Jul	29	12579	212	3066	18.9	1453.2	6.86		567	193	124	12
11-Jul	29.5	12665	188	3124	0	1534.8	6.85		567	195	117	15
12-Jul	30	12610	198	3184	4.9	1513.2	6.83	191	560	192	130	15
12-Jul	30.5	12373	181	3600	7.1	1503.4	6.83	187	560	193	117	15
Mean		12595	200	3124	19	1504	6.86	190	581	196	124	15
S.D.		239	12	109	13	27	0.05	3	28	2	5	1
Data points		12	13	9	13	13	6	7	13	12	11	13

Steady state No 8**Table B.26:** Operating conditions for steady state number 8

Feed batch number	F13
Mass of PSS in feed (g)	790
Total Mass of feed (g)	1400
Reactor Volume (L)	16
Retention time (day)	5.71
Sulfate addition (gSO₄/L)	0
pH	steady state
Biological groups present	Acidogens and methanogens

This experiment followed directly from steady state number 7. The feed volume was incremented by 50g with each feed cycle until the new operating feed volume was achieved. The same feed concentration was maintained.

Table B.27: Results summary for steady state number 8

Feed total COD (mg/L)	24960
Feed soluble COD (mg/L)	2516
Feed TKN (mgN/L)	616
Feed FSA (mgN/L)	124
Feed Total P (mgP/L)	142
Feed soluble P (mgP/L)	32
Steady state measured after 21 days (3.675 x R_h)	
Effluent total COD (mg/L)	12729 ± 297 (11)
Effluent soluble COD (mg/L)	205 ± 12 (11)
Suspended solids (mgCOD/L)	4445
Effluent VFA (mg/L as HAc)	32 ± 10 (10)
Effluent Alkalinity (mg/L as CaCO₃)	1463 ± 16 (10)
Reactor pH	6.93 ± 0.01 (11)
Gas Produced (units/day)	[216 ± 4 (10)] twice = 432
Volume per unit (ml)	49.7 ± 0.4
Gas composition (%CH₄)	*61.67
Methane production (L/day)	13.24
Methane production (gCOD/day)	35.2
Effluent TKN (mgN/L)	574 ± 6 (8)
Effluent FSA (mgN/L)	200 ± 4 (10)
Effluent Total P (mgP/L)	98 ± 4 (9)
Effluent soluble P (mgP/L)	9 ± 1 (9)
COD balance (%)	101.4
TKN balance (%)	93.2
Total P balance (%)	68.9

* Average of 9 measurements made

Appendix B: Steady State Data

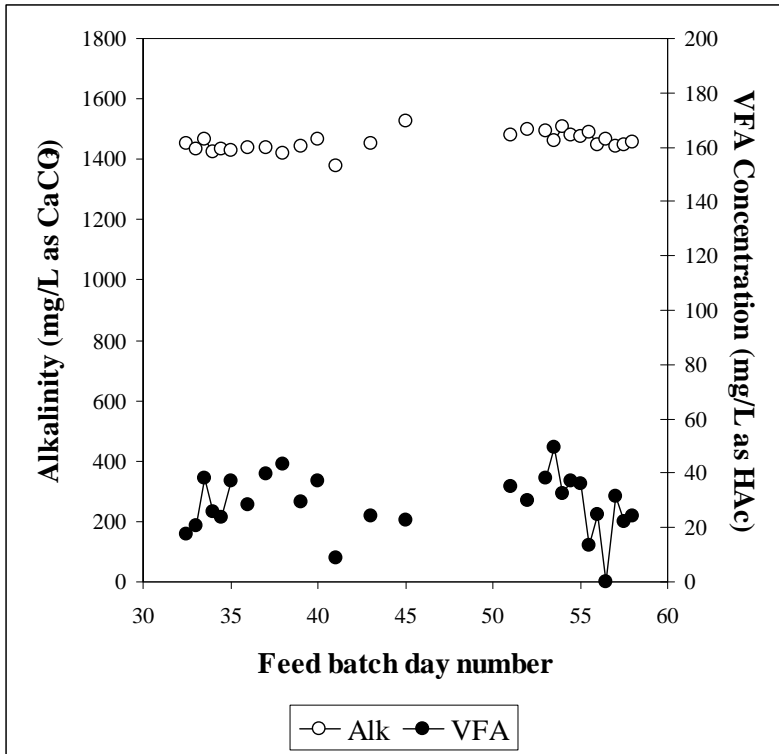


Figure B.16: Daily measurements of the VFA and alkalinity leading up to and including steady state number 8 (steady state from day 53)

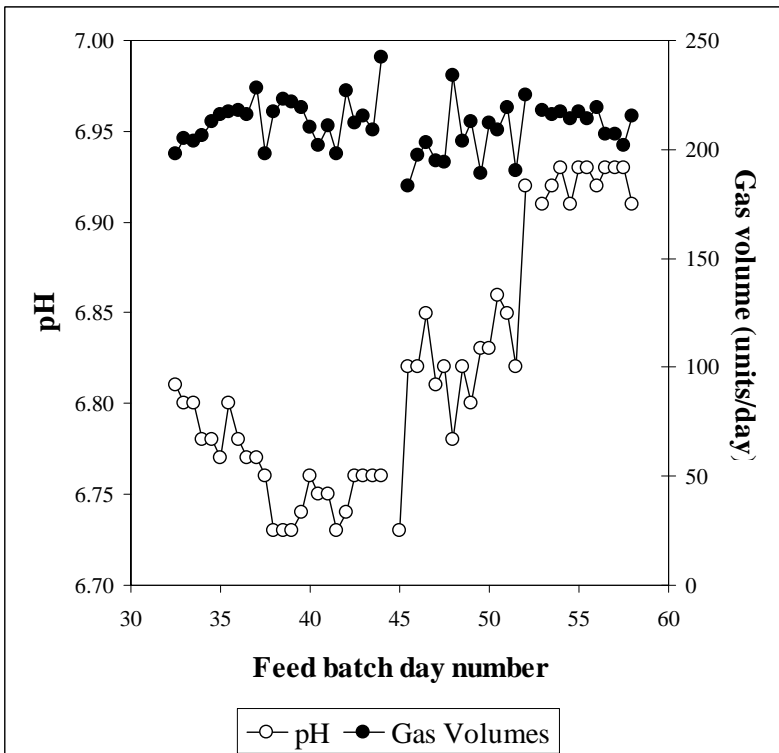


Figure B.17: Daily measurements of the pH and volumetric gas production leading up to and including steady state number 8 (steady state from day 53)

Appendix B: Steady State Data

Table B.28: Daily measured data for steady state number 8

Date	Day	Total COD (mgCOD/L)	Soluble COD (mgCOD/L)	Suspended Solids (mgCOD/L)	VFA (mg/L as HAc)	Alkalinity (mg/L as CaCO ₃)	pH	Gas Volume (Units/day)	TKN (mgN/L)	NH ₃ (mgN/L)	TP (mgP/L)	PO ₄ (mgP/L)
04-Aug	53	12210	205	4106	38.3	1491.5	6.91	218	581	202	98	9
04-Aug	53.5	12810	205	5298	49.4	1460.3	6.92	216	574	199	92	9
05-Aug	54	12532	205	4149	32.4	1505.9	6.93	217	581	200	98	9
05-Aug	54.5	12499	210	4650	37.2	1479.2	6.91	214	574	196	92	9
06-Aug	55	12577	219	6858	36.3	1477.1	6.93	217	567	202	98	7
06-Aug	55.5	12729	184	5059	13.4	1487.5	6.93	214	574	199	98	9
07-Aug	56	13226	218		24.9	1449.3	6.92	219	588	203	104	7
07-Aug	56.5	12659	215	4746	0	1466.1	6.93	207	574	196	104	9
08-Aug	57	12871	191	4279	31.3	1442.8	6.93	207		200	98	9
08-Aug	57.5	12736	184	4432	22.1	1447.5	6.93	202	455	188	168	18
09-Aug	58	13286	192	4874	24.1	1458.7	6.91	215	462	182	151	15
	Mean	12729	205	4650	32	1463	6.93	216	574	200	98	9
	S.D.	297	12	390	10	16	0.01	4	6	4	4	1
	Data points	11	11	9	10	10	11	10	8	10	9	9

Steady state No 9**Table B.29:** Operating conditions for steady state number 9

Feed batch number	F13
Mass of PSS in feed (g)	900
Total Mass of feed (g)	1600
Reactor Volume (L)	16
Retention time (day)	5
Sulfate addition (gSO₄/L)	0
pH	steady state
Biological groups present	Acidogens and methanogens

This experiment followed directly from steady state number 8. The feed volume was incremented over seven feeds until the new operating feed volume was achieved. The same feed concentration was maintained.

Table B.30: Results summary for steady state number 9

Feed total COD (mg/L)	24881
Feed soluble COD (mg/L)	2703
Feed TKN (mgN/L)	614
Feed FSA (mgN/L)	131
Feed Total P (mgP/L)	142
Feed soluble P (mgP/L)	33
Steady state measured after 9 days (1.8 x R_h)	
Effluent total COD (mg/L)	12610 ± 262 (11)
Effluent soluble COD (mg/L)	301 ± 15 (11)
Suspended solids (mgCOD/L)	5180
Effluent VFA (mg/L as HAc)	87 ± 7 (12)
Effluent Alkalinity (mg/L as CaCO₃)	1359 ± 18 (11)
Reactor pH	6.78 ± 0.02 (10)
Gas Produced (units/day)	[223 ± 4 (10)] twice = 446
Volume per unit (ml)	49.7 ± 0.4
Gas composition (%CH₄)	*61.23
Methane production (L/day)	13.57
Methane production (gCOD/day)	36.1
Effluent TKN (mgN/L)	455 ± 6 (11)
Effluent FSA (mgN/L)	193 ± 4 (10)
Effluent Total P (mgP/L)	151 ± 5 (11)
Effluent soluble P (mgP/L)	20 ± 1 (11)
COD balance (%)	96.0
TKN balance (%)	74.1
Total P balance (%)	106.5

* Average of 9 measurements made

Appendix B: Steady State Data

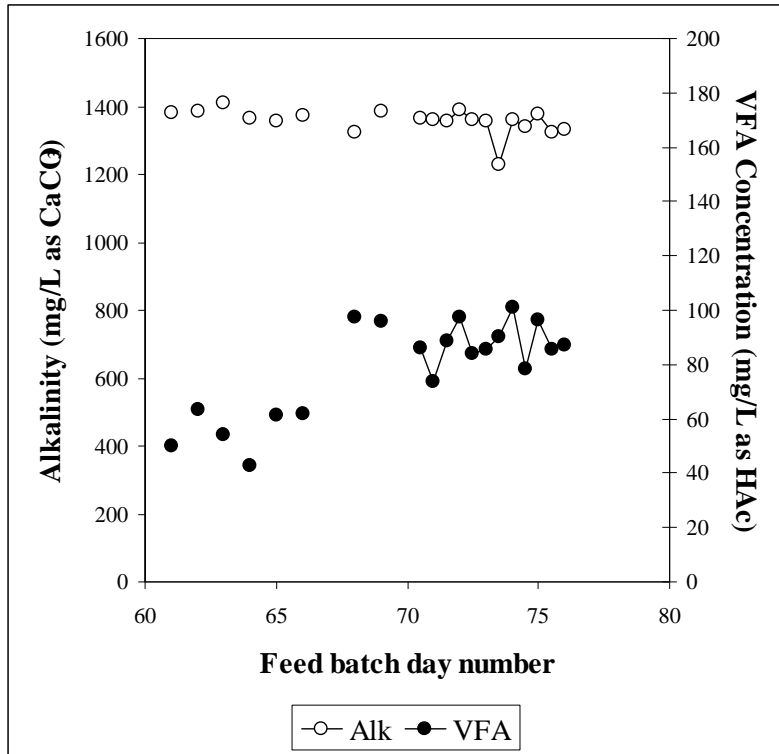


Figure B.18: Daily measurements of the VFA and alkalinity leading up to and including steady state number 9 (steady state from day 70.5)

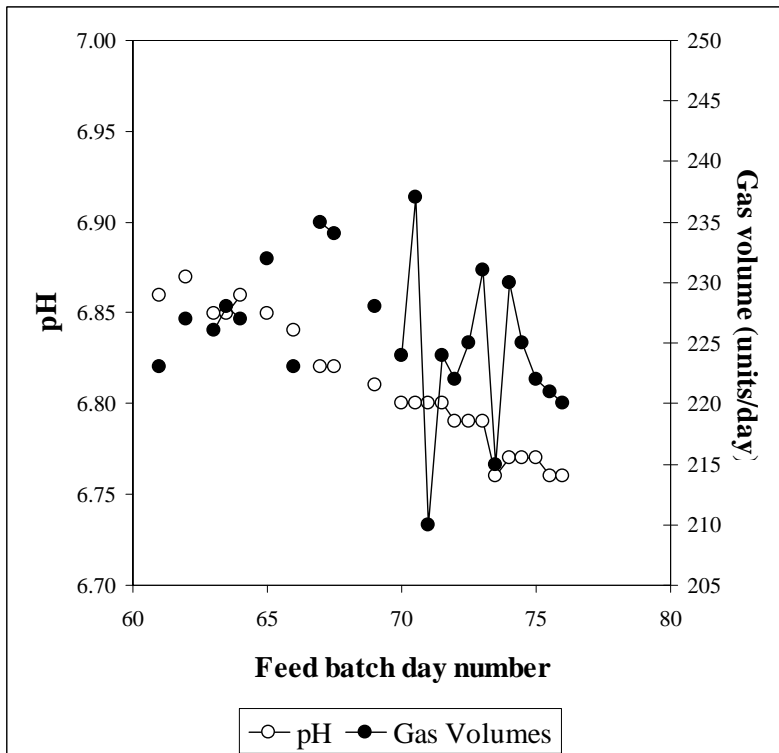


Figure B.19: Daily measurements of the pH and volumetric gas production leading up to and including steady state number 9 (steady state from day 70.5)

Appendix B: Steady State Data

Table B.31: Daily measured data for steady state number 9

Date	Day	Total COD (mgCOD/L)	Soluble COD (mgCOD/L)	Suspended Solids (mgCOD/L)	VFA (mg/L as HAc)	Alkalinity (mg/L as CaCO ₃)	pH	Gas Volume (Units/day)	TKN (mgN/L)	NH ₃ (mgN/L)	TP (mgP/L)	PO ₄ (mgP/L)
21-Aug	70.5	12473	257	5623	86.3	1365.4	6.80	237	455	218	126	18
22-Aug	71	12316	284	5211	73.8	1358.8	6.80	210	462	196	143	18
22-Aug	71.5	12468	272		88.9	1356.9	6.80	224	448		151	
23-Aug	72	12610	309	4091	97.3	1390.3	6.79	222	441	196	143	20
23-Aug	72.5	12383	283	4030	84	1358.9	6.79	225	448	193	151	20
24-Aug	73	12265	269	5348	85.6	1355.1	6.79	231	448	193	151	22
24-Aug	73.5	12754	301	5659	90.3	1230.2	6.76	215	448	196	143	20
25-Aug	74	12905	284	6603	101.1	1358.9	6.77	230	455	193	151	17
25-Aug	74.5	12833	312	6691	78.2	1341.9	6.77	225	455	182	151	20
26-Aug	75	12625	309	4827	96.2	1376.1	6.77	222	462	188	151	20
26-Aug	75.5	13159	301		85.6	1325.5	6.76	221	455	190	151	20
27-Aug	76	13215	311	5613	87.1	1332.2	6.76	220	462	190	160	20
	Mean	12610	301	5481	87	1359	6.78	223	455	193	151	20
	S.D.	262	15	850	7	18	0.02	4	6	4	5	1
	Data points	11	11	10	12	11	10	10	11	10	11	11

Steady state No 10**Table B.32:** Operating conditions for steady state number 10

Feed batch number	F13
Mass of PSS in feed (g)	600
Total Mass of feed (g)	667
Reactor Volume (L)	20
Retention time (day)	15
Sulfate addition (gSO₄/L)	0
pH	steady state
Biological groups present	acidogenic and methanogenic

This experiment followed steady state number 4. The feed was changed from F12 to F13, and the dilution was changed to increase the feed concentration from 25 gCOD/L to 40 gCOD/L. Transient data from the first 16 days after the change in concentration is available. The system was fed once daily until day 21, when it was changed to twice daily

Table B.33: Results summary for steady state number 10

Feed total COD (mg/L)	39790
Feed soluble COD (mg/L)	3550
Feed TKN (mgN/L)	982
Feed FSA (mgN/L)	180
Feed Total P (mgP/L)	227
Feed soluble P (mgP/L)	45
Steady state measured after 30 days (2 x R_h)	
Effluent total COD (mg/L)	16972 ± 322 (10)
Effluent soluble COD (mg/L)	250 ± 7 (9)
Suspended solids (mgCOD/L)	4924
Effluent VFA (mg/L as HAc)	28 ± 7 (11)
Effluent Alkalinity (mg/L as CaCO₃)	2446 ± 25 (10)
Reactor pH	6.98 ± 0.02 (11)
Gas Produced (units/day)	[215 ± 8 (11)] twice = 430
Volume per unit (ml)	45.9 ± 0.2
Gas composition (%CH₄)	*61.40
Methane production (L/day)	12.12
Methane production (gCOD/day)	32.3
Effluent TKN (mgN/L)	854 ± 14 (10)
Effluent FSA (mgN/L)	347 ± 8 (9)
Effluent Total P (mgP/L)	178 ± 4 (10)
Effluent soluble P (mgP/L)	12 ± 1 (10)
COD balance (%)	103.4
TKN balance (%)	86.9
Total P balance (%)	78.5

* Average of 6 measurements made

Appendix B: Steady State Data

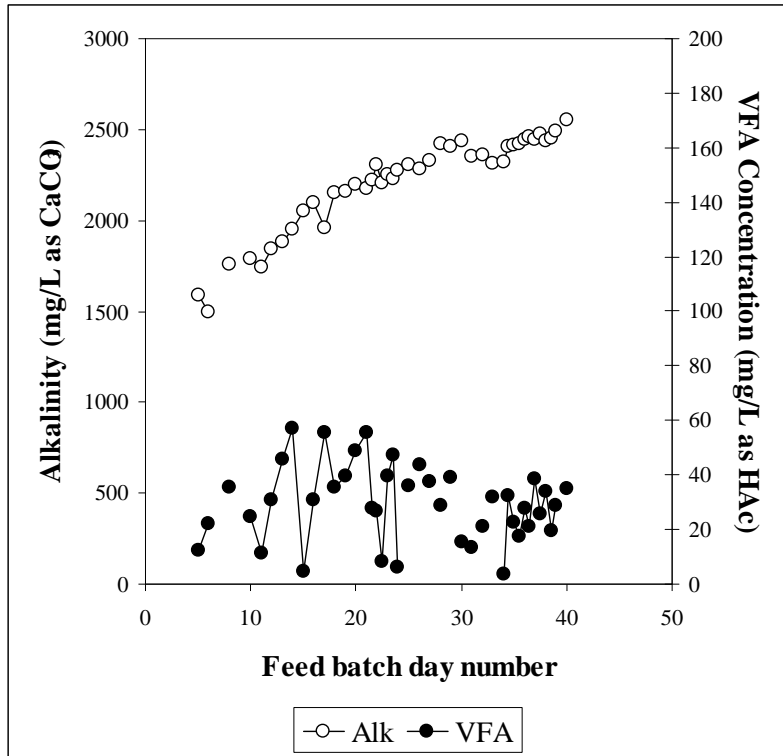


Figure B.20: Daily measurements of the VFA and alkalinity leading up to and including steady state number 10 (steady state from day 34.5)

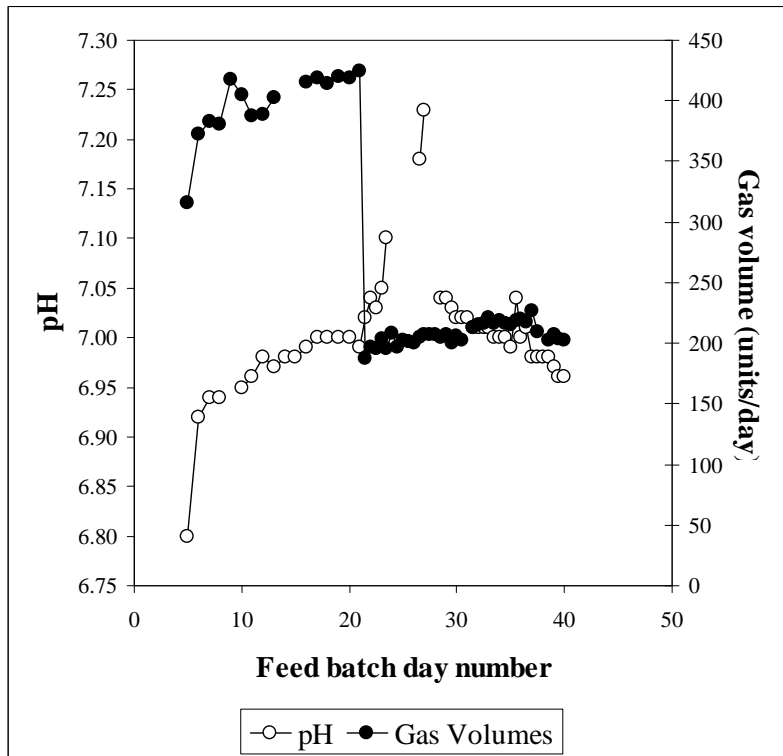


Figure B.21: Daily measurements of the pH and volumetric gas production leading up to and including steady state number 10 (steady state from day 34.5)

Appendix B: Steady State Data

Table B.34: Daily measured data for steady state number 10

Date	Day	Total COD (mgCOD/L)	Soluble COD (mgCOD/L)	Suspended Solids (mgCOD/L)	VFA (mg/L as HAc)	Alkalinity (mg/L as CaCO ₃)	pH	Gas Volume (Units/day)	TKN (mgN/L)	NH ₃ (mgN/L)	TP (mgP/L)	PO ₄ (mgP/L)
16-Jul	34.5	16887	242	5256	32.5	2409.9	7.00	216	882	333	184	7
17-Jul	35	16587	248	5098	22.5	2413.9	6.99	215	868	343	178	12
17-Jul	35.5	16532	253	4753	17.5	2419.6	7.04	219	861	322	178	11
18-Jul	36	17570	258	5174	27.9	2447.4	7.00	220	868	347	166	12
18-Jul	36.5	16879	243	5132	21.1	2461.2	7.01	218	854	342	178	12
19-Jul	37	16879	244	5219	38.7	2444.1	6.98	227	847	346	178	12
19-Jul	37.5	17388	250	5095	25.9	2474.1	6.98	209	840	364	178	11
20-Jul	38	15494	252	5033	33.7	2439.1	6.98		840	350	172	12
20-Jul	38.5	17153	272	5418	19.6	2453.9	6.98	203	840	347	178	12
21-Jul	39	17056	266	5258	28.6	2492.6	6.97	207	854	349	178	12
21-Jul	39.5						6.96	204				
22-Jul	40	17329			34.8	2550.3	6.96	202	798		146	
Mean		16972	250	5174	28	2446	6.98	215	854	347	178	12
S.D.		322	7	109	7	25	0.02	8	14	8	4	1
Data points		10	9	9	11	10	11	11	10	9	10	10

Steady state No 11**Table B.35:** Operating conditions for steady state number 11

Feed batch number	F13
Mass of PSS in feed (g)	600
Total Mass of feed (g)	667
Reactor Volume (L)	20
Retention time (day)	15
Sulfate addition (gSO₄/L)	0
pH	steady state
Biological groups present	acidogenic and methanogenic

This experiment was a duplicate of steady state number 10. The system was operated identically to steady state 10 for a further 13 days and the steady state operation reassessed.

Table B.36: Results summary for steady state number 11

Feed total COD (mg/L)	39790
Feed soluble COD (mg/L)	4012
Feed TKN (mgN/L)	982
Feed FSA (mgN/L)	198
Feed Total P (mgP/L)	227
Feed soluble P (mgP/L)	51
Steady state measured after 48 days (3.2 x R_h)	
Effluent total COD (mg/L)	17167 ± 283 (10)
Effluent soluble COD (mg/L)	299 ± 13 (10)
Suspended solids (mgCOD/L)	6779
Effluent VFA (mg/L as HAc)	35 ± 17 (11)
Effluent Alkalinity (mg/L as CaCO₃)	2491 ± 73 (11)
Reactor pH	7.12 ± 0.01 (10)
Gas Produced (units/day)	[205 ± 8 (8)] twice = 410
Volume per unit (ml)	45.9 ± 0.2
Gas composition (%CH₄)	*61.17
Methane production (L/day)	11.51
Methane production (gCOD/day)	30.6
Effluent TKN (mgN/L)	840 ± 12 (9)
Effluent FSA (mgN/L)	370 ± 3 (9)
Effluent Total P (mgP/L)	159 ± 11 (10)
Effluent soluble P (mgP/L)	9 ± 2 (10)
COD balance (%)	100.9
TKN balance (%)	85.5
Total P balance (%)	70.1

*Average of 9 measurements made

Appendix B: Steady State Data

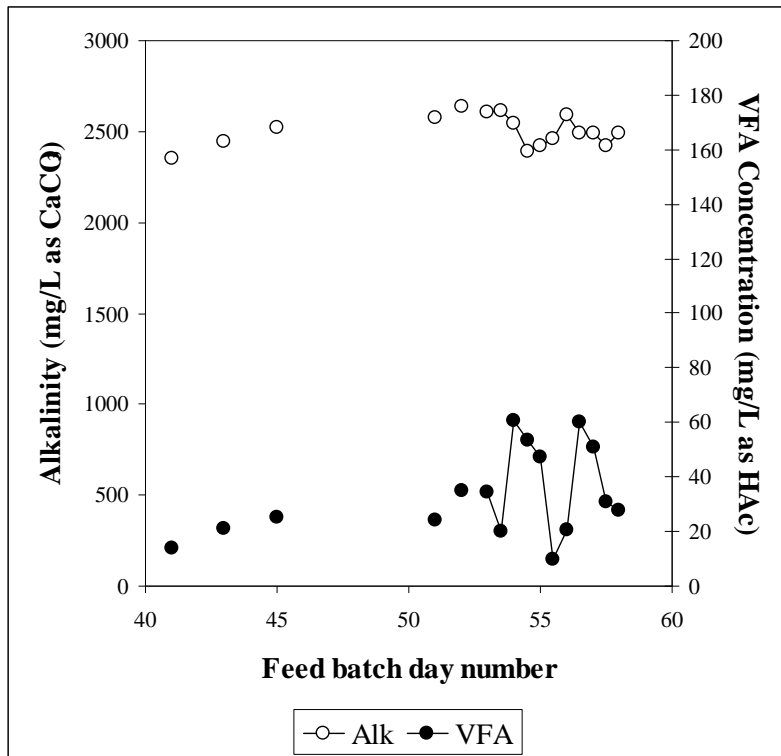


Figure B.22: Daily measurements of the VFA and alkalinity leading up to and including steady state number (steady state from day 53)

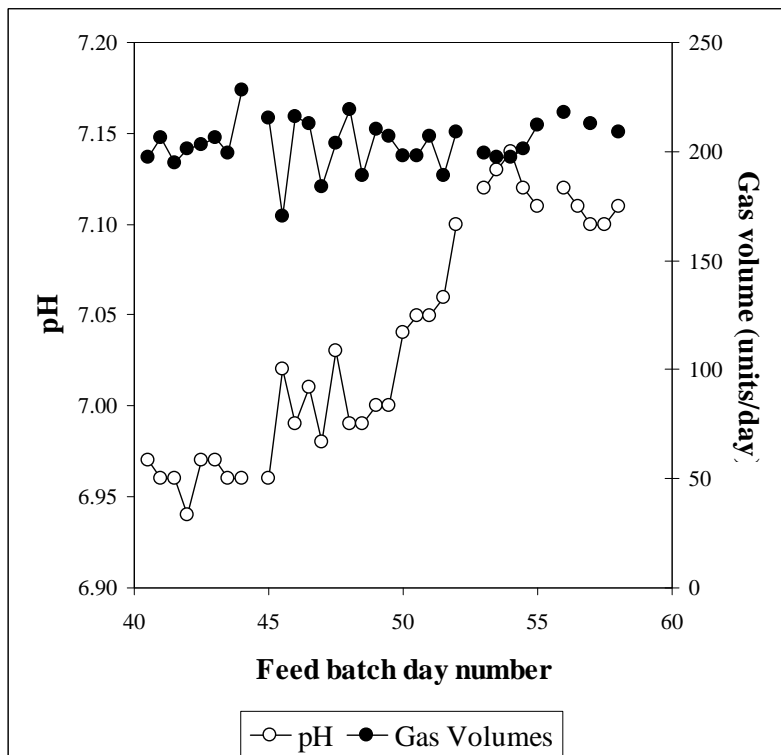


Figure B.23: Daily measurements of the pH and volumetric gas production leading up to and including steady state number 11 (steady state from day 53)

Appendix B: Steady State Data

Table B.37: Daily measured data for steady state number 11

Date	Day	Total COD (mgCOD/L)	Soluble COD (mgCOD/L)	Suspended Solids (mgCOD/L)	VFA (mg/L as HAc)	Alkalinity (mg/L as CaCO ₃)	pH	Gas Volume (Units/day)	TKN (mgN/L)	NH ₃ (mgN/L)	TP (mgP/L)	PO ₄ (mgP/L)
04-Aug	53	17357	288	6761	34.6	2605.4	7.12	199	840	368	159	7
04-Aug	53.5	17306	295	6755	20.3	2614.4	7.13	197	805	371	159	7
05-Aug	54	15993	304	7078	60.6	2542.1	7.14	197	833	370	165	9
05-Aug	54.5	17079	317	7401	53.5	2393.9	7.12	201	833	370	159	10
06-Aug	55	16599	302	7312	47.1	2422.6	7.11	212	847	371	159	9
06-Aug	55.5	17069	310	7306	9.7	2457.6			847	364	165	7
07-Aug	56	17239	336		20.5	2592.2	7.12	218	847	371	152	7
07-Aug	56.5	16456	314	6924	60.4	2488	7.11		833	364	159	10
08-Aug	57	17208	295	7100	51.0	2491.8	7.10	213	840	364	165	11
08-Aug	57.5	17176	279	6562	30.8	2425	7.10		644	333	193	15
09-Aug	58	17157	279		27.7	2491.4	7.11	209	679	336	227	18
Mean		17167	299	7078	35	2491	7.12	205	840	370	159	9
S.D.		283	13	275	17	73	0.01	8	12	3	11	2
Data points		10	10	9	11	11	10	8	9	9	10	10

Steady state No 12**Table B.38:** Operating conditions for steady state number 12

Feed batch number	F13
Mass of PSS in feed (g)	900
Total Mass of feed (g)	1000
Reactor Volume (L)	20
Retention time (day)	10
Sulfate addition (gSO₄/L)	0
pH	steady state
Biological groups present	acidogenic and methanogenic

This experiment followed from steady state number 11. The feed volume was increased over seven increments.

Table B.39: Results summary for steady state number 12

Feed total COD (mg/L)	39810
Feed soluble COD (mg/L)	4446
Feed TKN (mgN/L)	983
Feed FSA (mgN/L)	214
Feed Total P (mgP/L)	227
Feed soluble P (mgP/L)	54
Steady state measured after 16 days (1.6 x R_h)	
Effluent total COD (mg/L)	18085 ± 589 (11)
Effluent soluble COD (mg/L)	256 ± 10 (12)
Suspended solids (mgCOD/L)	4296
Effluent VFA (mg/L as HAc)	27 ± 8 (11)
Effluent Alkalinity (mg/L as CaCO₃)	2362 ± 25 (11)
Reactor pH	6.92 ± 0.01 (12)
Gas Produced (units/day)	[301 ± 2 (12)] twice = 602
Volume per unit (ml)	45.9 ± 0.2
Gas composition (%CH₄)	*62.73
Methane production (L/day)	17.33
Methane production (gCOD/day)	46.1
Effluent TKN (mgN/L)	770 ± 14 (11)
Effluent FSA (mgN/L)	260 ± 22 (9)
Effluent Total P (mgP/L)	251 ± 3 (11)
Effluent soluble P (mgP/L)	16 ± 2 (11)
COD balance (%)	103.4
TKN balance (%)	78.3
Total P balance (%)	110.7

*Average of 4 measurements made

Appendix B: Steady State Data

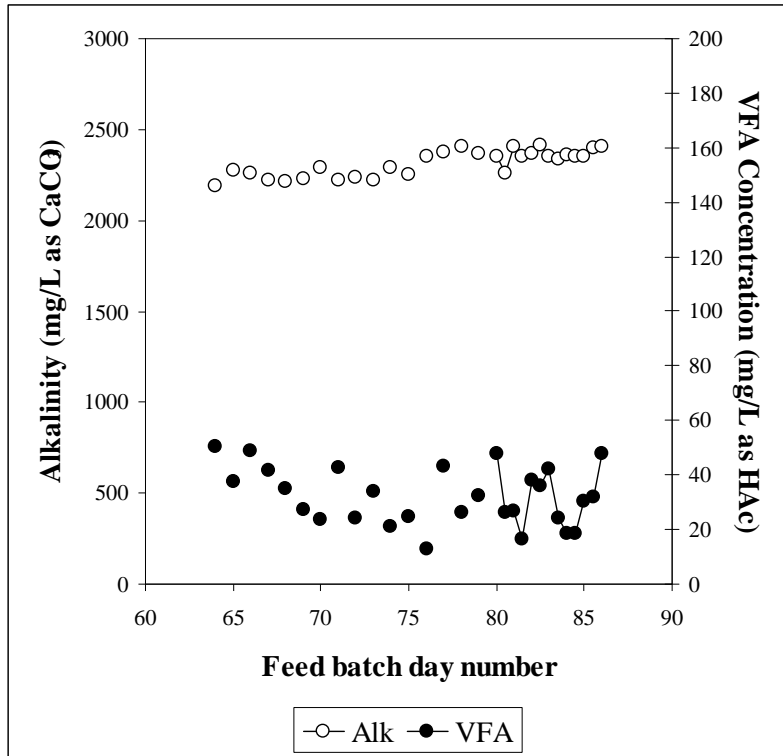


Figure B.24: Daily measurements of the VFA and alkalinity leading up to and including steady state number 12 (steady state from day 80.5)

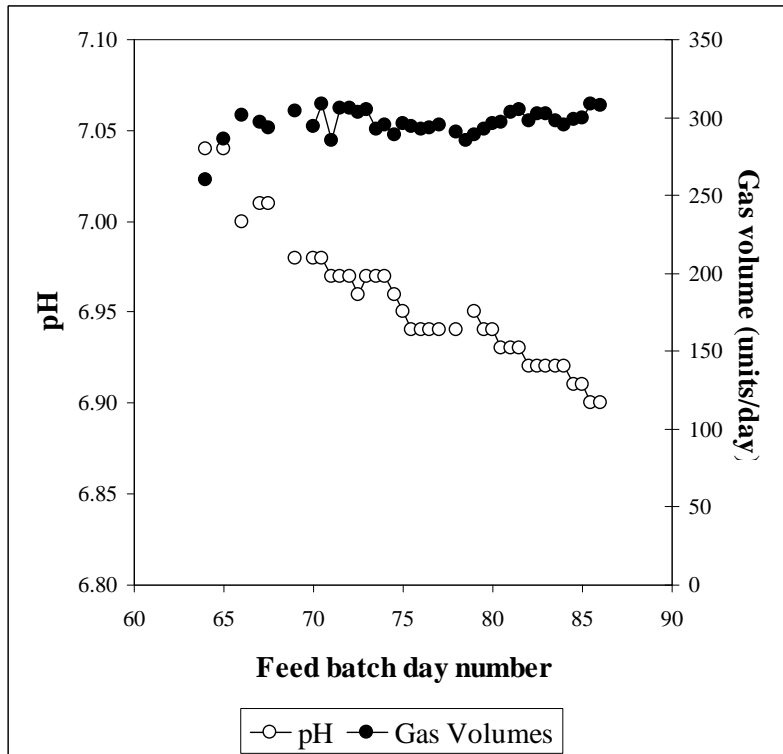


Figure B.25: Daily measurements of the pH and volumetric gas production leading up to and including steady state number 12 (steady state from day 80.5)

Appendix B: Steady State Data

Table B.40: Daily measured data for steady state number 12

Date	Day	Total COD (mgCOD/L)	Soluble COD (mgCOD/L)	Suspended Solids (mgCOD/L)	VFA (mg/L as HAc)	Alkalinity (mg/L as CaCO ₃)	pH	Gas Volume (Units/day)	TKN (mgN/L)	NH ₃ (mgN/L)	TP (mgP/L)	PO ₄ (mgP/L)
31-Aug	80.5	18673	255	6065	26.3	2260.7	6.93	297	777	312	251	11
01-Sep	81	18133	270	4909	26.8	2404.7	6.93	303	735	322	251	14
01-Sep	81.5	18055	259	4816	16.7	2348.7	6.93	305	798	321	251	16
02-Sep	82	18035	267		37.9	2368.9	6.92	298	763	317	251	18
02-Sep	82.5	18085	257	4804	35.8	2411.0	6.92	302	770	322	251	13
03-Sep	83	17075	248	4152	42.2	2354.5	6.92	302	777	260	259	13
03-Sep	83.5	16852	252	5718	24.3	2338.8	6.92	298	770	260	251	17
04-Sep	84	16626	247	4299	18.7	2361.6	6.92	295	791	260	234	15
04-Sep	84.5	18646	253	8379	18.7	2351.2	6.91	299	749	266	251	18
05-Sep	85	18498	276	4163	30.3	2355.4	6.91	300	763	261	251	17
05-Sep	85.5	18226	271	3948	31.8	2398.4	6.90	309	770	259	259	16
06-Sep	86	17320	242	4010	48.0	2403.8	6.90	308	756	260	251	17
	Mean	18085	256	4552	27	2362	6.92	301	770	260	251	16
	S.D.	589	10	690	8	25	0.01	4	14	22	3	2
	Data points	11	12	10	11	11	12	12	11	9	11	11

Steady state No 13**Table B.41:** Operating conditions for steady state number 13

Feed batch number	F13
Mass of PSS in feed (g)	300
Total Mass of feed (g)	1000
Reactor Volume (L)	20
Retention time (day)	10
Sulfate addition (gSO₄/L)	0
pH	steady state
Biological groups present	acidogenic and methanogenic

This experiment followed from steady state number. The feed was changed from F12 to F13. The feed volume was changed in a single step from 1.334 L/d to 2 L/d, and the system was fed twice a day instead of once a day.

Table B.42: Results summary for steady state number 13

Feed total COD (mg/L)	13270
Feed soluble COD (mg/L)	1164
Feed TKN (mgN/L)	328
Feed FSA (mgN/L)	59
Feed Total P (mgP/L)	76
Feed soluble P (mgP/L)	15
Steady state measured after 32ays (3.2 x R_h)	
Effluent total COD (mg/L)	6249 ± 109 (11)
Effluent soluble COD (mg/L)	108 ± 5 (10)
Suspended solids (mgCOD/L)	1823
Effluent VFA (mg/L as HAc)	8 ± 3 (11)
Effluent Alkalinity (mg/L as CaCO₃)	854 ± 9 (12)
Reactor pH	6.69 ± 0.01 (12)
Gas Produced (units/day)	[84 ± 3 (12)] twice = 168
Volume per unit (ml)	48.8 ± 0.5
Gas composition (%CH₄)	*60.98
Methane production (L/day)	5.0
Methane production (gCOD/day)	13.3
Effluent TKN (mgN/L)	302 ± 11 (10)
Effluent FSA (mgN/L)	127 ± 2 (11)
Effluent Total P (mgP/L)	65 ± 6 (11)
Effluent soluble P (mgP/L)	12 ± 1 (12)
COD balance (%)	97.2
TKN balance (%)	92.2
Total P balance (%)	86.0

* Average of 8 measurements made

Appendix B: Steady State Data

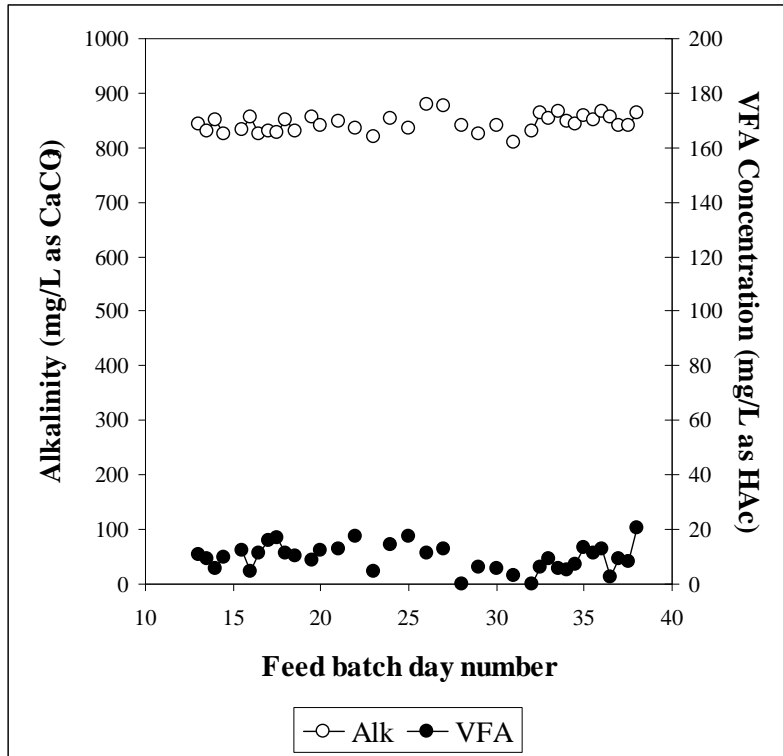


Figure B.26: Daily measurements of the VFA and alkalinity leading up to and including steady state number 13 (steady state from day 32.5)

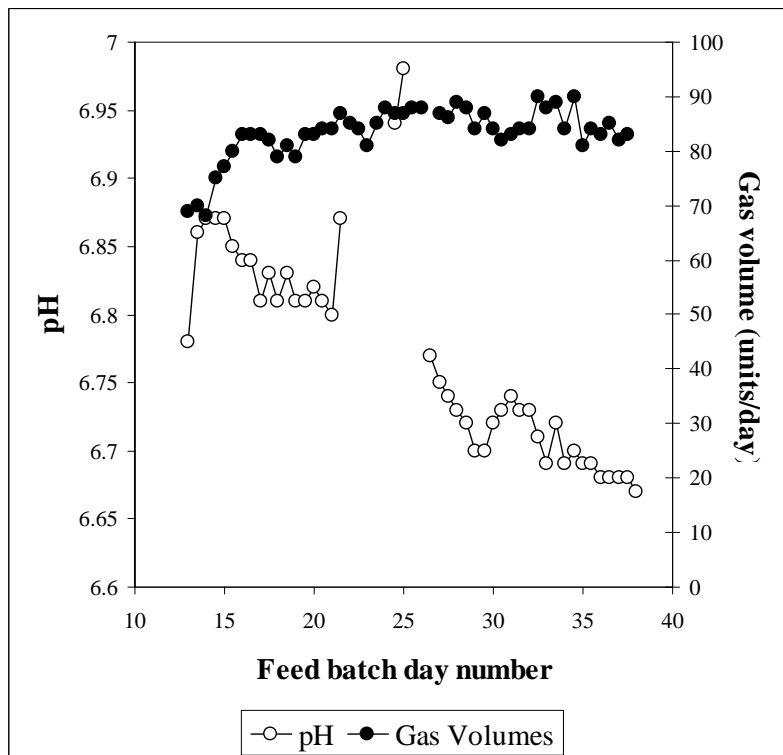


Figure B.27: Daily measurements of the pH and volumetric gas production leading up to and including steady state number 13 (steady state from day 32.5)

Appendix B: Steady State Data

Table B.43: Daily measured data for steady state number 13

Date	Day	Total COD (mgCOD/L)	Soluble COD (mgCOD/L)	Suspended Solids (mgCOD/L)	VFA (mg/L as HAc)	Alkalinity (mg/L as CaCO ₃)	pH	Gas Volume (Units/day)	TKN (mgN/L)	NH ₃ (mgN/L)	TP (mgP/L)	PO ₄ (mgP/L)
16-Jul	32.5	6389	108	1899	6.4	863.2	6.71	84	305	129	83	11
17-Jul	33	6733	110	1861	9.2	852.4	6.69	90	291	127	62	12
17-Jul	33.5	6304	121	1518	5.9	867.2	6.72	88	294	125	65	12
18-Jul	34	6185	109	1735	5.0	848.7	6.69	89		125	65	12
18-Jul	34.5	6249		2350	7.4	842.1	6.70	84	305	120	62	11
19-Jul	35	6238	104	1999	13.4	857.4	6.69	90	298	126	68	12
19-Jul	35.5	6260	117	1956	11.1	850.6	6.69	81	305	127	65	12
20-Jul	36	6015	111	1928	13.1	866.7	6.68	84	294	127	68	12
20-Jul	36.5	6203	100	1991	2.6	854.9	6.68	83	298	125	62	12
21-Jul	37	6237	108	1988	9.0	841.5	6.68	85	305	127	68	12
21-Jul	37.5	6279	108	1890	8.3	841	6.68	82	357	123	52	13
22-Jul	38	6466	100	1933	20.6	864.2	6.67	83	333	129	49	12
	Mean	6249	108	1931	8	854	6.69	84	302	127	65	12
	S.D.	109	5	75	3	9	0.01	3	11	2	6	1
	Data points	11	10	10	11	12	12	12	10	11	11	12

Steady state No 14**Table B.44:** Operating conditions for steady state number 14

Feed batch number	F13
Mass of PSS in feed (g)	375
Total Mass of feed (g)	1250
Reactor Volume (L)	20
Retention time (day)	8
Sulfate addition (gSO₄/L)	0
pH	steady state
Biological groups present	acidogenic and methanogenic

Following steady state number 13, the methanogenic bacteria failed resulting in an increase in the VFA concentration, even though the feed volume was increased incrementally. Further investigation showed that the gas seals had worn and needed replacing. The reactor was reseeded with waste sludge and the feed volume increased from initially a 20-day retention time until finally an 8-day retention time.

Table B.45: Results summary for steady state number 14

Feed total COD (mg/L)	13270
Feed soluble COD (mg/L)	1525
Feed TKN (mgN/L)	328
Feed FSA (mgN/L)	73
Feed Total P (mgP/L)	76
Feed soluble P (mgP/L)	17
Steady state measured after 19 days (2.375 x R_h)	
Effluent total COD (mg/L)	6299 ± 86 (13)
Effluent soluble COD (mg/L)	104 ± 4 (12)
Suspended solids (mgCOD/L)	1697
Effluent VFA (mg/L as HAc)	7 ± 6 (14)
Effluent Alkalinity (mg/L as CaCO₃)	863 ± 7 (14)
Reactor pH	6.78 ± 0.01 (21)
Gas Produced (units/day)	[104 ± 2 (20)] twice = 208
Volume per unit (ml)	48.8 ± 0.5
Gas composition (%CH₄)	*63.06
Methane production (L/day)	6.40
Methane production (gCOD/day)	17.4
Effluent TKN (mgN/L)	143 ± 28 (13)
Effluent FSA (mgN/L)	112 ± 3 (13)
Effluent Total P (mgP/L)	63 ± 3 (14)
Effluent soluble P (mgP/L)	12 ± 0 (13)
COD balance (%)	98.8
TKN balance (%)	43.7
Total P balance (%)	83.3

*Average of 12 measurements made

Appendix B: Steady State Data

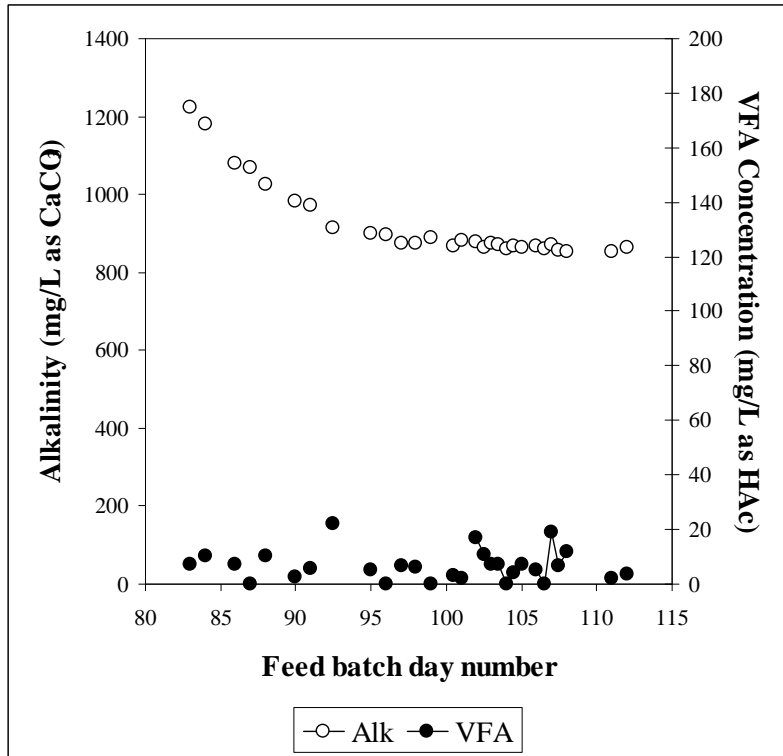


Figure B.28: Daily measurements of the VFA and alkalinity leading up to and including steady state number 14 (steady state from day 102)

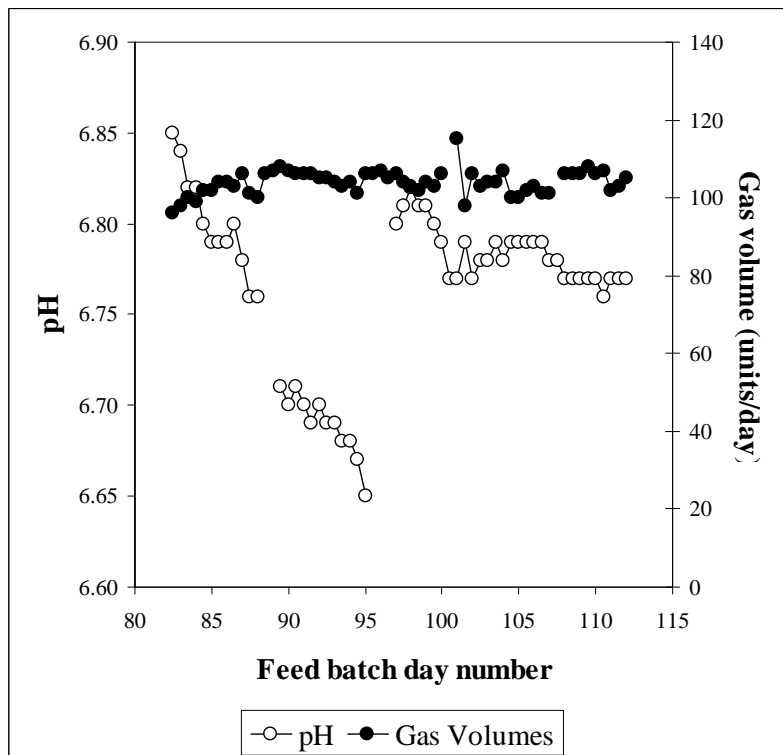


Figure B.29: Daily measurements of the pH and volumetric gas production leading up to and including steady state number 14 (steady state from day 102)

Appendix B: Steady State Data

Table B.46: Daily measured data for steady state number 14

Date	Day	Total COD (mgCOD/L)	Soluble COD (mgCOD/L)	Suspended Solids (mgCOD/L)	VFA (mg/L as HAc)	Alkalinity (mg/L as CaCO ₃)	pH	Gas Volume (Units/day)	TKN (mgN/L)	NH ₃ (mgN/L)	TP (mgP/L)	PO ₄ (mgP/L)
22-Sep	102	6251	108	1721	17.1	878.2	6.77	106	204	128	58	12
22-Sep	102.5	6238	106		10.8	862.8	6.78	103	140	112	63	12
23-Sep	103	6299	99	2197	7.2	874.9	6.78	104	143	118	65	3
23-Sep	103.5	6325	109		7.1	872.4	6.79	104	143	116	63	12
24-Sep	104	6406	103		0.0	859.1	6.78	107	195	116	63	12
24-Sep	104.5	6511	98		4.0	867.9	6.79	100	133	113	58	12
25-Sep	105	6299	104	1575	7.2	862.7	6.79	100	251	112	65	5
25-Sep	105.5	6402					6.79	102	202		63	12
26-Sep	106	6349	107	1816	5.2	867.9	6.79	103	136	108	63	11
26-Sep	106.5	6501	102	2038	0.0	859.3	6.79	101	150	112	65	12
27-Sep	107	6295	102	1621	18.9	869.3	6.78	101	175	111	65	11
27-Sep	107.5	6418	97	2270	6.6	855.5	6.78		140	111	70	11
28-Sep	108	6201	108	1652	11.7	853.6	6.77	106	206	111	65	11
28-Sep	108.5						6.77	106				
29-Sep	109			2164			6.77	106				
29-Sep	109.5			1743			6.77	108				
30-Sep	110			1801			6.77	106				
30-Sep	110.5						6.76	107				
01-Oct	111	6209	115	1806	2.0	853.9	6.77	102	141	109	63	11
01-Oct	111.5						6.77	103				
02-Oct	112				3.7	862.8	6.77	105	242	110	58	12
02-Oct	112.5								204	128	58	12
Mean		6299	104	1801	7	863	6.78	104	143	112	63	12
S.D.		86	4	202	6	7	0.01	2	28	3	3	0
Data points		13	12	11	14	13	21	20	13	13	14	13

Steady state No 15**Table B.47:** Operating conditions for steady state number 15

Feed batch number	F13
Mass of PSS in feed (g)	300
Total Mass of feed (g)	1000
Reactor Volume (L)	16
Retention time (day)	8
Sulfate addition (gSO₄/L)	9.6
pH	Controlled to ~ 6.8
Biological groups present	acidogens and sulfidogens

This experiment followed steady state number 6. The feed sulfate concentration was increased, the feed PSS was changed from F12 to F13, and ferrous chloride was added to precipitate aqueous sulfide as FeS.

Table B.48: Results summary for steady state number 15

Feed total COD (mg/L)	13270
Feed soluble COD (mg/L)	1503
Feed TKN (mgN/L)	328
Feed FSA (mgN/L)	72
Feed Total P (mgP/L)	76
Feed soluble P (mgP/L)	18
Steady state measured after 35 days (4.375 x R_h)	
Effluent total COD (mg/L)	13001 ± 457 (12)
Effluent soluble COD (mg/L)	197 ± 19 (11)
Effluent VFA (mg/L as HAc)	6 ± 6 (10)
Effluent Alkalinity (mg/L as CaCO₃)	2894 ± 54 (11)
Effluent Sulfate Concentration (mgSO₄/L)	733 ± 35 (7)
Reactor pH	6.87
Gas Produced (units/day)	[37 ± 2 (16)] twice = 74
Volume per unit (ml)	47.3 ± 0.4
Gas composition (%CH₄)	0.53
Methane production (L/day)	0.02
Methane production (gCOD/day)	0.05
Effluent TKN (mgN/L)	270 ± 24 (11)
Effluent FSA (mgN/L)	69 ± 5 (9)
Effluent Total P (mgP/L)	56 ± 12 (10)
Effluent soluble P (mgP/L)	9 ± 2 (11)
COD balance (%)	98.2
TKN balance (%)	82.4
Total P balance (%)	74.1

*Average for 6 measurements made

Appendix B: Steady State Data

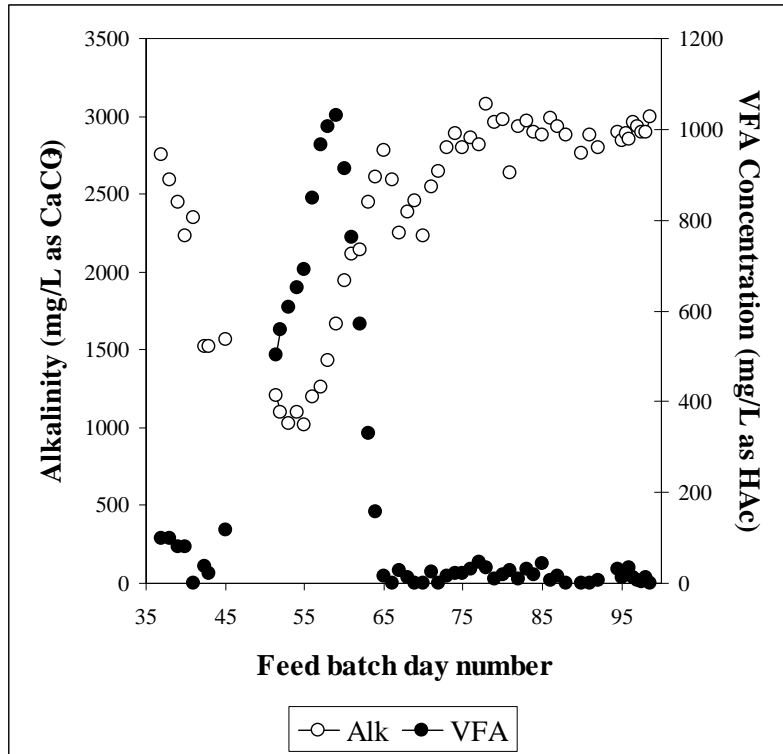


Figure B.30: Daily measurements of the VFA and alkalinity leading up to and including steady state number 15 (steady state from day 90)

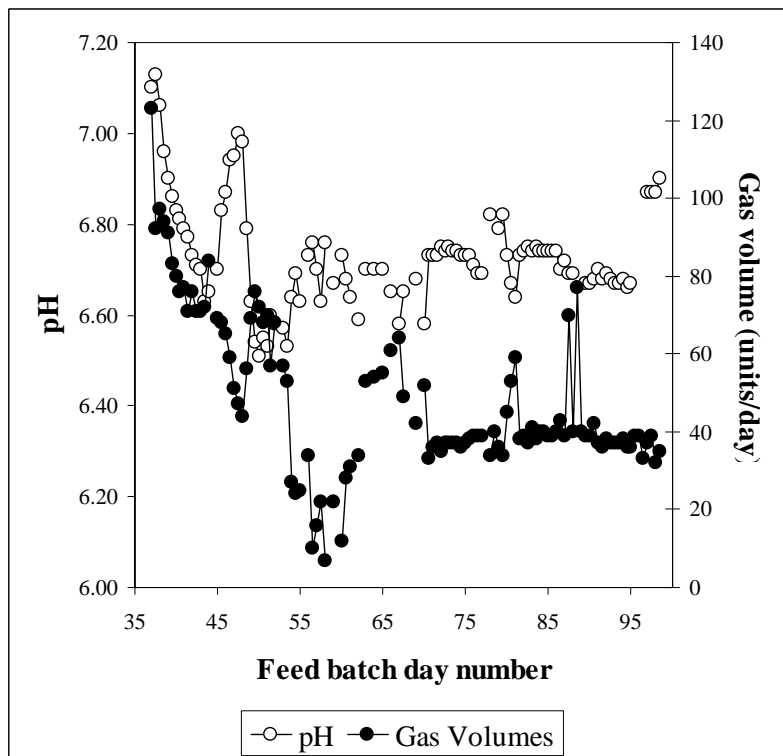


Figure B.31: Daily measurements of the pH and volumetric gas production leading up to and including steady state number 15 (steady state from day 90)

Appendix B: Steady State Data

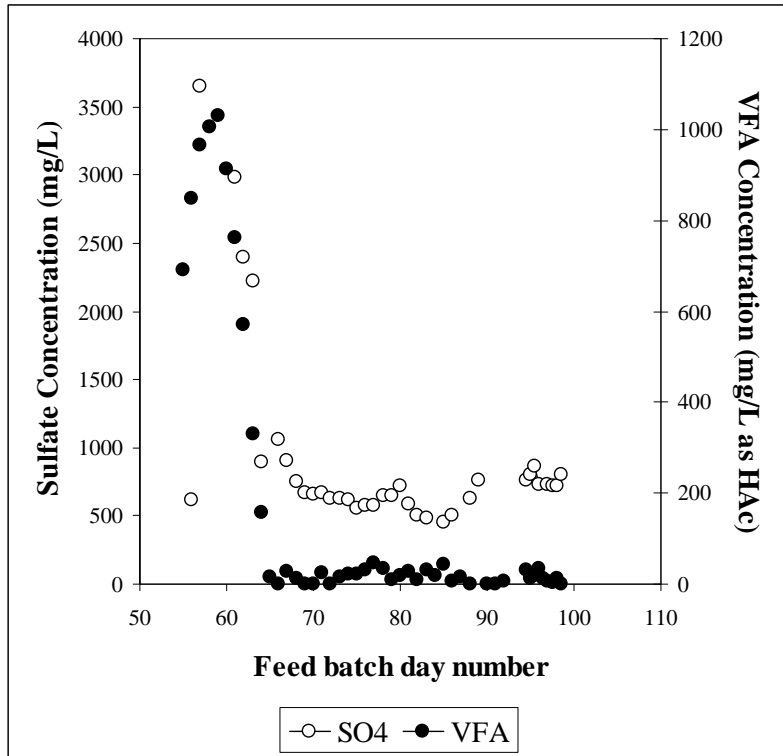


Figure B.32: Daily measurements of the VFA and sulfate concentration leading up to and including steady state number 15 (steady state from day 90)

Appendix B: Steady State Data

Table B.49: Daily measured data for steady state number 15

Date	Day	Total COD (mgCOD/L)	Soluble Organic COD (mgCOD/L)	Sulfate (mgSO ₄ /L)	VFA (mg/L as HAC)	Alkalinity (mg/L as CaCO ₃)	pH	Gas Volume (Units/day)	TKN (mgN/L)	NH ₃ (mgN/L)	TP (mgP/L)	PO ₄ (mgP/L)
10-Sep	90	13635	245		1.2	2760.5	6.67	39	287		104	
10-Sep	90.5						6.68	42				
11-Sep	91	13359	192		0	2878.3	6.70	37	270	32	75	12
11-Sep	91.5						6.68	36				
12-Sep	92	13550	201		6.3	2794.3	6.69	38	280	32	88	11
12-Sep	92.5						6.68	37				
13-Sep	93						6.67	37				
13-Sep	93.5						6.67	37				
14-Sep	94						6.68	38				
14-Sep	94.5	12668	197	760	31.4	2901.6	6.66	36	238	61	56	12
15-Sep	95	13137	210	801	12.3	2841.4	6.67	36		64		9
15-Sep	95.5	13633	233	862	20	2892		39	245	81	56	9
16-Sep	96	13604	202	733	34.5	2855.4		39	263	63	63	9
16-Sep	96.5	12864	169		11.6	2962.6		33	315	70	56	7
17-Sep	97	12638	167	726	6.1	2933.4	6.87	37	273	69	79	7
17-Sep	97.5	12498	190	718	3.6	2895	6.87	39	270	70	53	9
18-Sep	98	12620	179	716	11.3	2893.8	6.87	32	249	69	53	6
18-Sep	98.5	12483	221	801	0	2999	6.90	35	228	69	56	6
	Mean	13001	197	733	6	2894	6.87	37	270	69	56	9
	S.D.	457	19	35	6	54	0	2	24	5	12	2
	Data points	12	11	7	10	11	3	16	11	9	10	11

Steady state No 16**Table B.50:** Operating conditions for steady state number 16

Feed batch number	F13
Mass of PSS in feed (g)	300
Total Mass of feed (g)	1000
Reactor Volume (L)	16
Retention time (day)	8
Sulfate addition (gSO₄/L)	9.6
pH	Controlled to ~ 6.8
Biological groups present	acidogens and sulfidogens

After steady state 15 was analysed, the ferrous chloride addition was stopped. As soon as the residual ferrous in the system was precipitated, sulfide gas was smelled. The system was operated for 20 days with intermittent analyses performed. No steady state operation was observed.

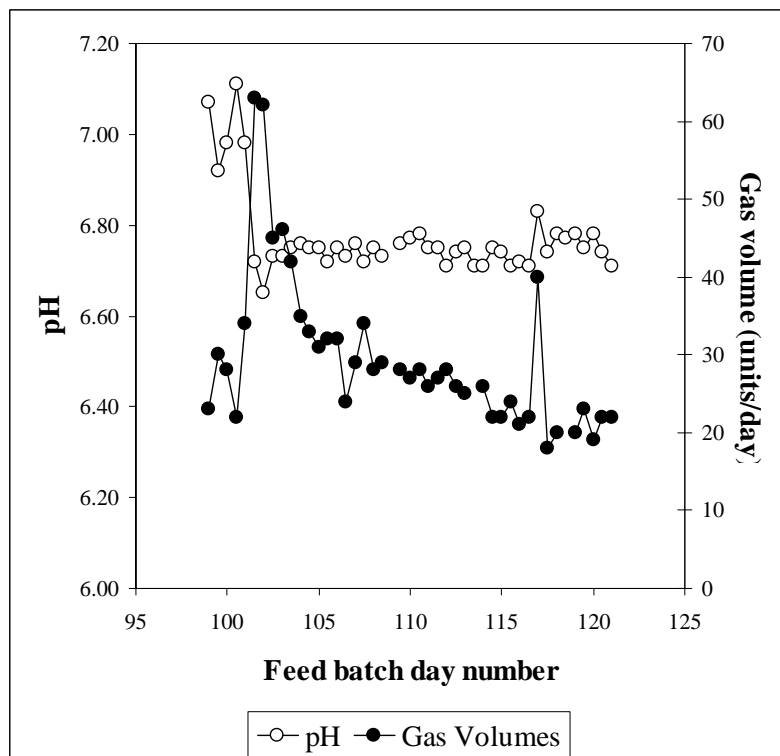


Figure B.33: Daily measurements of the pH and volumetric gas production for steady state number 16

Appendix B: Steady State Data

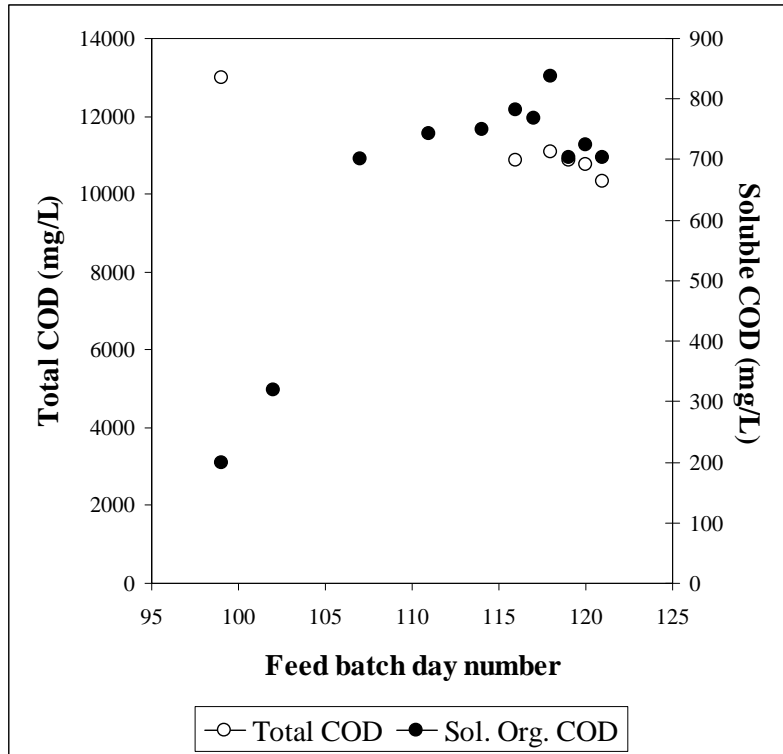


Figure B.34: Daily measurements of total COD and soluble organic COD for steady state number 16

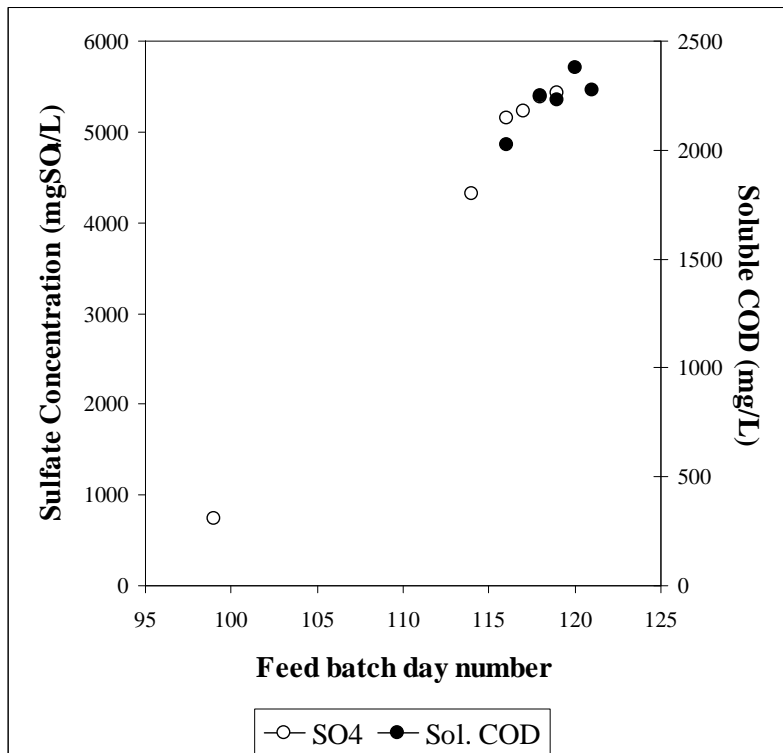


Figure B.35: Daily measurements of total soluble COD (including sulfide) and sulfate concentration for steady state number 16

Appendix B: Steady State Data

Table B.51: Daily measured data for steady state number 16

Date	Day	Total COD (mgCOD/L)	Soluble Organic COD (mgCOD/L)	Total Soluble COD (mgCOD/L)	Suspended Solids (mgCOD/L)	Suspended Solids Soluble COD (mgCOD/L)	Sulfate (mgSO ₄ /L)	pH	Gas Volume (Units/day)
04-Oct	114		750				4319	6.71	26
04-Oct	114.5							6.75	22
05-Oct	115							6.74	22
05-Oct	115.5							6.71	24
06-Oct	116	10879	782	2023			5150	6.72	21
06-Oct	116.5							6.71	22
07-Oct	117		769				5235	6.83	40
07-Oct	117.5							6.74	18
08-Oct	118	11082	837	2250	5514	2034	5390	6.78	20
08-Oct	118.5							6.77	
09-Oct	119	10870	704	2230	5481	1829	5435	6.78	20
09-Oct	119.5							6.75	23
10-Oct	120	10744	724	2378	5515	1995		6.78	19
10-Oct	120.5							6.74	22
11-Oct	121	10324	704	2276	5763	1839		6.71	22

Steady state No 17**Table B.52:** Operating conditions for steady state number 17

Feed batch number	F12
Mass of PSS in feed (g)	189
Total Mass of feed (g)	1000
Reactor Volume (L)	20
Retention time (day)	60
Sulfate addition (gSO₄/L)	0
pH	steady state
Biological groups present	acidogens and methanogens

The system was seeded with waste digester sludge consisting mostly of waste from systems fed with PSS at 25 and 40gCOD/L. The system was initially fed a third of the feed every day, but after 72 days, this was changed to the above volumes every third day.

Table B.53: Results summary for steady state number 17

Feed total COD (mg/L)	9810
Feed soluble COD (mg/L)	1204
Feed TKN (mgN/L)	182
Feed FSA (mgN/L)	15
Feed Total P (mgP/L)	47
Feed soluble P (mgP/L)	6
Steady state measured after 180 days (3 x R_h)	
Effluent total COD (mg/L)	3590 ± 119 (11)
Effluent soluble COD (mg/L)	88 ± 7 (12)
Suspended solids (mgCOD/L)	1648
Effluent VFA (mg/L as HAc)	5 ± 2 (12)
Effluent Alkalinity (mg/L as CaCO₃)	775 ± 13 (11)
Reactor pH	6.74 ± 0.03 (10)
Gas Produced (units/day)	[79 ± 1 (11)]/3 days = 26.3
Volume per unit (ml)	44.5 ± 0.5
Gas composition (%CH₄)	66.51
Methane production (L/day)	0.78
Methane production (gCOD/day)	2.1
Effluent TKN (mgN/L)	189 ± 29 (10)
Effluent FSA (mgN/L)	101 ± 14 (11)
Effluent Total P (mgP/L)	46 ± 7 (10)
Effluent soluble P (mgP/L)	10 ± 3 (11)
COD balance (%)	100.0
TKN balance (%)	103.8
Total P balance (%)	97.0

* Average of 9 measurements made

Appendix B: Steady State Data

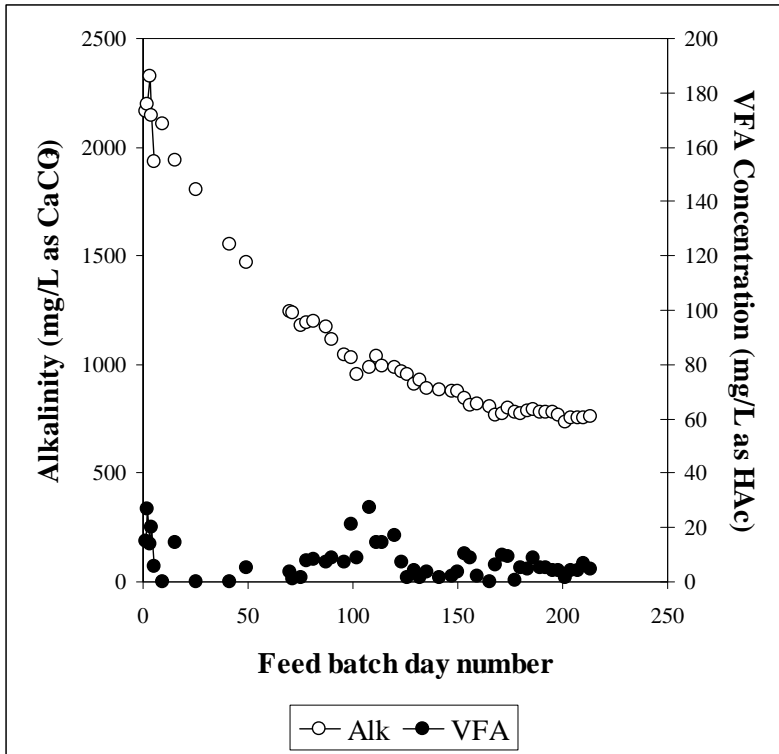


Figure B.36: Daily measurements of the VFA and alkalinity leading up to and including steady state number 17 (steady state from day 180)

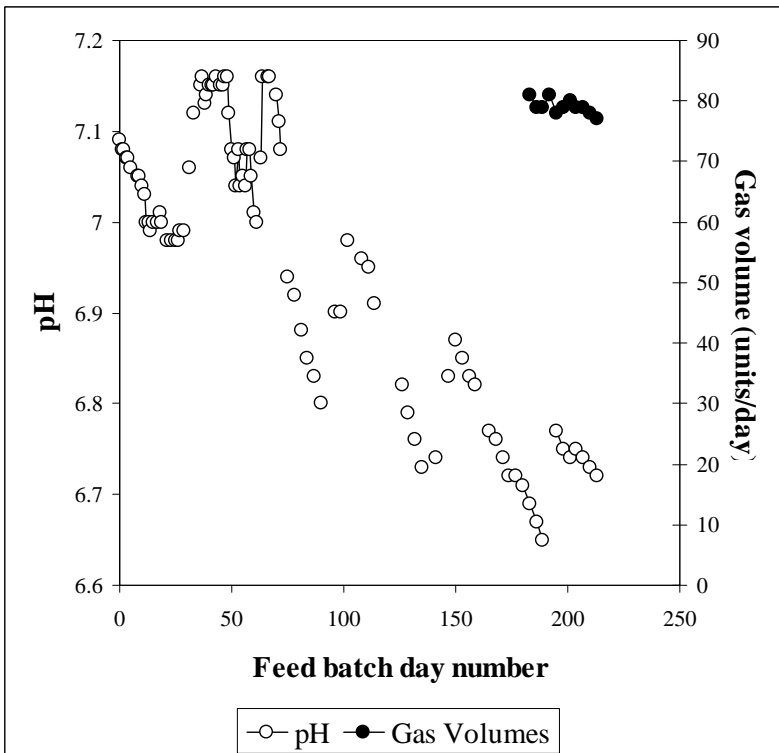


Figure B.37: Daily measurements of the pH and volumetric gas production leading up to and including steady state number 17 (steady state from day 180)

Appendix B: Steady State Data

Table B.54: Daily measured data for steady state number 17

Date	Day	Total COD (mgCOD/L)	Soluble COD (mgCOD/L)	Suspended Solids (mgCOD/L)	VFA (mg/L as HAc)	Alkalinity (mg/L as CaCO ₃)	pH	Gas Volume (Units/day)	TKN (mgN/L)	NH ₃ (mgN/L)	TP (mgP/L)	PO ₄ (mgP/L)
04-Sep	180	3453	85		5	774.7	6.71		186	64	74	13
07-Sep	183	3534	81		4.5	784.1	6.69	81	195	81	77	15
10-Sep	186	3663	97		8.6	789.9	6.67	79	195	79	68	13
13-Sep	189	2206	102		4.9	780.2	6.65	79	99	90	38	1
16-Sep	192	3952	92		5.1	779.8		81	190	161	46	10
19-Sep	195	3590	95		4.1	782.6	6.77	78	112	101	48	11
22-Sep	198	3589	82		4.1	769.2	6.75	79	115	109	42	12
25-Sep	201	3578	83		1.8	737.2	6.74	80	189	103	46	5
28-Sep	204	3608	86	1758	4	750.7	6.75	79	118	109	46	10
01-Oct	207	3564	77	1642	4.3	754.2	6.74	79	188	103	46	10
04-Oct	210	3655	96	1714	6.8	753.4	6.73	78	190	105	46	10
07-Oct	213	3618	89	1783	4.6	759.3	6.72	77	183	92	48	6
Mean		3590	88	1736	5	775	6.74	79	189	101	46	10
S.D.		119	7	53	2	13	0.03	1	29	14	7	3
Data points		11	12	4	12	11	10	11	10	11	10	11

Steady state No 18**Table B.55:** Operating conditions for steady state number 18

Feed batch number	F14
Mass of PSS in feed (g)	56
Total Mass of feed (g)	1000
Reactor Volume (L)	16
Retention time (day)	8
Sulfate addition (gSO₄/L)	0
pH	controlled to ~ 7.5
Biological groups present	acidogens and methanogens

The digester was seeded with diluted waste digester sludge since the feed concentration for this experiment was 2gCOD/L. The pH control was started after 4 feed cycles, and stepped to the final pH over 6 days. The pH was set to 7.5, with 1M NaOH additions only.

Table B.56: Results summary for steady state number 18

Feed total COD (mg/L)	1950
Feed soluble COD (mg/L)	280
Feed TKN (mgN/L)	43
Feed FSA (mgN/L)	7
Feed Total P (mgP/L)	10
Feed soluble P (mgP/L)	3
Steady state measured after 30 days (3.75 x R_H)	
Effluent total COD (mg/L)	827 ± 29 (12)
Effluent soluble COD (mg/L)	43 ± 6 (12)
Suspended solids (mgCOD/L)	276
Effluent VFA (mg/L as HAc)	0 ± 0 (11)
Effluent Alkalinity (mg/L as CaCO₃)	571 ± 13 (13)
Reactor pH	7.48 ± 0.02 (12)
Gas Produced (units/day)	[10 ± 1 (13)] twice = 20
Volume per unit (ml)	49.7 ± 0.4
Gas composition (%CH₄)	*84.69
Methane production (L/day)	0.84
Methane production (gCOD/day)	2.2
Effluent TKN (mgN/L)	17 ± 1 (11)
Effluent FSA (mgN/L)	18 ± 2 (13)
Effluent Total P (mgP/L)	12 ± 1 (12)
Effluent soluble P (mgP/L)	5 ± 1 (13)
COD balance (%)	99.9
TKN balance (%)	39.4
Total P balance (%)	124.6

* Average for 2 measurements made. The volume of gas produced per feed cycle was too small to be measured per cycle. Two gasbags were filled over the steady state period, and the results averaged.

Appendix B: Steady State Data

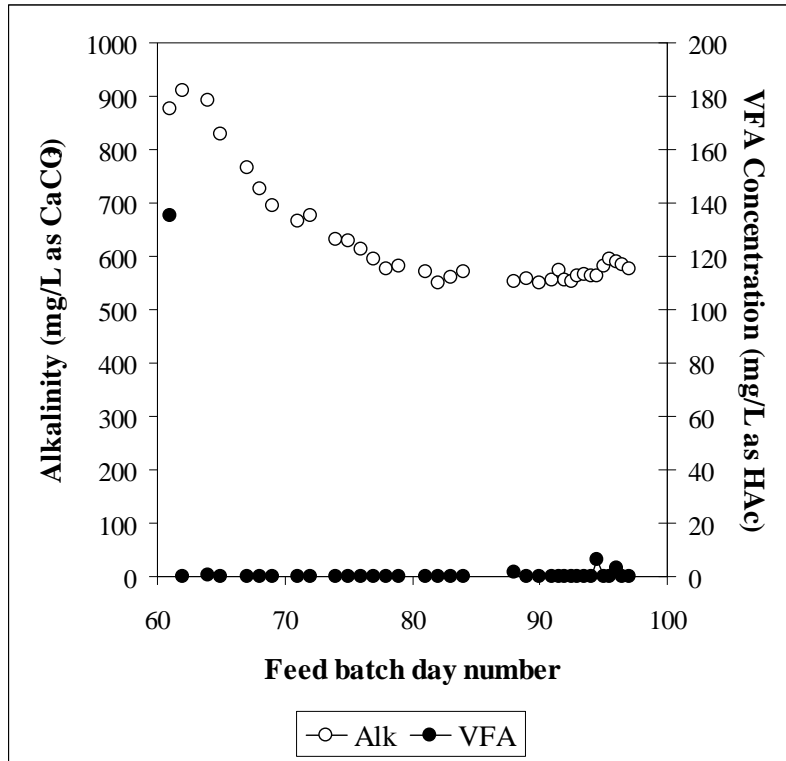


Figure B.38: Daily measurements of the VFA and alkalinity leading up to and including steady state number 18 (steady state from day 91)

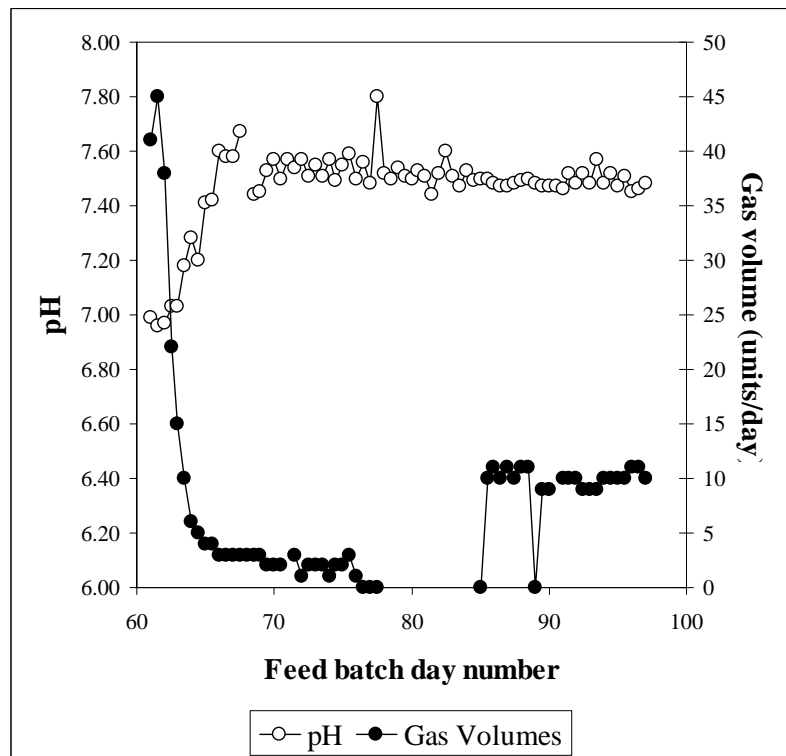


Figure B.39: Daily measurements of the pH and volumetric gas production leading up to and including steady state number 18 (steady state from day 91)

Appendix B: Steady State Data

Table B.57: Daily measured data for steady state number 18

Date	Day	Total COD (mgCOD/L)	Soluble COD (mgCOD/L)	Suspended Solids (mgCOD/L)	VFA (mg/L as HAc)	Alkalinity (mg/L as CaCO ₃)	pH	Gas Volume (Units/day)	TKN (mgN/L)	NH ₃ (mgN/L)	TP (mgP/L)	PO ₄ (mgP/L)
18-Dec	91	936	35	321	0	556.3	7.46	10	17	23	13	4
18-Dec	91.5	878	43	340	0	573.9	7.52	10	17	19	13	6
19-Dec	92	864	51	335	0	555.3	7.48	10	17	25	12	7
19-Dec	92.5	821	48	332	0	553.5	7.52	9	17	20	13	4
20-Dec	93	855	42	352	0	562.8	7.48	9	17	20	15	6
20-Dec	93.5	858	30	306	0	566.3	7.57	9	17	16	16	4
21-Dec	94	797	39	310	0	563.6	7.48	10	17	17	12	5
21-Dec	94.5	815	39	323	6.3	562.7	7.52	10	17	18	12	5
22-Dec	95	790	43	320	0	580.8	7.47	10	16	18	12	5
22-Dec	95.5	844	61	315	0	594.7	7.51	10	17	18	11	5
23-Dec	96	785	52	318	2.9	588.4	7.45	11	15	19	10	4
23-Dec	96.5	820	51	304	0	583.8	7.46	11	14	18	11	4
24-Dec	97	833	42	311	0	577.4	7.48	10	16	18	11	4
Mean		827	43	319	0	571	7.48	10	17	18	12	5
S.D.		29	6	11	0	13	0.02	1	1	2	1	1
Data points		12	12	12	11	13	12	13	11	12	12	13

Steady state No 19**Table B.58:** Operating conditions for steady state number 19

Feed batch number	F14
Mass of PSS in feed (g)	56
Total Mass of feed (g)	1000
Reactor Volume (L)	16
Retention time (day)	8
Sulfate addition (gSO₄/L)	0
pH	controlled to ~ 7.0
Biological groups present	acidogens and methanogens

This experiment followed directly from steady state number 18. The pH control was reset to a pH of 7.0, and the system pH allowed to drop to 7 over 3 days, when 1M NaOH addition resumed.

Table B.59: Results summary for steady state number 19

Feed total COD (mg/L)	1950
Feed soluble COD (mg/L)	293
Feed TKN (mgN/L)	43
Feed FSA (mgN/L)	8
Feed Total P (mgP/L)	10
Feed soluble P (mgP/L)	3
Steady state measured after 16 days (2 x R_h)	
Effluent total COD (mg/L)	815 ± 25 (12)
Effluent soluble COD (mg/L)	35 ± 7 (14)
Suspended solids (mgCOD/L)	269
Effluent VFA (mg/L as HAc)	0 ± 1 (14)
Effluent Alkalinity (mg/L as CaCO₃)	323 ± 21 (14)
Reactor pH	7.02 ± 0.02 (14)
Gas Produced (units/day)	[11 ± 1 (14)] twice = 22
Volume per unit (ml)	49.7 ± 0.4
Gas composition (%CH₄)	*72.2
Methane production (L/day)	0.78
Methane production (gCOD/day)	2.2
Effluent TKN (mgN/L)	20 ± 3 (13)
Effluent FSA (mgN/L)	23 ± 1 (13)
Effluent Total P (mgP/L)	9 ± 0 (13)
Effluent soluble P (mgP/L)	3 ± 0 (14)
COD balance (%)	95.8
TKN balance (%)	46.4
Total P balance (%)	93.4

* Single measurement made. Actual concentrations measured of 3.9% CH₄ and 1.5% CO₂, the majority being N₂, so not much confidence in this value

Appendix B: Steady State Data

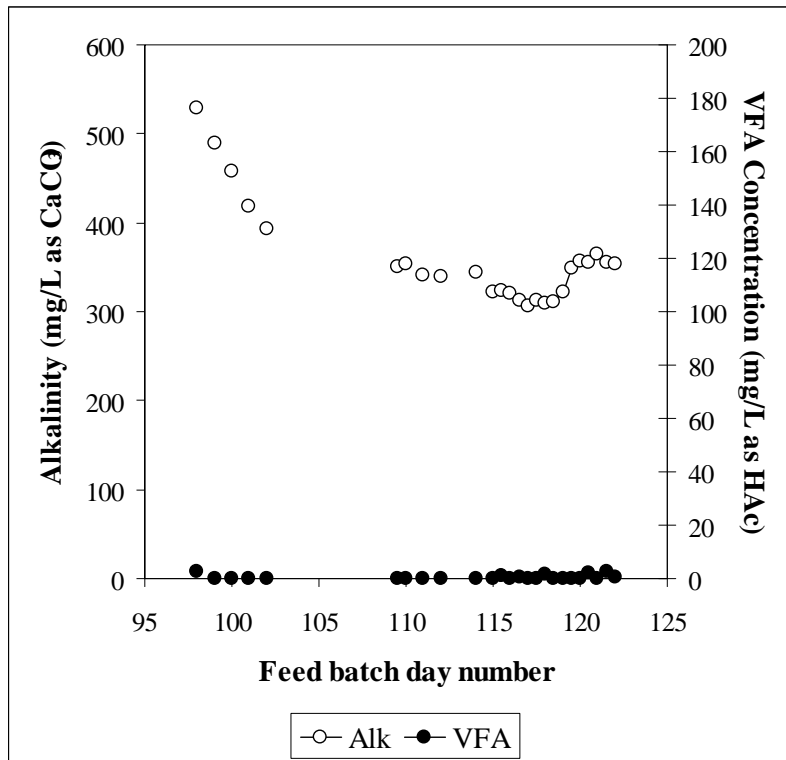


Figure B.40: Daily measurements of the VFA and alkalinity leading up to and including steady state number 19 (steady state from day 115.5)

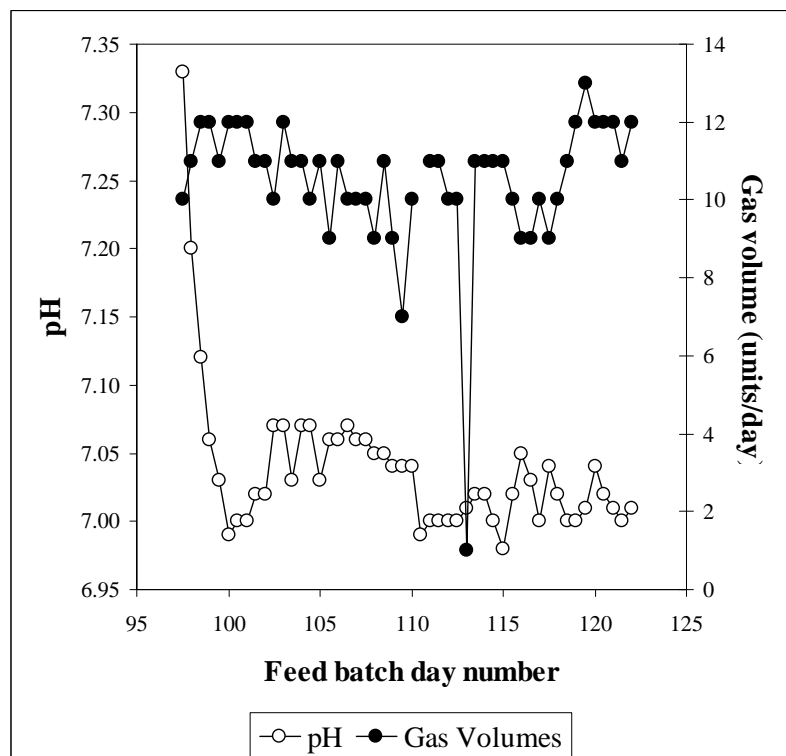


Figure B.41: Daily measurements of the pH and volumetric gas production leading up to and including steady state number 19 (steady state from day 115.5)

Appendix B: Steady State Data

Table B.60: Daily measured data for steady state number 19

Date	Day	Total COD (mgCOD/L)	Soluble COD (mgCOD/L)	Suspended Solids (mgCOD/L)	VFA (mg/L as HA _c)	Alkalinity (mg/L as CaCO ₃)	pH	Gas Volume (Units/day)	TKN (mgN/L)	NH ₃ (mgN/L)	TP (mgP/L)	PO ₄ (mgP/L)
11-Jan	115.5	829	41	276	1	324	7.02	10	18	24	49	3
12-Jan	116	845	33	276	0	320.3	7.05	9	16	22	10	3
12-Jan	116.5	926	35	280	0.6	312.5	7.03	9	34	24	9	4
13-Jan	117	921	30	281	0	306.5	7.00	10	21	23	9	4
13-Jan	117.5	892	37	265	0	312.1	7.04	9	21	22	10	4
14-Jan	118	916	28	278	1.4	310.1	7.02	10	26	26	10	3
14-Jan	118.5	814	26	316	0	310.3	7.00	11	24	25	9	4
15-Jan	119	818	32	307	0	322.6	7.00	12	17	22	9	3
15-Jan	119.5	809	21	302	0	349.5	7.01	13	19	22	9	3
16-Jan	120	815	48	336	0	357	7.04	12	19	23	10	3
16-Jan	120.5	818	34	312	2.1	355.6	7.02	12	22	23	10	3
17-Jan	121	803	38	312	0	364.2	7.01	12	20	23	10	3
17-Jan	121.5	794	36	323	2.5	354.7	7.00	11	20	22	9	3
18-Jan	122	813	45	305	0.7	353.1	7.01	12	20	22	9	3
Mean		815	35	304	0	323	7.02	11	20	23	9	3
S.D.		25	7	21	1	21	0.02	1	3	1	0	0
Data points		12	14	14	14	14	14	14	13	13	13	14

Steady state No 20**Table B.61:** Operating conditions for steady state number 20

Feed batch number	F14
Mass of PSS in feed (g)	56
Total Mass of feed (g)	1000
Reactor Volume (L)	16
Retention time (day)	8
Sulfate addition (gSO₄/L)	2
pH	controlled to ~ 7.5
Biological groups present	acidogens and sulfidogens

The digester was seeded from waste methanogenic sludge and operated for 10 days under methanogenic conditions. On day 42, sulfate was added at 2gSO₄/L. Methanogenesis failed completely (below detectable limits).

Table B.62: Results summary for steady state number 20

Feed total COD (mg/L)	1950
Feed soluble COD (mg/L)	292
Feed TKN (mgN/L)	43
Feed FSA (mgN/L)	8
Feed Total P (mgP/L)	10
Feed soluble P (mgP/L)	3
Steady state measured after 72 days (9 x R_n)	
Effluent total COD (mg/L)	1532 ± 58 (14)
Effluent soluble organic COD (mg/L)	61 ± 32 (13)
Effluent total soluble COD (mg/L)	790 ± 40 (14)
Suspended solids (mgCOD/L)	415 ± 43
Sulfate concentration (mgSO₄/L)	530 ± 26 (11)
Effluent VFA (mg/L as HAc)	0 ± 0 (14)
Effluent Alkalinity (mg/L as CaCO₃)	1386 ± 36 (13)
Reactor pH	7.52 ± 0.03 (14)
Gas Produced (units/day)	[3 ± 0 (14)] twice = 6
Volume per unit (ml)	47.3 ± 0.4
Gas composition (%CH₄)	*0
Methane production (L/day)	0
Methane production (gCOD/day)	0
Effluent TKN (mgN/L)	44 ± 1 (14)
Effluent FSA (mgN/L)	18 ± 1 (13)
Effluent Total P (mgP/L)	10 ± 1 (13)
Effluent soluble P (mgP/L)	4 ± 0 (14)
COD balance (%)	** Not possible
TKN balance (%)	102.0
Total P balance (%)	103.8

* Below detectable limits if present

** No gaseous sulfide measurement

Appendix B: Steady State Data

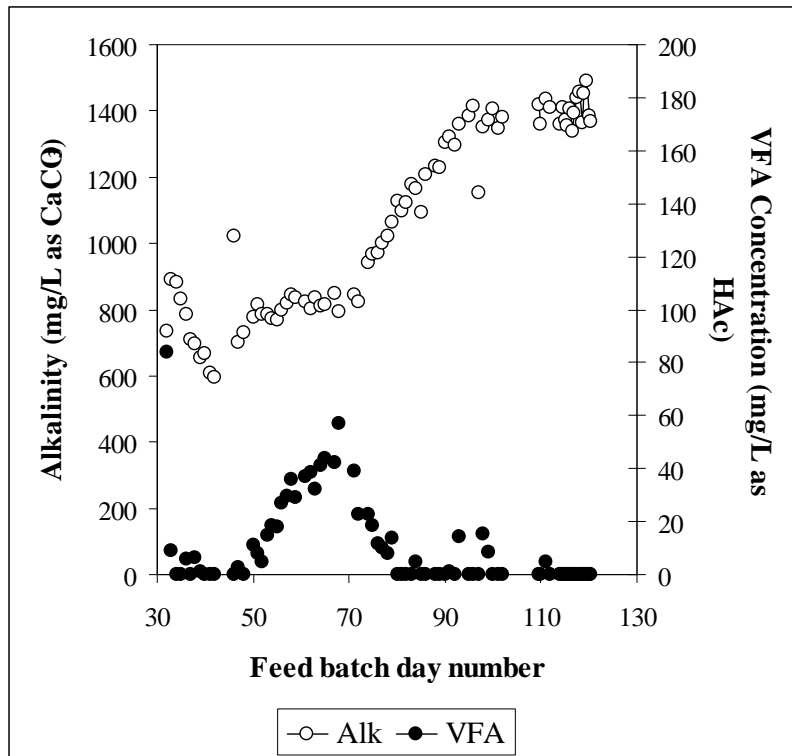


Figure B.42: Daily measurements of the VFA and alkalinity leading up to and including steady state number 20 (steady state from day 114)

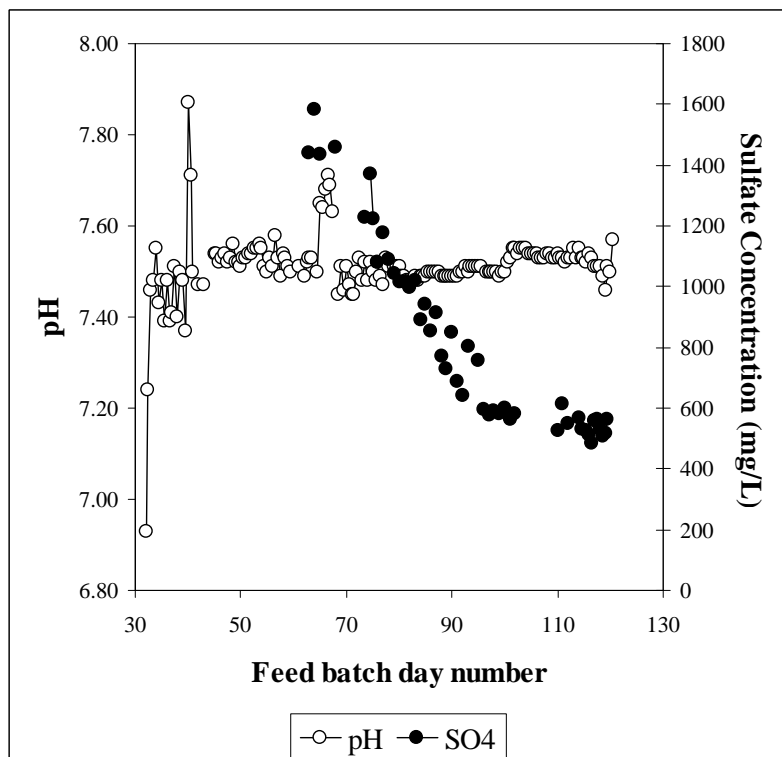


Figure B.43: Daily measurements of the pH and sulfate concentration leading up to and including steady state number 20 (steady state from day 114)

Appendix B: Steady State Data

Table B.63: Daily measured data for steady state number 20

Date	Day	Total COD (mgCOD/L)	Soluble Organic COD (mgCOD/L)	Total Soluble COD (mgCOD/L)	Suspended Solids (mgCOD/L)	Susp. Solids Soluble COD (mgCOD/L)	VFA (mg/L as HAc)	Alkalinity (mg/L as CaCO ₃)	pH	Sulfate (mgSO ₄ /L)	TKN (mgN/L)	NH ₃ (mgN/L)	TP (mgP/L)	PO ₄ (mgP/L)
10-Jan	114	1594	56	825		706	0	1358.7	7.55	568	44	19	10	4
10-Jan	114.5	1487	222	829	1182	746	0	1408.4	7.53	533	43	18	10	4
11-Jan	115	1448	134	844	1234	785	0	1371.1	7.53		43	19	10	4
11-Jan	115.5	1509	56	737	1138	795	0	1356.8	7.52	528	45	15	10	3
12-Jan	116	1520	150	722	1236	765	0	1405.4	7.54	513	44	19	10	4
12-Jan	116.5	1487	54	804	1207	761	0	1339.4	7.53	485	44	18	11	4
13-Jan	117	1476	58	746	1219	767	0	1392.2	7.51	560	44	17	11	4
13-Jan	117.5	1634	84	771	1128	703	0	1438.5	7.51	565	42	17	9	4
14-Jan	118	1615	64	803	1175	774	0	1455.8	7.51	530	31	17	10	4
14-Jan	118.5	1538	50	730	1175	743	0	1361.8	7.49	508	41	18	10	4
15-Jan	119	1540	51	826	1168	755	0	1450.8	7.46	515	43	18	9	5
15-Jan	119.5	1526	61	796	1180	749	0	1488.6	7.51	563	44	19	9	5
16-Jan	120	1616	104	740	1189	794	0	1386.2	7.50		44	17	10	4
16-Jan	120.5	1602	90	784	1136	809	0	1369.8	7.57		42	16	9	4
Mean		1532	61	790	1180	765	0	1386	7.52	530	44	18	10	4
S.D.		58	32	40	34	26	0	36	0.03	26	3	1	1	0
Data points		14	13	14	13	13	14	13	14	11	14	13	14	14

Steady state No 21**Table B.64:** Operating conditions for steady state number 21

Feed batch number	F14
Mass of PSS in feed (g)	1250
Total Mass of feed (g)	1250
Reactor Volume (L)	20
Retention time (day)	8
Sulfate addition (gSO₄/L)	0
pH	steady state
Biological groups present	acidogens and methanogens

This experiment followed from a 10-day retention time steady state after which the feed volume was increased, and then the feed changed from F13 to F14. There was no upset in the digester performance resulting from these changes.

Table B.65: Results summary for steady state number 21

Feed total COD (mg/L)	34818
Feed soluble COD (mg/L)	3828
Feed TKN (mgN/L)	770
Feed FSA (mgN/L)	44
Feed Total P (mgP/L)	172
Feed soluble P (mgP/L)	46
Steady state measured after 27 days (3.375 x R_h)	
Effluent total COD (mg/L)	15094 ± 493 (14)
Effluent soluble COD (mg/L)	205 ± 8 (13)
Suspended solids (mgCOD/L)	3426
Effluent VFA (mg/L as HAc)	22 ± 10 (14)
Effluent Alkalinity (mg/L as CaCO₃)	1868 ± 74 (14)
Reactor pH	6.90 ± 0.01 (14)
Gas Produced (units/day)	[359 ± 8 (12)] twice = 718
Volume per unit (ml)	45.9 ± 0.2
Gas composition (%CH₄)	*58.85
Methane production (L/day)	19.39
Methane production (gCOD/day)	51.6
Effluent TKN (mgN/L)	651 ± 14 (11)
Effluent FSA (mgN/L)	258 ± 10 (13)
Effluent Total P (mgP/L)	193 ± 6 (12)
Effluent soluble P (mgP/L)	22 ± 3 (11)
COD balance (%)	102.7
TKN balance (%)	84.5
Total P balance (%)	112.2

*Average of 12 measurements

Appendix B: Steady State Data

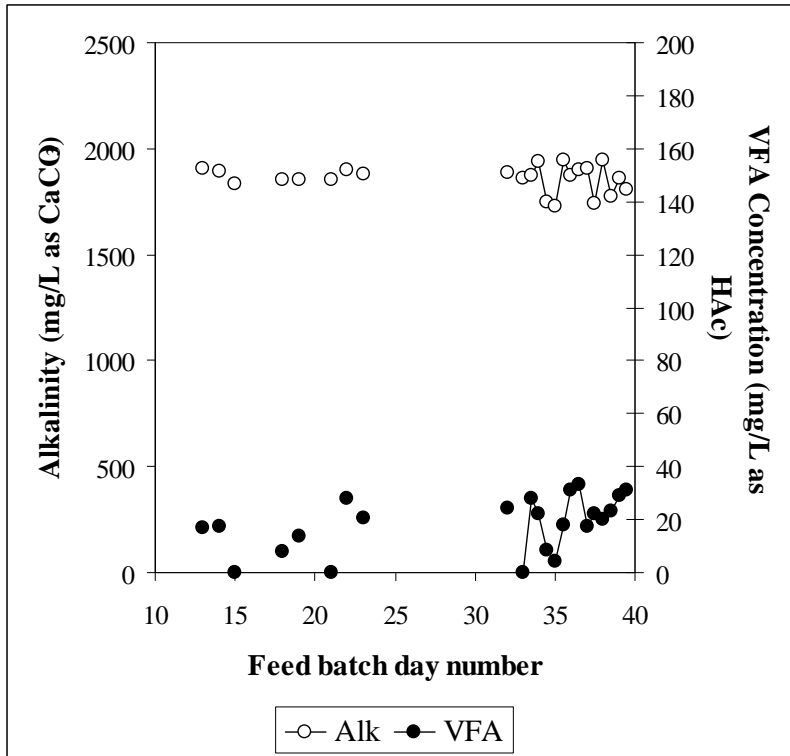


Figure B.44: Daily measurements of the VFA and alkalinity leading up to and including steady state number 21 (steady state from day 33)

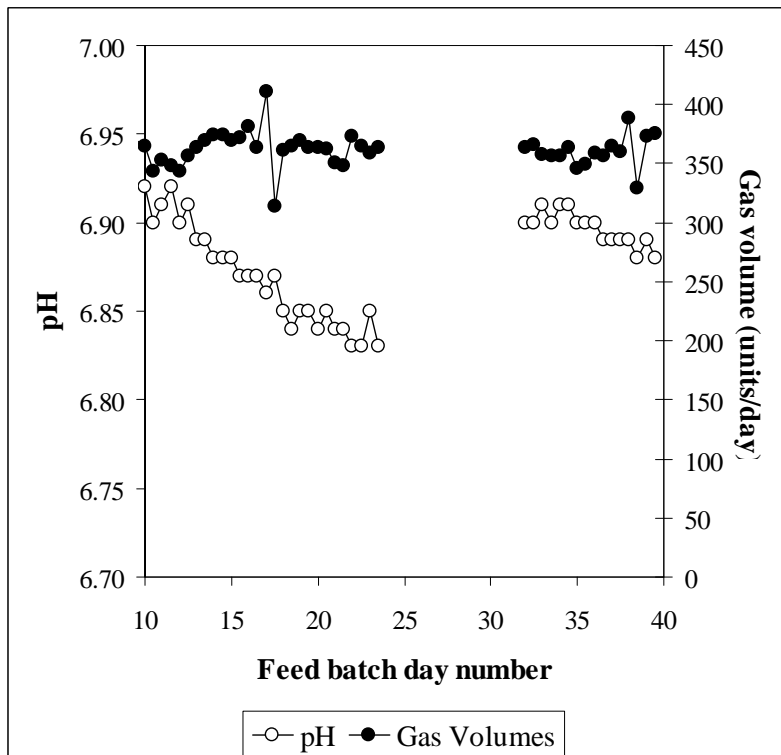


Figure B.45: Daily measurements of the pH and volumetric gas production leading up to and including steady state number 21 (steady state from day 33)

Appendix B: Steady State Data

Table B.66: Daily measured data for steady state number 21

Date	Day	Total COD (mgCOD/L)	Soluble COD (mgCOD/L)	Suspended Solids (mgCOD/L)	VFA (mg/L as HAc)	Alkalinity (mg/L as CaCO ₃)	pH	Gas Volume (Units/day)	TKN (mgN/L)	NH ₃ (mgN/L)	TP (mgP/L)	PO ₄ (mgP/L)
21-Oct	33	15579	216	3888	0.0	1862.9	6.91	358	399	266	189	28
21-Oct	33.5	15045	235	3898	27.8	1875.6	6.90	356	560	221	197	
22-Oct	34	14661	213		22.1	1938.3	6.91	356	553	273	193	22
22-Oct	34.5	15143	209	3970	8.3	1748.9	6.91	363	651	263	193	31
23-Oct	35	15175	210	3750	4.2	1730.4	6.90	346	637	273	197	22
23-Oct	35.5	15624	214	3631	18.2	1946.7	6.90	349	658	265	201	26
24-Oct	36	15606	208	3713	31.1	1873.6	6.90	359	634	262	164	22
24-Oct	36.5	15508	199	3491	33.0	1901.6	6.89	356	662	256	193	21
25-Oct	37	14719	198	3420	17.4	1905	6.89	365	630	258	184	31
25-Oct	37.5	15254	205		22.4	1738.4	6.89	360	655	257	180	21
26-Oct	38	14437	203	3571	19.8	1944.2	6.89	389	637	258	184	30
26-Oct	38.5	14256	189	2891	23.3	1776	6.88	329	651	255	193	22
27-Oct	39	14787	197	3552	28.9	1860.1	6.89	373	648	246	172	25
27-Oct	39.5	14639	199	3351	31.2	1807.7	6.88	375	679	237	197	20
	Mean	15094	205	3631	22	1868	6.9	359	651	258	193	22
	S.D.	493	8	195	8	74	0.01	8	14	10	6	3
	Data points	14	13	11	13	14	14	12	11	13	12	11

Steady state No 22**Table B.67:** Operating conditions for steady state number 22

Feed batch number	F14
Mass of PSS in feed (g)	56
Total Mass of feed (g)	1000
Reactor Volume (L)	16
Retention time (day)	8
Sulfate addition (gSO₄/L)	2
pH	controlled to ~ 7.0
Biological groups present	acidogens and sulfidogens

This experiment followed directly from steady state number 20. The pH was changed from 7.5 to 7.0 in two steps over two feed cycles by the addition of 1M HCl. Thereafter, the pH was controlled by addition of HCl only.

Table B.68: Results summary for steady state number 22

Feed total COD (mg/L)	1950
Feed soluble COD (mg/L)	298
Feed TKN (mgN/L)	43
Feed FSA (mgN/L)	10
Feed Total P (mgP/L)	10
Feed soluble P (mgP/L)	3
Steady state measured after 16 days (2 x R_n)	
Effluent total COD (mg/L)	1406 ± 17 (13)
Effluent soluble organic COD (mg/L)	155 ± 15 (13)
Effluent total soluble COD (mg/L)	655 ± 37 (13)
Suspended solids (mgCOD/L)	418 ± 49
Sulfate concentration (mgSO₄/L)	***770 ± 138 (13)
Effluent VFA (mg/L as HAc)	63 ± 8 (13)
Effluent Alkalinity (mg/L as CaCO₃)	782 ± 21 (13)
Reactor pH	6.99 ± 0.02 (14)
Gas Produced (units/day)	8 ± 0 (14)
Volume per unit (ml)	47.3 ± 0.4
Gas composition (%CH₄)	*0
Effluent TKN (mgN/L)	48 ± 1 (13)
Effluent FSA (mgN/L)	11 ± 1 (11)
Effluent Total P (mgP/L)	9 ± 1 (14)
Effluent soluble P (mgP/L)	5 ± 0 (12)
COD balance (%)	**Not possible
TKN balance (%)	111.3
Total P balance (%)	93.4

* Assume methanogenesis had not resumed in digester

** No gaseous sulfide measurement

*** Storage of samples questioned – may have increased

Appendix B: Steady State Data

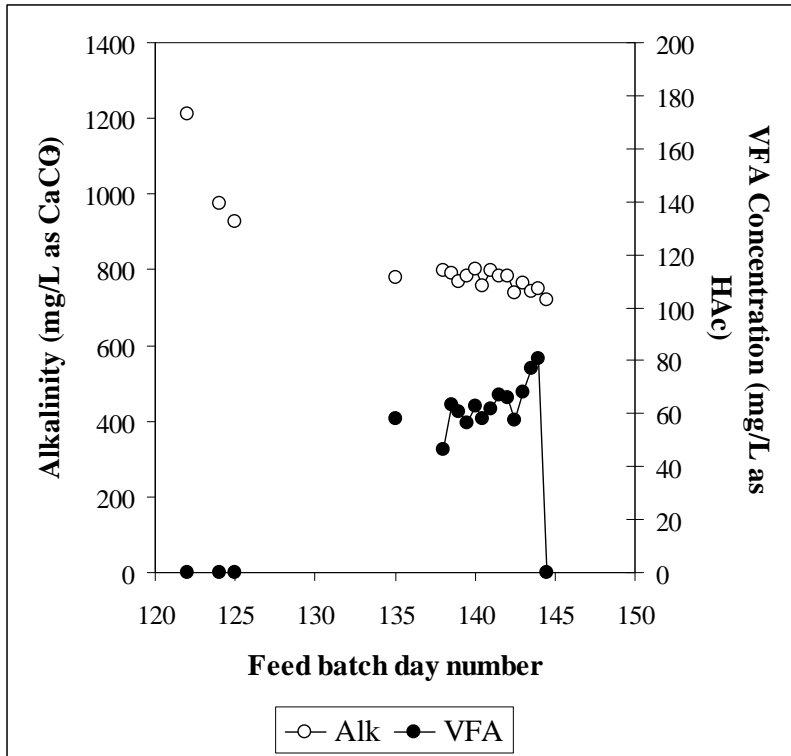


Figure B.46: Daily measurements of the VFA and alkalinity leading up to and including steady state number 22 (steady state from day 138)

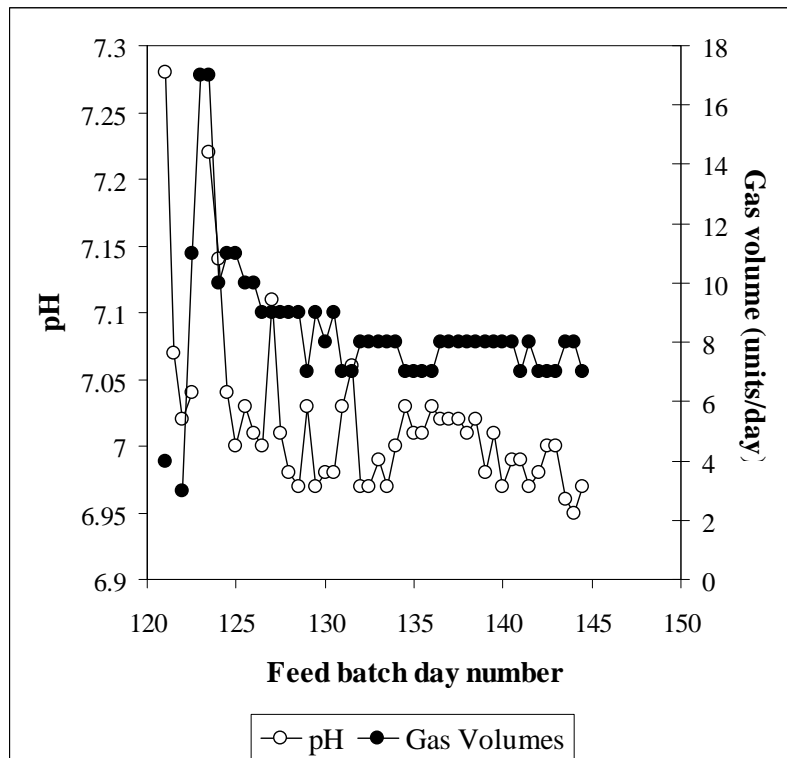


Figure B.47: Daily measurements of the pH and volumetric gas production leading up to and including steady state number 22 (steady state from day 138)

Appendix B: Steady State Data

Table B.69: Daily measured data for steady state number 22

Date	Day	Total COD (mg/L)	Soluble Organic COD (mg/L)	Total Soluble COD (mg/L)	Suspended Solids (mg/L)	Susp. Solids Soluble COD (mg/L)	VFA (mg/L as HAc)	Alkalinity (mg/L as CaCO ₃)	pH	Sulfate (mg/L)	TKN (mgN/L)	NH ₃ (mgN/L)	TP (mgP/L)	PO ₄ (mgP/L)
03-Feb	138	1427	155	766	1025	662	46.6	796.2	7.01	473	46	11	8	5
03-Feb	138.5	1400	132	642	956	600	63.3	790.9	7.02	460	49	14	9	5
04-Feb	139	1397	162	708	982	507	60.9	769	6.98	868	57	11	8	5
04-Feb	139.5	1416	150	741	1026	639	56.5	784.6	7.01	870	48	8	9	4
05-Feb	140	1446	148	679	1028	655	62.6	801.5	6.97	875	48	11	10	5
05-Feb	140.5	1448	156	678	1046	620	57.9	757.5	6.99	730	48	11	9	5
06-Feb	141	1474	139	709	996	641	62	798.1	6.99	785	47	12	8	4
06-Feb	141.5	1397	155	655	958	580	67.2	782.4	6.97	673	48	7	9	5
07-Feb	142	1397	124	639	1013	582	65.7	784.1	6.98	940	50	12	9	4
07-Feb	142.5	1403	145	618	960	536	57.7	740.3	7.00	850	48	12	8	4
08-Feb	143	1396	204	632	985	592	68.3	763.1	7.00	755	47	11	9	4
08-Feb	143.5	1413	187	629	1060	599	77.1	741.1	6.96	770	52	11	9	4
09-Feb	144	1407	158	695	1060	629	80.7	751.1	6.95	575	47		8	
09-Feb	144.5	1406	167	636	1022	575	0	720.2	6.97	545	49		9	
Mean		1406	155	655	1018	600	63	782	6.99	770	48	11	9	5
S.D.		17	15	37	35	35	8	21	0.02	138	1	1	1	0
Data points		13	13	13	14	13	13	13	14	13	13	11	14	12

Steady state No 23**Table B.70:** Operating conditions for steady state number 23

Feed batch number	F14
Mass of PSS in feed (g)	1500
Total Mass of feed (g)	1500
Reactor Volume (L)	20
Retention time (day)	6.67
Sulfate addition (gSO₄/L)	0
pH	steady state
Biological groups present	acidogens and methanogens

This experiment followed directly from steady state number 21. The feed volume was incremented by 50g per feed from 1250g to 1500g. Complete analysis of the digester was maintained over the entire period providing transient data (Transient state number 4, Appendix C).

Table B.71: Results summary for steady state number 23

Feed total COD (mg/L)	34818
Feed soluble COD (mg/L)	4354
Feed TKN (mgN/L)	770
Feed FSA (mgN/L)	70
Feed Total P (mgP/L)	172
Feed soluble P (mgP/L)	46
Steady state measured after 27 days (3.375 x R_h)	
Effluent total COD (mg/L)	14984 ± 431 (12)
Effluent soluble COD (mg/L)	207 ± 10 (13)
Suspended solids (mgCOD/L)	3407
Effluent VFA (mg/L as HAc)	12 ± 9 (13)
Effluent Alkalinity (mg/L as CaCO₃)	1821 ± 24 (13)
Reactor pH	6.83 ± 0.01 (14)
Gas Produced (units/day)	[417 ± 4 (13)] twice = 834
Volume per unit (ml)	45.9 ± 0.2
Gas composition (%CH₄)	*59.32
Methane production (L/day)	22.71
Methane production (gCOD/day)	60.4
Effluent TKN (mgN/L)	578 ± 65 (13)
Effluent FSA (mgN/L)	255 ± 4 (13)
Effluent Total P (mgP/L)	178 ± 3 (13)
Effluent soluble P (mgP/L)	27 ± 5 (13)
COD balance (%)	100.9
TKN balance (%)	75.1
Total P balance (%)	103.5

* Average for 2 measurements made

Appendix B: Steady State Data

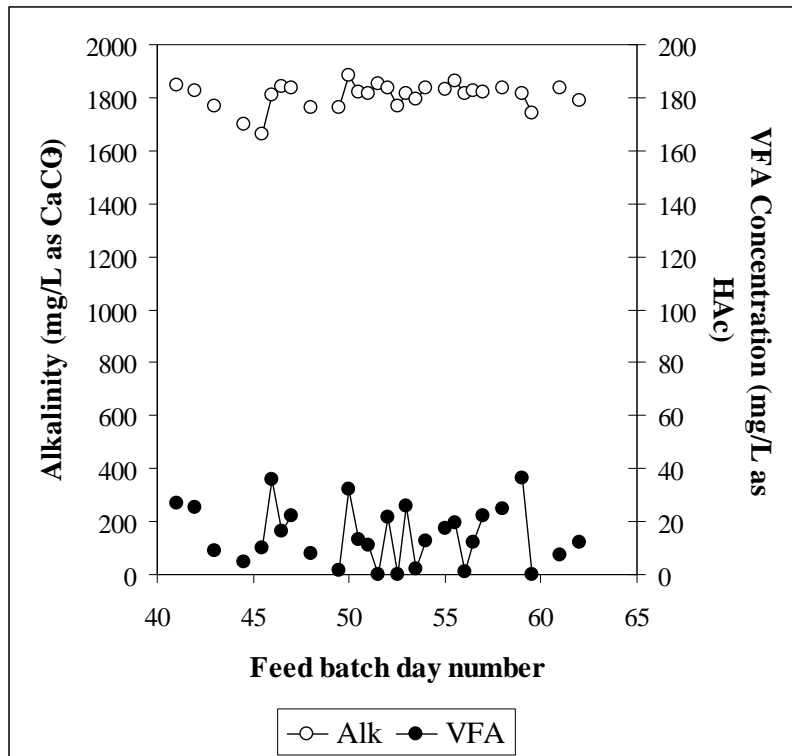


Figure B.48: Daily measurements of the VFA and alkalinity leading up to and including steady state number 23 (steady state from day 50.5)

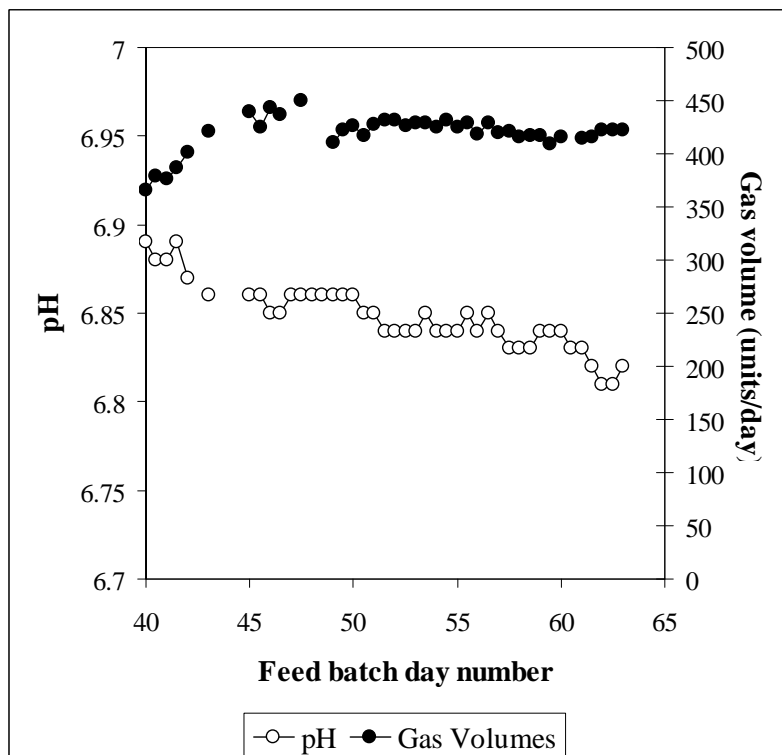


Figure B.49: Daily measurements of the pH and volumetric gas production leading up to and including steady state number 23 (steady state from day 50.5)

Appendix B: Steady State Data

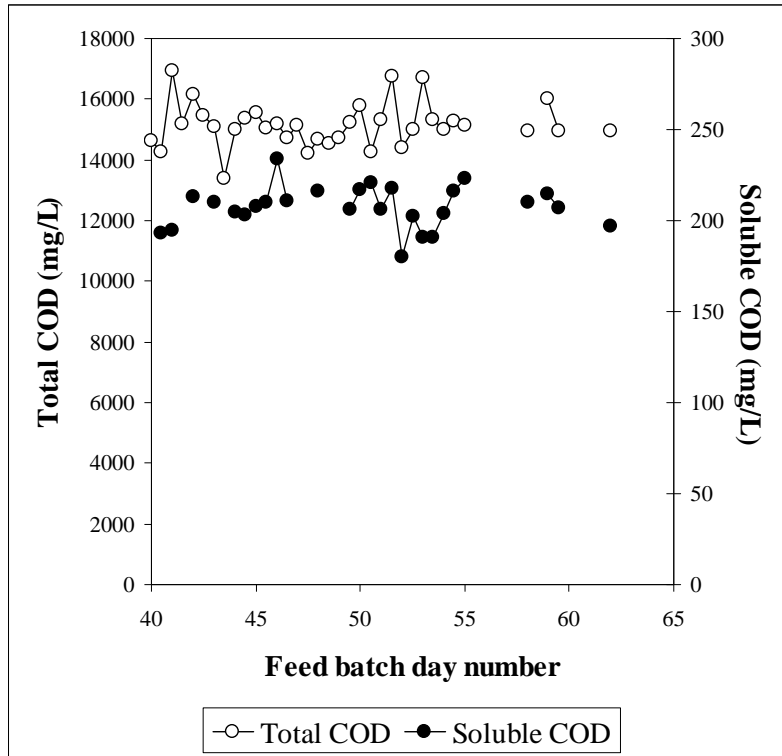


Figure B.50: Daily measurements of the total COD and soluble COD leading up to and including steady state number 23 (steady state from day 50.5)

Appendix B: Steady State Data

Table B.72: Daily measured data for steady state number 23

Date	Day	Total COD (mgCOD/L)	Soluble COD (mgCOD/L)	Suspended Solids (mgCOD/L)	VFA (mg/L as HAc)	Alkalinity (mg/L as CaCO ₃)	pH	Gas Volume (Units/day)	TKN (mgN/L)	NH ₃ (mgN/L)	TP (mgP/L)	PO ₄ (mgP/L)
28-Oct	40	14608					6.89	366	665		184	
28-Oct	40.5	14263	193				6.88	379	641	249	184	36
29-Oct	41	16937	195		27.0	1849.6	6.88	376	637	249	180	34
29-Oct	41.5	15191					6.89	387	644		184	
30-Oct	42	16163	213		25.3	1827.1	6.87	401	665	255	176	28
30-Oct	42.5	15459							655		176	
31-Oct	43	15085	210		8.9	1768.5	6.86	421	655	249	184	22
31-Oct	43.5	13396							616		172	
01-Nov	44	14984	205						648	256	197	30
01-Nov	44.5	15375	203		4.5	1700.9			665	248	172	34
02-Nov	45	15540	208				6.86	440	637	244	164	22
02-Nov	45.5	15057	210		10.1	1664.8	6.86	425	651	247	180	28
03-Nov	46	15180	234		35.8	1809.3	6.85	444	641	251	184	20
03-Nov	46.5	14705	211		16.3	1839.6	6.85	437	651	234	180	28
04-Nov	47	15142			21.9	1836	6.86		637		184	
04-Nov	47.5	14198					6.86	450	641		180	
05-Nov	48	14664	216		7.7	1762.7	6.86		658	242	180	19
05-Nov	48.5	14525					6.86		357			
06-Nov	49	14728					6.86	411	361		171	
06-Nov	49.5	15242	206		1.4	1764.1	6.86	423	438	250	174	29
07-Nov	50	15795	217		32.0	1882.2	6.86	426	490	258	174	22
07-Nov	50.5	14272	221		13.2	1822.6	6.85	417	375	245	159	21
08-Nov	51	15342	206		11.2	1814.3	6.85	428	525	252	174	21
08-Nov	51.5	16755	218		0.0	1853.2	6.84	432	585	237	174	32
09-Nov	52	14413	180		21.6	1837.4	6.84	431	396	248	171	27
09-Nov	52.5	14977	202		0.0	1768.2	6.84	426	399	255	171	24
10-Nov	53	16707	191	3618	25.7	1815.4	6.84	429	515	244	182	23
10-Nov	53.5	15345	191	4054	2.0	1792.3	6.85	429	431	255	178	27

Appendix B: Steady State Data

Date	Day	Total COD (mgCOD/L)	Soluble COD (mgCOD/L)	Suspended Solids (mgCOD/L)	VFA (mg/L as HAc)	Alkalinity (mg/L as CaCO ₃)	pH	Gas Volume (Units/day)	TKN (mgN/L)	NH ₃ (mgN/L)	TP (mgP/L)	PO ₄ (mgP/L)
11-Nov	54	14990	204		12.6	1839	6.84	425	494	256	174	29
11-Nov	54.5	15291	216	3591			6.84	431	515	253	174	33
12-Nov	55	15160	223	4285	17.4	1829.8	6.84	425	518	256	174	15
12-Nov	55.5				19.4	1864.2	6.85	429	560	260	178	30
13-Nov	56				1.1	1812.9	6.84	419	609	253	178	16
13-Nov	56.5				12.0	1826.7	6.85	429	602	248	155	28
14-Nov	57				22.0	1820.9	6.84	420	578	256	182	21
14-Nov	57.5						6.83	421				
15-Nov	58	14943	210	3567	25.0	1837.6	6.83	416	641	255	178	30
15-Nov	58.5						6.83	417				
16-Nov	59	16020	215	3464	36.2	1812.9	6.84	417	634	251	178	27
16-Nov	59.5	14943	207	3820	0.0	1738.8	6.84	409	641	253	182	18
17-Nov	60			3610								
17-Nov	60.5											
18-Nov	61				7.2	1837	6.83	414				
18-Nov	61.5											
19-Nov	62	14970	197	4033	12.1	1788.8	6.81	422	641	225	178	29
Mean		14984	207	3614	12	1821	6.83	417	578	255	178	27
S.D.		431	10	208	9	24	0.01	4	65	4	3	5
Data points		12	13	8	13	13	14	13	13	13	13	13

Steady state No 24**Table B.73:** Operating conditions for steady state number 24

Feed batch number	F14
Mass of PSS in feed (g)	585
Total Mass of feed (g)	1500
Reactor Volume (L)	20
Retention time (day)	6.67
Sulfate addition (gSO₄/L)	0
pH	steady state
Biological groups present	acidogens and methanogens

This experiment followed steady state number 14. The feed was changed from F13 to F14 at the same concentration and retention time. The volume was then incremented, but the digester became unstable. Without reseeded, the system was nursed back to the reported steady state.

Table B.74: Results summary for steady state number 24

Feed total COD (mg/L)	13579
Feed soluble COD (mg/L)	1845
Feed TKN (mgN/L)	300
Feed FSA (mgN/L)	37
Feed Total P (mgP/L)	67
Feed soluble P (mgP/L)	18
Steady state measured after 22 days (3.3 x R_h)	
Effluent total COD (mg/L)	5944 ± 140 (13)
Effluent soluble COD (mg/L)	96 ± 14 (10)
Suspended solids (mgCOD/L)	1329
Effluent VFA (mg/L as HAc)	5 ± 3 (11)
Effluent Alkalinity (mg/L as CaCO₃)	789 ± 11 (10)
Reactor pH	6.57 ± 0.01 (11)
Gas Produced (units/day)	[147 ± 3 (12)] twice = 294
Volume per unit (ml)	48.8 ± 0.5
Gas composition (%CH₄)	*60.95
Methane production (L/day)	8.74
Methane production (gCOD/day)	23.3
Effluent TKN (mgN/L)	246 ± 1 (12)
Effluent FSA (mgN/L)	104 ± 3 (12)
Effluent Total P (mgP/L)	72 ± 2 (12)
Effluent soluble P (mgP/L)	21 ± 1 (12)
COD balance (%)	100.9
TKN balance (%)	81.9
Total P balance (%)	107.3

*Average for 9 measurements made

Appendix B: Steady State Data

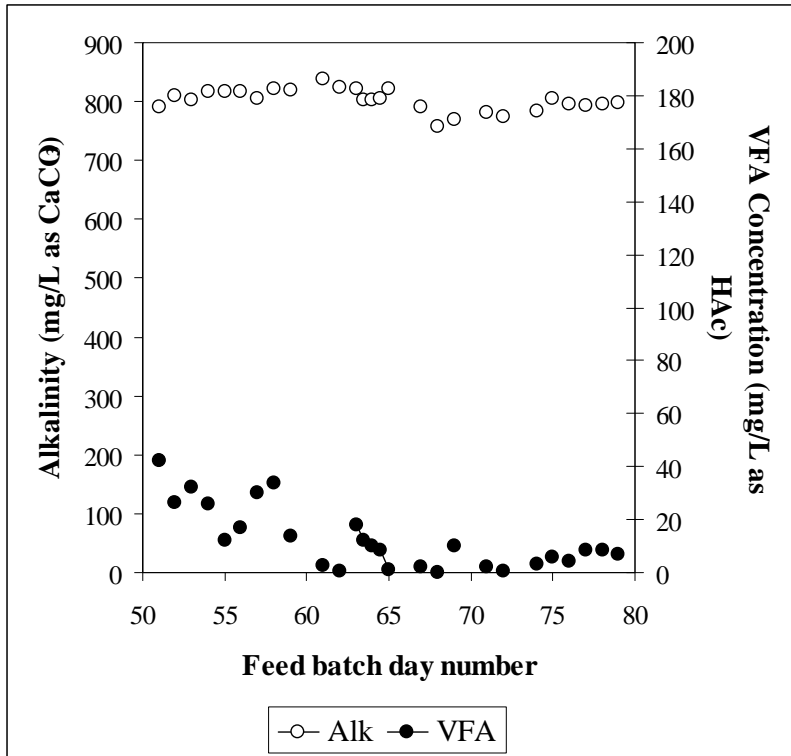


Figure B.51: Daily measurements of the VFA and alkalinity leading up to and including steady state number 24 (steady state from day 73)

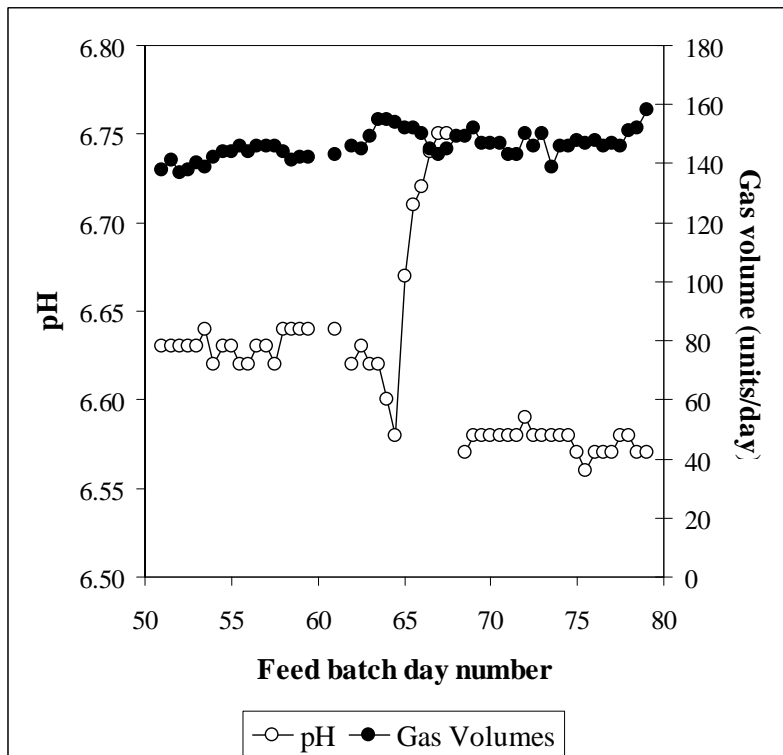


Figure B.52: Daily measurements of the pH and volumetric gas production leading up to and including steady state number 24 (steady state from day 73)

Appendix B: Steady State Data

Table B.75: Daily measured data for steady state number 24

Date	Day	Total COD (mgCOD/L)	Soluble COD (mgCOD/L)	Suspended Solids (mgCOD/L)	VFA (mg/L as HAc)	Alkalinity (mg/L as CaCO ₃)	pH	Gas Volume (Units/day)	TKN (mgN/L)	NH ₃ (mgN/L)	TP (mgP/L)	PO ₄ (mgP/L)
30-Nov	73	5982	111	1317			6.58	150	244	99	72	20
30-Nov	73.5	5990	113	1436			6.58	139	244	93	73	21
01-Dec	74	5953	112	1639	3.0	782.9	6.58	146	245	109	73	21
01-Dec	74.5	5977	108	1463			6.58	146	253	102	72	21
02-Dec	75	6165	93	1442	5.8	804.8	6.57	148	246	98	68	20
02-Dec	75.5	5956		1460			6.56	147	246	106	72	22
03-Dec	76	5760		1129	4.0	796.1	6.57	148	246	103	65	21
03-Dec	76.5	5797		1461			6.57	146	245	104	70	19
04-Dec	77	5843	76	1425	8.2	793.6	6.57	147	248	104	70	15
04-Dec	77.5	6104	79	1091			6.58	146	245	104	76	23
05-Dec	78	6136	91		8.5	795.1	6.58	151	246	105	75	22
05-Dec	78.5	5938	82	1752			6.57	152	245	103	72	23
06-Dec	79	5673	94	1484	6.8	798	6.57	158	246	105	73	20
Mean		5944	96	1425	5	789	6.57	147	246	104	72	21
S.D.		140	14	176	3	11	0.01	3	1	3	2	1
Data points		13	10	12	11	10	13	12	12	12	12	12

Steady state No 25**Table B.76:** Operating conditions for steady state number 25

Feed batch number	F14
Mass of PSS in feed (g)	56
Total Mass of feed (g)	1000
Reactor Volume (L)	20
Retention time (day)	10
Sulfate addition (gSO₄/L)	0
pH	steady state
Biological groups present	acidogens and methanogens

The digester was reseeded with waste digester sludge and fed immediately at the described feed concentration and retention time.

Table B.77: Results summary for steady state number 25

Feed total COD (mg/L)	1950
Feed soluble COD (mg/L)	254
Feed TKN (mgN/L)	43
Feed FSA (mgN/L)	5
Feed Total P (mgP/L)	10
Feed soluble P (mgP/L)	3
Steady state measured after 30 days (3 x R_h)	
Effluent total COD (mg/L)	905 ± 31 (14)
Effluent soluble COD (mg/L)	32 ± 2 (13)
Suspended solids (mgCOD/L)	235
Effluent VFA (mg/L as HAc)	0 ± 1 (11)
Effluent Alkalinity (mg/L as CaCO₃)	170 ± 7 (10)
Reactor pH	6.59 ± 0.07 (17)
Gas Produced (units/day)	[13 ± 0 (16)] twice = 26
Volume per unit (ml)	44.5 ± 0.5
Gas composition (%CH₄)	*53.2
Methane production (L/day)	0.62
Methane production (gCOD/day)	1.6
Effluent TKN (mgN/L)	40 ± 1 (14)
Effluent FSA (mgN/L)	19 ± 1 (14)
Effluent Total P (mgP/L)	11 ± 0 (14)
Effluent soluble P (mgP/L)	4 ± 1 (13)
COD balance (%)	88.4
TKN balance (%)	92.8
Total P balance (%)	114.2

* Average of 2 measurements made

Appendix B: Steady State Data

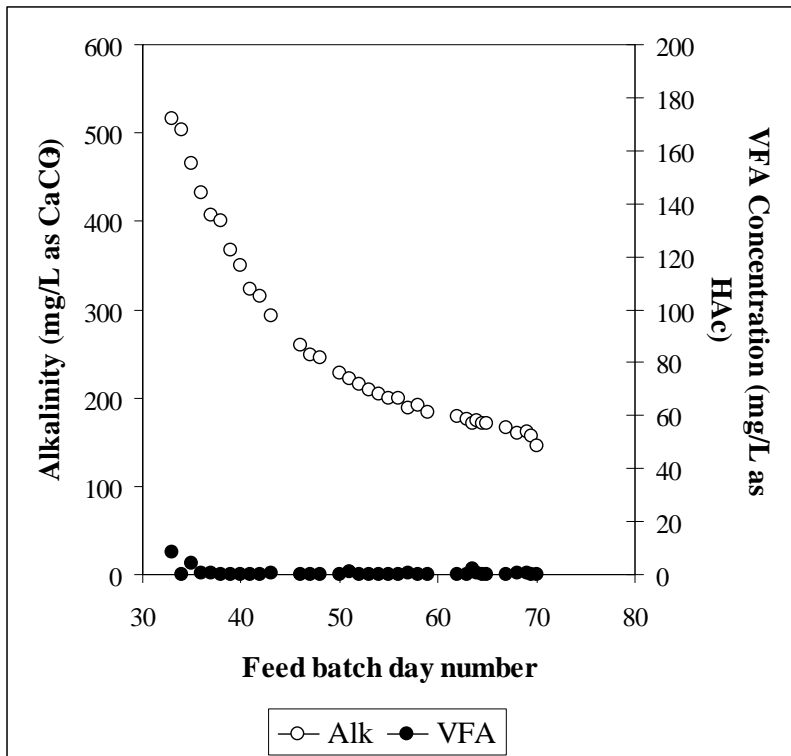


Figure B.53: Daily measurements of the VFA and alkalinity leading up to and including steady state number 25 (steady state from day 62)

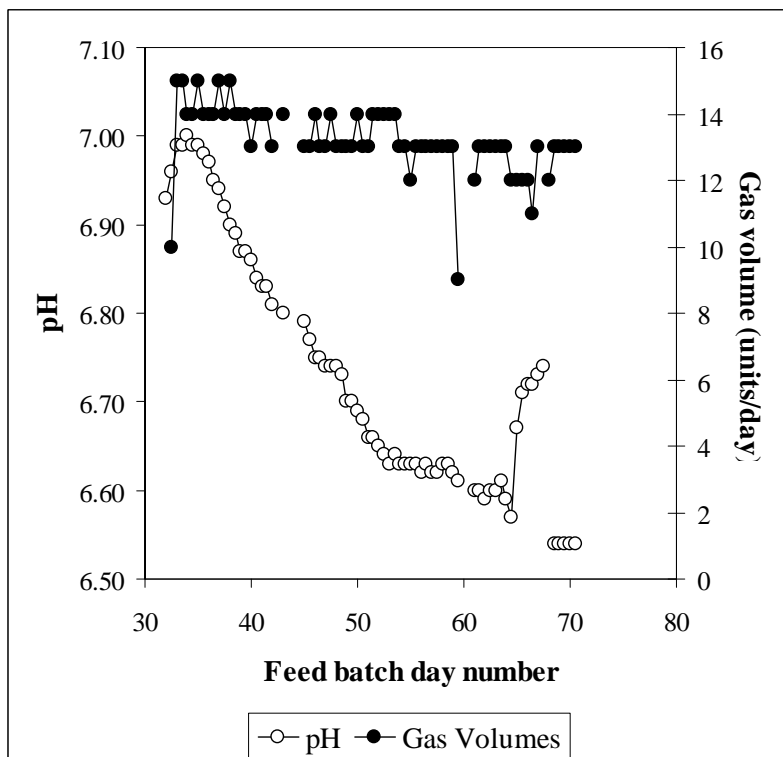


Figure B.54: Daily measurements of the pH and volumetric gas production leading up to and including steady state number 25 (steady state from day 62)

Appendix B: Steady State Data

Table B.78: Daily measured data for steady state number 25

Date	Day	Total COD (mgCOD/L)	Soluble COD (mgCOD/L)	Suspended Solids (mgCOD/L)	VFA (mg/L as HAc)	Alkalinity (mg/L as CaCO ₃)	pH	Gas Volume (Units/day)	TKN (mgN/L)	NH ₃ (mgN/L)	TP (mgP/L)	PO ₄ (mgP/L)
19-Nov	62	1014	27	275	0	178.5	6.59	13		20		6
19-Nov	62.5						6.60	13				
20-Nov	63	924	30	281	0	176.3	6.60	13	41	21	11	4
20-Nov	63.5	900	38	274	2.2	170.6	6.61	13	41	20	11	5
21-Nov	64	910	35	265	0.3	173.7	6.59	13	41	20	11	4
21-Nov	64.5	894	32	266	0.1	170.3	6.57	12	41	20	10	4
22-Nov	65	928	32		0	170.4	6.67	12	40	19	11	3
22-Nov	65.5						6.71	12				
23-Nov	66						6.72	12				
23-Nov	66.5	927	33				6.72	11	41	19	11	4
24-Nov	67	880	35	266	0.2	166.7	6.73	13	41	19	11	3
24-Nov	67.5	852	34	274			6.74		40	19	10	4
25-Nov	68	859	32	261	0.6	160.1		12	39	19	10	3
25-Nov	68.5	933	29	268			6.54	13	38	19	10	4
26-Nov	69	955	32	264	0.6	161.7	6.54	13	39	19	11	4
26-Nov	69.5	871	32		0	156	6.54	13	39	18	10	4
27-Nov	70	909	31	269	0	146.1	6.54	13	39	18	10	4
27-Nov	70.5	855		267			6.54	13	38		11	
Mean		905	32	267	0	170	6.59	13	40	19	11	4
S.D.		31	2	4	1	7	0.07	0	1	1	0	1
Data points		14	13	11	11	10	17	16	14	14	14	12

Steady state No 26**Table B.79:** Operating conditions for steady state number 26

Feed batch number	F14
Mass of PSS in feed (g)	70
Total Mass of feed (g)	1250
Reactor Volume (L)	20
Retention time (day)	8
Sulfate addition (gSO₄/L)	0
pH	steady state
Biological groups present	acidogens and methanogens

This experiment followed directly from steady state number 26. The feed was incremented by 50g over 5 feed cycles.

Table B.80: Results summary for steady state number 26

Feed total COD (mg/L)	1950
Feed soluble COD (mg/L)	284
Feed TKN (mgN/L)	43
Feed FSA (mgN/L)	7
Feed Total P (mgP/L)	10
Feed soluble P (mgP/L)	3
Steady state measured after 23 days (2.875 x R_h)	
Effluent total COD (mg/L)	892 ± 21 (13)
Effluent soluble COD (mg/L)	51 ± 8 (13)
Suspended solids (mgCOD/L)	304
Effluent VFA (mg/L as HAc)	10 ± 3 (11)
Effluent Alkalinity (mg/L as CaCO₃)	144 ± 1 (11)
Reactor pH	6.38 ± 0.02 (15)
Gas Produced (units/day)	[16 ± 1 (14)] twice = 32
Volume per unit (ml)	44.5 ± 0.5
Gas composition (%CH₄)	*59.3
Methane production (L/day)	0.84
Methane production (gCOD/day)	2.2
Effluent TKN (mgN/L)	36 ± 1 (11)
Effluent FSA (mgN/L)	15 ± 1 (12)
Effluent Total P (mgP/L)	10 ± 1 (12)
Effluent soluble P (mgP/L)	5 ± 1 (12)
COD balance (%)	91.9
TKN balance (%)	83.5
Total P balance (%)	103.8

* Average of 2 measurements made

Appendix B: Steady State Data

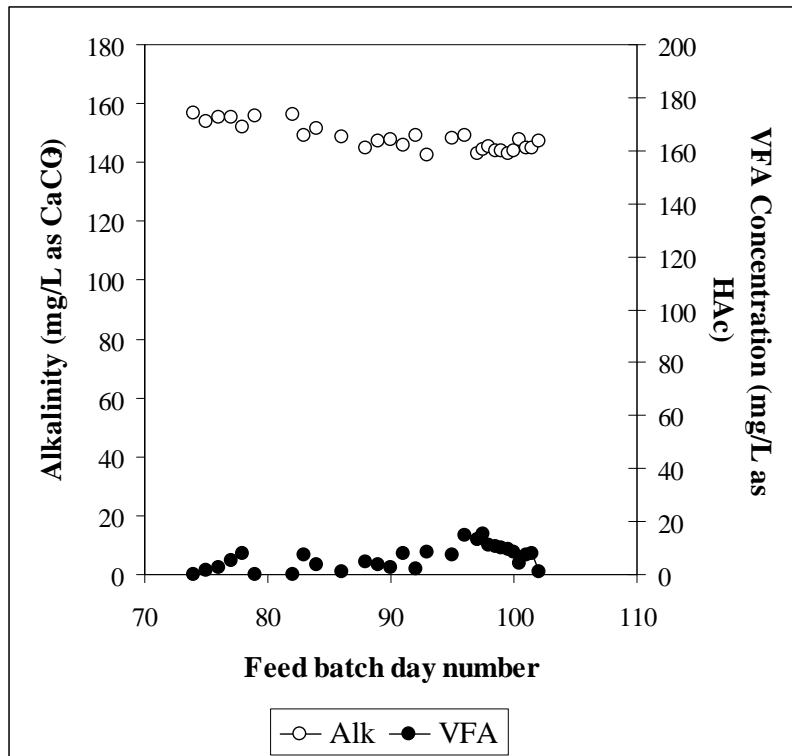


Figure B.55: Daily measurements of the VFA and alkalinity leading up to and including steady state number 26 (steady state from day 96)

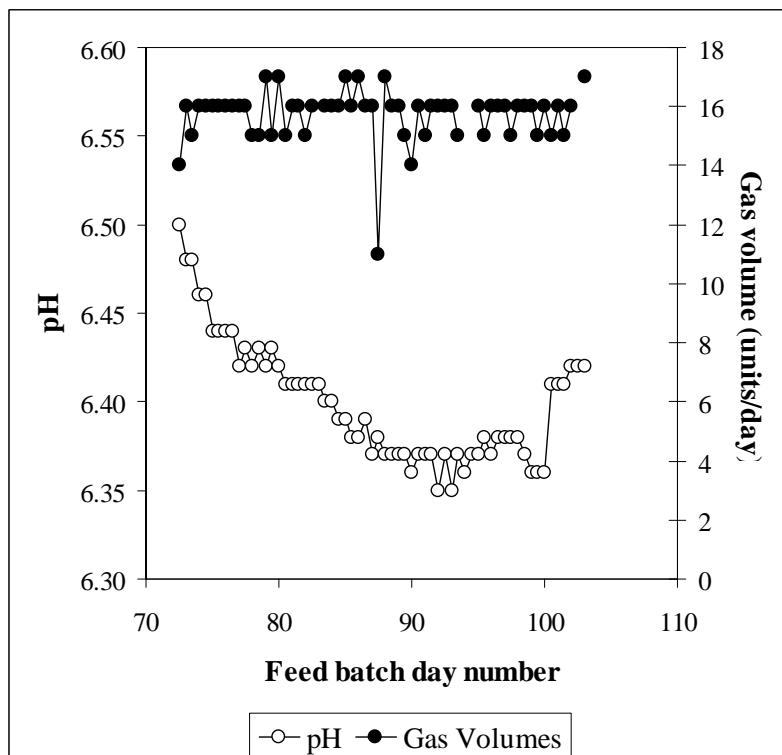


Figure B.56: Daily measurements of the pH and volumetric gas production leading up to and including steady state number 26 (steady state from day 96)

Appendix B: Steady State Data

Table B.81: Daily measured data for steady state number 26

Date	Day	Total COD (mgCOD/L)	Soluble COD (mgCOD/L)	Suspended Solids (mgCOD/L)	VFA (mg/L as HAc)	Alkalinity (mg/L as CaCO ₃)	pH	Gas Volume (Units/day)	TKN (mgN/L)	NH ₃ (mgN/L)	TP (mgP/L)	PO ₄ (mgP/L)
23-Dec	96	861	79	372	14.6	149.2	6.37	16	37	17	11	6
23-Dec	96.5						6.38	16				
24-Dec	97	905	59	356	13.2	143	6.38	16	36	18	10	5
24-Dec	97.5	931	68	362	15.4	144.2	6.38	15	37	17	11	8
25-Dec	98	892	67	346	11	145.3	6.38	16	36	15	10	7
25-Dec	98.5	892	41	340	10.8	143.8	6.37	16	36	17	8	6
26-Dec	99	852	45	340	10.1	143.9	6.36	16	36	16	10	5
26-Dec	99.5	988	50	343	9.4	142.9	6.36	15	36	15	10	5
27-Dec	100	937	47	356	8.6	144	6.36	16	36	15	10	5
27-Dec	100.5	828	49	365	4	147.7	6.41	15	34	15	10	4
28-Dec	101	881	51	355	7.6	144.7	6.41	16	35	14	11	4
28-Dec	101.5	879	48	353	7.9	144.7	6.41	15	36	15	10	4
29-Dec	102	885	52	355	1.1	147	6.42	16	36	14	10	4
29-Dec	102.5	891	51				6.42					
30-Dec	103	915	58	294			6.42	17				
	Mean	892	51	355	10	144	6.38	16	36	15	10	5
	S.D.	21	8	10	3	1	0.02	1	1	1	1	1
	Data points	13	13	12	11	11	15	14	11	12	12	12

Steady state No 27**Table B.82:** Operating conditions for steady state number 27

Feed batch number	F15
Mass of PSS in feed (g)	30.6
Total Mass of feed (g)	1000
Reactor Volume (L)	16
Retention time (day)	8
Sulfate addition (gSO₄/L)	0
pH	controlled to ~ 6.5
Biological groups present	acidogens and methanogens

The digester was reseeded with waste methanogenic sludge for this experiment. The pH was controlled to 6.5 by addition of 1M NaOH.

Table B.83: Results summary for steady state number 27

Feed total COD (mg/L)	2017
Feed soluble COD (mg/L)	222
Feed TKN (mgN/L)	39
Feed FSA (mgN/L)	8
Feed Total P (mgP/L)	9
Feed soluble P (mgP/L)	2
Steady state measured after 31 days (3.875 x R_h)	
Effluent total COD (mg/L)	913 ± 17 (12)
Effluent soluble COD (mg/L)	27 ± 3 (13)
Suspended solids (mgCOD/L)	398
Effluent VFA (mg/L as HAc)	1 ± 1 (14)
Effluent Alkalinity (mg/L as CaCO₃)	127 ± 3 (14)
Reactor pH	6.58 ± 0.01 (11)
Gas Produced (units/day)	[12 ± 0 (14)] twice = 24
Volume per unit (ml)	49.7 ± 0.4
Gas composition (%CH₄)	*58.46
Methane production (L/day)	0.70
Methane production (gCOD/day)	1.9
Effluent TKN (mgN/L)	36 ± 1 (11)
Effluent FSA (mgN/L)	15 ± 1 (12)
Effluent Total P (mgP/L)	10 ± 1 (12)
Effluent soluble P (mgP/L)	5 ± 1 (12)
COD balance (%)	91.3
TKN balance (%)	67.4
Total P balance (%)	108.6

* 1 measurement made – not too confident of the accuracy

Appendix B: Steady State Data

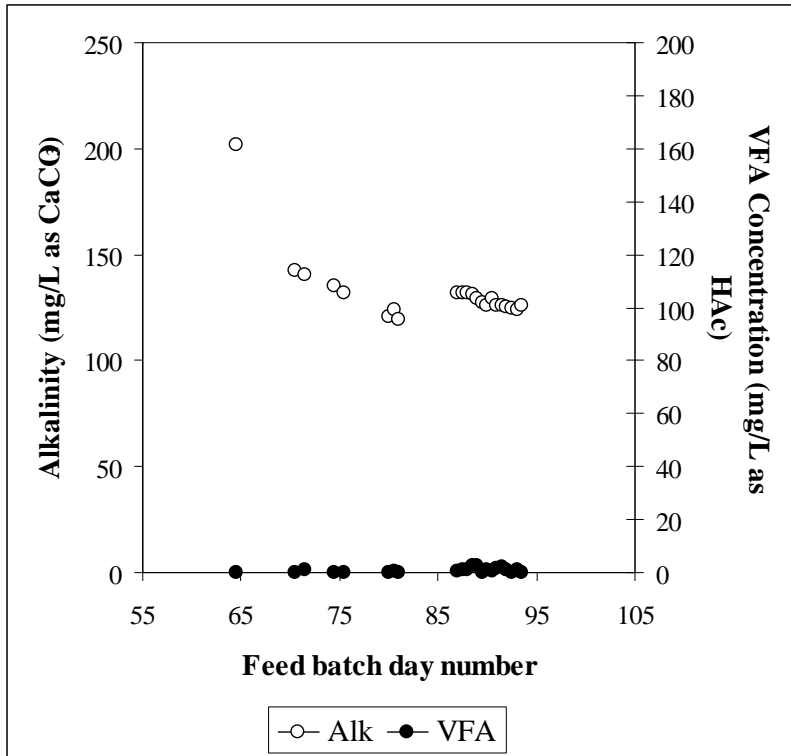


Figure B.57: Daily measurements of the VFA and alkalinity leading up to and including steady state number 27 (steady state from day 87)

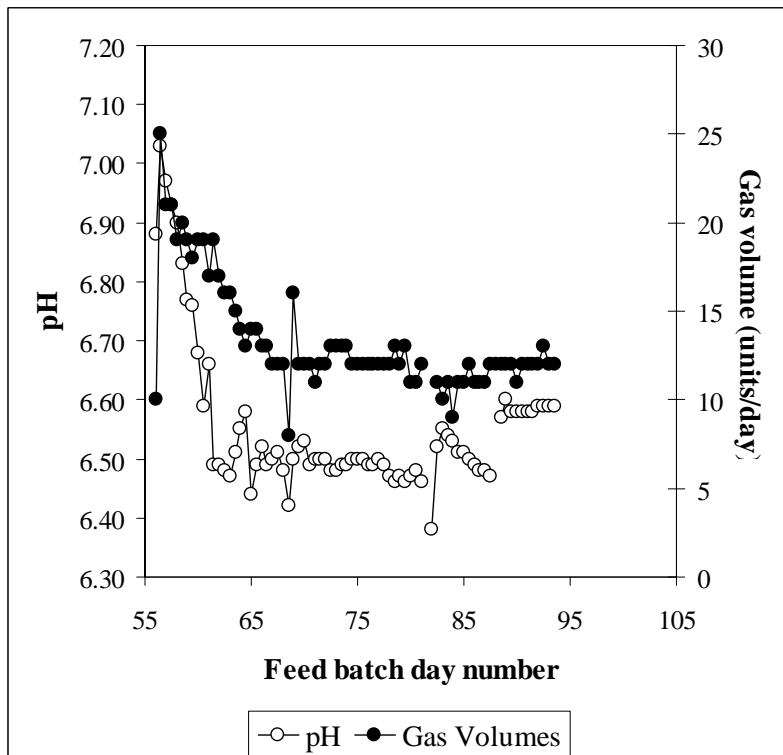


Figure B.58: Daily measurements of the pH and volumetric gas production leading up to and including steady state number 27 (steady state from day 87)

Appendix B: Steady State Data

Table B.84: Daily measured data for steady state number 27

Date	Day	Total COD (mgCOD/L)	Soluble COD (mgCOD/L)	Suspended Solids (mgCOD/L)	VFA (mg/L as HAc)	Alkalinity (mg/L as CaCO ₃)	pH	Gas Volume (Units/day)	TKN (mgN/L)	NH ₃ (mgN/L)	TP (mgP/L)	PO ₄ (mgP/L)
22-Feb	87	938	27	454	0.7	131.6	6.48	11	48	18	10	3
23-Feb	87.5	938	42	425	1.1	131.6	6.47	12	49	18	9	3
23-Feb	88	927	32	426	1.3	132.0		12	49	19	10	3
24-Feb	88.5	895	33	423	2.8	131.1	6.57	12	47	20	9	3
24-Feb	89	1107	32	442	2.9	129.6	6.60	12	52	19	10	2
25-Feb	89.5	913	33	420	0	127.2	6.58	12	50	19	9	3
25-Feb	90	1113	25	410	1.3	125.8	6.58	11	26	37	12	3
26-Feb	90.5	913	26	454	0.7	129.6	6.58	12	22	35	10	2
26-Feb	91	929	25	426	1.4	126.3	6.58	12	23	35	11	3
27-Feb	91.5	901	27	423	2.3	125.7	6.58	12	21	32	10	2
27-Feb	92	900	29	385	1.2	125.4	6.59	12	22	34	9	2
28-Feb	92.5	901	27	429	0	124.8	6.59	13	25	35	10	2
28-Feb	93	934	31	413	1.3	124.3	6.59	12	26	32	10	2
29-Feb	93.5	893	27	420	0	125.7	6.59	12	22	31	10	2
	Mean	913	27	425	1	127	6.58	12	26	32	10	3
	S.D.	17	3	13	1	3	0.01	0	12	8	1	1
	Data points	12	13	13	14	14	11	14	13	14	14	14

Steady state No 28**Table B.85:** Operating conditions for steady state number 28

Feed batch number	F15
Mass of PSS in feed (g)	1100
Total Mass of feed (g)	1750
Reactor Volume (L)	20
Retention time (day)	5.71
Sulfate addition (gSO₄/L)	0
pH	steady state
Biological groups present	acidogens and methanogens

This experiment followed steady state number 23. The feed was increased by 50g per cycle until the new retention time was reached. This was maintained for 6 days. The feed was then changed from F14 to F15 and the system allowed to reach steady state.

Table B.86: Results summary for steady state number 28

Feed total COD (mg/L)	41441
Feed soluble COD (mg/L)	2583
Feed TKN (mgN/L)	792
Feed FSA (mgN/L)	40
Feed Total P (mgP/L)	189
Feed soluble P (mgP/L)	37
Steady state measured after 15 days (2.6 x R_h)	
Effluent total COD (mg/L)	19737 ± 732 (13)
Effluent soluble COD (mg/L)	295 ± 36 (12)
Suspended solids (mgCOD/L)	6168
Effluent VFA (mg/L as HAc)	26 ± 16 (13)
Effluent Alkalinity (mg/L as CaCO₃)	1612 ± 25 (12)
Reactor pH	6.75 ± 0.01 (14)
Gas Produced (units/day)	[518 ± 16 (12)] twice = 1036
Volume per unit (ml)	45.9 ± 0.2
Gas composition (%CH₄)	*63.76
Methane production (L/day)	30.32
Methane production (gCOD/day)	80.7
Effluent TKN (mgN/L)	648 ± 22 (12)
Effluent FSA (mgN/L)	183 ± 5 (11)
Effluent Total P (mgP/L)	207 ± 10 (12)
Effluent soluble P (mgP/L)	17 ± 4 (12)
COD balance (%)	103.3
TKN balance (%)	81.8
Total P balance (%)	109.4

* Average of 7 measurements made

Appendix B: Steady State Data

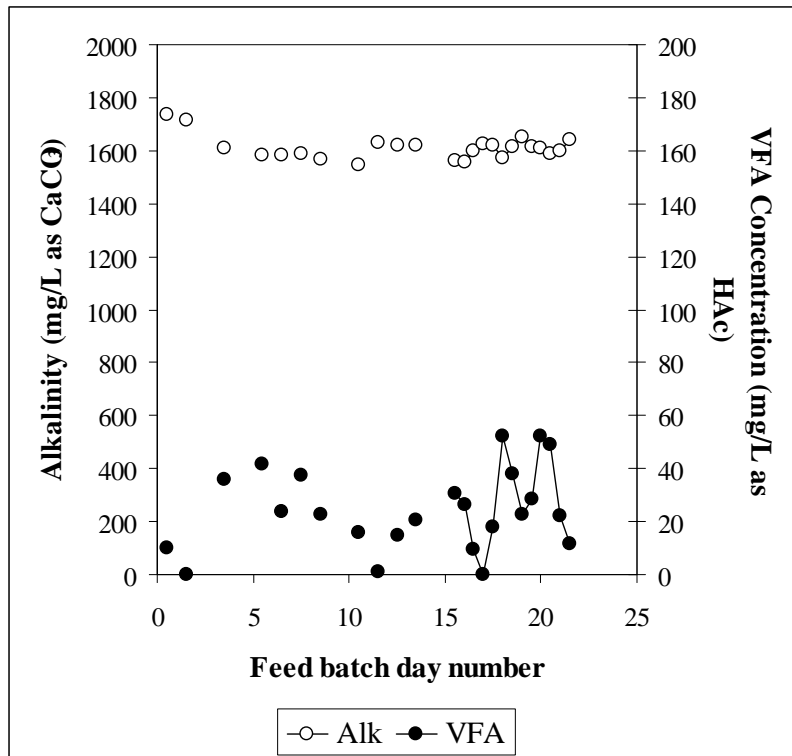


Figure B.59: Daily measurements of the VFA and alkalinity leading up to and including steady state number 28 (steady state from day 15.5)

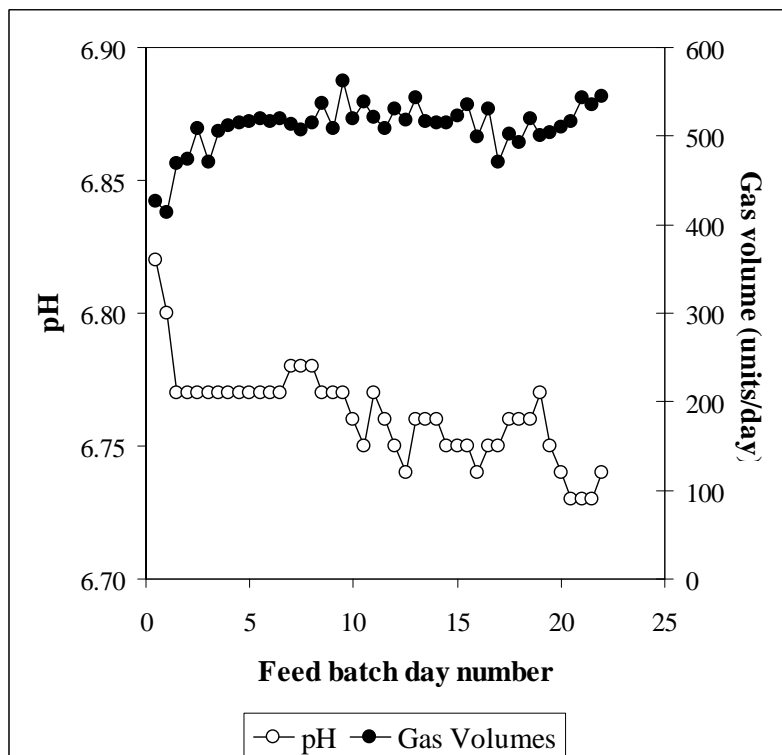


Figure B.60: Daily measurements of the pH and volumetric gas production leading up to and including steady state number 28 (steady state from day 15.5)

Appendix B: Steady State Data

Table B.87: Daily measured data for steady state number 28

Date	Day	Total COD (mgCOD/L)	Soluble COD (mgCOD/L)	Suspended Solids (mgCOD/L)	VFA (mg/L as HAc)	Alkalinity (mg/L as CaCO ₃)	pH	Gas Volume (Units/day)	TKN (mgN/L)	NH ₃ (mgN/L)	TP (mgP/L)	PO ₄ (mgP/L)
13-Dec	15.5	19018	230	6209	30.7	1560.2	6.75	536	714	217	224	18
13-Dec	16	19061	231	5887	26.2	1554.1	6.74	499	630	183	216	11
14-Dec	16.5	18315	229	6076	9.7	1601.5	6.75	530	637	181	232	18
14-Dec	17	19066	244	5867	0.0	1624.6	6.75	471	644	186	191	20
15-Dec	17.5	20331	279		18.2	1617.9	6.76	502	434	188	207	16
15-Dec	18	21024	288	7292	52.3	1574.7	6.76	492	672	192	207	18
16-Dec	18.5	20661	301	6643	38.0	1616.1	6.76	520	651	188	199	20
16-Dec	19	19737	304	6425	22.6	1652.7	6.77	500	630	171	199	10
17-Dec	19.5	19785		6463	28.5	1613.6	6.75	504	658		207	
17-Dec	20	19198	303	7015	52.0	1609.9	6.74	510	672	188	191	10
18-Dec	20.5	19896	316	9057	49.2	1586	6.73	516	651	182	207	20
18-Dec	21	20316	318	6802	22.3	1599.3	6.73	543	644	182	216	16
19-Dec	21.5	19567	328	6960	11.7	1638.9	6.73	535	644	181	216	10
Mean		19737	295	6463	26	1612	6.75	518	648	183	207	17
S.D.		732	36	453	16	25	0.01	16	22	5	10	4
Data points		13	12	11	13	12	14	12	12	11	12	12

Steady state No 29**Table B.88:** Operating conditions for steady state number 29

Feed batch number	F15
Mass of PSS in feed (g)	1875
Total Mass of feed (g)	3000
Reactor Volume (L)	20
Retention time (day)	3.33
Sulfate addition (gSO₄/L)	0
pH	steady state
Biological groups present	acidogens

Following on from steady state number 28, while reducing the retention time to 5 days, the VFA concentrations increased, and the washout point for the methanogens had been reached. The feed volume was then increased further to ensure that the methanogens were washout of the system.

Table B.89: Results summary for steady state number 29

Feed total COD (mg/L)	41206
Feed soluble COD (mg/L)	3896
Feed TKN (mgN/L)	788
Feed FSA (mgN/L)	99
Feed Total P (mgP/L)	188
Feed soluble P (mgP/L)	37
Steady state measured after 14 days (4.2 x R_h)	
Effluent total COD (mg/L)	37992 ± 892 (12)
Effluent soluble COD (mg/L)	6739 ± 173 (13)
Suspended solids (mgCOD/L)	7993
Reactor pH	4.80 ± 0.04 (13)
Gas Produced (units/day)	[38 ± 3 (11)] twice = 76
Volume per unit (ml)	45.9 ± 0.2
Gas composition (%CH₄)	*10.77
Methane production (L/day)	0.38
Methane production (gCOD/day)	1.0
Effluent TKN (mgN/L)	518 ± 57 (13)
Effluent FSA (mgN/L)	260 ± 4 (11)
Effluent Total P (mgP/L)	206 ± 11 (13)
Effluent soluble P (mgP/L)	66 ± 2 (12)
COD balance (%)	92.6
TKN balance (%)	65.8
Total P balance (%)	109.5

* Average of 2 measurements made

Appendix B: Steady State Data

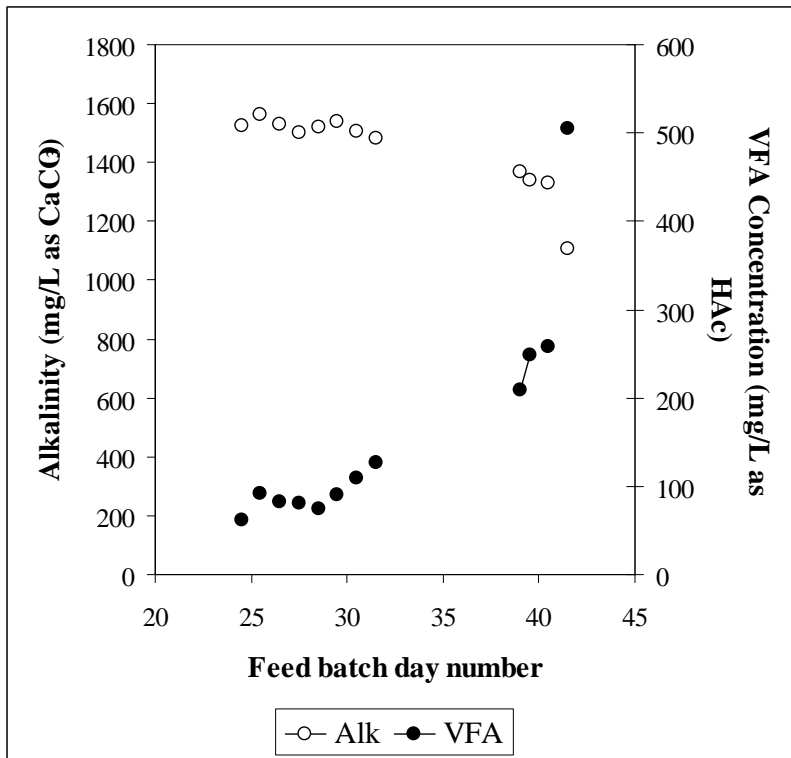


Figure B.61: Daily measurements of the VFA and alkalinity leading up to the point where the decision was made that the methanogens were washing out of the system

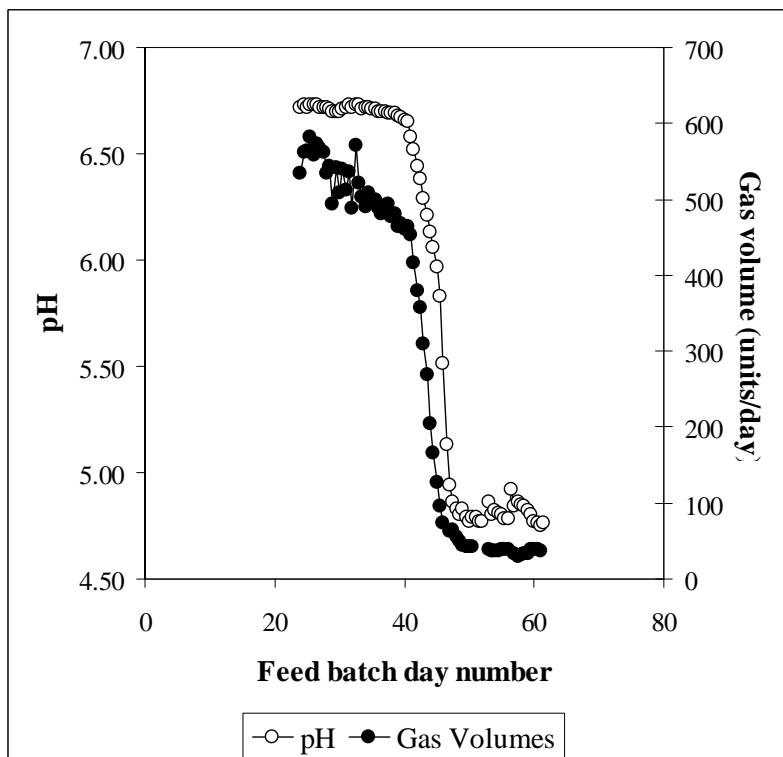


Figure B.62: Daily measurements of the pH and volumetric gas production leading up to and including steady state number 29 (steady state from day 55)

Appendix B: Steady State Data

Table B.90: Daily measured data for steady state number 29

Date	Day	Total COD (mgCOD/L)	Soluble COD (mgCOD/L)	Suspended Solids (mgCOD/L)	pH	Gas Volume (Units/day)	TKN (mgN/L)	NH ₃ (mgN/L)	TP (mgP/L)	PO ₄ (mgP/L)
21-Jan	55	37878	6800		4.80	39	441	350	190	77
22-Jan	55.5	36116	7028		4.78	39	574	371	190	77
22-Jan	56	39178	6491	15265	4.78	38	595	328	190	65
23-Jan	56.5	39291	6783	15908	4.92		560	256	221	65
23-Jan	57	37806	6635	15625	4.84	33	518	255	206	68
24-Jan	57.5	39475	6621	13659	4.86	30	616	260	190	63
24-Jan	58	38216	6584	14634	4.85	32	518	256	206	67
25-Jan	58.5	38134	6604	14003	4.84	34	532	265	190	66
25-Jan	59	37988	6768	14066	4.82	34		268	206	66
26-Jan	59.5	37179	6615	14637	4.80	39	448	256	206	61
26-Jan	60	37760	6739	14596	4.77	39	490	258	190	66
27-Jan	60.5	37995	6942	15667	4.76	39	476	261	206	66
27-Jan	61	41718	7074	14833	4.75	37	476	262	221	65
28-Jan	61.5	41290	7182	15167	4.76		609	266	253	62
Mean		37992	6739	14735	4.80	38	518	260	206	66
S.D.		892	173	681	0.04	3	57	4	11	2
Data points		12	13	12	13	11	13	11	13	12

Steady state No 30**Table B.91:** Operating conditions for steady state number 30

Feed batch number	F15
Mass of PSS in feed (g)	1275
Total Mass of feed (g)	2000
Reactor Volume (L)	20
Retention time (day)	5
Sulfate addition (gSO₄/L)	0
pH	steady state
Biological groups present	acidogens

This experiment followed steady state number 29. The feed volume was changed in a single step, and no methanogenesis was evident.

Table B.92: Results summary for steady state number 30

Feed total COD (mg/L)	42030
Feed soluble COD (mg/L)	4405
Feed TKN (mgN/L)	803
Feed FSA (mgN/L)	134
Feed Total P (mgP/L)	192
Feed soluble P (mgP/L)	38
Steady state measured after 15 days (3 x R_h)	
Effluent total COD (mg/L)	39889 ± 1580 (10)
Effluent soluble COD (mg/L)	7738 ± 146 (10)
Suspended solids (mgCOD/L)	7550
Reactor pH	4.71 ± 0.01 (12)
Gas Produced (units/day)	[36 ± 1 (12)] twice = 72
Volume per unit (ml)	45.9 ± 0.2
Gas composition (%CH₄)	*10.77
Methane production (L/day)	0.36
Methane production (gCOD/day)	0.9
Effluent TKN (mgN/L)	941 ± 52 (11)
Effluent FSA (mgN/L)	265 ± 62 (10)
Effluent Total P (mgP/L)	193 ± 12 (11)
Effluent soluble P (mgP/L)	68 ± 1 (10)
COD balance (%)	95.5
TKN balance (%)	117.1
Total P balance (%)	100.6

* Assumed the same as for steady state number 29

Appendix B: Steady State Data

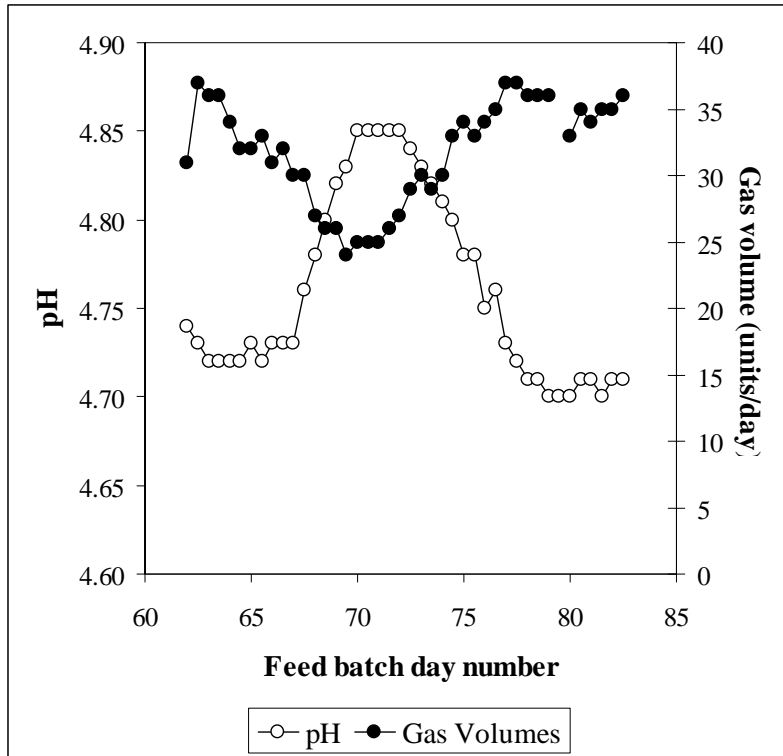


Figure B.63: Daily measurements of the pH and volumetric gas production leading up to and including steady state number 30 (steady state from day 76.5)

Appendix B: Steady State Data

Table B.93: Daily measured data for steady state number 30

Date	Day	Total COD (mgCOD/L)	Soluble COD (mgCOD/L)	Suspended Solids (mgCOD/L)	pH	Gas Volume (Units/day)	TKN (mgN/L)	NH ₃ (mgN/L)	TP (mgP/L)	PO ₄ (mgP/L)
12-Feb	76.5	40174	7219	14780	4.76	35	921	255	147	66
12-Feb	77	37511	7419	15790	4.73	37	910	493	177	68
13-Feb	77.5	40360	7522	14591	4.72	37	949	280	185	68
13-Feb	78	45041	7681	17385	4.71	36	1075	276	193	68
14-Feb	78.5	38940	7676	15579	4.71	36	1582	273	185	63
14-Feb	79	38579	7674	15083	4.70	36	941	256	193	66
15-Feb	79.5	39628	7794	14931	4.70		994	358	177	69
15-Feb	80	38889	7899	14990	4.70	33	896	277	209	69
16-Feb	80.5	40528	7841	15782	4.71	35	889	157	201	67
16-Feb	81	40150	7829	15565	4.71	34	966	155	216	67
17-Feb	81.5	43743	7833	15493	4.70	35	952	171	193	69
17-Feb	82				4.71	35	896		178	
Mean		39889	7738	15288	4.71	36	941	265	193	68
S.D.		1580	146	411	0.01	1	52	62	12	1
Data points		10	10	10	12	12	11	10	11	10

Steady state No 31**Table B.94:** Operating conditions for steady state number 31

Feed batch number	F15
Mass of PSS in feed (g)	350
Total Mass of feed (g)	1750
Reactor Volume (L)	20
Retention time (day)	5.71
Sulfate addition (gSO₄/L)	0
pH	steady state
Biological groups present	acidogens and methanogens

This experiment followed steady state number 24. The feed was changed from F14 to F15 at the same concentration and retention time and operated for three days before the feed volume was incremented until the new steady state operating condition.

Table B.95: Results summary for steady state number 31

Feed total COD (mg/L)	13186
Feed soluble COD (mg/L)	957
Feed TKN (mgN/L)	252
Feed FSA (mgN/L)	18
Feed Total P (mgP/L)	60
Feed soluble P (mgP/L)	12
Steady state measured after 13 days (2.3 x R_h)	
Effluent total COD (mg/L)	6757 ± 265 (14)
Effluent soluble COD (mg/L)	120 ± 10 (12)
Suspended solids (mgCOD/L)	2065
Effluent VFA (mg/L as HAc)	19 ± 2 (10)
Effluent Alkalinity (mg/L as CaCO₃)	564 ± 6 (10)
Reactor pH	6.45 ± 0.01 (15)
Gas Produced (units/day)	[144 ± 5 (14)] twice = 288
Volume per unit (ml)	48.8 ± 0.5
Gas composition (%CH₄)	*65.70
Methane production (L/day)	9.23
Methane production (gCOD/day)	24.6
Effluent TKN (mgN/L)	206 ± 2 (12)
Effluent FSA (mgN/L)	63 ± 1 (11)
Effluent Total P (mgP/L)	61 ± 2 (10)
Effluent soluble P (mgP/L)	12 ± 1 (11)
COD balance (%)	104.5
TKN balance (%)	81.7
Total P balance (%)	101.3

* Average for 6 measurements made

Appendix B: Steady State Data

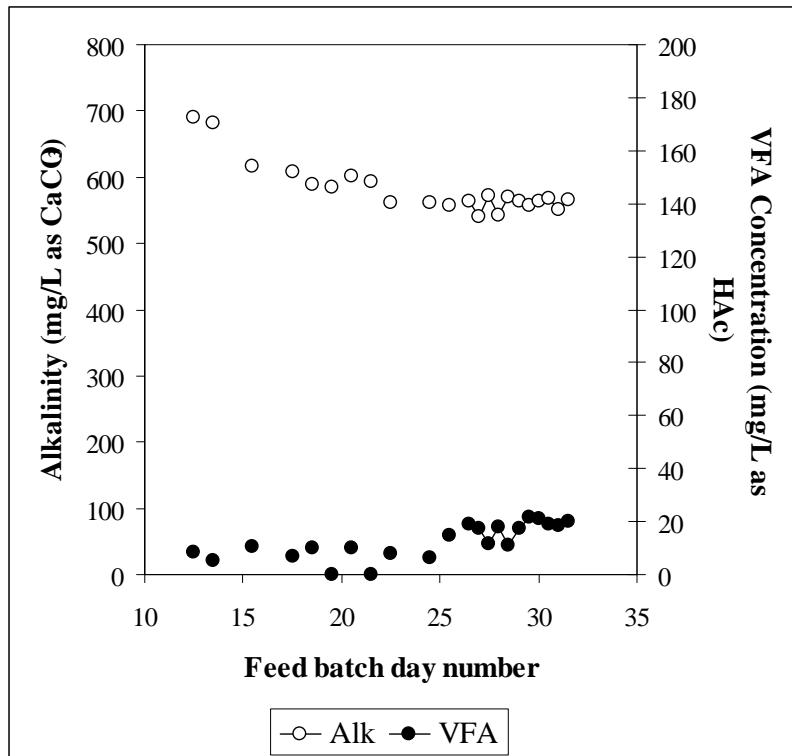


Figure B.64: Daily measurements of the VFA and alkalinity leading up to and including steady state number 31 (steady state from day 25.5)

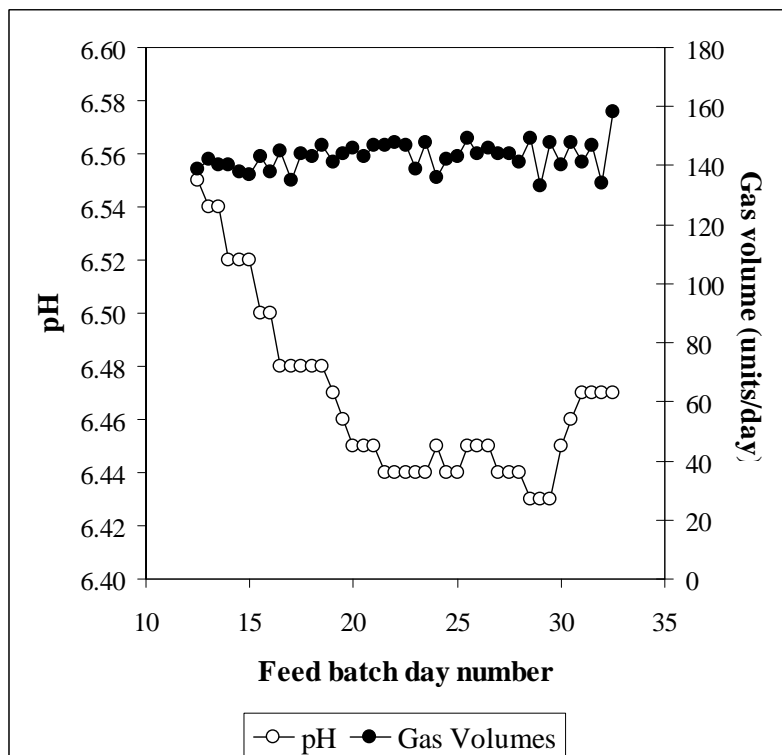


Figure B.65: Daily measurements of the pH and volumetric gas production leading up to and including steady state number 31 (steady state from day 25.5)

Appendix B: Steady State Data

Table B.96: Daily measured data for steady state number 31

Date	Day	Total COD (mgCOD/L)	Soluble COD (mgCOD/L)	Suspended Solids (mgCOD/L)	VFA (mg/L as HAc)	Alkalinity (mg/L as CaCO ₃)	pH	Gas Volume (Units/day)	TKN (mgN/L)	NH ₃ (mgN/L)	TP (mgP/L)	PO ₄ (mgP/L)
23-Dec	25.5	7221		2180	14.7	558.2	6.45	149	207		61	
23-Dec	26						6.45	144				
24-Dec	26.5	6736	123	2185	18.8	563.1	6.45	146	206	64	73	12
24-Dec	27	6650	112	2891	17.6	540.6	6.44	144	206	61	61	10
25-Dec	27.5	7073	115	2279	11.6	571.3	6.44	144	209	62	61	12
25-Dec	28	6536	108	2459	18.1	542.6	6.44	141	210	62	61	14
26-Dec	28.5	6533	107	2589	11.1	569.4	6.43	149	209	64	63	14
26-Dec	29	6750	114	2017	17.3	564.6	6.43	133	203	62	63	11
27-Dec	29.5	7158	127	2215	21.8	557.8	6.43	148	206	63	61	12
27-Dec	30	6763	121	2556	20.9	564.3	6.45	140	203	63	61	15
28-Dec	30.5	6427	119	2116	19.0	568.5	6.46	148	204	65	66	14
28-Dec	31	6694	121	2845	18.5	550.3	6.47	141	210	64	75	11
29-Dec	31.5	7265	128	2008	19.8	565.7	6.47	147	206	64	65	12
29-Dec	32	7082	145				6.47	134				
30-Dec	32.5	6881	160	1772			6.47	158				
Mean		6757	120	2185	19	564	6.45	144	206	63	61	12
S.D.		265	10	235	2	6	0.01	5	2	1	2	1
Data points		14	12	11	10	10	15	14	12	11	10	11

Steady state No 32**Table B.97:** Operating conditions for steady state number 32

Feed batch number	F15
Mass of PSS in feed (g)	600
Total Mass of feed (g)	3000
Reactor Volume (L)	20
Retention time (day)	3.33
Sulfate addition (gSO₄/L)	0
pH	steady state
Biological groups present	acidogens

After steady state 31, the system was operated at a 5-day retention time for 8 days. After day 42, when the VFA concentration was measured as 236.8 mg/L as HAc, it was decided that methanogenesis was failing and the retention time was decreased to 3.33 days.

Table B.98: Results summary for steady state number 32

Feed total COD (mg/L)	13186
Feed soluble COD (mg/L)	1222
Feed TKN (mgN/L)	252
Feed FSA (mgN/L)	30
Feed Total P (mgP/L)	60
Feed soluble P (mgP/L)	12
Steady state measured after 12 days (3.6 x R_h)	
Effluent total COD (mg/L)	12676 ± 289 (13)
Effluent soluble COD (mg/L)	2219 ± 47 (13)
Suspended solids (mgCOD/L)	3299
Reactor pH	4.83 ± 0.03 (14)
Gas Produced (units/day)	[12 ± 1 (13)] twice = 24
Volume per unit (ml)	48.8 ± 0.5
Gas composition (%CH₄)	*12.5
Methane production (L/day)	0.15
Methane production (gCOD/day)	0.4
Effluent TKN (mgN/L)	226 ± 7 (12)
Effluent FSA (mgN/L)	65 ± 7 (12)
Effluent Total P (mgP/L)	60 ± 2 (13)
Effluent soluble P (mgP/L)	28 ± 1 (13)
COD balance (%)	96.6
TKN balance (%)	89.7
Total P balance (%)	99.7

* Single measurement made for entire steady state

Appendix B: Steady State Data

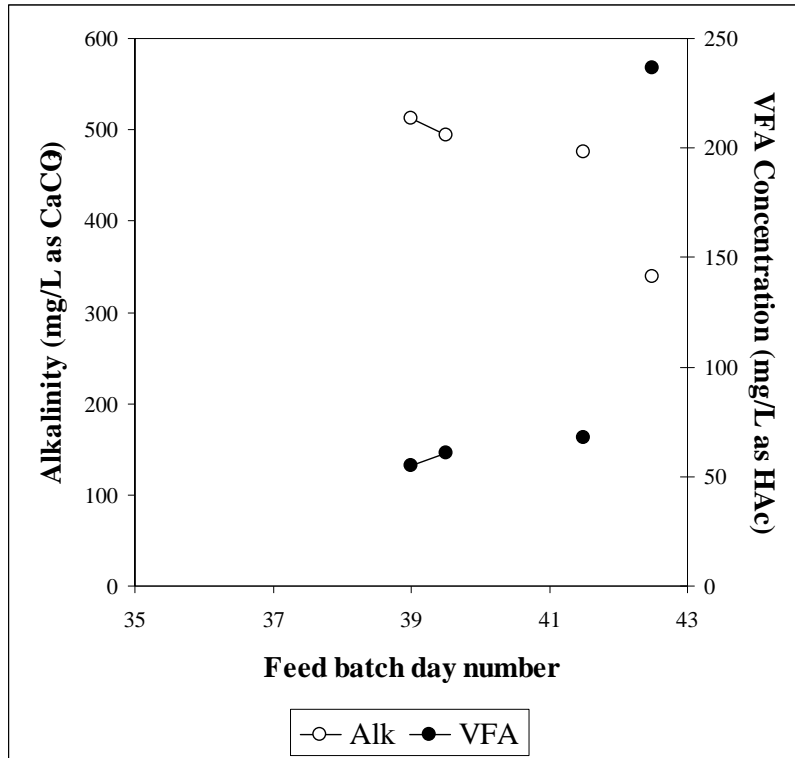


Figure B.66: Daily measurements of the VFA and alkalinity leading up the point where the decision was made that the methanogens were washing out of the system

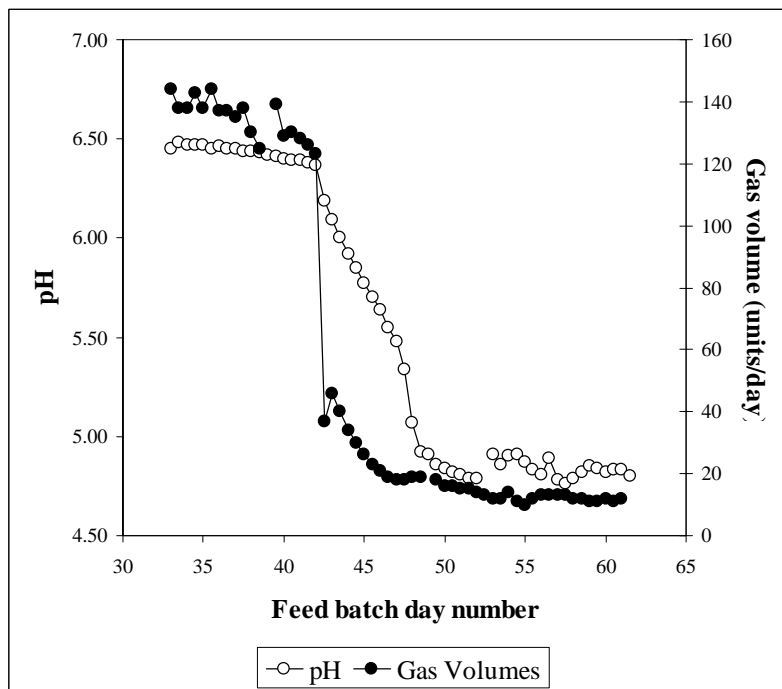


Figure B.67: Daily measurements of the pH and volumetric gas production leading up to and including steady state number 32 (steady state from day 55)

Appendix B: Steady State Data

Table B.99: Daily measured data for steady state number 32

Date	Day	Total COD (mgCOD/L)	Soluble COD (mgCOD/L)	Suspended Solids (mgCOD/L)	pH	Gas Volume (Units/day)	TKN (mgN/L)	NH ₃ (mgN/L)	TP (mgP/L)	PO ₄ (mgP/L)
21-Jan	55	12145	2144		4.87	10	249	133	60	31
22-Jan	55.5	12626	2211		4.83	12	255	126	60	31
22-Jan	56	12571	2236	5547	4.81	13	238	78	63	26
23-Jan	56.5	12632	2296	5513	4.89	13	241	59	60	27
23-Jan	57	12764	2211	5457	4.78	13	238	54	60	28
24-Jan	57.5	12676	2278	5584	4.76	13	224	65	51	9
24-Jan	58	12913	2075	5580	4.79	12	225	61	57	27
25-Jan	58.5	12829	2165	5568	4.82	12	227	64	63	28
25-Jan	59	12336	2139	5356	4.85	11	238	67	60	28
26-Jan	59.5	13185	2211	5458	4.84	11	227	66	57	29
26-Jan	60	12203	2219	5242	4.82	12	221	60	60	28
27-Jan	60.5	12934	2235	5523	4.83	11	224	78	60	30
27-Jan	61	13503	2221	5238	4.83	12	225	68	60	27
28-Jan	61.5	12874	2275	5478	4.80		221	64	63	28
Mean		12676	2219	5518	4.83	12	226	65	60	28
S.D.		289	47	67	0.03	1	7	7	2	1
Data points		13	13	10	14	13	12	12	13	13

Steady state No 33**Table B.100:** Operating conditions for steady state number 33

Feed batch number	F15
Mass of PSS in feed (g)	400
Total Mass of feed (g)	2000
Reactor Volume (L)	20
Retention time (day)	5
Sulfate addition (gSO₄/L)	0
pH	steady state
Biological groups present	acidogens

This experiment followed steady state number 32 with a single step decrease in the feed volume.

Table B.101: Results summary for steady state number 33

Feed total COD (mg/L)	13186
Feed soluble COD (mg/L)	1382
Feed TKN (mgN/L)	252
Feed FSA (mgN/L)	42
Feed Total P (mgP/L)	60
Feed soluble P (mgP/L)	12
Steady state measured after 15 days (3 x R_h)	
Effluent total COD (mg/L)	12823 ± 293 (10)
Effluent soluble COD (mg/L)	2405 ± 55 (11)
Suspended solids (mgCOD/L)	2802
Reactor pH	4.75 ± 0.03 (11)
Gas Produced (units/day)	[9 ± 0 (11)] twice = 18
Volume per unit (ml)	48.8 ± 0.5
Gas composition (%CH₄)	*12.5
Methane production (L/day)	0.11
Methane production (gCOD/day)	0.3
Effluent TKN (mgN/L)	297 ± 31 (11)
Effluent FSA (mgN/L)	71 ± 12 (10)
Effluent Total P (mgP/L)	58 ± 3 (10)
Effluent soluble P (mgP/L)	29 ± 0 (10)
COD balance (%)	97.8
TKN balance (%)	117.9
Total P balance (%)	96.3

*Not measured – assume the same as steady state number 32

Appendix B: Steady State Data

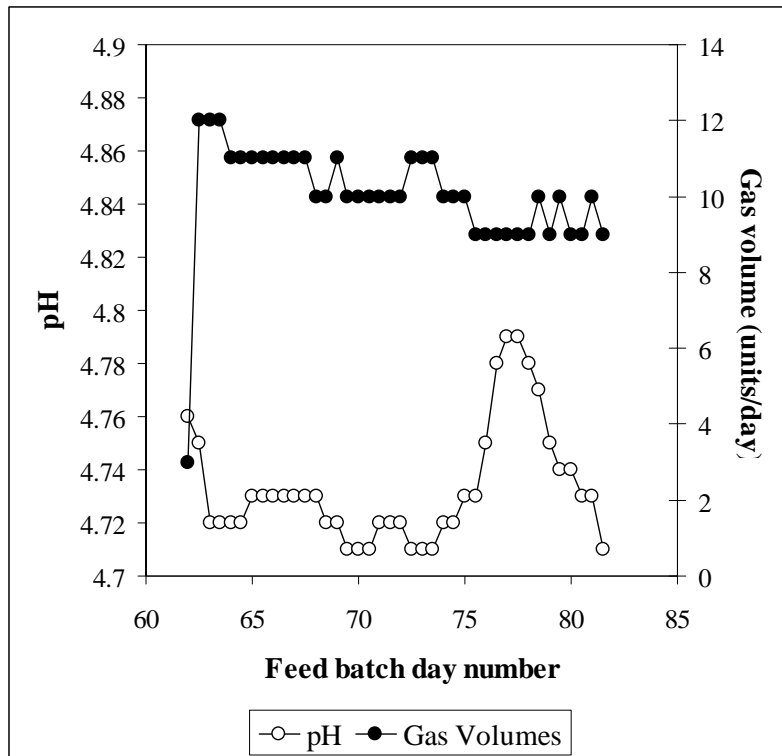


Figure B.68: Daily measurements of the pH and volumetric gas production leading up to and including steady state number 33 (steady state from day 76.5)

Appendix B: Steady State Data

Table B.102: Daily measured data for steady state number 33

Date	Day	Total COD (mgCOD/L)	Soluble COD (mgCOD/L)	Suspended Solids (mgCOD/L)	pH	Gas Volume (Units/day)	TKN (mgN/L)	NH ₃ (mgN/L)	TP (mgP/L)	PO ₄ (mgP/L)
12-Feb	76.5	12840	2352	5226	4.78	9	318	64	59	29
12-Feb	77	12284	2318	5208	4.79	9	356	82	52	29
13-Feb	77.5	12663	2316	4894	4.79	9	297	75	59	29
13-Feb	78	13413	2341	5215	4.78	9	312	74	62	29
14-Feb	78.5	13741	2381	5191	4.77	10	342	71	62	28
14-Feb	79	12627	2417	5203	4.75	9	308	66	2	29
15-Feb	79.5	12806	2405	5635	4.74	10	294	71	59	29
15-Feb	80	13022	2414	5217	4.74	9	260	71	56	28
16-Feb	80.5	13090	2484	5206	4.73	9	269	44	53	29
16-Feb	81	12875	2465	5224	4.73	10	259	35	56	17
17-Feb	81.5	12625	2446	5144	4.71	9	277	45	56	28
Mean		12823	2405	5207	4.75	9	297	71	58	29
S.D.		293	55	96	0.03	0	31	12	3	0
Data points		10	11	10	11	11	11	10	10	10

Steady state No 34**Table B.103:** Operating conditions for steady state number 34

Feed batch number	F15
Mass of PSS in feed (g)	91.6
Total Mass of feed (g)	3000
Reactor Volume (L)	20
Retention time (day)	3.33
Sulfate addition (gSO₄/L)	0
pH	steady state
Biological groups present	acidogens

Following steady state number 26, the retention time was reduced in the digester until a retention time of 6.67 days had been reached. After 10 days, the VFA concentration had increased to 99.6 mg/L as HAc, while the alkalinity had dropped to 70 mg/L as CaCO₃. The pH had also dropped to 5.89, and the methanogens were failing in the system. The feed was changed from F14 to F15, and the retention time reduced to 3.33 days.

Table B.104: Results summary for steady state number 34

Feed total COD (mg/L)	2013
Feed soluble COD (mg/L)	192
Feed TKN (mgN/L)	38
Feed FSA (mgN/L)	5
Feed Total P (mgP/L)	9
Feed soluble P (mgP/L)	2
Steady state measured after 12 days (3.6 x R_h)	
Effluent total COD (mg/L)	2053 ± 54 (10)
Effluent soluble COD (mg/L)	306 ± 14 (10)
Suspended solids (mgCOD/L)	824
Reactor pH	5.37 ± 0.02 (10)
Gas Produced (units/day)	[1 ± 1 (11)] twice = 2
Volume per unit (ml)	44.5 ± 0.5
Gas composition (%CH₄)	*12.5
Methane production (mL/day)	0.01
Methane production (mgCOD/day)	0.03
Effluent TKN (mgN/L)	32 ± 3 (9)
Effluent FSA (mgN/L)	15 ± 2 (10)
Effluent Total P (mgP/L)	9 ± 1 (11)
Effluent soluble P (mgP/L)	5 ± 1 (10)
COD balance (%)	102.2
TKN balance (%)	83.2
Total P balance (%)	97.9

*Not measured – assume the same as steady state number 33

Appendix B: Steady State Data

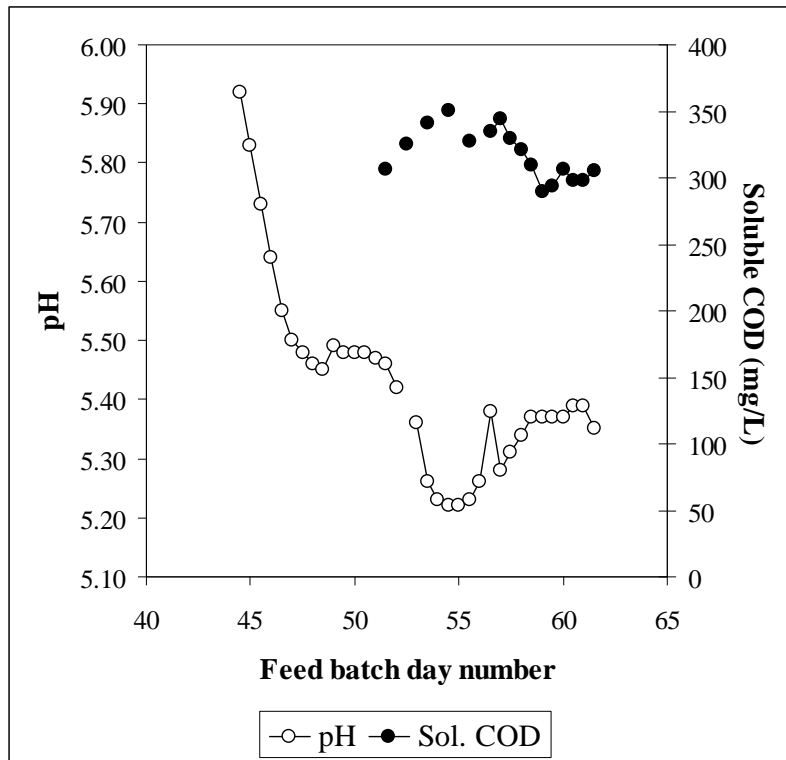


Figure B.69: Daily measurements of the pH and soluble COD concentration leading up to and including steady state number 34 (steady state from day 56.5)

Appendix B: Steady State Data

Table B.105: Daily measured data for steady state number 34

Date	Day	Total COD (mgCOD/L)	Soluble COD (mgCOD/L)	Suspended Solids (mgCOD/L)	pH	Gas Volume (Units/day)	TKN (mgN/L)	NH ₃ (mgN/L)	TP (mgP/L)	PO ₄ (mgP/L)
23-Jan	56.5	2080	335	1148	5.38	1	29	19	10	5
23-Jan	57	2060	344	1138	5.28	2	27	15	9	5
24-Jan	57.5	2058	329	1175	5.31	1	34	16	10	5
24-Jan	58	2047	321	1130	5.34	1	34	14	11	5
25-Jan	58.5	1997	310	1130	5.37	1	33	15	8	5
25-Jan	59	1974	290		5.37	1	32	12	9	6
26-Jan	59.5	2127	294	1096	5.37	1		16	10	7
26-Jan	60	2002	306	1056	5.37	1	27	6	9	9
27-Jan	60.5	1921	298		5.39	2	28	16	9	4
27-Jan	61	2062	298	1054	5.39	1	34	14	9	6
28-Jan	61.5	1933	305	1107	5.35	1		15	10	5
Mean		2053	306	1130	5.37	1	32	15	9	5
S.D.		54	14	34	0.02	1	3	2	1	1
Data points		10	10	8	10	11	9	10	11	10

Steady state No 35**Table B.106:** Operating conditions for steady state number 35

Feed batch number	F15
Mass of PSS in feed (g)	61
Total Mass of feed (g)	2000
Reactor Volume (L)	20
Retention time (day)	5
Sulfate addition (gSO₄/L)	0
pH	steady state
Biological groups present	acidogens

This experiment followed directly from steady state number 34, with a single step decrease in the feed volume.

Table B.107: Results summary for steady state number 35

Feed total COD (mg/L)	2011
Feed soluble COD (mg/L)	211
Feed TKN (mgN/L)	38
Feed FSA (mgN/L)	6
Feed Total P (mgP/L)	9
Feed soluble P (mgP/L)	2
Steady state measured after 14 days (2.8 x R_h)	
Effluent total COD (mg/L)	1915 ± 71 (11)
Effluent soluble COD (mg/L)	359 ± 7 (10)
Suspended solids (mgCOD/L)	880
Reactor pH	5.05 ± 0.01 (13)
Gas Produced (units/day)	[1 ± 0 (12)] twice = 2
Volume per unit (ml)	44.5 ± 0.5
Gas composition (%CH₄)	*12.5
Methane production (mL/day)	0.01
Methane production (mgCOD/day)	0.03
Effluent TKN (mgN/L)	44 ± 2 (12)
Effluent FSA (mgN/L)	9 ± 4 (11)
Effluent Total P (mgP/L)	9 ± 1 (12)
Effluent soluble P (mgP/L)	5 ± 1 (11)
COD balance (%)	95.6
TKN balance (%)	114.5
Total P balance (%)	98.0

*Not measured – assume the same as steady state number 34 –has insignificant influence

Appendix B: Steady State Data

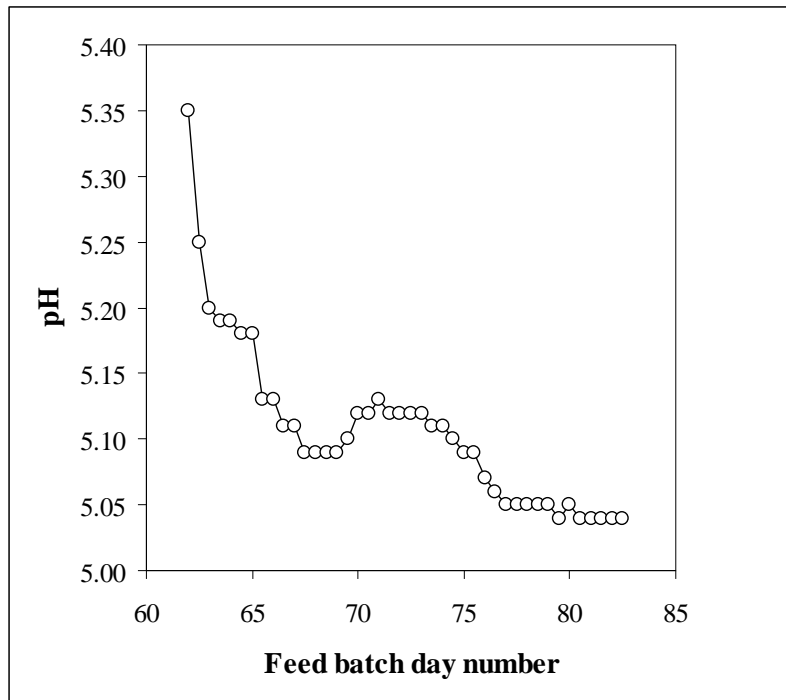


Figure B.70: Daily measurements of the pH leading up to and including steady state number 35 (steady state from day 76.5)

Appendix B: Steady State Data

Table B.108: Daily measured data for steady state number 35

Date	Day	Total COD (mgCOD/L)	Soluble COD (mgCOD/L)	Suspended Solids (mgCOD/L)	pH	Gas Volume (Units/day)	TKN (mgN/L)	NH ₃ (mgN/L)	TP (mgP/L)	PO ₄ (mgP/L)
12-Feb	76.5	1909	349		5.06	1	45	11	10	5
12-Feb	77	2074	353	1189	5.05	1	44	10	10	5
13-Feb	77.5	2139	359	1225	5.05	1	45	9	7	5
13-Feb	78	1980			5.05	1	45		10	
14-Feb	78.5	2094	363	1263	5.05	1	44	10	10	6
14-Feb	79	1884	368	1258	5.05	1	45	14	9	6
15-Feb	79.5	1896	367	1262	5.04	1	43	9	9	6
15-Feb	80	1983	372	1224	5.05	1	40	12	9	6
16-Feb	80.5	1875	351	1252	5.04	1	40	3	8	4
16-Feb	81	1915	357	1285	5.04	1	39	3	8	4
17-Feb	81.5	1951	358	1218	5.04	1	41	3	8	4
17-Feb	82	1915	333	1225	5.04	1	40	3	8	5
18-Feb	82.5				5.04		45	11	10	5
Mean		1915	359	1239	5.05	1	44	9	9	5
S.D.		71	7	27	0.01	0	2	4	1	1
Data points		11	10	10	13	12	12	11	12	11

Steady state No 36**Table B.109:** Operating conditions for steady state number 36

Feed batch number	F15
Mass of PSS in feed (g)	56
Total Mass of feed (g)	1000
Reactor Volume (L)	16
Retention time (day)	8
Sulfate addition (gSO₄/L)	2
pH	controlled to ~ 6.5
Biological groups present	acidogens and sulfidogens

This experiment followed steady state number 22. The pH was changed from 7.0 to 6.5 over 2 days, and then controlled by addition of 1M HCl only.

Table B.110: Results summary for steady state number 36

Feed total COD (mg/L)	1950
Feed soluble COD (mg/L)	278
Feed TKN (mgN/L)	43
Feed FSA (mgN/L)	13
Feed Total P (mgP/L)	10
Feed soluble P (mgP/L)	3
Steady state measured after 46 days (5.75 x R_h)	
Effluent total COD (mg/L)	1304 ± 48 (11)
Effluent soluble organic COD (mg/L)	80 ± 11 (12)
Effluent total soluble COD (mg/L)	521 ± 24 (12)
Suspended solids (mgCOD/L)	434 ± 30
Sulfate concentration (mgSO₄/L)	436 ± 20 (12)
Effluent VFA (mg/L as HAc)	0 ± 1 (11)
Effluent Alkalinity (mg/L as CaCO₃)	354 ± 10 (12)
Reactor pH	6.47 ± 0.01 (12)
Gas Produced (units/day)	9 ± 0 (12)
Volume per unit (ml)	47.3 ± 0.4
Gas composition (%CH₄)	*0
Effluent TKN (mgN/L)	46 ± 1 (8)
Effluent FSA (mgN/L)	16 ± 3 (12)
Effluent Total P (mgP/L)	8 ± 0 (8)
Effluent soluble P (mgP/L)	4 ± 0 (12)
COD balance (%)	** Not possible
TKN balance (%)	106.7
Total P balance (%)	83.1

* Assume methanogenesis had not resumed in digester

** No gaseous sulfide measurement

Appendix B: Steady State Data

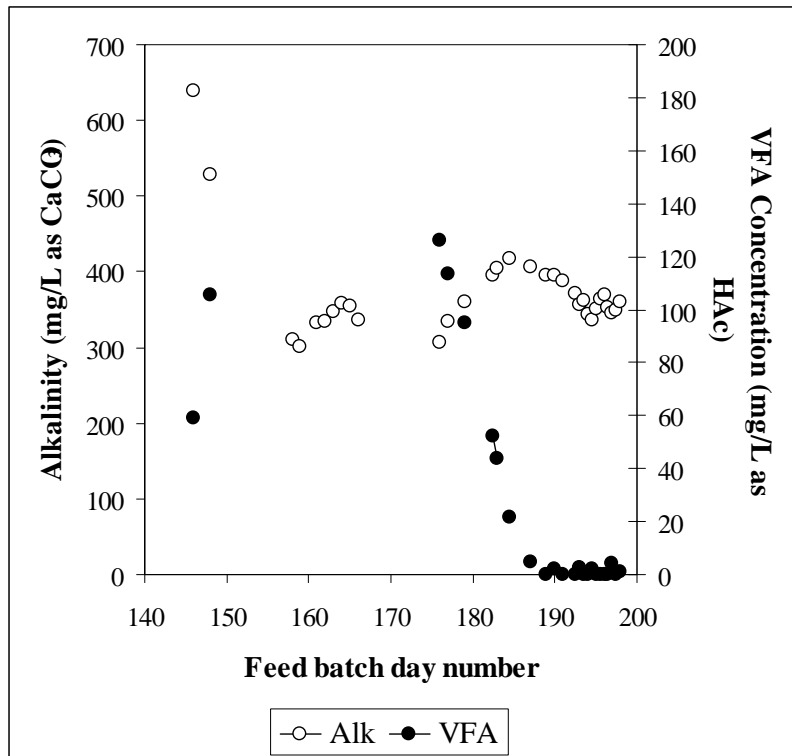


Figure B.71: Daily measurements of the VFA and alkalinity leading up to and including steady state number 36 (steady state from day 192.5)

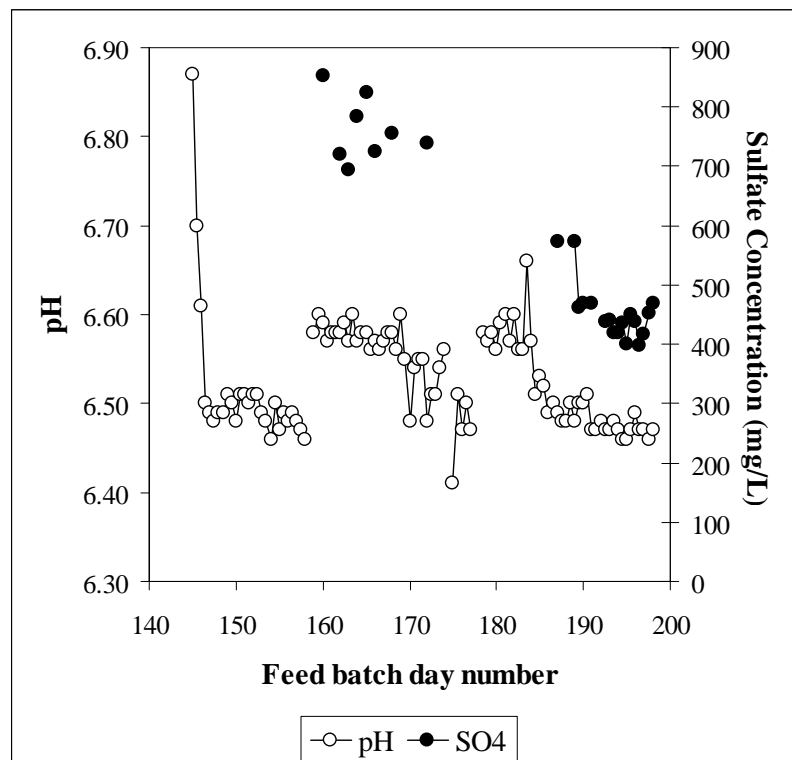


Figure B.72: Daily measurements of pH and sulfate concentration leading up to and including steady state number 36 (steady state from day 192.5)

Appendix B: Steady State Data

Table B.111: Daily measured data for steady state number 36

Date	Day	Total COD (mg/L)	Soluble Organic COD (mg/L)	Total Soluble COD (mg/L)	Suspended Solids (mg/L)	Susp. Solids Soluble COD (mg/L)	VFA (mg/L as HAc)	Alkalinity (mg/L as CaCO ₃)	pH	Sulfate (mg/L)	TKN (mgN/L)	NH ₃ (mgN/L)	TP (mgP/L)	PO ₄ (mgP/L)
28-Mar	192.5	1345	67	509	879	462	0	370.5	6.47	437		13		4
29-Mar	193	1457	67	522			2.7	355.7	6.47	440		13		4
29-Mar	193.5	1329	60	541	928	463	0	362	6.48	420	46	13	8	4
30-Mar	194	1331	81	514	931	469	0	342.7	6.47	420	46	21	8	5
30-Mar	194.5	1301	87	522	893	440	1.9	336.9	6.46	435	46	21	5	4
31-Mar	195	1284	83	496	892	410	0	350.3	6.46	400		15		4
31-Mar	195.5	1281	80	520	884	429	0	364.6	6.47	450	46	18	8	4
01-Apr	196	1285	73	556	902	482	0	368.9	6.49	437	46	18	8	4
01-Apr	196.5	1650	61	490	848	406	0	352.4	6.47	399	52	16	8	4
02-Apr	197	1304	79	550	830	439	4.3	344.8	6.47	418	48	18	8	4
02-Apr	197.5	1297	83	558	925	477	0.2	348.6	6.46	453	48	16	8	4
03-Apr	198	1313	102	484	901	472	1.3	360.9	6.47	468	46	15	7	4
	Mean	1304	80	521	897	463	0	354	6.47	436	46	16	8	4
	S.D.	48	11	24	24	18	1	10	0.01	20	1	3	0	0
	Data points	11	12	12	10	9	11	12	12	12	8	12	8	12

Steady state No 37**Table B.112:** Operating conditions for steady state number 37

Feed batch number	F15
Mass of PSS in feed (g)	30.6
Total Mass of feed (g)	1000
Reactor Volume (L)	16
Retention time (day)	8
Sulfate addition (gSO₄/L)	0
pH	Controlled to ~ 7.5
Biological groups present	Acidogens and methanogens

The digester was reseeded with waste methanogenic sludge. The pH was controlled immediately to 7.5 by addition of 1M NaOH.

Table B.113: Results summary for steady state number 37

Feed total COD (mg/L)	2017
Feed soluble COD (mg/L)	221
Feed TKN (mgN/L)	39
Feed FSA (mgN/L)	10
Feed Total P (mgP/L)	9
Feed soluble P (mgP/L)	2
Steady state measured after 26 days (3.25 x R_h)	
Effluent total COD (mg/L)	921 ± 18 (9)
Effluent soluble COD (mg/L)	33 ± 6 (9)
Suspended solids (mgCOD/L)	347
Effluent VFA (mg/L as HAc)	2 ± 2 (9)
Effluent Alkalinity (mg/L as CaCO₃)	421 ± 3 (9)
Reactor pH	7.49 ± 0.02 (9)
Gas Produced (units/day)	[10 ± 0 (9)] twice = 20
Volume per unit (ml)	49.7 ± 0.4
Gas composition (%CH₄)	*81.63
Methane production (L/day)	0.81
Methane production (gCOD/day)	2.2
Effluent TKN (mgN/L)	28 ± 3 (9)
Effluent FSA (mgN/L)	23 ± 1 (8)
Effluent Total P (mgP/L)	10 ± 0 (9)
Effluent soluble P (mgP/L)	3 ± 0 (9)
COD balance (%)	99.2
TKN balance (%)	72.6
Total P balance (%)	108.6

* One sample analysed for steady state period

Appendix B: Steady State Data

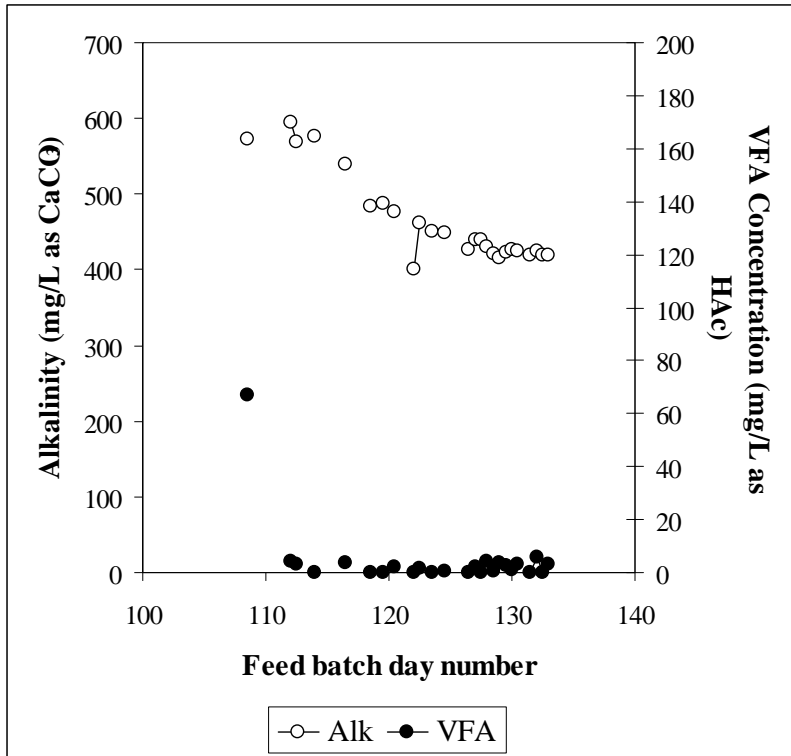


Figure B.73: Daily measurements of the VFA and alkalinity leading up to and including steady state number 37 (steady state from day 128.5)

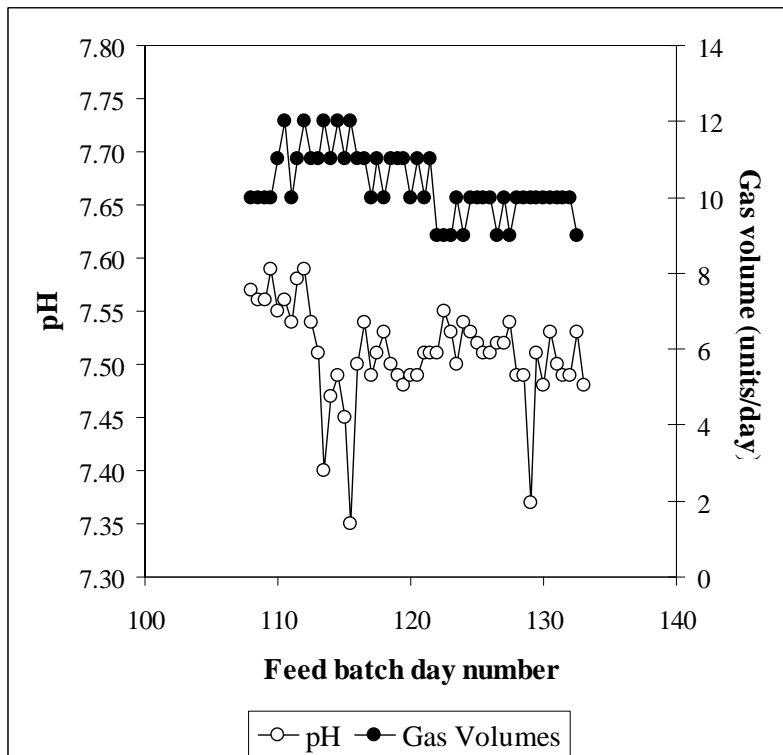


Figure B.74: Daily measurements of the pH and volumetric gas production leading up to and including steady state number 37 (steady state from day 128.5)

Appendix B: Steady State Data

Table B.114: Daily measured data for steady state number 37

Date	Day	Total COD (mgCOD/L)	Soluble COD (mgCOD/L)	Suspended Solids (mgCOD/L)	VFA (mg/L as HAc)	Alkalinity (mg/L as CaCO ₃)	pH	Gas Volume (Units/day)	TKN (mgN/L)	NH ₃ (mgN/L)	TP (mgP/L)	PO ₄ (mgP/L)
04-Apr	128.5	939	33	387	0.3	421.1	7.49	10	28	22	10	3
04-Apr	129	942	33	384	3.7	415.4	7.37	10	27	27	10	3
05-Apr	129.5	931	39	385	2.4	422.8	7.51	10	32	25	12	3
05-Apr	130	885	44	379	1.1	427.5	7.48	10	36	23	11	3
06-Apr	130.5	914	37	380	3.1	424.4	7.53	10	27	22	11	3
06-Apr	131	931					7.50	10	28		10	
07-Apr	131.5	921	36	368	0	420.1	7.49	10	24	22	10	3
07-Apr	132	916	25	353	5.9	424.5	7.49	10	32	24	11	3
08-Apr	132.5	986	26	373	0	418.6	7.53	9	33	22	10	3
08-Apr	133	896	25	365	3.4	419.5	7.48		25	24	10	3
	Mean	921	33	380	2	421	7.49	10	28	23	10	3
	S.D.	18	6	8	2	3	0.02	0	3	1	0	0
	Data points	9	9	8	9	9	9	9	9	8	9	9

Steady state No 38**Table B.115:** Operating conditions for steady state number 38

Feed batch number	F15
Mass of PSS in feed (g)	200
Total Mass of feed (g)	1000
Reactor Volume (L)	20
Retention time (day)	10
Sulfate addition (gSO₄/L)	0
pH	steady state
Biological groups present	acidogens

This experiment followed directly from steady state number 33. The system was fed once a day for the first 18 days, and then twice daily for the last 7 days.

Table B.116: Results summary for steady state number 38

Feed total COD (mg/L)	13186
Feed soluble COD (mg/L)	1467
Feed TKN (mgN/L)	252
Feed FSA (mgN/L)	57
Feed Total P (mgP/L)	60
Feed soluble P (mgP/L)	12
Steady state measured after 25 days (2.5 x R_h)	
Effluent total COD (mg/L)	12782 ± 222 (8)
Effluent soluble COD (mg/L)	2732 ± 31 (11)
Suspended solids (mgCOD/L)	3210
Reactor pH	4.83 ± 0.01 (13)
Gas Produced (units/day)	[7 ± 1 (13)] twice = 14
Volume per unit (ml)	48.8 ± 0.5
Gas composition (%CH₄)	*12.5
Methane production (mL/day)	85.4
Methane production (mgCOD/day)	227.2
Effluent TKN (mgN/L)	280 ± 8 (8)
Effluent FSA (mgN/L)	84 ± 1 (10)
Effluent Total P (mgP/L)	59 ± 2 (8)
Effluent soluble P (mgP/L)	31 ± 1 (11)
COD balance (%)	97.8
TKN balance (%)	111.1
Total P balance (%)	98.0

*Not measured – assume the same as steady state number 33 - has insignificant influence

Appendix B: Steady State Data

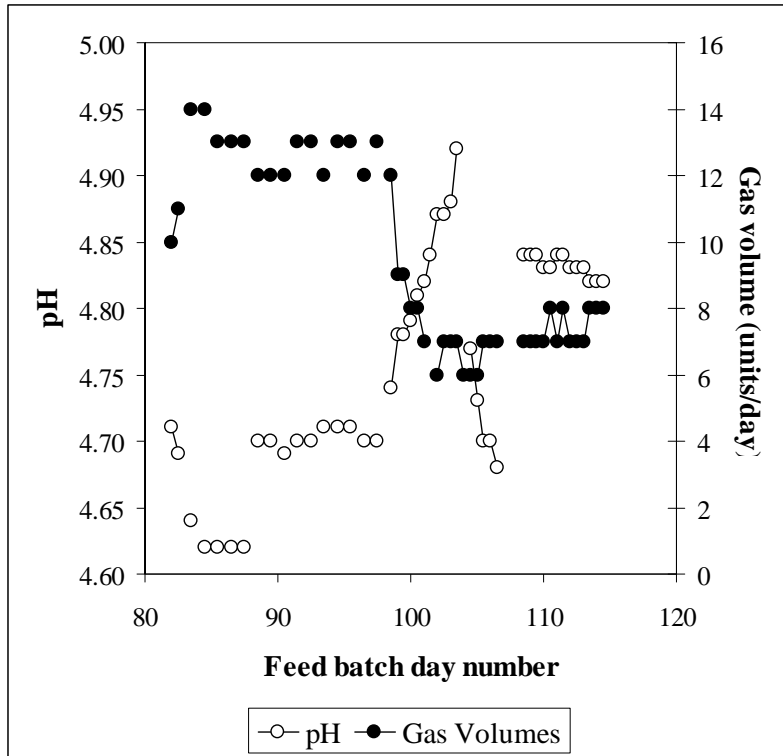


Figure B.75: Daily measurements of the pH and volumetric gas production leading up to and including steady state number 38 (steady state from day 108)

Appendix B: Steady State Data

Table B.117: Daily measured data for steady state number 38

Date	Day	Total COD (mgCOD/L)	Soluble COD (mgCOD/L)	Suspended Solids (mgCOD/L)	pH	Gas Volume (Units/day)	TKN (mgN/L)	NH ₃ (mgN/L)	TP (mgP/L)	PO ₄ (mgP/L)
14-Mar	108	12560	2714	6036			302	85	62	31
15-Mar	108.5	12704	2737	6180	4.84	7	286	85	59	31
15-Mar	109	13185	2759	6021	4.84	7	279	84	62	31
16-Mar	109.5	13120	2775	6151	4.84	7	283	80	59	31
16-Mar	110	12836	2694	5916	4.83	7	286	84	59	31
17-Mar	110.5				4.83	8				
17-Mar	111				4.84	7				
18-Mar	111.5	12754	2732	6096	4.84	8	260	84	56	30
18-Mar	112		2744	5904	4.83	7		82		31
19-Mar	112.5	12809	2786	5724	4.83	7	277	84	56	30
19-Mar	113		2617	5789	4.83	7		83		30
20-Mar	113.5		2711	5748	4.82	8				
20-Mar	114	12530	2714	5829	4.82	8	280	85	59	31
21-Mar	114.5	11975	2681	5968	4.82	8	277	85	65	31
Mean		12782	2732	5942	4.83	7	280	59	84	31
S.D.		222	31	148	0.01	1	8	2	1	1
Data points		8	11	12	13	13	8	8	10	11

Steady state No 39**Table B.118:** Operating conditions for steady state number 39

Feed batch number	F15
Mass of PSS in feed (g)	30.6
Total Mass of feed (g)	1000
Reactor Volume (L)	20
Retention time (day)	10
Sulfate addition (gSO₄/L)	0
pH	steady state
Biological groups present	acidogens

This experiment followed steady state 35 by decreasing the feed volume in a single step.

Table B.119: Results summary for steady state number 39

Feed total COD (mg/L)	2017
Feed soluble COD (mg/L)	224
Feed TKN (mgN/L)	39
Feed FSA (mgN/L)	9
Feed Total P (mgP/L)	9
Feed soluble P (mgP/L)	2
Steady state measured after 24 days (2.4 x R_h)	
Effluent total COD (mg/L)	1934 ± 65 (9)
Effluent soluble COD (mg/L)	434 ± 4 (11)
Suspended solids (mgCOD/L)	840
Reactor pH	5.19 ± 0.01 (14)
Gas Produced (units/day)	1 ± 0 (13)
Volume per unit (ml)	44.5 ± 0.5
Gas composition (%CH₄)	*12.5
Methane production (mL/day)	11.12
Methane production (mgCOD/day)	29.6
Effluent TKN (mgN/L)	47 ± 1 (8)
Effluent FSA (mgN/L)	17 ± 1 (12)
Effluent Total P (mgP/L)	9 ± 1 (8)
Effluent soluble P (mgP/L)	6 ± 0 (12)
COD balance (%)	96.6
TKN balance (%)	121.9
Total P balance (%)	97.7

*Not measured – assume the same as steady state number 35 – has insignificant influence

Appendix B: Steady State Data

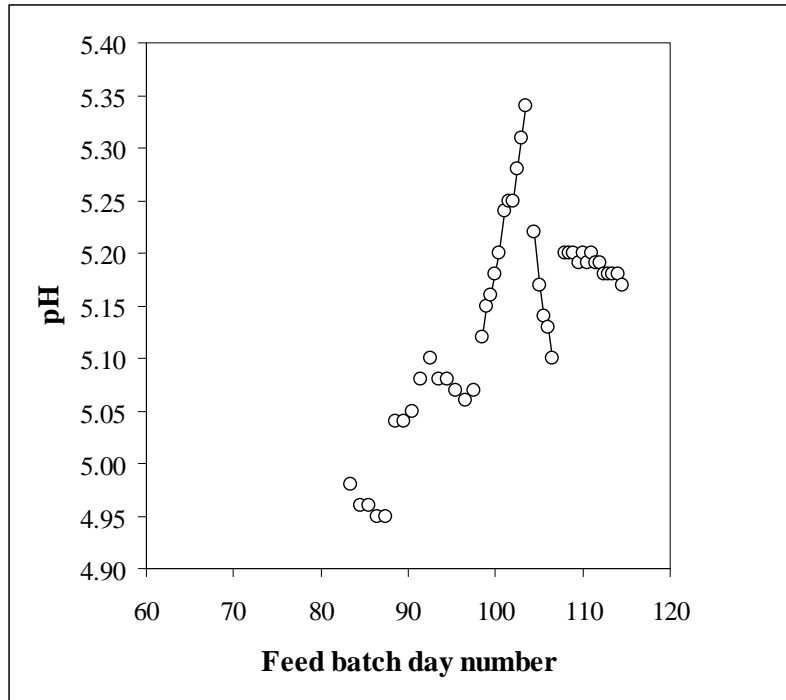


Figure B.76: Daily measurements of the pH leading up to and including steady state number 39 (steady state from day 108)

Appendix B: Steady State Data

Table B.120: Daily measured data for steady state number 39

Date	Day	Total COD (mgCOD/L)	Soluble COD (mgCOD/L)	Suspended Solids (mgCOD/L)	pH	Gas Volume (Units/day)	TKN (mgN/L)	NH ₃ (mgN/L)	TP (mgP/L)	PO ₄ (mgP/L)
14-Mar	108	1947	434	1247	5.20		48	15	10	6
15-Mar	108.5	1913	435	1284	5.20	1	50	16	9	6
15-Mar	109	2060	443	1286	5.20	1	46	17	9	6
16-Mar	109.5	1911	442	1315	5.19	1	53	14	9	6
16-Mar	110	1934	439	1182	5.20	1	46	15	10	6
17-Mar	110.5				5.19	1				
17-Mar	111				5.20	1				
18-Mar	111.5	2031	432	1301	5.19	1	48	18	11	6
18-Mar	112		444	1154	5.19	1		17		6
19-Mar	112.5	1927	436	1276	5.18	1	46	16	9	6
19-Mar	113		434	1166	5.18	1		15		6
20-Mar	113.5		432	1272	5.18	1		17		6
20-Mar	114	2005	432	1251	5.18	1	46	17	9	6
21-Mar	114.5	1837	434	1263	5.17	1	47	17	9	6
Mean		1934	434	1274	5.19	1	47	17	9	6
S.D.		65	4	35	0.01	0	1	1	1	0
Data points		9	11	10	14	13	8	12	8	12

Steady state No 40**Table B.121:** Operating conditions for steady state number 40

Feed batch number	F15
Mass of PSS in feed (g)	61
Total Mass of feed (g)	2000
Reactor Volume (L)	20
Retention time (day)	5
Sulfate addition (gSO₄/L)	0
pH	controlled to ~ 6.0
Biological groups present	acidogens

This experiment followed directly from steady state number 39. The feed volume was increased and the pH controlled to 6.0 in a single step.

Table B.122: Results summary for steady state number 40

Feed total COD (mg/L)	2011
Feed soluble COD (mg/L)	220
Feed TKN (mgN/L)	38
Feed FSA (mgN/L)	10
Feed Total P (mgP/L)	9
Feed soluble P (mgP/L)	2
Steady state measured after 15 days (3 x R_h)	
Effluent total COD (mg/L)	1969 ± 52 (11)
Effluent soluble COD (mg/L)	424 ± 33 (11)
Suspended solids (mgCOD/L)	726
Reactor pH	6.04 ± 0.02 (12)
Gas Produced (units/day)	2 ± 1 (11)
Volume per unit (ml)	44.5 ± 0.5
Gas composition (%CH₄)	*12.5
Methane production (mL/day)	22.2
Methane production (mgCOD/day)	59.2
Effluent TKN (mgN/L)	43 ± 1 (12)
Effluent FSA (mgN/L)	11 ± 4 (11)
Effluent Total P (mgP/L)	9 ± 0 (12)
Effluent soluble P (mgP/L)	4 ± 1 (12)
COD balance (%)	96.9
TKN balance (%)	111.9
Total P balance (%)	98.0

*Not measured – assume the same as steady state number 34 –has insignificant influence

Appendix B: Steady State Data

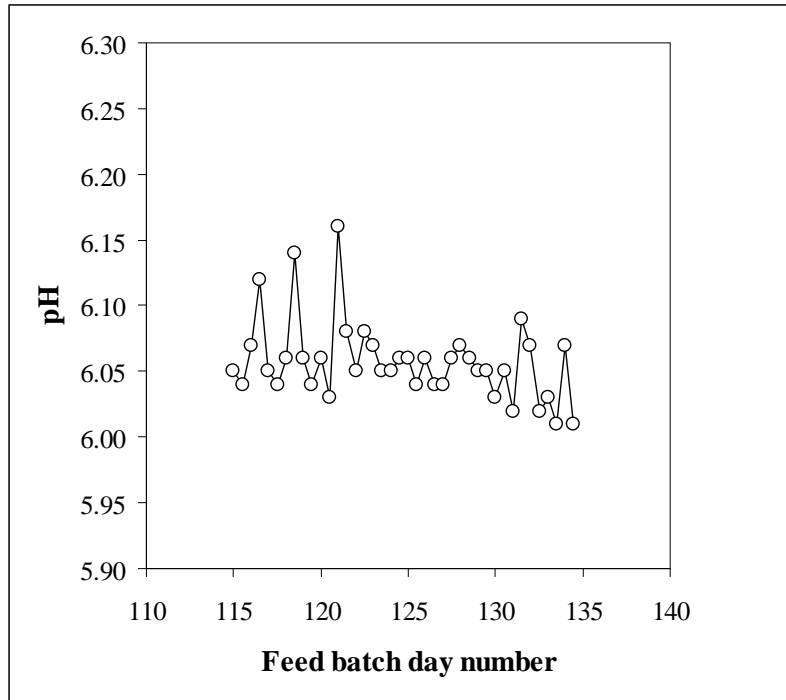


Figure B.77: Daily measurements of the pH leading up to and including steady state number 40 (steady state from day 129)

Appendix B: Steady State Data

Table B.123: Daily measured data for steady state number 40

Date	Day	Total COD (mgCOD/L)	Soluble COD (mgCOD/L)	Suspended Solids (mgCOD/L)	pH	Gas Volume (Units/day)	TKN (mgN/L)	NH ₃ (mgN/L)	TP (mgP/L)	PO ₄ (mgP/L)
04-Apr	129	1988	435		6.05	3	42	36	9	4
05-Apr	129.5	1929	427	1152	6.05	1	44	11	9	4
05-Apr	130	2062	428	1147	6.03		43	18	9	4
06-Apr	130.5	1969	427	1109	6.05	2	45	17	9	4
06-Apr	131	1923	415	1144	6.02	2	45	6	9	4
07-Apr	131.5	2004	424	1164	6.09	2	43	11	9	4
07-Apr	132	1969	330	1145	6.07	2	43	14	9	4
08-Apr	132.5	1890	376	1185	6.02	2	42	8	9	3
08-Apr	133	1988	427	1168	6.03	2	44	8	9	3
09-Apr	133.5	2129	407	1250	6.01	2	42	11	9	4
09-Apr	134	1870	141	1146	6.07	2	42	6	8	4
10-Apr	134.5	1978	361	1213	6.01	2	45	4	9	3
	Mean	1969	424	1150	6.04	2	43	11	9	4
	S.D.	52	33	26	0.02	1	1	4	0	1
	Data points	11	11	10	12	11	12	11	11	12

Steady state No 41**Table B.124:** Operating conditions for steady state number 41

Feed batch number	F15
Mass of PSS in feed (g)	38.2
Total Mass of feed (g)	1250
Reactor Volume (L)	20
Retention time (day)	16
Sulfate addition (gSO₄/L)	2
pH	steady state
Biological groups present	acidogens and sulfidogens

This digester was operated for 49 days at a 8-day retention time with the feed described in Table B.123 (38.2gF15 up to 1250g with water twice per day). Since the VFA concentration would not drop below about 200mg/L, the feed was changed from F14 to F15, and the retention time doubled.

Table B.125: Results summary for steady state number 41

Feed total COD (mg/L)	2015
Feed soluble COD (mg/L)	207
Feed TKN (mgN/L)	39
Feed FSA (mgN/L)	6
Feed Total P (mgP/L)	9
Feed soluble P (mgP/L)	2
Steady state measured after 26 days (1.625 x R_h)	
Effluent total COD (mg/L)	1697 ± 41 (13)
Effluent soluble organic COD (mg/L)	85 ± 10 (12)
Effluent total soluble COD (mg/L)	897 ± 41 (12)
Suspended solids (mgCOD/L)	454
Sulfate concentration (mgSO₄/L)	** no data
Effluent VFA (mg/L as HAc)	0 ± 1 (10)
Effluent Alkalinity (mg/L as CaCO₃)	1633 ± 41 (9)
Reactor pH	7.64 ± 0.01 (13)
Gas Produced (units/day)	0 ± 1 (13)
Volume per unit (ml)	~ 50
Gas composition (%CH₄)	*0
Effluent TKN (mgN/L)	45 ± 1 (12)
Effluent FSA (mgN/L)	11 ± 1 (10)
Effluent Total P (mgP/L)	8 ± 1 (11)
Effluent soluble P (mgP/L)	4 ± 1 (9)
COD balance (%)	** Not possible
TKN balance (%)	116.9
Total P balance (%)	87.0

* Assume methanogenesis had not resumed in digester

** No gaseous sulfide measurement

Appendix B: Steady State Data

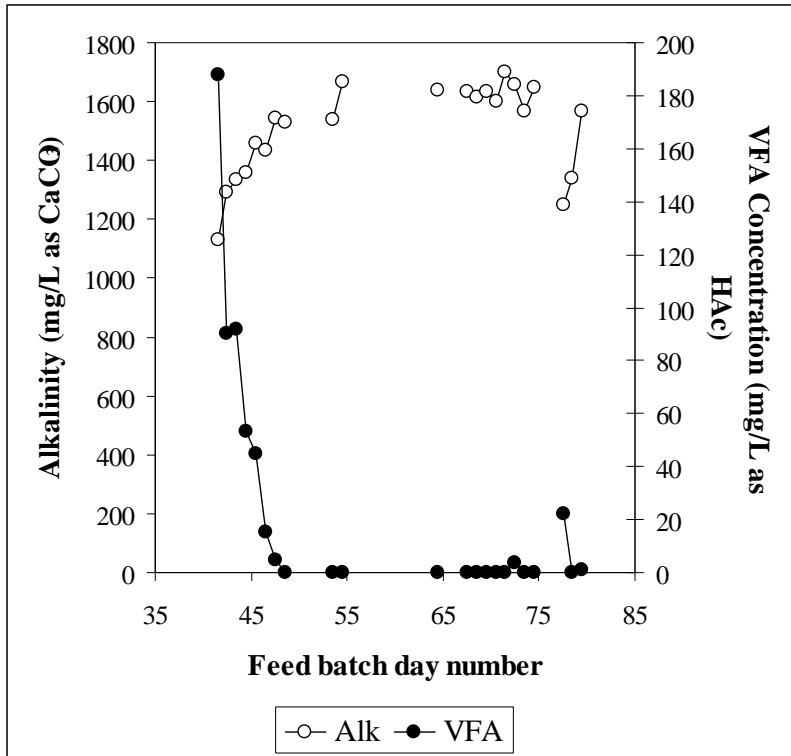


Figure B.78: Daily measurements of the VFA and alkalinity leading up to and including steady state number 41 (steady state from day 67.5)

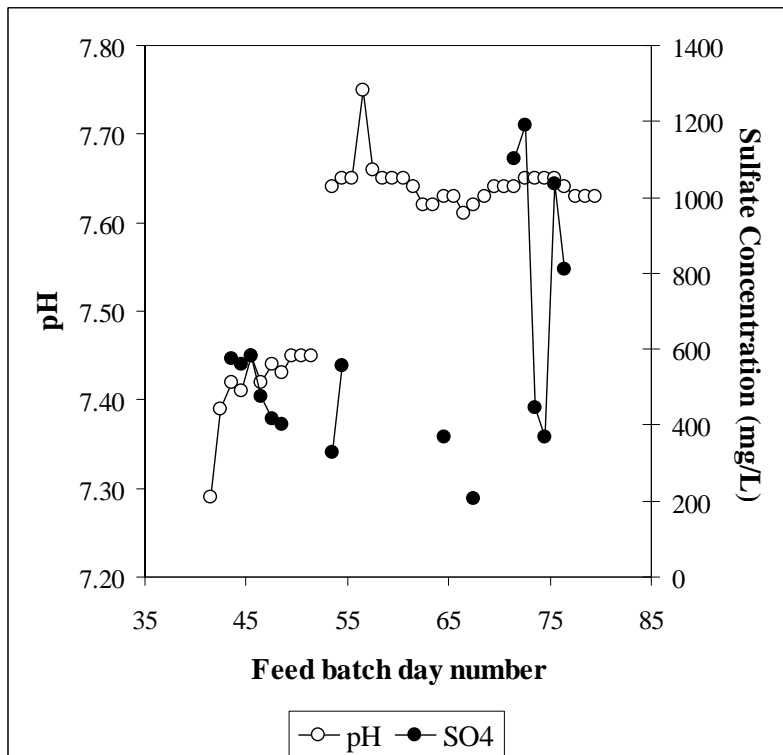


Figure B.79: Daily measurements of the pH and sulfate concentration leading up to and including steady state number 41 (steady state from day 67.5)

Appendix B: Steady State Data

Table B.126: Daily measured data for steady state number 41

Date	Day	Total COD (mgCOD/L)	Soluble Organic COD (mgCOD/L)	Total Soluble COD (mgCOD/L)	Suspended Solids (mgCOD/L)	Susp. Solids Soluble COD (mgCOD/L)	VFA (mg/L as HAC)	Alkalinity (mg/L as CaCO ₃)	pH	Sulfate (mgSO ₄ /L)	TKN (mgN/L)	NH ₃ (mgN/L)	TP (mgP/L)	PO ₄ (mgP/L)
03-Feb	67.5	1685	75	929	1284	898	0	1635.1	7.62	205	45	11	9	8
04-Feb	68.5	1768	87	856	1317	778	0	1612.7	7.63		45	13	9	4
05-Feb	69.5	1669	80	905	1348	693	0	1633.2	7.64		45	13	9	4
06-Feb	70.5	1697	70	892	1348	762	0	1599.9	7.64		44	13	8	4
07-Feb	71.5	1769	86	868	1287	827	0	1699.3	7.64	1102	45	10	8	5
08-Feb	72.5	1726	109	892	1322	788	3.6	1656.6	7.65	1190	44	11	8	3
09-Feb	73.5	1677	105	955	1356	905	0	1568.4	7.65	445	45	9	8	4
10-Feb	74.5	1709	85	860	1228	812	0	1649.3	7.65	370	45	10	11	4
11-Feb	75.5	1660	84	897	1357	895			7.65	1035	44	11	8	3
12-Feb	76.5	1737	88	896	1334	916			7.64	810	44	11	7	3
13-Feb	77.5	1629	108	977	1262	878	22.3	1249.3	7.63		44		7	
14-Feb	78.5	1673	85	978	1399	928	0	1339.4	7.63		44		7	
15-Feb	79.5	1743	83	991	1366	956	1.1	1565.4	7.63		15		3	
Mean		1697	85	897	1341	887	0	1633	7.64	problem with sample storage	45	11	8	4
S.D.		41	10	41	38	62	1	41	0.01		1	1	1	1
Data points		13	12	12	12	12	10	9	13		12	10	11	9

Steady state No 42**Table B.127:** Operating conditions for steady state number 42

Feed batch number	F15
Mass of PSS in feed (g)	45.8
Total Mass of feed (g)	1500
Reactor Volume (L)	20
Retention time (day)	13.3
Sulfate addition (gSO₄/L)	2
pH	steady state
Biological groups present	acidogens and sulfidogens

This experiment followed steady state number 42. The feed volume was incremented by 50g per feed until the new operating volume was reached.

Table B.128: Results summary for steady state number 42

Feed total COD (mg/L)	2013
Feed soluble COD (mg/L)	221
Feed TKN (mgN/L)	38
Feed FSA (mgN/L)	10
Feed Total P (mgP/L)	9
Feed soluble P (mgP/L)	2
Steady state measured after 40 days (3 x R_h)	
Effluent total COD (mg/L)	1749 ± 34 (12)
Effluent soluble organic COD (mg/L)	129 ± 23 (12)
Effluent total soluble COD (mg/L)	964 ± 63 (12)
Suspended solids (mgCOD/L)	448
Sulfate concentration (mgSO₄/L)	147 ± 39 (12)
Effluent VFA (mg/L as HAc)	57 ± 16 (11)
Effluent Alkalinity (mg/L as CaCO₃)	1573 ± 41 (11)
Reactor pH	7.75 ± 0.01 (10)
Gas Produced (units/day)	1 ± 1 (13)
Volume per unit (ml)	~ 50
Gas composition (%CH₄)	*0
Effluent TKN (mgN/L)	127 ± 3 (12)
Effluent FSA (mgN/L)	19 ± 1 (12)
Effluent Total P (mgP/L)	25 ± 1 (13)
Effluent soluble P (mgP/L)	4 ± 1 (13)
COD balance (%)	**Not possible
TKN balance (%)	335.3
Total P balance (%)	272.0

* Assume methanogenesis had not resumed in digester

** No gaseous sulfide measurement

No idea what happened to TKN and TP measurements

Appendix B: Steady State Data

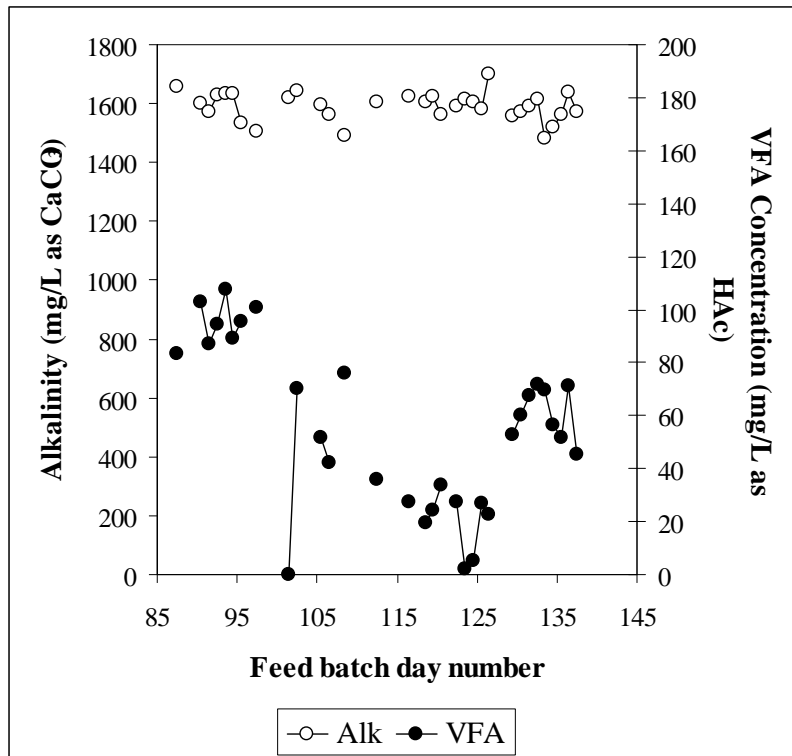


Figure B.80: Daily measurements of the VFA and alkalinity leading up to and including steady state number 42 (steady state from day 124.5)

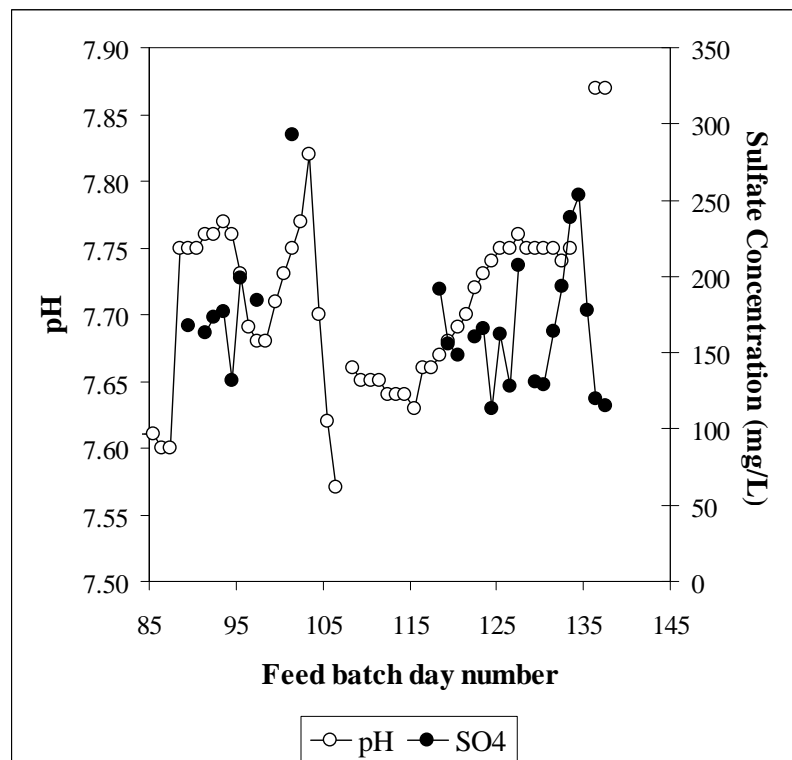


Figure B.81: Daily measurements of the pH and sulfate concentration leading up to and including steady state number 42 (steady state from day 124.5)

Appendix B: Steady State Data

Table B.129: Daily measured data for steady state number 42

Date	Day	Total COD (mgCOD/L)	Soluble Organic COD (mgCOD/L)	Total Soluble COD (mgCOD/L)	Suspended Solids (mgCOD/L)	Susp. Solids Soluble COD (mgCOD/L)	VFA (mg/L as HAC)	Alkalinity (mg/L as CaCO ₃)	pH	Sulfate (mgSO ₄ /L)	TKN (mgN/L)	NH ₃ (mgN/L)	TP (mgP/L)	PO ₄ (mgP/L)
31-Mar	124.5	1781	298	1410	1351	1352	5.4	1607.3	7.74	113	128	19	25	4
01-Apr	125.5	1804	125	1016	1302	1031	27	1580.9	7.75	162	129	18	23	4
02-Apr	126.5	1690	97	1035	1399	965	22.6	1701.1	7.75	128	133	19	25	4
03-Apr	127.5	1655	98	863	1275	814			7.76	207	127	17	24	5
04-Apr	128.5								7.75					
05-Apr	129.5	1746	112	893	1346	814	52.8	1560.0	7.75	131	138	18	25	4
06-Apr	130.5	1782	125	950	1378	879	60.3	1572.8	7.75	129	130	21	25	5
07-Apr	131.5	1755	126	947	1396	928	67.3	1593.2	7.75	164	129	19	24	4
08-Apr	132.5	1739	137	896	1326	825	72	1612.9	7.74	193	127	19	23	4
09-Apr	133.5	1712	169	1021	1324	928	69.9	1480.4	7.75	239	125	17	24	4
10-Apr	134.5	1798	169	983			56.6	1519.8		253	124	19	24	4
11-Apr	135.5	1746	151	989	1234	770	51.9	1563.8		178	127	21	25	3
12-Apr	136.5	1751	142	834	1246	778	71.2	1636.4	7.87	120	122	17	25	3
13-Apr	137.5	1713	131	977	1327	904	45.2	1573.1	7.87	115	126	14	25	4
Mean		1749	129	964	1327	879	57	1573	7.75	147	127	19	25	4
S.D.		34	23	63	52	79	16	41	0.01	39	3	1	1	1
Data points		12	12	12	12	11	11	11	10	12	12	12	13	13

Steady state No 43**Table B.130:** Operating conditions for steady state number 43

Feed batch number	F15
Mass of PSS in feed (g)	61
Total Mass of feed (g)	2000
Reactor Volume (L)	20
Retention time (day)	5
Sulfate addition (gSO₄/L)	0
pH	controlled to ~ 7.0
Biological groups present	acidogens

Following steady state number 40, the pH was adjusted to 7.0 in a single step.

Table B.131: Results summary for steady state number 43

Feed total COD (mg/L)	2011
Feed soluble COD (mg/L)	211
Feed TKN (mgN/L)	38
Feed FSA (mgN/L)	11
Feed Total P (mgP/L)	9
Feed soluble P (mgP/L)	2
Steady state measured after 15 days (3 x R_h)	
Effluent total COD (mg/L)	1914 ± 60 (10)
Effluent soluble COD (mg/L)	431 ± 8 (10)
Suspended solids (mgCOD/L)	812
Reactor pH	7.07 ± 0.02 (11)
Gas Produced (units/day)	2 ± 0 (11)
Volume per unit (ml)	44.5 ± 0.5
Gas composition (%CH₄)	*12.5
Methane production (mL/day)	22.2
Methane production (mgCOD/day)	59.2
Effluent TKN (mgN/L)	43 ± 3 (11)
Effluent FSA (mgN/L)	18 ± 3 (11)
Effluent Total P (mgP/L)	9 ± 0 (11)
Effluent soluble P (mgP/L)	3 ± 0 (11)
COD balance (%)	95.9
TKN balance (%)	111.9
Total P balance (%)	98.0

*Not measured – assume the same as steady state number 40 - has insignificant influence

Appendix B: Steady State Data

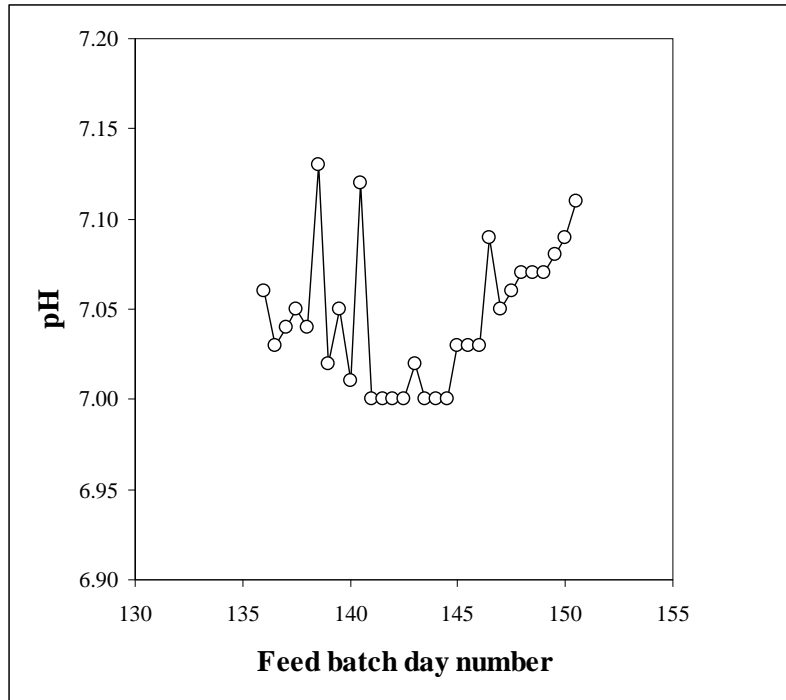


Figure B.82: Daily measurements of the pH leading up to and including steady state number 43 (steady state from day 145.5)

Appendix B: Steady State Data

Table B.132: Daily measured data for steady state number 43

Date	Day	Total COD (mgCOD/L)	Soluble COD (mgCOD/L)	Suspended Solids (mgCOD/L)	pH	Gas Volume (Units/day)	TKN (mgN/L)	NH ₃ (mgN/L)	TP (mgP/L)	PO ₄ (mgP/L)
21-Apr	145.5	1796	429	1265	7.03	2	38	18	9	3
21-Apr	146	2089	420	1134	7.03	2	42	18	8	3
22-Apr	146.5	1979	417	1212	7.09	2	46	15	9	2
22-Apr	147	1935	430	1304	7.05	2	45	11	9	3
23-Apr	147.5	1985	438	1262	7.06	2	42	17	8	3
23-Apr	148	1910	400	1190	7.07	2	40	20	8	3
24-Apr	148.5	1957	431	1240	7.07	2	37	20	8	3
24-Apr	149	1876	433	1245	7.07	2	43	18	9	3
25-Apr	149.5	1822	443	1292	7.08	2	44	15	9	3
25-Apr	150	1918	436	1239	7.09	2	47	21	9	3
26-Apr	150.5	1892	424	1202	7.11	2	43	16	8	3
Mean		1914	431	1243	7.07	2	43	18	9	3
S.D.		60	8	35	0.02	0	3	3	0	0
Data points		10	10	10	11	11	11	11	11	11

Steady state No 44**Table B.133:** Operating conditions for steady state number 44

Feed batch number	F15
Mass of PSS in feed (g)	30.6
Total Mass of feed (g)	1000
Reactor Volume (L)	16
Retention time (day)	8
Sulfate addition (gSO₄/L)	0
pH	controlled to ~ 8.0
Biological groups present	acidogens and methanogens

This experiment followed steady state number 37. The pH was increased over 4 feed cycles, and then maintained by addition of 1M NaOH only.

Table B.134: Results summary for steady state number 44

Feed total COD (mg/L)	2017
Feed soluble COD (mg/L)	208
Feed TKN (mgN/L)	39
Feed FSA (mgN/L)	12
Feed Total P (mgP/L)	9
Feed soluble P (mgP/L)	2
Steady state measured after 15 days (1.875 x R_h)	
Effluent total COD (mg/L)	866
Effluent soluble COD (mg/L)	38
Suspended solids (mgCOD/L)	383
Effluent VFA (mg/L as HAc)	7
Effluent Alkalinity (mg/L as CaCO₃)	545
Reactor pH	7.98
Gas Produced (units/day)	[8] twice = 16
Volume per unit (ml)	49.7
Gas composition (%CH₄)	86.36
Methane production (L/day)	0.69
Methane production (gCOD/day)	1.8
Effluent TKN (mgN/L)	24
Effluent FSA (mgN/L)	19
Effluent Total P (mgP/L)	9
Effluent soluble P (mgP/L)	3
COD balance (%)	88.2
TKN balance (%)	62.2
Total P balance (%)	97.7

* Only one measurement for entire steady state period

Appendix B: Steady State Data

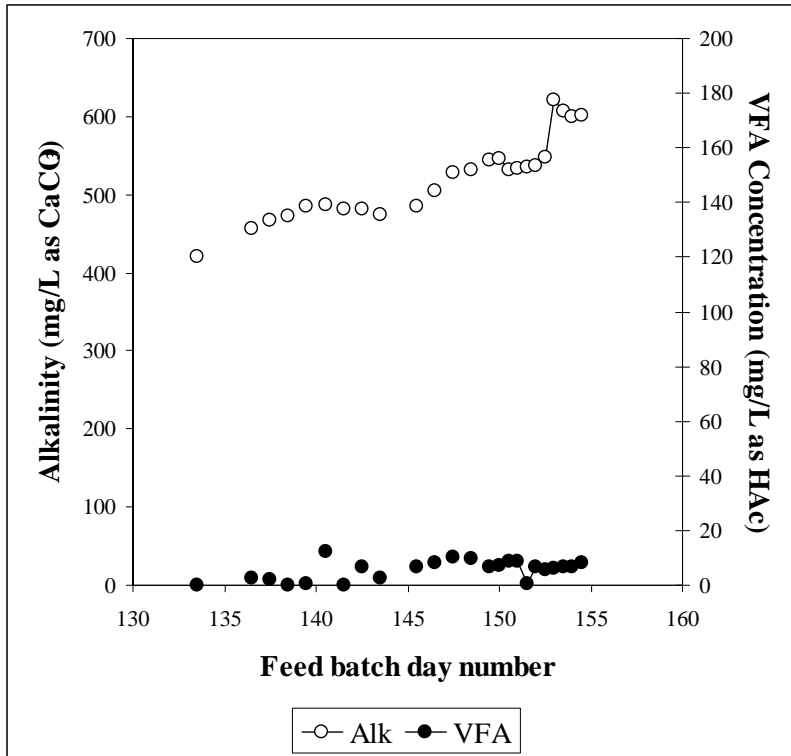


Figure B.83: Daily measurements of the VFA and alkalinity leading up to and including steady state number 44 (steady state from day 150)

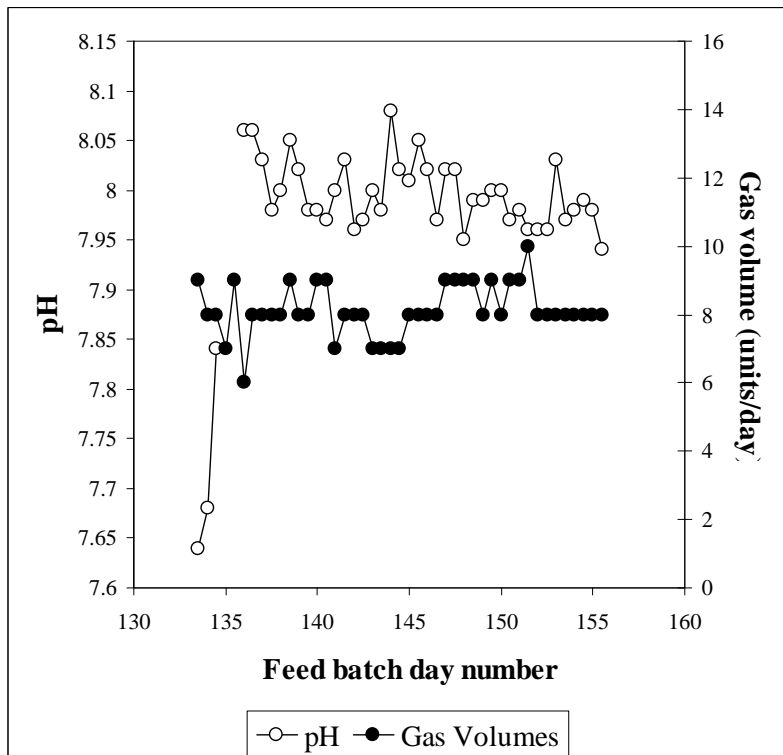


Figure B.84: Daily measurements of the pH and volumetric gas production leading up to and including steady state number 44 (steady state from day 150)

Appendix B: Steady State Data

Table B.135: Daily measured data for steady state number 44

Date	Day	Total COD (mgCOD/L)	Soluble COD (mgCOD/L)	Suspended Solids (mgCOD/L)	VFA (mg/L as HAc)	Alkalinity (mg/L as CaCO ₃)	pH	Gas Volume (Units/day)	TKN (mgN/L)	NH ₃ (mgN/L)	TP (mgP/L)	PO ₄ (mgP/L)
25-Apr	150	936	48	426	7.1	545.4	8.00	8	27	19	9	3
26-Apr	150.5	891	52	382	8.9	531.5	7.97	9	20	19	9	3
26-Apr	151	945	34	352	8.9	533.1	7.98	9	23	18	9	3
27-Apr	151.5	875	42	358	0.5	535.2	7.96	10	27	19	9	3
27-Apr	152	860	51	408	6.4	536.7	7.96	8	28	20	9	3
28-Apr	152.5	884	40	387	5.5	547.9	7.96	8	24	19	8	3
28-Apr	153	848	25	383	6.2	621.5	8.03	8	23	18	9	3
29-Apr	153.5	848	25		6.6	606.4	7.97	8	24	18	9	3
29-Apr	154	871	32		6.7	599.5	7.98	8	26	19	8	3
30-Apr	154.5	843	30		8	601.3	7.99	8	25	19	8	3
30-Apr	155	835	38				7.98	8	23	18	8	3
01-May	155.5						7.94	8				
	Mean	866	38	383	7	545	7.97	8	24	19	9	3
	S.D.	28	9	24	1	31	0.02	1	2	1	0	0
	Data points	10	11	7	9	9	11	12	11	11	11	11

Steady state No 45**Table B.136:** Operating conditions for steady state number 45

Feed batch number	F15
Mass of PSS in feed (g)	61
Total Mass of feed (g)	2000
Reactor Volume (L)	20
Retention time (day)	5
Sulfate addition (gSO₄/L)	0
pH	controlled to ~ 8.0
Biological groups present	acidogens

Following steady state number 40, the pH was adjusted to 8.0 in a single step.

Table B.137: Results summary for steady state number 45

Feed total COD (mg/L)	2011
Feed soluble COD (mg/L)	193
Feed TKN (mgN/L)	38
Feed FSA (mgN/L)	13
Feed Total P (mgP/L)	9
Feed soluble P (mgP/L)	2
Steady state measured after 14 days (2.8 x R_h)	
Effluent total COD (mg/L)	1846 ± 30 (8)
Effluent soluble COD (mg/L)	454 ± 14 (8)
Reactor pH	8.03 ± 0.04 (10)
Gas Produced (units/day)	2 ± 0 (9)
Volume per unit (ml)	44.5 ± 0.5
Gas composition (%CH₄)	*12.5
Methane production (mL/day)	22.2
Methane production (mgCOD/day)	59.2
Effluent TKN (mgN/L)	43 ± 2 (8)
Effluent FSA (mgN/L)	18 ± 2 (8)
Effluent Total P (mgP/L)	9 ± 0 (8)
Effluent soluble P (mgP/L)	3 ± 0 (8)
COD balance (%)	92.5
TKN balance (%)	111.9
Total P balance (%)	98.0

* Not measured – assume the same as steady state number 43 - has insignificant influence

Appendix B: Steady State Data

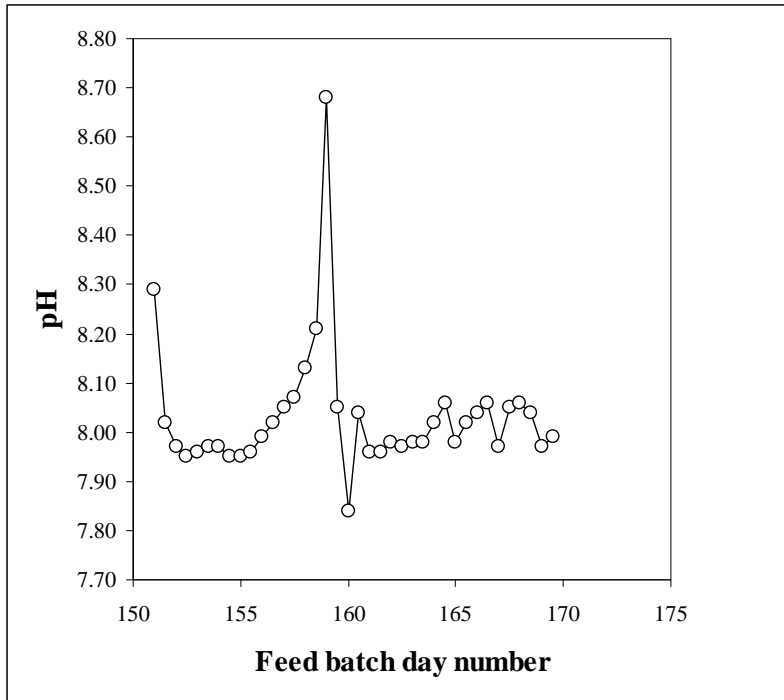


Figure B.85: Daily measurements of the pH leading up to and including steady state number 45. pH control pH probe failed on day 158 – replaced on day 159 (steady state from day 165)

Appendix B: Steady State Data

Table B.138: Daily measured data for steady state number 45

Date	Day	Total COD (mgCOD/L)	Soluble COD (mgCOD/L)	pH	Gas Volume (Units/day)	TKN (mgN/L)	NH ₃ (mgN/L)	TP (mgP/L)	PO ₄ (mgP/L)
10-May	165	1845	431	7.98	2	41	19	8	3
11-May	165.5	1815	453	8.02	2	45	16	8	3
11-May	166	1883	446	8.04	2	45	20	9	3
12-May	166.5	1816	457	8.06	2	49	21	9	3
12-May	167	1799	418	7.97	1	42	17	9	3
13-May	167.5	1848	460	8.05	2	41	17	9	3
13-May	168	1846	455	8.06	2	43	17	8	3
14-May	168.5	1889	456	8.04	5	43	21	9	3
14-May	169			7.97	1	41	19	8	3
15-May	169.5			7.99	2	45	16	8	3
Mean		1846	454	8.03	2	43	18	9	3
S.D.		30	14	0.04	0	2	2	0	0
Data points		8	8	10	9	8	8	8	8

Steady state No 46**Table B.139:** Operating conditions for steady state number 46

Feed batch number	F15
Mass of PSS in feed (g)	30
Total Mass of feed (g)	2000
Reactor Volume (L)	20
Retention time (day)	10
Sulfate addition (gSO₄/L)	1
pH	steady state
Biological groups present	acidogens and sulfidogens

This experiment followed steady state number 42. The feed concentration was halved and the feed volume increased to the new retention time. The system was fed once daily.

Table B.140: Results summary for steady state number 46

Feed total COD (mg/L)	989
Feed soluble COD (mg/L)	102
Feed TKN (mgN/L)	19
Feed FSA (mgN/L)	7
Feed Total P (mgP/L)	5
Feed soluble P (mgP/L)	1
Steady state measured after 29 days (2.9 x R_h)	
Effluent total COD (mg/L)	897 ± 25 (11)
Effluent soluble organic COD (mg/L)	42 ± 5 (10)
Effluent total soluble COD (mg/L)	466 ± 18 (10)
Sulfate concentration (mgSO₄/L)	51 ± 9 (8)
Effluent VFA (mg/L as HAc)	3 ± 6 (10)
Effluent Alkalinity (mg/L as CaCO₃)	1025 ± 26 (10)
Reactor pH	7.92 ± 0.04 (10)
Gas Produced (units/day)	0
Volume per unit (ml)	-
Gas composition (%CH₄)	not measured
Effluent TKN (mgN/L)	not measured
Effluent FSA (mgN/L)	not measured
Effluent Total P (mgP/L)	not measured
Effluent soluble P (mgP/L)	not measured
COD balance (%)	** Not possible
TKN balance (%)	Not possible
Total P balance (%)	Not possible

** No gaseous sulfide measurement

Appendix B: Steady State Data

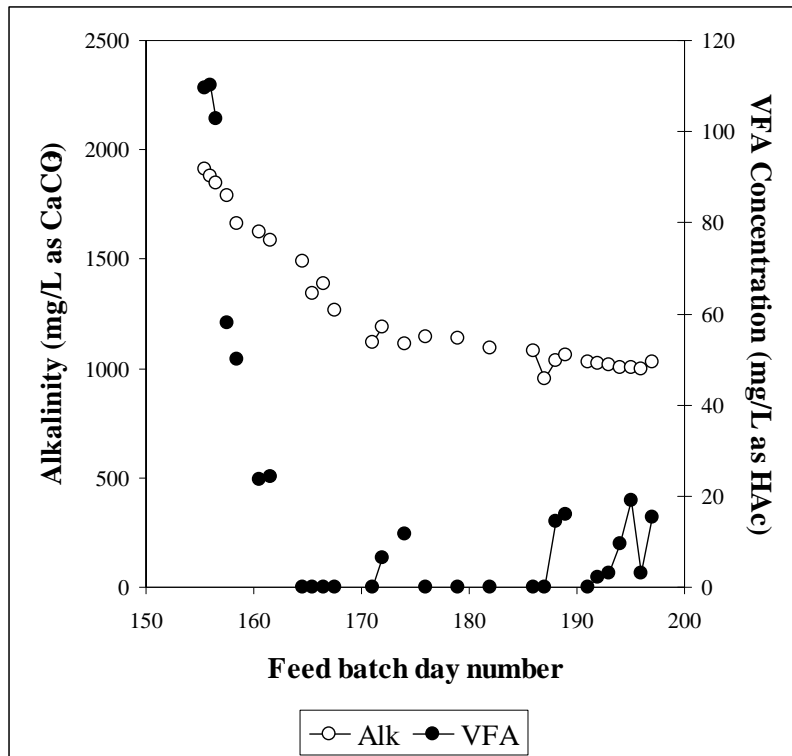


Figure B.86: Daily measurements of the VFA and alkalinity leading up to and including steady state number 46 (steady state from day 186)

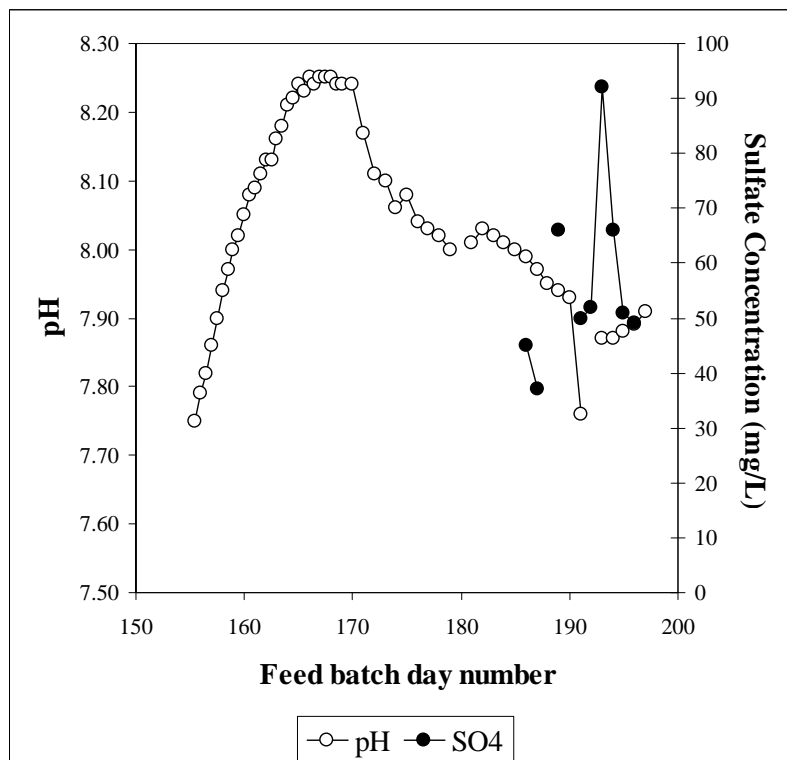


Figure B.87: Daily measurements of the pH and sulfate concentration leading up to and including steady state number 46 (steady state from day 186)

Appendix B: Steady State Data

Table B.141: Daily measured data for steady state number 46

Date	Day	Total COD (mgCOD/L)	Soluble Organic COD (mgCOD/L)	Total Soluble COD (mgCOD/L)	VFA (mg/L as HAc)	Alkalinity (mg/L as CaCO ₃)	pH	Sulfate (mgSO ₄ /L)
31-May	186	898	131	449	0	1080.1	7.99	45
01-Jun	187	914	33	475	0	953.7	7.97	37
02-Jun	188	856	30	462	14.4	1037.1	7.95	
03-Jun	189	891	46	451	16	1064.2	7.94	66
04-Jun	190						7.93	
05-Jun	191	910	42	504	0	1028.4	7.76	50
06-Jun	192	937	42	438	2.3	1020.7		52
07-Jun	193	920	44	469	3.2	1016.7	7.87	92
08-Jun	194	897	40	451	9.5	1005.9	7.87	66
09-Jun	195	866	41	479	19.1	1000.7	7.88	51
10-Jun	196	875	43	415	3	994.3	7.89	49
11-Jun	197	860	35	469	15.2	1032.4	7.91	
Mean		897	42	466	3	1025	7.92	51
S.D.		25	5	18	6	26	0.04	9
Data points		11	10	10	10	10	10	8

Steady state No 47**Table B.142:** Operating conditions for steady state number 47

Feed batch number	F16
Mass of PSS in feed (g)	51.2
Total Mass of feed (g)	2000
Reactor Volume (L)	16
Retention time (day)	8
Sulfate addition (gSO₄/L)	2
pH	~ 8.3
Biological groups present	acidogens and sulfidogens

This digester was reseeded with waste sulfate-reducing sludge. The pH was controlled by the addition of a 1M NaOH solution.

Table B.143: Results summary for steady state number 47

Feed total COD (mg/L)	1900
Feed soluble COD (mg/L)	203
Feed TKN (mgN/L)	46
Feed FSA (mgN/L)	4
Feed Total P (mgP/L)	8
Feed soluble P (mgP/L)	2
Steady state measured after 30 days (3.75 x R_h)	
Effluent total COD (mg/L)	2020 ± 43 (10)
Effluent soluble organic COD (mg/L)	84 ± 24 (10)
Effluent total soluble COD (mg/L)	926 ± 47 (10)
Sulfate concentration (mgSO₄/L)	47 ± 52 (8)
Effluent VFA (mg/L as HAc)	34 ± 14 (11)
Effluent Alkalinity (mg/L as CaCO₃)	1950 ± 50 (10)
Reactor pH	8.27 ± 0.04 (11)
Gas Produced (units/day)	0
Volume per unit (ml)	-
Gas composition (%CH₄)	not measured
Effluent TKN (mgN/L)	not measured
Effluent FSA (mgN/L)	not measured
Effluent Total P (mgP/L)	not measured
Effluent soluble P (mgP/L)	not measured
COD balance (%)	**Not possible
TKN balance (%)	Not possible
Total P balance (%)	Not possible

** No gaseous sulfide measurement

Appendix B: Steady State Data

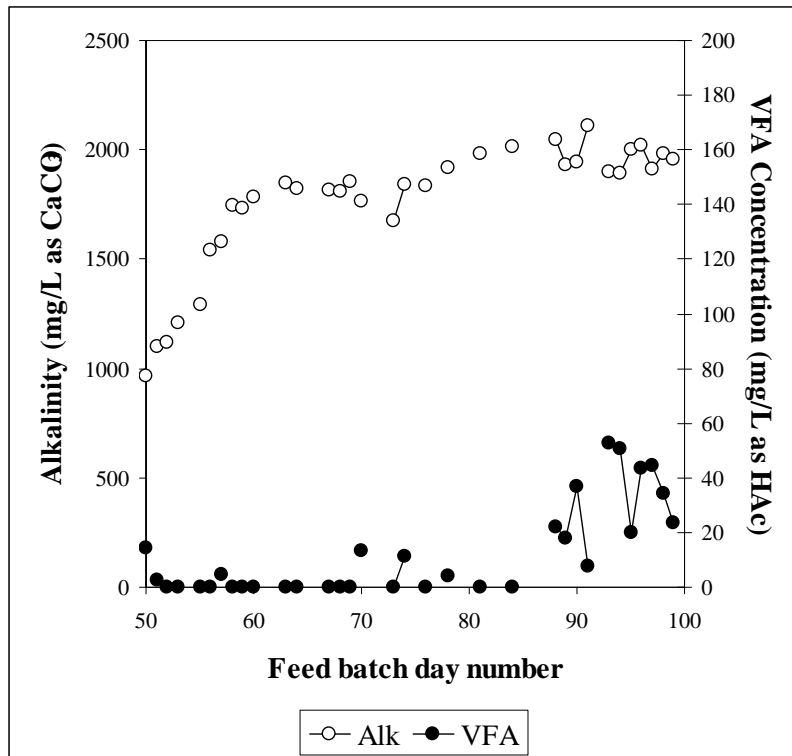


Figure B.88: Daily measurements of the VFA and alkalinity leading up to and including steady state number 47 (steady state from day 88)

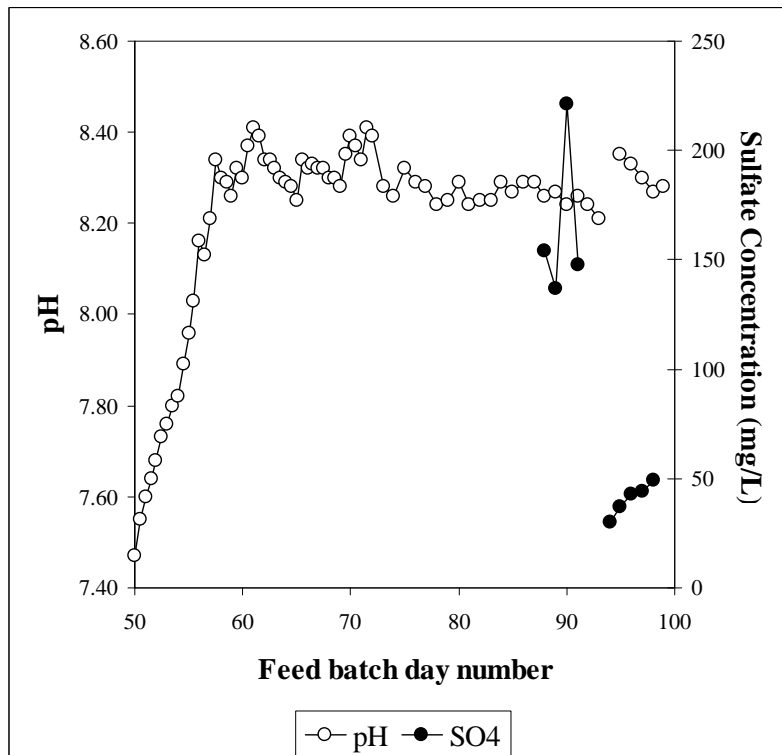


Figure B.89: Daily measurements of the pH and sulfate concentration leading up to and including steady state number 47 (steady state from day 88)

Appendix B: Steady State Data

Table B.144: Daily measured data for steady state number 47

Date	Day	Total COD (mgCOD/L)	Soluble Organic COD (mgCOD/L)	Total Soluble COD (mgCOD/L)	VFA (mg/L as HAc)	Alkalinity (mg/L as CaCO ₃)	pH	Sulfate (mgSO ₄ /L)
31-May	88	2101	71	869	22	2045.9	8.26	154
01-Jun	89	2053	153	914	17.8	1932.8	8.27	137
02-Jun	90	1887	60	884	36.6	1943.2	8.24	221
03-Jun	91	2037	84	724	7.9	2113.1	8.26	148
04-Jun	92						8.24	
05-Jun	93	2005	335	1003	52.7	1901.1	8.21	
06-Jun	94	1949	97	962	50.4	1891.8		30
07-Jun	95	2034	92	938	20.1	2002.6	8.35	37
08-Jun	96	2044	94	909	43.3	2021.6	8.33	43
09-Jun	97	1986	83	958	44.3	1908.9	8.30	44
10-Jun	98	1994	75	961	34.3	1979	8.27	49
11-Jun	99	1964	78	840	23.6	1956.7	8.28	
Mean		2020	84	926	34	1950	8.27	47
S.D.		43	24	47	14	50	0.04	52
Data points		10	10	10	11	10	11	8

Appendix C

Transient Operating Data

Anaerobic digesters were operated to collect steady state data at various retention time and feed COD concentrations, under methanogenic, acidogenic and sulfate-reducing conditions. Appendix B details the results of the steady states that were analysed in more detail, and shows the VFA and alkalinity measurements, and pH and gas unit productions on a daily basis as the system reached steady state. For some of the steady state changes, a step change was made in the feed volume or feed COD concentration, and the system was monitored on a daily basis to evaluate the transient state. This data is not analysed further in this thesis, but is available, and would be useful, for a more extensive modelling exercise than developed in this research.

Each of the transient states starts and ends with a steady state period as described in Appendix B. In order to properly analyse the transient state, these steady state periods need to be examined, and then the changes made to the model, as described in the following sections.

Transient state No 1

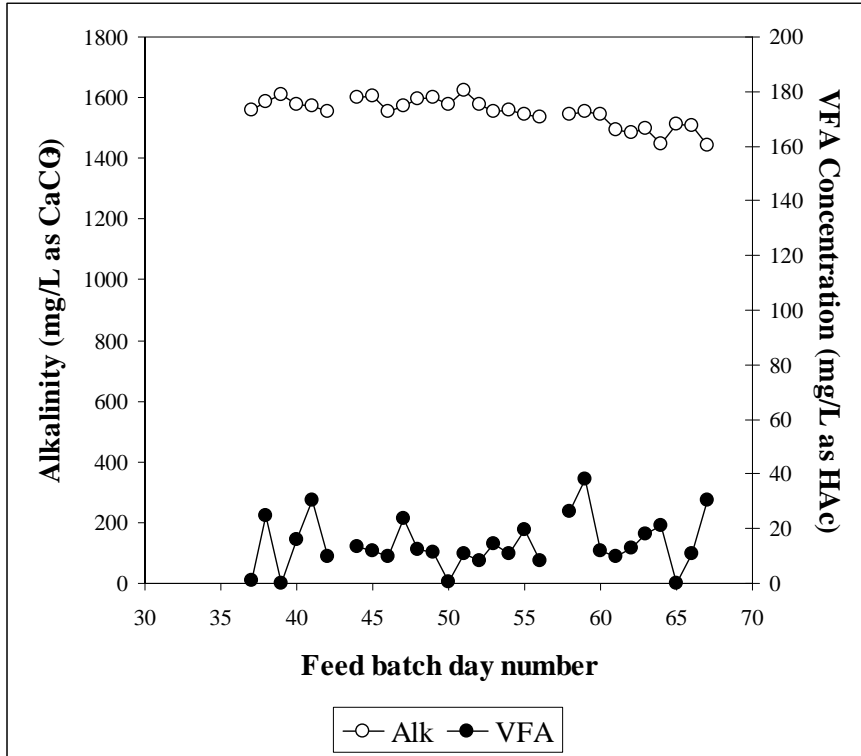


Figure C.1: Daily measurements of the VFA and alkalinity concentrations for steady state number 3 and the transient stage afterwards (feed increased on day 55)

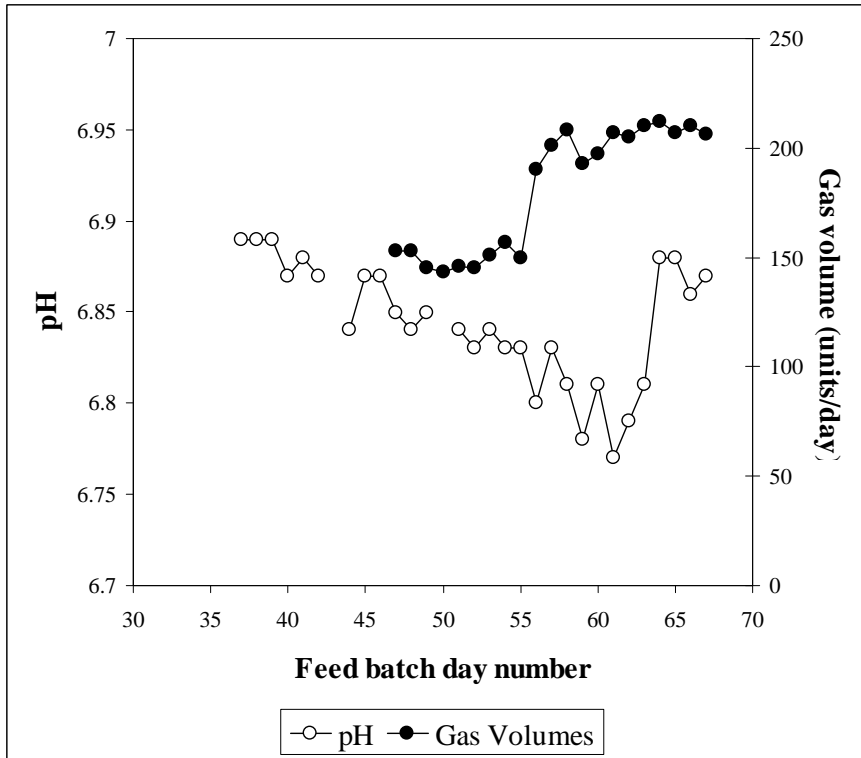


Figure C.2: Daily measurements of the pH and volumetric gas production for steady state number 3 and the transient stage afterwards (feed increased on day 55)

Appendix C: Transient Data

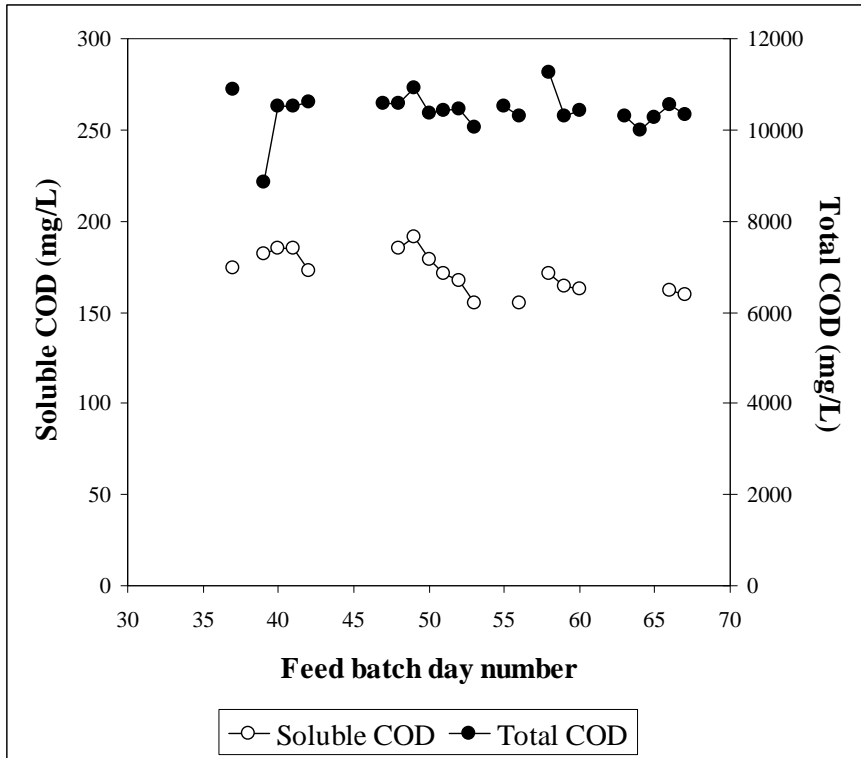


Figure C.3: Daily measurements of the total and soluble COD concentrations for steady state number 3 and the transient stage afterwards (feed increased on day 55)

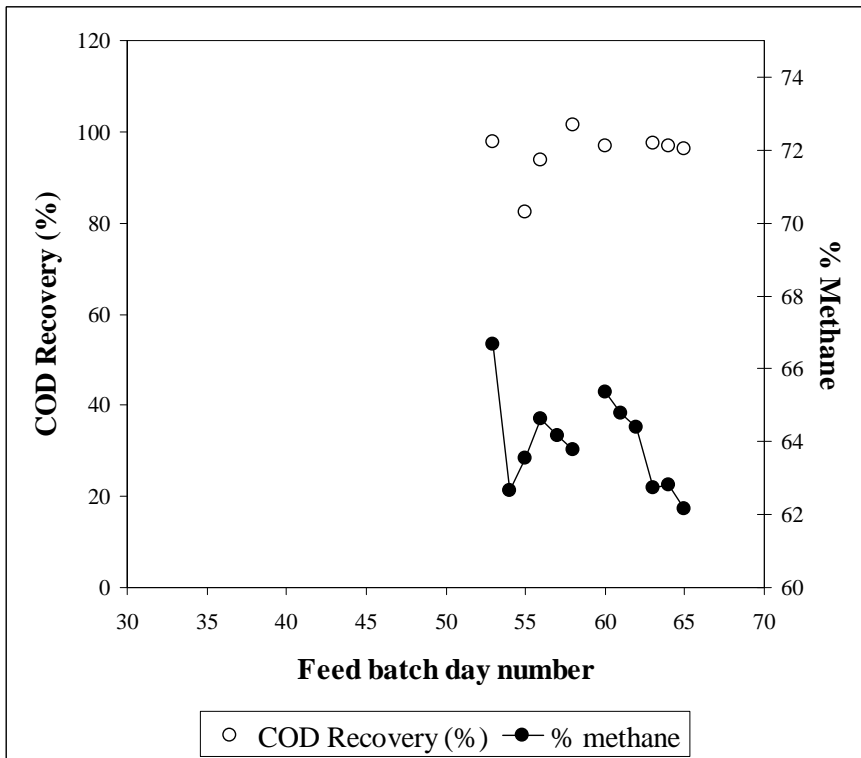


Figure C.4: Daily measurements of the gas composition (% methane calculated) and COD mass balance recovery for steady state number 3 and the transient stage afterwards (feed increased on day 55)

Appendix C: Transient Data

Table C.1: Daily measured data for steady

Date	Day	Total COD (mgCOD/L)	Soluble COD (mgCOD/L)	VFA (mg/L as HAc)	Alkalinity (mg/L as CaCO ₃)	pH	Gas Volume (Units/day)	%CH ₄	%CO ₂	Mass of PSS (g)	Total feed mass (g)	TKN (mgN/L)	NH ₃ (mgN/L)	TP (mgP/L)	PO ₄ (mgP/L)
14-Apr	37	10899	174	1.2	1557.1	6.89	15			500	1000	423			
15-Apr	38			24.9	1586.7	6.89	15			500	1000				
16-Apr	39	8847	182	0.0	1609	6.89	15			500	1000	525	223	125	22
17-Apr	40	10522	185	16.0	1578	6.87	15			500	1000	518	228	135	22
18-Apr	41	10525	185	30.5	1570.4	6.88	15			500	1000	522	232	147	22
19-Apr	42	10608	173	9.9	1553.2	6.87	16			500	1000	525	231	156	22
20-Apr	43									0	0				
21-Apr	44			13.3	1602	6.84				500	1000				
22-Apr	45			12.1	1605.1	6.87				500	1000				
23-Apr	46			9.7	1554.1	6.87				500	1000				
24-Apr	47	10578		23.5	1574.7	6.85	153			500	1000				
25-Apr	48	10588	185	12.6	1594.8	6.84	153			500	1000	511	238	150	23
26-Apr	49	10909	191	11.2	1602.3	6.85	145			500	1000	511	231	150	22
27-Apr	50	10369	179	0.4	1577.1		143			500	1000	508	230	147	22
28-Apr	51	10429	171	10.6	1624.8	6.84	146			500	1000	511	228	138	22
29-Apr	52	10455	167	8.2	1579	6.83	145			500	1000	515	220	138	22
30-Apr	53	10043	155	14.6	1554.1	6.84	151	51.2	25.6	500	1000	518	238	106	16
01-May	54			10.8	1560.6	6.83	157	35.6	21.2	500	1000				
02-May	55	10523		19.4	1544.3	6.83	150	35.9	20.6	666.667	1334	525	239	106	15
End of steady state number 3. The feed was from a 20-day retention time to a 15-day retention time on day 55															
03-May	56	10302	155	8.5	1536.4	6.8	190	41.5	22.7	666.667	1334	529	241	100	17
04-May	57					6.83	201	41.7	23.3	666.667	1334				
05-May	58	11245	171	26.4	1546.7	6.81	208	42.8	24.3	666.667	1334	522	234	106	15
06-May	59	10296	164	38.3	1555.4	6.78	193			666.667	1334	525	231	106	15
07-May	60	10428	163	12.0	1545.3	6.81	197	41.7	22.1	666.667	1334				
08-May	61			9.6	1494.7	6.77	207	42.3	23	666.667	1334				
09-May	62			12.9	1486.3	6.79	205	42.3	23.4	666.667	1334				
10-May	63	10291		18.0	1498.4	6.81	210	40.9	24.3	666.667	1334				
11-May	64	9987		20.9	1446.5	6.88	212	44.6	26.4	666.667	1334				
12-May	65	10276		0.0	1511.4	6.88	207	41.1	25	666.667	1334				
13-May	66	10555	162	10.6	1506.3	6.86	210			666.667	1334				
14-May	67	10326	160	30.6	1445	6.87	206			666.667	1334				

Transient state No 2

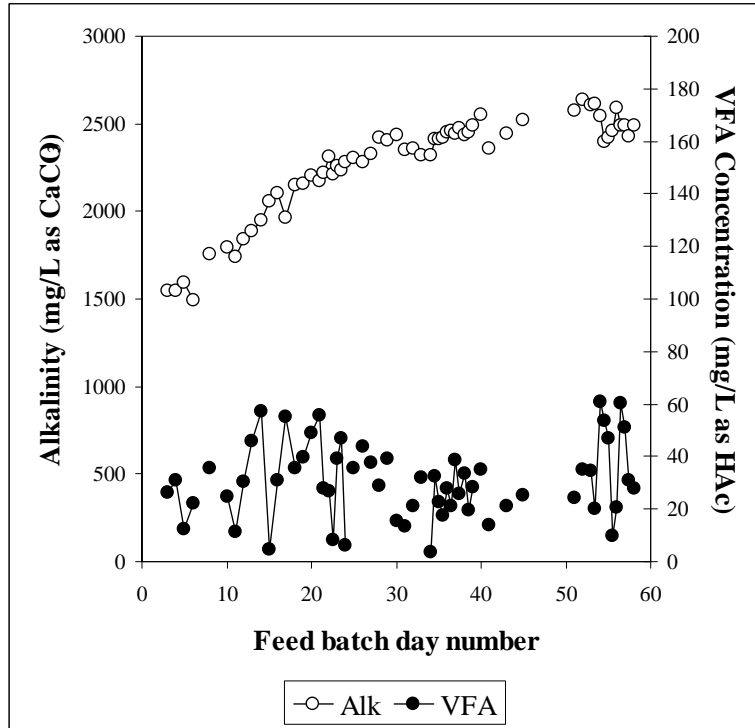


Figure C.5: Daily measurements of the VFA and alkalinity concentrations for the transient stages between steady states numbers 4, 10 and 11 (steady state 10 from day 34.5 to 40 and steady state number 11 from day 53 to 58)

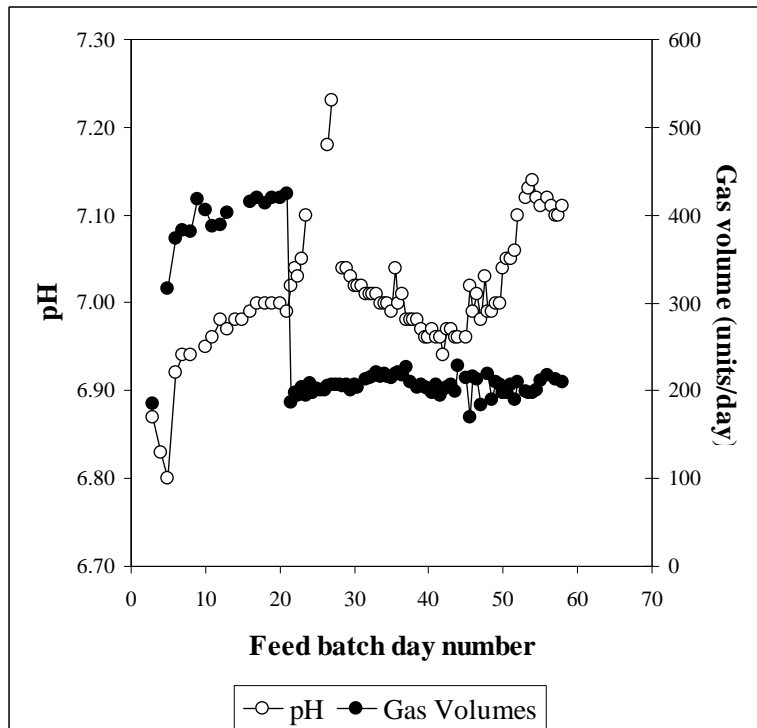


Figure C.6: Daily measurements of the pH and volumetric gas production for the transient stages between steady states numbers 4, 10 and 11 (steady state 10 from day 34.5 to 40 and steady state number 11 from day 53 to 58)

Appendix C: Transient Data

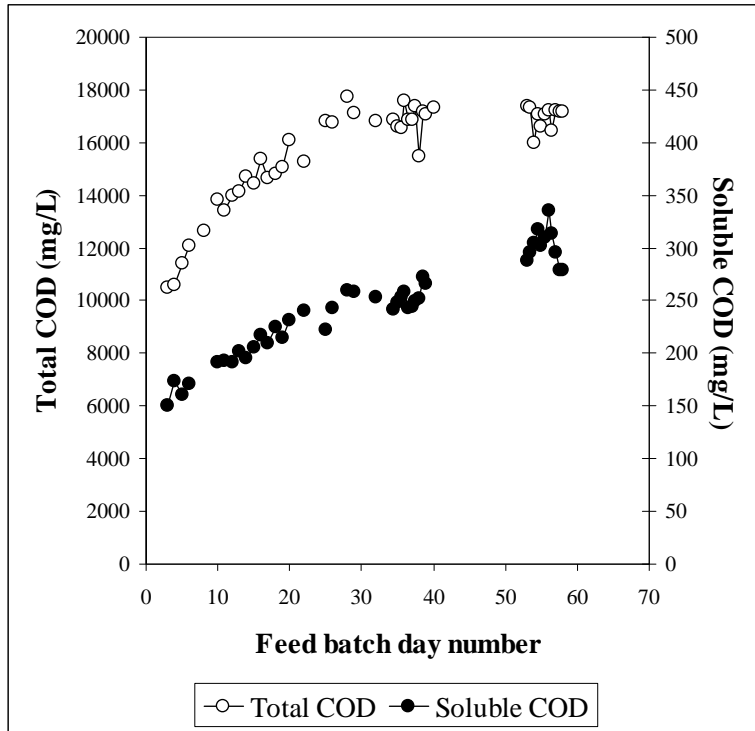


Figure C.7: Daily measurements of the total and soluble COD concentrations for the transient stages between steady states numbers 4, 10 and 11 (steady state 10 from day 34.5 to 40 and steady state number 11 from day 53 to 58)

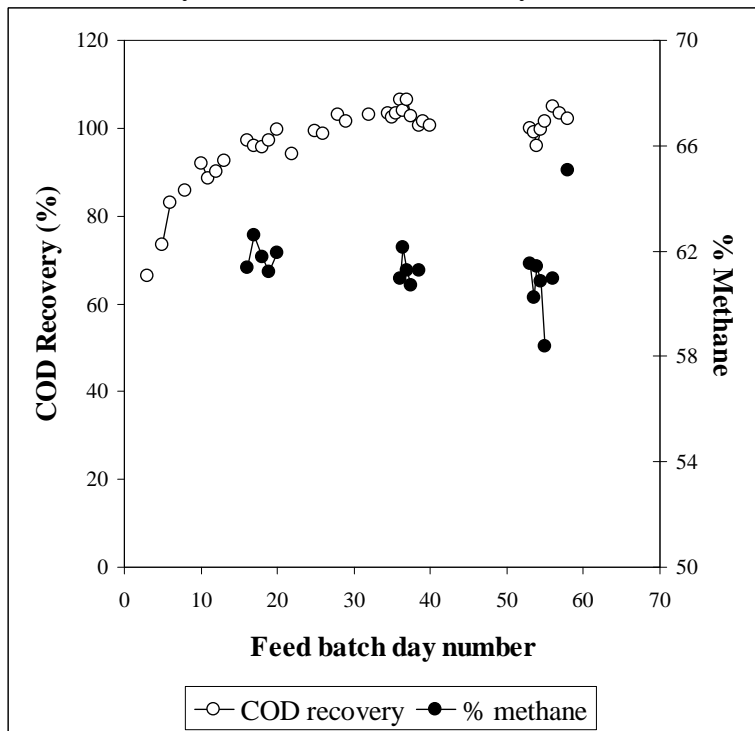


Figure C.8: Daily measurements of the gas composition (% methane calculated) and COD mass balance recovery for the transient stages between steady states numbers 4, 10 and 11 (steady state 10 from day 34.5 to 40 and steady state number 11 from day 53 to 58)

Appendix C: Transient Data

Table C.2: Daily measured data for steady

Date	Day	Total COD (mgCOD/L)	Soluble COD (mgCOD/L)	Suspended Solids (mgCOD/L)	VFA (mg/L as HAc)	Alkalinity (mg/L as CaCO ₃)	pH	Gas Volume (Units/day)	%CH ₄	%CO ₂	Mass of PSS (g)	Total feed mass (g)	TKN (mgN/L)	NH ₃ (mgN/L)	TP (mgP/L)	PO ₄ (mgP/L)	
04-Jun	88	10232	164	2221	17.3	1651.8	6.81	203			667	1334	553	221	111	14	
05-Jun	89	10283	155	2257	14.2	1512.8	6.78	213			667	1334	525	230	114	16	
06-Jun	90	10173	161	2177	8.5	1636.6	6.77	214	40.8	24.5	667	1334	518	218	114	16	
07-Jun	91	10028	156	2178	33.2	1594.4	6.77	216	42.5	25.9	667	1334	525		114		
08-Jun	92	10369	174	2265	10.8	1518.4	6.85	214	42.9	25	667	1334	511	218	111	16	
09-Jun	93	10013	155	2195	8.3	1572.3	6.85	212	44.4	24.4	667	1334	525	207	111	18	
10-Jun	94	9960	165	2288	23.8	1531.2	6.86	217			667	1334	511	213	114	20	
11-Jun	95	10322	157	2195	29.6	1545.8	6.87	214			667	1334	525	210	117	17	
12-Jun	96				32.4	1499.1	6.86	217			667	1334					
13-Jun	97	10191	159	2165	40	1528.9	6.84	217			667	1334		206	140	18	
14-Jun	98	10235	157	2185	17.5	1563.3	6.86	193			667	1334	518	203	137	18	
End of steady state number 4. The feed was changed from F12 to F13 on the 14 June 2003 as follows:																	
14-Jun	2										950	1334					
15-Jun	3	10497	150	2254	26.1	1550	6.87	185			950	1334					
16-Jun	4	10596	173		31.1	1542.8	6.83				950	1334	672	196	131	19	
17-Jun	5	11433	161		12.4	1591.9	6.80	316			1200	1334	672	207	147	20	
18-Jun	6	12064	171		22.0	1496	6.92	373			1200	1334	588	218	147	18	
19-Jun	7						6.94	383			1200	1334					
20-Jun	8	12647			35.5	1754.8	6.94	381			1200	1334	644		152		
21-Jun	9							418			1200	1334					
22-Jun	10	13813	192	2809	24.6	1790.7	6.95	405			1200	1334	637	210	156	14	
23-Jun	11	13433	193		11.3	1740.9	6.96	387			1200	1334	728	269	165	10	
24-Jun	12	13981	191		30.6	1841.1	6.98	389			1200	1334	735	245	159	14	
25-Jun	13	14157	202		46.0	1885.2	6.97	403			1200	1334	700	255	159	15	
26-Jun	14	14695	196		57.2	1948.7	6.98				1200	1334	693	263	165	18	
27-Jun	15	14443	206		4.4	2054	6.98				1200	1334	693	266	159	17	
28-Jun	16	15365	217		30.8	2100.8	6.99	415			1200	1334	609	269	89	17	
29-Jun	17	14651	209		55.3	1960.2	7.00	419	47	28.1	1200	1334	595	266	86	17	
30-Jun	18	14813	225		35.6	2148.6	7.00	414	47.2	29.2	1200	1334		279		14	
01-Jul	19	15089	215		39.5	2159.4	7.00	420	46.9	29.7	1200	1334	714	288	154	15	

Appendix C: Transient Data

Table C.2: Continued

Date	Day	Total COD (mgCOD/L)	Soluble COD (mgCOD/L)	Suspended Solids (mgCOD/L)	VFA (mg/L as HAc)	Alkalinity (mg/L as CaCO ₃)	pH	Gas Volume (Units/day)	%CH ₄	%CO ₂	Mass of PSS (g)	Total feed mass (g)	TKN (mgN/L)	NH ₃ (mgN/L)	TP (mgP/L)	PO ₄ (mgP/L)
02-Jul	20	16085	231		49.1	2201.6	7.00	419	49.1	30.2	1200	1334	749	307	154	16
03-Jul	21				55.6	2174.2	6.99	424			600	667				
03-Jul	21.5				27.7	2220.4	7.02	187			600	667				
04-Jul	22	15276	241	3589	26.7	2309.1	7.04	197			600	667	721	308	173	14
04-Jul	22.5				8.1	2208.1	7.03	195			600	667				
05-Jul	23				39.4	2254.1	7.05	204			600	667				
05-Jul	23.5				47.1	2232.5	7.10	195			600	667				
06-Jul	24				6.0	2278.9		208			600	667				
06-Jul	24.5							197			600	667				
07-Jul	25	16834	222	4188	35.8	2307.3		202			600	667	735	311	179	12
07-Jul	25.5							201			600	667				
08-Jul	26	16755	243		43.7	2283.6		200			600	667	784	315	161	15
08-Jul	26.5						7.18	205			600	667				
09-Jul	27				37.5	2328.8	7.23	207			600	667				
09-Jul	27.5							207			600	667				
10-Jul	28	17756	259		28.9	2418.6		207			600	667	777	316	161	12
10-Jul	28.5						7.04	205			600	667				
11-Jul	29	17136	258		39.1	2405.9	7.04	207			600	667	784	315	161	14
11-Jul	29.5						7.03	200			600	667				
12-Jul	30				15.3	2435.8	7.02	206			600	667				
12-Jul	30.5						7.02	203			600	667				
13-Jul	31				13.5	2350.8	7.02				600	667				
13-Jul	31.5						7.01	213			600	667				
14-Jul	32	16806	253		21.3	2357.7	7.01	215			600	667	784	315	185	12
14-Jul	32.5						7.01	216			600	667				
15-Jul	33				32.1	2316.9	7.01	221			600	667				
15-Jul	33.5						7.00	216			600	667				
16-Jul	34				3.8	2321.8	7.00	219			600	667				

Steady state period started as measured in steady state number 10

Appendix C: Transient Data

Table C.2: Continued

Date	Day	Total COD (mgCOD/L)	Soluble COD (mgCOD/L)	Suspended Solids (mgCOD/L)	VFA (mg/L as HAc)	Alkalinity (mg/L as CaCO ₃)	pH	Gas Volume (Units/day)	%CH ₄	%CO ₂	Mass of PSS (g)	Total feed mass (g)	TKN (mgN/L)	NH ₃ (mgN/L)	TP (mgP/L)	PO ₄ (mgP/L)
16-Jul	34.5	16887	242	5256	32.5	2409.9	7.00	216			600	667	882	333	184	7
17-Jul	35	16587	248	5098	22.5	2413.9	6.99	215			600	667	868	343	178	12
17-Jul	35.5	16532	253	4753	17.5	2419.6	7.04	219			600	667	861	322	178	11
18-Jul	36	17570	258	5174	27.9	2447.4	7.00	220	34.5	22.1	600	667	868	347	166	12
18-Jul	36.5	16879	243	5132	21.1	2461.2	7.01	218	38.1	23.2	600	667	854	342	178	12
19-Jul	37	16879	244	5219	38.7	2444.1	6.98	227	35.7	22.6	600	667	847	346	178	12
19-Jul	37.5	17388	250	5095	25.9	2474.1	6.98	209	36.3	23.5	600	667	840	364	178	11
20-Jul	38	15494	252	5033	33.7	2439.1	6.98				600	667	840	350	172	12
20-Jul	38.5	17153	272	5418	19.6	2453.9	6.98	203	36.2	22.9	600	667	840	347	178	12
21-Jul	39	17056	266	5258	28.6	2492.6	6.97	207			600	667	854	349	178	12
21-Jul	39.5						6.96	204	38.8	23.7	600	667				
22-Jul	40	17329			34.8	2550.3	6.96	202			600	667	798		146	
End of steady state period for steady state number 10 – decided to repeat steady state analyses after another 2 weeks																
22-Jul	40.5						6.97	197			600	667				
23-Jul	41				14.1	2355.6	6.96	206			600	667				
23-Jul	41.5						6.96	195			600	667				
24-Jul	42						6.94	201			600	667				
24-Jul	42.5						6.97	203			600	667				
25-Jul	43				21.1	2443.3	6.97	206			600	667				
25-Jul	43.5						6.96	199			600	667				
26-Jul	44						6.96	228			600	667				
26-Jul	44.5										600	667				
27-Jul	45				25.2	2519.9	6.96	215			600	667				
27-Jul	45.5						7.02	170			600	667				
28-Jul	46						6.99	216			600	667				
28-Jul	46.5						7.01	213			600	667				
29-Jul	47						6.98	184			600	667				

Appendix C: Transient Data

Table C.2: Continued

Date	Day	Total COD (mgCOD/L)	Soluble COD (mgCOD/L)	Suspended Solids (mgCOD/L)	VFA (mg/L as HAc)	Alkalinity (mg/L as CaCO ₃)	pH	Gas Volume (Units/day)	%CH ₄	%CO ₂	Mass of PSS (g)	Total feed mass (g)	TKN (mgN/L)	NH ₃ (mgN/L)	TP (mgP/L)	PO ₄ (mgP/L)
29-Jul	47.5						7.03	604			600	667				
30-Jul	48						6.99	219			600	667				
30-Jul	48.5						6.99	189			600	667				
31-Jul	49						7.00	210			600	667				
31-Jul	49.5						7.00	207			600	667				
01-Aug	50						7.04	198			600	667				
01-Aug	50.5						7.05	198			600	667				
02-Aug	51				24.3	2578.5	7.05	207			600	667				
02-Aug	51.5						7.06	189			600	667				
03-Aug	52				34.8	2634.9	7.10	209			600	667				
03-Aug	52.5										600	667				
Steady state period started as measured in steady state number 11																
04-Aug	53	17357	288	6761	34.6	2605.4	7.12	199	37.4	23.4	600	667	840	368	159	7
04-Aug	53.5	17306	295	6755	20.3	2614.4	7.13	197	35	23.1	600	667	805	371	159	7
05-Aug	54	15993	304	7078	60.6	2542.1	7.14	197	36.8	23.1	600	667	833	370	165	9
05-Aug	54.5	17079	317	7401	53.5	2393.9	7.12	201	37.9	24.4	600	667	833	370	159	10
06-Aug	55	16599	302	7312	47.1	2422.6	7.11	212	33.8	24.1	600	667	847	371	159	9
06-Aug	55.5	17069	310	7306	9.7	2457.6			38.5	25.2	600	667	847	364	165	7
07-Aug	56	17239	336		20.5	2592.2	7.12	218	36.8	23.6	600	667	847	371	152	7
07-Aug	56.5	16456	314	6924	60.4	2488	7.11				600	667	833	364	159	10
08-Aug	57	17208	295	7100	51.0	2491.8	7.10	213			600	667	840	364	165	11
08-Aug	57.5	17176	279	6562	30.8	2425	7.10		34.1	21.2	600	667	644	333	193	15
09-Aug	58	17157	279		27.7	2491.4	7.11	209	38.2	20.5			679	336	227	18

Transient state No 3

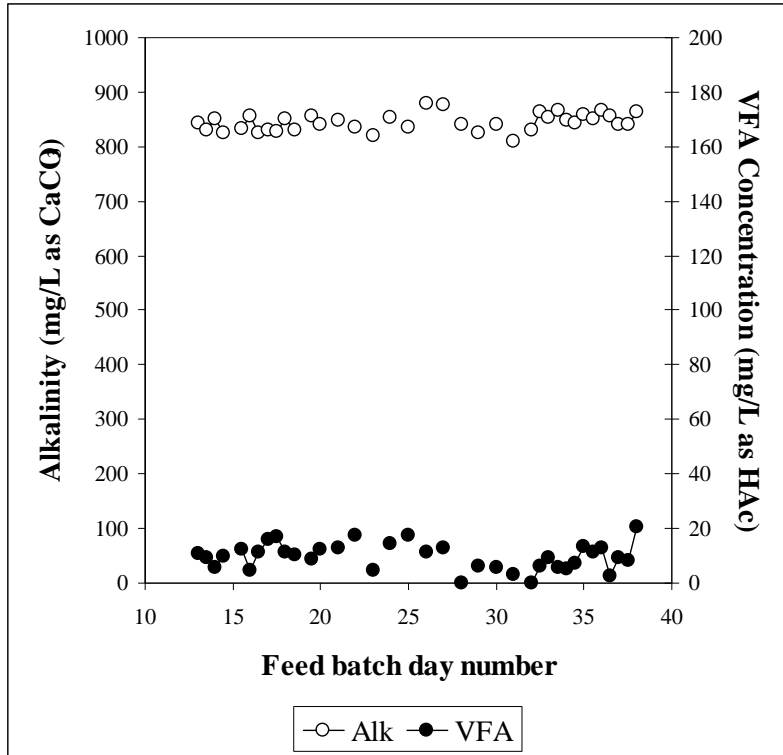


Figure C.9: Daily measurements of the VFA and alkalinity concentrations for the transient stage between steady states number 5 and 13 (steady state 13 from day 32.5)

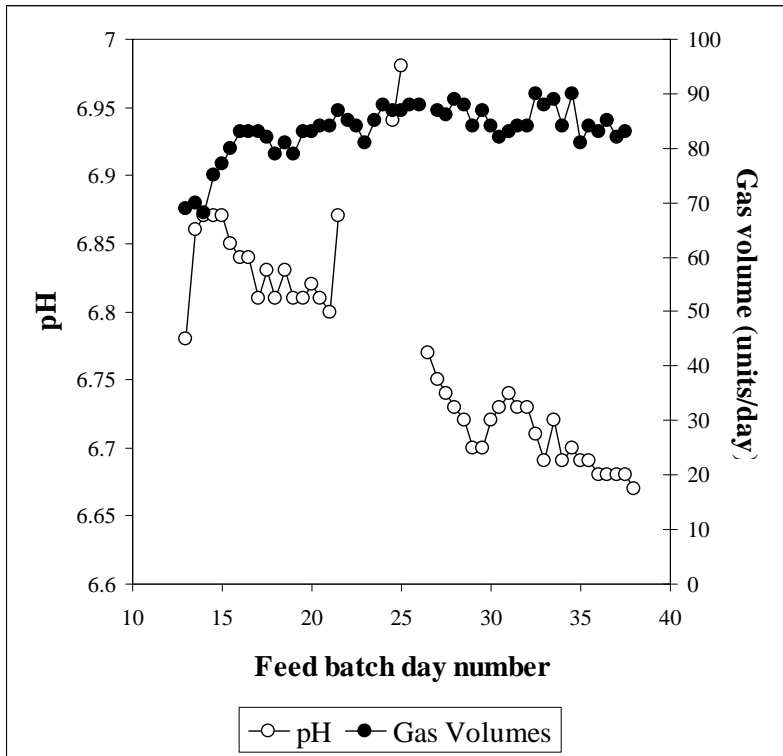


Figure C.10: Daily measurements of the pH and volumetric gas production for the transient stage between steady states number 5 and 13 (steady state 13 from day 32.5)

Appendix C: Transient Data

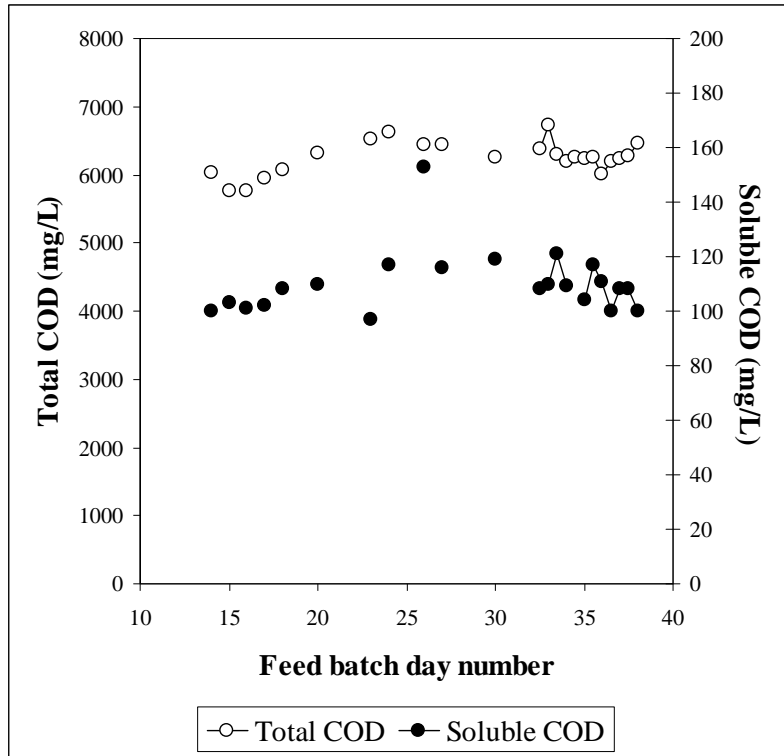


Figure C.11: Daily measurements of the total and soluble COD concentrations for the transient stage between steady states number 5 and 13 (steady state 13 from day 32.5)

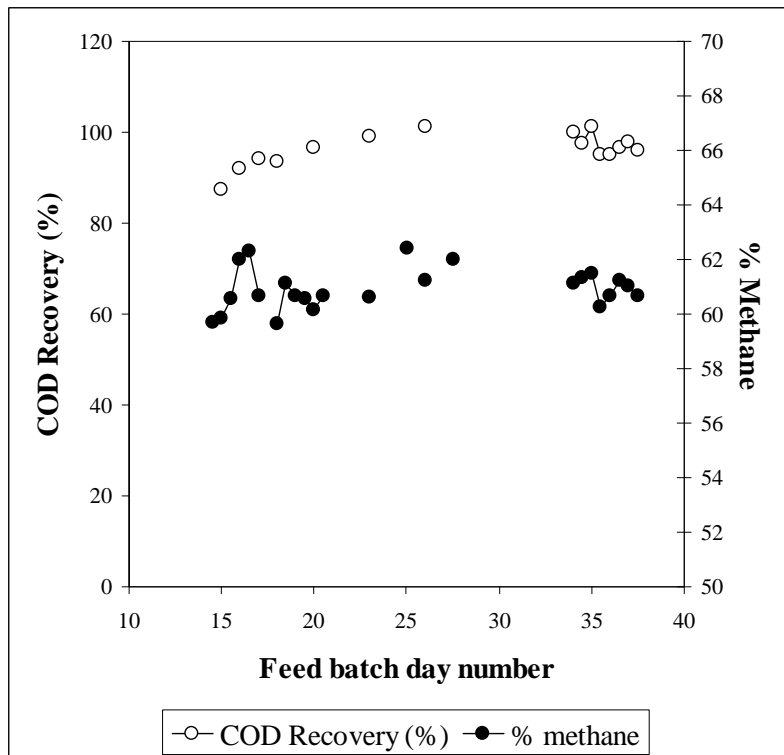


Figure C.12: Daily measurements of the gas composition (% methane calculated) and COD mass balance recovery for the transient stage between steady states number 5 and 13 (steady state 13 from day 32.5)

Appendix C: Transient Data

Table C.3: Daily measured data for steady

Date	Day	Total COD (mgCOD/L)	Soluble COD (mgCOD/L)	Suspended Solids (mgCOD/L)	VFA (mg/L as HAc)	Alkalinity (mg/L as CaCO ₃)	pH	Gas Volume (Units/day)	%CH ₄	%CO ₂	Mass of PSS (g)	Total feed mass (g)	TKN (mgN/L)	NH ₃ (mgN/L)	TP (mgP/L)	PO ₄ (mgP/L)	
15-Jun	99	5538			11.7	860.8	6.75	132			350	1334	294		83		
16-Jun	100	5632	110	1632	32.6	865.9	6.72	131			350	1334	284	108	83	13	
17-Jun	101	6204	98	1518	5.8	865.2	6.70	128	32.4	18.3	350	1334	280	108	86	13	
18-Jun	102	5796			5.1	806.7	6.80	128	33.4	18.4	350	1334					
19-Jun	103						6.82	126			350	1334					
20-Jun	104	5871			18.8	879.1	6.81	135	33.8	19.2	350	1334					
21-Jun	105						6.81	129			350	1334					
22-Jun	106	5829	99	1587	0.0	845.2	6.79	126			350	1334	315	115	76	11	
23-Jun	107	5811	97	1503	14.3	833.1	6.80	127			350	1334	298	112	79	9	
24-Jun	108	5809	95	1422	15.5	810.6	6.80	125	31.9	19.6	350	1334	280	116	79	13	
25-Jun	109	5706	101	1459	3.1	837.3	6.78	131	32.6	18.7	350	1334	298	115	79	13	
26-Jun	110	5696	92	1416	6.8	830	6.78	128	31.4	18.8	350	1334	294	116	73	15	
27-Jun	111	5600	93	1451	5.5	847.7	6.78	128	32	19.1	350	1334	294	111	67	13	
End of steady state number 5. The feed was changed from F12 to F13 on the 27 June 2003 as follows:																	
27-Jun	13										300	1000					
27-Jun	13.5				9.4	829.4	6.86	69			300	1000					
28-Jun	14	6026	100		5.7	851.8	6.87	70			300	1000		115	64	15	
28-Jun	14.5				10.0	824.1	6.87	68	20	13.5	300	1000	298	113		13	
29-Jun	15	5764	103				6.87	75	20.7	13.9	300	1000	294	116	67	13	
29-Jun	15.5				12.3	831.7	6.85	77	21.5	14	300	1000					
30-Jun	16	5770	101		4.6	857.2	6.84	80	23.5	14.4	300	1000					
30-Jun	16.5				11.5	825.9	6.84	83	22.3	13.5	300	1000					
01-Jul	17	5941	102		16.1	829.3	6.81	83	23.3	15.1	300	1000	284	123	62	14	
01-Jul	17.5				17.1	827.9	6.83	83			300	1000					
02-Jul	18	6066	108		11.2	851.9	6.81	82	22.9	15.5	300	1000	280	126	62	14	
02-Jul	18.5				10.4	829.1	6.83	79	22.8	14.5	300	1000					
03-Jul	19						6.81	81	22.2	14.4	300	1000					
03-Jul	19.5				8.7	855.2	6.81	79	21.8	14.2	300	1000					
04-Jul	20	6317	110	1659	12.3	840.3	6.82	83	22.5	14.9	300	1000	284	123	62	12	

Appendix C: Transient Data

Table C.3: Continued

Date	Day	Total COD (mgCOD/L)	Soluble COD (mgCOD/L)	Suspended Solids (mgCOD/L)	VFA (mg/L as HAc)	Alkalinity (mg/L as CaCO ₃)	pH	Gas Volume (Units/day)	%CH ₄	%CO ₂	Mass of PSS (g)	Total feed mass (g)	TKN (mgN/L)	NH ₃ (mgN/L)	TP (mgP/L)	PO ₄ (mgP/L)
04-Jul	20.5						6.81	83	22.5	14.6	300	1000				
05-Jul	21				12.8	849.4	6.80	84			300	1000				
05-Jul	21.5						6.87	84			300	1000				
06-Jul	22				17.7	834.4		87			300	1000				
06-Jul	22.5							85			300	1000				
07-Jul	23	6516	97	1905	4.4	820.5		84	23.1	15	300	1000	280	120	68	12
07-Jul	23.5							81			300	1000				
08-Jul	24	6627	117		14.6	852.4		85			300	1000	280	122	74	11
08-Jul	24.5						6.94	88			300	1000				
09-Jul	25				17.7	835.1	7.0	87	24.4	14.7	300	1000				
09-Jul	25.5							87			300	1000				
10-Jul	26	6448	153		11.3	879.2		88	24	15.2	300	1000	280	116	80	12
10-Jul	26.5						6.77	88			300	1000				
11-Jul	27	6436	116		12.8	876.4	6.75				300	1000	284	118	80	11
11-Jul	27.5						6.74	87	27.9	17.1	300	1000				
12-Jul	28				0.0	840.9	6.73	86			300	1000				
12-Jul	28.5						6.72	89			300	1000				
13-Jul	29				6.2	826.2	6.70	88			300	1000				
13-Jul	29.5						6.70	84			300	1000				
14-Jul	30	6264	119		5.4	840.1	6.72	87			300	1000	287	115	93	11
14-Jul	30.5						6.73	84			300	1000				
15-Jul	31				3.2	810.8	6.74	82			300	1000				
15-Jul	31.5						6.73	83			300	1000				
16-Jul	32				0.0	830.5	6.73	84			300	1000				

Steady state period started as measured in steady state number 13

Appendix C: Transient Data

Table C.3: Continued

Date	Day	Total COD (mgCOD/L)	Soluble COD (mgCOD/L)	Suspended Solids (mgCOD/L)	VFA (mg/L as HAc)	Alkalinity (mg/L as CaCO ₃)	pH	Gas Volume (Units/day)	%CH ₄	%CO ₂	Mass of PSS (g)	Total feed mass (g)	TKN (mgN/L)	NH ₃ (mgN/L)	TP (mgP/L)	PO ₄ (mgP/L)
16-Jul	32.5	6389	108	1899	6.4	863.2	6.71	84			300	1000	305	129	83	11
17-Jul	33	6733	110	1861	9.2	852.4	6.69	90			300	1000	291	127	62	12
17-Jul	33.5	6304	121	1518	5.9	867.2	6.72	88			300	1000	294	125	65	12
18-Jul	34	6185	109	1735	5.0	848.7	6.69	89	23.9	15.2	300	1000		125	65	12
18-Jul	34.5	6249		2350	7.4	842.1	6.70	84	23.8	15	300	1000	305	120	62	11
19-Jul	35	6238	104	1999	13.4	857.4	6.69	90	23.8	14.9	300	1000	298	126	68	12
19-Jul	35.5	6260	117	1956	11.1	850.6	6.69	81	22	14.5	300	1000	305	127	65	12
20-Jul	36	6015	111	1928	13.1	866.7	6.68	84	23	14.9	300	1000	294	127	68	12
20-Jul	36.5	6203	100	1991	2.6	854.9	6.68	83	23.2	14.7	300	1000	298	125	62	12
21-Jul	37	6237	108	1988	9.0	841.5	6.68	85	22.7	14.5	300	1000	305	127	68	12
21-Jul	37.5	6279	108	1890	8.3	841	6.68	82	23.3	15.1	300	1000	357	123	52	13
22-Jul	38	6466	100	1933	20.6	864.2	6.67	83			300	1000	333	129	49	12

Transient state No 4

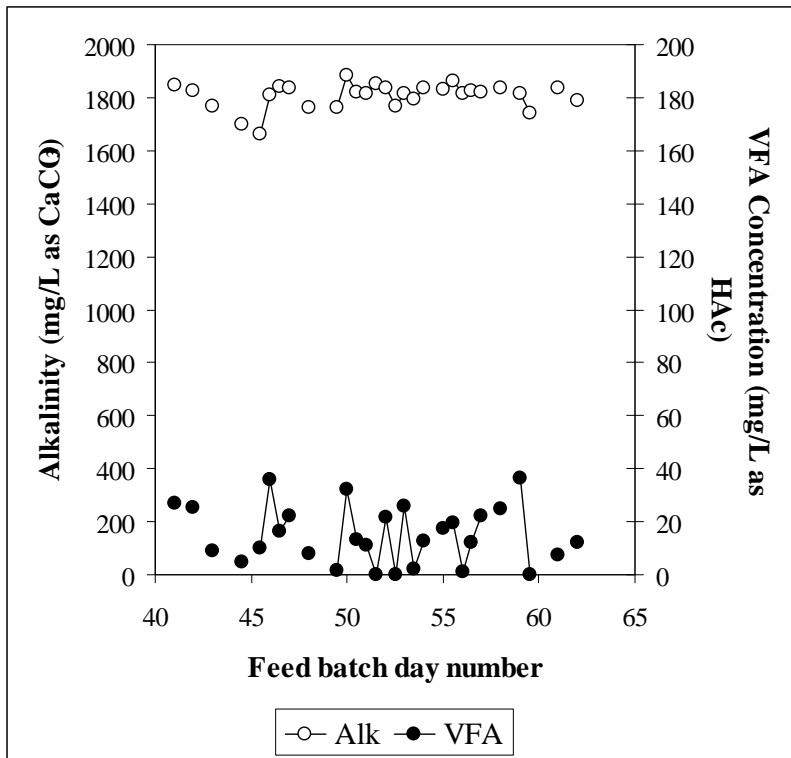


Figure C.13: Daily measurements of the VFA and alkalinity for the transient stage between steady states number 21 and 23 (steady state 23 from day 50.5)

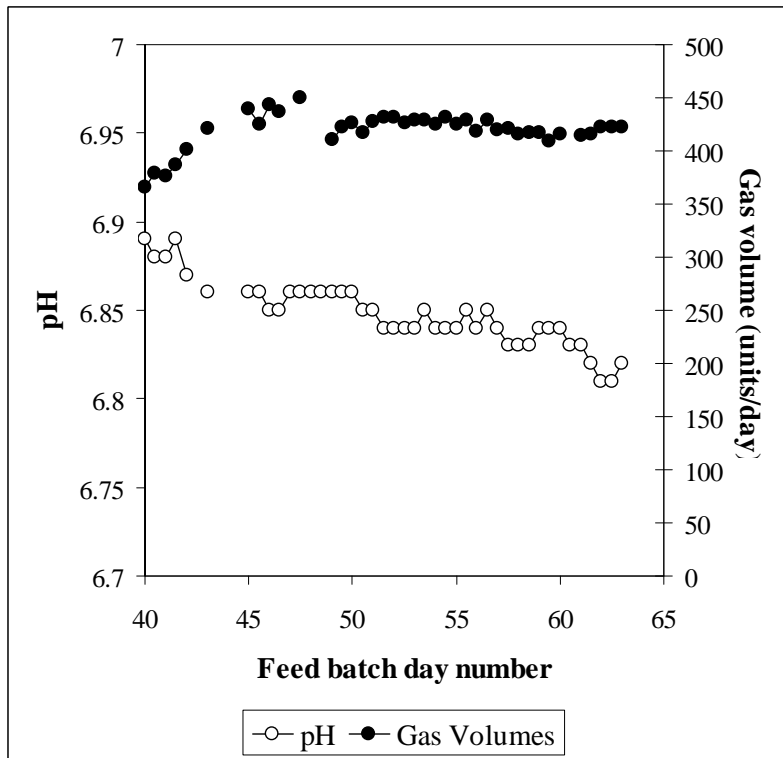


Figure C.14: Daily measurements of the pH and volumetric gas production for the transient stage between steady states number 21 and 23 (steady state 23 from day 50.5)

Appendix C: Transient Data

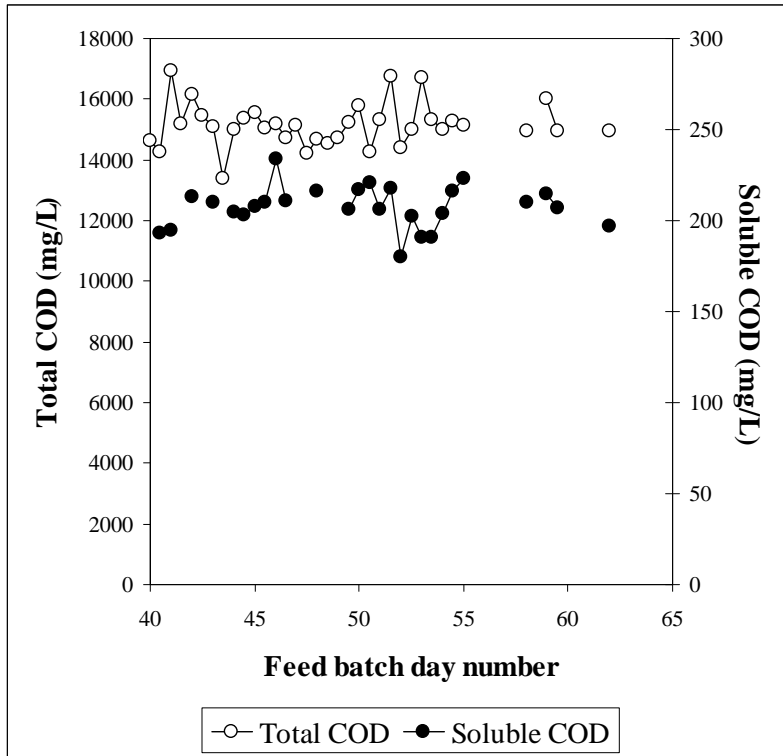


Figure C.15: Daily measurements of the total COD and soluble COD for the transient stage between steady states number 21 and 23 (steady state 23 from day 50.5)

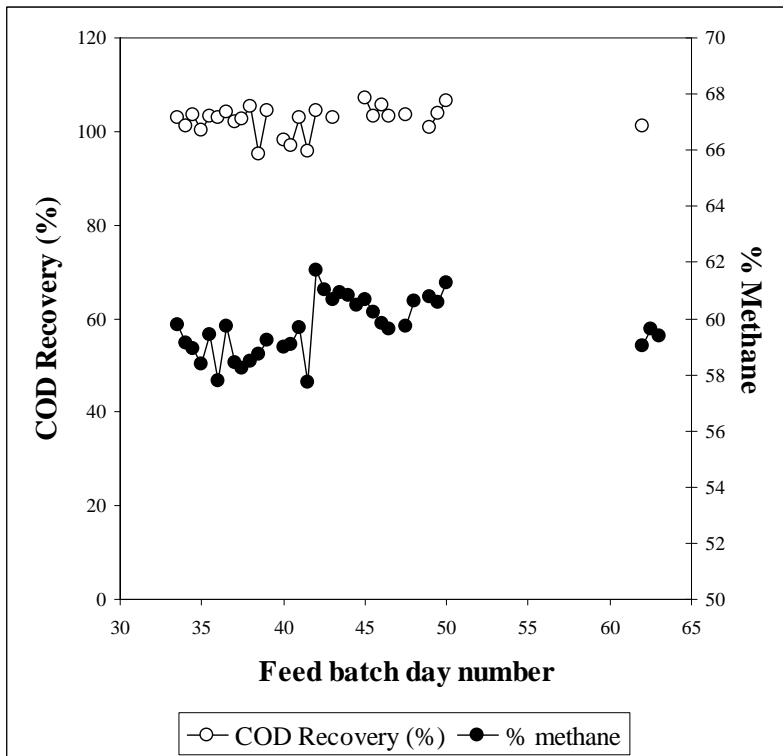


Figure C.16: Daily measurements of the gas composition (% methane calculated) and COD mass balance recovery for the transient stage between steady states number 21 and 23 (steady state 23 from day 50.5)

Appendix C: Transient Data

Table C.4: Daily measured data for steady

Date	Day	Total COD (mgCOD/L)	Soluble COD (mgCOD/L)	Suspended Solids (mgCOD/L)	VFA (mg/L as HAc)	Alkalinity (mg/L as CaCO ₃)	pH	Gas Volume (Units/day)	%CH ₄	%CO ₂	Mass of PSS (g)	Total feed mass (g)	TKN (mgN/L)	NH ₃ (mgN/L)	TP (mgP/L)	PO ₄ (mgP/L)	
21-Oct	33	15579	216	3888	0.0	1862.9	6.91	358			1250	1250	399	266	189	28	
21-Oct	33.5	15045	235	3898	27.8	1875.6	6.90	356	49.2	33.1	1250	1250	560	221	197		
22-Oct	34	14661	213		22.1	1938.3	6.91	356	45.3	31.3	1250	1250	553	273	193	22	
22-Oct	34.5	15143	209	3970	8.3	1748.9	6.91	363	45.5	31.7	1250	1250	651	263	193	31	
23-Oct	35	15175	210	3750	4.2	1730.4	6.90	346	39.7	28.3	1250	1250	637	273	197	22	
23-Oct	35.5	15624	214	3631	18.2	1946.7	6.90	349	46.6	31.8	1250	1250	658	265	201	26	
24-Oct	36	15606	208	3713	31.1	1873.6	6.90	359	39	28.5	1250	1250	634	262	164	22	
24-Oct	36.5	15508	199	3491	33.0	1901.6	6.89	356	46.4	31.3	1250	1250	662	256	193	21	
25-Oct	37	14719	198	3420	17.4	1905	6.89	365	40.6	28.9	1250	1250	630	258	184	31	
25-Oct	37.5	15254	205		22.4	1738.4	6.89	360	41.4	29.7	1250	1250	655	257	180	21	
26-Oct	38	14437	203	3571	19.8	1944.2	6.89	389	44.5	31.6	1250	1250	637	258	184	30	
26-Oct	38.5	14256	189	2891	23.3	1776	6.88	329	43.5	30.6	1250	1250	651	255	193	22	
27-Oct	39	14787	197	3552	28.9	1860.1	6.89	373	48.8	33.6	1250	1250	648	246	172	25	
27-Oct	39.5	14639	199	3351	31.2	1807.7	6.88	375			1300	1300	679	237	197	20	
End of steady state number 21. The feed was changed from an 8-day retention time to a 6.67-day retention time as follows:																	
27-Oct	39.5	14639	199	3351	31.2	1807.7	6.88	375			1300	1300	679	237	197	20	
28-Oct	40	14608					6.89	366	45.3	31.5	1350	1350	665		184		
28-Oct	40.5	14263	193				6.88	379	47.6	33	1400	1400	641	249	184	36	
29-Oct	41	16937	195		27.0	1849.6	6.88	376	49	33.1	1450	1450	637	249	180	34	
29-Oct	41.5	15191					6.89	387	39.6	29	1500	1500	644		184		
30-Oct	42	16163	213		25.3	1827.1	6.87	401	49.3	30.6	1500	1500	665	255	176	28	
30-Oct	42.5	15459							48.4	30.9	1500	1500	655		176		
31-Oct	43	15085	210		8.9	1768.5	6.86	421	47.5	30.8	1500	1500	655	249	184	22	
31-Oct	43.5	13396							47.1	30.2	1500	1500	616		172		
01-Nov	44	14984							48.6	31.3	1500	1500	648	256	197	30	
01-Nov	44.5	15375	203		4.5	1700.9			46.8	30.6	1500	1500	665	248	172	34	
02-Nov	45	15540	208				6.86	440	47.4	30.7	1500	1500	637	244	164	22	
02-Nov	45.5	15057	210		10.1	1664.8	6.86	425	47.7	31.5	1500	1500	651	247	180	28	
03-Nov	46	15180	234		35.8	1809.3	6.85	444	45.4	30.5	1500	1500	641	251	184	20	
03-Nov	46.5	14705	211		16.3	1839.6	6.85	437	44.9	30.4	1500	1500	651	234	180	28	
04-Nov	47	15142			21.9	1836	6.86				1500	1500	637		184		
04-Nov	47.5	14198					6.86	450	45.5	30.7	1500	1500	641		180		

Appendix C: Transient Data

Table C.4: Continued

Date	Day	Total COD (mgCOD/L)	Soluble COD (mgCOD/L)	Suspended Solids (mgCOD/L)	VFA (mg/L as HAc)	Alkalinity (mg/L as CaCO ₃)	pH	Gas Volume (Units/day)	%CH ₄	%CO ₂	Mass of PSS (g)	Total feed mass (g)	TKN (mgN/L)	NH ₃ (mgN/L)	TP (mgP/L)	PO ₄ (mgP/L)
05-Nov	48	14664	216		7.7	1762.7	6.86		44.5	28.9	1500	1500	658	242	180	19
05-Nov	48.5	14525					6.86				1500	1500	357			
06-Nov	49	14728					6.86	411	45.4	29.3	1500	1500	361		171	
06-Nov	49.5	15242	206		1.4	1764.1	6.86	423	46.9	30.5	1500	1500	438	250	174	29
07-Nov	50	15795	217		32.0	1882.2	6.86	426	50.6	32	1500	1500	490	258	174	22
07-Nov	50.5	14272	221		13.2	1822.6	6.85	417			1500	1500	375	245	159	21
08-Nov	51	15342	206		11.2	1814.3	6.85	428			1500	1500	525	252	174	21
08-Nov	51.5	16755	218		0.0	1853.2	6.84	432			1500	1500	585	237	174	32
09-Nov	52	14413	180		21.6	1837.4	6.84	431			1500	1500	396	248	171	27
09-Nov	52.5	14977	202		0.0	1768.2	6.84	426			1500	1500	399	255	171	24
10-Nov	53	16707	191	3618	25.7	1815.4	6.84	429			1500	1500	515	244	182	23
10-Nov	53.5	15345	191	4054	2.0	1792.3	6.85	429			1500	1500	431	255	178	27
11-Nov	54	14990	204		12.6	1839	6.84	425			1500	1500	494	256	174	29
11-Nov	54.5	15291	216	3591			6.84	431			1500	1500	515	253	174	33
12-Nov	55	15160	223	4285	17.4	1829.8	6.84	425			1500	1500	518	256	174	15
12-Nov	55.5				19.4	1864.2	6.85	429			1500	1500	560	260	178	30
13-Nov	56				1.1	1812.9	6.84	419			1500	1500	609	253	178	16
13-Nov	56.5				12.0	1826.7	6.85	429			1500	1500	602	248	155	28
14-Nov	57				22.0	1820.9	6.84	420			1500	1500	578	256	182	21
14-Nov	57.5						6.83	421			1500	1500				
15-Nov	58	14943	210	3567	25.0	1837.6	6.83	416			1500	1500	641	255	178	30
15-Nov	58.5						6.83	417			1500	1500				
16-Nov	59	16020	215	3464	36.2	1812.9	6.84	417			1500	1500	634	251	178	27
16-Nov	59.5	14943	207	3820	0.0	1738.8	6.84	409			1500	1500	641	253	182	18
17-Nov	60			3610			6.84	416			1500	1500				
17-Nov	60.5						6.83				1500	1500				
18-Nov	61				7.2	1837	6.83	414			1500	1500				
18-Nov	61.5						6.82	416			1500	1500				
19-Nov	62	14970	197	4033	12.1	1788.8	6.81	422	44.5	30.9	1500	1500	641	225	178	29
19-Nov	62.5						6.81	422	46.8	31.7	1500	1500				
20-Nov	63						6.82	422	46	31.5	1550	1550				

Appendix C: Transient Data

Appendix D: Sulfate measurement in organic-rich solutions: Carbonate fusion pretreatment to remove colour interference

Ristow, N.E., Sötemann, S.W., Wentzel*, M.C., Loewenthal, R.E. and Ekama, G.A.

Water Research Group, Department of Civil Engineering, University of Cape Town, South Africa, *markw@ebe.uct.ac.za, tel: + 27 21 650 2583, fax: + 27 21 689 7471

Abstract

Sulfate measurement using a barium sulfate turbidimetric method in solutions with high concentrations of organic material is shown to be problematic. The organics give background colour, which introduces a positive error to the measured absorption, and inhibit the barium sulfate precipitate, which results in a negative error. A carbonate fusion pretreatment of the sample results in the removal of the organic matter and associated interferences. With this pretreatment, excellent sulfate recoveries were obtained (100%). Rigorous testing of the method shows that reproducible and accurate results are obtainable.

Introduction

In a variety of applications of biological sulfate reduction, measurement of sulfate in the presence of elevated concentrations of organic materials is required. Such measurements have proved problematic due to the organic interferences. This paper investigates the interference of organics in sulfate measurement by standard methods, and proposes modifications to the prescribed methods to overcome these interferences.

Standard Methods (1985) describes four methods for the determination of sulfate in water: Methods 426A, B, C and D. Two of these methods (426A and 426B) involve the formation of a barium sulfate precipitate in hydrochloric acid at near boiling temperature, followed by a period of digestion (>2h), filtration of the barium sulfate, which is then either dried (426B) or ignited (426A), and the residue weighed. However, both methods are described as being subject to much interference, leading to both positive and negative errors. Interferences include suspended matter, silica, barium chloride, nitrate, sulfite and alkali metals, all of which add to the mass of the dried or ignited residue, or substitute the barium ion with one of a lower or higher molecular weight. Accordingly, these two test methods were rejected for further evaluation.

Method 426D requires the availability of an autoanalyser, which would render it unfeasible unless large quantities of samples were being tested and hence was not investigated further. Method 426C requires the formation of a barium sulfate precipitate in an acetic acid buffer solution, and the measurement of the absorbance of the precipitate using a spectrophotometer at 420nm wavelength. However, Standard Methods (1985) lists colour, suspended matter and organic material as the major interferences. If the organic material and colour can be removed from the sample to allow for the accurate measurement of the sulfate concentration, the method would seem practical and feasible. Accordingly, a preliminary evaluation of the method was undertaken.

Appendix D: Sulfate Measurement Method

Preliminary Evaluation

Method 426C can be used automated with an autoanalyser, and the accuracy of this automated method was evaluated and also compared with a commercially available sulfate test kit (Merck, Method No 14791). A standard sulfate solution (100 mgSO₄/L) was prepared and increasing amounts of sulfate free soluble organic solution (soluble fraction of methanogenic anaerobic digester effluent, filtered through a 0.45µm filter paper, S&S ME 25/21) were added to the standard solution. Table 1 shows the results of this experiment. Clearly, for both methods, as the organic concentration in the sample increases, the accuracy of the analysis deteriorates. The accuracy of the test kit was inferior both for the solution without sulfate present and for the standard sulfate solution without organic matter, and accordingly the test kit version of the method was discarded.

Table 1: Sulfate concentrations of two experiments to determine the effects of a sulfate free soluble organic solution on the analysis of a standard sulfate solution

Sulfate Concentration (mgSO ₄ /L)	Volume organics added (mL)	Sulfate Concentration (mgSO ₄ /L)	
		Merck method	Autoanalyser
0	10	112; 83; 42	0; 0; 0
0	20	77; 66; 78	5; 0; 0
100	0	134; 149; 130	103; 101; 100
100	10	108; 132; 152	112; 113; 112
100	20	119; 123; 120	138; 138; 18

Although Table 1 clearly illustrates the interference of soluble organic matter on the accuracy of Method 426C using an autoanalyser, the accuracy of the method for samples without organic interference was encouraging. Also, the method shows that the organic solution added to the sulfate standard solution was indeed sulfate free (of importance in the experiments that follow). Accordingly, the method was selected for modification, to develop pretreatments to remove the organics prior to application.

Method Development

As noted above, Standard Methods (1985) lists colour, suspended matter and organic material as the major interferences in Method 426C. The method is based on the formation of a barium sulfate (BaSO₄) precipitate of uniform size under controlled pH conditions using an acetate buffer, and then measuring the absorbance of the BaSO₄ suspension using a spectrophotometer. Filtration of the sample will remove the suspended matter and particulate organic material, especially if used in conjunction with a flocculent, and hence these interferences can be readily overcome. However, interference by the colour of the sample, and particularly soluble organics, would be problematic, and need to be addressed.

Appendix D: Sulfate Measurement Method

Calibration Curve

The turbidimetric method (Method 426C) requires the generation of a standard calibration curve. To overcome the colour interference (and the soluble organic interference if this is due to colour only), the standard sulfate samples could be measured in the presence of the same, or similar, background matrix as the sulfate samples, so that the colour interferences would be incorporated into the calibration curve. Comparison of the calibration curve with one in which the background matrix is distilled water would also allow the magnitude of the interferences to be observed. Thus, a calibration curve was generated using a standard sulfate solution to which different amounts of methanogenic anaerobic digestion filtered effluent, in which the sulfate concentration would be zero, was added (similar to the experiments of Table 1).

The calibration curves generated in this manner were inconsistent. The addition of a fixed volume of organic matter to varying sulfate concentrations resulted in a consistent curve, but this curve was not reproducible. Further, when the organic addition was either halved or doubled, the curves generated gave no correlation to the amount of organic addition. Thus, the generation of a general calibration curve in the presence of the background organic matrix was not possible, nor would it be possible to use a series of calibration curves at different organic concentrations if the organic concentration of the sample was known. Thus, it was concluded that it is imperative that the organic background be removed from the sample prior to sulfate analysis.

To remove the organics from the sample, several alternatives were investigated but did not prove feasible. For example, with dichromate and nitric acid pre-digestion, the colour of the dichromate gave an absorbance greater than the barium sulfate precipitate. One method did appear promising, that of carbonate fusion, and this was investigated further. This carbonate fusion method proved very successful for removal of colour interference in total phosphorous measurement in municipal wastewater (Marton and Marias, 1975).

Organic interference removal by carbonate fusion

Prior to sulfate analysis (Method 426C above), the sample was to be passed through a carbonate fusion pretreatment, which would oxidize the organics and possibly remove both the colour and organic interferences. The carbonate fusion method involved drying a measured volume (10mL) of the filtered sample (0.45µm membrane filter) in a crucible. Both platinum and nickel crucibles were used without any difference in the results. Drying was achieved using either a steam bath or an oven. The advantage of using an oven was that the samples could be left unattended, while the steam bath required supervision. However, if the temperature of the oven was too high (> 150°C), the dried residue tended to splatter and flake, and part of the sample was lost from the crucible.

Once dry, a half-teaspoon of sodium carbonate (Na_2CO_3) was added, and the crucible heated over a powerful Bunsen burner until the sodium carbonate melted, forming a sodium meta-sulfate salt. This took around 30 seconds on a powerful burner, or several minutes on a normal Bunsen burner. Once the sodium carbonate had melted, the molten contents were swirled so that it came into contact with the entire initial sample. This was then allowed to cool. The cooled sodium meta-sulfate salt was then dissolved by adding sufficient (~10mL) 1:1 concentrated (12N) HCl: H_2O solution via a pipette. The acid reacted vigorously with the salt as carbon

Appendix D: Sulfate Measurement Method

dioxide was expelled, so that a watch glass was required to cover the crucible to prevent loss of sample. Once the sample ceased fizzing, the crucible contents were poured into a 50mL or 100mL volumetric flask, depending on the dilution required for the final sample. The crucible and cover glass were rinsed with distilled water and the rinse water captured into the volumetric flask. A drop of phenolphthalein indicator was added to the volumetric flask, followed by 10M sodium hydroxide solution (drop wise) until the solution turned pink. The flask was then made up to volume with distilled water. This solution was then further diluted into 50mL volumetric flasks so that the final concentration was in the recommended range of 10 – 40mgSO₄/L. The diluted sample then was subjected to the standard sulfate measurement method, Method 426C.

Carbonate fusion calibration curve

A calibration curve was generated by first making up standard sulfate solutions with the methanogenic organic sample as background. These standards were then pretreated using the carbonate fusion method above, and then subjected to the sulfate measurement method 426C. Two further calibration curves were generated in the same way, but with different dilutions of the same methanogenic organic sample as background. Table 2 lists the absorbance values for the three calibration curves, while Figure 1 plots these calibration curves.

From Table 2 and Figure 1, there is little difference between the absorbances from the standard curves with the three different organic concentrations. Clearly, the carbonate fusion pretreatment of the samples successfully removed all organic interferences. This allows for a single calibration curve to be used for all sample initial organic concentrations and background matrices.

Table 2: Values for the absorbances obtained from standard sulfate concentrations at difference concentrations of background organics, all pretreated by the carbonate fusion method

SO ₄ Concentration	Absorption with x50 organic dilution	Absorption with x100 organic dilution	Absorption with x200 organic dilution
0 (blank)	0.000	0.000	0.000
10	0.070	0.064, 0.070	0.070, 0.065
15		0.123, 0.123	
20	0.170, 0.178	0.170, 0.170	0.176, 0.171
25		0.220, 0.240	
30	0.298	0.316, 0.303	0.313, 0.314
35		0.352, 0.374	
40	0.428, 0.428	0.410, 0.430	0.380, 0.382
50	0.572	0.555, 0.570	0.558

Appendix D: Sulfate Measurement Method

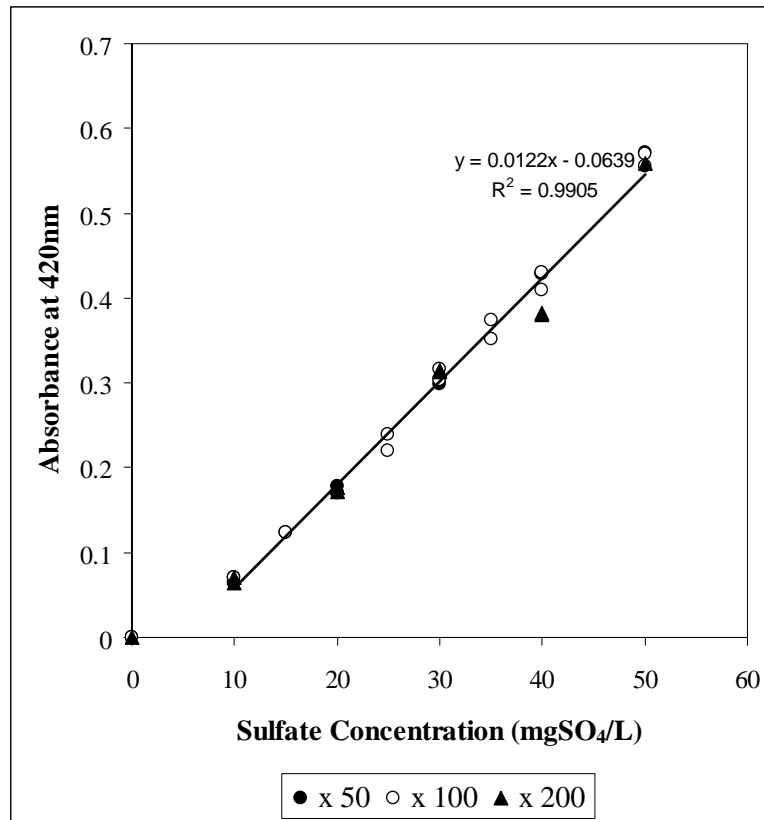


Figure 2: Sulfate calibration curves with three different background organic concentrations; all samples pretreated with the carbonate fusion method

Standard Methods (1985) states that the BaSO₄ turbidity method 426C is restricted to the range of 10 to 40mgSO₄/L. In the study here, although the absorbance at zero sulfate concentration is zero, the relationship between the sulfate concentration and the absorbance is non-linear between 0 and 10mgSO₄/L (Figure 1), confirming the lower measurement limit. As expected, the relationship is linear between 10 and 40mgSO₄/L, but the linearity continues above 40mgSO₄/L, suggesting a higher upper limit of at least 50mgSO₄/L. This possibly could be extended further, but was not evaluated here.

To test whether standard samples used to generate the calibration curve require carbonate fusion pretreatment or not, a calibration curve was generated using a standard sulfate solution and deionised water only. A sample of the standard sulfate solution was put through the carbonate fusion pretreatment, and the absorbance compared to the calibration curve. The 120mgSO₄/L sample was analyzed at 119 and 122mgSO₄/L (99.17 and 101.17% respectively). Thus, irrespective of whether the standard samples in the calibration curve are pretreated with carbonate fusion or not, the same absorbance is obtained. This indicates that the carbonate fusion pretreatment does not impact the subsequent sulfate measurement method (Method 426C). Hence, a standard curve using deionised water will suffice for samples that are being treated by the carbonate fusion method.

Appendix D: Sulfate Measurement Method

Method verification

To verify the proposed method, two samples (S1 and S2) were drawn from two laboratory-scale anaerobic digesters (one from each) being fed a mixture of primary settled sludge (PSS) and sulfate. A third sample (M1) was drawn from a purely methanogenic laboratory-scale anaerobic digester. A few grains of zinc acetate (ZnAc) were added to the two samples (S1 and S2) (sulfate-reducing systems) to precipitate any sulfide present, since these systems generate sulfide: aqueous sulfide would be oxidized to sulfate in the carbonate fusion pretreatment step and hence add to the sulfate measured in the subsequent BaSO₄ turbidity step. NaOH was added to precipitate the residual Zn as Zn(OH)₂, which also acted as a flocculent. The samples were settled for 1 minute, and the supernatant then filtered through a 0.45µm membrane filter paper (S&S ME25/21). The filtrate samples were used for a series of experiments to demonstrate the effects of the background matrix on the sulfate analysis. Sample S1 and S2 0.45µm filtrate were analyzed directly, but with appropriate dilution with distilled water to bring the sulfate concentrations into the measurement range (see above), Table 3. A third sample (S2 and M1) was made up from a mixture of sample S2 and M1 filtrates, with the addition of M1 to S2 to give the same dilution as for S2 above. It is important to note that the methanogenic anaerobic digester from which sample M1 was drawn was operating under very stable conditions, and thus the VFA concentration was negligible. However, the sample M1 was visibly brown in colour.

The three samples (S1, S2 and S2 + M1) were divided into two duplicates. The one set of samples had no pretreatment, while the other set was subjected to pretreatment using the carbonate fusion method above. The absorbances of the three blank samples (S1, S2 and S2 + M1) were measured, without barium chloride addition, for both the non-treated and carbonate-fusion pretreated sets of samples. Each sample in both sets was then divided into two and the BaSO₄ turbidity method (426C) applied to the duplicates, and the absorbance measured. Absorbances were converted to “equivalent” sulfate concentrations with the calibration curve in Figure 1, and the dilution taken into account, see Table 3.

Table 3: Equivalent sulfate concentrations for samples S1, S2 and S2 + M1, with and without organic and barium chloride (BaCl₂) addition, and with and without carbonate fusion pretreatment

Treatment	Sulfate Concentration (mgSO ₄ /L)		
	S1 Sulfate sample 1	S2 Sulfate sample 2	S2 + M1 Sulfate sample + soluble organic solution
Dilution	20	6.66	6.66
Blank (no BaCl₂; no carbonate fusion)	135	83	93
BaCl₂ added; no carbonate fusion	246; 352	85; 85	96; 97
Blank (no BaCl₂; carbonate fusion)	0	0	0
Carbonate fusion; BaCl₂ added	276; 262	99; 99	98; 98

Appendix D: Sulfate Measurement Method

From Table 3, it is clear that the presence of the organic solution significantly effects the measurement of the sulfate. For the sample set without carbonate fusion pretreatment, the colour in the blanks results in significant absorbances, which translated to significant sulfate concentrations (83 – 135mgSO₄/L). Method 426C suggests that the absorbance of the blank sample be subtracted from absorbance of the sample to which the barium chloride has been added. In this case, for sample S2, the calculated sulfate concentration would be 2mg SO₄/L (85 – 83mgSO₄/L), and when the organic solution (M1) was added, it would increase to 3 – 4 mgSO₄/L (96 or 97 – 93mgSO₄/L). For sample S1, the difference between the two duplicate measured concentrations (246 and 352mgSO₄/L) is so great that an accurate estimate is not possible. However, for all three samples, the carbonate fusion pretreatment successfully removed all colour interferences, in that no absorbance and hence sulfate concentrations were measured for the blank samples. Further, the measured concentrations were more consistent, 276 and 262mgSO₄/L for S1, 99 and 99 and 98 and 98mgSO₄/L for S2 with and without M1 addition respectively. Additionally, a third S1 sample at a different dilution was analyzed including carbonate fusion pretreatment, and gave a concentration of 288 mgSO₄/L (compared with 276 and 262mgSO₄/L, Table 3). With the carbonate fusion pretreatment, the sulfate concentration in sample S1 (98 – 99mgSO₄/L) is significantly higher than that obtained without the pretreatment (2 – 4mgSO₄/L). This, and the change in sulfate concentration induced by adding organics would suggest that the organics interference in the test method is not only background colour, but also in the BaSO₄ precipitate. However, since the actual sulfate concentration in the samples is not known, it cannot be stated unequivocally that the carbonate fusion pretreatment measurement is superior. Accordingly, sulfate recovery tests were undertaken.

Following the procedures above, a standard sulfate solution was added to a sulfate-reducing system sample with unknown sulfate concentration. Additions were made to the equivalent of 0, 20 and 40mgSO₄/L, and the respective measured concentrations were 44, 64 and 84mgSO₄/L, indicating a 100% sulfate recovery. This substantially verifies the carbonate fusion pretreatment modification to the test method (426C).

To test the reproducibility of the carbonate fusion pretreatment method, four samples were drawn separately from a single anaerobic digester being fed a sulfate and primary sewage sludge (PSS) mixture and analyzed following the procedures detailed above. The results for the four samples were 129, 122, 119 and 124 mgSO₄/L, showing excellent reproducibility (coefficient of variation = 0.03).

To further demonstrate the interference of organics in the method, a soluble organic solution (methanogenic supernatant, brown in colour, no sulfate, see above) was added to the samples after the carbonate fusion pretreatment step, but before the BaSO₄ precipitation. The results showed that the addition of 5 and 10mL of methanogenic organic solution (no SO₄) gave an increase in the equivalent measured sulfate concentration (128mgSO₄/L (no organic); 142mgSO₄/L (5mL organic); 170 mgSO₄/L (10mL organic)). This re-enforces the interferences in measuring sulfate in high organic solutions.

Conclusions

The presence of organic matter interferes with the BaSO₄ turbidimetric method (Method 426C, Standard Methods, 1985) for the determination of sulfate in organic-rich solutions. The

Appendix D: Sulfate Measurement Method

interference of the organics in the method is due both to their background colour, and to their interference in the BaSO_4 precipitation. Carbonate fusion pretreatment has been shown to remove the interference, and excellent recoveries of added sulfate were obtained.

Acknowledgements

This research was supported by the Water Research Commission, National Research Foundation and the University of Cape Town, and is published with their permission.

Reference

Marton, K.A.C. and Marias, G.v.R. 1975. Kinetics of enhanced phosphorous removal in the activated sludge process. Research Report W14, Department of Civil Engineering, University of Cape Town, Rondebosch, 7701, South Africa.

Standard Methods for the Examination of Water and Wastewater (1985). 19th edn, American Public Health Association/American Water Works Association/Water Environment Federation, Washington DC, USA.